

Extracellular Vesicles as a Non-Invasive Endometrial Receptivity Biomarker

Amber Rose Hart

A thesis submitted in partial fulfilment of the requirement of the degree of Doctor of Philosophy

The University of Sheffield

Division of Clinical Medicine,
School of Medicine and Population Health.

Submitted April 2024

Authors Declaration.

I, the author, confirm that the work within this thesis is an original report of my research and composed by myself. The work contained herein is my own except where explicitly stated and appropriate credit has been given where work has formed part of a joint authored publication. This thesis has never been previously submitted at this university or any other institution.

Amber Rose Hart

April 2024

Abstract.

Infertility is a pressing global issue, impacting the mental well-being, financial stability, and societal aspects of aspiring parents facing challenges in conception. Assisted reproductive technologies (ART) offer hope, yet their efficiency remains suboptimal, marked by a considerable 70% rate of implantation failure. In response, efforts have been directed towards identifying assays and markers to assess endometrial receptivity; however, existing methods are often unreliable, controversial, and invasive.

This thesis explores the potential use of the small nanoparticles extracellular vesicles (EVs), as a non-invasive biomarker for endometrial receptivity. Drawing upon years of research on the role of EVs in maternal communication, the study investigates whether EVs can address the escalating global infertility crisis. The primary objective is to establish a proof of concept for this novel idea while advancing our comprehension of endometrial EV characteristics.

To achieve this, an *in vitro* model simulating the menstrual cycle's phases under the influence of sex hormones was employed, enabling the isolation and analysis of resulting endometrial EVs. Our results demonstrated that while endometrial-derived EVs were secreted in numbers independent of hormonal stimulation, the size and proteomic profile of these EVs were significantly influenced by hormonal conditions, particularly during the receptive window of implantation phase, with proteins involved in embryo implantation, endometrial receptivity, and embryo development being notably enhanced.

The model was expanded by incorporating a trophoblast cell line and a binding assay, elucidating the functional and transcriptomic effects of endometrial EVs. Notably, hormonally stimulated endometrial-derived EVs reflecting the window of implantation were shown to significantly enhance trophoblast binding affinity, with mRNA sequencing revealing critical changes in gene expression related to glycosphingolipid biosynthesis, immune modulation, and cellular signalling, underscoring the role of EVs in embryo-endometrial communication.

In response to the imperative for non-invasive biomarkers, the thesis also explores the isolation and optimisation of urine-derived EVs (uEVs), examining their proteomic profile in samples from female volunteers across different menstrual cycle phases. Our findings indicate that while the concentration of uEVs varies with the menstrual cycle, their size remains consistent. Importantly, the proteomic profile of uEVs was significantly altered during the window of implantation, highlighting their potential as biomarkers for enhancing fertility.

This comprehensive investigation significantly contributes to our understanding of EVs in reproductive processes and introduces a groundbreaking perspective on uEVs as a promising biofluid for endometrial receptivity biomarkers. The study's insights lay the groundwork for future research, paving the way for the development of much-needed non-invasive biomarker-based approaches to enhance implantation and pregnancy success.

Thesis outline.

This thesis is presented in publication format. Chapter 1 is an introduction in which we introduce the topics that will be found in each of the proceeding chapters. It will give background context into why this research is being conducted and the wider implications this work could have. First it will introduce infertility and receptivity and the role that cell-to-cell communication has within this. It will then introduce the new research area of EVs in this communication, giving a background into EVs in terms of their biogenesis and function. The chapter will then go on to reference endometrial-derived EVs and how previous publications have shown them to have a role in this communication and receptivity. From this discussion, the question will be raised: can endometrial EVs be exploited in diagnosis and treatment in a clinical setting? This will lead onto the non-invasive aspect of the thesis: the work on urine and uEVs as biomarkers. Referenced will be how biomarker discovery in urine is advantageous and how this area can be explored to determine receptivity and improve pregnancy rates.

Chapter 2 will focus on the *in vitro* work conducted on the endometrial cell line RL95-2 in which the sex hormones estrogen and progesterone were used in various combinations and concentrations to mimic the different phases of the menstrual cycle. The results in this chapter will have a proteomic focus. The areas discussed will be how receptive phase EVs are enriched in protein known to have a role in embryo implantation, endometrial receptivity, and embryo development, supporting the concept of a communication system between the embryo and the maternal endometrium via EVs.

Chapter 3 focuses on examining EVs from an endometrial receptive cells line under the influence of sex hormones and exploring their effect on trophoblast binding and Messenger ribonucleic acid (mRNA) expression in trophoblasts. This chapter confirms, in a functional way, that endometrial EVs from the hormone-stimulated receptive phase have a role in implantation.

Chapter 4 focuses on the optimisation and repeatability of isolating EVs from urine biofluid, as well as an assessment of the effect of storage conditions on EV isolation yield. This chapter will form as the basis for the following chapter on uEVs for evaluating them as a non-invasive EV biomarker.

Chapter 5 will focus on urine samples from participants to explore the effects of the menstrual cycle on urine EVs. This chapter will have a proteomic focus, with the EV proteome from the urine samples assessed and the different phases compared. This chapter will help characterise the uEVs proteome across the menstrual phases and will begin the identification of potential biomarkers of the receptive period.

Reflecting on the results from the proceeding chapters, chapter 6 will provide a review of the current landscape of endometrial receptivity tests as well as proposing how the future direction of endometrial receptivity test research should proceed.

Finally, Chapter 7 will bring together the discussions from all the other chapters to form a cohesive story about research into EVs as a non-invasive receptivity marker. It will

summarise the work carried out, examine further work that is required, and explore the prospects and implications this research could lead to.

Acknowledgements.

I would like to thank my supervisors Professor Alireza Fazeli, Dr Paul Heath and Dr Saji Eapen for their help and support, being inspirational supervisors and for providing me with the opportunity to become involved in many research projects and collaborations. Thank you also to all the students and staff within the Fazeli Lab for the opportunities to present and discuss my work and the excellent supportive atmosphere. I would also like to thank the University of Sheffield and Swiss Precision Diagnostic Limited for the studentship that allowed me to carry out these studies and make these advancements in science discoveries. Finally thank you to my parents and friends for their support, time, and unwavering belief in me over the years.

Contents

AUTHORS DECLARATION **P2**

ABSTRACT **P3**

THESIS OUTLINE **P5**

ACKNOWLEDGMENTS **P8**

CONTENT **P9**

FIGURE LIST **P16**

TABLE LIST **P21**

ABBREVIATIONS **P23**

CHAPTER 1: INTRODUCTION

1.1 AUTHORS CONTRIBUTIONS **P29**

1.2 INFERTILITY **P30**

1.3 ESTABLISHMENT AND MAINTENANCE OF PREGNANCY

1.3.1 CHARACTERISATION OF DECIDUALISATION P34

1.3.2 WINDOW OF UTERINE RECEPTIVITY P37

1.3.3 IMMUNOTOLERANCE P39

1.4 EXTRACELLULAR VESICLES

1.4.1 DEFINITION AND BIOGENESIS P43

1.4.2 CONTENT AND FUNCTION P45

1.5 EMBRYO DERIVED EXTRACELLULAR VESICLES AND THEIR FUNCTION **P49**

1.6 ENDOMETRIAL DERIVED EXTRACELLULAR VESICLES AND THEIR FUNCTION **P55**

1.7 CAN ENDOMETRIAL AND EMBRYO DERIVED EVS BE EXPLOITED IN DIAGNOSTICS AND TREATMENT? **P59**

1.8 URINE AS BIOMARKER BIOFLUID **P64**

1.9 URINARY EXTRACELLULAR VESICLES DEFINITION AND BIOGENESIS **P65**

1.10 URINARY EXTRACELLULAR ISOLATION AND BIOMARKER DISCOVERIES **P68**

1.11 THE FUTURE OF URINARY EXTRACELLULAR VESICLES IN CLINICAL APPLICATION **P72**

1.12 CONCLUSION **P73**

1.13 THESIS AIMS **P74**

1.14 REFERENCES.....**P76**

CHAPTER 2: THE EFFECT OF SEX HORMONE ON ENDOMETRIAL EVS PROTEOME

2.1 AUTHORS CONTRIBUTIONS **P94**

2.2 CHAPTER AIM.....**P95**

2.3 ABSTRACT **P95**

2.4 INTRODUCTION **P74**

2.5 MATERIALS AND METHODS

2.5.1 CELL CULTURE P98

2.5.2 DIFFERENTIAL CENTRIFUGATION.....P99

2.5.3 SIZE EXCLUSION CHROMATOGRAPHY.....P99

2.5.4 NANOPARTICLE TRACKING ANALYSIS.....P100

2.5.5 RL95-2 CELL CONDITION MEDIA EV ISOLATION OPTIMISATION P100

2.5.6 HORMONE TREATMENT OF RL95-2 CELLS.....P101

2.5.7 TRANSMISSION ELECTRON MICROSCOPY (TEM) P102

2.5.8 PROTEOMIC ANALYSIS – LABEL-FREE LIQUID CHROMATOGRAPHY TANDEM MASS SPECTROMETRY (LC-MS/MS).....P102

2.5.9 PROTEOMIC DATA ANALYSIS.....P103

2.5.10 WESTERN BLOT.....P104

2.5.11 STATISTICAL ANALYSIS P105

2.6 RESULTS

2.6.1 CHARACTERISATION OF EVS RELEASED ROM RL95-2 CELLS P106

2.6.2 CONCENTRATION AND SIZE DISTRIBUTION OF EVS RELEASED FROM HORMONE TREATED RL95-2 CELLS P109

2.6.3 COMPARATIVE PROTEOMIC ANALYSIS OF ENDOMETRIAL EVS UNDER HORMONAL TREATMENT P111

2.6.4 VALIDATION OF LC/MS-MS RESULTS.....P124

2.7 DISCUSSION P124

2.7.1 RECEPTIVE PHASE ENDOMETRIAL CELL EVS WERE ENRICHED WITH PROTEIN INVOLVED IN EMBRYO IMPLANTATION P126

2.7.2 RECEPTIVE PHASE ENDOMETRIAL EVS WERE ENRICHED IN PROTEINS INVOLVED IN EMBRYO DEVELOPMENT P128

2.7.3 RECEPTIVE PHASE ENDOMETRIAL EVS WERE ENRICHED IN PROTEINS INVOLVED IN ENDOMETRIAL RECEPTIVITY P129
2.7.4 RECEPTIVE PHASE ENDOMETRIAL EVS GO TERMS AND KEGG PATHWAYS ARE ASSOCIATED WITH RECEPTIVITY AND IMPLANTATION SUCCESS...P130
2.8 CONCLUSION **P132**
2.9 REFERENCES **P134**
2.10 SUPPLEMENTARY MATERIALS.....**P142**
CHAPTER 3: HORMONAL TREATED ENDOMETRIAL CELL DERIVED EVS ALTER THE BINDING AFFINITY OF TROPHOBLAST TO ENDOMETRIAL CELLS
3.1 AUTHORS CONTRIBUTIONS **P153**
3.2 INTERCONNECTING CHAPTERS **P153**
3.3 CHAPTER AIM.....**P153**
3.4 ABSTRACT **P154**
3.5 INTRODUCTION.....**P155**
3.6 MATERIALS AND METHODS
3.6.1 CELL CULTURE P157
3.6.2 DIFFERENTIAL CENTRIFUGATION P158
3.6.3 SIZE EXCLUSION CHROMATOGRAPHY P159
3.6.4 NANOPARTICLE TRACKING ANALYSIS P159
3.6.5 EV CHARACTERISATION.....P160
3.6.6 HORMONE TREATMENT OF RL95-2 CELLS.....P160
3.6.7 FORMATION AND TREATMENT OF JAR SPHEROIDS.....P160
3.6.8 FORMATION OF RL95-2 MONOLAYER.....P161
3.6.9 BINDING ASSAY P161
3.6.10 RNA EXTRACTION AND MRNA SEQUENCING P163
3.6.11 PROCESSING, ALIGNMENT, AND QUANTIFICATION OF RNA SEQUENCING (RNASEQ) READS.....P164
3.6.12 DIFFERENTIAL GENE EXPRESSION ANALYSIS P164
3.6.13 STATISTICAL ANALYSIS P165
3.6.14 EXPERIMENTAL DESIGN P165

3.7 RESULTS

3.7.1 EFFECT OF HORMONE STIMULATED ENDOMETRIAL EVS ON TROPHOBLAST BINDING.....P167

3.7.2 PRINCIPAL COMPONENT ANALYSIS (PCA) AND HEAT MAP VISUALISATION OF MRNA GENE EXPRESSION PATTERNS.....P168

3.7.3 DIFFERENTIAL ENRICHMENT ANALYSIS (DEA). P172

3.7.4 GENE SET ENRICHMENT ANALYSIS (GSEA) P178

3.8 DISCUSSION **P184**

3.9 CONCLUSION.....**P189**

3.10 REFERENCES **P190**

3.11 SUPPLEMENTARY MATERIALS **P194**

CHAPTER 4: COMPARISON OF URINE EV ISOLATION AND STORAGE METHODS FOR SUBSEQUENT BIOMARKER RESEARCH

4.1 AUTHORS CONTRIBUTIONS......**P225**

4.2 INTERCONNECTING CHAPTERS **P225**

4.3 CHAPTER AIM **P225**

4.4 ABSTRACT.....**P226**

4.5 INTRODUCTION **P227**

4.6 MATERIALS AND METHODS

4.6.1 URINE SAMPLES.....P229

4.6.2 DIFFERENTIAL CENTRIFUGATION P230

4.6.3 SIZE EXCLUSION CHROMATOGRAPHY.....P230

4.6.4 SALT PRECIPITATION P231

4.6.5 NANOPARTICLE TRACKING ANALYSIS P231

4.6.6 BICINCHONINIC ACID ASSAY P232

4.6.7 TRANSMISSION ELECTRON MICROSCOPY (TEM).....P232

4.6.8 EXPERIMENTAL DESIGN: URINE EV ISOLATION METHOD COMPARISON.....P233

4.6.9 EXPERIMENTAL DESIGN: STORAGE COMPARISON P235

4.6.10 STATISTICAL ANALYSIS P236

4.7 RESULTS

4.7.1 URINE EV ISOLATION OPTIMISATION METHOD COMPARISON P236

4.7.2 STORAGE COMPARISON P241

4.8 DISCUSSION P244

4.9 CONCLUSION P249

4.10 REFERENCES P251

4.11 SUPPLEMENTARY MATERIAL P255

CHAPTER 5: COMPARISON OF THE MENSTRUAL CYCLE PHASE ON URINE AND URINE EVS

5.1 AUTHORS CONTRIBUTIONS P257

5.2 INTERCONNECTING CHAPTERS P257

5.3 CHAPTER AIM.....P257

5.4 ABSTRACT P258

5.5 INTRODUCTION P259

5.6 MATERIALS AND METHODS

5.6.1 URINE SAMPLE COLLECTION P261

5.6.2 PRELIMINARY URINALYSIS P262

5.6.3 URINE SAMPLE CYCLE DAY SELECTION P263

5.6.4 URINE EV ISOLATION.....P263

5.6.5 NANOPARTICLE TRACKING ANALYSIS P264

5.6.6 TRANSMISSION ELECTRON MICROSCOPY (TEM).....P265

5.6.7 PROTEOMIC ANALYSIS- LABEL-FREE LIQUID CHROMATOGRAPHY TANDEM MASS SPECTROMETRY (LC-MS/MS).....P266

5.6.8 PROTEOMIC DATA ANALYSIS P267

5.6.9 DATA AVAILABILITY P267

5.6.10 STATISTICAL ANALYSIS.....P267

5.6.11 EXPERIMENTAL DESIGN P268

5.7 RESULTS

5.7.1 CHARACTERISATION OF URINE EVS P269

5.7.2 CONCENTRATION AND SIZE DISTRIBUTION OF URINE EVS FROM THE MENSTRUAL PHASES P272

5.7.3 COMPARATIVE PROTEOMIC ANALYSIS OF URINE EVS NEAT FROM THE MENSTRUAL PHASES P273

5.7.4 COMPARATIVE PROTEOMIC ANALYSIS OF NEAT URINE FROM THE MENSTRUAL PHASES P278

5.8 DISCUSSION P285

5.9 REFERENCES P292

5.10 SUPPLEMENTARY MATERIALS.....P301

CHAPTER 6: RETHINKING ENDOMETRIAL RECEPTIVITY TESTS: A CALL FOR INNOVATION

6.1 AUTHORS CONTRIBUTIONS.....P312

6.2 INTERCONNECTING CHAPTERS ...P312

6.3 ABSTRACT P313

6.4 INTRODUCTION P313

6.5 TRADITIONAL ENDOMETRIAL RECEPTIVITY TIMING.....P315

6.6 CURRENT PRACTICES.....P316

6.7 AVAILABLE ENDOMETRIAL RECEPTIVITY TESTS.....P317

6.8 WHAT AN IDEAL TEST NEEDS.....P323

6.9 FUTURE DIRECTION P325

6.10 CONCLUSION P328

6.11 REFERENCES P330

CHAPTER 7: DISCUSSION AND FUTURE DIRECTION

7.1 INTEGRATED DISCUSSION.....P337

7.1.1 ENDOMETRIAL EVS AND TROPHOBLAST INTERACTION P337

7.1.2 URINE EV ISOLATION, STORAGE AND OPTIMISATION.....P338

7.1.3 URINE EV PROTEOMIC PROFILING ACROSS MENSTRUAL CYCLE PHASES.....P339

7.1.4 RETHINKING ENDOMETRIAL RECEPTIVITY TESTING P339

7.2 FUTURE DIRECTION.....P340

7.3 CONCLUSION P342

CHAPTER 8: PUBLICATIONS

8.1 THE ROLE OF EXTRACELLULAR VESICLES IN ENDOMETRIAL RECEPTIVITY AND THEIR POTENTIAL IN REPRODUCTIVE THERAPEUTICS AND DIAGNOSIS.....P345

8.2 THE EXTRACELLULAR VESICLES PROTEOME OF ENDOMETRIAL CELLS SIMULATING THE RECEPTIVE MENSTRUAL PHASE DIFFERS FROM THAT OF ENDOMETRIAL CELLS SIMULATING THE NON-RECEPTIVE MENSTRUAL PHASE .....P 354

Figure list.

Figure 1.1. Ovarian hormones, folliculogenesis and uterine cycle throughout the normal human menstrual cycle.....P31

Figure 1.2. Extracellular vesicles produced from different cell types vary in size P44

Figure 1.3. Schematic representation of Extracellular vesicle structure and content.P46

Figure 1.4. Embryo-endometrium mutual crosstalk via Exosomes and Microvesicles.....P48

Figure 1.5. The origin of urinary EVs.....P67

Figure 1.6 Exploring EV isolation methods from human urine: insights from 2017 to 2022 publications via Using EV-TRACK P69

Figure 2.1. Protein content–based EV characterisation P107

Figure 2.2. Principal component analysis (PCA) of top 100 variable proteins in the study groups.....P108

Figure 2.3. TEM Image based characterisation of endometrial EVs from the different hormone treatment groups.....P108

Figure 2.4. Concentration and size distribution of EVs released from RL95-2 hormone-treated cells.....P110

Figure 2.5. Heatmap shows the log2 centred intensity of all significant proteins with the data centred per protein.....P113

Figure 2.6. Differential enrichment of EV proteins in different comparison groups...P114

Figure 2.7. GO enrichment of SAP in the different comparison groups.....P120

Figure 2.8. GO enrichment of SAP in the different comparison groups.....P121

Figure 2.9. KEGG Pathway analysis of SAP in the comparison groups and control...P123

Supplementary Figure 2.1. Isolation of extracellular vesicles sized particles secreted by the endometrial cell line RL95-2 using differential centrifugation and size exclusion chromatography.....P142

Supplementary Figure 2.2. Mass spectrometry validation.....P150

Supplementary Figure 2.3. Venn diagram of proteins enriched in the Control EV group versus the conditioned media control compared to the top 100 Vesiclepedia EV markers.....P151

Figure 3.1. Experimental design: determining the effect of EVs derived from hormone treated RL95-2 cells on trophoblast binding and transcriptional changed in JAr cells.....P166
Figure 3.2. JAr spheroid RL95-2 binding affinity after JAr cell spheroid treatment with EVs derived from hormone treated RL95-2 cells.....P167
Figure 3.3. Principal component analysis (PCA) of variable proteins in the study groups from 3 replicates P169
Figure 3.4. Principal component analysis (PCA) of variable proteins in the study groups, based on 2 replicates P170
Figure 3.5. Sample-to-sample clustering heat map.....P171
Figure 3.6. Sample-to-sample clustering heat map.....P171
Figure 3.7. Differential enrichment analysis of JAr genes in different comparison groups with the different EV treatment.....P173
Figure 3.8. Differential enrichment analysis of JAr genes in different comparison groups with the different EV treatment compared to untreated JAr cells.....P176
Figure 3.9. KEGG pathway analysis of GSEA in the different comparison groups, displaying the top 20 up and down regulated pathways P179
Figure 3.10. KEGG pathway analysis of GSEA in the different comparison groups....P180
Figure 3.11. KEGG pathway analysis of GSEA in the different comparison groups....P181
Figure 3.12. KEGG pathway analysis of GSEA in the different comparison groups....P182
Figure 3.13. KEGG pathway analysis of GSEA in the different comparison groups....P183
Figure 3.14. Venn diagram of GSEA KEGG pathways upregulated in JAr spheroid group treated with EVs derived from estrogen and progesterone treated RL95-2 cells compared to all other treatment and control groups.....P184
Supplementary Figure 3.1. Concentration and size distribution of EVs released from RL95-2 hormone-treated cells. P194
Supplementary Figure 3.2. Example image of JAr Spheroid formation after 24h formation period captured by an inverted microscope.....P194
Supplementary Figure 3.3. Optimisation of binding assay incubation time.....P195
Supplementary Figure 3.4. Example image of JAr spheroids binding to RL95-2 monolayer after 30 incubation period captured by an inverted microscope.....P195

Supplementary Figure 3.5. Principal component analysis (PCA) of variable proteins in the study groups from 3 replicates with batch effect not adjusted.....P196
Figure 4.1. Experimental Design for optimisation of EV Particle Isolation from Urine Using a Combination of Isolation Methods of Differential Centrifugation and Size Exclusion Chromatography and Analysis via Nanoparticle Tracking and Bicinchoninic Acid Assay.....P233
Figure 4.2. Experimental design for benchmarking EV particle isolation from urine Using a Combination of Isolation Methods of Differential Centrifugation, Salt Precipitation and Size Exclusion Chromatography and Analysis via Nanoparticle Tracking and Bicinchoninic Acid Assay.....P234
Figure 4.3. Experimental design for storage comparison of urine EVs.....P235
Figure 4.4 Comparison of particle concentration and protein concentration in SEC fractions from different urine starting volumes using isolation method 1.....P237
Figure 4.5 Comparison of particle concentration and protein concentration in SEC fractions from different urine starting volumes using isolation method 2.....P238
Figure 4.6. Comparison of Particle concentration among the different isolation methods and starting volumes.....P239
Figure 4.7. Particle concentration comparison of the different isolation methods with a change in the salt precipitation incubation temperature.....P240
Figure 4.8. Comparison of particle concentration yield under different storage conditions.....P242
Figure 4.9. Comparison of size distribution under different storage conditions.....P243
Figure 4.10. TEM Image-based characterisation of uEVs under different storage conditions.....P244
Figure 5.1. Study Experimental Design.....P269
Figure 5.2. Protein content-based uEV characterisation.....P270
Figure 5.3. Principal component analysis (PCA) of top 1500 variable proteins in the study groups.....P271
Figure 5.4. Transmission electron microscopy (TEM) Image based characterisation of urine EVs from the different menstrual cycle phases.....P271
Figure 5.5. Concentration and size distribution of EVs released from urine EVs from different menstrual cycle phases.....P272

Figure 5.6. Heatmap shows the log2 centred intensity of all significant proteins with the data centred per protein.....P274
Figure 5.7. Differential enrichment of uEV proteins in different comparison groups.P275
Figure 5.8. GO enrichment of SAP in the different comparison groups.....P276
Figure 5.9. KEGG Pathway analysis of SAP in the comparison groups.....P277
Figure 5.10. Heatmap shows the log2 centred intensity of all significant proteins with the data centred per protein. P280
Figure 5.11. Differential enrichment of neat urine proteins in different comparison groups.....P281
Figure 5.12. GO enrichment of SAP in the different neat urine comparison groups..P283
Figure 5.13. KEGG Pathway analysis of SAP in the neat urine comparison groups....P284
Figure 5.14. Non-invasive urine biofluid proteomic analysis could identify the personalised optimum embryo transfer day, promoting improved implantation outcomes for assisted reproductive technology patients.....P292
Supplementary Figure 5.1. Urinalysis of subject 1 urine across the collection period.....P301
Supplementary Figure 5.2. Urinalysis of subject 2 urine across the collection period.....P302
Supplementary Figure 5.3. Urinalysis of subject 3 urine across the collection period.....P303
Supplementary Figure 5.4. Isolation of urine extracellular vesicles sized particles using differential centrifugation and size exclusion chromatography.....P307
Supplementary Figure 5.5. Combined concentration of EVs for urine from SEC fractions 6-8.....P307
Supplementary Figure 5.6. Venn diagram of uEV proteins in all the comparison groups.....P308
Supplementary Figure 5.7. Venn diagram of proteins in the uEV groups versus the compared to the top 100 Vesiclepedia EV markers P309
Supplementary Figure 5.8. Venn diagram of proteins found in the neat urine versus the number of proteins found in uEVs P309
Supplementary Figure 5.9. Venn diagram of proteins reported in peptide atlas human urine 2022-02 database versus the proteins found in uEVs P310

Figure 6.1. Workflow of future direction for the development of an endometrial receptivity test.....P325

Table list.

Table 1.1. Current major findings about embryo derived extracellular vesicles.....P54

Table 1.2. Current major findings about endometrial derived extracellular vesicles...P58

Table 2.1. Proteins differentially enriched in the E2P4 receptive group EVs related to implantation success P117

Supplementary Table 2.1. Differential enrichment of EV proteins of E2P4 Group compared to E2.....P142

Supplementary Table 2.2. Differential enrichment of EV proteins of E2P4 Group compared to P4.....P144

Supplementary Table 2.3 Differential enrichment of EV proteins of E2 Group compared to P4.....P145

Supplementary Table 2.4 . Differential enrichment of EV proteins of E2P4 Group compared to C..... .....P147

Supplementary Table 2.5. Differential enrichment of EV proteins of E2 Group compared to C.....P148

Supplementary Table 2.6. Differential enrichment of EV proteins of P4 Group compared to C. P149

Supplementary Table 3.1. Differential expression results of JAr E2P4 v JAr E2.....P197

Supplementary Table 3.2. Differential expression results of JAr E2P4 v JAr P4.....P199

Supplementary Table 3.3. Differential expression results of JAr E2 v JAr P4.....P201

Supplementary Table 3.4. Differential expression results of Jar C v JAr E2.....P203

Supplementary Table 3.5. Differential expression results of JAr C v JAr P4.....P205

Supplementary Table 3.6. Differential expression results of JAr C v JAr E2P4.....P208

Supplementary Table 3.7. Differential expression results of JAr P4 v JAr UN.....P210

Supplementary Table 3.8. Differential expression results of JAr E2P4 v JAr UN.....P213

Supplementary Table 3.9. Differential expression results of JAr E2 v JAr UN.....P216

Supplementary Table 3.10. Differential expression results of JAr C v JAr UN.....P218

Supplementary Table 3.11. KEGG terms of all pathways identified to be upregulated in the E2P4 treated groups in all comparison groups with the normalised enrichment scores displayed. P221

Supplementary Table 4.1. Clinical profile of female urine donors P255

Supplementary Table 5.1. Differential enrichment of urine proteins of WOI Group compared to O.....P304
Supplementary Table 5.2. Differential enrichment of urine proteins of WOI Group compared to P.....P304
Supplementary Table 5.3. Differential enrichment of urine proteins of P Group compared to WOI.....P305
Supplementary Table 5.4. Differential enrichment of EV proteins of WOI Group compared to O..... .....P306
Supplementary Table 5.5. Differential enrichment of EV proteins of WOI Group compared to P..... .....P306
Table 6.1. Summary of study's Assessment of Endometrial Receptivity Array.....P320

Abbreviations.

°C	Degree Celsius
3D	Three dimensional
Å	Angstrom
ACE2	Angiotensin-converting enzyme 2
AI	Artificial intelligence
AKT	Protein kinase B
ANGPTs	Angiopoietins
ANGPTL2	Angiopoietin Like 2
ANXA2	Annexin A2
AR	Abortion rate
ART	Assisted reproductive technologies
ATCC	American Type Culture Collection
AUC	Area under the curve
BCA	Bicinchoninic acid
BP_1	Biological process
BP_2	Biochemical pregnancy
BSA	bovine serum albumin
C	Conception
Ca^{2+}	Calcium ions
cAMP	Cyclic adenosine monophosphate
CAMs	Cellular adhesion molecules
CANX	Calnexin
CAT	Catalase
CDH5	Chadherin-5
C/EBPβ	CCAAT/enhancer binding protein beta
CHAPS	3-[(3- Cholamidopropyl)dimethylammonio]-1-propanesulfonate hydrate
CI	Confidence Interval
circRNAs	Circular RNAs
CLU	Clusterin
cm	Centimeters
CM	Conditioned media
CPR	Clinical pregnancy rate
CPM	Counts per million
ddH2O	Double distilled water
DE	Differential expression
DEA	Differential expression analysis
DEGs	Differentially expressed genes
DELFIA	Dissociation-enhanced lanthanide fluorescence immunoassay
DG	Density gradient
DMEM/F12	Dulbecco’s Modified Eagles Medium
DNA	Deoxyribonucleic acid
DOT	Digital Ovulation Test
DOX	Doxorubicin
DPBS	Dulbecco's Phosphate-Buffered Saline
DRE	Digital rectal examination
DSC	Decidual cells
DTT	Dithiothreitol
dUC	Differential ultracentrifugation
E2	Estrogen

E2P4	Estrogen plus progesterone
E3G	Estrone-3-glucuronide
ECM	Extracellular matrix
EDTA	Ethylenediaminetetraacetic acid
EGF	Epidermal growth factor
EGFR	Epidermal growth factor receptor
EIF4E	Eukaryotic translation initiation factor 4E
ERA	Endometrial receptivity array
ERG	Erythroblast transformation-specific – related gene
ESC	Endometrial stromal cells
ESCRT	Endosomal sorting complex required for transport
ET	Embryo transfer
EVs	Extracellular vesicles
FA	Formic acid
FAK	Focal adhesion kinase
Fas	Fatty acid synthase
FasL	Fatty acid synthase ligand
FBS	Fetal bovine serum
FBT	Frozen blastocyst transfer
FDR	False discovery rate
FET	Frozen embryo transfer
FGB	Fibrinogen beta chain
FOXO1	Forkhead box protein O1
FOXP3	Forkhead box P3
FSH	Follicle stimulating hormone
FUCA1	Tissue alpha-L-fucosidase,
GO	Gene Ontology
GSEA	Gene set enrichment analysis
GTPases	Guanosine triphosphate
h	Hour
HAND2	heart and neural crest derivatives expressed transcript 2
HB-EGF	Heparin-binding epidermal growth factor
HFEA	Human fertilisation and embryology Authorities
HLA	Histocompatibility Locus Antigen
HLA-G	Histocompatibility Locus Antigen G
HOXA10	Homeobox A10
HRP	Horseradish peroxidase
HSP	Heat shock proteins
HSP70,	Heat shock protein 70
HSP90	Heat shock protein 90
HSPG2	Heparan sulfate proteoglycan core protein
IAF	Immuno-affinity capture
IDHC	Isocitrate Dehydrogenase (NADP(+)) 1
IDO	Indoleamine 2,3-Dioxygenase
IgG	Immunoglobulin G
IGF-1	Insulin-like growth factor 1
IGF-2	Insulin-like growth factor 2
IGFBP-1	Insulin-like growth factor binding protein-1
IL-6	Interleukin-6
IL-10	Interleukin-10
IL-11	Interleukin-11

IL-15	Interleukin 15
INHBB	Inhibin beta B chain
IR	Implantation rate
ISEV	International Society for Extracellular Vesicles
ITGAM	Integrin alpha M chain
ITGB6	Integrin Subunit Beta 6
IU	International Units
IVF	In vitro fertilisation
JAM2	Junctional Adhesion Molecule 2
kDa	Kilodalton
KEGG	Kyoto Encyclopedia of Genes and Genomes
KIF5C	Kinesin heavy chain isoform 5C
KRT6B	Keratin 6B
kV	Kilovolt
LBR	Live birth rate
LC/MS-MS	Liquid chromatography tandem mass spectrometry
LDHA1	l-lactate dehydrogenase A chain
LEFTY2	Left-right determination factor 2
LFQ	Label-free protein quantification
LH	Luteinizing hormone
lncRNAs	Long non-coding RNAs
m/z	Mass to charge ratio
MF	Molecular function
Mg^{2+}	Magnesium
MHC	Major histocompatibility complex
Min	Minutes
miRNAs	Micro ribonucleic acid
MISEV	Minimal information for studies of extracellular vesicles
mL	Milliliters
mm	Millimeters
MR	Miscarriage rate
mRNA	Messenger ribonucleic acid
MS	Mass spectrometer
ms	Millisecond
MS/MS	Tandem mass spectrometry
MSigDB	Molecular Signatures Database
mTOR	Mammalian target of rapamycin
MUC-1	Mucin-1
MUC16	Mucin-16
MVs	Microvesicles
NaCl	Sodium chloride
ncRNA	Noncoding ribonucleic acid
NGS	Next generation sequencing
NK	Natural killer
nl	Nanoliters
nM	Nanomole
nm	Nanometers
NTA	Nanoparticle tracking analysis
O_2	Oxygen
ORP	Ongoing pregnancy rate
P3G	Pregnanediol-3- glucuronide

P4	Progesterone
PCA	Principal component analysis
PCA3	Prostate cancer antigen 3
PCDHB8	Protocadherin Beta 8
PCDHGA9	Protocadherin Gamma Subfamily A, 9
PCR	Polymerase chain reaction
PEG	Polyethylene glycol precipitation
PGR	Progesterone receptor
PKA	Protein Kinase
PL	Pregnancy loss
PLAT	Tissue-type plasminogen activator
PLGF	Placental growth factor
PPIA	Peptidylprolyl isomerase A
PR	Pregnancy rate
PRDX2	Peroxiredoxin-2
PRL	Prolactin
PSA	Prostate specific antigen
PTX	Paclitaxel
QSOX1	Quiescin Sulfhydryl Oxidase 1
RCT	Randomised controlled trial
RIF	Recurrent implantation failure
RM	Repeated measures
RNA	Ribonucleic acid
rpm	Revolutions per minute
s	Seconds
S100A4	S100 Calcium Binding Protein A4
SAPs	Significant altered proteins
SEC	Size exclusion chromatography
SEM	Standard error of the mean
SERPING1	Serpin family G member 1
sncRNAs	Small noncoding RNAs
SOC	Standard of care
SPD	Swiss Pression Diagnostics Limited
STARD	Standards for reporting diagnostic accuracy studies
TEM	Transmission electron microscopy
TGF- β	Transforming growth factor-beta
THP	Tamm–Horsfall Protein
TLR	Toll like receptor
TMM	Trimmed Mean of M-values
Tregs	Regulatory T cells
TSG101	Tumor susceptibility gene 101
uEVs	Urine-derived EVs
UF	Ultra-filtration
UF-EVs	Uterine fluid EVs
UMOD	Uromodulin
uNK	Uterine natural killer cells
UP	unpurified
VEGF	Vascular endothelial growth factor
WB	Western Blot
WOI	Window of implantation
ZP	Zona pellucida

ZP1	ZP glycoprotein -1
ZP2	ZP glycoprotein -2
ZP3	ZP glycoprotein -3
ZP4	ZP glycoprotein -4
µg	Microgram
µl	Microliters
µm	Micrometers

CHAPTER 1

INTRODUCTION.

Chapter 1. Introduction.

1.1 Author's contribution.

This chapter forms part of the review publication "**The role of extracellular vesicles in endometrial receptivity and their potential in reproductive therapeutics and diagnosis**" published in reproductive biology (2022), the published version of which is included in chapter 8 of this thesis.

Hart AR, Khan NLA, Godakumara K, Dissanayake K, Piibor J, Muhandiram S, et al. The role of extracellular vesicles in endometrial receptivity and their potential in reproductive therapeutics and diagnosis. Reprod Biol. 2022 Jun;22(2):100645.

Amber Rose Hart: Conceptualisation, Writing – original draft. Norhayati Liaqat Ali Khan: Writing– review & editing. Kasun Godakumara: Writing– review & editing. Keerthie Dissanayake: Writing– review & editing. Johanna Piibor: Writing– review & editing. Subhashini Muhandiram: Writing– review & editing. Saji Eapen: Writing– review & editing, Supervision. Paul R. Heath: Writing– review & editing, Supervision. Alireza Fazeli: Conceptualisation, Writing – review & editing, Supervision, Funding acquisition.

1.2 Infertility.

The human endometrium experiences significant cyclical growth and regeneration approximately 450 times during the reproductive age of a woman (1). It undergoes regular cycles of menstruation, repair, proliferation, and secretory differentiation, all regulated by a precisely timed sequence of female sex hormones throughout the menstrual cycle, typically lasting 24-28 days (2). The cycle can be divided into four main phases: menstrual, follicular/proliferative, ovulation, and luteal/secretory (3) (Figure 1.1). During the follicular phase, which follows menstruation, the endometrium (the lining of the uterus) thickens in response to rising estrogen levels due to the growth of ovarian follicles, preparing the uterus for potential embryo implantation (3,4). Ovulation marks the release of an egg from the ovary, after which the luteal phase begins. In this phase, progesterone levels rise, secreted from the corpus luteum, further preparing the endometrium for implantation by transforming it into a hospitable environment (3,4). In addition to hormones, various local levels of autocrine and paracrine molecules fluctuate during the menstrual cycle, profoundly impacting uterine function and implantation success (5).

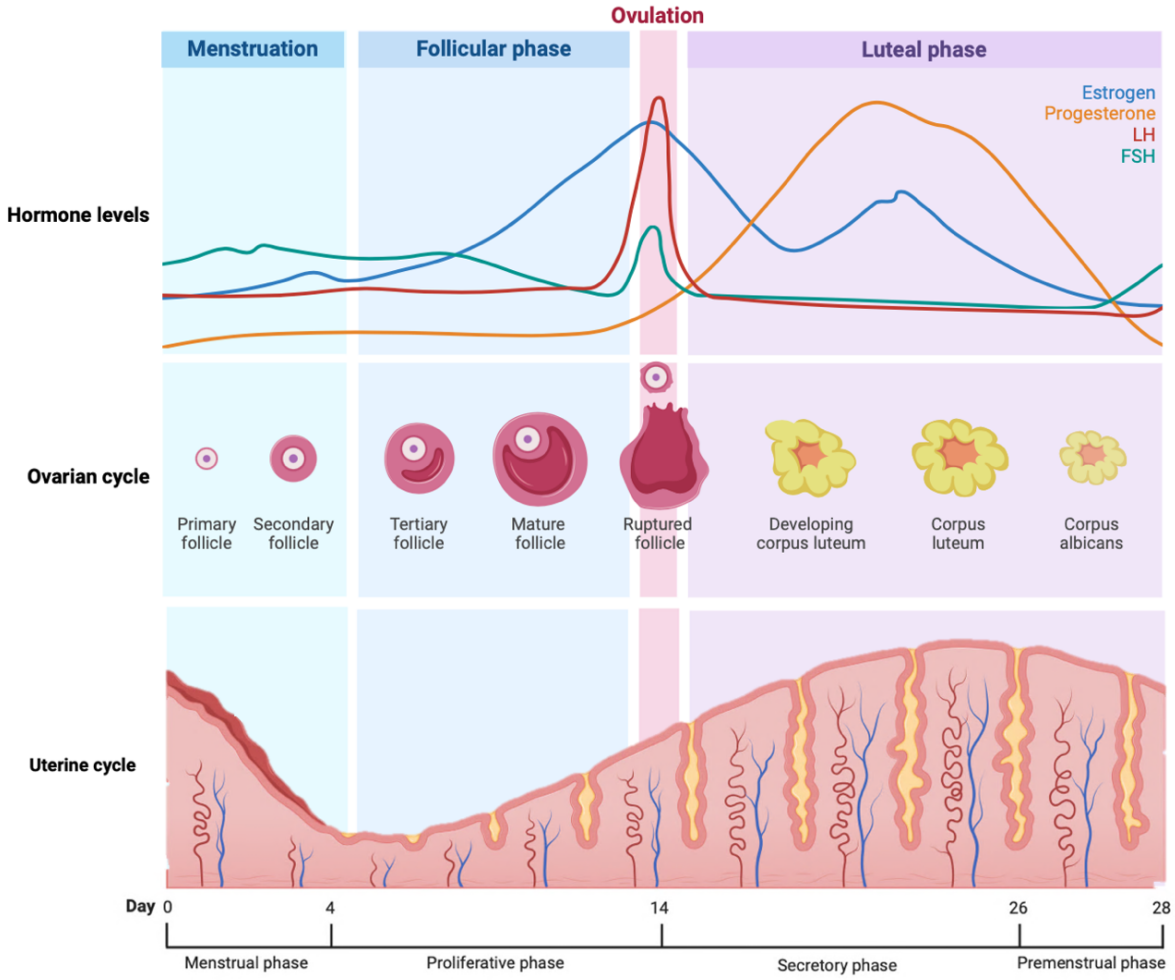


Figure 1.1 Ovarian hormones, folliculogenesis and uterine cycle throughout the normal human menstrual cycle. (Created with BioRender.com.).

Successful implantation into the uterine wall is critical in the development of the mammalian embryo into a complete organism (6). However, infertility poses a significant challenge in human reproduction, with epidemiological studies suggesting that merely 30% of all conceptions get clinically recognised (7), with most lost spontaneously. Within couples of reproductive age, 55% of those affected by infertility will seek medical services to try and achieve parenthood (8). Within the UK the use of assisted reproductive technologies (ART) is linked to nearly 3% of births (9). Despite momentous advances and progression in ART in the recent decade, a low implantation rate per transferred embryo remains a key setback in achieving higher successful pregnancy rates (10). This is probably owing to uterine receptivity being suboptimal and inadequate communication between embryo and uterus, despite high-grade morphologically and genetically normal embryos being selected and transferred.

Studies have previously discovered that failure in pregnancy arises mostly during the period of embryo implantation (11). The complex but vital step of embryo implantation in establishing pregnancy can only occur in a limited window once the unreceptive uterine lining converts to a hospitable environment that is able to receive the embryo (12). This functional endometrium is established in the secretory phase through the action of progesterone on an estrogen-primed endometrium (2) (Figure 1.1). During this period, the uterine cavity is prepared to accept a blastocyst and support further implantation through mediation and communication by cytokines (e.g. Interleukin 6 (IL6) (13)), growth factors (e.g. Insulin-like growth factor 2 (IGF-2) (14)), chemokines (e.g. CX3CL1 (15)) and adhesion molecules (e.g. integrins like αvβ3 (16)).

Additionally, as a non-self- entity, due to half of the genetic information coming from the father and unique embryo antigens, the semi-allogenic embryo must also avoid immune system rejection by the mother, demanding complex communication before implantation can occur (17). Hence, the preparation for receptivity of the endometrium is a complex molecular and morphologic course requiring mutual crosstalk between endometrial cells and the embryo (18). However, little is known about this communication. Previously it has been presumed that the endometrial tissue is passive in its nature and should readily accept an embryo. Outmost the general view was (and probably still is) that the endometrium gets to a receptive stage as a result of the reproductive cycle and the influence of the sex hormones on the endometrial cells. Recent experimental evidence has expanded on this view , confirming a complex mutual communication among the foetal and maternal compartments during implantation in addition to these hormonal effects (19). A new dogma is emerging that emphasises the role that embryo signals play on preparation of the receptive endometrium for embryo implantation as well as signals produced by the endometrium on initiation of final stages of development of the embryo and its preparation for implantation (19).

Given the intricate processes involved in establishing and maintaining pregnancy, it is essential to delve deeper into the characterisation of decidualisation, the window of uterine receptivity, and immunotolerance. These processes are critical for understanding infertility and improving ART outcomes, as will be discussed in detail in the following section.

1.3. Establishment and maintenance of pregnancy.

1.3.1 Characterisation of decidualisation.

Decidualisation is the functional and morphological change that occurs within the endometrium to form the decidual lining into which the blastocyst implants (20). This process is characterised by the differentiation of the endometrial stromal cells (ESC), which are elongated fibroblast-like cells, into decidual cells (DSC), which are rounded epithelial-like cells, during the menstrual cycle and pregnancy (21). This transformation occurs after ovulation and is essential for the preparation of the endometrium for embryo implantation (20). Decidualisation not only supports the embryo but also plays a crucial role in forming the maternal-foetal interface (22).

The molecular mechanisms involved in decidualisation involve a complex interplay of hormonal signals and transcription factors, with many studies investigating the regulation (20). Progesterone, secreted by the corpus luteum, is thought to be the primary hormone driving decidualisation (20). Progesterone binding to and activating progesterone receptor (PGR) in stromal cells leads to the activation of downstream pathways, including the cyclic adenosine monophosphate (cAMP) / protein kinase (PKA) pathway (23,24). This cascade results in the upregulation of intracellular complex networks and secreted proteins necessary for decidualisation, such as prolactin (PRL) and insulin-like growth factor binding protein-1 (IGFBP-1) (24,25). PRL is suggested to possibly play a role in implantation via immune environment modification and/or regulation of the factors that govern trophoblast proliferation and invasion into the endometrium (26,27). Various other secretory molecules from DSC have been reported, include interleukin-11 (IL-11), epidermal growth factor (EGF), heparin-binding epidermal

growth factor (HB-EGF), neuropeptides, activin A, and Left-right determination factor 2 (LEFTY2), which help contribute to the creation of a receptive and supportive environment for the embryo and facilitate embryo adhesion and invasion (28).

In addition to progesterone and cAMP, transcription factors, including Forkhead box protein O1 (FOXO1) (29), Homeobox A10 (HOXA10) (30), heart and neural crest derivatives expressed transcript 2 (HAND2) (31), and CCAAT/enhancer binding protein β (C/EBPβ) (32), play pivotal roles in regulating gene expression during decidualisation. These factors control the expression of genes involved in cell cycle regulation, differentiation, and secretion of extracellular matrix components, which are necessary for the structural and functional changes in the endometrium (21). For example, HANDS2 has recently been confirmed to directly upregulate human interleukin 15 (*IL-15)* transcription in ESC, with IL15 having a suggested essential function in the regulation of the differentiation and function of uterine natural killer cells (uNK) in the human endometrium (33).

Morphologically, decidualisation involves significant changes in endometrial stromal cells, identified through ultrastructural studies (34). These cells increase in size, acquire a polygonal shape, and develop abundant cytoplasm and secretory granules (34). Cytoskeletal reorganisation and accumulation of lipid droplets are also notable features of decidual cells (35), possibly thought to be an essential source of histiotrophic support for the early conceptus; however, further studies are necessary to fully understand their function. Additionally, decidualisation involves the extensive remodelling of the extracellular matrix (ECM), which is crucial for creating a supportive environment for the

implanting embryo and which the trophoblast cells interact with during invasion and limit the extent of the aggressive invasion of trophoblast cells (27). ECM proteins produced by decidualized stromal cells include laminin, heparan sulfate proteoglycans, decorin, fibronectin, and type IV collagen (36–39).

In addition to the previous discussed functional roles of DSC in supporting the developing embryo through various secretions, formatting the ECM, and producing factors that regulate trophoblast invasion, DSC also contribute to the immunological environment of the uterus by creating a balanced immune response that favours pregnancy maintenance (40). They secrete various cytokines and chemokines, such as interleukins (e.g., interleukin 10 (IL-10)) (41) and transforming growth factor-beta (TGF-β) (42), that help modulate the maternal immune response, promoting tolerance towards the semi-allogeneic foetus while protecting against infections (40). The decidua also serves as a barrier, preventing the direct contact of maternal immune cells with the foetal trophoblast, thereby protecting the foetus from immune attack (40,43). Details of this immunotolerance is discussed in more detail below (1.3.3).

In addition to these roles, DSC are crucial for angiogenesis, the formation and maturation of blood vessels within the uterus (44). They secrete angiogenic factors such as vascular endothelial growth factor (VEGF) (45) and placental growth factor (PlGF) (46), which stimulate the development of a robust vascular network essential for adequate blood supply to the placenta and the growing foetus (44). This vascular remodelling improves nutrient and oxygen delivery while supporting the long-term viability of the pregnancy by stabilising blood flow and ensuring proper placental function (44).

In summary, decidualisation is a multifaceted process involving hormonal regulation, molecular signalling, and cellular transformation. The successful decidualisation of the endometrium is essential for embryo implantation and the maintenance of early pregnancy.

1.3.2 Window of uterine receptivity.

The window of uterine receptivity, or widow of implantation (WOI), is a crucial period during which the endometrium undergoes morphological and biochemical changes to become receptive to embryo implantation (2,3). This period is a short, specific time in the menstrual cycle, typically occurring between days 19 and 23 of a 28-day cycle, coinciding with the mid-secretory phase of the endometrial cycle (2,3). During this time, the endometrium is optimally prepared to accept and support a developing blastocyst (47).

In terms of morphological changes, several distinct changes occur in the endometrium to signify uterine receptivity (48). For example, a receptive endometrium is characterised by the presence of small, finger like projections on the apical surface of the luminal epithelial cells called pinopodes (49,50). These pinopodes typically appear for 1 to 2 days, usually around days 20 and 21 of the menstrual cycle during the widow of implantation (50), though the timing can vary by up to 5 days between women (48). They are considered potential clinical markers for assessing uterine receptivity, with studies indicating a correlation between the number of pinopodes and the endometrial receptivity for blastocyst implantation (51,52). Pinopodes are also believed to play a role in the absorption of uterine fluid, facilitating closer contact between the blastocyst and

the endometrial surface (53). In addition to these pinopodes, there is changes in the epithelial cell height, with the epithelial cells of the endometrium become more cuboidal, a change thought to enhance cell-to-cell contact between the embryo and the endometrium (54)

Several biochemical changes also characterise the preparation of the endometrium for embryo implantation (20). In addition to the previously mentioned hormonal regulation, the expression of cellular adhesion molecules (CAMs) family such integrins, cadherins (55) and selectins (56) helps regulate the window of implantation and facilitates the initial adhesion of the blastocyst to the endometrial surface (57). Looking into the example of integrins, in mammals, various integrin isoforms are involved, with α1β1, α4β1, and αVβ3 being particularly important (58). In humans, these isoforms are expressed in the endometrium during the implantation window and are thought to facilitate cell attachment to the ECM and initiate signalling from the embryo to the ECM, triggering gene expression crucial for implantation(59).

In addition to CAMS, various cytokine and chemokines are involved in the maternal-embryo interaction during the WOI (40). For example, the secretion of the cytokine leukemia inhibitory factor (LIF), a pleiotropic cytokine that belongs to the IL-6 family, plays a crucial role during the attachment of the blastocyst and promotes the appearance of the previously mentioned pinopodes (60). Similar to the upregulation of LIF, IL-6 is also upregulated with IL-6 involved in the acute inflammatory response, a key regulator of implantation success (13).

Growth factors are an addition example of a biochemical change during the WOI (20). This includes insulin-like growth factor-1 (IGF-1) and HB-EGF (61), both of which are critical for modulating endometrial receptivity. These factors influence cell proliferation, differentiation, and survival, which are essential for successful implantation (61). However, not all biochemical and morphological changes associate with implantation require upregulation. The glycosylated transmembrane glycoprotein mucin-1 (MUC-1), expressed at the apical surface of the human endometrial epithelium, although upregulated in the secretory phase and seen as a barrier to implantation (62), is seen to be removed directly at the implantation site at the time of impanation, thought to be performed by signals produced by the blastocyst itself (63).

In summary, the window of uterine receptivity is a critical period marked by specific morphological and biochemical changes that prepare the endometrium for embryo implantation. These changes are regulated by hormonal and local factors, and their precise timing is essential for successful pregnancy establishment. Further exploration of this window and its regulation may lead to improved diagnostics and treatments for infertility.

1.3.3 Immunotolerance.

The significance of immunological primming of the endometrium is becoming more evident, with the decidua playing a vital part in ensuring immune tolerance for the semi-allogeneic foetal–placental unit, protecting the conceptus from the mother's immune system (64,65). This complex process involves various immune cells, cytokines, and

mechanisms that create a tolerogenic environment, allowing for the successful establishment and maintenance of pregnancy (40).

One of the key features of this adaptation is the modulation of immune cell activity within the decidua. These key immune cells include uNK cells, the most abundant immune cells in the decidua during early pregnancy (66). Unlike the cytotoxic peripheral NK cells, uNK cells have regulatory roles in the establishing and maintaining pregnancy, such as angiogenesis promotion in the decidua, remodelling spiral arteries, and aiding trophoblast invasion (67). For example, angiogenesis is aided through the uNK secreting interferon-γ and angiogenic factors (e.g. VEGF and angiopoietins (ANGPTs)), which cause remodelling of maternal spiral arteries, enhancing blood flow to the developing placenta, a crucial step in establishing pregnancy (68,69).

Other key immune cells that play a pivotal role in maintaining immune tolerance during pregnancy include CD4 + CD25 + forkhead box P3 (FOXP3) + regulatory T cells (Tregs) (40). These cells help suppress the maternal immune response against foetal antigens, preventing immune-mediated damage to the developing foetus (70). This is achieved via the Tregs producing anti-inflammatory cytokines, such as the anti-inflammatory cytokine IL-10 and TGF-β, which help maintain a tolerant environment (40). The recruitment of Tregs is controlled by the same cytokines produced by the DSC (IL-10 and TGF-β), creating a positive feedback loop where DSC and Tregs mutually support each other's functions to ensure a successful pregnancy by maintain a tolerant environment (70). The importance of Tregs in pregnancy establishment is highlighted through studies in women

showing that insufficient numbers of Treg cells or their functional deficiency have been linked to infertility, miscarriage, and preeclampsia (71,72).

In addition to IL-10 and TGF-β, DSC and immune cells within the decidua secrete other cytokines and growth factors that contribute to immunotolerance, including Indoleamine 2,3-Dioxygenase (IDO) (73). Produced by DCS, IDO is an enzyme known to deplete tryptophan, an essential amino acid for T-cell proliferation (73). By reducing local tryptophan levels, IDO inhibits T-cell activity and promotes tolerance, creating an immunosuppressive environment conducive to foetal survival (74). This enzyme plays a critical role in maintaining the balance between protecting the foetus from maternal immune attack and allowing sufficient immune function to prevent infections, with evidences suggesting higher expression of IDO during mid-luteal phase being correlated with an increased live birth rate during in vitro fertilisation (IVF) (75).

In addition to these immune cells, cytokines and secretory molecules, several other key mechanisms are involved in establishing and maintaining immunotolerance during pregnancy (40). This includes the expression of Histocompatibility Locus Antigen (HLA)-G (HLA-G), a non-classical major histocompatibility complex (MHC) class I molecule expressed on foetal trophoblast, which interact with inhibitory receptors on uNK cells and other immune cells (40,76). This interaction prevents the activation of cytotoxic responses against the foetus, thus safeguarding it from maternal immune attacks (76). Therefore, HLA-G plays a crucial role in creating a tolerogenic environment at the maternal-foetal interface, contributing to successful pregnancy outcomes. Additionally, the Fatty acid synthase (Fas) ligand (FasL), expressed on trophoblast cells, induces

apoptosis in activated maternal T cells that express the Fas receptor (77). This mechanism effectively eliminates maternal immune cells that could potentially target and harm the foetus(77). By inducing cell death in these activated T cells, the Fas/FasL system plays a vital role in protecting the foetus from immune attack and ensuring maternal-foetal tolerance.

In conclusion immunotolerance is essential for the successful establishment and maintenance of pregnancy. It involves a complex interplay of immune cells, cytokines, and molecular mechanisms that create a supportive and protective environment for the developing foetus. Understanding these processes provides valuable insights into the causes of pregnancy complications, such as recurrent miscarriage and preeclampsia, and can inform the development of therapeutic interventions to improve pregnancy outcomes.

However, recent research has highlighted the importance of cellular communication in these processes, with extracellular vesicles (EVs) emerging as critical mediators (78–80). Studies are suggesting that EVs facilitate the transfer of bioactive molecules between cells, playing a significant role in embryo-maternal interactions (81). The next section will explore the definition, biogenesis, content, and function of extracellular vesicles, and their potential implications in pregnancy and fertility treatments.

1.4 Extracellular vesicles.

1.4.1 Definition and biogenesis.

A general definition of EVs is a membrane-enclosed nano-sized vesicle discharged by a cell that carry Deoxyribonuclease acid (DNA), Ribonucleic acid (RNA), and proteins between different cells (82). Most cell types have been shown to discharge EVs, such as haematopoietic cells, B- and T-lymphocytes, endometrial cells, reticulocytes, platelets, mast cells, dendritic cells, neurons, astrocytes, placenta, intestinal epithelial cells, and tumour cells (83). Originally membrane-enclosed microparticles isolated first from a variety of biological materials including human seminal plasma (84), animal platelet-free plasma (85), and from various mammalian cell lines were presumed to derive from plasma membrane outward budding (86). Years later Johnstone *et al* described in reticulocytes a new theory of active vesicle secretion, here exosomes were described as being discharged via exocytosis (87).

Though EV's have been identified in a range of organisms, they are classified into different categories including microvesicles (MVs), exosomes, and apoptotic bodies, depending on the biogenesis, size and discharge pathway (81). MVs discharged from budding of plasma membrane facilitated by restructuring of the actin-myosin cytoskeleton, range in size between 100 nm and 1 μm, while the smaller exosomes, originating from the multivesicular endolytic compartment via the merging of the plasma membrane with the multivesicular endosome, range between 40 and 120 nm (81). Oncosomes, released from cancer cells, range between 1–10 μm and apoptotic bodies produced by dying cells range between 50 nm–2 μm (19) (Figure 1.2). The umbrella term,

EVs, is often used due to the difficulty in separating the nanoparticles, with all three categories of particles being found in all biological samples.

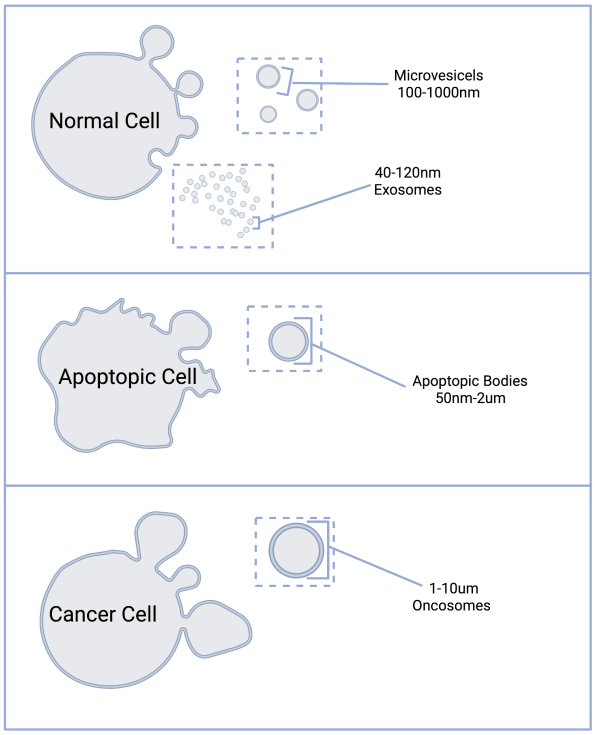


Figure 1.2 Extracellular vesicles produced from different cell types vary in size (Created with BioRender.com.).

EVs comprise of cell lineage markers, phosphatidylserine, cell surface receptors, and specialised cell membrane microdomains, hence MVs membrane structure mirrors the parent cell more than those of the exosomes (88). Regulation of the MV biogenesis is controlled via specific series of molecular occurrences, including acidic sphingomyelinase and Protein kinase B (AKT) activation (89), flux variations in intracellular calcium, and enzymes implicated in upholding the asymmetry of the membrane phospholipid (90). Unlike the outward budding of MVs, exosomes have a buoyant density and are formed via inward budding of the luminal membrane of endosomal multivesicular bodies (81). Exosomes are enriched in tetraspanins and their biogenesis is managed by multiple regulatory mechanisms (88). This includes the endosomal sorting complex required for transport (ESCRT), RabGTPase proteins, syndecan-syntenin-Alix, proteins from the p53/TSAP6 pathway, phospholipase D, ceramide, oligomerization, and neutral sphingomyelinase 2 (88).

1.4.2 Content and function.

EVs package and transport multiple molecules such as, membrane-bound and soluble proteins, lipids, DNA, and RNA including mRNA and Micro ribonucleic acid (miRNAs) (91). This content varies conditional on the phenotype and origin of the cell, they can then transfer to other cells horizontally, where they become functional (91). A great diversity of elements has been discovered in EVs from various cells (both prokaryote, non-mammalian and mammalian eukaryotic), this includes around 4400 proteins, 194 lipids, 1639 mRNAs, and 764 miRNAs, illustrating the intricacy of EVs and possible variation in their function (92) (Figure 1.3).

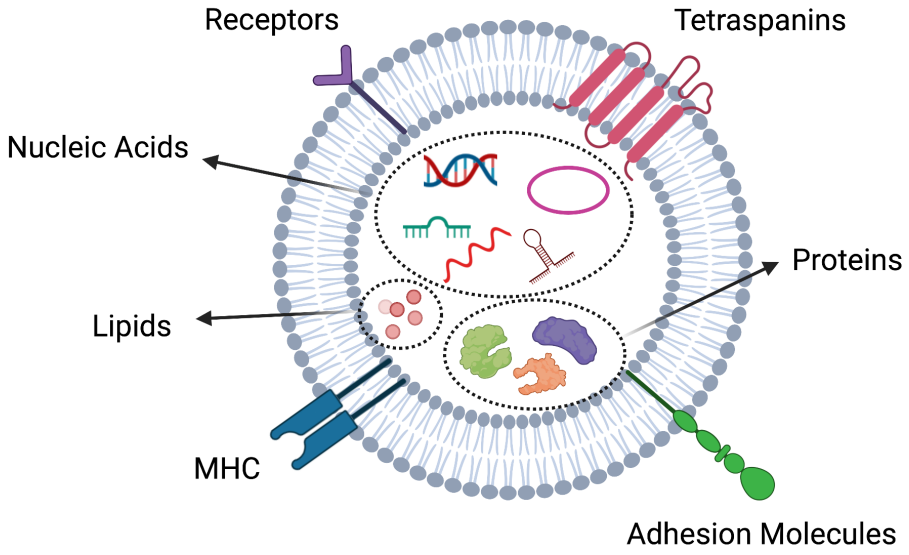


Figure 1.3. Schematic representation of Extracellular vesicle structure and content. The phospholipid bilayer is integrated with membrane proteins such as tetraspanins (CD9, CD63, CD81), adhesion molecules (integrins, EpCAM) MHC and receptors. This membrane surrounds the content of nucleic acids (mRNA,miRNA, DNA, long non-coding RNAs (LncRNAs), and circular RNAs (circRNAs)), proteins (HSP70, HSP90, EGFR), and lipids. (Created with BioRender.com.).

Proteomic content of EVs have been extensively investigated owing to their significant role in cell signalling (93). These studies demonstrated that proteins are transported from one tissue or cell to others by EVs, influencing the bioactivity of the target cells or tissues. EVs have been shown to be enriched in a range of proteins with various functions, for example, heat shock proteins (HSP70 and HSP90) that are involved in the stress response in antigen binding and presentation, and tetraspanins (CD9, CD37, CD53, CD63, CD81, and CD82) which are involved in cell penetration, invasion, and fusion events (94). Furthermore, endosomal sorting complex proteins needed for exosome release, such as Alix and Tumor susceptibility gene 101 (TSG101), as well as protein markers chaperones are also found (81). EVs have also been shown to contain

transmembrane proteins and glycoproteins comparative to the cells they originated from, including integrins, glycoprotein and P-selectin (81). Furthermore, enriched in EVs are receptors such as membrane trafficking proteins (Guanosine triphosphate (GTPases), Flotillin and Annexins), epidermal growth factor receptor, cytoskeletal proteins (tubulin and actin), and cytosolic proteins (81).

Besides proteins, EVs also contain a noteworthy component, RNAs, which can integrate into the receiving cells (91). miRNA are considered to be especially enriched, signifying that EVs could aid in the route of transmission of genetic material between cells (95). miRNAs can regulate the expression of genes of target cells, with the miRNAs acting intracellularly or discharged in EVs bound or free form (96). Within pregnancy and implantation, miRNAs have been shown to be isolated from embryo conditioned media and cultured trophoblasts (97). A variety of RNA and miRNA from embryo and trophoblastic EVs have been identified that have various targets in epithelial and stromal cells (97). The miRNA targeted genes are thought to control cellular functions like migration and adhesion, implying embryos can alter genomes of the endometrium to improve trophoblast adhesion. Within a study by Cuman *et al.,* it has been shown that secreted miRNA profiles significantly vary among implantation incompetent/competent and developmentally different blastocysts (98). This included miR-166, that is most highly expressed in non-implanting blastocysts when compared to implanted blastocysts (98). Further i*n vitro* analysis of miR-166 showed that its transfection into human endometrial epithelial cultured cells caused a decrease in trophoblast adhesion to the epithelium (98). Hence this study indicated embryos only release appropriate signals to aid apposition via modification of the luminal epithelium.

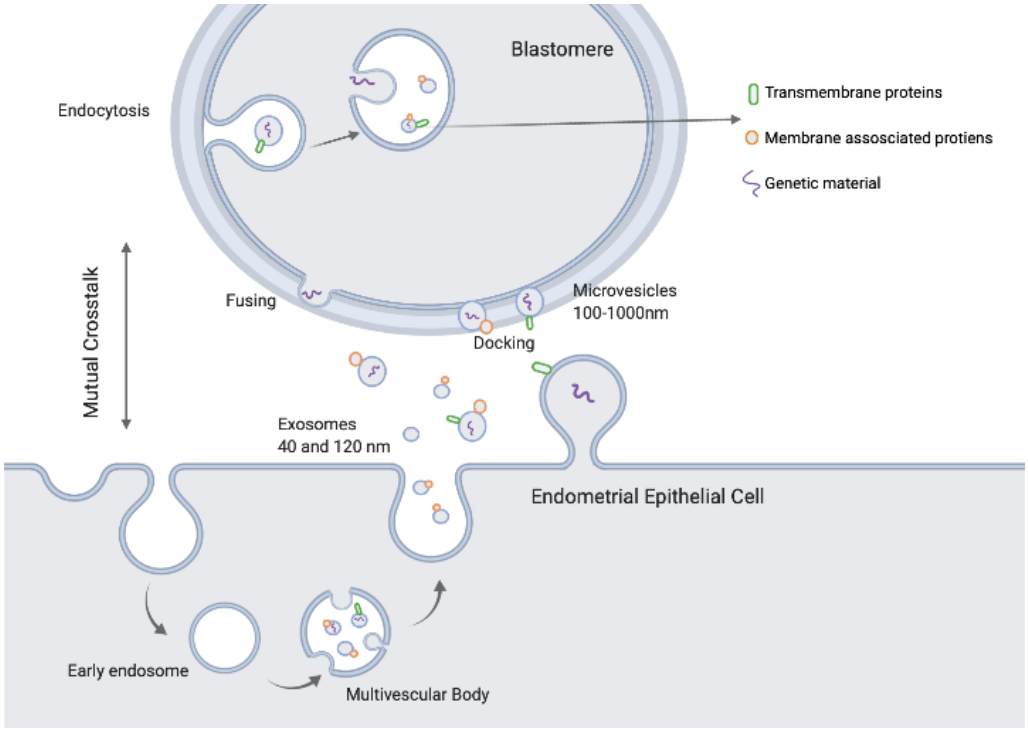


Figure 1.4. Embryo-endometrium mutual crosstalk via Exosomes and Microvesicles. Depiction of the production of Exosomes from inward budding of the endosomal membrane and Microvesicles produced from plasma membrane outward budding. Via this mutual communication, EVs can fuse or dock with the membrane or enter via endocytosis with bidirectional movement across the zona pellucida (Created with BioRender.com.).

EVs are known to have other diverse roles, including angiogenesis stimulation (99), formation of lymphatic vessels (100), and epithelial-mesenchymal transition (101). In terms of roles within pregnancy and implantation, EVs of placental (102), embryonic and uterine origin (103) are being investigated to improve understanding of their function within uterine receptivity. Within this review the already known roles of EVs within the uterine microenvironment are examined, however it is speculated that these will be the first phases in EVs discovery within the dynamic system of fertility and gestation. We will examine the current literature on potential production of EVs during the window of implantation (WOI) by both embryo and endometrium leading to implantation and establishment of the pregnancy. This information will include, for example, as discussed below, the recently suggested roles of EVs mutual communication between blastocyst and endometrium (Figure 1.4) (78,104).

1.5 Embryo-derived Extracellular Vesicles and their potential function.

It is apparent that embryos produce EVs and the rate of EVs production as well as type of EVs produced is altered as they undergo development (104–107). Currently we are not aware what type of EVs are produced or if the cargo of EVs produced changes as embryos develop further. However, embryo derived EVs, seem to have a role as communications vectors within the dialogue of early embryo-maternal communication, as well as embryo-embryo communication and having a regulatory role in the embryo's development (Figure 1.4) (104,108,109).

First, when thinking about embryo EV uptake or release it's important to consider if EVs can pass through the intact zona pellucida (ZP). The answer to this question lies in the ZP

porosity and permeability. The ZP is an extracellular matrix surrounding the oocyte and early embryo, composed primarily of the four glycoproteins ZP glycoprotein -1 (ZP1), -2 (ZP2), -3 (ZP3), and -4 (ZP4) that form a porous, mesh-like structure (110). The pore size of the ZP typically ranges from 60 to 200 nm, which allows the passage of smaller molecules and certain types of EVs (111).

During oocyte maturation, the ZP undergoes significant changes (112). It hardens post-fertilization to prevent polyspermy, involving cross-linking of the ZP proteins, which can reduce pore size and alter permeability (113). The release of cortical granules upon fertilization further modifies the ZP, making it more resistant to enzymatic digestion by additional sperm (114). As the embryo develops from a zygote to a blastocyst, the ZP may expand and thin out slightly(113). Eventually, the blastocyst must hatch from the ZP for implantation, involving enzymatic digestion that partially breaks down the ZP (113).

Nevertheless, hydrophilic–lipophilic properties like that of lipid-containing molecules can penetrate the zona pellucida easily, and similarly, lipid bilayer membrane EVs are expected to pass through (115). Many studies have supported this theory with EV being shown to pass through the ZP (116,117). EVs could play a role in the required breakdown of the ZP and hatching for implantation and pregnancy establishment. A recent study has shown that blastocysts release EVs that contain a specific miRNA (miR-378a-3p) and when embryos are supplemented with this miRNA improved hatching is seen and the opposite seen with an inhibitor (118). These studies highlight that not only EVs are being released from blastocysts and passing through the ZP, but perhaps blastocyst EVs are

also acting in an autocrine way and play a crucial role in promoting blastocyst hatching which is an established parameter of embryo quality associated with implantation.

However, embryo-derived EVs secretion is dependent on various factors (119). Nonetheless, when comparing current published work, there is an agreement that the concentration of embryo derived EVs upsurges in parallel to the embryonic developmental phase (104,105,107,120). For example, within human embryos it has been shown that day 3 early cleaved embryos compared to the day 5 blastocyst stage, release a lower concentration of EVs (104). Similarly, it has been shown that conditioned media from embryos that are degenerated after day 8 contained a larger EVs mean concentration as opposed to embryos developing into blastocysts on day 8 (105). Additional factors that affect EVs concentration have also been shown such as the embryo's sex and the *in vitro* embryo culture conditions. For example, Taqi et al (2019) demonstrated that a higher concentration and larger sized EVs were released by male bovine embryos under 20% oxygen (O_2) conditions, whereas female bovine embryos released larger and more EVs under 5% O_2 conditions (107). Similarly, higher concentrations of EVs were shown in bovine embryos at day 7 in comparison to day 3 embryos subjected to 20% O_2 conditions, and the inverse was seen in 5% O_2 conditions (120).

Regarding correlation between embryo competency and embryo derived EVs, studies have also been conducted, with a relationship between higher concentration of embryo derived EVs and less competent embryos is suggested (121,122). For example, using flow cytometry on spent embryo culture medium, there was shown to be a correlation

between lower concentration of EVs within embryos ending in pregnancy (122). However, when considering this study, it should be noted that this study design was based on DNA detection in EVs, with no EVs isolation step, therefore this data could be subjective to a bias selection of EVs subpopulations and that simply incompetent embryos could contain greater apoptotic cells releasing greater volumes of DNA within EVs. Nevertheless, other studies have shown a similar positive correlation between low EVs concentration in media culture leading to pregnancy and higher EVs concentration not leading to pregnancy (121). Yet a more recent *in vitro* study utilising bovine embryos the reduction of EVs from the culture media negatively impacted the embryo culture, demonstrated by a reduced blastocyst formation (105).

Embryo-derived EVs have been shown to play a multi-signal messenger part in embryo-maternal communication, with labelled embryo derived EVs shown in *in vitro* cultured human primary endometrial epithelial and stromal cells (104). Within this study using non-manipulated human embryos cultured *in vitro*, it was also shown that day 3 and day 5 pre-implanted embryos released a heterogeneous population of EVs containing embryonic specific molecules and were shown to be incorporated by an *in vitro* endometrial epithelial cell line (104). Crucially, within the protein supplement normally used with embryo culture media, EVs were also found (104). However, interestingly in the uptake assessment that used EVs isolated from control media containing no embryos but still containing these protein supplements, these EVs were shown to not be up taken by endometrial epithelial cells (104). More recently it has been shown, in a study examining bovine embryo derived EVs and their effect on oviductal cells, that molecular signatures are displayed by pre-implanted embryos indicating their developmental

success, such a signal could be displayed on the surface or within the cargo of EVs (123). Taken together, this implies the maternal tract is capable of differentiating the EVs origin or molecular content, ultimately regulating embryo EVs uptake by the endometrium. Such results suggest EVs are involved with a maternal-embryo recognition process.

Supporting this *in vitro* data, a study in sheep demonstrated that EVs harvested on gestation day 14 and derived from elongating conceptuses *in vivo* are capable of releasing EVs *in vitro* following 24 hours of *in vitro* embryo culture (124). Additionally, within this study they showed that *in vivo* intrauterine instillation of labelled conceptus-derived EVs were up taken by uterine luminal epithelium as well as some glandular epithelial cells but were not detected to be taken up by the uterine stroma or myometrium or any other analysed organ such as the ovaries (124). These observations demonstrate that EVs uptake is targeted locally to the endometrial epithelium, acting as a new method of cell-to-cell interaction for pregnancy establishment, however, whether these EVs altered the endometrial epithelium gene expression profiles or cell physiology was not investigated.

Embryo derived EVs have also been shown to have a role in embryo-to-embryo communication signalling, with embryo EVs entering embryos via the zona pellucida bringing in new factors for their development (117,125,126). For example, in a study which simulated paracrine communication in a co-culture among different porcine embryos (125) it was demonstrated that the co-culture enhanced significantly the development of *in vitro* cloned embryos, mirroring previous results by Saadeldin et al (2014) (117). It was revealed that this communication could be via EVs, with these EVs

shown to enclose different pluripotency gene mRNA of which their embryonic expression increased (117). Similarly, in a different study with bovine embryos, it was shown that labelled PKH67 embryo derived EVs were up taken by zona-intact bovine embryos, and this in addition to embryo derived EVs enriched embryo culture media improved significantly the day 7 and 8 blastocyst rates with a lower apoptotic cell ratio (126).

Generally, the current literature supports the assumption that embryos from the moment of their establishment are producing EVs and releasing them to their environment whether *in vivo* or *in vitro* (Table 1.1). The number, type, and cargo of these EVs are different and is dependent on the embryo developmental stage, embryo gender and embryo's ability for further development. These EVs seems to have a function in communication with other embryos and with the maternal tract.

Table 1.1. Current major findings about embryo derived extracellular vesicles.

Subtopic	Key Findings	Reference
EVs derived from *in vitro* produced embryos	Both IVF and parthenogenetic embryos release EVs but differ in concentration and diameter.	(106)
	Bovine somatic cell nuclear transfer embryos secrete EVs, transfer of these EVs to other embryos increased blastocyst formation and quality.	(127)
	EVs from parthenogenetic embryos increasing cleavage rate and blastocyst formation in the cloned embryos.	(117)
	Labelled embryo derived EVs shown in *in vitro* cultured human primary endometrial epithelial and stromal cells are up taken.	(104)
	The number and molecular cargo of bovine embryo EVs differed between male and female embryos exposed to environmental stresses.	(107)
	miRNA expression of EVs secreted during blastulation vary depending on embryo quality.	(128)

	Bovine embryos under different oxygen tensions changed the EVs concentration and the EVs miRNA contents.	(120)
	EVs secreted by pre-implantation bovine embryos can alter the expression of genes of primary oviductal epithelial cells, with the response varying depending on the embryo quality.	(123)
	Cultured pre-implantation bovine embryos release EVs with their concentration and size subjective to embryo quality.	(105)
EVs derived from *in vitro* models	Trophectoderm-cells EVs release miRNAs and proteins that stimulate the angiogenesis pathway in maternal endothelial cells.	(129)
	Trophoblast spheroids secrete EVs that contain RNA and when incubated with endometrial cells induced down-regulation of transcripts in endometrial cells.	(78)
	Multiple signalling pathways may underlie receptor stimulated EVs release besides, or in addition to, calcium.	(130)
	Trophectoderm cells EVs are up taken by endometrial cells and alter transepithelial electrical resistance, and upregulated proteins implicated in embryo attachment, immune regulation, and antioxidant activity.	(131)
	Trophoblast derived EVs can modify the endometrial gene expression.	(132)

1.6 Endometrial derived extracellular vesicles and their function.

Successful pregnancy seems to also necessitate EVs production by the endometrium, with several studies demonstrating endometrial EVs being isolated from bovine (133) , human (83) and equine (134) uterine aspirates (135), mucus, cultured uterine epithelial cells, stromal cells and mesenchymal stromal cells (Table 1.2).

The initial evidence of existence of endometrial EVs was observed by assessing uterine aspirates (83). Here EVs positive for tetraspanins, CD9 and CD63 were detected in samples from fertile women within their secretory phase (83). Via utilisation of cell-

surface marker immunostaining, EVs were shown to be localised on the luminal epithelial cells apical surface proposing that secreted uterine EVs originated from the endometrial epithelial cells (83). Also, within this study the miRNA cargo of endometrial derived EVs from the endometrial epithelial cell line, ECC1 was characterised (83). Of the miRNAs profiled, 214 miRNAs were found in EVs and ECC1 cells, suggesting many host miRNAs are sorted within EVs (83). However, interestingly the ECC1 derived EV's had 13 unique miRNA transcripts as well as a group of Noncoding RNAs (ncRNAs) such as small nuclear RNA U6 (involved in the spliceosome), and RNU44 and RNU48 (involved in chemical modifications of other RNAs) (83). The biological relevance of EVs sorting these ncRNA is unknown but is predicted to target embryo implantation genes. For example, when examining the exosomal miRNAs found most abundantly, (hsa-miR-200c, hsa-miR-17 and hsa-miR-106a), bioinformatic analysis suggests a role for these miRNAs in the implantation biological process (83). However experimental and mechanistic data on the role of endometrial EVs on the embryo implantation process is still required.

In an *in vitro* study by Greening et al (2016) it was demonstrated that endometrial derived EVs play an important role in the endometrium-blastocyst interactions within the uterine cavity that is essential for establishing pregnancy, within which these EVs are regulated by hormones and menstrual phases (136). In this study the proteomic profile of endometrial derived EVs influenced by estrogen plus progesterone (to mimic the receptive endometrium) and estrogen (to mimic the proliferative phase) were investigated to study their possible ability to modify trophoblast function (136). Estrogen influenced EVs were shown to be enriched with 254 proteins and estrogen plus

progesterone influenced EVs enriched with 126 (136). Interestingly, estrogen plus progesterone influenced EVs proteins were related to implantation changes such as adhesion, migration and invasion (136). These EVs where shown to be up taken by human trophoblast cells and changed their properties, enhancing their adhesion capability at implantation, a response shown to be mediated partly through active focal adhesion kinase (FAK) signalling (136). Interestingly, FAK is a pathway recently identified in EVs-blastocyst communication and between inner cell mass and the trophectodermal cells (137). Thus, this study demonstrates endometrial exosomes aid in the endometrial-embryo interactions within a simulated uterine microenvironment.

Similarly, it has been shown in other studies that endometrial EVs play a role in implantation, again with their protein cargo varying during embryo implantation (138). A study by Kusama et al (2018), examined effects of bovine intrauterine exosomes on conceptus implantation (138). This study revealed that numerous proteins are differentially abundantly expressed in the EVs isolated from pre-implantation stage bovine endometrial epithelium in comparison to the post-implantation group (138). In addition to this, protein analysis was carried out on isolated EVs from bovine uterine flushing fluids during pre- and post-implantation windows (138). The analysis revealed that the addition of EVs from post-implantation stage to the primary bovine endometrial epithelial cells up regulated the expression of proteins involved in cell adhesion while the pre-implantation endometrial EVs had a greater up regulation of proteins involved in cell apoptosis (138). These results could suggest a paracrine effect of endometrial EVs in receptivity and implantation regulation, however, these changes might instead just reflect the occurrence of epithelial physiological alterations.

It seems EVs, both from the endometrium and the embryo, have significant functionality in numerous physiological and pathological events within implantation and fertility. Convincing investigations have begun to suggest uses of EVs as possible biomarkers in a clinical setting, such as liquid biopsies in diagnostics (139) and therapeutics (140), suggesting a possible means for helping to defeat infertility.

Table 1.2. Current major findings about endometrial derived extracellular vesicles.

Subtopic	Key Findings	Reference
EVs obtained from uterine flushing	Uterine flush EVs are up taken by conceptuses trophectoderm cells and the uterine epithelia.	(124)
	Progesterone increases the release of EVs from endometrial cells, in addition to increasing the release of miRNAs contained in EVs that target PI3K/AKT and BMP signaling pathways.	(141)
	EVs from uterine fluid regulate implantation, with EVs from post-implantation up-regulating the expression of genes related to adhesion molecule and EV's from pre-implantation up-regulating the expression of apoptosis-related genes.	(138)
	Cows' uterine fluid EVs with endometritis impact IVF embryo development with exosomes miRNAs is the main molecule that impeded the quality of IVF embryos.	(142)
	EVs isolated from Avian uterine fluid contain proteins that may be essential in the preservation of sperm functions within the female genital tract.	(143)
	Endometrial derived EVs transport miRNAs that are internalised by the trophectoderm, influencing the embryo transcriptomic for genes involved in embryonic adhesion.	(144)
	Uterine Flush EVs contain various small RNAs that are involved in regulating pathways or processes related to endometrial remodelling and immune processes.	(145)
	The transcriptomic cargo of uterine flush EVs reflects the RNA profile of the endometrial tissue as well as changes between the non-receptive and the receptive phase.	(146)

	Uterine lavage EVs from fertile versus infertile women contain known predictors of embryo implantation, endometrial receptivity, and implantation success.	(103)
	Endometrial-derived EVs increased adhesion and invasion of human trophectodermal to endometrial epithelium. Transfer of endometrial EV cargo proteins to trophectoderm mediate changes in trophectoderm function was also shown.	(147)
	Endometrial derived EVs contain specific miRNA that could be involved in endometrial-embryo cross talk and embryo implantation.	(83)
Endometrial EVs from *in vitro* cell models	Endometrial EVs from recurrent implantation failure patients inhibited the functions of trophoblasts by decreasing their proliferation, migration, and invasive capacity.	(148)
	EVs are released by the endometrium, and the miRNA profile of the secreted EVs varies with the physiological states of the uterus.	(149)
	Recurrent implantation failure EVs decrease embryo development via inhibition of blastocyst formation, reducing the embryos total cell number and the embryos invasion capability.	(150)

1.7 Can endometrial and embryo derived EVs be exploited in diagnostics and treatment?

EV's involvement in a diverse range of pathophysiological processes makes them a promising entity to be utilised in a diagnostic and therapeutic setting. Application of EVs within a clinical setting can be categorised into 4 potential groups of tools. This includes treatment, a diagnostic biomarker for diseases, a drug delivery tool and finally in vaccinations and immune response.

At the onset and during disease, cell physiology, behaviour and metabolism are altered triggering modification in cell's protein content, gene expression and cargo content of cell produced EVs (151). These alterations therefore make EVs a plausible interesting

target as a biomarker in the clinical field. Genomic and proteomic profiling of endometrial EVs in different pathological reproductive conditions has been conducted to help discover these diagnostic biomarkers (152). This potential of EVs being used as endometrial receptivity biomarkers is further highlighted by a meta-analysis of endometrial tissue implantation-associated genes from nine different studies which showed 28 of 57 receptivity markers transcripts are also found in EVs (153). Contrary to the investigations of endometrial EVs, very few studies have researched the possibility of embryo derived EVs as a quality biomarker for pre- implanted embryos. It has been reported that EVs composition and secretions are not accidental and can alter depending on internal signalling and external stimulation (154). Hence embryonic EVs could be used to predict the embryo quality or health. However, it is important to draw attention to the fact that the only method to research mammalian embryo EVs is via *in vitro* embryo production and culture media analysis. Such methodology results in studies with small sample sizes and contamination with EVs not derived from embryos.

A study by Rai *et al* (2021) investigated uterine lavage derived EVs proteome from proven fertile and non-fertile women to provide an insight into endometrial receptivity (155). Intriguingly, previously known predicted proteins of embryo implantation (Peroxiredoxin-2 (PRDX2), Isocitrate Dehydrogenase (NADP(+)) 1 (IDHC)), endometrial receptivity (S100 Calcium Binding Protein A4 (S100A4), Fibrinogen beta chain (FGB), serpin family G member 1 (SERPING1), Clusterin (CLU), Annexin A2 (ANXA2)), and implantation success (Catalase (CAT), YWHAE, Peptidylprolyl isomerase A (PPIA)) were detected in EVs and differed between fertile and non-fertile women (155). This indicated their potential for diagnostic purposes in endometrial receptivity status and hence pregnancy outcome.

Transcriptomic analysis of endometrial EVs have also been investigated with the goal of classifying new receptivity-associated biomarkers (149,156). A study recently profiled small noncoding RNAs (sncRNAs) in endometrial EVs and identified markers of endometrial receptivity and implantation success through analysis of uterine fluid samples from fertile and patients receiving IVF treatment (156). 12 endometrial EVs-sncRNAs, which are related with biological functions related to immune response, extracellular matrix, and cell junction, were identified as receptivity-associated transcripts in both subject groups (156). Similarly, in an *in vivo* mouse study of endometrium EVs MicroRNAs, the upregulation of miR-34c-5p was identified during implantation, suggesting a possible receptivity biomarker for successful embryo implantation (149). From these studies and others about miRNA, it is reasonable to speculate that in the future, non-invasive EVs-based genomic diagnostics will enable precision health applications.

There are nevertheless endometrial receptivity array (ERA) commercial tests available which, on an endometrial biopsy at the presumed time of WOI, evaluate the gene expression profiles to identify a precise transcriptomic signature to allow a more accurate time of embryo transfer for IVF (157). However, a recent random control trial based on live birth outcome analysing the use of ERA compared to standardised timing from single euploid frozen blastocyst transfer (FBT) showed no improvement in live births (158). Additionally, a recent retrospective study showed that on 488 subjects with recurrent implantation failure (RIF) using an ERA test could not show any improved outcome though use of the test (159). Collectively these findings suggest that ERA is not

yet a reliable tool to improve pregnancy rates, with conditions such as RIF being multi-faceted hence ERA alone does not assist when failure is due to embryo quality or other potential issues with pregnancy establishment. This coupled with the requirement of an invasive endometrial biopsy, EVs could prove as a reliable alternative, by instead assessing the embryos quality through analysis of the EVs being released by the embryo prior to artificial implantation and assessment of endometrial EVs to assess receptivity.

In terms of treatment, EVs have been shown to increase the secretion of proinflammatory cytokines, and therefore this property could be utilised for inflammatory reproductive disease treatment by reducing the absorption or production of EVs (160). For example, in a study in which endothelial cells were treated with EVs derived from endometrial epithelial cells they displayed an increased release of proinflammatory cytokines such a tumour necrosis factor-alpha as well as a reduction in macrophage-derived chemokines (161). EVs appear to be emerging frontiers in anti-inflammatory therapy (162). Within reproduction, the common inflammatory condition, endometritis, could benefit from these emerging therapies, with either anti-inflammatory targeting EVs by surface engineering or cargo loading. Similar to treatment regimens, there is increasing evidence showing that EVs have potential for successful drug delivery mechanism (163). Since EVs are vesicles for transporting different RNAs and proteins and during pathological conditions as discussed, the speculation of application in drug delivery has gained scientific interest (163).

Within reproduction, research into the use of EVs as a treatment delivery tool is limited. However, within cancer research this area is progressing owing to EVs numerous

advantages over other nanocarriers (164,165). For example, the chemotherapy drug doxorubicin (DOX) is used to treat different tumours, however it has multiple side effects including its cardiotoxicity (164). Encapsulation of DOX within EVs in both *in vitro* and *in vivo* experiments have shown to reduce these toxicity effects of the free drug whilst not inhibiting its anticancer effectiveness (164). Similarly, paclitaxel (PTX), an anti-mitotic chemotherapeutic, loaded into EVs to treat pancreatic cancer cells, showed an improved target cell internalisation via the endocytic pathways and improved its cytotoxicity (165). Like EVs, liposomes have been used successfully as drug delivery tool, however EVs do have reported advantages over these (163). For example, in a study which compared the uptake dynamic of exosomes and a liposome nanoparticle via confocal live cell imaging, liposomes were shown to accumulate on the cell surface and only a few being endocytoses after a few hours, whereas the exosomes entered the cells within minutes without accumulation at the cell surface (166). Such results suggest EVs uptake is more efficient which could then result in an improved cargo delivery and therefore a better delivery system. These advantages of EVs, including their stability, obtainable from multiple sources and having low immunogenicity, shows an opportunity to utilise EVs as a reproductive treatment tool. Perhaps artificial EVs or EVs loaded with a drug could treat and improve the implantation environment, reducing common problems such as recurrent implantation failure and recurrent pregnancy loss.

Overall, EVs have the potential to be involved in all aspects of clinical application. However, to improve fertility via such applications, it's vital to further increase our knowledge on EVs biology in reproductive tissues. With this knowledge, research should then aim to advance non-invasive biomarker discoveries, devising new methods to

determine receptivity, and replacing the unproven and unreliable technologies currently used at present such as ERA.

1.8 Urine as biomarker biofluid.

Biomarkers, defined as "any substance, structure, or process that can be measured in the body or its products and influence or predict the incidence of outcome or disease" (167) are helpful indicators of pathological developments connected with a particular disease (168). Biomarkers are regularly utilised in disease diagnosis or to follow up on a therapeutic intervention pharmacological response, as unlike subjective disease symptoms, biomarkers provide an objective measurable way to assess disease status (168). The application of urine biomarkers in disease diagnosis is an age-old practice (169). Throughout history various publications and claims on the interpretation of urine have been made, but evaluation of urine truly didn't begin until alchemists commenced purifying and identifying its various components (170). In 1771 Roulle discovered Urea, and Dobson thereafter provided proof that urine sweetness in diabetes was owed to glucose (171). In the early mid-1800s, the English physician, Bright, who was termed the "father of nephrology", pioneered kidney research (172). He was followed by Henry Bence Jones who methodically examined healthy and diseased urine chemical compositions and subsequently characterised kappa and lambda light chains within multiple myeloma patients urine, identifying the first tumour marker (173).

Urinalysis still today remains a powerful instrument in acquiring vital data for diagnostic purposes (174). Numerous semiquantitative and qualitative analyses via reagent strips and tablets, as well as quantitative tests, are utilised to assess protein,

electrolytes, and porphyrin concentrations (175). Reports on ascertaining disease biomarkers within urine have been a fundamental area of investigative medicine during the 20th and 21st century (174). Such investigations are constructed on disease pathophysiology knowledge to ascertain putative biomarkers that can subsequently be verified within clinical trials and then moved into clinical practice (174). Urine has been utilised as a biofluid for biomarkers for diseases of not only the kidney but also the urinary tract (176) and prostate (177). On account of the expanding development in the recent decade of liquid biopsies, customary old biopsies are demonstrating considerably more limitations. Introduction of liquid biopsies into the clinical setting is crucial in helping limit invasive operations and encourage more specific and personalised interventions.

1.9 Urinary extracellular vesicles definition and biogenesis.

Urine is a complex fluid mostly made up of water but also containing various cells, nucleic acids, proteins, bacteria and EVs. As described above (Figure 1.2), EVs, including that of urine EVs (uEVs), consist of a heterogeneous population with a variety of vesicles of variable sizes (178). uEVs are largely thought to derive from the urogenital tract cell such as epithelial lining of nephrons and kidney parenchyma but also from residing bacteria and viruses (Figure 1.5) (179). The quantification of the contribution of the various urogenital tract origin organs to the whole uEV population is unknown, but studies have demonstrated the possibility of enrichment of subpopulations of uEVs by altered collection protocols such as a digital rectal examination (DRE) which increases the prostatic fluid secretion and hence an increase in the uEV originating from prostatic luminal epithelium cells (180). Nevertheless, due to their urogenital origin, uEVs

represent a great potential source of biomarkers of disease of organs such as the bladder, kidneys and prostate and probably have a function in these organs' physiology and pathology.

Interestingly, however, proteins originating from distal anatomical sites have also been found in uEVs. For example studies have explored EVs as biomarkers in the urinary system from sites and diseases such as Parkinson's disease (181), brain tumours (182), lung cancer (183,184) and pulmonary arterial hypertension (185). These studies highlight the potential of uEVs in identifying diseases unrelated to the urinary system via a non-invasive sampling. However, a limitation in uEVs biomarker discovery is that the content of urine, including the uEVs, are very variable and dynamic, and influenced by different factors including, fluid intake, diet (186), age, exercise (187), gender (188) and time of collection. Such factors can complicate the interpretation of urine biomarker data in diagnostics, this as well as the lack of standardisation is discussed below in more detail.

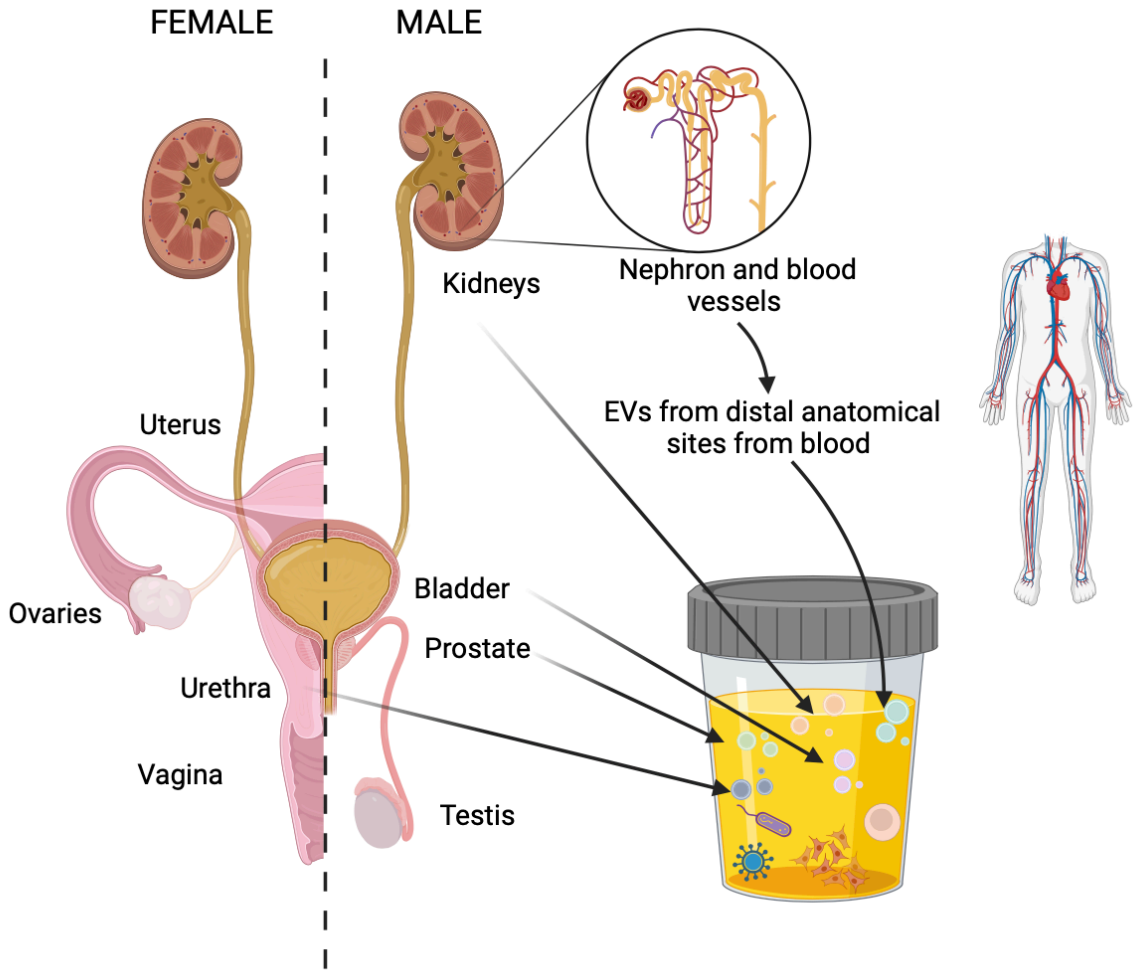


Figure 1.5. The origin of urinary EVs. Depiction of the origin of urinary EVs with EVs deriving from various organs and structure of the urinary system in both females and males in addition to distal anatomical sites via nephron and blood vessels. Components such as bacteria, viruses and epithelial cells are also shown in the urine (Created with BioRender.com.).

1.10 Urinary extracellular isolation and biomarker discoveries.

A large variety of methods used to isolate EVs from urine are published within the literature with the purification methods dependent on the EVs physicochemical properties (179). These methods include those that utilise centrifugation, filtration, precipitation and affinity interaction, of which each have limitations and advantages for their downstream application (189). The best method of isolation and purification should take into account the source of the sample (including the volume), sample integrity, yield of EVs required for subsequent analyses as well as time limitations and available instruments. The classic and most widely used method (Figure 1.6), is differential ultracentrifugation (dUC) in which a step wise increase in centrifugation speed is used to pellet EVs based on size density (190). In addition to this method many studies opt to perform a combination of dUC and other methods, such that many of the experiments use a combination of 2 or 3 isolation methods (Figure 1.6) (191). Ultimately, the selection of an isolation method or combination of methods not only depend on the type of biofluid but also any further downstream analyses such as 'omics' like proteomics and transcriptomics.

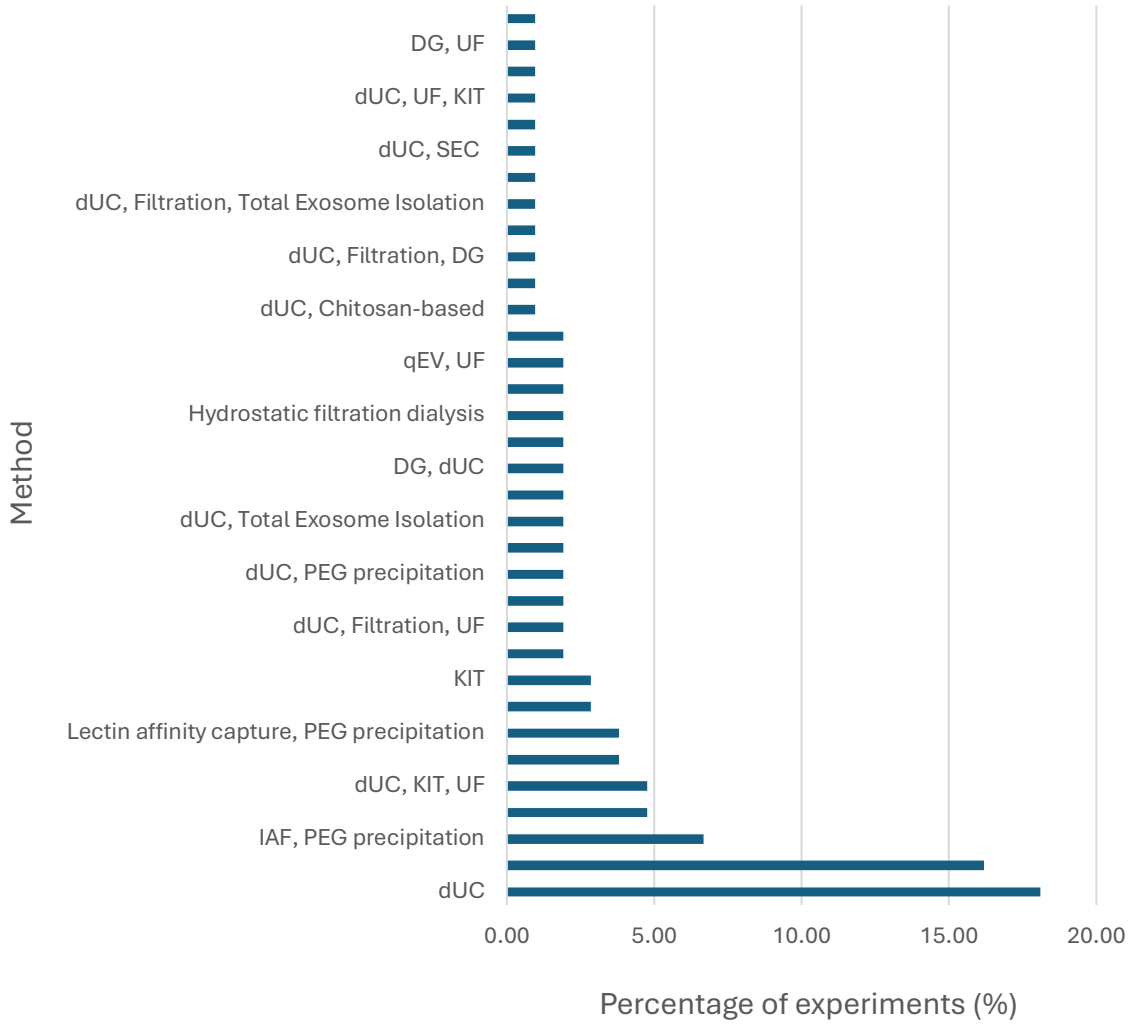


Figure 1.6. Exploring EV isolation methods from human urine: insights from 2017 to 2022 publications via Using EV-TRACK. A total of 105 experiments were included and showed that dUC was the most common method for uEV isolation (18.1%) and that many of the experiments used a combination of 2 or 3 isolation methods (72.4%). DG (Density gradient)), UF (ultra-filtration), dUC (differential ultracentrifugation), KIT (EV isolation kits), SEC (Size exclusion chromatography), qEV (qEV size exclusion column) IAF (Immuno-affinity capture) PEG precipitation (polyethylene glycol precipitation).

Despite these mixed isolation methods, further challenges arise from EV isolation from urine due to their different components. Urine sample EV preparation is challenged by the presence of abundant proteins including , human serum albumin, Tamm–Horsfall Protein (THP), Aquaporin-1, Aquaporin-2, uroplakin in addition to apolipoproteins, immunoglobulins, and other soluble proteins (192). THP, being the most abundant urinary protein (a daily excretion of 50–100 mg/day), can interfere with EV isolation and proteomic discovery (193). THP forms a gel-like 3D network that retains a variety of vesicles, decreasing the EV yield (194). Numerous approaches have been suggested to release the EVs from this THP matrix, including treatment with dithiothreitol (DTT) (194), CHAPS (3-[(3- Cholamidopropyl)dimethylammonio]-1-propanesulfonate hydrate) (195) or salt precipitation (196).

The reducing agent DTT is the most common method used to release EVs from the polymeric THP by reducing the THP ZP module that causes polymerization of filaments (197). Despite being widely used and shown to release vessels connected to the polymeric network, the monomeric THP and some part of the polymers are still shown to be present in the isolated EV pellet and could therefore go onto interfere with EV component analysis (194). Additionally, the treatment is considered to be harsh and also reduces disulphide bonds and intramolecular disulphide bridges, altering the protein's native activity and structure, including those on the EV surface (198). The zwitterionic detergent CHAPS, a suggested alternative to DTT, works by destroying protein-protein interactions by dissolving THP releasing EV while preserving their protein functional and morphological integrity (195).

These challenges in EV isolation from urine may account for only 14% of EV biomarker research performed in urine despite its non-invasive ease of collection, sterility and richness in biomolecules (199). Nevertheless, since the landmark study that first described EV within the urine (178), indicating the potential of EVs in urine as a non-invasive biofluid, many EV derived molecules have been investigated in a wide variety of diseases and conditions (181,200–203).

For example, prostate cancer is the second most frequent malignancy in men worldwide and the fifth leading cause of death (204), hence lots of research goes into the early diagnosis of prostate cancer. Currently four commercial urine based biomarker tests are available for prostate cancer (205) one of which utilises EVs (206). This test, the ExoDx Prostate IntelliScore from Exome Diagnostics, is the most progressive and vigorously validated tool which distinguished between Gleason 7 or higher-grade prostate cancer and those with Gleason 6 or benign tumour via measurement of mRNA levels of EV Erythroblast transformation-specific – related gene (ERG*)* and Prostate cancer antigen 3 (PCA3)*,* using reverse transcription quantitative PCR (139). This test is based on the knowledge that within prostate cancer, ERG is frequently shown to be overexpressed (207) along with the ncRNA PCA3 (208). The test examines first-catch urine samples without digital prostate manipulation and shows advantages over other urine tests available (209). In a validation study for ExoDx, 519 patients were used to test the gene expression signature's ability to recognise Gleason 7 or higher disease along with prostate specific antigen (PSA) level, age, race, and family history compared to the current standard of care (SOC) which involves just PSA, age, race, and family history alone (209). It was reported that the gene expression assay plus standard care methods

had an area under the curve (AUC) of 0.73 (a Confidence Interval (CI) of 95%) and SOC AUC of 0.63 (CI 95%) (209). This reported better identification of patients could therefore be used to reduce the need for an invasive biopsy. This available test highlights the importance of preliminary biomarker discoveries and the need for further research and validation in other diseases and condition before more test kits can be created and be publicly available for diagnostic usage.

1.11 The future of urinary extracellular vesicles in clinical application.

Despite the advances of using urine as a non-invasive biofluid, and the previously discussed urine biomarker discoveries, multiple hurdles are still prevalent and need to be overcome before urinary exosomes can be used within a clinical setting (210). For example, urine biomarkers can be affected by substances within the urine as well as urine volume concentration correction, highlighting that one of the key challenges is quantification (210). Preferably the absolute excretion rate of each protein and comparison between patient groups and matched controls should be known, as the current simple measurement of individual protein concentration in studies is of limited use due to the differences in subject-to-subject water excretion which would be the key determinate of biomarker concentration (211). A method of normalising such variables is via urinary creatinine concentration, however excretion rate of creatinine varies between person to person (212), possibly leading to camouflaging of changes in protein marker excretion. To overcome this, normalisation of excretion of specific exosomal proteins should be compared to excretion of known markers of exosomes like Alix or TSG101 (213).

Another barrier in urinary EV transition into clinical practice is standardisation of EV extraction methodology (211). Current EV extraction methods are too diverse to confirm their purity, this protocol wide diversity (even within the same approaches) hinders the comparison, verification and subsequent analysis by different research teams and studies. In conjunction with this issue are the various contaminants within urine that could result from these isolation methods, notably the issue of THP excretion as discussed above. Thus, the development of a standard international consensus of EV isolation should include or consider this THP issue, either through its elimination or prevention of its aggregation.

Furthermore, proposed EV biomarkers will have to be validated in large prospective trials to prove their clinical benefit in comparison with established standards, as many of the previously discussed biomarkers are being identified in very small-scale studies with small patient numbers. This, in conjunction with the additional disadvantages mentioned, need to be overcome before the next step of urine EV clinical translation and application. Current commercial EV available testing highlights that such challenges can be overcome, and hence future biomarker discovers should use studies leading to the commercial test development and approval as guidance in study planning.

1.12 Conclusion.

For a successful pregnancy, a continuous molecular dialogue is vital, with this communication based on endocrine, paracrine, and autocrine factors. EVs signify a possible direct and dynamic communication method between the embryo and the mother in the development of the blastocyst, embryo modulation of the receptive

endometrium, and trophoblast invasion. However, the precise courses of this communication are not fully comprehended, and additional investigations are needed. Improved knowledge of molecular mechanisms facilitating this cross talk could lead to new regulating agent development, with novel diagnostic, biological, and therapeutic possibilities in assisting reproduction and ultimately increasing healthy birth rates. Due to the advantages and advancement in urine and uEV biomarker discoveries, more research into the biofluid of urine in the context of reproduction could lead to the development of a non-invasive method of improving these birth rates. Finally, reliable biomarkers should be confirmed, while various EVs derived molecules have been recognised as possible biomarkers, few are qualified for therapeutic application. However, consensus has established that EVs are a biological element that could have physiological and diagnostic relevance within pregnancy establishment and so further research into this area is essential.

1.13 Thesis aims.

Successful embryo implantation into a receptive endometrium requires mutual endometrial-embryo communication. EVs derived from the endometrium are increasingly being reported to be involved in embryo-maternal interactions during implantation. Through the knowledge gained from the analysis of these EVs and their cargos could lead to EVs being exploited as an implantation receptivity biomarker. Currently the method used to assess endometrial receptivity involves the use of endometrial biopsies in an invasive clinical procedure and doubts about its reliability exist. Hence the need for a non-invasive reliable assessment is high. Consequently, we set out the following aims to explore the cargo of endometrial EVs and the non-invasive

biofluid of urine during the receptive implantation period to help identify potential biomarkers with clinical implications:

- Investigate the proteomic profile, as well as the size and concentration, of endometrial cells EVs *in vitro* under the influence of sex hormones, specifically estrogen and progesterone, to mimic different phases of the menstrual cycle.
- Investigate the impact of sex hormone-influenced endometrial EVs from receptive endometrial cells on trophoblast binding and trophoblast mRNA expression *in vitro*.
- Optimising the isolation of EVs from urine to ensure the repeatability, purity, and storage condition is sufficient for the subsequent investigation into urine EVs as non-invasive biomarker.
- Explore the effects of the menstrual cycle on neat urine and urine EVs using a proteomic approach aiming to characterise and identify potential biomarkers associated with receptivity.

1.14 References.

1. Fraser I, Critchley H, Broder M, Munro M. The FIGO Recommendations on Terminologies and Definitions for Normal and Abnormal Uterine Bleeding. Semin Reprod Med. 2011 Sep;29(05):383–90.

2. Jabbour HN, Kelly RW, Fraser HM, Critchley HOD. Endocrine regulation of menstruation. Vol. 27, Endocrine Reviews. 2006.

3. Draper CF, Duisters K, Weger B, Chakrabarti A, Harms AC, Brennan L, et al. Menstrual cycle rhythmicity: metabolic patterns in healthy women. Sci Rep. 2018 Oct 1;8(1):14568.

4. Farage MA, Neill S, MacLean AB. Physiological Changes Associated with the Menstrual Cycle: A Review. Obstet Gynecol Surv. 2009 Jan;64(1):58–72.

5. Hillier SG. Paracrine support of ovarian stimulation. Mol Hum Reprod. 2009 Dec 1;15(12):843–50.

6. Ashary N, Tiwari A, Modi D. Embryo Implantation: War in times of love. Endocrinology. 2018.

7. Jarvis GE. Early embryo mortality in natural human reproduction: What the data say. F1000Research. 2016.

8. Boivin J, Griffiths E, Venetis CA. Emotional distress in infertile women and failure of assisted reproductive technologies: Meta-analysis of prospective psychosocial studies. BMJ. 2011.

9. Fertility treatment 2018: trends and figures. Human Fertilisation & Embryology Authority. 2020.

10. Apter S, Balaban B, Campbell A, Catt J, Coticchio G, Jose de los Santos M, et al. The Vienna consensus: report of an expert meeting on the development of ART laboratory performance indicators. In: Reproductive BioMedicine Online. 2017. p. 494–510.

11. Wilcox AJ, Baird DD, Weinberg CR. Time of Implantation of the Conceptus and Loss of Pregnancy. N Engl J Med. 1999.

12. Ashary N, Tiwari A, Modi D. Embryo Implantation: War in times of love. Endocrinology. 2018.

13. Cork BA, Tuckerman EM, Li TC, Laird SM. Expression of interleukin (IL)-11 receptor by the human endometrium in vivo and effects of IL-11, IL-6 and LIF on the production of MMP and cytokines by human endometrial cells in vitro. Mol Hum Reprod. 2002;8(9).

14. Fowler DJ, Nicolaides KH, Miell JP. Insulin-like growth factor binding protein-1 (IGFBP-1): A multifunctional role in the human female reproductive tract. Vol. 6, Human Reproduction Update. 2000.

15. Hannan NJ, Jones RL, White CA, Salamonsen LA. The chemokines, CX3CL1, CCL14, and CCL4, promote human trophoblast migration at the feto-maternal interface. Biol Reprod. 2006;74(5).

16. He Z, Ma Y, Li L, Liu J, Yang H, Chen C, et al. Osteopontin and Integrin αvβ3 Expression during the Implantation Window in IVF Patients with Elevated Serum Progesterone and Oestradiol Level. Geburtshilfe Frauenheilkd. 2016;76(6).

17. Warning JC, McCracken SA, Morris JM. A balancing act: Mechanisms by which the fetus avoids rejection by the maternal immune system. Reproduction. 2011;141(6):715–24.

18. Bhagwat SR, Chandrashekar DS, Kakar R, Davuluri S, Bajpai AK, Nayak S, et al. Endometrial Receptivity: A Revisit to Functional Genomics Studies on Human Endometrium and Creation of HGEx-ERdb. PLoS ONE. 2013.

19. Modi D, Bhartiya P. Physiology of embryo-endometrial cross talk. Biomed Res J. 2015.

20. Ochoa-Bernal MA, Fazleabas AT. Physiologic Events of Embryo Implantation and Decidualization in Human and Non-Human Primates. Int J Mol Sci. 2020 Mar 13;21(6):1973.

21. Ng SW, Norwitz GA, Pavlicev M, Tilburgs T, Simón C, Norwitz ER. Endometrial Decidualization: The Primary Driver of Pregnancy Health. Int J Mol Sci. 2020 Jun 8;21(11):4092.

22. Greenbaum S, Averbukh I, Soon E, Rizzuto G, Baranski A, Greenwald NF, et al. A spatially resolved timeline of the human maternal–fetal interface. Nature. 2023 Jul 20;619(7970):595–605.

23. Gellersen B, Brosens J. Cyclic AMP and progesterone receptor cross-talk in human endometrium: a decidualizing affair. J Endocrinol. 2003 Sep 1;178(3):357–72.

24. Gellersen B, Brosens JJ. Cyclic Decidualization of the Human Endometrium in Reproductive Health and Failure. Endocr Rev. 2014 Dec 1;35(6):851–905.

25. Jabbour HN, Critchley HOD, Boddy SC. Expression of Functional Prolactin Receptors in Nonpregnant Human Endometrium: Janus Kinase-2, Signal Transducer and Activator of Transcription-1 (STAT1), and STAT5 Proteins Are Phosphorylated after Stimulation with Prolactin. J Clin Endocrinol Metab. 1998 Jul 1;83(7):2545–53.

26. Pellegrini I, Lebrun JJ, Ali S, Kelly PA. Expression of prolactin and its receptor in human lymphoid cells. Mol Endocrinol. 1992 Jul;6(7):1023–31.

27. Sharma S, Godbole G, Modi D. Decidual Control of Trophoblast Invasion. Am J Reprod Immunol. 2016;75(3):341–50.

28. Dimitriadis E, White CA, Jones RL, Salamonsen LA. Cytokines, chemokines and growth factors in endometrium related to implantation. Hum Reprod Update. 2005 Nov 1;11(6):613–30.

29. Kajihara T, Brosens JJ, Ishihara O. The role of FOXO1 in the decidual transformation of the endometrium and early pregnancy. Med Mol Morphol. 2013 Jun;46(2):61–8.

30. Xu Y, Lu J, Wu J, Jiang R, Guo C, Tang Y, et al. HOXA10 co-factor MEIS1 is required for the decidualization in human endometrial stromal cell. J Mol Endocrinol. 2020 May;64(4):249–58.

31. Cho H, Okada H, Tsuzuki T, Nishigaki A, Yasuda K, Kanzaki H. Progestin-induced heart and neural crest derivatives expressed transcript 2 is associated with fibulin-1 expression in human endometrial stromal cells. Fertil Steril. 2013 Jan;99(1):248-255.e2.

32. Tamura I, Maekawa R, Jozaki K, Ohkawa Y, Takagi H, Doi-Tanaka Y, et al. Transcription factor C/EBPβ induces genome-wide H3K27ac and upregulates gene expression during decidualization of human endometrial stromal cells. Mol Cell Endocrinol. 2021 Jan;520:111085.

33. Murata H, Tanaka S, Tsuzuki-Nakao T, Kido T, Kakita-Kobayashi M, Kida N, et al. The transcription factor HAND2 up-regulates transcription of the IL15 gene in human endometrial stromal cells. J Biol Chem. 2020 Jul;295(28):9596–605.

34. Wynn RM. Ultrastructural development of the human decidua. Am J Obstet Gynecol. 1974 Mar;118(5):652–70.

35. Kajihara T, Tanaka K, Oguro T, Tochigi H, Prechapanich J, Uchino S, et al. Androgens Modulate the Morphological Characteristics of Human Endometrial Stromal Cells Decidualized In Vitro. Reprod Sci. 2014 Mar;21(3):372–80.

36. Ramathal C, Wang W, Hunt E, Bagchi IC, Bagchi MK. Transcription Factor CCAAT Enhancer-binding Protein β (C/EBPβ) Regulates the Formation of a Unique Extracellular Matrix That Controls Uterine Stromal Differentiation and Embryo Implantation. J Biol Chem. 2011 Jun;286(22):19860–71.

37. Glasser SR, Lampelo S, Munir MI, Julian J. Expression of desmin, laminin and fibronectin during in situ differentiation (decidualization) of rat uterine stromal cells. Differentiation. 1987 Oct;35(2):132–42.

38. Kisalus LL, Herr JC. Immunocytochemical Localization of Heparan Sulfate Proteoglycan in Human Decidual Cell Secretory Bodies and Placental Fibrinoid1. Biol Reprod. 1988 Sep 1;39(2):419–30.

39. Oefner CM, Sharkey A, Gardner L, Critchley H, Oyen M, Moffett A. Collagen type IV at the fetal–maternal interface. Placenta. 2015 Jan;36(1):59–68.

40. Murata H, Tanaka S, Okada H. Immune Tolerance of the Human Decidua. J Clin Med. 2021 Jan 18;10(2):351.

41. Robertson SA, Care AS, Skinner RJ. Interleukin 10 Regulates Inflammatory Cytokine Synthesis to Protect Against Lipopolysaccharide-Induced Abortion and Fetal Growth Restriction in Mice1. Biol Reprod. 2007 May 1;76(5):738–48.

42. Yang D, Dai F, Yuan M, Zheng Y, Liu S, Deng Z, et al. Role of Transforming Growth Factor-β1 in Regulating Fetal-Maternal Immune Tolerance in Normal and Pathological Pregnancy. Front Immunol. 2021 Aug 31;12:689181.

43. Llorca T, Ruiz-Magaña MJ, Martinez-Aguilar R, García-Valdeavero OM, Rodríguez-Doña L, Abadia-Molina AC, et al. Decidualized human decidual stromal cells inhibit chemotaxis of activated T cells: a potential mechanism of maternal-fetal immune tolerance. Front Immunol. 2023 Aug 23;14:1223539.

44. Plaisier M. Decidualisation and angiogenesis. Best Pract Res Clin Obstet Gynaecol. 2011 Jun;25(3):259–71.

45. Guo X, Yi H, Li TC, Wang Y, Wang H, Chen X. Role of Vascular Endothelial Growth Factor (VEGF) in Human Embryo Implantation: Clinical Implications. Biomolecules. 2021 Feb 10;11(2):253.

46. De Falco S. The discovery of placenta growth factor and its biological activity. Exp Mol Med. 2012;44(1):1.

47. Diedrich K, Fauser BCJM, Devroey P, Griesinger G. The role of the endometrium and embryo in human implantation. Hum Reprod Update. 2007 Jul 1;13(4):365–77.

48. Nikas G. Endometrial Receptivity: Changes in Cell-Surface Morphology. Semin Reprod Med. 2000;18(03):229–36.

49. Nikas G, Makrigiannakis A. Endometrial Pinopodes and Uterine Receptivity. Ann N Y Acad Sci. 2003 Nov;997(1):120–3.

50. Stavreus-Evers A, Nikas G, Sahlin L, Eriksson H, Landgren BM. Formation of pinopodes in human endometrium is associated with the concentrations of progesterone and progesterone receptors. Fertil Steril. 2001 Oct;76(4):782–91.

51. Nikas G. Pinopodes as markers of endometrial receptivity in clinical practice. Hum Reprod. 1999 Dec 1;14(suppl 2):99–106.

52. D'Ippolito S, Di Nicuolo F, Papi M, Castellani R, Palmieri V, Masciullo V, et al. Expression of Pinopodes in the Endometrium from Recurrent Pregnancy Loss Women. Role of Thrombomodulin and Ezrin. J Clin Med. 2020 Aug 13;9(8):2634.

53. Nikas G, Psychoyos A. Uterine Pinopodes in Peri-implantation Human Endometrium Clinical Relevance. Ann N Y Acad Sci. 1997 Jun;816(1):129–42.

54. Sternberg AK, Buck VU, Classen-Linke I, Leube RE. How Mechanical Forces Change the Human Endometrium during the Menstrual Cycle in Preparation for Embryo Implantation. Cells. 2021 Aug 6;10(8):2008.

55. Alikani M. Epithelial cadherin distribution in abnormal human pre-implantation embryos. Hum Reprod. 2005 Dec 1;20(12):3369–75.

56. Feng Y, Ma X, Deng L, Bin Yao, Xiong Y, Wu Y, et al. Role of Selectins and their Ligands in Human Implantation Stage. Glycobiology. 2017 Jan 23;cwx009.

57. Singh H, Aplin JD. Adhesion molecules in endometrial epithelium: tissue integrity and embryo implantation. J Anat. 2009 Jul;215(1):3–13.

58. Aplin JD, Spanswick C, Behzad F, Kimber SJ, Vićovac L. Integrins beta 5, beta 3 and alpha v are apically distributed in endometrial epithelium. Mol Hum Reprod. 1996;2(7):527–34.

59. Johnson GA, Burghardt RC, Bazer FW, Seo H, Cain JW. Integrins and their potential roles in mammalian pregnancy. J Anim Sci Biotechnol. 2023 Sep 8;14(1):115.

60. Aghajanova L. Leukemia Inhibitory Factor and Human Embryo Implantation. Ann N Y Acad Sci. 2004 Dec;1034(1):176–83.

61. Chobotova K, Karpovich N, Carver J, Manek S, Gullick WJ, Barlow DH, et al. Heparin-Binding Epidermal Growth Factor and Its Receptors Mediate Decidualization and Potentiate Survival of Human Endometrial Stromal Cells. J Clin Endocrinol Metab. 2005 Feb;90(2):913–9.

62. Hey NA, Graham RA, Seif MW, Aplin JD. The polymorphic epithelial mucin MUC1 in human endometrium is regulated with maximal expression in the implantation phase. J Clin Endocrinol Metab. 1994 Feb;78(2):337–42.

63. Meseguer M, Aplin JD, Caballero-Campo P, O'Connor JE, Martín JC, Remohí J, et al. Human Endometrial Mucin MUC1 Is Up-Regulated by Progesterone and Down-Regulated In Vitro by the Human Blastocyst1. Biol Reprod. 2001 Feb 1;64(2):590–601.

64. Monin L, Whettlock EM, Male V. Immune responses in the human female reproductive tract. Immunology. 2020 Jun;160(2):106–15.

65. Vinketova K, Mourdjeva M, Oreshkova T. Human Decidual Stromal Cells as a Component of the Implantation Niche and a Modulator of Maternal Immunity. J Pregnancy. 2016;2016:1–17.

66. Sojka DK, Yang L, Yokoyama WM. Uterine Natural Killer Cells. Front Immunol. 2019 May 1;10:960.

67. Wallace AE, Fraser R, Cartwright JE. Extravillous trophoblast and decidual natural killer cells: a remodelling partnership. Hum Reprod Update. 2012 Jul 1;18(4):458–71.

68. Quenby S, Nik H, Innes B, Lash G, Turner M, Drury J, et al. Uterine natural killer cells and angiogenesis in recurrent reproductive failure. Hum Reprod. 2008 Oct 14;24(1):45–54.

69. Wang F, Qualls AE, Marques-Fernandez L, Colucci F. Biology and pathology of the uterine microenvironment and its natural killer cells. Cell Mol Immunol. 2021 Sep;18(9):2101–13.

70. Okeke EB, Uzonna JE. The Pivotal Role of Regulatory T Cells in the Regulation of Innate Immune Cells. Front Immunol. 2019 Apr 9;10:680.

71. Zhang XX, Kang XM, Zhao AM. Regulation of CD4+FOXP3+ T cells by CCL20/CCR6 axis in early unexplained recurrent miscarriage patients. Genet Mol Res. 2015;14(3):9145–54.

72. Sasaki Y. Decidual and peripheral blood CD4+CD25+ regulatory T cells in early pregnancy subjects and spontaneous abortion cases. Mol Hum Reprod. 2004 Mar 25;10(5):347–53.

73. Kudo Y. Mechanisms regulating the expression of indoleamine 2,3-dioxygenase during decidualization of human endometrium. Hum Reprod. 2004 Mar 25;19(5):1222–30.

74. Mbongue J, Nicholas D, Torrez T, Kim NS, Firek A, Langridge W. The Role of Indoleamine 2, 3-Dioxygenase in Immune Suppression and Autoimmunity. Vaccines. 2015 Sep 10;3(3):703–29.

75. Liu S, Hong L, Li Y, Lian R, Wang X, Zeng Y. Association between endometrial indoleamine 2,3-dioxygenase expression level and pregnancy outcomes in women undergoing first in vitro fertilization treatment. BMC Pregnancy Childbirth. 2021 Dec;21(1):33.

76. Gregori S, Amodio G, Quattrone F, Panina-Bordignon P. HLA-G Orchestrates the Early Interaction of Human Trophoblasts with the Maternal Niche. Front Immunol [Internet]. 2015 Mar 30 [cited 2024 Jul 26];6. Available from: http://journal.frontiersin.org/Article/10.3389/fimmu.2015.00128/abstract.

77. Abrahams VM. First trimester trophoblast cells secrete Fas ligand which induces immune cell apoptosis. Mol Hum Reprod. 2004 Jan 1;10(1):55–63.

78. Es-Haghi M, Godakumara K, Häling A, Lättekivi F, Lavrits A, Viil J, et al. Specific trophoblast transcripts transferred by extracellular vesicles affect gene expression in endometrial epithelial cells and may have a role in embryo-maternal crosstalk. Cell Commun Signal. 2019.

79. O'Neil E V., Burns GW, Ferreira CR, Spencer TE. Characterization and regulation of extracellular vesicles in the lumen of the ovine uterus. Biol Reprod. 2020;102(5).

80. Nakamura K, Kusama K, Ideta A, Kimura K, Hori M, Imakawa K. Effects of miR-98 in intrauterine extracellular vesicles on maternal immune regulation during the peri-implantation period in cattle. Sci Rep. 2019;9(1).

81. Zaborowski MP, Balaj L, Breakefield XO, Lai CP. Extracellular Vesicles: Composition, Biological Relevance, and Methods of Study. BioScience. 2015.

82. Xu R, Greening DW, Zhu HJ, Takahashi N, Simpson RJ. Extracellular vesicle isolation and characterization: Toward clinical application. Journal of Clinical Investigation. 2016.

83. Ng YH, Rome S, Jalabert A, Forterre A, Singh H, Hincks CL, et al. Endometrial Exosomes/Microvesicles in the Uterine Microenvironment: A New Paradigm for Embryo-Endometrial Cross Talk at Implantation. PloS One. 2013;8(3):p.e58502.

84. Stegmayr B, Ronquist G. Promotive effect on human sperm progressive motility by prostasomes. Urol Res. 1982.

85. Crawford N. The Presence of Contractile Proteins in Platelet Microparticles Isolated from Human and Animal Platelet-free Plasma. Br J Haematol. 1971.

86. Trams EG, Lauter CJ, Norman Salem J, Heine U. Exfoliation of membrane ecto-enzymes in the form of micro-vesicles. BBA - Biomembr. 1981.

87. Johnstone RM, Adam M, Hammond JR, Orr L, Turbide C. Vesicle formation during reticulocyte maturation. Association of plasma membrane activities with released vesicles (exosomes). J Biol Chem. 1987.

88. Villarroya-Beltri C, Baixauli F, Gutiérrez-Vázquez C, Sánchez-Madrid F, Mittelbrunn M. Sorting it out: Regulation of exosome loading. Seminars in Cancer Biology. 2014.

89. Bianco F, Perrotta C, Novellino L, Francolini M, Riganti L, Menna E, et al. Acid sphingomyelinase activity triggers microparticle release from glial cells. EMBO J. 2009;28(8):1043–54.

90. Piccin A, Murphy WG, Smith OP. Circulating microparticles: pathophysiology and clinical implications. Blood Rev. 2007;21(3):157–71.

91. Yáñez-Mó M, Siljander PRM, Andreu Z, Zavec AB, Borràs FE, Buzas EI, et al. Biological properties of extracellular vesicles and their physiological functions. Journal of Extracellular Vesicles. 2015.

92. Kim DK, Kang B, Kim OY, Choi DS, Lee J, Kim SR, et al. EVpedia: An integrated database of high-throughput data for systemic analyses of extracellular vesicles. J Extracell Vesicles. 2013;2(10).

93. Yeung CYC, Schoof EM, Tamáš M, Mackey AL, Kjaer M. Proteomics identifies differences in fibrotic potential of extracellular vesicles from human tendon and muscle fibroblasts. Cell Commun Signal. 2020;18(1).

94. Vlassov A V., Magdaleno S, Setterquist R, Conrad R. Exosomes: Current knowledge of their composition, biological functions, and diagnostic and therapeutic potentials. Biochim Biophys Acta - Gen Subj. 2012;1820(7):940–8.

95. Huang X, Yuan T, Tschannen M, Sun Z, Jacob H, Du M, et al. Characterization of human plasma-derived exosomal RNAs by deep sequencing. BMC Genomics. 2013;14(319).

96. Capalbo A, Ubaldi FM, Cimadomo D, Noli L, Khalaf Y, Farcomeni A, et al. MicroRNAs in spent blastocyst culture medium are derived from trophectoderm cells and can be explored for human embryo reproductive competence assessment. Fertil Steril. 2016;105(1):225-235.e3.

97. Gross N, Kropp J, Khatib H. MicroRNA signaling in embryo development. Biology. 2017;6(3):34.

98. Cuman C, Van Sinderen M, Gantier MP, Rainczuk K, Sorby K, Rombauts L, et al. Human Blastocyst Secreted microRNA Regulate Endometrial Epithelial Cell Adhesion. EBioMedicine. 2015.

99. Taraboletti G, D'Ascenzo S, Borsotti P, Giavazzi R, Pavan A, Dolo V. Shedding of the matrix metalloproteinases MMP-2, MMP-9, and MT1-MMP as membrane vesicle-associated components by endothelial cells. Am J Pathol. 2002.

100. Carrasco-Ramírez P, Greening DW, Andrés G, Gopal SK, Martín-Villar E, Renart J, et al. Podoplanin is a component of extracellular vesicles that reprograms cell-derived exosomal proteins and modulates lymphatic vessel formation. Oncotarget. 2016.

101. He S, Chen D, Hu M, Zhang L, Liu C, Traini D, et al. Bronchial epithelial cell extracellular vesicles ameliorate epithelial–mesenchymal transition in COPD pathogenesis by alleviating M2 macrophage polarization. Nanomedicine Nanotechnol Biol Med. 2019.

102. Han C, Wang C, Chen Y, Wang J, Xu X, Hilton T, et al. Placenta-derived extracellular vesicles induce preeclampsia in mouse models. Haematologica. 2020;105(6).

103. Rai A, Poh QH, Fatmous M, Fang H, Gurung S, Vollenhoven B, et al. Proteomic profiling of human uterine extracellular vesicles reveal dynamic regulation of key players of embryo implantation and fertility during menstrual cycle. Proteomics. 2021;21(13–14).

104. Giacomini E, Vago R, Sanchez AM, Podini P, Zarovni N, Murdica V, et al. Secretome of in vitro cultured human embryos contains extracellular vesicles that are uptaken by the maternal side. Sci Rep. 2017.

105. Dissanayake K, Nõmm M, Lättekivi F, Ressaissi Y, Godakumara K, Lavrits A, et al. Individually cultured bovine embryos produce extracellular vesicles that have the potential to be used as non-invasive embryo quality markers. Theriogenology. 2020;149.

106. Mellisho EA, Velásquez AE, Nuñez MJ, Cabezas JG, Cueto JA, Fader C, et al. Identification and characteristics of Extracellular vesicles from bovine blastocysts produced in vitro. PLoS ONE. 2017.

107. Taqi MO, Saeed-Zidane M, Gebremedhn S, Salilew-Wondim D, Khdrawy O, Rings F, et al. Sexual dimorphic expression and release of transcription factors in bovine embryos exposed to oxidative stress. Mol Reprod Dev. 2019.

108. Es-Haghi M, Godakumara K, Häling A, Lättekivi F, Lavrits A, Viil J, et al. Specific trophoblast transcripts transferred by extracellular vesicles affect gene expression in endometrial epithelial cells and may have a role in embryo-maternal crosstalk. Cell Commun Signal. 2019.

109. Mellisho EA, Velásquez AE, Nuñez MJ, Cabezas JG, Cueto JA, Fader C, et al. Identification and characteristics of Extracellular vesicles from bovine blastocysts produced in vitro. PLoS ONE. 2017.

110. Gupta SK. Human Zona Pellucida Glycoproteins: Binding Characteristics With Human Spermatozoa and Induction of Acrosome Reaction. Front Cell Dev Biol. 2021 Feb 11;9:619868.

111. Vanroose G, Nauwynck H, Soom AV, Ysebaert MT, Charlier G, Oostveldt PV, et al. Structural Aspects of the Zona Pellucida of In Vitro-Produced Bovine Embryos: A Scanning Electron and Confocal Laser Scanning Microscopic Study1. Biol Reprod. 2000 Feb 1;62(2):463–9.

112. Wassarman PM, Litscher ES. Female fertility and the zona pellucida. eLife. 2022 Jan 25;11:e76106.

113. Familiari G. Structural changes of the zona pellucida during fertilization and embryo development. Front Biosci. 2008;Volume(13):6730.

114. Cheeseman LP, Boulanger J, Bond LM, Schuh M. Two pathways regulate cortical granule translocation to prevent polyspermy in mouse oocytes. Nat Commun. 2016 Dec 19;7(1):13726.

115. Turner K, Horobin RW. Permeability of the mouse zona pellucida: A structure-staining-correlation model using coloured probes. J Reprod Fertil. 1997;111(2).

116. Vyas P, Balakier H, Librach CL. Ultrastructural identification of CD9 positive extracellular vesicles released from human embryos and transported through the zona pellucida. Syst Biol Reprod Med. 2019;65(4).

117. Saadeldin IM, Kim SJ, Choi Y Bin, Lee BC. Improvement of cloned embryos development by co-culturing with parthenotes: A possible role of exosomes/microvesicles for embryos paracrine communication. Cell Reprogramming. 2014;16(3):223–34.

118. Pavani KC, Meese T, Pascottini OB, Guan X, Lin X, Peelman L, et al. Hatching is modulated by microRNA-378a-3p derived from extracellular vesicles secreted by blastocysts. Proc Natl Acad Sci. 2022 Mar 22;119(12).

119. Chen K, Liang J, Qin T, Zhang Y, Chen X, Wang Z. The Role of Extracellular Vesicles in Embryo Implantation. Front Endocrinol. 2022 Jan 28;13:809596.

120. Andrade GM, Bomfim MM, del Collado M, Meirelles FV, Perecin F, da Silveira JC. Oxygen tension modulates extracellular vesicles and its miRNA contents in bovine embryo culture medium. Mol Reprod Dev. 2019;86:1067–80.

121. Abu-Halima M, Häusler S, Backes C, Fehlmann T, Staib C, Nestel S, et al. Micro-ribonucleic acids and extracellular vesicles repertoire in the spent culture media is altered in women undergoing In Vitro Fertilization. Sci Rep. 2017;7:13525.

122. Pallinger E, Bognar Z, Bodis J, Csabai T, Farkas N, Godony K, et al. A simple and rapid flow cytometry-based assay to identify a competent embryo prior to embryo transfer. Sci Rep. 2017;7:39927.

123. Dissanayake K, Nõmm M, Lättekivi F, Ord J, Ressaissi Y, Godakumara K, et al. Oviduct as a sensor of embryo quality: deciphering the extracellular vesicle (EV)-mediated embryo-maternal dialogue. J Mol Med. 2021;99(5).

124. Burns GW, Brooks KE, Spencer TE. Extracellular vesicles originate from the conceptus and uterus during early pregnancy in sheep. Biol Reprod. 2016;94(56).

125. Terashita Y, Sugimura S, Kudo Y, Amano R, Hiradate Y, Sato E. Improving the Quality of Miniature Pig Somatic Cell Nuclear Transfer Blastocysts: Aggregation of SCNT Embryos at the Four-cell Stage. Reprod Domest Anim. 2011;46(2):189–96.

126. Pavani KC, Hendrix A, Van Den Broeck W, Couck L, Szymanska K, Lin X, et al. Isolation and characterization of functionally active extracellular vesicles from culture medium conditioned by bovine embryos in vitro. Int J Mol Sci. 2019;20(1):38.

127. Qu P, Qing S, Liu R, Qin H, Wang W, Qiao F, et al. Effects of embryo-derived exosomes on the development of bovine cloned embryos. PLoS ONE. 2017;12(3).

128. Mellisho EA, Briones MA, Velásquez AE, Cabezas J, Castro FO, Rodríguez-Álvarez L. Extracellular vesicles secreted during blastulation show viability of bovine embryos. Reproduction. 2019;158(6).

129. Bidarimath M, Khalaj K, Kridli RT, Kan FWK, Koti M, Tayade C. Extracellular vesicle mediated intercellular communication at the porcine maternal-fetal interface: A new paradigm for conceptus-endometrial cross-talk. Sci Rep. 2017;7.

130. Conrad KP, Tuna KM, Mestre CT, Banwatt ES, Alli AA. Activation of multiple receptors stimulates extracellular vesicle release from trophoblast cells. Physiol Rep. 2020;8(20).

131. Poh QH, Rai A, Carmichael II, Salamonsen LA, Greening DW. Proteome reprogramming of endometrial epithelial cells by human trophectodermal small extracellular vesicles reveals key insights into embryo implantation. Proteomics. 2021;21(13–14).

132. Godakumara K, Ord J, Lättekivi F, Dissanayake K, Viil J, Boggavarapu NR, et al. Trophoblast derived extracellular vesicles specifically alter the transcriptome of endometrial cells and may constitute a critical component of embryo-maternal communication. Reprod Biol Endocrinol. 2021;19(1):115.

133. Nakamura K, Kusama K, Ideta A, Imakawa K, Hori M. IFNT-independent effects of intrauterine extracellular vesicles (EVs) in cattle. Reproduction. 2020;159(5).

134. Almiñana C, Vegas AR, Tekin M, Hassan M, Uzbekov R, Fröhlich T, et al. Isolation and characterization of equine uterine extracellular vesicles: A comparative methodological study. Int J Mol Sci. 2021;22(2).

135. Ng YH, Rome S, Jalabert A, Forterre A, Singh H, Hincks CL, et al. Endometrial Exosomes/Microvesicles in the Uterine Microenvironment: A New Paradigm for Embryo-Endometrial Cross Talk at Implantation. PloS One. 2013;8(3):p.e58502.

136. Greening DW, Nguyen HPT, Elgass K, Simpson RJ, Salamonsen LA. Human endometrial exosomes contain hormone-specific cargo modulating trophoblast adhesive capacity: Insights into endometrial-embryo interactions. Biol Reprod. 2016.

137. Desrochers LM, Bordeleau F, Reinhart-King CA, Cerione RA, Antonyak MA. Microvesicles provide a mechanism for intercellular communication by embryonic stem cells during embryo implantation. Nat Commun. 2016;7:11958.

138. Kusama K, Nakamura K, Bai R, Nagaoka K, Sakurai T, Imakawa K. Intrauterine exosomes are required for bovine conceptus implantation. Biochem Biophys Res Commun. 2018;495(1):1370–5.

139. Tutrone R, Donovan MJ, Torkler P, Tadigotla V, McLain T, Noerholm M, et al. Clinical utility of the exosome based ExoDx Prostate(IntelliScore) EPI test in men presenting for initial Biopsy with a PSA 2–10 ng/mL. Prostate Cancer Prostatic Dis. 2020;23:607–14.

140. Alvarez-Erviti L, Seow Y, Yin H, Betts C, Lakhal S, Wood MJA. Delivery of siRNA to the mouse brain by systemic injection of targeted exosomes. Nat Biotechnol. 2011;29(4).

141. Burns GW, Brooks KE, O'Neil E V., Hagen DE, Behura SK, Spencer TE. Progesterone effects on extracellular vesicles in the sheep uterus. Biol Reprod. 2018;98(5).

142. Wang X, Tian F, Chen C, Feng Y, Sheng X, Guo Y, et al. Exosome-derived uterine microRNAs isolated from cows with endometritis impede blastocyst development. Reprod Biol. 2019;19(2).

143. Riou C, Brionne A, Cordeiro L, Harichaux G, Gargaros A, Labas V, et al. Avian uterine fluid proteome: Exosomes and biological processes potentially involved in sperm survival. Mol Reprod Dev. 2020;87(4).

144. Vilella F, Moreno-Moya JM, Balaguer N, Grasso A, Herrero M, Martínez S, et al. Hsa-miR-30d, secreted by the human endometrium, is taken up by the pre-implantation embryo and might modify its transcriptome. Dev Camb. 2015;142(18).

145. Xie Y, Liu G, Zang X, Hu Q, Zhou C, Li Y, et al. Differential Expression Pattern of Goat Uterine Fluids Extracellular Vesicles miRNAs during Peri-Implantation. Cells. 2021;10(2309).

146. Giacomini E, Scotti GM, Vanni VS, Lazarevic D, Makieva S, Privitera L, et al. Global transcriptomic changes occur in uterine fluid-derived extracellular vesicles during the endometrial window for embryo implantation. Hum Reprod Oxf Engl. 2021;36(8).

147. Evans J, Rai A, Nguyen HPT, Poh QH, Elglass K, Simpson RJ, et al. Human Endometrial Extracellular Vesicles Functionally Prepare Human Trophectoderm Model for Implantation: Understanding Bidirectional Maternal-Embryo Communication. Proteomics. 2019;19(23).

148. Liu C, Li L, Wang M, Shui S, Yao H, Sui C, et al. Endometrial extracellular vesicles of recurrent implantation failure patients inhibit the proliferation, migration, and invasion of HTR8/SVneo cells. J Assist Reprod Genet. 2021;38(4).

149. Tan Q, Shi S, Liang J, Zhang X, Cao D, Wang Z. MicroRNAs in Small Extracellular Vesicles Indicate Successful Embryo Implantation during Early Pregnancy. Cells. 2020.

150. Liu C, Yao W, Yao J, Li L, Yang L, Zhang H, et al. Endometrial extracellular vesicles from women with recurrent implantation failure attenuate the growth and invasion of embryos. Fertil Steril. 2020;114(2).

151. Yáñez-Mó M, Siljander PRM, Andreu Z, Zavec AB, Borràs FE, Buzas EI, et al. Biological properties of extracellular vesicles and their physiological functions. J Extracell Vesicles. 2015.

152. Esfandyari S, Elkafas H, Chugh RM, Park H soo, Navarro A, Al-Hendy A. Exosomes as Biomarkers for Female Reproductive Diseases Diagnosis and Therapy. Int J Mol Sci. 2021 Feb 22;22(4):2165.

153. Altmäe S, Koel M, Võsa U, Adler P, Suhorutšenko M, Laisk-Podar T, et al. Meta-signature of human endometrial receptivity: A meta-analysis and validation study of transcriptomic biomarkers. Sci Rep. 2017;7(1).

154. Verweij FJ, Bebelman MP, Jimenez CR, Garcia-Vallejo JJ, Janssen H, Neefjes J, et al. Quantifying exosome secretion from single cells reveals a modulatory role for GPCR signaling. J Cell Biol. 2018;217(3).

155. Rai A, Greening DW, Xu R, Chen M, Suwakulsiri W, Simpson RJ. Secreted midbody remnants are a class of extracellular vesicles molecularly distinct from exosomes and microparticles. Commun Biol. 2021;4(1).

156. Li T, Greenblatt EM, Shin MEJ, Brown TJ, Chan C. Cargo small non-coding RNAs of extracellular vesicles isolated from uterine fluid associate with endometrial receptivity and implantation success. Fertil Steril. 2021;115(5):1327–36.

157. Mahajan N. Endometrial receptivity array: Clinical application. J Hum Reprod Sci. 2015;8(3).

158. Doyle N, Jahandideh S, Hill MJ, Widra EA, Levy M, Devine K. A Randomized Controlled Trial Comparing Live Birth From SingleI Euploid Frozen Blastocyst Transfer Using Standardized Timing Versus Timing By Endometrial Receptivity Analysis. Fertil Steril. 2021;116(3).

159. Cozzolino M, Diaz-Gimeno P, Pellicer A, Garrido N. Evaluation of the endometrial receptivity assay and the preimplantation genetic test for aneuploidy in overcoming recurrent implantation failure. J Assist Reprod Genet. 2020;37(12).

160. Kumar MA, Baba SK, Sadida HQ, Marzooqi SAl, Jerobin J, Altemani FH, et al. Extracellular vesicles as tools and targets in therapy for diseases. Signal Transduct Target Ther. 2024 Feb 5;9(1):27.

161. Khalaj K, Miller JE, Lingegowda H, Fazleabas AT, Young SL, Lessey BA, et al. Extracellular vesicles from endometriosis patients are characterized by a unique miRNA-lncRNA signature. JCI Insight. 2019;4(18).

162. Lou K, Luo H, Jiang X, Feng S. Applications of emerging extracellular vesicles technologies in the treatment of inflammatory diseases. Front Immunol. 2024 Mar 13;15:1364401.

163. Herrmann IK, Wood MJA, Fuhrmann G. Extracellular vesicles as a next-generation drug delivery platform. Nat Nanotechnol. 2021 Jul;16(7):748–59.

164. Toffoli G, Hadla M, Corona G, Caligiuri I, Palazzolo S, Semeraro S, et al. Exosomal doxorubicin reduces the cardiac toxicity of doxorubicin. Nanomed. 2015;10(19).

165. Saari H, Lázaro-Ibáñez E, Viitala T, Vuorimaa-Laukkanen E, Siljander P, Yliperttula M. Microvesicle- and exosome-mediated drug delivery enhances the cytotoxicity of Paclitaxel in autologous prostate cancer cells. J Controlled Release. 2015;220.

166. Heusermann W, Hean J, Trojer D, Steib E, von Bueren S, Graff-Meyer A, et al. Exosomes surf on filopodia to enter cells at endocytic hot spots, traffic within endosomes, and are targeted to the ER. J Cell Biol. 2016;213(2).

167. WHO. Biomarkers In Risk Assessment: Validity And Validation. Environ Health. 2001.

168. Strimbu K, Tavel JA. What are biomarkers?: Curr Opin HIV AIDS. 2010 Nov;5(6):463–6.

169. Pisitkun T, Johnstone R, Knepper MA. Discovery of Urinary Biomarkers. Mol Cell Proteomics. 2006 Oct;5(10):1760–71.

170. Echeverry G, Hortin GL, Rai AJ. Introduction to urinalysis: historical perspectives and clinical application. Methods in molecular biology (Clifton, N.J.). 2010.

171. Eknoyan G, Nagy J. A history of diabetes mellitus or how a disease of the kidneys evolved into a kidney disease. Adv Chronic Kidney Dis. 2005.

172. Bright R. Cases and observations illustrative of renal disease accompanied with the secretion of albumin. Guy's Hospital Reports. 1836.

173. Jones HB. III. On a new substance occurring in the urine of a patient with mollities ossium. Philos Trans R Soc Lond. 1848.

174. Sequeira-Antunes B, Ferreira HA. Urinary Biomarkers and Point-of-Care Urinalysis Devices for Early Diagnosis and Management of Disease: A Review. Biomedicines. 2023 Mar 29;11(4):1051.

175. Penders J, Fiers T, Delanghe JR. Quantitative evaluation of urinalysis test strips. Clin Chem. 2002.

176. Xu WC, Qian G, Liu AQ, Li YQ, Zou HQ. Urinary Extracellular Vesicle: A Potential Source of Early Diagnostic and Therapeutic Biomarker in Diabetic Kidney Disease. Chinese Medical Journal. 2018.

177. Nilsson J, Skog J, Nordstrand A, Baranov V, Mincheva-Nilsson L, Breakefield XO, et al. Prostate cancer-derived urine exosomes: A novel approach to biomarkers for prostate cancer. Br J Cancer. 2009.

178. Pisitkun T, Shen RF, Knepper MA. Identification and proteomic profiling of exosomes in human urine. Proc Natl Acad Sci U S A. 2004.

179. Svenningsen P, Sabaratnam R, Jensen BL. Urinary extracellular vesicles: Origin, role as intercellular messengers and biomarkers; efficient sorting and potential treatment options. Acta Physiol. 2020.

180. Hendriks RJ, Dijkstra S, Jannink SA, Steffens MG, Van Oort IM, Mulders PFA, et al. Comparative analysis of prostate cancer specific biomarkers PCA3 and ERG in whole urine, urinary sediments and exosomes. Clin Chem Lab Med. 2016;54(3).

181. Fraser KB, Rawlins AB, Clark RG, Alcalay RN, Standaert DG, Liu N, et al. Ser(P)-1292 LRRK2 in urinary exosomes is elevated in idiopathic Parkinson's disease. Mov Disord. 2016;31(10).

182. Chattrairat K, Yasui T, Suzuki S, Natsume A, Nagashima K, Iida M, et al. All-in-One Nanowire Assay System for Capture and Analysis of Extracellular Vesicles from an ex Vivo Brain Tumor Model. ACS Nano. 2023;17(3):2235–44.

183. Zhang C, Leng W, Sun C, Lu T, Chen Z, Men X, et al. Urine Proteome Profiling Predicts Lung Cancer from Control Cases and Other Tumors. EBioMedicine. 2018;30.

184. Li Y, Zhang Y, Qiu F, Qiu Z. Proteomic identification of exosomal LRG1: A potential urinary biomarker for detecting NSCLC. Electrophoresis. 2011;32(15).

185. Rose JA, Wanner N, Cheong HI, Queisser K, Barrett P, Park M, et al. Flow cytometric quantification of peripheral blood cell β-adrenergic receptor density and urinary endothelial cell-derived microparticles in pulmonary arterial hypertension. PLoS ONE. 2016;11(6).

186. Garcia-Perez I, Posma JM, Gibson R, Chambers ES, Hansen TH, Vestergaard H, et al. Objective assessment of dietary patterns by use of metabolic phenotyping: a randomised, controlled, crossover trial. Lancet Diabetes Endocrinol. 2017;5(3).

187. JC M. Renal function during exercise and recovery. J Sports Med Ther. 2019;4(1).

188. Shao C, Zhao M, Chen X, Sun H, Yang Y, Xiao X, et al. Comprehensive analysis of individual variation in the urinary proteome revealed significant gender differences. Mol Cell Proteomics. 2019;18(6).

189. Svenningsen P, Sabaratnam R, Jensen BL. Urinary extracellular vesicles: Origin, role as intercellular messengers and biomarkers; efficient sorting and potential treatment options. Acta Physiologica. 2020.

190. Teixeira-Marques A, Monteiro-Reis S, Montezuma D, Lourenço C, Oliveira MC, Constâncio V, et al. Improved recovery of urinary small extracellular vesicles by differential ultracentrifugation. Sci Rep. 2024 May 28;14(1):12267.

191. Stam J, Bartel S, Bischoff R, Wolters JC. Isolation of extracellular vesicles with combined enrichment methods. J Chromatogr B. 2021 Apr;1169:122604.

192. Musante L, Tataruch DE, Holthofer H. Use and isolation of urinary exosomes as biomarkers for diabetic nephropathy. Front Endocrinol. 2014;5:149.

193. Serafini-Cessi F, Malagolini N, Cavallone D. Tamm-Horsfall glycoprotein: Biology and clinical relevance. Am J Kidney Dis. 2003;42(4):658–76.

194. Fernández-Llama P, Khositseth S, Gonzales PA, Star RA, Pisitkun T, Knepper MA. Tamm-Horsfall protein and urinary exosome isolation. Kidney Int. 2010;77:736–42.

195. Musante L, Saraswat M, Duriez E, Byrne B, Ravidà A, Domon B, et al. Biochemical and physical characterisation of urinary nanovesicles following CHAPS treatment. PLoS ONE. 2012;7(7).

196. Tamm I, Horsfall FL. Characterization and Separation of an Inhibitor of Viral Hemagglutination Present in Urine. Proc Soc Exp Biol Med. 1950;74(1).

197. Bokhove M, Nishimura K, Brunati M, Han L, De Sanctis D, Rampoldi L, et al. A structured interdomain linker directs self-polymerization of human uromodulin. Proc Natl Acad Sci U S A. 2016;113(6):1552–7.

198. Wachalska M, Koppers-Lalic D, van Eijndhoven M, Pegtel M, Geldof AA, Lipinska AD, et al. Protein Complexes in Urine Interfere with Extracellular Vesicle Biomarker Studies. J Circ Biomark. 2016;5(4).

199. Gardiner C, Vizio D Di, Sahoo S, Théry C, Witwer KW, Wauben M, et al. Techniques used for the isolation and characterization of extracellular vesicles: Results of a worldwide survey. J Extracell Vesicles. 2016.

200. Abe H, Sakurai A, Ono H, Hayashi S, Yoshimoto S, Ochi A, et al. Urinary exosomal mRNA of WT1 as diagnostic and prognostic biomarker for diabetic nephropathy. J Med Invest. 2018;65(3–4).

201. Bourderioux M, Nguyen-Khoa T, Chhuon C, Jeanson L, Tondelier D, Walczak M, et al. A new workflow for proteomic analysis of urinary exosomes and assessment in cystinuria patients. J Proteome Res. 2015;14(1).

202. Chun-yan L, Zi-yi Z, Tian-lin Y, Yi-li W, Bao L, Jiao L, et al. Liquid biopsy biomarkers of renal interstitial fibrosis based on urinary exosome. Exp Mol Pathol. 2018;105(2).

203. Erdbrügger U, Blijdorp CJ, Bijnsdorp I V., Borràs FE, Burger D, Bussolati B, et al. Urinary extracellular vesicles: A position paper by the Urine Task Force of the International Society for Extracellular Vesicles. J Extracell Vesicles. 2021;10(7).

204. Rawla P. Epidemiology of Prostate Cancer. World J Oncol. 2019;10(2):63–89.

205. Fujita K, Nonomura N. Urinary biomarkers of prostate cancer. International Journal of Urology. 2018.

206. Narayan VM. A critical appraisal of biomarkers in prostate cancer. World J Urol. 2020.

207. Berg KD, Røder MA, Thomsen FB, Vainer B, Gerds TA, Brasso K, et al. The predictive value of ERG protein expression for development of castration-resistant prostate cancer in hormone-naïve advanced prostate cancer treated with primary androgen deprivation therapy. Prostate. 2015.

208. De Kok JB, Verhaegh GW, Roelofs RW, Hessels D, Kiemeney LA, Aalders TW, et al. DD3PCA3, a very sensitive and specific marker to detect prostate tumors. Cancer Res. 2002.

209. McKiernan J, Donovan MJ, O'Neill V, Bentink S, Noerholm M, Belzer S, et al. A novel urine exosome gene expression assay to predict high-grade prostate cancer at initial biopsy. JAMA Oncol. 2016.

210. Thomas CE, Sexton W, Benson K, Sutphen R, Koomen J. Urine Collection and Processing for Protein Biomarker Discovery and Quantification. Cancer Epidemiol Biomarkers Prev. 2010 Apr 1;19(4):953–9.

211. Erdbrügger U, Blijdorp CJ, Bijnsdorp IV, Borràs FE, Burger D, Bussolati B, et al. Urinary extracellular vesicles: A position paper by the Urine Task Force of the International Society for Extracellular Vesicles. J Extracell Vesicles. 2021;10(7).

212. Delanaye P, Cavalier E, Pottel H. Serum Creatinine: Not so Simple! Nephron. 2017.

213. Zhou H, Yuen PST, Pisitkun T, Gonzales PA, Yasuda H, Dear JW, et al. Collection, storage, preservation, and normalization of human urinary exosomes for biomarker discovery. Kidney Int. 2006.

CHAPTER 2

THE EFFECT OF SEX HORMONE ON ENDOMETRIAL EVs PROTEOME.

Chapter 2. The effect of sex hormone on endometrial EVs proteome.

2.1 Authors contribution.

This work forms part of the article publication "The Extracellular Vesicles Proteome of Endometrial Cells Simulating the Receptive Menstrual Phase Differs from That of Endometrial Cells Simulating the Non-Receptive Menstrual Phase" published in Biomolecules (2023), the published version of which is included in chapter 8.

Hart AR, Khan NLA, Dissanayake K, Godakumara K, Andronowska A, Eapen S, Heath PR, Fazeli A. The Extracellular Vesicles Proteome of Endometrial Cells Simulating the Receptive Menstrual Phase Differs from That of Endometrial Cells Simulating the Non-Receptive Menstrual Phase. *Biomolecules*. 2023; 13(2):279. https://doi.org/10.3390/biom13020279

Amber Rose Hart: design or conceptualisation of the study, performing experiments, analysis and interpretation of data, and drafted and revised the manuscript. Norhayati Liaqat Ali Khan: revised the manuscript. Keerthie Dissanayake: assisted in analysis of data and revised the manuscript. Kasun Godakumara: assisted in analysis of data and revised the manuscript. Aneta Andronowska: Assisted in TEM analysis and revised the manuscript. Saji Eapen: revised the manuscript. Paul Roy Heath: design or conceptualisation of the study and revised the manuscript. Alireza Fazeli: design or conceptualisation of the study and revised the manuscript.

2.2 Chapter aim.

Investigate the proteomic profile, as well as the size and concentration, of endometrial cells EVs *in vitro* under the influence of sex hormones, specifically estrogen and progesterone, to mimic different phases of the menstrual cycle.

2.3 Abstract.

Successful embryo implantation into a receptive endometrium requires mutual endometrial-embryo communication. Recently, the function of extracellular vesicles (EVs) in cell-to-cell interaction in embryo-maternal interactions has been investigated. We explored isolated endometrial-derived EVs, using RL95-2 cells, which are human endometrial cells, as a model of a receptive endometrium, influenced by the menstrual cycle hormones estrogen (E2; proliferative phase), progesterone (P4; secretory phase), and estrogen plus progesterone (E2P4; the receptive phase). EV sized particles were isolated by differential centrifugation and size exclusion chromatography. Nanoparticle tracking analysis was used to examine the different concentrations and sizes of particles, while EV proteomic analysis was performed using shotgun label-free mass spectrometry. Our results showed that although endometrial-derived EVs were secreted in numbers independent of hormonal stimulation, EV sizes were statistically modified by it. Proteomics analysis showed that hormone treatment changes affect the endometrial EV proteome, with proteins enhanced within the EV E2P4 group shown to be involved in different processes, such as embryo implantation, endometrial receptivity, and embryo development, supporting the concept of a communication system between the embryo and the maternal endometrium via EVs.

2.4 Introduction.

The development of the mammalian embryo into a complete organism is dependent on the successful implantation of the embryo into the uterus wall within a limited window of implantation during the menstrual cycle (1). In humans, the menstrual cycle refers to cyclic changes under the control of several molecules, including the sex hormones estrogen and progesterone, working in a negative and positive feedback mechanism (1). These resulting changes in the endometrium lead to a receptive period during the secretory phase for blastocyst arrival and implantation. However, there is only around a 30% chance of conception occurring in one menstrual cycle; such a low percentage is due to many factors including the short receptive period of 4–5 days (2). Studies have suggested that by controlling these cyclic changes, the endometrium modulates the uterine environment, leading to the secretion of various molecules, factors, and proteins that aid in conception (3). Accordingly, this complex process of receptive endometrial remodelling and embryo implantation likely requires a sophisticated exchange of signals between embryo and endometrium (4). However, the mechanisms involved in this process are not yet fully understood.

Recently, extracellular vesicles (EVs), which are lipid bilayer particles secreted into the extracellular space, have been shown to be released from the endometrium and to have a key functional role in cell-to-cell communication, including embryo-maternal interactions (5–8). The cargos and size distribution of endometrial EVs at different phases of the cycle could affect the functionality of EVs. In terms of the physical properties of vesicles, including size and distribution, these factors previously have been shown to have a determining effect on the recipient cell ability to be internalised (9). Regarding

cargo, endometrial EVs are known to contain various biological molecules, such as proteins, lipids, and nucleic acids, including mRNA, with studies beginning to suggest that they may be up taken by trophoblastic cells, with this content being transferred to the blastocyst to improve or aid in the invasion or adhesion capacity of the embryo during the implantation process (10–12). The cargos of endometrial EVs, including proteins, DNA, and RNA, have previously been shown in various models (13–15); however, throughout the menstrual cycle phase of humans, the question remains if the proteomic profile and the size of the endometrial EVs differ or remains constant. This recent experimental data emphasises the role that endometrial signalling may play via EVs on the preparation of the receptive endometrium for embryo implantation (16–20). The current investigation builds on this data and aims to identify the characteristics of endometrial EVs at different phases of the menstrual cycle by testing the hypothesis that the characteristics of endometrial EVs change across the different stages of the menstrual cycle. This information has huge potential in clinical applications in therapeutics and biomarker discovery for assisted reproductive treatments.

Many studies have employed *in vitro* cell culture systems to advance the understanding of the role of EVs in the female reproductive tract and the intercellular communications (8,17,21). To produce beneficial conclusions from such experiments, it is paramount that cell culture models are optimised for the production and recovery of EVs, whilst mimicking the true *in vivo* conditions as much as possible. To clarify the mechanisms involved in implantation success and endometrial receptivity, in the present study we isolated EVs secreted by RL95-2 cells under conditions that mimic the menstrual cycle phases and analysed their protein content via proteomic approaches. The Rl95-2 cell line

is an extensively used *in vitro* model due to its well-characterised features and ability to produced relevant biological responses (22,23). However, the use of a single cell line also has limitations, such as potentially not fully replicating the diversity of cellular responses found in the human endometrium (24). Despite these limitations, the study revealed new characteristics and dynamics of endometrial EVs at different phases of the menstrual cycle and thus revealed physiological and pathological changes associated with the menstrual cycle.

2.5 Materials and methods.

2.5.1 Cell culture.

Two types of media have been used: (i) Dulbecco's Modified Eagles Medium (DMEM/F12) culture media (Sigma-Aldrich, Dorset, UK), supplemented with 10% fetal bovine serum (FBS) (Sigma-Aldrich, Dorset, UK), 1% l-glutamine (Sigma-Aldrich, Dorset, UK), 1% penicillin (100 IU/mL)/streptomycin (100 µg/mL) (Sigma-Aldrich, Dorset, UK), and 5 µg/mL insulin (human recombinant insulin; Gibco Invitrogen, Roskilde, Denmark); and (ii) Dulbecco's Modified Eagles Medium lacking phenol red (Thermo Fisher, Scotland, UK). The final variation (iii) was phenol red free media (ii) with charcoal stripped FBS (10%) (Sigma-Aldrich, Dorset, UK).

RL95-2 cells obtained from American Type Culture Collection (ATCC, Cat. No. CRL-1671, Teddington, UK) were used to simulate receptive endometrial cells *in vitro*. RL95-2 cells were cultured in T75 flasks (Greiner, bio-one, Gloucestershire, UK) in culture media (i). Cells were incubated at 37°C in a 5% CO_2 atmosphere until confluent. At confluence, cells were washed using calcium (Ca^{2+}) and magnesium (Mg^{2+}) free Dulbecco's

phosphate-buffered saline (Sigma-Aldrich, Dorset, UK). The cells were then harvested using trypsin-EDTA (Sigma-Aldrich, Dorset, UK) and pelleted by centrifugation at 300× *g* for 4 min.

2.5.2 Differential centrifugation.

Conditioned media was centrifuged for 10 min at 400× *g* at 4°C in a Sigma swinging-out rotor centrifuge (catalogue number 11,180). The pellet was discarded, and the supernatant was centrifuged for 10 min at 4000× *g* at 4°C; again, the pellet was discarded, and the supernatant was centrifuged for 10 min at 10,000× *g* at 4°C. Following centrifugation, the final resulting supernatant was concentrated using a 10kDa ultrafiltration tube (Sartorius, Hampshire, UK) to 500µl. Retentates were then stored at −80°C for further isolation procedures and experiments. An aliquot was reserved from the control group as a conditioned media control.

2.5.3 Size exclusion chromatography.

For the preparation of a size exclusion chromatography (SEC) column, 14-mL of Sepharose CL-2B slurry (GE Healthcare, Uppsala, Sweden) was poured into an empty gravity chromatography column (Bio-Rad, Watford, UK). After settling of the Sepharose beads, a nylon net filter was inserted at the ethanol/Sepharose separation interface at about 10mL. The ethanol was eluted followed by washing the column with molecular grade water (3 × 5 mL) and then with Ca^{2+} and Mg^{2+} free Dulbecco's phosphate-buffered saline (3 × 5 mL) (Sigma-Aldrich, Dorset, UK). On top of the filter, 0.5 mL of the concentrated conditioned medium was loaded, and fractions of 0.5 mL were collected

in 20 fractions with a Ca^{2+} and Mg^{2+} free Dulbecco's phosphate-buffered saline eluent. The resulting fractions were stored at −80°C for further EV characterisation.

2.5.4 Nanoparticle tracking analysis.

For nanoparticle tracking analysis (NTA) (ZetaView PMX 110, Particle Metrix, Meerbusch, Germany) all samples were diluted in milliQ water. Ideal measurement concentrations were found by pre-testing the ideal particles per frame value (140–200 particles/frame). For each measurement, three cycles were performed by scanning 11 cell positions each and capturing 30 frames per position under the following settings: focus: auto-focus; camera sensitivity for all samples: 50; shutter: 70; scattering intensity: detected automatically; and cell temperature: 25°C. After capture, the videos were analysed by the in-built ZetaView Software 8.04.02 SP2 with specific analysis parameters: maximum size: 500; minimum size: 5; minimum brightness: 25; hardware: embedded laser: 40 mW at 488 nm; and camera: CMOS.

2.5.5 RL95-2 Cell conditioned media EV isolation optimisation.

This experiment was carried out to determine which of the size exclusion fractions contain EV particles. RL95-2 cells were cultured in T75 flasks with complete DMEM culture media until ~70/80% confluent. Cells were washed using DPBS without Ca2+ and Mg2+ 3 times and FBS free Dulbecco's Modified Eagles Medium (DMEM/F12) culture media added and incubated for 24 h. After 24 h the conditioned media was collected, and differential centrifugation was performed. Conditioned media underwent differential centrifugation followed by concentration using a 10kDa ultrafiltration tube (Sartorius, Hampshire, UK) to 500µL. Retentates were subjected to size exclusion chromatography

with 20 × 0.5 mL fractions collected. The protein content of the fractions was determined using the bicinchoninic acid assay kit (Pierce™ BCA Protein Assay Kit, Thermo Scientific, Scotland, UK), according to the manufacturer's instructions, and particle concentration was determined by NTA. Experiments were performed in triplicate on 3 different days. From this optimisation, it was determined that fractions 5–8 will be collected as these were shown to contain the highest concentration of EV sized particles free from protein contaminants (Supplementary Figure 2.1).

2.5.6 Hormone treatment of RL95-2 cells.

This experiment was designed to determine the hormonal effect on EVs produced by endometrial cells. RL95-2 cells were cultured in T75 flasks with complete DMEM culture media until ~60/70% confluent. The media was changed after being washed using DPBS without Ca^{2+} and Mg^{2+} 3 times before being incubated with phenol red free DMEM culture media with charcoal stripped FBS (10%) to adapt similar conditions and avoid possible hormone-like (estrogenic) activity of phenol red for 24h. The appropriate hormone treatment was then added to the cells in phenol red-free DMEM culture media at either a final concentration of 10 nM of progesterone (water soluble, Sigma-Aldrich, Dorset, UK) (P4) or 10 nM of estrogen (water soluble, Sigma-Aldrich, Dorset, UK) (E2) or estrogen (10 nM) plus progesterone (100 nM) (E2P4), as described before (25,26). A control group containing equal amounts of the solubility complexing agent, cyclodextrin, found within the hormone mixtures was also performed. Following a 24h incubation period, conditioned media was collected, and differential centrifugation was performed, followed by concentration and size exclusion chromatography, as described above. Samples were then analysed for particle concentration via NTA and protein

concentration using the BCA assay. Experiments were performed in triplicates on 3 different days.

2.5.7 Transmission electron microscopy (TEM).

After SEC, 100 µL of the concentrated EVs were mixed with 100µL of 4% paraformaldehyde (Polyscience, Warrington, USA) to fix the EVs. On the day of analysis, 20µL of an EVs droplet was covered by a 200-mesh formvar and carbon coated grid (Electron Microscopy Sciences). The EVs droplet was incubated for 20 min at room temperature. After 20 min, the grid was tapped on filter paper to remove excess DPBS. Later the grid was rinsed once by gently touching the surface of the grid onto 50 µL of ddH2O droplet and tapped on filter paper to remove the excess water. For negative staining, the grid was transferred onto a droplet of 4% of uranyl acetate (Polyscience Warrington, USA) for 5 min incubation at room temperature. Samples were observed with a JEM 1400 transmission electron microscope (JEOL Ltd. Tokyo, Japan) at 80 kV, and digital images were acquired with a numeric camera (Morada TEM CCD camera, Olympus, Germany).

2.5.8 Proteomic analysis- Label-free liquid chromatography tandem mass spectrometry (LC-MS/MS).

EV samples (100µL each) were transported to Proteomic Core Facility, University of Tartu, Estonia in dry ice for proteomic analysis. 1µg of protein was injected onto an Easy-nLC 1000 system (Thermo Scientific, Scotland, UK). The sample was eluted at 250 nl/min from the trap to a 75 µm ID x 50 cm emitter-column (New Objective) packed with C18 material (3 µm, 300 Å particles, Dr Maisch). The separating gradient was 2-35% B for 60

min and 40-100% B for 5 min (A: 0.1% formic acid (FA), B: 80% Acetonitrile (CAN) + 0.1% FA). Eluted peptides were sprayed onto a Q Exactive Plus (Thermo Fisher Scientific, Scotland, UK) quadrupole-orbitrap mass spectrometer (MS) using nano-electrospray ionisation at 2.4 kV (applied through liquid-junction). The MS was operated with a top-5 data-dependent acquisition strategy. Briefly, one 350-1400 m/z MS scan at a resolution setting of R=70 000 at 200 m/z was followed by five higher-energy collisional dissociation fragmentation (normalised collision energy of 26) of 5 most intense ions (z: +2 to +6) at R=17 500. MS and MS/MS ion target values were 3e6 and 5e4, respectively with 50 ms injection time. Dynamic exclusion was limited to 40 s.

2.5.9 Proteomic data analysis.

Mass spectrometric raw files were processed with the MaxQuant software package (versions 1.6.15.0 and 2.0.3.0). Methionine oxidation, asparagine and glutamine deamidation and protein N-terminal acetylation were set as variable modifications, while cysteine carbamidomethylation was defined as a fixed modification. Label-free protein quantification (LFQ) was enabled with LFQ and the protein minimum ratio count set to 1. The search was performed against *Homo sapiens* and *Bos taurus* reference proteomes, using the tryptic digestion rule. The peptide-spectrum match and protein false discovery rate (FDR) were kept below 1% using a target-decoy approach. All other parameters were default. Protein-coding of significant altered proteins (SAPs) in EVs were identified based on a fold change cut-off of 1 and a p-value cut-off of 0.05. An analysis of SAPs was performed in R studio (version 4.2.1) using the Bioconductor "DEP" package (version 3.1.5). Identified duplicates and contaminants were excluded from the list of each sample, and only proteins detected in at least two of the replicates were

considered. After a literature review of these proteins enriched in the E2P4 group, 17 were selected for their functional relevance in implantation success and were divided into three groups depending on their involvement in embryo implantation, endometrial receptivity, and embryo development (Table 2.1). Gene Ontology (GO) and Kyoto Encyclopedia of Genes and Genomes (KEGG) pathway enrichment analyses were performed by the "clusterProfiler" R package (version 4.4.4). Volcano plots, GO terms, and KEGG pathways were visualised by the "ggplot2" R packages (version 3.3.6). The mass spectrometry proteomics data have been deposited to the ProteomeXchange Consortium via the PRIDE (27) partner repository with the dataset identifier PXD039764.

2.5.10 Western Blot.

Sample preparation.

Western Blot (WB) analysis was performed on EVs isolated from the hormone-treated RL95-2 cells. For lysis and extraction of proteins, RIPA buffer (Thermo fisher Scientific, Scotland, UK) with protease inhibitor cocktail (Thermo fishers Scientific, Scotland, UK) was used. Briefly, the buffer solution was used in 1:1 ratio with the EV samples, mixed thoroughly, and incubated on ice for 15 min. Following this, the samples were centrifuged at 15,000 g for 5 mins at 4°C, and the supernatant was collected for evaluation of protein content. The quantification of protein in the samples was performed using Pierce BCA Protein Assay Kit (Thermo Fisher Scientific, Scotland, UK) according to manufacturer's instructions. The absorbance of standards and the samples was measured with a spectrophotometer (Ledetect 96 Microplate Reader, Biomed Dr Wieser GmbH) at 540 nm wavelength. The protein concentrations of each EV sample were calculated and normalised to the total protein content. Finally, the samples were

denatured at 95°C for 5 mins in loading buffer with β-mercaptoethanol, and equal volumes were loaded into the wells.

Gel Electrophoresis and Blotting.

The separation of proteins was performed in a 12% SDS-PAGE. The separated proteins were then transferred to polyvinylidene difluoride membranes and blocked with 5% non-fat milk for 1 h at room temperature before being incubated overnight at 4°C with the primary antibodies. The antibodies used were Eukaryotic translation initiation factor 4E (eIF4E) (Cell Signalling Technology, MA, USA), integrin alpha M chain (ITGAM) (Cell Signalling Technology, MA, USA), Quiescin Sulfhydryl Oxidase 1 (QSOX1) (Proteintech group, Manchester, UK), at the concentration of 1:1000. Washed membranes were then incubated with HRP-conjugated goat anti-Rabbit IgG secondary antibody for 1 h (1:10,000, Thermo Fisher Scientific, Scotland, UK). After washing, bands were detected by enhanced chemiluminescence (Amersham Pharmacia Biotech, Cytiva, MA, USA) and imaged using ImageQuant RT ECL machine coupled with IQuantaCapture software (GE Healthcare Bio-Sciences AB). Band intensities were quantified using ImageJ software.

2.5.11 Statistical analysis.

GraphPad Prism version 9.2.0 was used for all statistical analysis. The comparison of particle concentration between the hormonal conditions and the control was analysed with repeated measure one-way ANOVA. When comparing the different sizes and the different treatment groups, a two-way ANOVA with multiple comparisons was performed. All data presented as mean plus/minus standard error of the mean (mean ± SEM). In all analyses, $p < 0.05$ was considered to be statistically significant.

2.6 Results.

2.6.1 Characterisation of EVs released from RL95-2 cells.

Purified EVs were shown to be positive for markers of transmembrane proteins associated with the EV plasma membrane CD9 and CD81 which were not seen in the conditioned media control (Figure 2.1A). EVs isolated from the control group conditions were also positive for TSG10, a marker of cytosolic protein recovered in EVs (Figure 2.1B) and negative for the negative marker Calnexin (CANX), a major component of non-EV co-isolated structures (Figure 2.1C). The PCA analysis also showed clear clustering between the control EV group and the control CM group (Figure 2.2). Transmission electron microscopy confirmed that EVs were intact, spherical in morphology, and with the expected EV size range within all four experimental conditions (Figure 2.3). Combined, these results fulfil the minimal information for studies of extracellular vesicles (MISEV) criteria and demonstrate that EVs have been successfully isolated from the endometrial conditioned media.

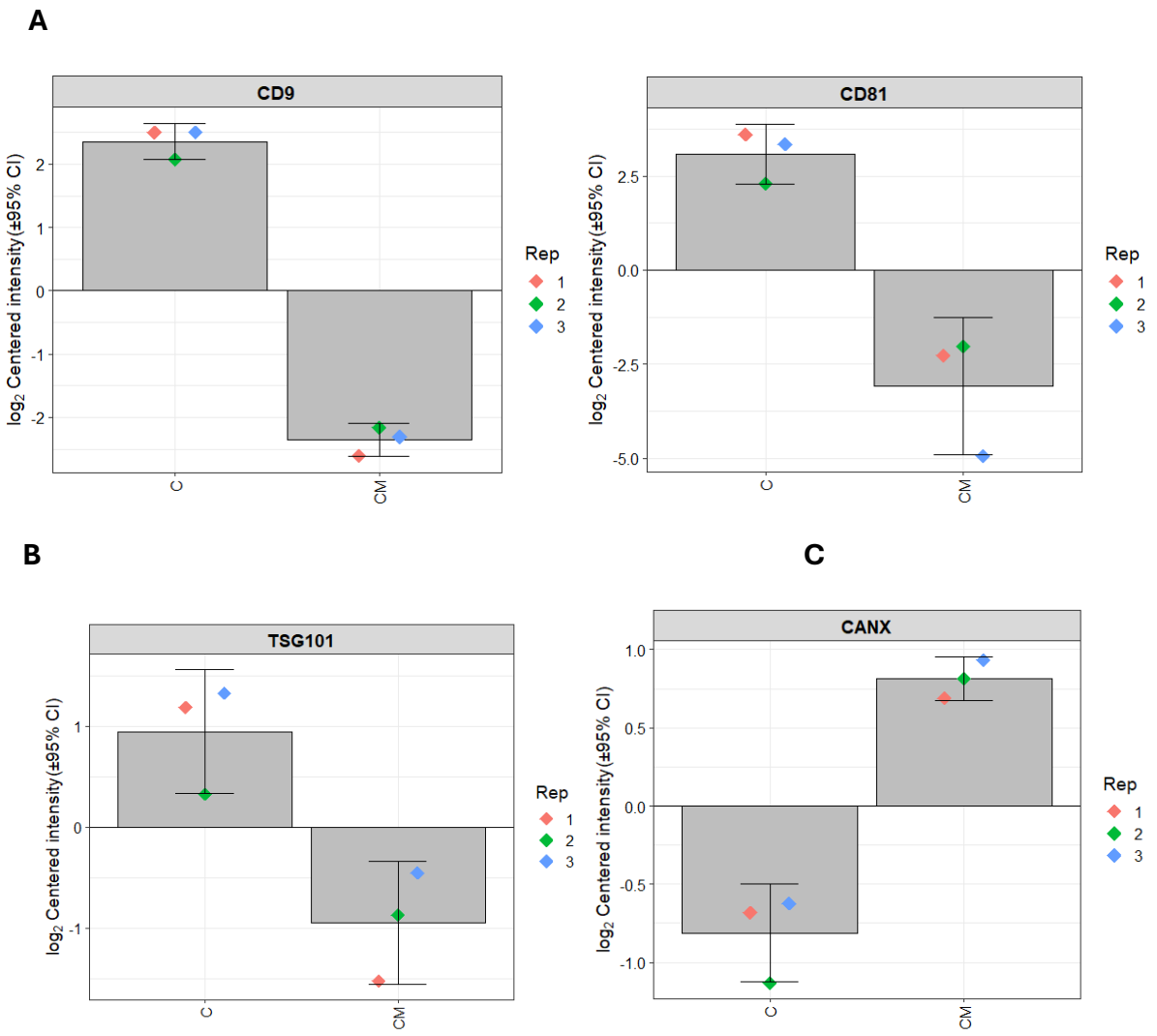


Figure 2.1. Protein content–based EV characterisation from the Label-free liquid chromatography tandem mass spectrometry data. Graphs representing the log2 centred intensity of various protein markers in the control, as well as the conditioned media control, validating the presence of EVs according to the MISEV guidelines. (A) represents is the intensity of the markers CD9 and CD81 to fulfil the MISEV criteria for markers of transmembrane or GPI-anchored proteins associated to plasma membrane and/or endosomes. (B) represents is the intensity of TSG101 to fulfil the MISEV criteria for a marker of cytosolic protein recovered in EVs. (C) represents is the intensity of the marker CANX to fulfil the MISEV criteria for a marker of a major components of non-EV co-isolated structures. C represents the Control EV sample and CM the condition media control, non-EV enriched, from the same Control EV sample.

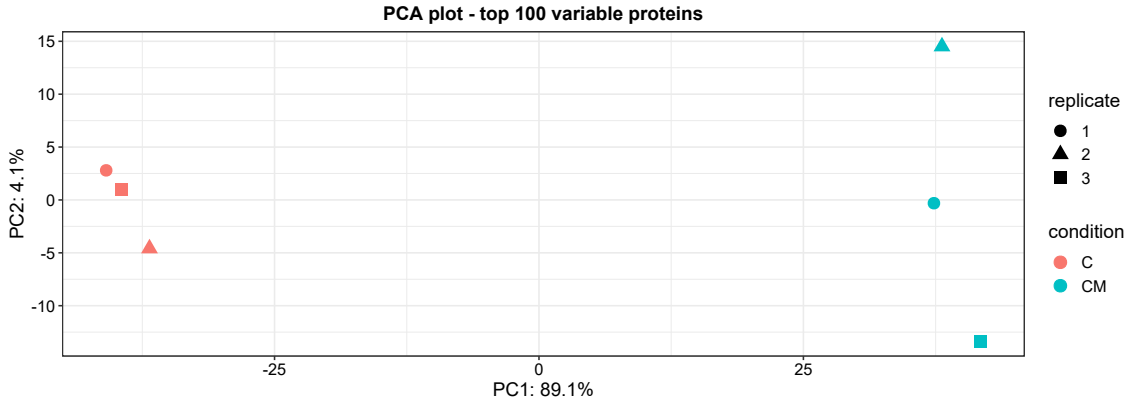


Figure 2.2. Principal component analysis (PCA) of top 100 variable proteins in the study groups. With C representing the EVs from the control group and CM representing the control conditioned media group. *n* = 3 for each experimental condition.

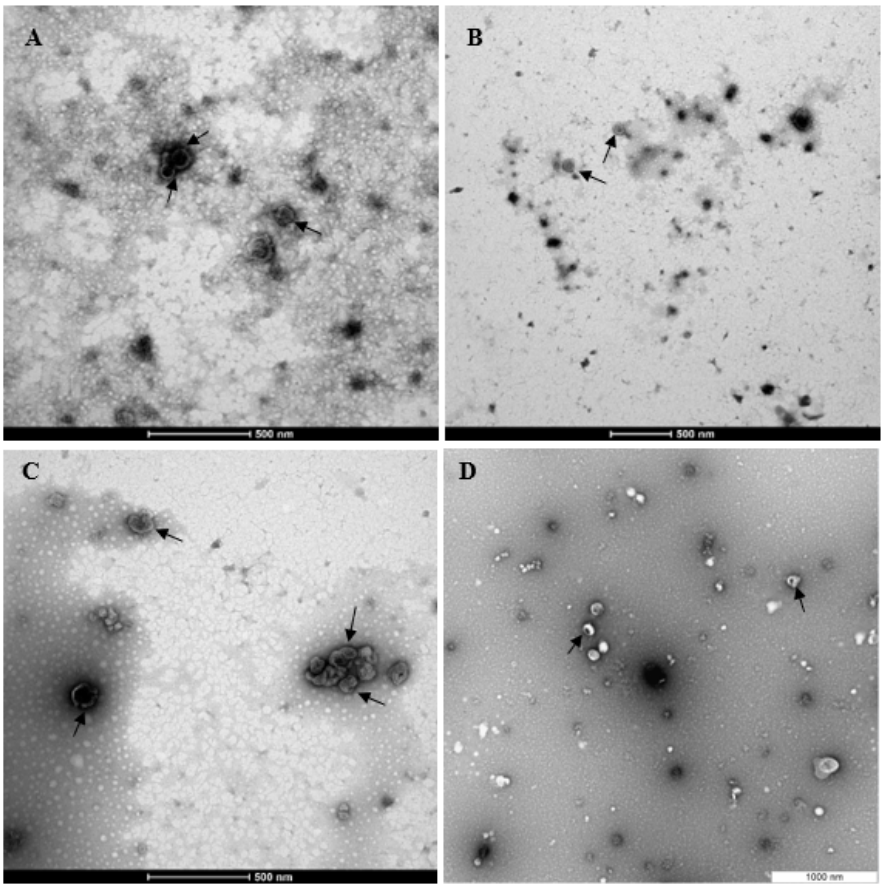
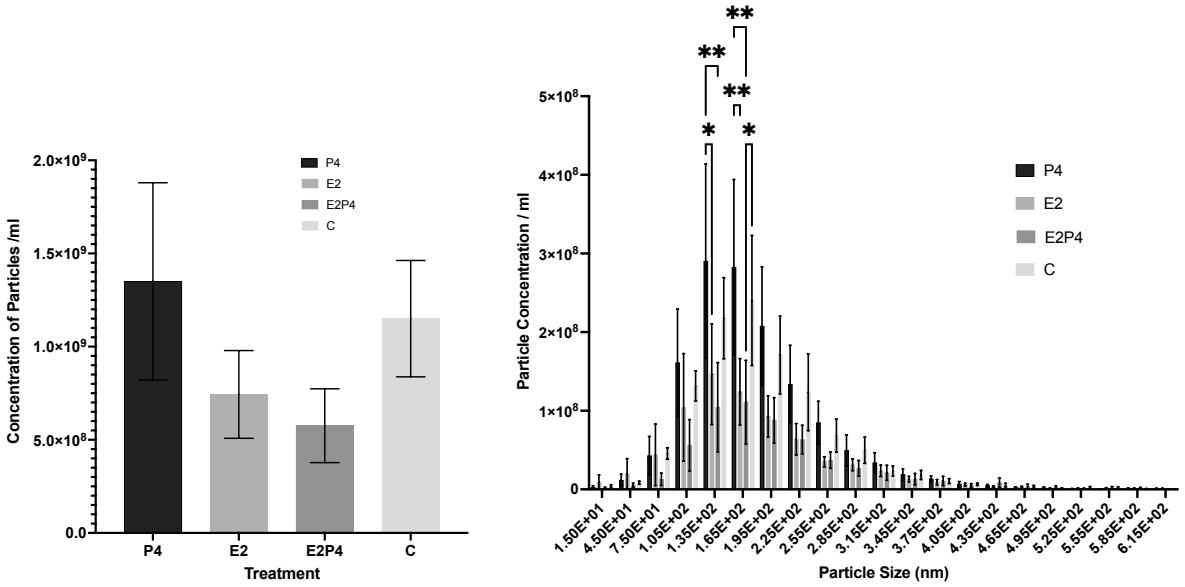


Figure 2.3. TEM Image based characterisation of endometrial EVs from the different hormone treatment groups**.** Representative TEM images of endometrial EVs from the control group (**A**), the progesterone treatment group (P4) (**B**), the estrogen treatment group (E2) (**C**), and the combined estrogen and progesterone treatment group (E2P4) (**D**). Scale bars: 500 nm (**A**–**C**); 1000 nm (**D**).

2.6.2 Concentration and size distribution of EVs released from hormone treated RL95-2 cells.

To assess the effect of the different menstrual cycle hormones on EV production, a comparison of the concentration and size of EVs produced from estrogen (E2), progesterone (P4), or estrogen plus progesterone (E2P4)-treated cells were compared to a control group, using nanoparticle tracking analysis. The addition of the hormones in the three different treatment groups showed no difference between the amount of EV sized particles produced (Figure 2.4A). A size comparison analysis of the concentration of particles in the different size classes of the particles was also produced and the different treatment groups were compared (Figure 2.4B). A significant difference can be seen between the 135nm and 165nm size groups, with more EV sized particles being released by the P4-treated group compared to the E2 group or the E2P4 group.



A B

Figure 2.4. Concentration and size distribution of EVs released from RL95-2 hormone-treated cells, obtained from the nanoparticle tracking analysis. (**A**) The bars represent the mean concentration (particles/mL) ±SEM of EV sized particles from the SEC fractions 5–8. The treatment groups include estrogen (E2), progesterone (P4), estrogen plus progesterone (E2P4), and the control. Data were from 3 biological replicates and 3 technical replicates from each group. RM one-way ANOVA was performed with Dunnett post hoc test performed, but no results were considered significant ($P \leq 0.05$) (**B**) The bars represent the mean concentration of the indicated particle size ± SEM from the SEC fractions 5–8. A 2way ANOVA was performed with a Tukey post hoc test with significant difference marked with 1 asterisk symbol (*) to denote $P \leq 0.05$ and 2 asterisk symbols (**) to denote $P \leq 0.01$. Data are from 3 biological replicates and 3 technical replicates.

2.6.3 Comparative proteomic analysis of endometrial EVs under hormonal treatment.

A heatmap of the log2 centred intensity of all significant proteins with the data centred per protein from the four experimental conditions showed a clear grouping of the four experimental conditions with six cluster groups, showing clear varied intensities between the EV isolated groups (Figure 2.5). There were 60 significantly altered proteins (SAP) identified from the differential enrichment of EV proteins from the E2P4 group compared to E2 (Supplementary Table 2.1), 35 SAP identified from differential enrichment of EV proteins from the E2P4 group compared to the P4 group (Supplementary Table 2.2), 50 SAP identified from differential enrichment of EV proteins from E2vP4 (Supplementary Table 2.3), 31 SAP identified from the differential enrichment of EV protein from E2P4vC (Supplementary Table 2.4), 41 SAP identified from the differential enrichment of EV protein from E2vC (Supplementary Table 2.5), and five SAP identified from the differential enrichment of EV protein from P4vC (Supplementary Table 2.6). In the E2P4 group compared to the E2 group, 37 SAP were upregulated and 23 were downregulated. In the E2P4 group compared to the P4 group, 18 SAP were upregulated and 17 were down regulated. Volcano plots of these result show a direct indication of SAP (Figure 2.6). After a literature review of these proteins enriched in the E2P4 group, 17 were selected for their functional relevance in implantation success and were divided into three groups depending on their involvement in embryo implantation, endometrial receptivity, and embryo development (Table 2.1).

To further analyse the biological function of SAPs, GO terms and KEGG pathway enrichment analyses were performed on the three comparison groups (E2P4vE2,

E2P4vP4, and E2vP4) and the controls (E2P4vC, E2vC, and P4vC) (Figures 2.7–9). GO function analysis was conducted first. Regarding the biological process (BP_1), in E2P4vE2, the enriched SAP were involved in the regulation of cell communication, RNA transport, the movement of the cell or subcellular component, and protein modification (Figure 2.7A). In E2P4vP4, the SAP were enriched in endosomal transport, dephosphorylation, RNA transport, and mRNA transport (Figure 2.7B). In E2vP4, the SAP were enriched in protein-containing complex assembly, RNA catabolic process, translation, and mRNA metabolic processes (Figure 2.7C). In terms of molecular function (MF), in the E2P4vE2 group, enrichment was seen in cytoskeletal protein binding, microtubule binding, and GTPase regulator activity (Figure 2.7A). In E2P4vP4 the SAP were enriched in phosphatidylinositol phosphate binding, RNA cap binding, and ubiquitin conjugating enzyme activity (Figure 2.7B). In E2vP4, enrichment was seen in rRNA binding, DNA binding, and translation regulator activity (Figure 2.7C).

KEGG pathway analysis showed various pathways enriched in the comparison groups and control (Figure 2.9A,B). In E2P4vE2, enriched pathways included the mammalian target of rapamycin (mTOR) signalling pathway, prolactin signalling pathway, and ErbB signalling pathway. In E2P4vP4, pathways that were intensified included the insulin signalling pathway, natural killer cell mediated cytotoxicity, and estrogen signalling pathway. In E2vP4, supressed pathways included cytokine-cytokine receptor interaction, lysosomes, and chemokine signalling pathways.

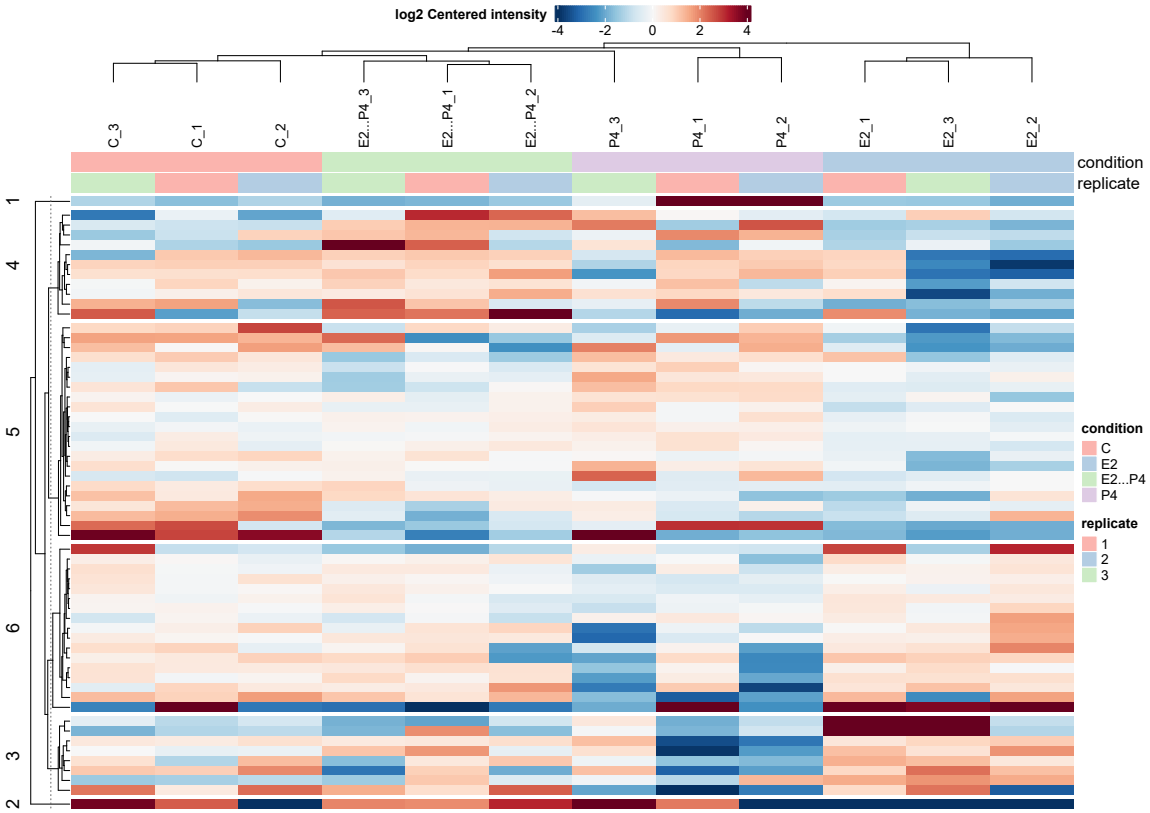
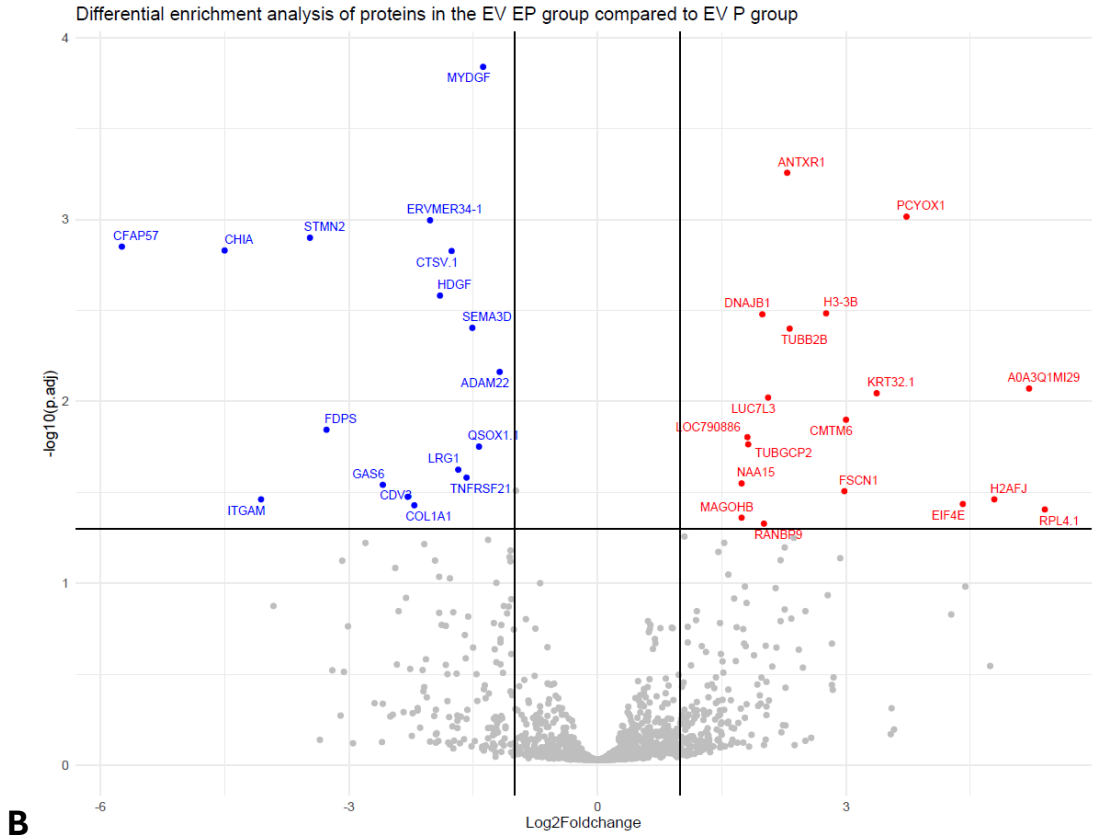


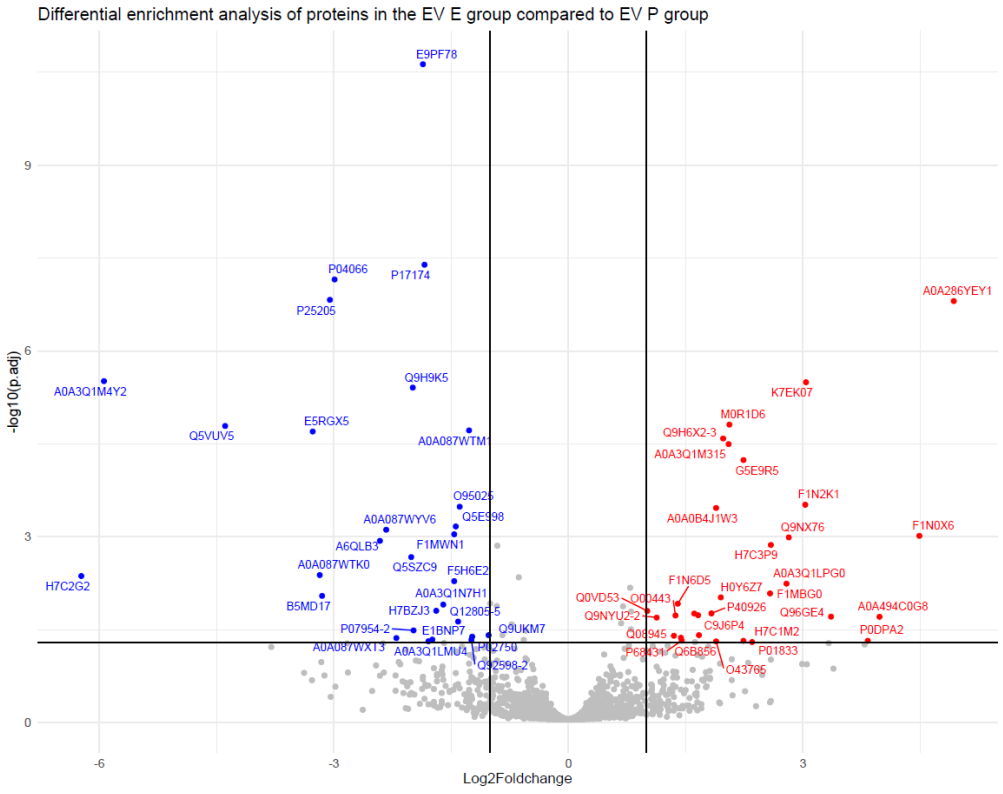
Figure 2.5. Heatmap shows the log2 centred intensity of all significant proteins with the data centred per protein. The rows represent all significant proteins and are clustered in 6 groups by k-means clustering (numbers on the left). C (control group), E2 (estrogen group), E2...P4 (estrogen and progesterone group), and P4 (progesterone group). Colours represent the abundance of significantly altered proteins (red: higher; blue: lower).


Differential enrichment analysis of proteins in the EV EP group compared to EV E group
-log10(p.adj)
Log2Foldchange
FUCA1
SCLT1
QSOX1.1
IGLL5
NAE1
TSPAN6
CARM1
MDH2
RARS1.1
MST1L
PHLDA2
KRT32.1
ART4
IGHA1
MCM3
SLC29A1.1
GOT1
FSTL1.1
TLL1
A0A3Q1LPG0
SPARC
THOC6
ITGB5.1
NDST1
TM9SF2
EIF4E
HSPG2.1
KRT31
KRT79
CEP95
GAS6
PDGFA
SFRP1
CDH5
NECTIN1
KIF5C
ITGAM
NCAM1
DLD
RNASET2
ARL1
MFGE8.1
IGFBP2
PDLIM1

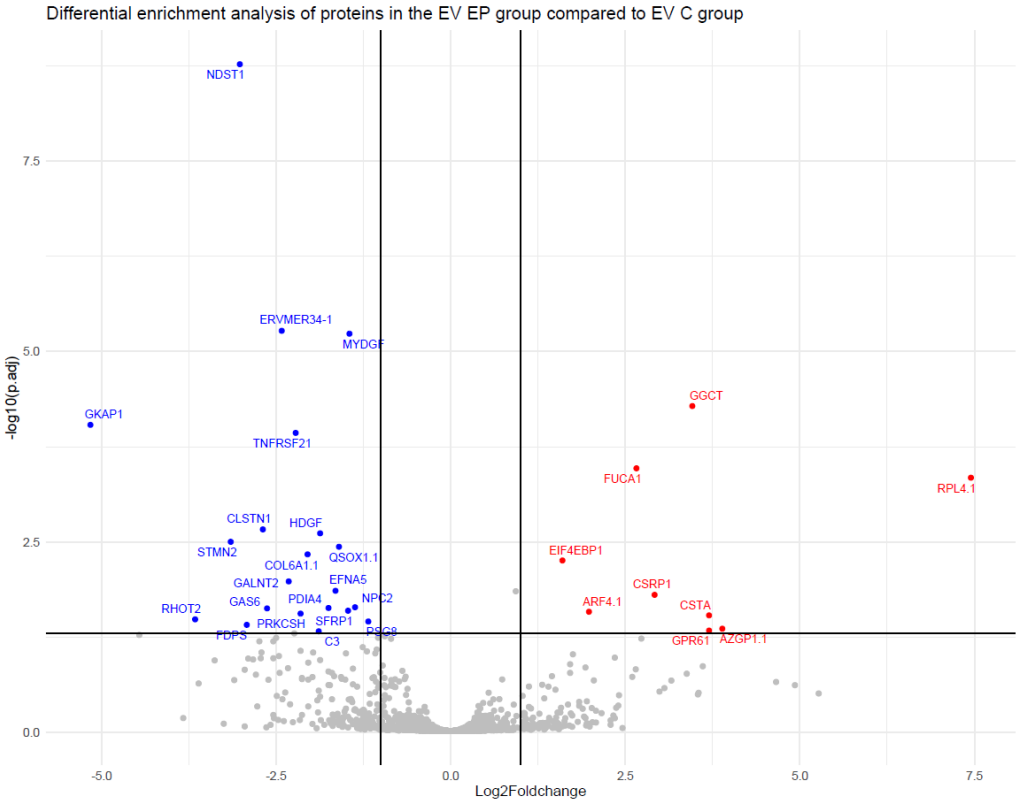
A


Differential enrichment analysis of proteins in the EV EP group compared to EV P group
-log10(p.adj)
Log2Foldchange
MYDGF
ANTXR1
ERVMER34-1
PCYOX1
CFAP57
CHIA
STMN2
CTSV.1
HDGF
DNAJB1
H3-3B
SEMA3D
TUBB2B
ADAM22
KRT32.1
A0A3Q1MI29
LUC7L3
FDPS
LOC790886
CMTM6
QSOX1.1
TUBGCP2
LRG1
NAA15
GAS6
FSCN1
TNFRSF21
H2AFJ
ITGAM
CDV3
MAGOHB
EIF4E
RPL4.1
COL1A1
RANBP9

B


Differential enrichment analysis of proteins in the EV E group compared to EV P group
-log10(p.adj)
Log2Foldchange
E9PF78
P04066
P17174
P25205
A0A286YEY1
A0A3Q1M4Y2
Q9H9K5
K7EK07
M0R1D6
Q5VUV5
E5RGX5
A0A087WTM1
Q9H6X2-3
A0A3Q1M315
G5E9R5
Q95025
F1N2K1
Q5E998
A0A087WYV6
A0A0B4J1W3
Q9NX76
F1N0X6
A6QLB3
F1MWN1
H7C3P9
A0A087WTK0
Q5SZC9
F5H6E2
A0A3Q1LPG0
H7C2G2
F1N6D5
H0Y6Z7
F1MBG0
A0A3Q1N7H1
Q0VD53
Q0D443
B5MD17
H7BZJ3
Q12805-5
P40926
Q96GE4
A0A494C0G8
Q9NYU2-2
P07954-2
E1BNP7
Q9UKM7
C9J6P4
H7C1M2
P0DPA2
Q08945
A0A087WX13
A0A3Q1LMU4
P68431
Q6B856
P01833
Q92598-2
O43765

C


Differential enrichment analysis of proteins in the EV EP group compared to EV C group
-log10(p.adj)
Log2Foldchange
NDST1
ERVMER34-1
MYDGF
GKAP1
GGCT
TNFRSF21
FUCA1
RPL4.1
CLSTN1
HDGF
STMN2
QSOX1.1
COL6A1.1
EIF4EBP1
GALNT2
EFNA5
CSRP1
RHOT2
GAS6
PDIA4
NPC2
ARF4.1
CSTA
PRKCSH
SFRP1
PDPS
C3
PSG8
GPR61
AZGP1.1

D

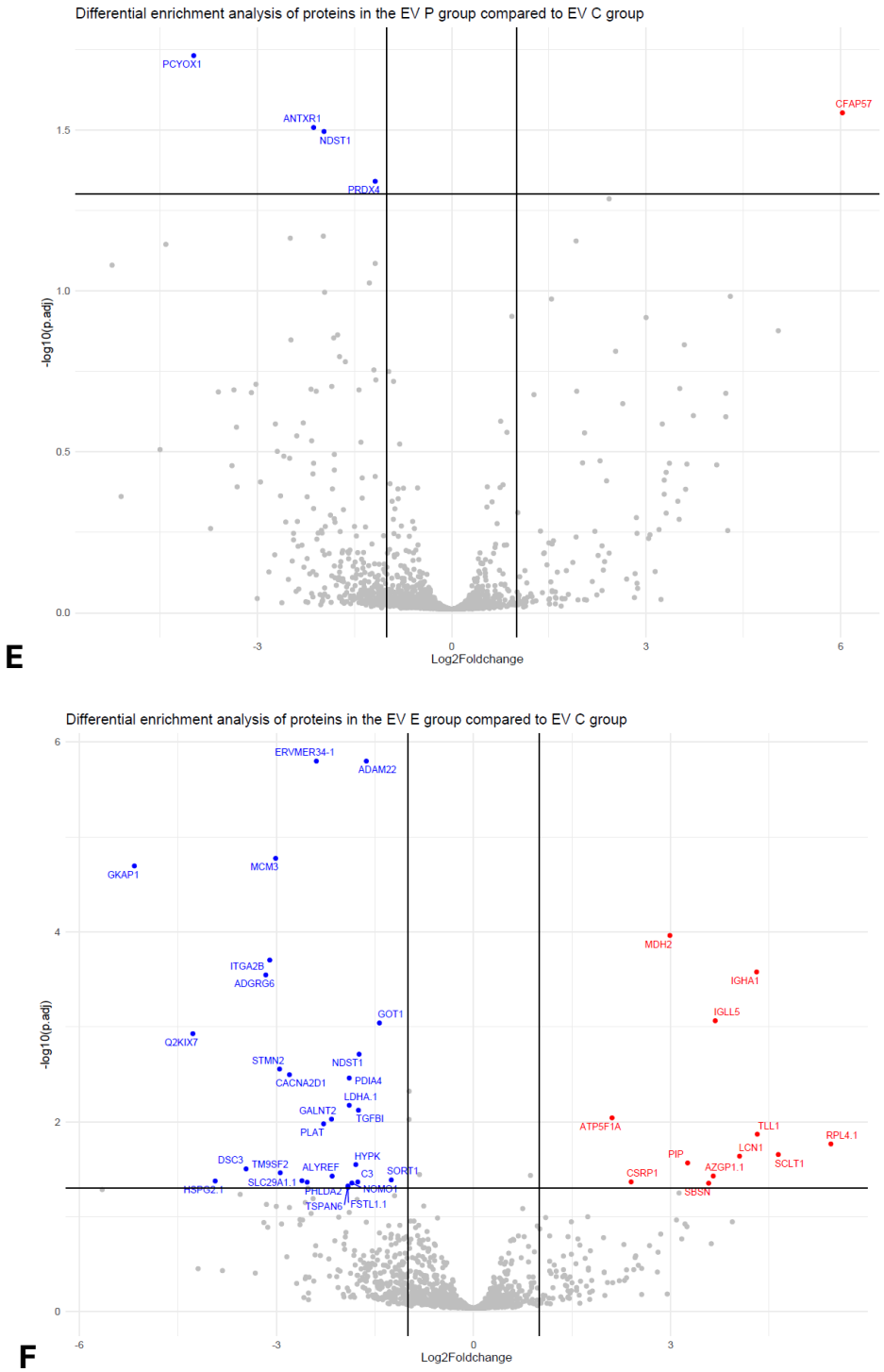


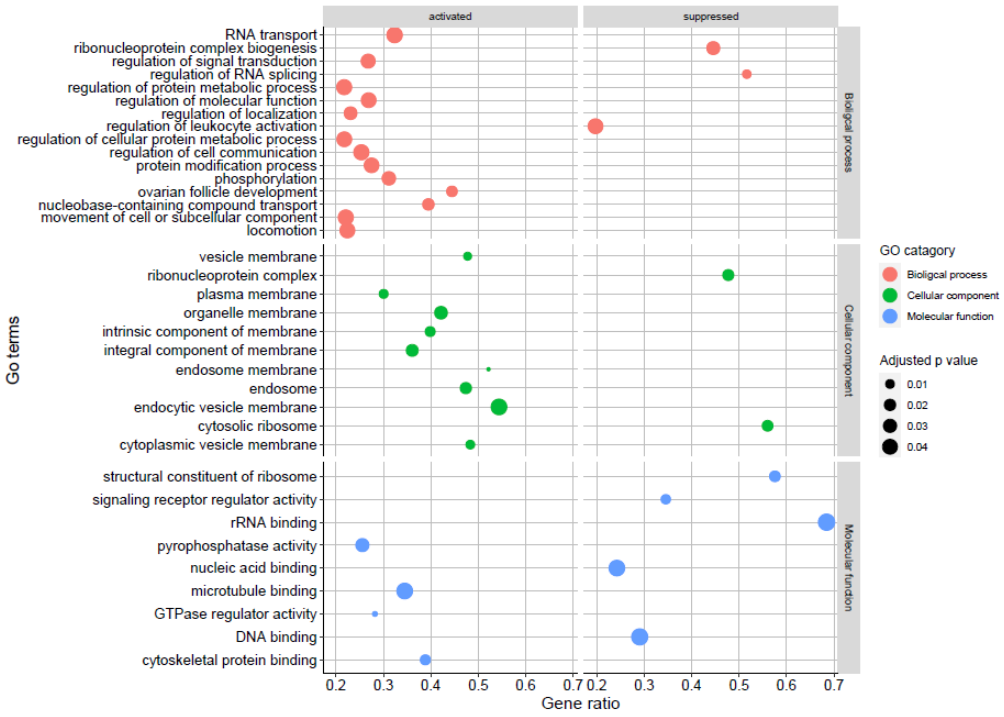
Figure 2.6. Differential enrichment of EV proteins in different comparison groups. (**A**) Volcano plot of the differentially expressed proteins in the estrogen plus progesterone supplemented groups (E2P4) compared to the estrogen group (E2); (**B**) estrogen plus progesterone supplemented groups (E2P4) compared to the progesterone group (P4); (**C**) estrogen supplemented groups (E2) compared to the progesterone group (P4); (**D**) estrogen plus progesterone group (E2P4) compared to the control (C); (**E**) progesterone (P4) compared to the control (C); and (**F**) estrogen (E2) compared to control. Adjusted *p* values (−log10) are plotted against the fold changes (log2). Red dots represent enriched proteins whereas blue dots represent depleted proteins in the respective comparisons.

Table 2.1. Proteins differentially enriched in the E2P4 receptive group EVs related to implantation success.

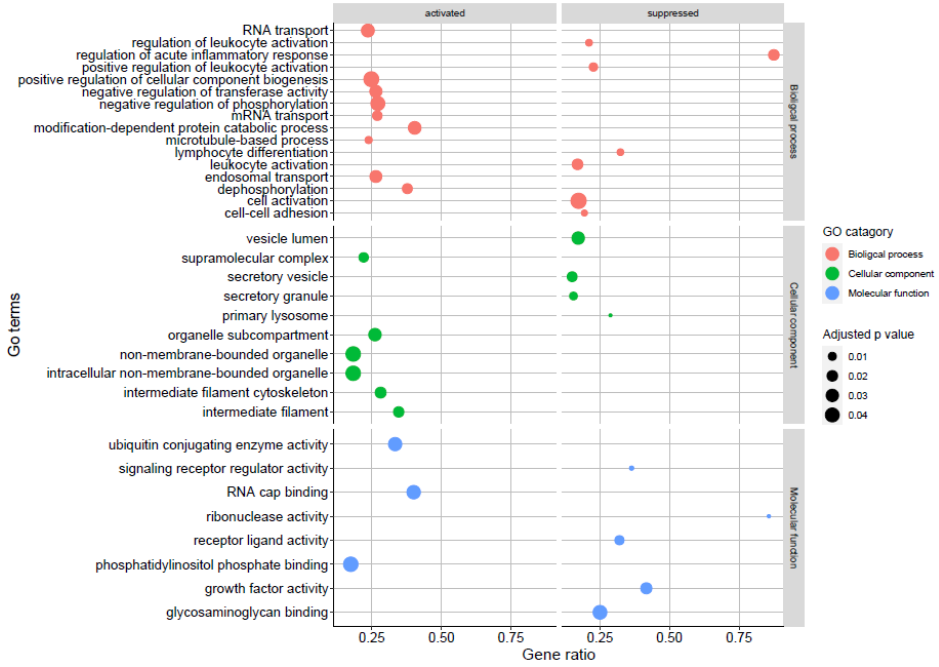
UniProt accession	Gene name	Protein description	Evidence	Reference
	Embryo Implantation			
Q6URK6	CDH5	Cadherin-5	CDH5 has been shown to be expressed in the late proliferative phase in endometrium. A mouse *in vitro* study has demonstrated that expression of CDH5 in trophectoderm helps facilitates embryo implantation.	(28) 29)
F1MER7	HSPG2	Basement membrane-specific heparan sulfate proteoglycan core protein	Shown to be an abundant cargo of the luteal phase EVs and have a specific role in embryo implantation. HSPG2 within the uterine epithelium has been shown to facilitate trophoblast attachment and adhesion.	(26) (30)
F6RAG5	KIF5C	Kinesin heavy chain isoform 5C	Gene expression increased in embryo-endometrium contact co cultures as well as being shown to plays a role during different. morphogenetic processes in early embryo development.	(31,32)
A0A452DJ21	EIF4E	Eukaryotic translation initiation factor 4E	The expression if EIF4E has been examined in porcine endometrium during implantation, with truncated EIF4E shown to particularly regulate protein synthesis during conceptus attachment at the time of implantation.	(33)
Q58D84	FSTL1	Follistatin-related protein 1	Identified in menstrual fluid samples and is a	(34)

			common inflammatory and repair proteins.	
A6QLB3	ITGA2B	Integrin subunit alpha 2b	ITGA2B has been identified during the stages of bovine trophectoderm cell migration and fusion with the uterine epithelial cells.	(35)
Q9NRN7	AASDHPPT	L-aminoadipate-semialdehyde dehydrogenase-phosphopantetheinyl transferase	Found to be upregulated in the endometrium during pregnancy compared to genes during estrous cycle.	(36)
	Endometrial Receptivity			
A0A452DJE0	ACE2	Angiotensin-converting enzyme 2	ACE2 within the female reproductive system is abundantly expressed and plays a crucial role in regulating levels of angiotensin, which has been shown to stimulate ovarian follicle growth, ovulation and oocyte maturation, and within the human endometrium.	(37)
H7BZJ3	PDIA3	Protein disulfide-isomerase A3	PDIA3 upregulated in fertile endometrium's during secretory phase as compared to proliferative phase.	(38)
P00750	PLAT	Tissue-type plasminogen activator	In the reproductive system PLAT mediates tissue remodeling required for ovulation and endometrial receptivity.	(39)
C9JPV1	SLC6A6	Sodium- and chloride-dependent taurine transporter	SLC6A6 gene expression has been shown to be greater in cow endometria in the large preovulatory follicle compared to the small preovulatory follicles. This gene is thought to have a role in amino acid metabolism which is linked to the	(40)

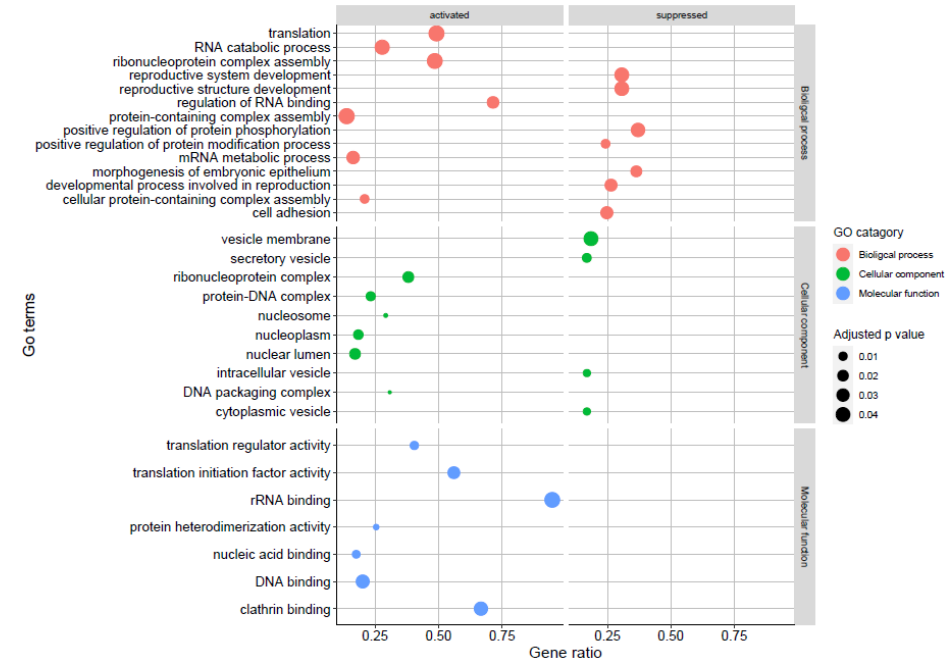
			receptive state of the endometrial tissue.	
A0A087WYV6	TSPAN6	Tetraspanin-6	Found in endometrial exosomes and thought to have functional and regulatory roles.	(41)
M0R1D6	DNAJB1	DnaJ homolog subfamily B member 1	One of many novel genes identified and associated with the biological process of menstrual cycle.	(42)
D6RDI2	LUC7L3	Luc7-like protein 3	Upregulated in human endometrial sample in women who exhibited implantation failure.	(43)
A0A3Q1LMU4	INHBB	Inhibin beta B chain	Known marker gene of decidualization.	(44)
	Embryo Development			
P04066	FUCA1	Tissue alpha-L-fucosidase	FUCA1 was seen to be higher abundant at elongation as well upregulated during day 15 of the cycle compared to day 7.	(45) (46)
P00338	LDHA	L-lactate dehydrogenase A chain	When LDHA is inhibited, histone lactylation level is reduced and an impaired rate of development of pre-implantation mice embryos is seen.	(47)


activated
suppressed
RNA transport
ribonucleoprotein complex biogenesis
regulation of signal transduction
regulation of RNA splicing
regulation of protein metabolic process
regulation of molecular function
regulation of localization
regulation of leukocyte activation
regulation of cellular protein metabolic process
regulation of cell communication
protein modification process
phosphorylation
ovarian follicle development
nucleobase-containing compound transport
movement of cell or subcellular component
locomotion
vesicle membrane
ribonucleoprotein complex
plasma membrane
organelle membrane
intrinsic component of membrane
integral component of membrane
endosome membrane
endosome
endocytic vesicle membrane
cytosolic ribosome
cytoplasmic vesicle membrane
structural constituent of ribosome
signaling receptor regulator activity
rRNA binding
pyrophosphatase activity
nucleic acid binding
microtubule binding
GTPase regulator activity
DNA binding
cytoskeletal protein binding
Biological process
Cellular component
Molecular function
Go terms
0.2
0.3
0.4
0.5
0.6
0.7
Gene ratio
GO catagory
Biological process
Cellular component
Molecular function
Adjusted p value
0.01
0.02
0.03
0.04

A

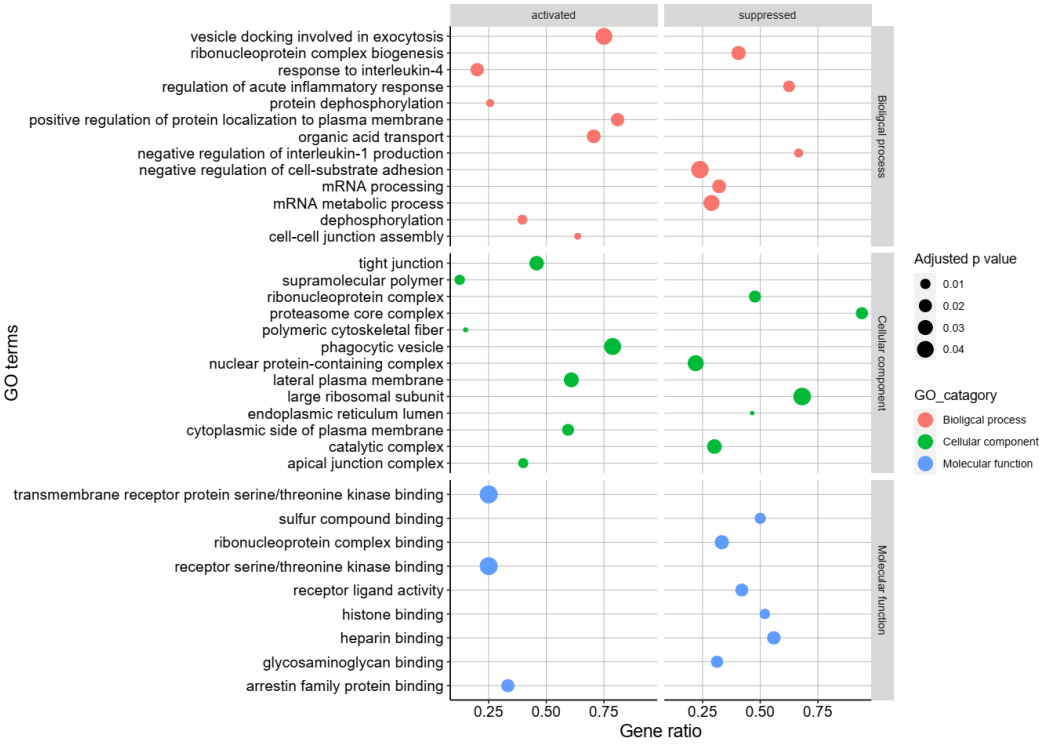

activated
suppressed
RNA transport
regulation of leukocyte activation
regulation of acute inflammatory response
positive regulation of leukocyte activation
positive regulation of cellular component biogenesis
negative regulation of transferase activity
negative regulation of phosphorylation
mRNA transport
modification-dependent protein catabolic process
microtubule-based process
lymphocyte differentiation
leukocyte activation
endosomal transport
dephosphorylation
cell activation
cell-cell adhesion
vesicle lumen
supramolecular complex
secretory vesicle
secretory granule
primary lysosome
organelle subcompartment
non-membrane-bounded organelle
intracellular non-membrane-bounded organelle
intermediate filament cytoskeleton
intermediate filament
ubiquitin conjugating enzyme activity
signaling receptor regulator activity
RNA cap binding
ribonuclease activity
receptor ligand activity
phosphatidylinositol phosphate binding
growth factor activity
glycosaminoglycan binding
Biological process
Cellular component
Molecular function
Go terms
0.25
0.50
0.75
Gene ratio
GO catagory
Biological process
Cellular component
Molecular function
Adjusted p value
0.01
0.02
0.03
0.04

B

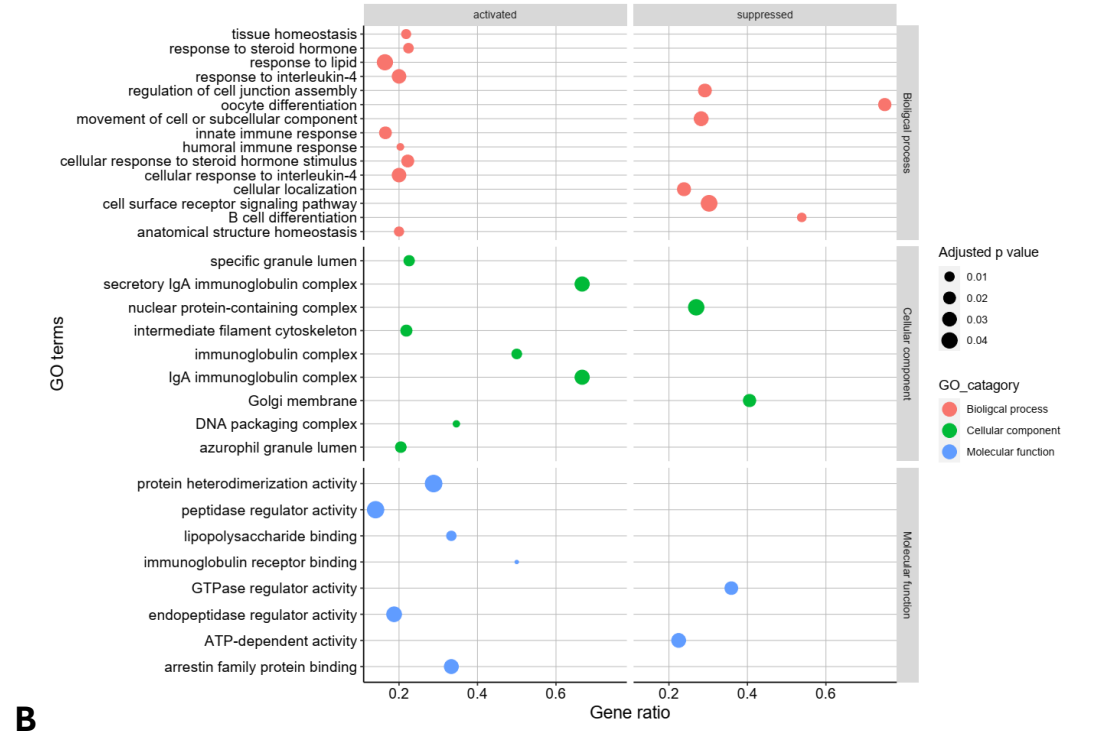


C

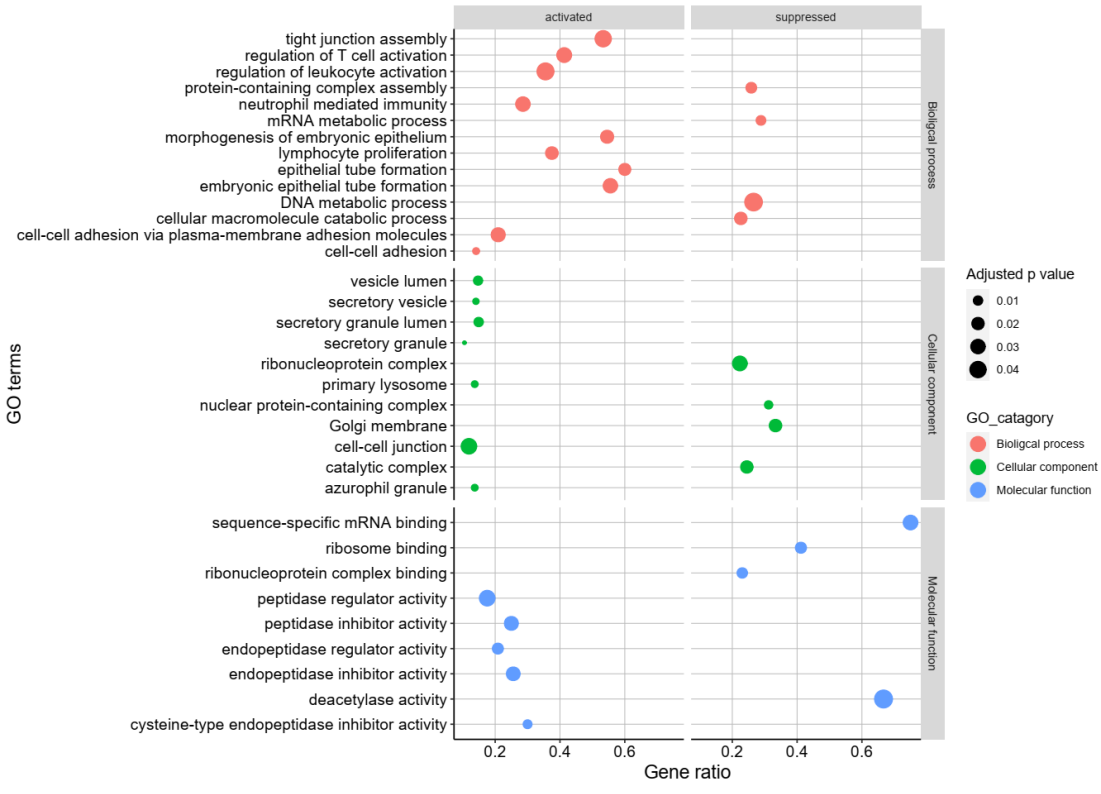
Figure 2.7. GO enrichment of SAP in the different comparison groups. (A) E2P4 v E2, (B) E2P4 v P4, (C) E2vP4. The size and colour of points represents the GO category and the q-values respectively.



A



B



C

Figure 2.8. GO enrichment of SAP in the different comparison groups. (A) E2P4 v C, (B) E2 v C, (C) P4 v C. The size and colour of points represents the GO category and the q-values respectively.

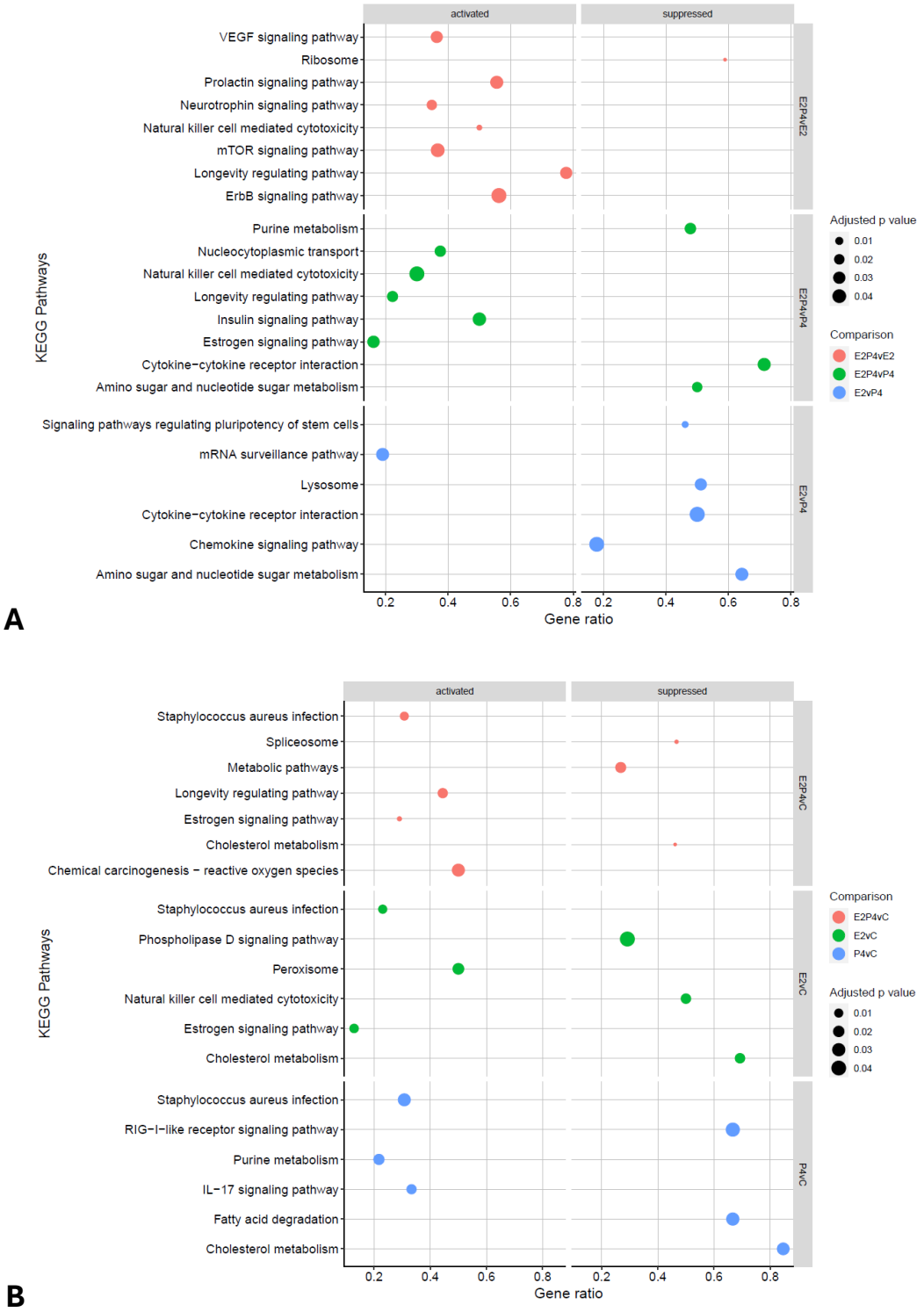


Figure 2.9. KEGG Pathway analysis of SAP in the comparison groups and control. (A) Pathway analysis of SAP in the comparison groups, the size and colour of points represents the *p*-values and the comparison groups respectively. (B) KEGG Pathway analysis of SAP in the treatment groups versus the control, the size and colour of points represents the *p*-values and the comparison groups respectively.

2.6.4 Validation of LC/MS-MS Results.

To validate the LC/MS-MS results, we selected ITGAM and QSOX1, which were measured as lower in the EP group compared to the progesterone and control groups, retrospectively, and EIF4E, which was measured as higher in the EP group compared to the control group (Supplementary Figure 2.2). The WB results showed similar results compared to the LC-MS/MS analysis, therefore indicating the trend we observed from the MS/MS analysis is correct.

2.7 Discussion.

A successful pregnancy requires a receptive endometrium and a good quality embryo and optimum communication between these two entities (48). Locally, this complex process involves mutual communication between the incoming embryo and the endometrium in the uterine milieu (49–52). Recently, it has been suggested that EVs regulate early embryo development as it reaches the uterus, in addition to priming the endometrium for embryo implantation (5,53,54). The EVs lipid-bilayer protects the cargo, including proteins, from degradation, making them highly stable (55). However, a complete understanding of EV and their cargo's role in mediating implantation has not been demonstrated. This study comprehensively evaluates the proteome of EVs secreted by RL95-2 cells, an analogue of receptive endometrial epithelial cells, under a hormone stimulation mimicking the menstrual cycle to help begin to define novel biomarkers of endometrial receptivity and implantation success.

RL95-2 has been used in a number of papers and is a well-established model of a receptive endometrium (22,56,57); additionally this cell line has been used in many

implantation and adhesion related assays (58–60). Thus, by using this cell line, we can provide novel insights into the complex process of human embryo implantation regulation. Via this *in vitro* modulation, discrepancies and variations between endocrinologic milieu among the individuals in a population can be avoided. An *in vitro* endometrial cell culture-based model, despite its simplicity, can offer a simple and a general characterisation and understanding of the EV proteome. Interestingly, 112 proteins were seen to be upregulated in the control EV samples compared to the conditioned medium, and of these proteins only 12 have been previously identified as exosome markers in Vesiclepedia, (ANXA6, ANXA7, ATP1A1, BSG, CD9, FLOT1, GNAS, GNB2, ITGB1, RAB7A, SDCBP, TFRC) (Supplementary Figure 2.3). The presence of these markers further supports their use as indicators of the enrichment of EVs. The additional 100 proteins enriched in EVs could be additional potential new markers for EVs or endometrial EVs, such as integrin alpha-3, a membrane protein that regulates multiple biological processes, including cell adhesion, cell differentiation, and cell migration.

Moreover, the results indicate that the effects of all the hormone experimental conditions when compared to the control had no statistically significant differences in terms of EV concentration *in vitro*. A similar *in vitro* study showed results comparable to ours in that EVs were secreted in numbers independent of hormonal regulation, with similar concentrations seen between the estrogen and progesterone-treated groups (61). However, these results and ours contradict those of an *in vivo* study which demonstrated that P4 increased the concentration of EVs in the uterine lumen (62). However, it is important to note the different cell lines used when comparing studies, as well as the complex microenvironmental influences from different *in vivo* models.

In terms of EV size distribution, it was observed that the EV fractions from all four treatment conditions were within the expected EV size range but also, interestingly, there was a significant difference seen between the 135 nm and 165 nm size groups with more EV being released by the P4-treated group compared to the E2 group or the E2P4 group. This could suggest that higher amounts of EVs within this size range in the progesterone group, the hormone most prominent during the secretory phase when the endometrium is fertile, is due to an increase in communication signalling occurring, either sending a signal to the incoming embryo or in an autocrine way for the endometrium to prime itself for the incoming embryo. Alternatively, the larger size could be the presence of more cargo due to induction of secretory activity of the epithelial cells by the progesterone, which indirectly improves communications. However, when interpreting these results, it is Important to remember the limitations of NTA, the lack of specificity means differentiation between non-EV-structures, such as lipoproteins or residual reagent residues, could influence these results. Thus, only limited conclusions can be drawn from this method alone.

2.7.1 Receptive phase endometrial cell EVs were enriched with proteins involved in embryo implantation.

Proteomic assessment by the mass spectrometry of EVs allows a broader analysis to be performed. It has previously been shown that EVs derived from the endometrium can signal to the embryo to promote implantation (16,29,63). However, their composition, function, and influence on the uterine microenvironment and embryo remain unknown. Through proteomic analysis, we identified some key proteins that were significantly

increased in E2P4-treated endometrial cell EVs compared to both E2 or P4 endometrial cell derived EVs, and these proteins may have a specific role in embryo implantation. Several of these proteins (including Cadherin-5 "CDH5", heparan sulfate proteoglycan core protein "HSPG2", Kinesin heavy chain isoform 5C "KIF5C" and Eukaryotic translation initiation factor 4E "EIF4E") have previously been identified in various embryo implantation models (31,33,64,65). Cadherin are cell adhesion molecules of which there are more than eighty members and are key regulators of cell adhesion, sorting and invasion (28). In the current study, CDH5, was shown to be upregulated in EVs from the E2P4-treated cells, and has similarly been shown to be expressed in the late proliferative phase in endometrial explants (64) as well as endometrial mesenchymal stromal cells (66) . In addition an *in vitro* mouse study demonstrated that expression of CDH5 in the trophectoderm facilitates embryo implantation (29). Such studies suggest that the upregulation of CDH5 in EVs specifically in the stimulated receptive period could be contributing to embryo implantation. Of further interest to the developmental progress of pregnancy is our identification of Perlecan (HSPG2) as intrinsic to the EV proteome. This molecule has been shown to be highly regulated at the time of blastocyst apposition and attachment, with previous studies demonstrating this role and its presence in the uterine epithelium (67,68). All this data point towards the role of the receptive endometrium in contributing to the implantation interface through the release of EVs, potentially by signalling to, and preparing the endometrium to support implantation during this specific period dictated by hormones.

2.7.2 Receptive phase endometrial EVs were enriched in proteins involved in embryo development.

The analysis of our dataset from the E2P4 EVs showed further proteins to be increased that are important in embryo development. These include proteins (including, “FUCA1” tissue alpha-L-fucosidase, and “LDHA1” l-lactate dehydrogenase A chain) that have previously been identified in various models assessing embryonic development (45,69). For example, the protein FUCA1 was seen in higher amounts in the EV isolated from the receptive phase induced endometrium condition in our study. Interestingly this protein was one of many that have also been seen at a higher level in the uterus of deer while embryos were at elongation rather than during diapause (45). This suggests that changes occur upon embryo elongation in the uterine environment to support early development and survival, and perhaps our study suggests that endometrial EVs are contributing to transporting these proteins. Additionally, LDHA was seen to be upregulated in the E2P4 group and has also been shown to have a role in embryo development (47,69). Within pre-implantation, embryo glycolysis is regulated by LDHA, with LDHA catalysing the conversion of pyruvate to lactate. It has been shown that when LDHA is inhibited, the histone acetylation level is reduced and an impaired rate of development of pre-implantation mice embryos is seen (47). Taken together this data suggest that endometrial EVs during the receptivity period could contain proteins associated with embryo development and that these are mutually communicated between the embryo and mother.

2.7.3 Receptive phase endometrial EVs were enriched in proteins involved in endometrial receptivity.

On further analysis of our dataset, we observed an increase in proteins within E2P4 EVs compared to both E2 or P4 that are important in endometrial receptivity. These include proteins (including "PLAT" tissue-type plasminogen activator, angiotensin-converting enzyme 2 "ACE2" and inhibin beta B chain "INHBB"), that have previously been identified in various endometrial receptivity models (39,44,70). ACE2 has been found previously to be highly expressed within the reproductive system and is responsible for generating angiotensin-derived peptides from precursor peptides produced locally or taken from the circulation (70). Angiotensin within various mammalian species is seen to stimulate ovarian follicle growth, ovulation and oocyte maturation, and, within the human endometrium, it is seen at its highest levels during the window of implantation (71). In addition, it has previously been discovered in airway epithelial cells that estrogen stimulated ACE2 expression, suggesting that the expression seen here also could also be mediated by steroid hormones (72). However, the precise role of ACEs in the human endometrium is yet to be revealed and more evidence is required. In addition to ACE2, the protein PLAT was also seen to be upregulated in the stimulated receptive phase EVs. Again this protein has also been suggested to have a role in endometrial receptivity with PLAT seen to be involved in the extracellular matrix degradation essential for embryo adhesion and placental angiogenesis (39). Finally, an increase in INHBB is seen in the receptive phase stimulated EVs. It has been previously reported that INHBB gene expression within the human uterus is related to the onset of decidualisation (73), with its expression increasing in human endometrial stromal cells during decidualisation *in vitro* (74). In addition to this, a reduced expression and reduced decidualization has been

shown in ectopic pregnancies, implying that INHBB expression within human pregnancy is dependent on decidualisation (74). These studies support the theory that the proteins found within the endometrial EV within the receptive phase have a role in endometrial receptivity too.

2.7.4 Receptive phase endometrial EVs GO terms and KEGG pathways are associated with receptivity and implantation success.

GO and KEGG analyses reinforced the above findings and identified key pathways associated with receptivity and implantation success in the receptive group. In the E2P4 group, in both the E2P4vE2 and E2P4vP4 group, key pathways in immune modulation, specifically natural killer cells (NK), were activated. It has been previously reported that the levels of NK cells change during the menstrual cycle and pregnancy (75), with increases seen during the secretory phase followed by a peak during the early stages of pregnancy (76). There are various publications that support the theory that NK cells help in the regulation of pregnancy establishment and maintenance through many mechanisms, such as cytokine production that directly influence trophoblast growth (77), in addition to the vascularization and implantation of the decidua (78), immune modulating protein production that has a role in regulation of the immune response at the maternal-foetal interface (79), as well as the regulation of trophoblast invasion by cell-mediated cytotoxicity (77). Despite this activation, cytokine-cytokine receptor interaction was shown to be supressed in the E2P4 group. This contradiction has been suggested to derive from the concept that endometrial NK cells are special immature cells that await pregnancy, with the NK cells lacking NK-specific functional phenotype and activity, such as cytokine secretion and cytotoxicity (80). Hence the activation and

suppression of these pathways reflects the phases stimulated in this model, with no influence of pregnancy or embryo stimulus.

In addition to the immune modulation, the KEGG pathway analysis also revealed many pathways known to support implantation in the E2P4 group, including the mTOR signalling pathway and VEGF signalling pathway. The mTOR pathway is known to play a role in cellular functions, such as cell proliferation, differentiation, apoptosis, autophagy, and decidualization (81), all of which are requirements for modulating a receptive endometrium. Similarly to what is seen in our data, it has previously been shown that mTOR increases during the implantation window in mice, with its role in receptivity further highlighted in a study in which an intrauterine injection of an inhibitor of mTOR, rapamycin, compromised the endometrial receptivity in mice (82). Like mTOR, VEGF is also well reported to have a role in improving endometrial receptivity and facilitating the interactions between the embryo and the endometrium (83). VEGF, is an endothelial-specific mitogen *in vitro*, and is a main physiological and pathological angiogenesis regulator in the endometrium (84). Within rodents, it has been shown that VEGF regulates endometrial vascular permeability and endothelial cell proliferation at the implantation site, indicating a key role of the VEGF pathway in embryonic-endometrial interaction (85,86). It is well established that expression of VEGF dynamically changes within the oestrus cycle period and has been shown to be highly expressed in the endometrium in the middle stage of secretion (86,87), which mimics results seen in this study with the pathways activated in the E2P4 EV group. None of these pathways were seen to be activated in the E2- or P4-only-treated endometrial cell EVs, suggesting that the EV proteome is changing during the menstrual phases but a

mechanism of how/if these proteins physiologically affect the endometrium/embryo requires further investigation.

A limitation and implication of interpreting this proteomic data, however, lies in the use of the proteomic method of shotgun label free proteomics. One issue that this approach highlights is that only the most abundant proteins are identified due to limitations in detection methods; hence, further proteins could be identified as being altered in the various groups, had an alternative method been used. This might have identified other pathways or roles that endometrial EVs contribute to during the menstrual cycle. Additionally, the results relate to the sample's total proteome, and it cannot be determined if they are located on the EVs cell surface or exist as cargo. Instead, the results are of a complex total EV proteome and further investigation via other means, such as antibody microarray, would be needed to understand their precise origin (i.e., cargo, surface, or both). Thus, whether these proteins are surface bound or cargos of EVs, and hence how, and if, they are of physiological significance in embryo-maternal signalling, remains an open question.

2.8 Conclusion.

In summary, findings of the present study provide a new insight into the characteristics of EV from endometrial cells under hormonal control. Results from this study have provided new information on the effect menstrual cycles have on EV production, demonstrating a contribution of endometrial-derived EVs to endometrial-embryo cross talk, showing an effect even without the known contributions of other players, such as spermatozoa, oocyte, and the developing embryo in an environment that is constantly

changing and sending and receiving signals. Here the total proteome of endometrial EVs has been shown to be regulated by estrogen and progesterone, as physiologically relevant to the phases of the menstrual cycle. Significantly, our study shows that endometrial EVs within the receptive phase of the menstrual cycle consists of proteins associated with embryo implantation, endometrial receptivity, and embryo development, and key pathways identified in immune modulation and implantation processes. The application of this knowledge may allow EVs to be exploited as an endometrial tissue biopsy alternative and have a range of applications, such as monitoring the window of implantation, identifying the underlying aetiology of recurrent implantation failure, better prediction and increased implantation success in IVF, and enabling the design of non-hormonal-based contraceptives.

2.9 References.

1. Reed BG. The Normal Menstrual Cycle and the Control of Ovulation. Endotext - NCBI. 2021.

2. Taylor A. ABC of subfertility: Extent of the problem. Vol. 327, British Medical Journal. 2003.

3. Okada H, Tsuzuki T, Murata H. Decidualization of the human endometrium. Vol. 17, Reproductive Medicine and Biology. 2018.

4. Bhagwat SR, Chandrashekar DS, Kakar R, Davuluri S, Bajpai AK, Nayak S, et al. Endometrial Receptivity: A Revisit to Functional Genomics Studies on Human Endometrium and Creation of HGEx-ERdb. PLoS ONE. 2013.

5. Es-Haghi M, Godakumara K, Häling A, Lättekivi F, Lavrits A, Viil J, et al. Specific trophoblast transcripts transferred by extracellular vesicles affect gene expression in endometrial epithelial cells and may have a role in embryo-maternal crosstalk. Cell Communication and Signaling. 2019.

6. O'Neil E V., Burns GW, Ferreira CR, Spencer TE. Characterization and regulation of extracellular vesicles in the lumen of the ovine uterus. Biology of Reproduction. 2020;102(5).

7. Nakamura K, Kusama K, Ideta A, Kimura K, Hori M, Imakawa K. Effects of miR-98 in intrauterine extracellular vesicles on maternal immune regulation during the peri-implantation period in cattle. Scientific Reports. 2019;9(1).

8. Dissanayake K, Nõmm M, Lättekivi F, Ord J, Ressaissi Y, Godakumara K, et al. Oviduct as a sensor of embryo quality: deciphering the extracellular vesicle (EV)-mediated embryo-maternal dialogue. Journal of Molecular Medicine. 2021;99(5).

9. Caponnetto F, Manini I, Skrap M, Palmai-Pallag T, Di Loreto C, Beltrami AP, et al. Size-dependent cellular uptake of exosomes. Nanomedicine: Nanotechnology, Biology, and Medicine. 2017;13(3).

10. Li T, Greenblatt EM, Shin MEJ, Brown TJ, Chan C. Cargo small non-coding RNAs of extracellular vesicles isolated from uterine fluid associate with endometrial receptivity and implantation success. Fertility and Sterility. 2021;115(5):1327–36.

11. Segura-Benítez M, Carbajo-García MC, Corachán A, Faus A, Pellicer A, Ferrero H. Proteomic analysis of extracellular vesicles secreted by primary human epithelial endometrial cells reveals key proteins related to embryo implantation. Reproductive Biology and Endocrinology. 2022;20(1).

12. Giacomini E, Scotti GM, Vanni VS, Lazarevic D, Makieva S, Privitera L, et al. Global transcriptomic changes occur in uterine fluid-derived extracellular vesicles during the endometrial window for embryo implantation. Human reproduction (Oxford, England). 2021;36(8).

13. Burns GW, Brooks KE, Spencer TE. Extracellular vesicles originate from the conceptus and uterus during early pregnancy in sheep. Biology of Reproduction. 2016;94(56).

14. Almiñana C, Vegas AR, Tekin M, Hassan M, Uzbekov R, Fröhlich T, et al. Isolation and characterization of equine uterine extracellular vesicles: A comparative methodological study. International Journal of Molecular Sciences. 2021;22(2).

15. Nakamura K, Kusama K, Ideta A, Imakawa K, Hori M. IFNT-independent effects of intrauterine extracellular vesicles (EVs) in cattle. Reproduction. 2020;159(5).

16. Evans J, Rai A, Nguyen HPT, Poh QH, Elglass K, Simpson RJ, et al. Human Endometrial Extracellular Vesicles Functionally Prepare Human Trophectoderm Model for Implantation: Understanding Bidirectional Maternal-Embryo Communication. Proteomics. 2019;19(23).

17. Ng YH, Rome S, Jalabert A, Forterre A, Singh H, Hincks CL, et al. Endometrial Exosomes/Microvesicles in the Uterine Microenvironment: A New Paradigm for Embryo-Endometrial Cross Talk at Implantation. PloS one. 2013;8(3):p.e58502.

18. Liu C, Li L, Wang M, Shui S, Yao H, Sui C, et al. Endometrial extracellular vesicles of recurrent implantation failure patients inhibit the proliferation, migration, and invasion of HTR8/SVneo cells. Journal of Assisted Reproduction and Genetics. 2021;38(4).

19. Liu C, Yao W, Yao J, Li L, Yang L, Zhang H, et al. Endometrial extracellular vesicles from women with recurrent implantation failure attenuate the growth and invasion of embryos. Fertility and Sterility. 2020;114(2).

20. Tan Q, Shi S, Liang J, Zhang X, Cao D, Wang Z. MicroRNAs in Small Extracellular Vesicles Indicate Successful Embryo Implantation during Early Pregnancy. Cells. 2020.

21. Thippabhotla S, Zhong C, He M. 3D cell culture stimulates the secretion of in vivo like extracellular vesicles. Scientific Reports. 2019;9(1).

22. Way DL, Grosso DS, Davis JR, Surwit EA, Christian CD. Characterization of a new human endometrial carcinoma (RL95-2) established in tissue culture. In Vitro. 1983;19(3).

23. Fitzgerald HC, Schust DJ, Spencer TE. In vitro models of the human endometrium: evolution and application for women's health+. Biology of Reproduction. 2021 Feb 11;104(2):282–93.

24. Garcia-Alonso L, Handfield LF, Roberts K, Nikolakopoulou K, Fernando RC, Gardner L, et al. Mapping the temporal and spatial dynamics of the human endometrium in vivo and in vitro. Nat Genet. 2021 Dec;53(12):1698–711.

25. Yang H, Lei C, Cheng C, Feng Y, Zhang W, Petracco RG, et al. The antiapoptotic effect of galectin-3 in human endometrial cells under the regulation of estrogen and progesterone. Biology of Reproduction. 2012.

26. Greening DW, Nguyen HPT, Elgass K, Simpson RJ, Salamonsen LA. Human endometrial exosomes contain hormone-specific cargo modulating trophoblast adhesive capacity: Insights into endometrial-embryo interactions. Biology of Reproduction. 2016.

27. Perez-Riverol Y, Bai J, Bandla C, García-Seisdedos D, Hewapathirana S, Kamatchinathan S, et al. The PRIDE database resources in 2022: A hub for mass spectrometry-based proteomics evidences. Nucleic Acids Research. 2022;50(D1).

28. Zhou W, Santos L, Dimitriadis E. Characterization of the role for cadherin 6 in the regulation of human endometrial receptivity. Reproductive Biology and Endocrinology. 2020;18(1).

29. Vilella F, Moreno-Moya JM, Balaguer N, Grasso A, Herrero M, Martínez S, et al. Hsa-miR-30d, secreted by the human endometrium, is taken up by the pre-implantation embryo and might modify its transcriptome. Development (Cambridge). 2015;142(18).

30. Slater M, Murphy CR. Chondroitin sulphate and heparan sulfate proteoglycan are sequentially expressed in the uterine extracellular matrix during early pregnancy in the rat. Matrix Biology. 1999;18(2).

31. Sponchiado M, Marei WFA, Beemster GTS, Bols PEJ, Binelli M, Leroy JLMR. Molecular interactions at the bovine embryo–endometrial epithelium interface. Reproduction. 2020;160(6).

32. Dathe V, Pröls F, Brand-Saberi B. Expression of kinesin kif5c during chick development. Anatomy and Embryology. 2004;207(6).

33. Wollenhaupt K, Reinke K, Brüssow KP, Albrecht D, Tiemann U, Seyfert HM, et al. Natural occurrence and physiological role of a truncated eIF4E in the porcine endometrium during implantation. Biochemical Journal. 2010;432(2).

34. Salamonsen LA. Menstrual Fluid Factors Mediate Endometrial Repair. Frontiers in Reproductive Health. 2021;3.

35. Imakawa K, Bai R, Fujiwara H, Kusama K. Conceptus implantation and placentation: molecules related to epithelial–mesenchymal transition, lymphocyte homing, endogenous retroviruses, and exosomes. Reproductive Medicine and Biology. 2016;15(1).

36. Kim M, Seo H, Choi Y, Shim J, Kim H, Lee CK, et al. Microarray analysis of gene expression in the uterine endometrium during the implantation period in pigs. Asian-Australasian Journal of Animal Sciences. 2012;25(8).

37. Reis FM, Reis AM. Angiotensin-converting enzyme 2 (ACE2), angiotensin-(1-7) and Mas receptor in gonadal and reproductive functions. Vol. 134, Clinical Science. 2020.

38. Rai P, Kota V, Sundaram CS, Deendayal M, Shivaji S. Proteome of human endometrium: Identification of differentially expressed proteins in proliferative and secretory phase endometrium. Proteomics - Clinical Applications. 2010;4(1).

39. Hoirisch-Clapauch S, Brenner B. The role of the fibrinolytic system in female reproductive disorders and depression. Thrombosis Update. 2020;1.

40. França MR, da Silva MIS, Pugliesi G, Van Hoeck V, Binelli M. Evidence of endometrial amino acid metabolism and transport modulation by peri-ovulatory endocrine profiles driving uterine receptivity. Journal of Animal Science and Biotechnology. 2017;8(1).

41. Koh YQ, Peiris HN, Vaswani K, Reed S, Rice GE, Salomon C, et al. Characterization of exosomal release in bovine endometrial intercaruncular stromal cells. Reproductive Biology and Endocrinology. 2016;14(1).

42. Groothuis PG, Dassen HHNM, Romano A, Punyadeera C. Estrogen and the endometrium: Lessons learned from gene expression profiling in rodents and human. Vol. 13, Human Reproduction Update. 2007.

43. Tapia-Pizarro A, Figueroa P, Brito J, Marín JC, Munroe DJ, Croxatto HB. Endometrial gene expression reveals compromised progesterone signaling in women refractory to embryo implantation. Reproductive Biology and Endocrinology. 2014;12(1).

44. Griffiths IV RM, Pru CA, Behura SK, Cronrath AR, McCallum ML, Kelp NC, et al. AMPK is required for uterine receptivity and normal responses to steroid hormones. Reproduction. 2020;159(6).

45. van der Weijden VA, Bick JT, Bauersachs S, Arnold GJ, Fröhlich T, Drews B, et al. Uterine fluid proteome changes during diapause and resumption of embryo development in roe deer (Capreolus capreolus). Reproduction. 2019;158(1).

46. Faulkner S, Elia G, O'Boyle P, Dunn M, Morris D. Composition of the bovine uterine proteome is associated with stage of cycle and concentration of systemic progesterone. Proteomics. 2013;13(22).

47. Yang W, Wang P, Cao P, Wang S, Yang Y, Su H, et al. Hypoxic in vitro culture reduces histone lactylation and impairs pre-implantation embryonic development in mice. Epigenetics and Chromatin. 2021;14(1).

48. Massimiani M, Lacconi V, La Civita F, Ticconi C, Rago R, Campagnolo L. Molecular signaling regulating endometrium–blastocyst crosstalk. International Journal of Molecular Sciences. 2020;21(1).

49. Legato MJ. Principles of Gender-Specific Medicine: Gender in the Genomic Era: Third Edition. Principles of Gender-Specific Medicine: Gender in the Genomic Era: Third Edition. 2017.

50. Fazeli A, Pewsey E. Maternal communication with gametes and embryos: A complex interactome. Briefings in Functional Genomics and Proteomics. 2008;7(2).

51. Fazeli A, Holt W V. Cross talk during the periconception period. Vol. 86, Theriogenology. 2016.

52. Fazeli A, Moein Vaziri N, Holt WV. Proteomics of the periconception milieu. Vol. 15, Proteomics. 2015.

53. Hart AR, Khan NLA, Godakumara K, Dissanayake K, Piibor J, Muhandiram S, et al. The role of extracellular vesicles in endometrial receptivity and their potential in reproductive therapeutics and diagnosis. Reproductive Biology. 2022 Jun;22(2):100645.

54. Godakumara K, Ord J, Lättekivi F, Dissanayake K, Viil J, Boggavarapu NR, et al. Trophoblast derived extracellular vesicles specifically alter the transcriptome of endometrial cells and may constitute a critical component of embryo-maternal communication. Reproductive Biology and Endocrinology. 2021;19(1):115.

55. Skotland T, Sagini K, Sandvig K, Llorente A. An emerging focus on lipids in extracellular vesicles. Advanced Drug Delivery Reviews. 2020;159.

56. Harduf H, Goldman S, Shalev E. Human uterine epithelial RL95-2 and HEC-1A cell-line adhesiveness: the role of plexin B1. Fertility and Sterility. 2007;87(6).

57. Thie M, Denker HW. In vitro studies on endometrial adhesiveness for trophoblast: Cellular dynamics in uterine epithelial cells. Cells Tissues Organs. 2002;172(3).

58. Harduf H, Goldman S, Shalev E. Progesterone receptor A and c-Met mediates spheroids-endometrium attachment. Reproductive Biology and Endocrinology. 2009;7.

59. Thie M, Herter P, Pommerenke H, Dürr F, Sieckmann F, Nebe B, et al. Adhesiveness of the free surface of a human endometrial monolayer for trophoblast as related to actin cytoskeleton. Molecular Human Reproduction. 1997;3(4).

60. Heneweer C, Kruse LH, Kindháuser F, Schmidt M, Jakobs KH, Denker HW, et al. Adhesiveness of human uterine epithelial RL95-2 cells to trophoblast: Rho protein regulation. Molecular Human Reproduction. 2002;8(11).

61. Greening DW, Nguyen HPT, Elgass K, Simpson RJ, Salamonsen LA. Human endometrial exosomes contain hormone-specific cargo modulating trophoblast adhesive capacity: Insights into endometrial-embryo interactions. Biology of Reproduction. 2016.

62. Burns GW, Brooks KE, O'Neil E V., Hagen DE, Behura SK, Spencer TE. Progesterone effects on extracellular vesicles in the sheep uterus. Biology of Reproduction. 2018;98(5).

63. Rai A, Poh QH, Fatmous M, Fang H, Gurung S, Vollenhoven B, et al. Proteomic profiling of human uterine extracellular vesicles reveal dynamic regulation of key players of embryo implantation and fertility during menstrual cycle. Proteomics. 2021;21(13–14).

64. Dassen H, Punyadeera C, Kamps R, Klomp J, Dunselman G, Dijcks F, et al. Progesterone regulation of implantation-related genes: New insights into the role of oestrogen. Cellular and Molecular Life Sciences. 2007;64(7–8).

65. Mishra A, Ashary N, Sharma R, Modi D. Extracellular vesicles in embryo implantation and disorders of the endometrium. American Journal of Reproductive Immunology. 2021;85(2).

66. Gargett CE, Schwab KE, Deane JA. Endometrial stem/progenitor cells: The first 10 years. Vol. 22, Human Reproduction Update. 2016.

67. Yin Y, Wang A, Feng L, Wang Y, Zhang H, Zhang I, et al. Heparan sulfate proteoglycan sulfation regulates uterine differentiation and signaling during embryo implantation. Endocrinology. 2018;159(6).

68. Carson DD, Tang JP, Julian J. Heparan sulfate proteoglycan (perlecan) expression by mouse embryos during acquisition of attachment competence. Developmental Biology. 1993;155(1).

69. Pierzchała D, Liput K, Korwin-Kossakowska A, Ogłuszka M, Poławska E, Nawrocka A, et al. Molecular characterisation of uterine endometrial proteins during early stages of pregnancy in pigs by maldi tof/tof. International Journal of Molecular Sciences. 2021;22(13).

70. Reis FM, Reis AM. Angiotensin-converting enzyme 2 (ACE2), angiotensin-(1-7) and Mas receptor in gonadal and reproductive functions. Clinical Science. 2020;134(22).

71. Henarejos-Castillo I, Sebastian-Leon P, Devesa-Peiro A, Pellicer A, Diaz-Gimeno P. SARS-CoV-2 infection risk assessment in the endometrium: viral infection-related gene expression across the menstrual cycle. Fertility and Sterility. 2020;114(2).

72. Stelzig KE, Canepa-Escaro F, Schiliro M, Berdnikovs S, Prakash YS, Chiarella SE. Estrogen regulates the expression of SARS-CoV-2 receptor ACE2 in differentiated airway epithelial cells. American Journal of Physiology - Lung Cellular and Molecular Physiology. 2020;318(6).

73. McConaha ME, Eckstrum K, An J, Steinle JJ, Bany BM. Microarray assessment of the influence of the conceptus on gene expression in the mouse uterus during decidualization. Reproduction. 2011;141(4).

74. Horne AW, Van Den Driesche S, King AE, Burgess S, Myers M, Ludlow H, et al. Endometrial inhibin/activin β-B subunit expression is related to decidualization and is reduced in tubal ectopic pregnancy. Journal of Clinical Endocrinology and Metabolism. 2008;93(6).

75. Xu B, Wang J, Xia L, Zhang D, Wu X, Zhang A. Increased Uterine NK cell numbers and perforin expression during the implantation phase in IVF Cycles with GnRH Antagonist Protocol. Scientific Reports. 2017;7.

76. Bulmer JN, Morrison L, Longfellow M, Ritson A, Pace D. Granulated lymphocytes in human endometrium: Histochemical and immunohistochemical studies. Human Reproduction. 1991;6(6).

77. Lash GE, Otun HA, Innes BA, Percival K, Searle RF, Robson SC, et al. Regulation of extravillous trophoblast invasion by uterine natural killer cells is dependent on gestational age. Human Reproduction. 2010;25(5).

78. El-Azzamy H, Dambaeva S V., Katukurundage D, Salazar Garcia MD, Skariah A, Hussein Y, et al. Dysregulated uterine natural killer cells and vascular remodeling in women with recurrent pregnancy losses. American Journal of Reproductive Immunology. 2018;80(4).

79. Fu B, Li X, Sun R, Tong X, Ling B, Tian Z, et al. Natural killer cells promote immune tolerance by regulating inflammatory TH17 cells at the human maternal-fetal interface. Proceedings of the National Academy of Sciences of the United States of America. 2013;110(3).

80. Manaster I, Mizrahi S, Goldman-Wohl D, Sela HY, Stern-Ginossar N, Lankry D, et al. Endometrial NK Cells Are Special Immature Cells That Await Pregnancy. The Journal of Immunology. 2008;181(3).

81. Laplante M, Sabatini DM. Regulation of mTORC1 and its impact on gene expression at a glance. Journal of Cell Science. 2013;126(8).

82. Chen X, He J, Ding Y, Zeng L, Gao R, Cheng S, et al. The role of MTOR in mouse uterus during embryo implantation. Reproduction. 2009;138(2).

83. Guo X, Yi H, Li TC, Wang Y, Wang H, Chen X. Role of Vascular Endothelial Growth Factor (VEGF) in Human Embryo Implantation: Clinical Implications. Biomolecules. 2021 Feb 10;11(2):253.

84. Salmasi S, Sharifi M, Rashidi B. Evaluating the effect of ovarian stimulation and exogenous progesterone on CD31-positive cell density, VEGF protein, and miR-17-5p expression of endometrium immediately before implantation. Biomedicine and Pharmacotherapy. 2021;133.

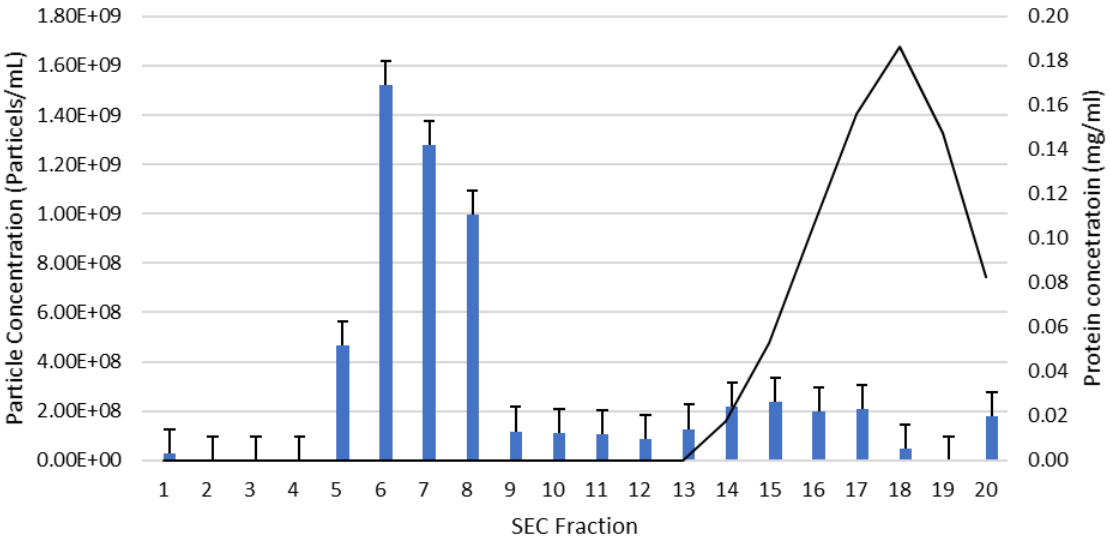
85. Lofti-Miri Rabbani M, Rogers PAW. Role of vascular endothelial growth factor in endometrial vascular events before implantation in rats. Reproduction. 2001;122(1).

86. Shao L, Wang H, Duan E, Zhu C. Expression of vascular endothelial growth factor in rat uterus during peri-implantation. Chinese Science Bulletin. 2001;46(14).

87. Tasaki Y, Nishimura R, Shibaya M, Lee HY, Acosta TJ, Okuda K. Expression of VEGF and Its Receptors in the Bovine Endometrium Throughout the Estrous Cycle: Effects of VEGF on Prostaglandin Production in Endometrial Cells. Journal of Reproduction and Development. 2010;56(2):223–9.

88. Heberle H, Meirelles VG, da Silva FR, Telles GP, Minghim R. InteractiVenn: A web-based tool for the analysis of sets through Venn diagrams. BMC Bioinformatics. 2015;16(1).

2.10 Supplementary materials.



Supplementary Figure 2.1. Isolation of extracellular vesicles sized particles secreted by the endometrial cell line RL95-2 using differential centrifugation and size exclusion chromatography. The height of the bars represents the mean concentration (particles/ml) of EVs from three biological replicates. The majority of EVs sized particles were eluted in fractions 5-8. The line graph represents the mean concentration of protein (mg/ml) in each SEC fraction from three biological replicates. Error bars represent the standard error from the mean.

Supplementary Table 2.1. Differential enrichment of EV proteins of E2P4 Group compared to E2. Protein identified in EVs released from estrogen- plus progesterone-treated RL95-2 cells to estrogen-treated RL95-2 cells.

Uniport accession	Gene Name	Adjusted p value	Fold change
A0A494C0G8	SCLT1	1.25E-06	-7.18
F1N0X6	TLL1	0.00812	-4.13
Q148H7	KRT79	0.0257	-4.09
A0A0B4J231	IGLL5	6.93E-05	-3.88
A0A286YEY1	IGHA1	0.00132	-3.59
Q96GE4	CEP95	0.0334	-3.36
F1MBG0	CARM1	0.00067	-3.29
P11215	ITGAM	0.0409	-3.24
Q95114	MFGE8.1	0.0437	-3.13
A0A3Q1N1J8	NCAM1	0.0388	-3.08
A0A3Q1LPG0	A0A3Q1LPG0	0.0112	-2.82
A7YW98	RARS1.1	0.00077	-2.53
P40926	MDH2	0.00076	-2.49

Q14393-5	GAS6	0.0345	-2.09
P18065	IGFBP2	0.0372	-2.07
H7BYW6	PDGFA	0.0352	-1.85
F1MM32	QSOX1.1	2.18E-05	-1.81
O00151	PDLIM1	0.048	-1.34
E9PEX6	DLD	0.0367	-1.31
A0A3Q1M688	NDST1	0.0262	-1.28
Q8N474	SFRP1	0.0377	-1.15
D6RHI9	RNASET2	0.0423	-1.14
F5GY03	SPARC	0.0108	-1.11
Q99523	SORT1	0.0345	1.15
P17174	GOT1	0.0018	1.24
Q2TV78-2	MST1L	0.00107	1.24
A0A3Q1MNL9	TGFBI	0.0424	1.3
Q17QQ1	LAMTOR3	0.045	1.31
P19858	LDHA.1	0.0277	1.51
A0A3Q1N7H1	CYRIB	0.0317	1.53
Q3SZF2	ARF4.1	0.04	1.55
H7BZJ3	PDIA3.1	0.0277	1.69
E9PAM4	PI4K2A	0.0367	1.81
Q9NRN7	AASDHPPT	0.0231	1.86
A6QLB3	ITGA2B	0.0406	1.86
O75223	GGCT	0.0362	1.88
A0A3Q1LMU4	INHBB	0.0451	1.88
Q13564-3	NAE1	0.00023	1.88
P00750	PLAT	0.026	1.91
A0A452DJE0	ACE2	0.0394	1.95
C9JPV1	SLC6A6	0.0256	2.03
Q58D84	FSTL1.1	0.00488	2.2
P25205	MCM3	0.00115	2.25
Q86W42	THOC6	0.00806	2.28
A0A087WXT3	ZNF33B	0.0408	2.32
A0A087WYV6	TSPAN6	0.00054	2.56
Q6URK6	CDH5	0.0369	2.71
F1N672	TM9SF2	0.0266	2.75
B4DZG7	ARL1	0.0398	2.83
Q53GA4	PHLDA2	0.00138	3.1
Q3ZC83	SLC29A1.1	0.00147	3.16
A6QP90	KRT32.1	0.00142	3.19

P04066	FUCA1	2.81E-08	3.22
A0A3Q1M5K6	ITGB5.1	0.0168	3.53
Q15223	NECTIN1	0.0316	3.68
A0A452DJ21	EIF4E	0.0265	3.83
F1MER7	HSPG2.1	0.0246	3.83
F6RAG5	KIF5C	0.0315	3.97
Q148I8	KRT31	0.0246	5.61
H7C2G2	ART4	0.00122	7.2

Supplementary Table 2.2. Differential enrichment of EV proteins of E2P4 Group compared to P4. Protein identified in EVs released from estrogen plus progesterone-treated RL95-2 compared to progesterone-treated RL95-2 cells.

Uniport accession	Gene Name	Adjusted p value	Fold change
A0A3Q1M4Y2	CFAP57	0.00141	-5.74
Q5VUV5	CHIA	0.00148	-4.5
P11215	ITGAM	0.0345	-4.06
E5RGX5	STMN2	0.00126	-3.47
P14324-2	FDPS	0.0143	-3.27
Q14393-5	GAS6	0.0287	-2.59
H0Y8K3	CDV3	0.0334	-2.29
P02453	COL1A1	0.0372	-2.21
Q9H9K5	ERVMER34-1	0.00101	-2.02
P51858	HDGF	0.00262	-1.9
Q5E998	CTSV.1	0.00149	-1.76
P02750	LRG1	0.0237	-1.68
O75509	TNFRSF21	0.0262	-1.58
O95025	SEMA3D	0.00394	-1.51
F1MM32	QSOX1.1	0.0177	-1.43
Q969H8	MYDGF	0.000145	-1.38
E9PF78	ADAM22	0.00688	-1.18
F5H6P7	MAGOHB	0.0435	1.74
A0A0B4J1W3	NAA15	0.0282	1.74
A0A3Q1M315	LOC790886	0.0157	1.81
Q9BSJ2-3	TUBGCP2	0.0172	1.82
M0R1D6	DNAJB1	0.00332	1.99
Q96S59	RANBP9	0.0469	2.01
D6RDI2	LUC7L3	0.00952	2.06
Q9H6X2-3	ANTXR1	0.000554	2.29
Q6B856	TUBB2B	0.00398	2.32
K7EK07	H3-3B	0.00328	2.76
C9JPH9	FSCN1	0.0311	2.98
Q9NX76	CMTM6	0.0126	3

A6QP90	KRT32.1	0.00901	3.37
F1N2K1	PCYOX1	0.000965	3.73
A0A452DJ21	EIF4E	0.0366	4.41
Q3ZBX9	H2AFJ	0.0345	4.79
A0A3Q1MI29	A0A3Q1MI29	0.00849	5.21
A0A3Q1MM65	RPL4.1	0.0392	5.4

Supplementary Table 2.3. Differential enrichment of EV proteins of E2 Group compared to P4. Protein identified in EVs released from estrogen plus progesterone-treated RL95-2 compared to control treated RL95-2 cells.

Uniport accession	Gene Name	Adjusted p value	Fold change
H7C2G2	ART4	0.00429	-6.23
A0A3Q1M4Y2	CFAP57	0.00000306	-5.94
Q5VUV5	CHIA	0.0000162	-4.39
E5RGX5	STMN2	0.0000199	-3.27
A0A087WTK0	PTPRJ	0.00414	-3.18
B5MD17	CBX1	0.00897	-3.15
P25205	MCM3	0.000000149	-3.05
P04066	FUCA1	6.98E-08	-2.99
A6QLB3	ITGA2B	0.00116	-2.41
A0A087WYV6	TSPAN6	0.000767	-2.33
A0A087WXT3	ZNF33B	0.043	-2.2
Q5SZC9	ABRACL	0.00212	-2.01
Q9H9K5	ERVMER34-1	0.00000389	-1.99
P07954-2	FH	0.0324	-1.98
E9PF78	ADAM22	2.34E-11	-1.86
P17174	GOT1	4.04E-08	-1.84
A0A3Q1LMU4	INHBB	0.0485	-1.79
E1BNP7	TFAP2D	0.0455	-1.74
H7BZJ3	PDIA3	0.0156	-1.69
A0A3Q1N7H1	CYRIB	0.0124	-1.6
F1MWN1	CSE1L	0.000909	-1.46
F5H6E2	MYO1C	0.00519	-1.46
Q5E998	CTSV	0.000679	-1.44
Q12805-5	EFEMP1	0.0233	-1.41
O95025	SEMA3D	0.000326	-1.39
A0A087WTM1	ROBO1	0.0000191	-1.27
Q92598-2	HSPH1	0.046	-1.24

P02750	LRG1	0.0408	-1.23
Q9UKM7	MAN1B1	0.0387	-1.02
C9JFR7	CYCS	0.0119	-1
Q0VD53	VPS26A	0.0157	1.01
Q9NYU2-2	UGGT1	0.0201	1.13
Q08945	SSRP1	0.0395	1.35
O00443	PIK3C2A	0.0186	1.37
F1N6D5	EFTUD2	0.012	1.4
Q6B856	TUBB2B	0.0425	1.44
P68431	H3C1	0.0474	1.45
Q5E9X4	LRRC59	0.0173	1.61
O97593	SMC1A	0.05	1.62
C9J6P4	ZC3HAV1	0.0184	1.66
P24627	LTF	0.0386	1.67
P40926	MDH2	0.0172	1.83
A0A0B4J1W3	NAA15	0.000341	1.89
O43765	SGTA	0.0487	1.89
H0Y6Z7	PTPRF	0.00948	1.95
Q9H6X2-3	ANTXR1	0.0000258	1.98
A0A3Q1M315	LOC790886	0.0000318	2.05
M0R1D6	DNAJB1	0.0000154	2.06
G5E9R5	ACP1	0.0000576	2.24
H7C1M2	SON	0.0476	2.24
P01833	PIGR	0.0499	2.35
F1MBG0	CARM1	0.00819	2.58
H7C3P9	COPS3	0.00135	2.59
A0A3Q1LPG0	A0A3Q1LPG0	0.00569	2.79
Q9NX76	CMTM6	0.00102	2.82
F1N2K1	PCYOX1	0.000303	3.03
K7EK07	H3-3B	0.00000319	3.04
Q96GE4	CEP95	0.0194	3.36
P0DPA2	VSIG8	0.0476	3.83
A0A494C0G8	SCLT1	0.0195	3.98
F1N0X6	TLL1	0.000963	4.49
A0A286YEY1	IGHA1	0.000000156	4.93

Supplementary Table 2.4. Differential enrichment of EV proteins of E2P4 Group compared to C. Protein identified in EVs released from estrogen plus progesterone-treated RL95-2 compared to control treated RL95-2 cells.

Uniport accession	Gene Name	Adjusted p value	Fold change
Q5VSY0-2	GKAP1	9.18E-05	-5.16
Q5E9M9	RHOT2	0.0327	-3.66
E5RGX5	STMN2	0.00314	-3.15
A0A3Q1M688	NDST1	1.7E-09	-3.02
P14324-2	FDPS	0.0386	-2.92
O94985-2	CLSTN1	0.00216	-2.69
Q14393-5	GAS6	0.0235	-2.63
Q9H9K5	ERVMER34-1	5.35E-06	-2.42
Q10471	GALNT2	0.0104	-2.32
Q56K13	SF3B5	0.05	-2.24
O75509	TNFRSF21	0.000117	-2.22
K7ELL7	PRKCSH	0.0275	-2.15
A0A087X0S5	COL6A1	0.00459	-2.05
P01024	C3	0.0469	-1.89
P51858	HDGF	0.00243	-1.87
P13667	PDIA4	0.0232	-1.75
A0A3Q1MRC3	EFNA5	0.0138	-1.65
F1MM32	QSOX1	0.00365	-1.6
Q8N474	SFRP1	0.0252	-1.47
Q969H8	MYDGF	5.84E-06	-1.45
J3KMY5	NPC2	0.0227	-1.37
Q9UQ74-2	PSG8	0.0349	-1.18
Q13541	EIF4EBP1	0.00552	1.6
Q3SZF2	ARF4	0.026	1.98
P04066	FUCA1	0.000341	2.66
E9PS42	CSRP1	0.0156	2.92
O75223	GGCT	0.000052	3.46
P01040	CSTA	0.029	3.7
Q9BZJ8	GPR61	0.0459	3.7
P25311	AZGP1	0.0434	3.89
A0A3Q1MM65	RPL4	0.000453	7.45

Supplementary Table 2.5. Differential enrichment of EV proteins of E2 Group compared to C. Protein identified in EVs released from estrogen treated RL95-2 compared to control treated RL95-2 cells.

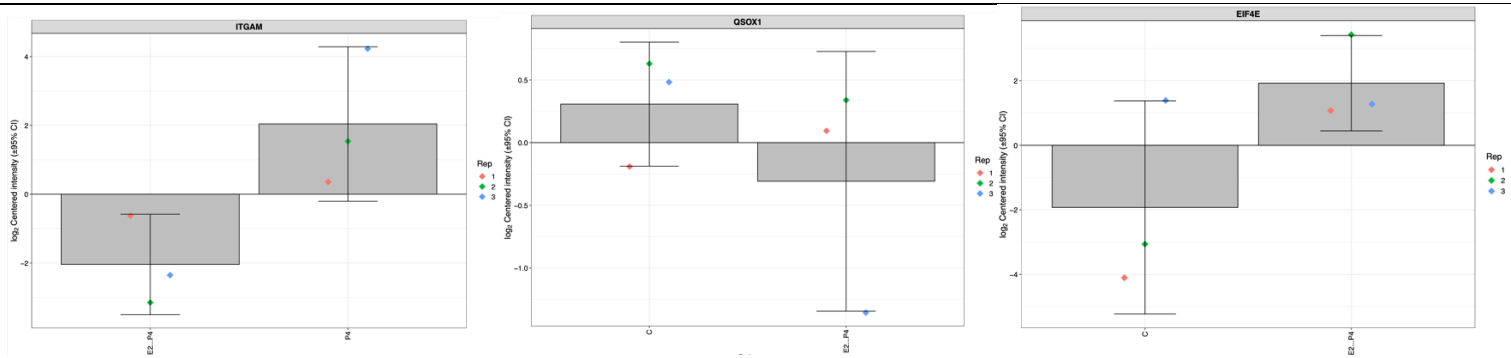
Uniport accession	Gene Name	Adjusted p value	Fold change
Q5VSY0-2	GKAP1	0.0000202	-5.16
Q2KIX7	Q2KIX7	0.00118	-4.27
F1MER7	HSPG2	0.042	-3.93
Q14574	DSC3	0.0313	-3.46
Q86SQ4-2	ADGRG6	0.000284	-3.16
A6QLB3	ITGA2B	0.000198	-3.1
P25205	MCM3	0.0000168	-3.01
E5RGX5	STMN2	0.00278	-2.95
F1N672	TM9SF2	0.0344	-2.94
A0A3Q1NFD1	CACNA2D1	0.00319	-2.8
Q3ZC83	SLC29A1.1	0.0417	-2.61
Q53GA4	PHLDA2	0.0432	-2.53
G3N1U4	SERPINA3-3	0.05	-2.52
Q9H9K5	ERVMER34-1	0.00000159	-2.39
P00750	PLAT	0.0105	-2.28
Q10471	GALNT2	0.00937	-2.16
E9PB61	ALYREF	0.0373	-2.15
Q58D84	FSTL1	0.0491	-1.91
A0A087WYV6	TSPAN6	0.0474	-1.91
P19858	LDHA	0.0067	-1.89
P13667	PDIA4	0.00346	-1.89
A0A0G2JP90	NOMO1	0.0441	-1.85
F1MGE9	HYPK	0.0282	-1.79
P01024	C3	0.043	-1.76
A0A3Q1MNL9	TGFBI	0.00755	-1.75
A0A3Q1M688	NDST1	0.00194	-1.74
E9PF78	ADAM22	0.00000159	-1.63
P17174	GOT1	0.00091	-1.43
Q99523	SORT1	0.0409	-1.25
K7ENJ4	ATP5F1A	0.00908	2.11
E9PS42	CSRP1	0.0429	2.4
P40926	MDH2	0.000109	2.99
P12273	PIP	0.0271	3.26
Q6UWP8	SBSN	0.0443	3.58
P25311	AZGP1	0.0372	3.65

A0A0B4J231	IGLL5	0.000862	3.68
P31025	LCN1	0.023	4.05
A0A286YEY1	IGHA1	0.000264	4.31
F1N0X6	TLL1	0.0135	4.32
A0A494C0G8	SCLT1	0.0221	4.64
A0A3Q1MM65	RPL4	0.0171	5.44

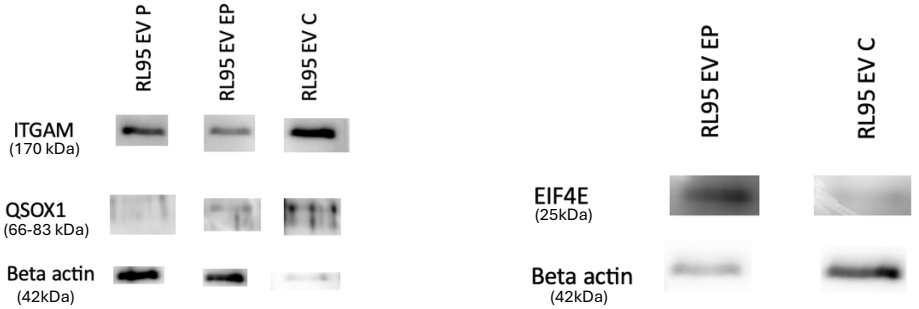
Supplementary Table 2.6. Differential enrichment of EV proteins of P4 Group compared to C. Protein identified in EVs released from progesterone treated RL95-2 compared to control treated RL95-2 cells.

Uniport accession	Gene Name	Adjusted p value	Fold change
F1N2K1	PCYOX1	0.0186	-3.98
Q9H6X2-3	ANTXR1	0.0311	-2.13
A0A3Q1M688	NDST1	0.032	-1.97
Q13162	PRDX4	0.0457	-1.18
A0A3Q1M4Y2	CFAP57	0.028	6.03

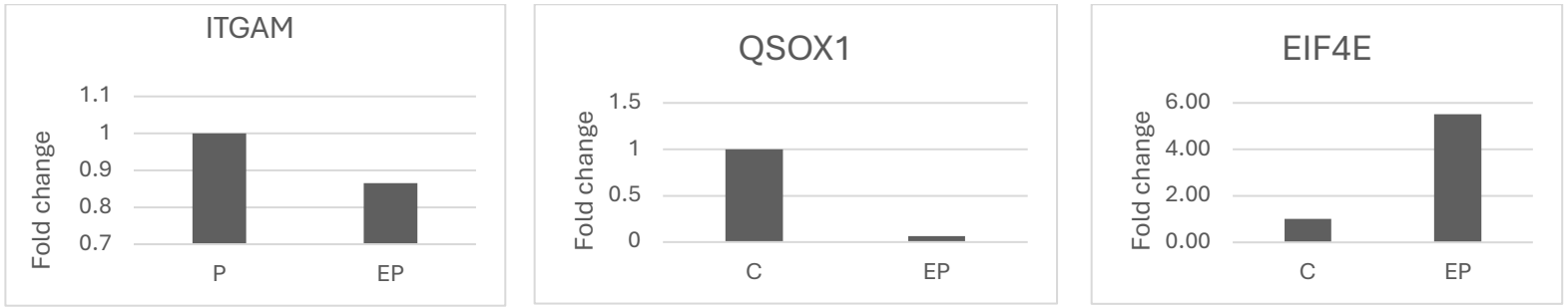
A



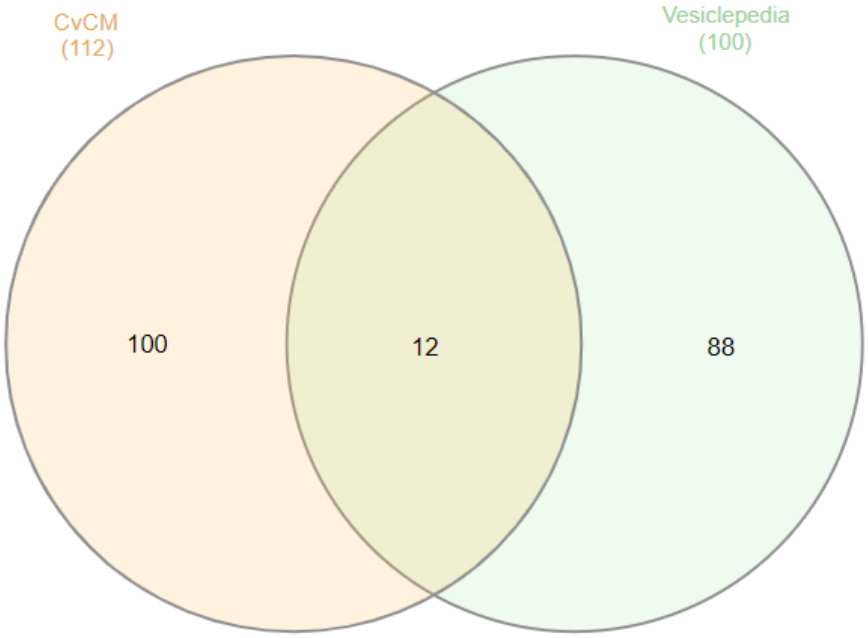
B



C



Supplementary Figure 2.2. Mass spectrometry validation. Validation of integrin alpha M chain (ITGAM), Quiescin Sulfhydryl Oxidase 1 (QSOX1) and Eukaryotic translation initiation factor 4E (EIF4E) protein change measured in the EV from hormone treated RL95-2 cells. The liquid chromatography/mass-spectrometry (LC-MS/MS) results showed reduced differential enrichment of ITGAM and QSOX1 in E2P4 EV than their comparison groups and increase in deferential enrichment in EIF4E in E2P4 EVs than their comparison (A). The LC-MS/S results of ITGAM, QSOX1 and EIF4E was validated with western blot analysis (WB) using EV samples from hormone treated RL95-2 cells which were previously used in the LC-MS/MS analysis (B). The intensity was confirmed via fold change of WB band intensity normalised to beta actin control.



Supplementary Figure 2.3. Venn diagram of proteins enriched in the Control EV group versus the conditioned media control compared to the top 100 Vesiclepedia EV markers. (Made in Heberle, H.; Meirelles, G. V.; da Silva, F. R.; Telles, G. P.; Minghim, R. *InteractiVenn: a web-based tool for the analysis of sets through Venn diagrams*. BMC Bioinformatics 16:169 (2015) (88)).

CHAPTER 3

HORMONAL TREATED ENDOMETRIAL CELL DERIVED EVS ALTER THE BINDING AFFINITY OF TROPHOBLAST TO ENDOMETRIAL CELLS.

Chapter 3. Hormonal treated endometrial cell derived EVs alter the binding affinity of trophoblast to endometrial cells.

3.1 Authors contribution.

This chapter is presented in a publication format and currently is not under review.

3.2 Interconnecting chapters.

After identifying that the endometrial EV proteome differs under hormonal stimulation, and proteins were identified that have a role in implantation, this chapter continues to explore the suggested role of endometrial EVs in implantation. Experimentation into this suggested role described in this chapter was via a functional assay whilst also exploring the concept that the transcriptional effect that EVs derived from hormone treated endometrial cells have on the *in vitro* embryo mimics produced from JAr cells in spheroid form.

3.3 Chapter aim.

Investigate the impact of sex hormone-influenced endometrial EVs from receptive endometrial cells on trophoblast binding and trophoblast mRNA expression *in vitro*.

3.4 Abstract.

Embryo binding and subsequent implantation are pivotal events in a successful human pregnancy, involving complicated communication between the embryonic trophectoderm and the maternal endometrium. Although various biochemical and physiological changes involved in this process are mediated by numerous factors, the specifics of the signalling between the embryo and endometrium are not fully understood. This study explores the role of endometrial extracellular vesicles (EVs) in mediating communication between surrogate endometrial cells (RL95-2) and trophoblasts (JAr) during simulated implantation. Previous work demonstrated the impact of trophoblast derived EVs on endometrial gene expression, prompting investigation into the reverse hypothesis. Our results showed that hormonally stimulated endometrial-derived EVs, replicating the window of implantation, significantly enhance trophoblast binding affinity. mRNA sequencing of EV-treated trophoblast spheroids revealed changes in gene expression and gene set enrichment analysis identified key pathways associated with glycosphingolipid biosynthesis, immune modulation, and cellular signalling with hormonally stimulated endometrial-derived EV treatment. This study has highlighted some of the intrinsic molecular mechanisms governing implantation, emphasising the need for further research to unravel the complexities of bidirectional embryo-endometrium communication. Insights gained may have implications for fertility treatments and addressing implantation failure in clinical settings.

3.5 Introduction.

Embryo implantation is a pivotal point in the establishment of human pregnancy. The initial stages involve the apposition of the embryonic trophectoderm and the maternal endometrium, followed by adhesion and subsequent invasion of the trophectoderm across the luminal epithelium of the endometrium(1). To facilitate this process, different biochemical and physiological changes occur which are mediated via different factors (2). However, the factors that regulate the initial embryo-endometrium signalling interaction are subject to limited understanding.

In each step of implantation, it is understood that there is a crosstalk between the endometrium and the trophoblast (3). This interaction helps facilitate implantation during the window of implantation (WOI), a process believed to be regulated by steroid hormones (2,3). During this crosstalk, the endometrium and embryo are prepared for successful implantation through different functional and molecular alterations, promoting synchronisation in the endometrium, embryo, and the overall uterine microenvironment (2,3). The consequences of a lack of communication result in embryo implantation failure, with 75% of all pregnancy losses being due to implantation failure (4). Hence, embryo implantation is an intricately sensitive process, and it is probable that several lesser-known mechanisms are involved, arising from both the embryo and the endometrium.

One of these alternative methods of communication that has been increasingly investigated in recent years is extracellular vesicle (EV)-mediated communication (5,6). These nanosized particles have been shown to influence functions via the transfer of

information either by their extensive surface proteome or via their cargo of RNAs, lipids, and proteins (7). During the last few years, it has been well evidenced that EVs act as a communication method between cells, enabling intercellular communication within the female reproductive microenvironment and tract (8–10). Additionally, the EVs involved in this communication via their content have been shown to originate from various cells and tissues, including the oviduct (11,12), the endometrium (13,14), the placenta (15), the pre implanted embryo (16–18), and the embryonic stem cells (19).

In our previous study, it was shown that the proteome of endometrial cell-derived EVs differs under hormonal stimulation (14). In addition, another earlier study demonstrated that labelled RNA can be transferred from trophoblast cells to endometrial cells via EVs (16). This EV-mediated embryo-maternal communication was further investigated using an *in vitro* model of embryo-maternal communication by supplementing trophoblast analogue spheroid (JAr) derived EVs to an endometrial analogue (RL95-2) cell layer and characterising the transcriptomic alterations using RNA sequencing (17). This study revealed that trophoblast-derived EVs can modify endometrial gene expression, potentially with functional importance for embryo-maternal communication during implantation (17). In the current study, using a similar *in vitro* system, we explored the reverse hypothesis: that endometrial-derived EVs, specifically from hormone-treated endometrial cells, are capable of altering the mRNA profiles of JAr (trophoblast) cells spheroids. Additionally, we explored the effects of the same EVs derived from hormone treated endometrial cells on trophoblast binding in an *in vitro* assay mimicking embryo implantation.

3.6 Material and methods.

3.6.1 Cell culture.

Three types of media were used for the culturing of RL95-2 cells: (i) Dulbecco's Modified Eagles Medium (DMEM/F12) culture media (Sigma-Aldrich, Dorset, UK), supplemented with 10% fetal bovine serum (FBS) (Sigma-Aldrich, Dorset, UK), 1% l-glutamine (Sigma-Aldrich, Dorset, UK), 1% penicillin (100 IU/mL)/streptomycin (100 µg/mL) (Sigma-Aldrich, Dorset, UK), and 5 µg/mL insulin (human recombinant insulin; Gibco Invitrogen, Roskilde, Denmark); and (ii) Dulbecco's Modified Eagles Medium lacking phenol red (Thermo Fisher, Scotland, UK). The final variation (iii) was phenol red free media (ii) with charcoal stripped FBS (10%) (Sigma-Aldrich, Dorset, UK).

For JAr cells, one type of media has been used for the culture of the cells, consisting of RPMI-1640 culture media (Sigma-Aldrich, Dorset, UK), supplemented with 10% fetal bovine serum (FBS) (Sigma-Aldrich, Dorset, UK), 1% l-glutamine (Sigma-Aldrich, Dorset, UK), and 1% penicillin (100 IU/mL)/streptomycin (100 µg/mL) (Sigma-Aldrich, Dorset, UK). During the binding assay, RPMI-1640 culture media (Sigma-Aldrich, Dorset, UK), was used without any supplementation.

RL95-2 cells obtained from the American Type Culture Collection (ATCC, Cat. No. CRL-1671, Teddington, UK) were used to simulate receptive endometrial cells *in vitro*. RL95-2 cells were cultured in T75 flasks (Greiner, bio-one, Gloucestershire, UK) in culture media (i). Cells were incubated at 37 °C in a 5% CO_2 atmosphere until confluent. At confluence, cells were washed using Ca^{2+} and Mg^{2+} free Dulbecco's phosphate-buffered saline (Sigma-Aldrich, Dorset, UK). The cells were then harvested using 1 x trypsin-EDTA

(Sigma-Aldrich, Dorset, UK) and pelleted by centrifugation at 300× *g* for 4 min. RL95-2 Cell line has been authenticated by ATCC.

JAr cells obtained from American Type Culture Collection (ATCC, Cat. No. HTB-144, Teddington, UK) were used to simulate the trophoblast *in vitro*. JAr was cultured in in T75 flasks (Greiner, bio-one, Gloucestershire, UK) in the supplemented RMPI-1640 culture media. Cells were incubated at 37 °C in a 5% CO_2 atmosphere until confluent. At confluence, cells were washed using Ca^{2+} and Mg^{2+} free Dulbecco's phosphate-buffered saline (Sigma-Aldrich, Dorset, UK). The cells were then harvested using 1x trypsin-EDTA (Sigma-Aldrich, Dorset, UK) and pelleted by centrifugation at 300× *g* for 4 min. JAr cell line has been authenticated by ATCC.

3.6.2 Differential centrifugation.

Conditioned media was centrifuged for 10 min at 400× *g* at 4 °C in a Sigma swing-out rotor centrifuge (catalogue number 11,180). The pellet was discarded, and the supernatant was centrifuged for 10 min at 4000× *g* at 4 °C; again, the pellet was discarded, and the supernatant was centrifuged for 10 min at 10,000× *g* at 4 °C. Following centrifugation, the final resulting supernatant was concentrated using a 10kDa ultrafiltration tube (Sartorius, Hampshire, UK) to 500µl. Retentates were then subjected to size exclusion chromatography. An aliquot was reserved from the control group, prior to concentration as a conditioned media control.

3.6.3 Size exclusion chromatography.

For the preparation of a size exclusion chromatography (SEC) column, 14-mL of Sepharose CL-2B slurry (GE Healthcare, Uppsala, Sweden) was packed into an empty gravity chromatography column (Bio-Rad, Watford, UK). After settling of the Sepharose beads, a nylon net filter was inserted at the ethanol/Sepharose separation interface at about 10 mL. The ethanol was eluted followed by washing the column with molecular-grade water (3 × 5 mL) and then with Ca^{2+} and Mg^{2+} free Dulbecco's phosphate-buffered saline (3 × 5 mL) (Sigma-Aldrich, Dorset, UK). On top of the filter, 0.5 mL of the concentrated conditioned medium was loaded, and fractions 5-8 (as previous optimised(14)) of 0.5 mL were collected with a Ca^{2+} and Mg^{2+} free Dulbecco's phosphate-buffered saline eluent. The resulting fractions were stored at −80°C for further EV treatment and analysis.

3.6.4 Nanoparticle tracking analysis.

For nanoparticle tracking analysis (NTA) (ZetaView, PMX 110, Particle Metrix, Meerbusch, Germany) all samples were diluted in milliQ water. Ideal measurement concentrations were found by pre-testing the ideal particles per frame value (140–200 particles/frame). For each measurement, three cycles were performed by scanning 11 cell positions each and capturing 30 frames per position under the following settings: Focus: autofocus; Camera sensitivity for all samples: 50; Shutter: 70; Scattering intensity: detected automatically; Cell temperature: 25°C. After capture, the videos were analysed by the in-built ZetaView Software 8.04.02 SP2 with specific analysis parameters: maximum size: 500; minimum size: 5; minimum brightness: 25; hardware: embedded laser: 40 mW at 488 nm; and camera: CMOS.

3.6.5 EV characterisation.

Characterisation of the isolated EVs was carried out using methods described in our previous publication (14) and according to ISEV 2018 guidelines (20). In summary, the nanoparticle size and concentration in EV fractions were measured using NTA (ZetaView, Particle Metrix, Meerbusch, Germany). The original nanoparticle concentrations and size profiles of RL95-2 EVs used in this experiment are shown in Supplementary Figure 3.1. Transmission electron microscopy was used previously for the physical characterisation of EVs (14). Enrichment of EV surface protein markers, CD9, CD81 and TSG101 was previously confirmed by Label-free liquid chromatography tandem mass spectrometry (LC-MS/MS) (14). The methods used for RL95-2 cell-derived EV characterisation were fully described in our previous publications (14) and chapter 2.

3.6.6 Hormone treatment of RL95-2 cells.

RL95-2 cells were treated with hormone treatment as previously described (14). Following a 24h incubation period, conditioned media was collected, and differential centrifugation was performed, followed by concentration and size exclusion chromatography, as described above. Enriched EV samples were then analysed for particle concentration via NTA and then stored at -80°C. The experiment was performed once, with aliquots of the same EV sample used to treat the JAr spheroids in triplicates.

3.6.7 Formation and treatment of JAr spheroids.

JAr cells at confluency in a T75 flask were harvested via 1 x trypsin-EDTA and centrifuged to form a pellet. From a 1:3 dilution of these pelleted cells ($8x10^8$ cells), 265µl was

transferred into a 60x15mm cell culture dish with 5ml supplemented RMPI-1640 culture media. These were then incubated on a gyrating shaker (300 rpm) at 37°C in a 5% CO_2 atmosphere incubator for 24h. After 24h, spheroids were washed with RMPI-1640 media with no supplementation and transferred to a 60x15mm cell culture dish with 4ml RMPI-1640 culture media with no supplementation. For treatment, EVs were added into the culture dishes at a concentration of $3x10^8$ EVs/ml from the RL95-2 hormone-treated conditions (E2, P4, E2P4, C), and a control containing no EVs was incubated for a further 24h on a gyrating shaker (300 rpm) at 37°C in a 5% CO_2 atmosphere incubator. After this 48h total incubation, approximately 5000 spheroids were formed. Example images of JAr spheroids can be seen in Supplementary Figure 3.2.

3.6.8 Formation of RL95-2 monolayer.

Confluent RL95-2 cells from a T75 flask were subcultured via trypsin-EDTA, as mentioned above, and the cell pellet resuspended in a 1:3 dilution ($4x10^6$ cells), with 50µl of these cells transferred into a 12-well plate with 1ml DEMEM-supplemented media (i). Once confluent, these cells were used in the binding assay.

3.6.9 Binding assay.

For optimisation, JAr spheroids were grown for 48 hours on a gyrating shaker (300rpm) at 37°C in a 5% CO_2 atmosphere incubator. After the first 24 hours, spheroids were washed and incubated with FBS-free media for a further 24 hours. After the 48hours, the monolayer of RL95-2 cells were washed with Ca^{2+} and Mg^{2+} Dulbecco's phosphate-buffered saline (Sigma-Aldrich, Dorset, UK), and non-supplemented DMEM/F12 media added into each well (1ml). JAr spheroids were selected under the microscope, and 35

round and compound spheroids were transferred into each well, 3 wells per condition per replicate. The plate was then incubated at 37°C in a 5% CO_2 atmosphere incubator for 30mins, 20mins, or 15mins. After the incubation time, the amounts of transferred spheroids in each well were counted and recorded. The plate was then placed on shaker at 15.5V for 4 minutes. Following this, media from the wells was discarded with a hard shake, and the wells were washed with 1ml Ca^{2+} and Mg^{2+} Dulbecco's phosphate-buffered saline before being placed on the shaker for a further 4 mins at 15.5V. This was again discarded with a hard shake, and the attached spheroids were counted under the microscope (results of the optimisation can be seen in Supplementary Figure 3.3).

For the EV-treated experiment, on the day of the binding assay, the RL95-2 monolayer was confluent and was formed as described as above. Additionally, the JAr spheroids have formed and been treated for 24h, also as described above. First, the RL95-2 were washed with Ca^{2+} and Mg^{2+} Dulbecco's phosphate-buffered saline (Sigma-Aldrich, Dorset, UK) then non-supplemented DMEMD/F12 media was added into each well (1ml). Following this, JAr spheroids were selected under microscope, and 35 round and compound spheroids were transferred into each well, with 3 wells per condition per replicate. The plate was then incubated in a 37°C, 5% CO_2 atmosphere incubator for 30 minutes. After the incubation time, the number of transferred spheroids in each well were counted and recorded. The plate was then placed on a shaker at 15.5V for 4 minutes. Following this, media from the wells were discarded with a hard shake, and the wells washed with 1ml Ca^{2+} and Mg^{2+} Dulbecco's phosphate-buffered saline before being placed on the shaker for a further 4 minutes at 15.5V. This was again discarded with a hard shake, and the attached spheroids were counted under the microscope. Example

images of JAr spheroids binding to Rl95-2 can be seen in Supplementary Figure 3.4. The images of JAr spheroids and RL95-2s co-culture were captured by a Nikon DS-Fi1 camera (Nikon, Kingston Upon Thames, UK) connected to an inverted CKX41 fluorescent microscope (OLYMPUS, Tokyo, Japan).

3.6.10 RNA extraction and mRNA sequencing.

For RNA extraction, all the remaining JAr spheroids were collected and centrifuged at 200g for 2 minutes to pellet cells. Cell media supernatant was discarded, and 1ml TRIzol reagent was added (Thermo Fisher, Scotland, UK) to homogenise the sample. RNA was then isolated from the samples via the Direct-zol RNA MicroPrep Kit (Zymo Research, Irvine, CA, USA) according to the manufacturer's instructions, with a 25µl final sample eluate. The extracted RNA was assessed for purity and concentration using a The NanoDrop® ND-1000 UV-Vis Spectrophotometer (Thermo Fisher Scientific, Scotland, UK) to ensure the samples were of a sufficient quality for transcriptomic sequencing. Samples were then stored at -80°C. The samples were shipped frozen to Biomarker Technologies (Münster, Germany) for mRNA sequencing. Nanodrop 2000 (Thermo Fisher Scientific) and Agilent 2100 LabChip GX (PerkinElmer, MA, USA) instruments were used to measure RNA concentration and integrity, respectively. cDNA libraries were constructed using the Hieff NGS Ultima Dual-mode mRNA Library Prep Kit (Yeasen Biotechnology, Shanghai, China). HieffNGS DNA selection beads (Superior Ampure XP alternative, Yeasen Biotechnology, Shanghai, China) were used for library purification. Library quality was assessed using Qsep-4, and sequencing was performed on the Illumina Novaseq 6000 platform (Illumina, SanDiego, CA) with a paired-end read length of 6 Gb and 20 million reads per library.

3.6.11 Processing, alignment, and quantification of RNA sequencing (RNAseq) reads.

Raw sequencing data (FASTQ) were processed using the nf-core/rnaseq pipeline (21). The quality of raw reads was assessed using FASTQC v3.12.0. Reads of low quality (those with Phred scores under 20) and adapter sequences were filtered out using Cutadapt v3.4. Reads passing the quality check were then aligned to the GRCh38.110 human reference genome. The alignment was performed using STAR aligner v2.7.10a and quantification via RSEM.

3.6.12 Differential gene expression analysis.

Differential expression (DE) analysis was carried out in R Studio (version 4.2.2) using the edgeR package (version 3.40.2) with the quasi-likelihood functionality. The design of the experiment, inclusive of linear model coefficients and their parameterisation, was integrated into a model matrix used for analysing differential expression. To mitigate the impact of genes with low expression levels, only those with counts per million (CPM) exceeding a set threshold (k) in n samples were considered. This threshold (k) was established based on the sizes of the sample libraries and the number of samples (n) as inferred from the design matrix. Normalisation for library size was achieved through the Trimmed Mean of M-values (TMM) method. Estimates of negative binomial dispersions were made at common, trended and gene-specific levels through the weighted likelihood empirical Bayes approach. Then, a quasi-likelihood negative binomial generalised log-linear model was applied to the dataset for gene expression pattern analysis, taking these dispersions into account. Batch effect was adjusted using ComBat-seq. Genes were considered differentially expressed if they exhibited a log2 fold-change beyond 1

and a p Value of <0.05, indicating statistical significance. FDR was not considered as a threshold cut off. Gene Set Enrichment Analysis (GSEA) on gene sets sourced from the Molecular Signatures Database (MSigDB) was performed using the fgsea version 11.28.0 and msigdbr version 7.5.1 packages.

3.6.13 Statistical analysis.

All binding assays were performed in 3 biological replicates and 3 technical replicates. In this context, biological replicates pertain to experiments performed on different days with different passage numbers, and technical replicates refers to the different wells on the same plate with the same passage number. For the binding assay result a one-way ANOVA was performed with Tukey post hoc test, with (*) indicating a $P \leq 0.05$ and (**) $P \leq 0.01$.

3.6.14 Experimental design.

EVs were isolated from hormone-treated RL95-2 cells, as per our previous publication (14), and used to assess the impact of these EVs on the binding of JAr spheroids to a RL95-2 monolayer using a 3D optimised model of implantation. At confluency, JAr cells were trypsinised, and $3X10^5$ cells were cultured in a 60x15mm cell culture dish with 5ml supplemented RMPI-1640 culture media. The cells were incubated on a gyratory shaker set at 300 rpm in a 5% CO_2 atmosphere incubator at 37°C for 24 hours to form 3D spheroids. After this incubation period, EVs from the hormone-treated RL95-2 cells in different conditions (E2, P4, E2P4 and C) were added to the media at $3x10^8$ concentration and incubated for a further 24 hours. Around 5000 spheroids were formed following this period; 35 from each condition were transferred into one well of a 12-well plate

monolayer of RL95-2 cells. This was performed in 3 technical replicates per condition. The binding assay was performed, and the binding percentage calculated. The remaining spheroids were collected, and RNA extracted via Direct-zol RNA MicroPrep Kit, and mRNA sequencing was performed. A diagrammatic representation of the experimental design can be seen in Figure 3.1.

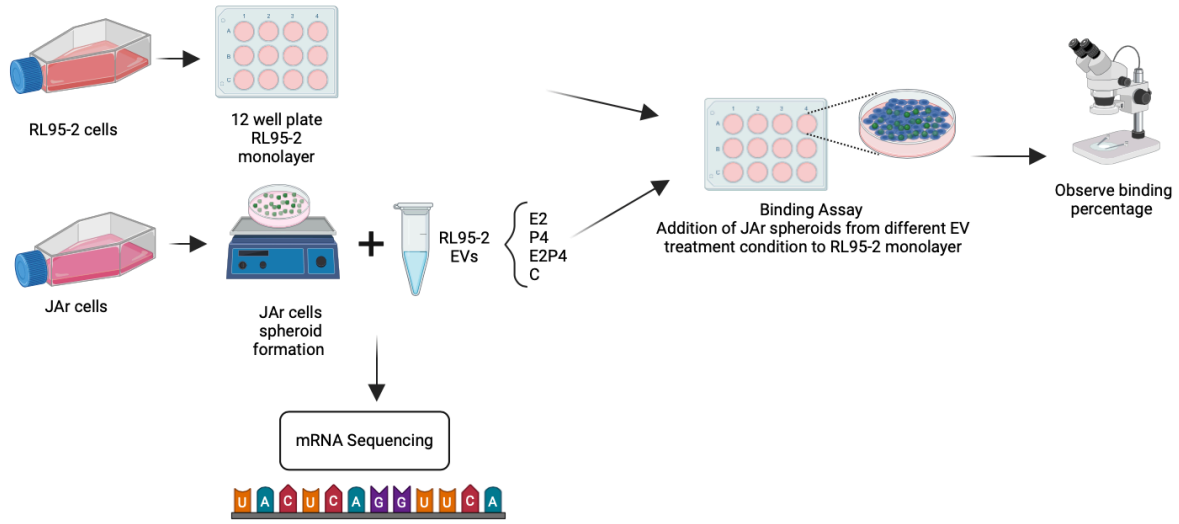


Figure 3.1. Experimental design: determining the effect of EVs derived from hormone-treated RL95-2 cells on trophoblast binding and transcriptional changes in JAr cells. (Created with BioRender.com).

3.7 Results.

3.7.1 Effect of hormone stimulated endometrial EVs on trophoblast binding.

The treatment of JAr spheroids with EVs derived from hormone-treated RL95-2 cells showed a statistically significant increase in binding affinity when treated with estrogen plus progesterone (E2P4) compared to all other groups (Figure 3.2).

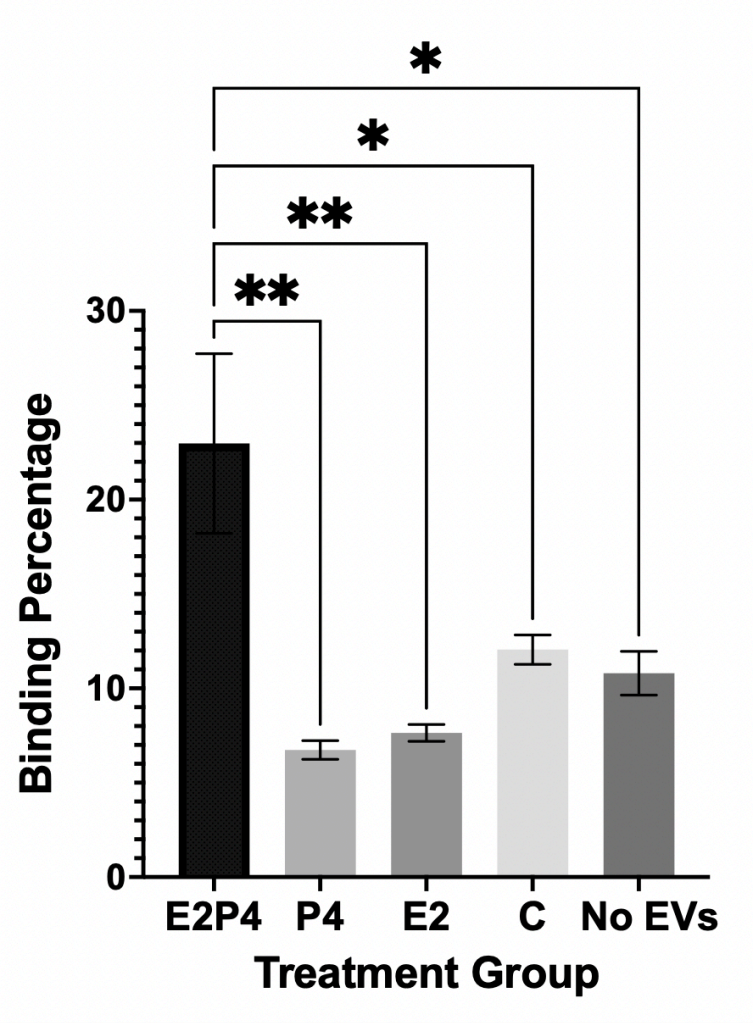


Figure 3.2. JAr spheroid RL95-2 binding affinity after JAr cell spheroid treatment with EVs derived from hormone treated RL95-2 cells. With E2P4 referring to JAr spheroids treated with EVs derived from RL95-2 cells treated with estrogen and progesterone, P4 referring to JAr spheroids treated with EVs derived from RL95-2 cells treated with progesterone, E2 referring to JAr spheroids treated with EVs derived from RL95-2 cells treated with estrogen, C referring to JAr spheroids treated with EVs derived from RL95-2 cells treated with the control and No EVs referring to JAr spheroids not treated with anything. The height of the bars represents the mean binding percentage from 3 biological replicates and 3 technical replicates. Error bars represent the standard error from the mean. One-way ANOVA was performed with Tukey post hoc test, with (*) indicating a $P \leq 0.05$ and (**) $P \leq 0.01$.the mean of each column was compared to every other column.

3.7.2 Principal component analysis (PCA) and Heat map visualisation of mRNA gene expression patterns.

The expression profile of JAr spheroids treated with EVs derived from hormone-treated RL95-2 and untreated control was analysed. The PCA plot visualises the patterns and trends (Figure 3.3), revealing subtle grouping among the different treatment groups. Sample-to-sample clustering heat maps were also generated, displaying agglomerative hierarchical clustering based on the Euclidean distances and the optimal linkage method for the various treatments and replicates (Figure 3.4).

The removal of the potential outlier replicate, replicate 1, identified during pre-batch effect adjustment (Supplementary Figure 3.5), slightly improved PCA group patterns and heatmap grouping but still resulted in overlapping expression patterns (Figure 3.4 and Figure 3.6). Further analysis was conducted on all 3 replicates due to the lack of justification to remove replicate 1 and the reduced statistical power the removal creates.

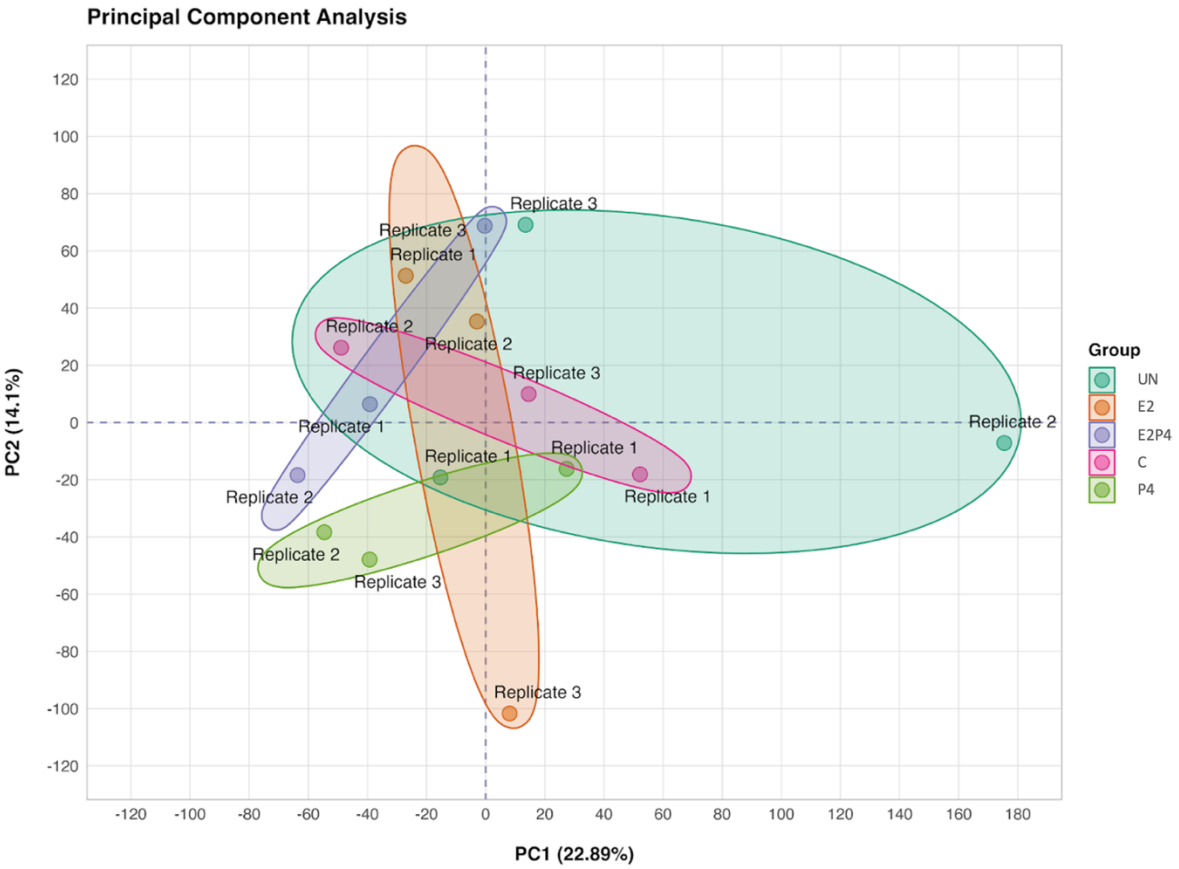


Figure 3.3. Principal component analysis (PCA) of variable proteins in the study groups from 3 replicates. With the "UN" group representing JAr cells that haven't been treated with any EVS, "E2" group representing JAr spheroids treated with EVs derived from RL95-2 cells treated with Estrogen, "E2P4" group representing JAr spheroids treated with EVs derived from RL95-2 cells treated with estrogen and progesterone, "C" group representing JAr spheroids treated with EVs derived from RL95-2 cells treated with the control and "P4" group representing JAr spheroids treated with EVs derived from RL95-2 cells treated with progesterone. *n* = 3 for each experimental condition.

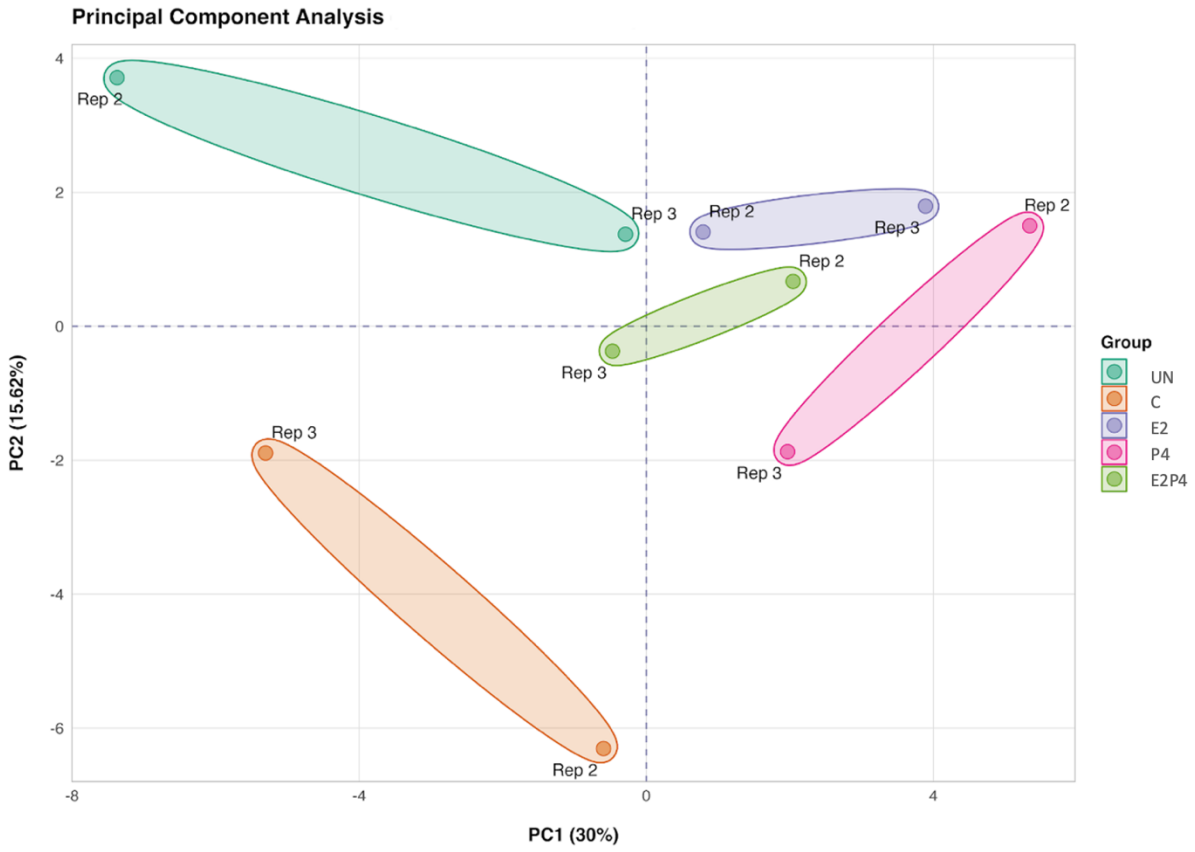


Figure 3.4. Principal component analysis (PCA) of variable proteins in the study groups, based on 2 replicates. The "UN" group represents JAr cells that haven't been treated with any EVs, "E2" group representing JAr spheroids treated with EVs derived from RL95-2 cells treated with Estrogen, the "E2P4" group represents JAr spheroids treated with EVs derived from RL95-2 cells treated with estrogen and progesterone, the "C" groups represents JAr spheroids treated with EVs derived from RL95-2 cells treated with the control, and the "P4" group only represents JAr spheroids treated with EVs derived from RL95-2 cells treated with progesterone. *n* = 2 for each experimental condition.

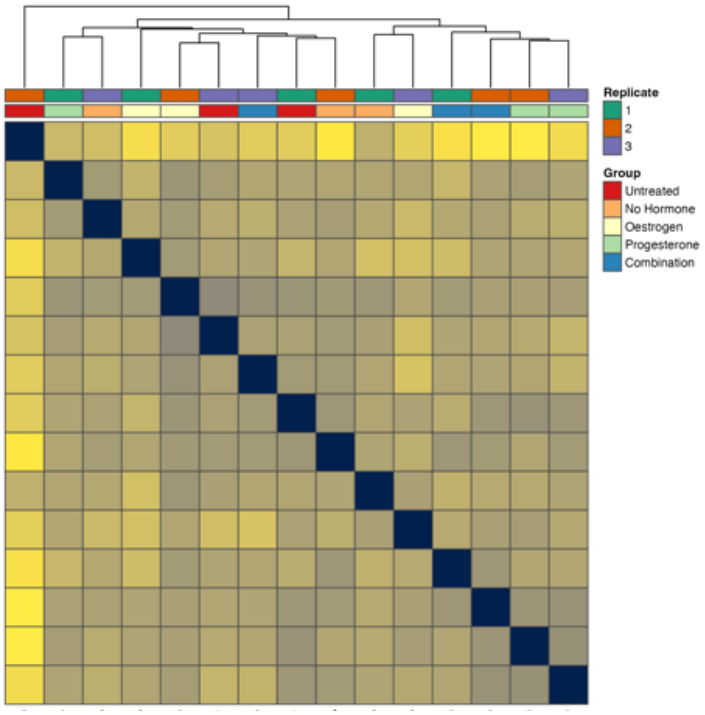


Figure 3.5. Sample-to-sample clustering heat map. Showing agglomerative hierarchical clustering based on the Euclidean distances and the Ward linkage method for all three replicates.

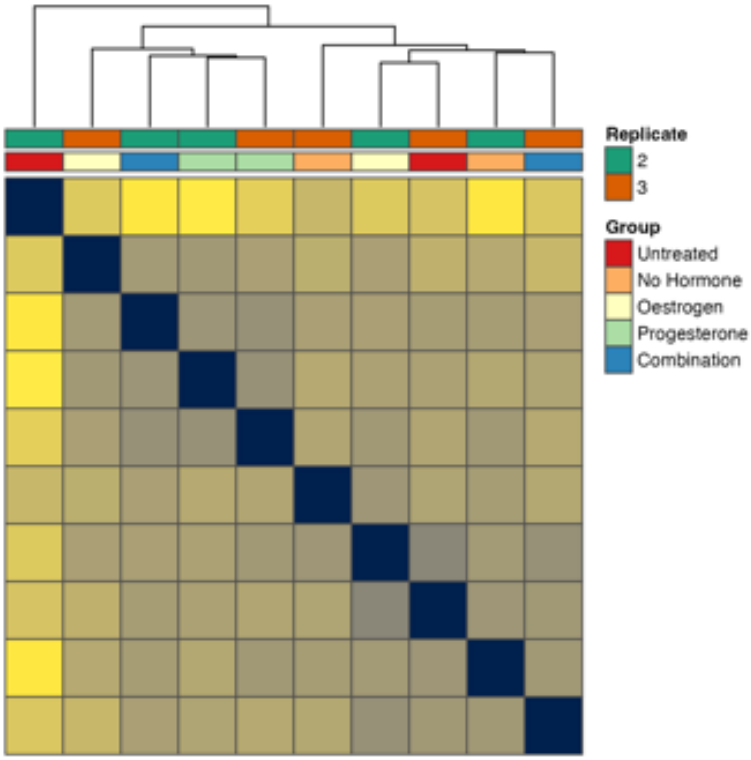
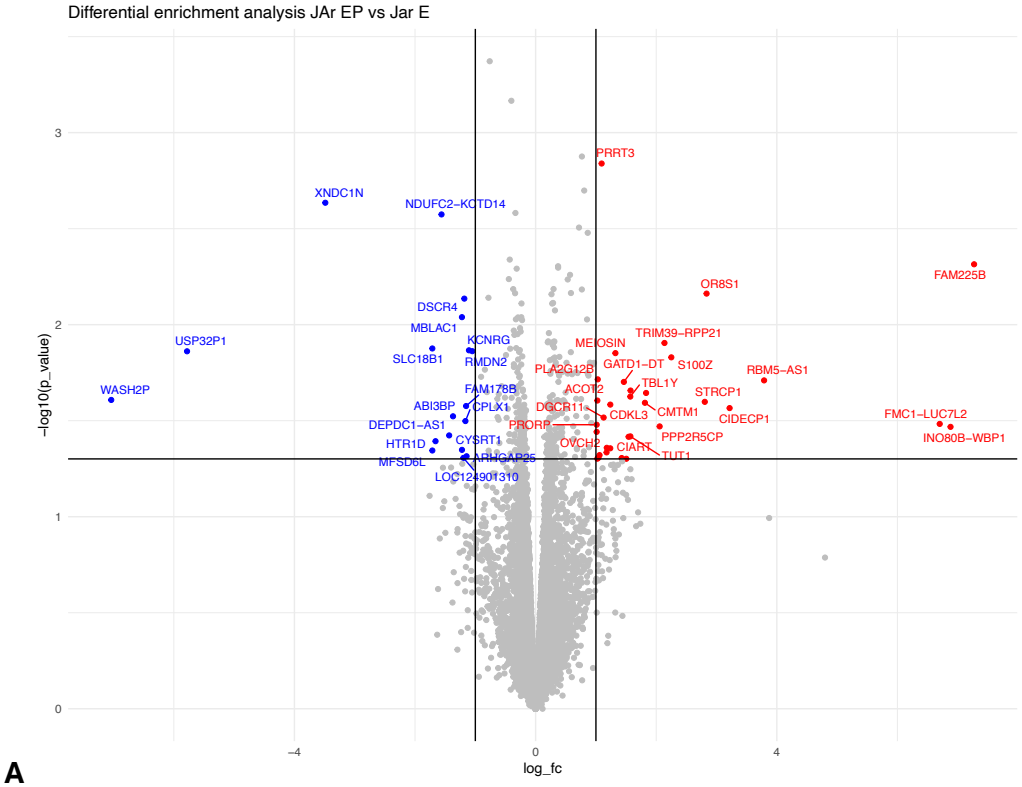


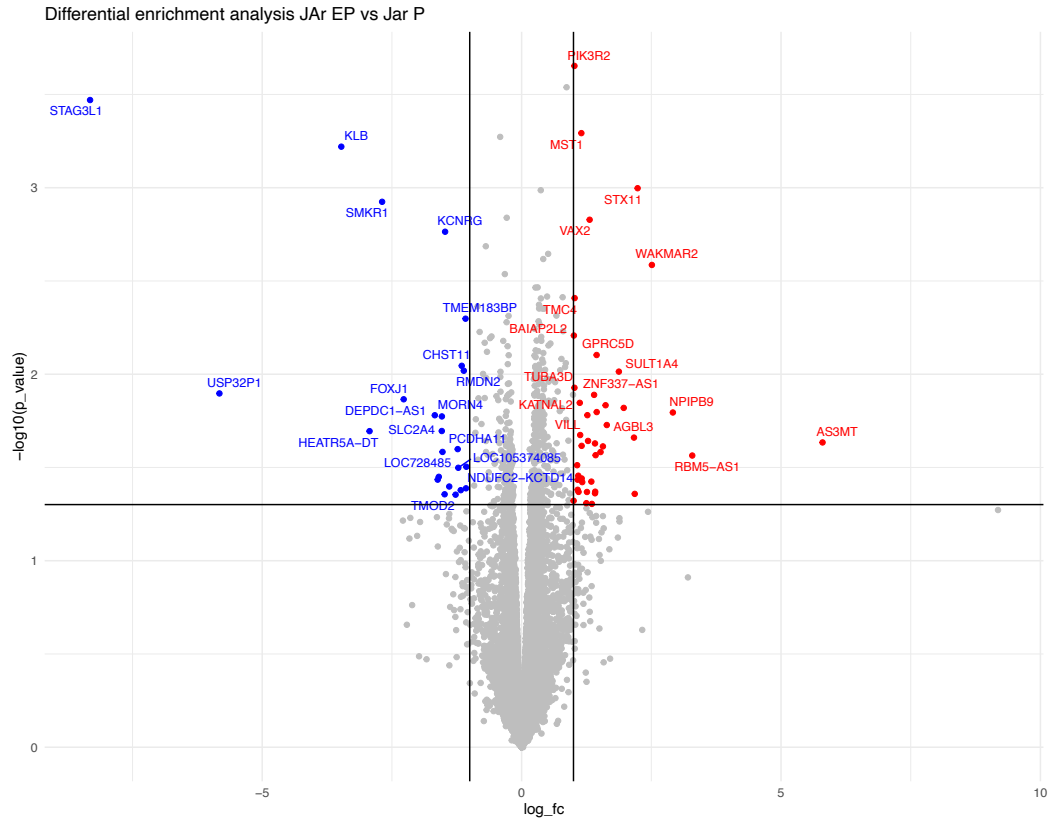
Figure 3.6. Sample-to-sample clustering heat map. Showing agglomerative hierarchical clustering based on the Euclidean distances and the Ward linkage method for two replicates, with outlier replicate 1 removed.

3.7.3 Differential enrichment analysis (DEA).

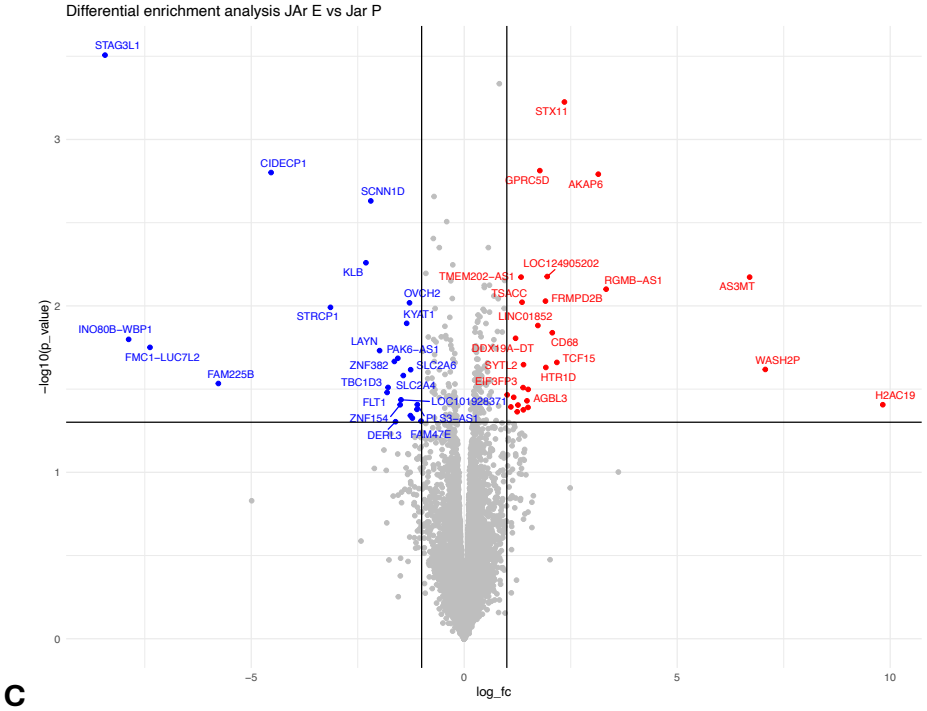
The results of the differential enrichment analysis revealed significant differences in gene expression across various comparisons. Specifically, there were a total of 51 significant genes when comparing EP v E group (Figure 3.7 A), 67 when comparing EP v P (Figure 3.7 B) , 52 when comparing E v P (Figure 3.7 C), 59 when comparing C v E (Figure 3.7 D), 78 when comparing C v P (Figure 3.7 E) , 64 when comparing C v EP (Figure 3.7 F), 79 when comparing P v UN (Figure 3.8A) , 68 when comparing EP v UN (Figure 3.8 B), 68 when comparing E v UN (Figure 3.8 C) and 71 when comparing C v UN (Figure 3.8 D). These results were obtained when employing a fold change cut-off of 1 and a p-value cut-off of 0.05. (All significant DEA results with a fold change cut-off of 1 and a p-value cut-off of 0.05 for all comparison groups with the FDR are shown in Supplementary Table 3.1 – 3.10). These findings indicate alterations in biological processes and molecular pathways under the condition's studies, specifically, the effect of the addition of EV from endometrial cells (RL95-2) on trophoblast (JAr) spheroid cell mRNA. Genes identified to be unregulated in the EP treated group compared to untreated are associated with roles in cellular adhesion. Among these, Protocadherin Gamma Subfamily A, 9 (PCDHGA9) , Protocadherin Beta 8 (PCDHB8), and Junctional Adhesion Molecule 2 (JAM2) stand out as key players, each contributing distinctively to the regulation and maintenance of cell adhesion mechanisms .


Differential enrichment analysis JAr EP vs Jar E
−log10(p_value)
log_fc
PRRT3
XNDC1N
NDUFC2−KCTD14
FAM225B
OR8S1
DSCR4
MBLAC1
USP32P1
KCNRG
SLC18B1
RMDN2
MEIOSIN
TRIM39−RPP21
GATD1−DT
S100Z
RBM5−AS1
PLA2G12B
TBL1Y
WASH2P
FAM178B
ACOT2
STRCP1
ABI3BP
CPLX1
DGCR11
CDKL3
CMTM1
CIDECP1
FMC1−LUC7L2
DEPDC1−AS1
PRORP
PPP2R5CP
INO80B−WBP1
HTR1D
CYSRT1
OVCH2
CIART
TUT1
MFSD6L
ARHGAP26
LOC123901310

A


Differential enrichment analysis JAr EP vs Jar P
−log10(p_value)
log_fc
PIK3R2
STAG3L1
KLB
MST1
STX11
SMKR1
KCNRG
VAX2
WAKMAR2
TMEM183BP
TMC4
BAIAP2L2
GPRC5D
CHST11
SULT1A4
TUBA3D
USP32P1
RMDN2
ZNF337−AS1
FOXJ1
KATNAL2
NPIPB9
DEPDC1−AS1
MORN4
VIL1
AGBL3
AS3MT
SLC2A4
HEATR5A−DT
PCDHA11
LOC728485
LOC105374085
RBM5−AS1
NDUFC2−KCTD14
TMOD2

B


Differential enrichment analysis JAr E vs Jar P
STAG3L1
STX11
CIDECP1
GPRC5D
AKAP6
SCNN1D
KLB
LOC124905202
TMEM202−AS1
RGMB−AS1
AS3MT
OVCH2
TSACC
FRMPD2B
STRCP1
KYAT1
LINC01852
INO80B−WBP1
LAYN
CD68
FMC1−LUC7L2
PAK6−AS1
DDX19A−DT
TCF15
WASH2P
ZNF382
SLC2A6
SYTL2
FAM225B
TBC1D3
SLC2A4
EIF3FP3
HTR1D
H2AC19
FLT1
LOC101928371
AGBL3
ZNF154
CPLX3−AS1
DERL3
FAM47E
−log10(p_value)
log_fc
C


Differential enrichment analysis JAr C vs Jar E
MECOM
TMEM63C
LINC01852
OR7E14P
ZNF528−AS1
GPER1
LRRC24
NEDD8−MDP1
DLL4
MAK
ZNF747−DT
TIMP3
ANKRD31
LOC100419515
PRDZ
RPS27AP5
PTP4A1
SMIM5
LOC101927401
STAG3L1
SLC27A1
LINC00926
PAK6−AS1
TCAP
RRP12
ZNF75
SLC2A6
RRP7BP
TBC1D3K
MFSD4A
KCP
H2AC19
VPS37D
PTPRQ
NTS
ZNF154
RBM5−AS1
SLC6A13
CLEC7A
SNX22
IFITM2
LOC105374085
THSD4
HPSE2
−log10(p_value)
log_fc
D

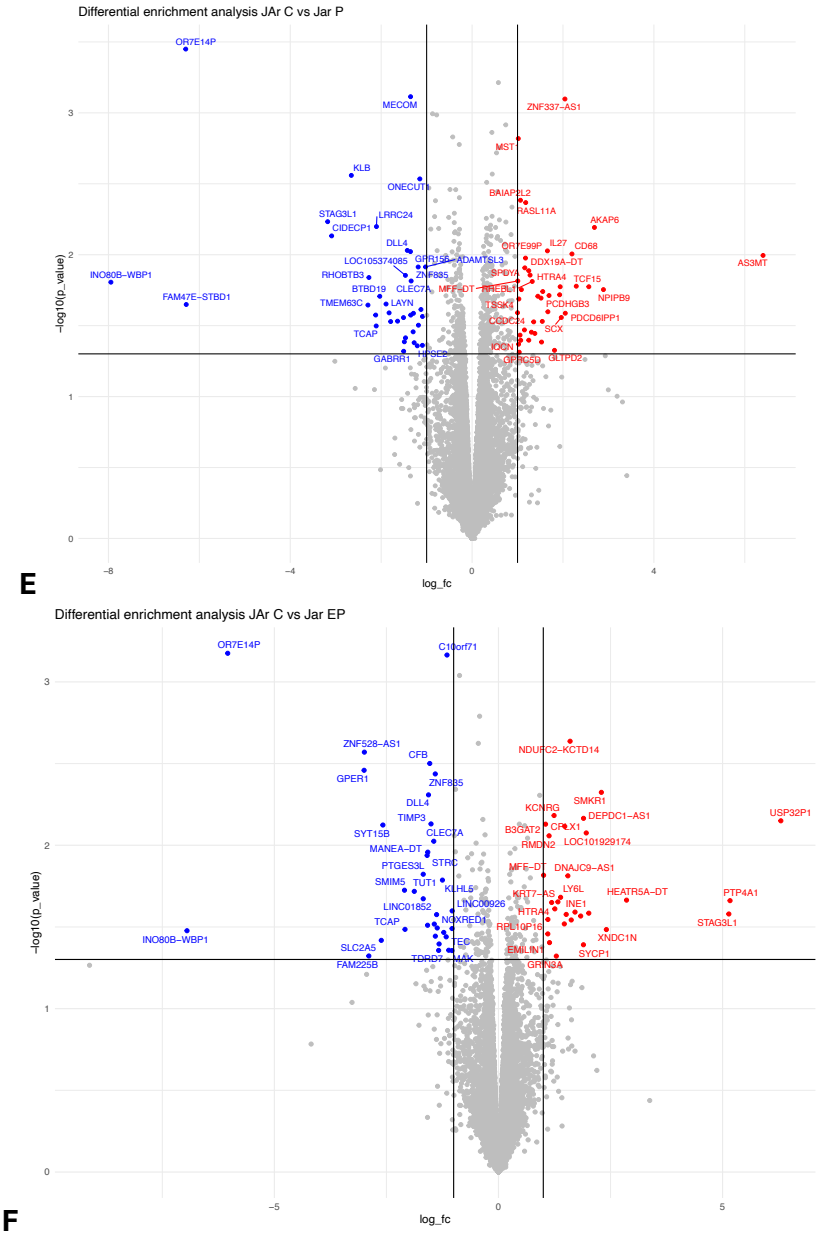
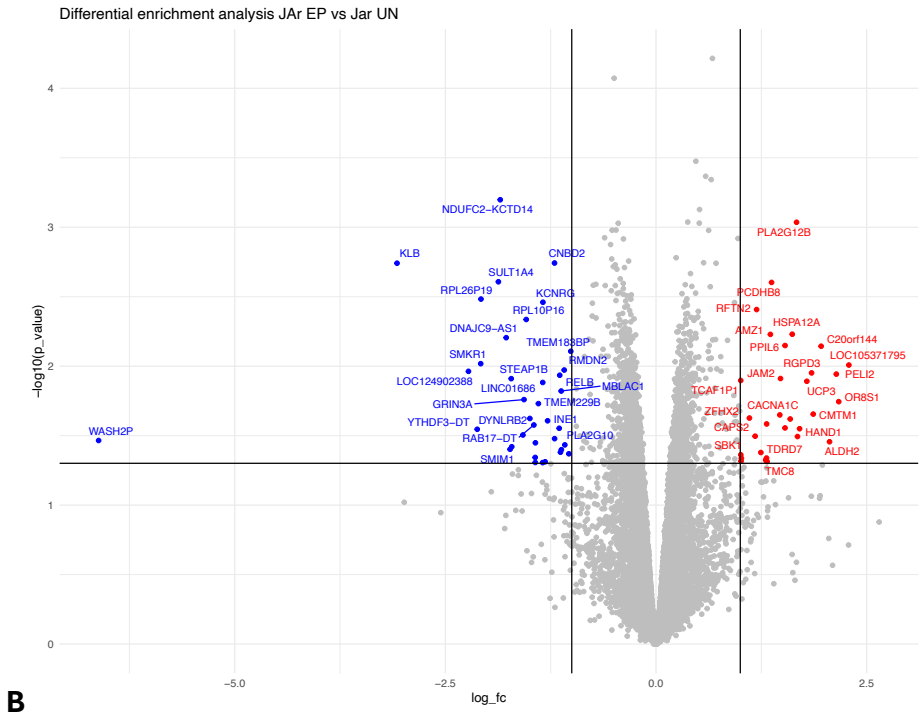
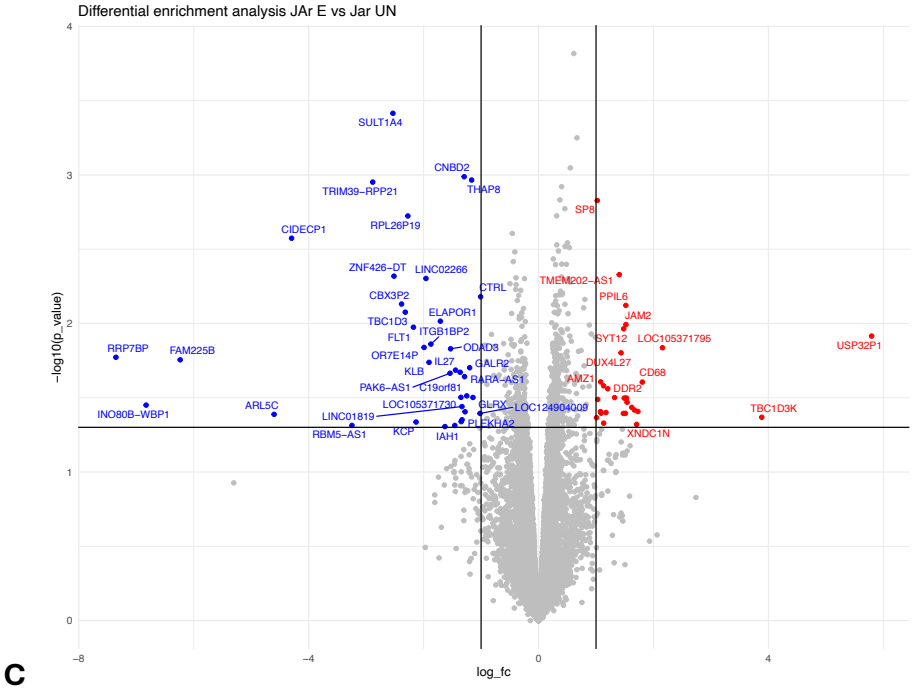


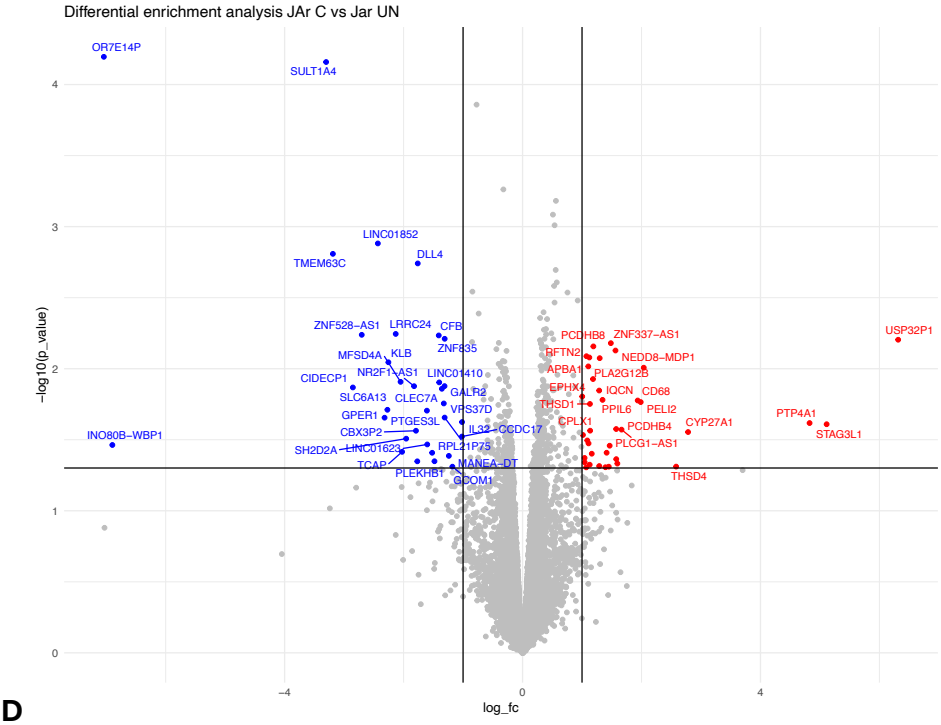
Figure 3.7. Differential enrichment analysis of JAr genes in different comparison groups with the different EV treatment. (**A**) Volcano plot of the differentially expressed genes of JAr cell in the EV estrogen plus progesterone treated group (EP) compared to the estrogen treated group (E); (**B**) estrogen plus progesterone supplemented groups (EP) compared to the progesterone group (P). (**C**) Volcano plot of the differentially expressed genes of JAr cell in the EV estrogen treated groups (E) compared to the progesterone treated group (P); (**D**) control supplemented groups (C) compared to the estrogen group (E). (**E**) Volcano plot of the differentially expressed genes of JAr cell in the EV control treated groups (C) compared to the progesterone treated group (P); (**F**) control supplemented groups (C) compared to the estrogen and progesterone treated group (EP). Adjusted *p* values (−log10) are plotted against the fold changes (log2) based on a fold change cut-off of 1 and a p-value cut-off of 0.05. Red dots represent enriched proteins whereas blue dots represent depleted proteins in the respective comparisons.


Differential enrichment analysis JAr P vs Jar UN
SULT1A4
STAG3L1
LDHD
ADAMTSL3
LOC105371795
LINC01852
GPRC5D
RFTN2
PLA2G12B
AKAP6
RPL26P19
DDX19A-DT
SLC26A4
AS3MT
STPG3-AS1
HSPA12A
GBP3
IL27
VAX2
APBA1
SYT12
USP32P1
NPIPB9
PELI2
ZDHHC11B
RHOBTB3
ARLNC1
CYP27A1
WASH2P
GPR156
TNKS2-DT
TTLL2
SNX10-AS1
−log10(p_value)
log_fc
A


Differential enrichment analysis JAr EP vs Jar UN
NDUFC2-KCTD14
PLA2G12B
KLB
CNBD2
SULT1A4
PCDHB8
RPL26P19
KCNRG
RFTN2
RPL10P16
HSPA12A
DNAJC9-AS1
AMZ1
C20orf144
TMEM183BP
PPIL6
LOC105371795
SMKR1
RMDN2
RGPD3
STEAP1B
JAM2
PELI2
LOC124902388
RELB
LINC01686
MRLAC1
TCAF1P1
UCP3
GRIN3A
TMEM229B
OR8S1
CACNA1C
YTHDF3-DT
DYNLRB2
INE1
ZFHX2
CMTM1
RAB17-DT
PLA2G10
CAPS2
HAND1
WASH2P
SBK1
TDRD7
ALDH2
SMIM1
TMC8
−log10(p_value)
log_fc
B



C



D

Figure 3.8. Differential enrichment analysis of JAr genes in different comparison groups with the different EV treatment compared to untreated JAr cells. (**A**) Volcano plot of the differentially expressed genes of JAr cell in the EV progesterone treated groups (P) compared to the untreated group (UN); (**B**) estrogen and progesterone supplemented groups (EP) compared to the untreated group (UN). (**C**) Volcano plot of the differentially expressed genes of JAr cell in the EV estrogen treated groups (E) compared to the untreated group (UN); (**D**) control groups (C) compared to the untreated group (UN). Adjusted *p* values (−log10) are plotted against the fold changes (log2) based on a fold change cut-off of 1 and a p-value cut-off of 0.05. Red dots represent enriched proteins whereas blue dots represent depleted proteins in the respective comparisons.

3.7.4 Gene set enrichment analysis (GSEA).

GSEA was conducted on all possible comparisons (Figure 3.9, 3.10, 3.11, 3.12 and 3.13) to identify pathways of potential biological importance. Due to the inter-group relatedness, very few significantly enriched pathways were identified. The pathways “ribosome” and “oxidative phosphorylation” were significantly down-regulated in the EP v UN, P v UN, and E v EP comparison groups, and significantly upregulated in the C v EP comparison group. When comparing all pathways shown to be upregulated in the EP treated groups in all comparisons, 52 pathways (listed in Supplementary Table 3.11) were commonly identified (Figure 3.14). Among these pathways, several key KEGG pathways were identified in roles suspected to be involved in the pregnancy and implantation processes. Notably, pathways associated with glycosphingolipid biosynthesis, such as "Glycosphingolipid Biosynthesis Globo Series" and "Glycosphingolipid Biosynthesis Lacto and Neolacto Series," displayed alterations, suggesting a potential impact on cellular membrane composition. Immune-related pathways, including "FC Gamma R Mediated Phagocytosis," "T Cell Receptor Signalling Pathway," and "Natural Killer Cell Mediated Cytotoxicity," were also markedly affected, implying a modulation of immune responses critical for pregnancy success. Additionally, pathways associated with cellular signalling, metabolism, and DNA repair mechanisms, such as " Insulin Signalling Pathway," "VEGF Signalling Pathway," and "Non-Homologous End Joining," exhibited significant dysregulation, highlighting the intricate interplay between hormonal influences and cellular functions.

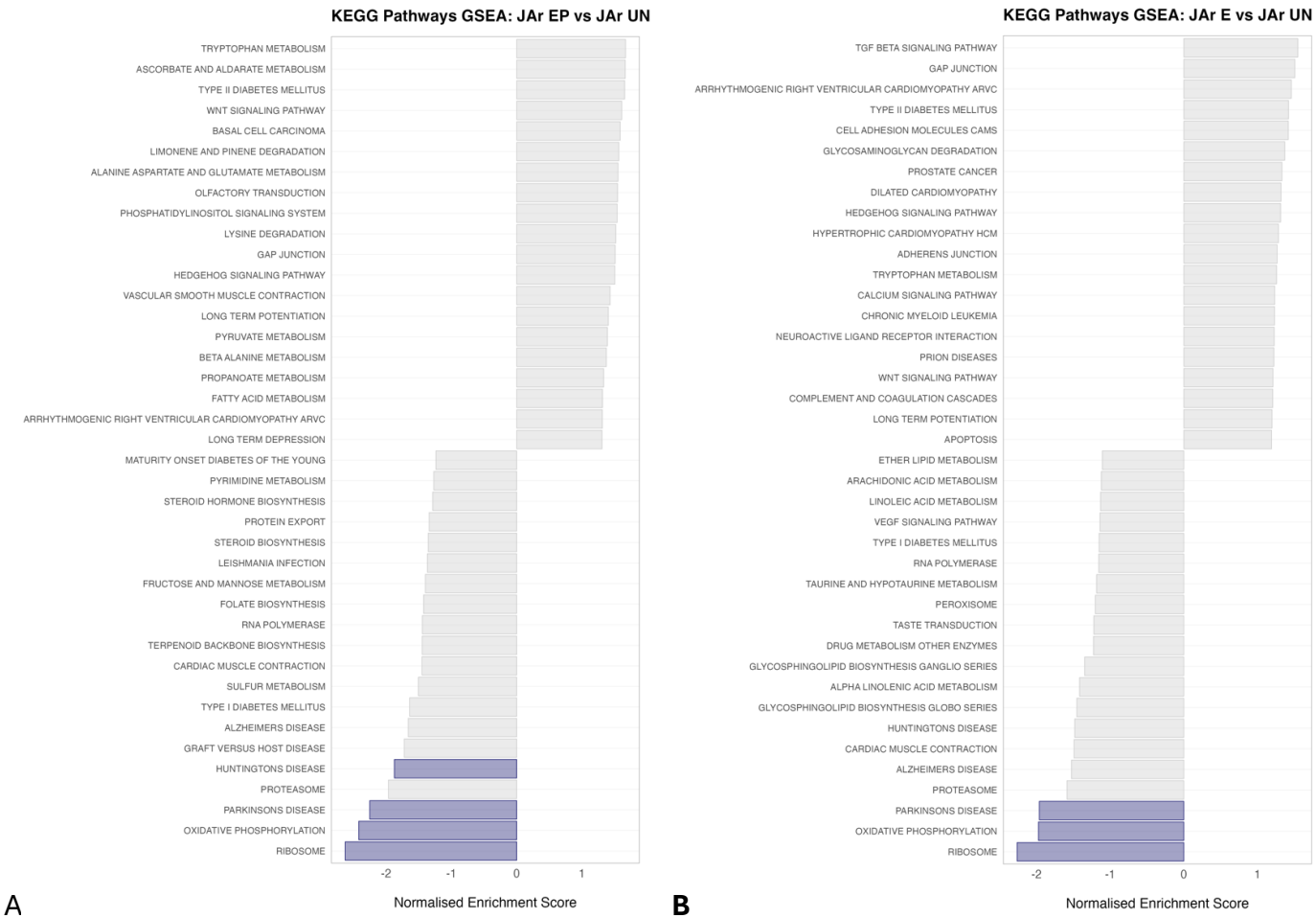


Figure 3.9. KEGG pathway analysis of GSEA in the different comparison groups, displaying the top 20 up and down regulated pathways. (A) KEGG pathway analysis of JAr cell spheroids treated with EV derived from Estrogen and progesterone treated RL95-2 cells versus JAr cell spheroids untreated. (B) KEGG pathway analysis of JAr cell spheroids treated with EV derived from Estrogen treated RL95-2 cells versus JAr call spheroids untreated. The length of the bar indicating the normalised enrichment score, with significant results (Padj ≤ 0.05) shown in blue.

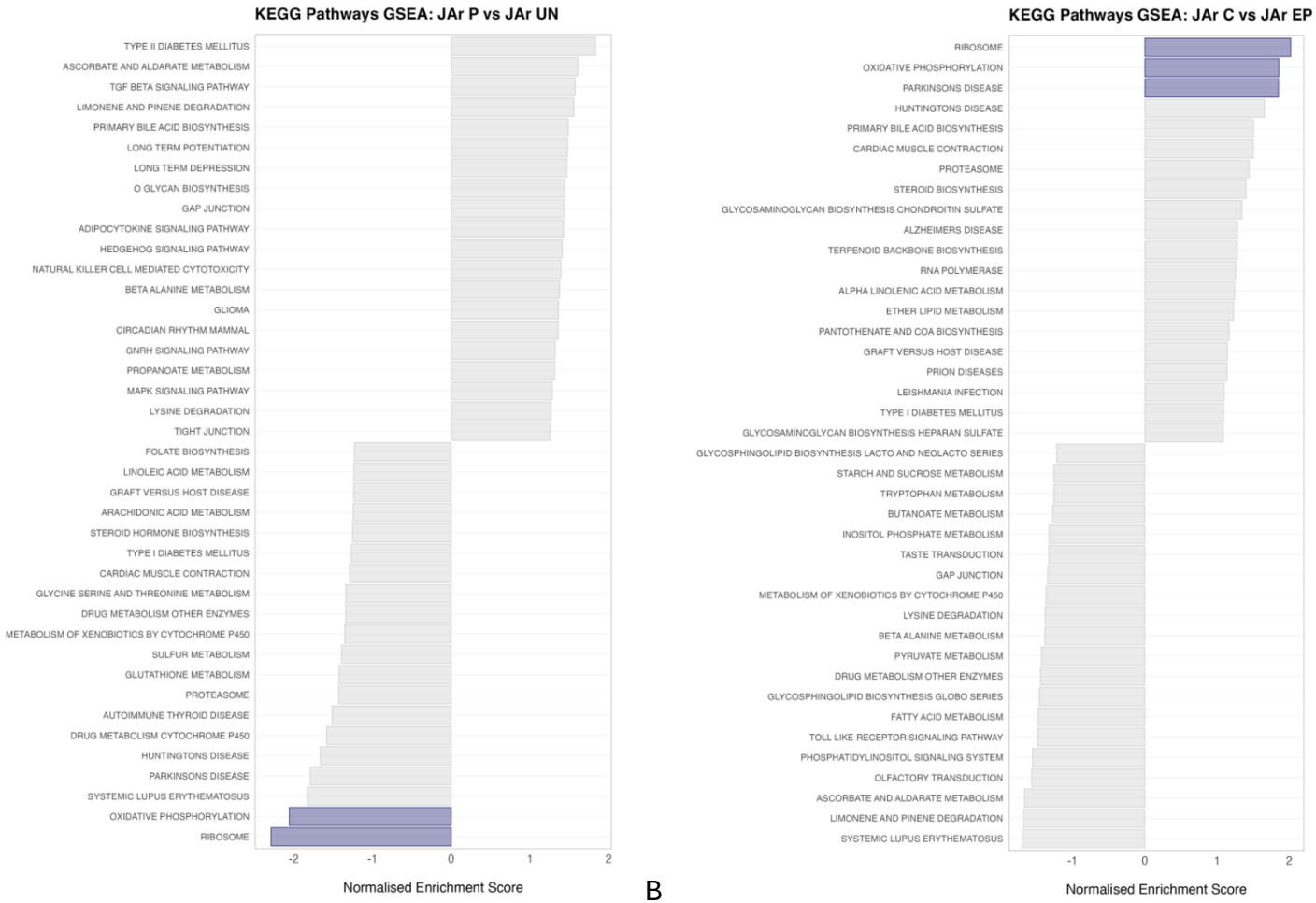


Figure 3.10. KEGG pathway analysis of GSEA in the different comparison groups, displaying the top 20 up and down regulated pathways. (A) KEGG pathway analysis of JAr cell spheroids treated with EV derived from progesterone treated RL95-2 cells versus JAr cell spheroids untreated. (B) KEGG pathway analysis of JAr cell spheroids treated with EV derived from control treated RL95-2 cells versus JAr cell spheroids treated with EV derived from Estrogen and progesterone treated RL95-2 cells The length of the bar indicating the normalised enrichment score, with significant results (Padj ≤ 0.05) shown in blue.

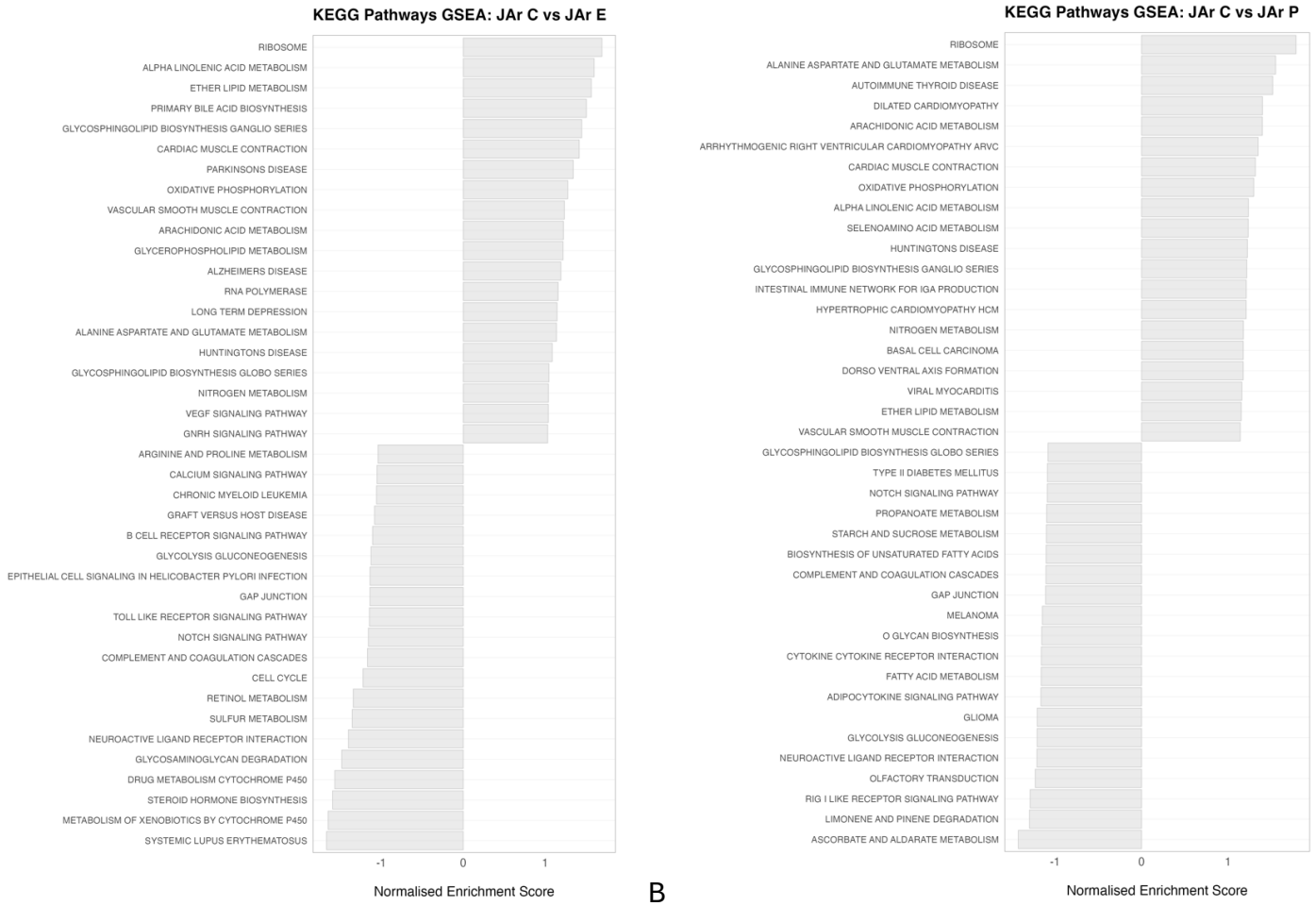


Figure 3.11. KEGG pathway analysis of GSEA in the different comparison groups, displaying the top 20 up and down regulated pathways. (A) KEGG pathway analysis of JAr cell spheroids treated with EV derived from control treated RL95-2 cells versus JAr cell spheroids treated with EVs derived from estrogen treated RL95-2 cells.(B) KEGG pathway analysis of JAr cell spheroids treated with EV derived from control treated RL95-2 cells versus JAr cell spheroids treated with EV derived from progesterone treated RL95-2 cells The length of the bar indicating the normalised enrichment score.

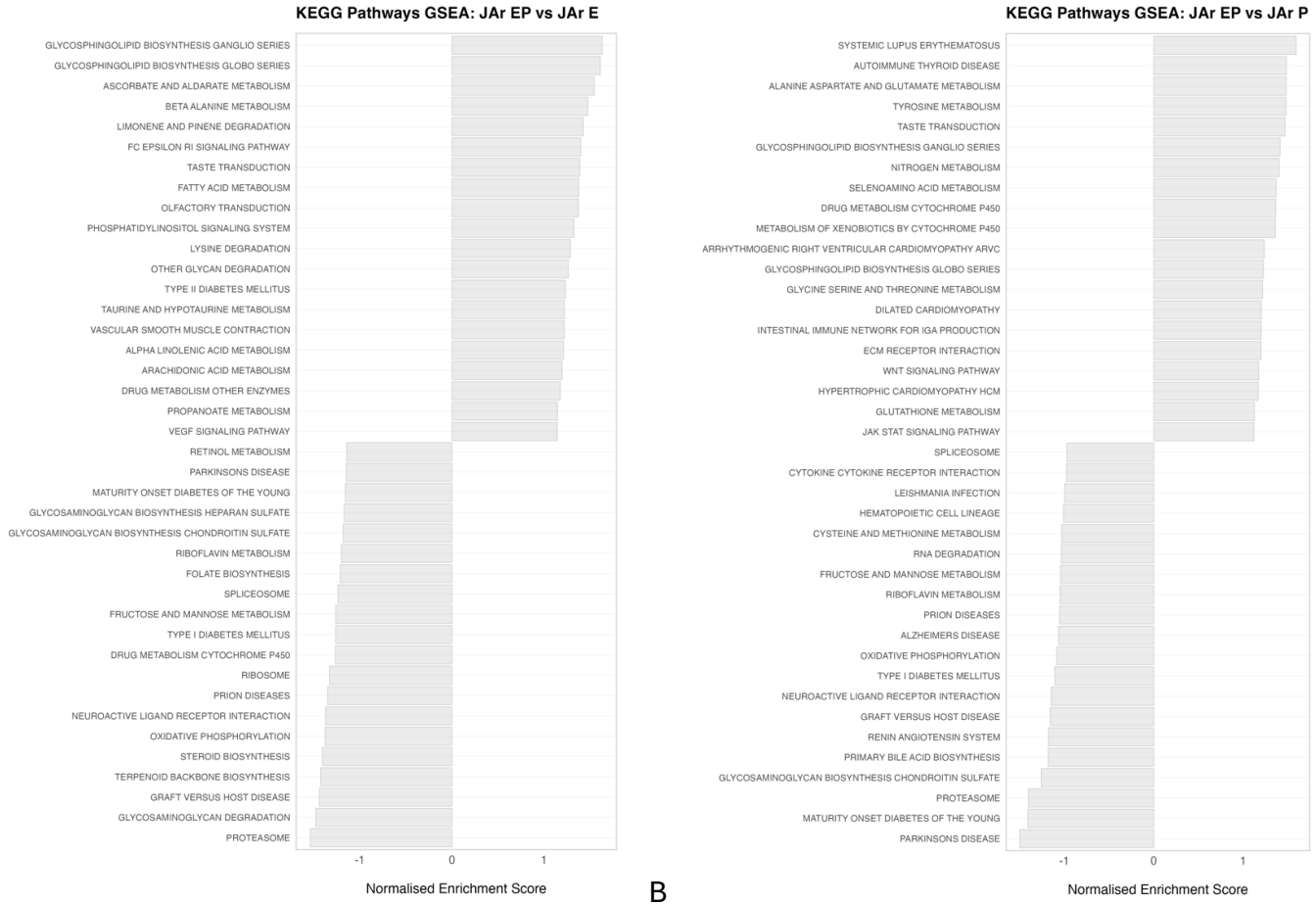


Figure 3.12. KEGG pathway analysis of GSEA in the different comparison groups, displaying the top 20 up and down regulated pathways. (A) KEGG pathway analysis of JAr cell spheroids treated with EV derived from EP treated RL95-2 cells versus JAr cell spheroids treated with EVs derived from estrogen treated RL95-2 cells. (B) KEGG pathway analysis of JAr cell spheroids treated with EV derived from estrogen and progesterone treated RL95-2 cells versus JAr cell spheroids treated with EV derived from progesterone treated RL95-2 cells. The length of the bar indicating the normalised enrichment score.

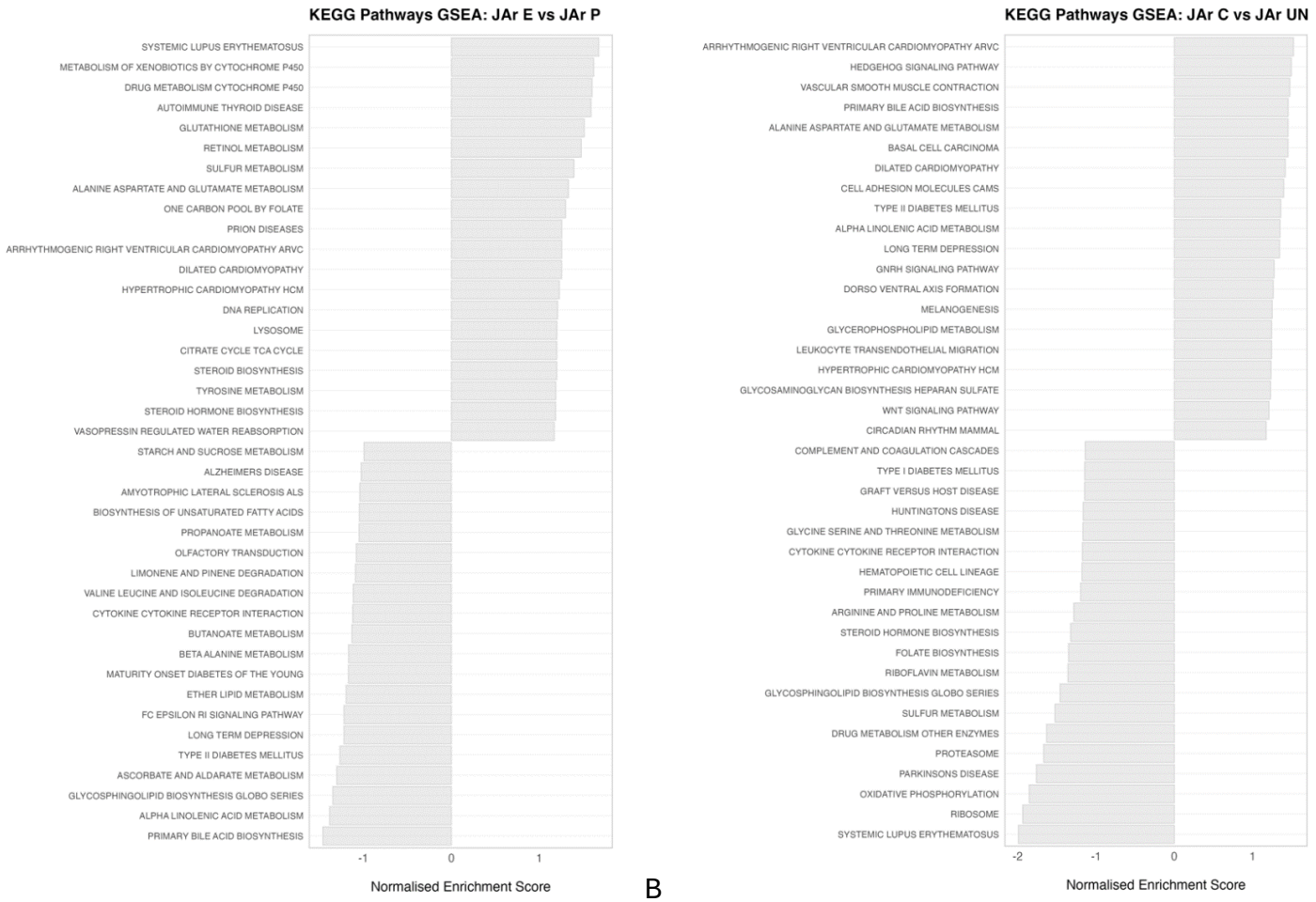


Figure 3.13. KEGG pathway analysis of GSEA in the different comparison groups, displaying the top 20 up and down regulated pathways. (A) KEGG pathway analysis of JAr cell spheroids treated with EV derived from estrogen treated RL95-2 cells versus JAr cell spheroids treated with EVs derived from progesterone treated RL95-2 cells. (B) KEGG pathway analysis of JAr cell spheroids treated with EV derived from control treated RL95-2 cells versus JAr cell spheroids untreated. The length of the bar indicating the normalised enrichment score.

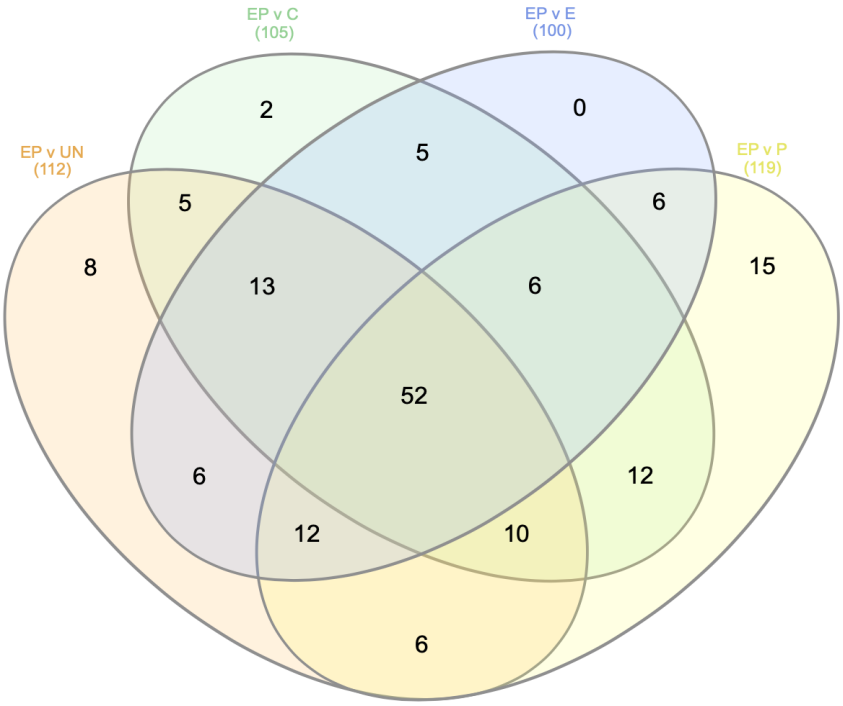


Figure 3.14. Venn diagram of GSEA KEGG pathways upregulated in JAr spheroid group treated with EVs derived from estrogen and progesterone treated RL95-2 cells compared to all other treatment and control groups.

3.8 Discussion.

We have previously suggested that the hormonal treatment of RL95-2 cells, mimicking the menstrual cycle, resulted in distinct proteomic changes in the EVs derived from these cells (14). This previous study as well as other reports have suggested that EVs derived from the endometrium could contribute to embryo-maternal communication to promote embryo implantation (13,22). The current investigation explores further the functional role of EVs during the menstrual cycle, with subsequent co-incubation of endometrial EVs with JAr spheroids. Results revealed a significant increase in trophoblast binding affinity in the presence of estrogen and progesterone (E2P4), which mimics the WOI environment, compared with the other treatment groups. This result emphasises the potential regulatory roles of hormones in modulating endometrial EVs and their impact

on trophoblast behaviour during implantation. The significant increase in trophoblast binding suggests potential mechanisms or regulation induced by the presence of the EVs released at the time of the WOI to aid in trophoblast binding. Previous studies have suggested that such regulation could come from complex interplay of various molecular mechanisms including proteomics signalling pathways or transcriptomic modulation (8,17). Explored within this study was the potential transcriptomic modulation. Here we observed differential enrichment of genes and alterations in GSEA KEGG pathways, particularly those associated with implantation.

While trying to uncover a mechanism associated with the increase in trophoblast binding upon the addition of EV from endometrial cells under estrogen and progesterone conditions, differential enrichment analysis revealed a modulation in gene expression of trophoblast cells when compared to the untreated group. Notably, pivotal genes such as PCDHGA9, PCDHB8, and JAM2 are seen to be upregulated in response to this EV treatment. Among these genes, PCDHGA9 and PCDHB8, members of the protocadherin gene family, are recognised for their roles in mediating cell-cell adhesion and facilitating tissue morphogenesis (23), crucial processes in embryo implantation and placental development. Additionally, the heightened expression of JAM2, a junctional adhesion molecule, suggests a reinforcement of cell-cell interactions and barrier functions essential for successful embryo implantation and subsequent placental formation. It has been evidenced in a previous study that also demonstrated an increase in JAM2 expression in preimplantation embryos, which was also associated with an increase in adhesion rate in an adhesion assay, further supporting the role JAM2 potentially facilitated in embryo implantation (24). These findings illuminate the significant impact

of EV-mediated communication in coordinating the molecular dialogues necessary for the establishment and maintenance of pregnancy.

In addition to differential enrichment analysis, GSEA provided insights into the potential pathways involved in the observed changes in the binding assay. Again, we see very few individual KEGG pathways showing significant effects in isolation, however, they can still be influential on cellular function or biological processes through their interactions with other pathways, their context-dependent roles, or their contributions to regulatory networks. Our results reveal pathways that could play various roles in the process of implantation in the binding assay, contributing to aspects such as cellular adhesion, immune modulation, and signalling. For example, upregulation of the "Glycosphingolipid Biosynthesis Globo Series" and "Glycosphingolipid Biosynthesis Lacto and Neolacto Series" gene sets in the JAr spheroids treated with EVs derived from estrogen and progesterone-treated RL95-2 indicates a potential effect on cellular adhesion processes during embryo implantation. These complex pathways are involved in glycosphingolipids biosynthesis, molecules known for their vital roles in cell recognition and adhesion (25,26). The alteration in these pathways may have influenced the adhesive properties of the cells, affecting their interaction with the endometrium, hence increasing the binding affinity. Modulation of glycosphingolipid biosynthesis pathways suggests a multifaceted regulatory mechanism that plays a crucial role in facilitating the initial attachment and subsequent interactions between the developing embryo and the maternal environment.

Other pathways seen to be upregulated in JAr cells with the same treatment mimicking the window of implantation collectively indicate a complex cellular response involving immune activation. The upregulation in pathways such as “B Cell Receptor Signalling Pathway” and “T Cell Receptor Signalling Pathway” indicates an activation of adaptive immune responses through B and T cells (27). The upregulation of this pathway with the treatment is consistent with publications that B and T cells increase at the time of implantation, helping with immune regulation and promoting trophoblast invasion, vascular and tissue remodelling (28–30). The involvement of “Natural Killer Cell Mediated Cytotoxicity” suggests an enhanced cytotoxic capability of natural killer cells (31). This finding supports a number of studies suggesting sex hormones govern natural killer cell migration into the endometrium and their accumulation around the invading trophoblasts (32,33), with our data also suggesting that this in turn affects the trophoblast cells. Moreover, the upregulation in the “Toll Like Receptor Signalling Pathway” signifies an increased sensitivity to microbial components, indicating a possible activated state of the innate immune response. While some TLRs are closely associated with innate immunity, it's important to note that not all TLRs exclusively function within this domain. Nevertheless, this finding is consistent with previous studies, suggesting that embryos and trophoblast express TLR receptors and respond to TLR ligands (34), with a study showing that when blastocysts with TLR5 were stimulated with ligands Poly (I: C) (a synthetic analogy of double stranded RNA to mimic viral infection) and flagellin this caused changes in mRNA expression levels of TLR genes (35). The immune modulation is further supported by the upregulation in “Complement and Coagulation Cascades'', highlighting potential involvement in complement activation, with roles of the complement system well recognised in implantation and having

hormonal regulation throughout the menstrual cycle (36–38). The pathway "Fc Epsilon RI Signalling Pathway", associated with allergic responses and mast cell activation, adds another layer to the immune activation profile. Collectively, these findings underscore the intricate immunological responses elicited by the endometrial extracellular vesicles on the trophoblast and point toward a potential influence on cellular processes, with implications for embryo implantation and broader physiological outcomes.

It is worth noting that the utilisation of mRNA sequencing in genetic research is contingent on robust experimental design and significance cut-off values. In this study, the mRNA sequencing analysis was performed with only three biological replicates, a limitation that could compromising the statistical power but also exacerbate the challenge of distinguishing genuine biological signals from background noise. A higher number of replicates would facilitate a more accurate estimation of the true distribution of expression values, reducing the influence of outliers and increasing the confidence in identifying statistically significant differences (39). Our DEA also doesn't consider FDR, so the reported significant enrichments should be interpreted cautiously, as they may include a proportion of false positives, however, they may be indicative of an important underlying mechanism. While our study provides some insight, the use of a limited number of biological replicates and significant cut-off values means mRNA results should be interpreted cautiously. Future studies are warranted to strengthen the robustness of the findings.

Nevertheless, the observed pathways and gene alterations collectively suggest potential roles of EVs derived from estrogen and progesterone-treated RL95-2 cells on JAr

spheroids, including cellular adhesion, immune modulation, and signalling during embryo implantation. Notably, the significant change in trophoblast binding observed with the addition of EVs derived from the endometrium simulating the window of implantation suggests the involvement of a mechanism to aid in embryo implantation. However, further experimental investigation and validation are required to reveal the specific mechanisms and functional consequences associated with the reported pathways activated in this context. Additional experiments, such as pathway-specific inhibition or activation using specific inhibitors or activators for key components within the identified pathways to assess their direct impact on cellular functions related to implantation would be advantageous in providing insight. The current findings simply provide a framework for further investigations to elucidate the specific mechanisms and functional consequences associated with the observed pathway activations in the context of implantation.

3.9 Conclusion.

In conclusion, our study has begun to provide an insight into the intricate interplay between endometrial-derived EVs and trophoblasts during the implantation process. Our findings reveal significant alteration in trophoblast binding affinity, accompanied by changes in pathways known to have roles in implantation. While further research is required to understand the precise molecular mechanisms involved, these contribute to the growing understanding of the complex communication networks that regulate embryo implantation.

3.10 References.

1. Ochoa-Bernal MA, Fazleabas AT. Physiologic Events of Embryo Implantation and Decidualization in Human and Non-Human Primates. Int J Mol Sci. 2020 Mar 13;21(6):1973.

2. Kim SM, Kim JS. A Review of Mechanisms of Implantation. Dev Reprod. 2017;21(4).

3. Massimiani M, Lacconi V, La Civita F, Ticconi C, Rago R, Campagnolo L. Molecular signaling regulating endometrium–blastocyst crosstalk. Int J Mol Sci. 2020;21(1).

4. Bashiri A, Halper KI, Orvieto R. Recurrent Implantation Failure-update overview on etiology, diagnosis, treatment and future directions. Reprod Biol Endocrinol. 2018;16(1).

5. Chen K, Liang J, Qin T, Zhang Y, Chen X, Wang Z. The Role of Extracellular Vesicles in Embryo Implantation. Front Endocrinol. 2022 Jan 28;13:809596.

6. Fazeli A, Godakumara K. The evolving roles of extracellular vesicles in embryo-maternal communication. Commun Biol. 2024 Jun 21;7(1):754.

7. Van Niel G, D'Angelo G, Raposo G. Shedding light on the cell biology of extracellular vesicles. Nat Rev Mol Cell Biol. 2018 Apr;19(4):213–28.

8. Piibor J, Waldmann A, Dissanayake K, Andronowska A, Ivask M, Prasadani M, et al. Uterine Fluid Extracellular Vesicles Proteome Is Altered During the Estrous Cycle. Mol Cell Proteomics. 2023;22(11):100642.

9. Muhandiram S, Dissanayake K, Orro T, Godakumara K, Kodithuwakku S, Fazeli A. Secretory Proteomic Responses of Endometrial Epithelial Cells to Trophoblast-Derived Extracellular Vesicles. Int J Mol Sci. 2023;24(15).

10. Piibor J, Dissanayake K, Midekessa G, Andronowska A, Kavak A, Waldmann A, et al. Characterization of bovine uterine fluid extracellular vesicles proteomic profiles at follicular and luteal phases of the oestrous cycle. Vet Res Commun. 2023;47(2).

11. Almiñana C, Corbin E, Tsikis G, Soleilhavoup C, Galio L, Sandra O, et al. 108 Characterization Of Bovine Oviductal Exosomes From In Vivo And In Vitro Origin. Reprod Fertil Dev. 2015;27(1).

12. Dissanayake K, Nõmm M, Lättekivi F, Ord J, Ressaissi Y, Godakumara K, et al. Oviduct as a sensor of embryo quality: deciphering the extracellular vesicle (EV)-mediated embryo-maternal dialogue. J Mol Med. 2021;99(5).

13. Ng YH, Rome S, Jalabert A, Forterre A, Singh H, Hincks CL, et al. Endometrial Exosomes/Microvesicles in the Uterine Microenvironment: A New Paradigm for Embryo-Endometrial Cross Talk at Implantation. PloS One. 2013;8(3):p.e58502.

14. Hart AR, Khan NLA, Dissanayake K, Godakumara K, Andronowska A, Eapen S, et al. The Extracellular Vesicles Proteome of Endometrial Cells Simulating the Receptive Menstrual Phase Differs from That of Endometrial Cells Simulating the Non-Receptive Menstrual Phase. Biomolecules. 2023;13(2).

15. Sarker S, Scholz-Romero K, Perez A, Illanes SE, Mitchell MD, Rice GE, et al. Placenta-derived exosomes continuously increase in maternal circulation over the first trimester of pregnancy. J Transl Med. 2014;12(1).

16. Es-Haghi M, Godakumara K, Häling A, Lättekivi F, Lavrits A, Viil J, et al. Specific trophoblast transcripts transferred by extracellular vesicles affect gene expression in endometrial epithelial cells and may have a role in embryo-maternal crosstalk. Cell Commun Signal. 2019.

17. Godakumara K, Ord J, Lättekivi F, Dissanayake K, Viil J, Boggavarapu NR, et al. Trophoblast derived extracellular vesicles specifically alter the transcriptome of endometrial cells and may constitute a critical component of embryo-maternal communication. Reprod Biol Endocrinol. 2021;19(1):115.

18. Giacomini E, Vago R, Sanchez AM, Podini P, Zarovni N, Murdica V, et al. Secretome of in vitro cultured human embryos contains extracellular vesicles that are uptaken by the maternal side. Sci Rep. 2017.

19. Khan M, Nickoloff E, Abramova T, Johnson J, Verma SK, Krishnamurthy P, et al. Embryonic Stem Cell-Derived Exosomes Promote Endogenous Repair Mechanisms and Enhance Cardiac Function Following Myocardial Infarction. Circ Res. 2015;117(1).

20. Théry C, Witwer KW, Aikawa E, Alcaraz MJ, Anderson JD, Andriantsitohaina R, et al. Minimal information for studies of extracellular vesicles 2018 (MISEV2018): a position statement of the International Society for Extracellular Vesicles and update of the MISEV2014 guidelines. J Extracell Vesicles. 2018;7(1).

21. Ewels PA, Peltzer A, Fillinger S, Patel H, Alneberg J, Wilm A, et al. The nf-core framework for community-curated bioinformatics pipelines. Nat Biotechnol. 2020 Mar;38(3):276–8.

22. Greening DW, Nguyen HPT, Elgass K, Simpson RJ, Salamonsen LA. Human endometrial exosomes contain hormone-specific cargo modulating trophoblast adhesive capacity: Insights into endometrial-embryo interactions. Biol Reprod. 2016.

23. Pancho A, Aerts T, Mitsogiannis MD, Seuntjens E. Protocadherins at the Crossroad of Signaling Pathways. Front Mol Neurosci. 2020 Jun 30;13:117.

24. Su RW, Jia B, Ni H, Lei W, Yue SL, Feng XH, et al. Junctional Adhesion Molecule 2 Mediates the Interaction between Hatched Blastocyst and Luminal Epithelium: Induction by Progesterone and LIF. Wang H, editor. PLoS ONE. 2012 Apr 12;7(4):e34325.

25. Yamashita T, Wada R, Sasaki T, Deng C, Bierfreund U, Sandhoff K, et al. A vital role for glycosphingolipid synthesis during development and differentiation. Proc Natl Acad Sci U S A. 1999;96(16).

26. Regina Todeschini A, Hakomori S itiroh. Functional role of glycosphingolipids and gangliosides in control of cell adhesion, motility, and growth, through glycosynaptic microdomains. Biochim Biophys Acta - Gen Subj. 2008;1780(3).

27. Marshall JS, Warrington R, Watson W, Kim HL. An introduction to immunology and immunopathology. Allergy Asthma Clin Immunol. 2018;14.

28. Wu HX, Jin LP, Xu B, Liang SS, Li DJ. Decidual stromal cells recruit Th17 cells into decidua to promote proliferation and invasion of human trophoblast cells by secreting IL-17. Cell Mol Immunol. 2014;11(3).

29. Wu HM, Chen LH, Hsu LT, Lai CH. Immune Tolerance of Embryo Implantation and Pregnancy: The Role of Human Decidual Stromal Cell- and Embryonic-Derived Extracellular Vesicles. Int J Mol Sci. 2022;23(21).

30. Schumacher A, Sharkey DJ, Robertson SA, Zenclussen AC. Immune Cells at the Fetomaternal Interface: How the Microenvironment Modulates Immune Cells To Foster Fetal Development. J Immunol. 2018;201(2).

31. Topham NJ, Hewitt EW. Natural killer cell cytotoxicity: How do they pull the trigger? Immunology. 2009;128(1).

32. Mahajan D, Sharma NR, Kancharla S, Kolli P, Tripathy A, Sharma AK, et al. Role of Natural Killer Cells during Pregnancy and Related Complications. Biomolecules. 2022;12(1).

33. Lee JY, Lee M, Lee SK. Role of endometrial immune cells in implantation. Clin Exp Reprod Med. 2011;38(3).

34. Koga K, Mor G. Toll-Like Receptors at the Maternal-Fetal Interface in Normal Pregnancy and Pregnancy Disorders. Am J Reprod Immunol. 2010;63(6).

35. Aboussahoud WS, Smith H, Stevens A, Wangsaputra I, Hunter HR, Kimber SJ, et al. The expression and activity of Toll-like receptors in the preimplantation human embryo suggest a new role for innate immunity. Hum Reprod. 2021;36(10).

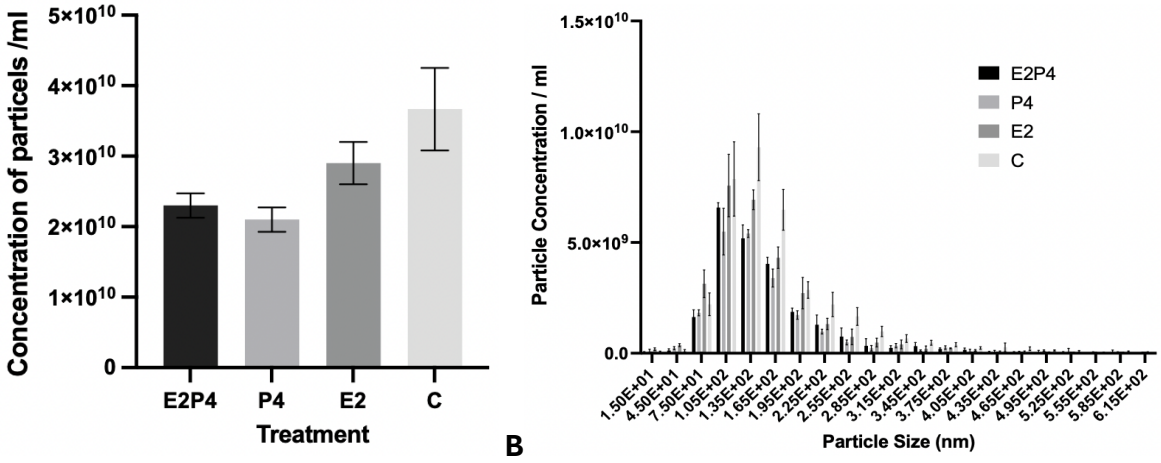
36. Hasty LA, Lambris JD, Lessey BA, Pruksananonda K, Lyttle CR. Hormonal regulation of complement components and receptors throughout the menstrual cycle. Am J Obstet Gynecol. 1994;170(1).

37. Li SH, Huang HL, Chen YH. Ovarian steroid-regulated synthesis and secretion of complement C3 and factor B in mouse endometrium during the natural estrous cycle and pregnancy period. Biol Reprod. 2002;66(2).

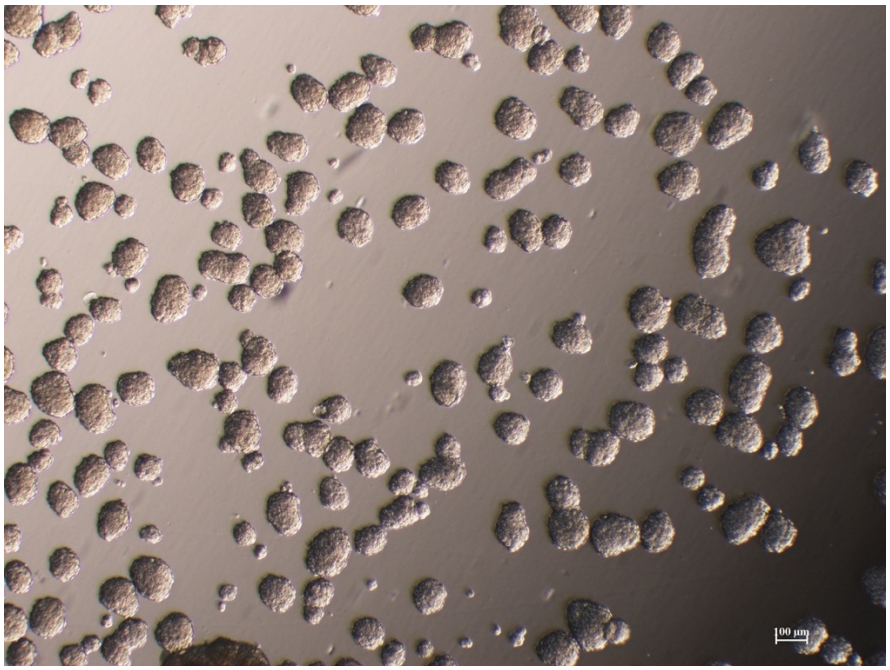
38. Smith-Jackson K, Harrison RA. Alternative pathway activation in pregnancy, a measured amount “complements” a successful pregnancy, too much results in adverse events. Immunol Rev. 2023;313(1).

39. Love MI, Huber W, Anders S. Moderated estimation of fold change and dispersion for RNA-seq data with DESeq2. Genome Biol. 2014;15(12).

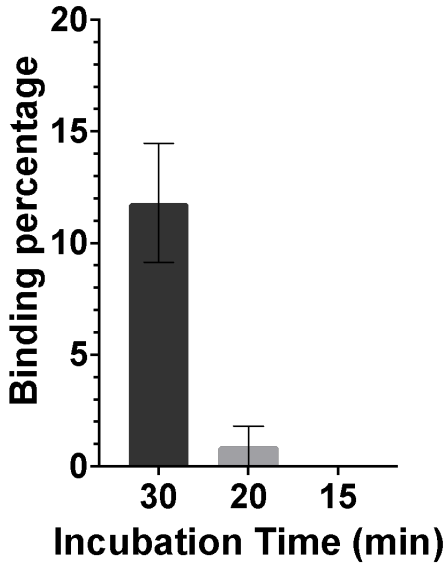
3.11 Supplementary materials.



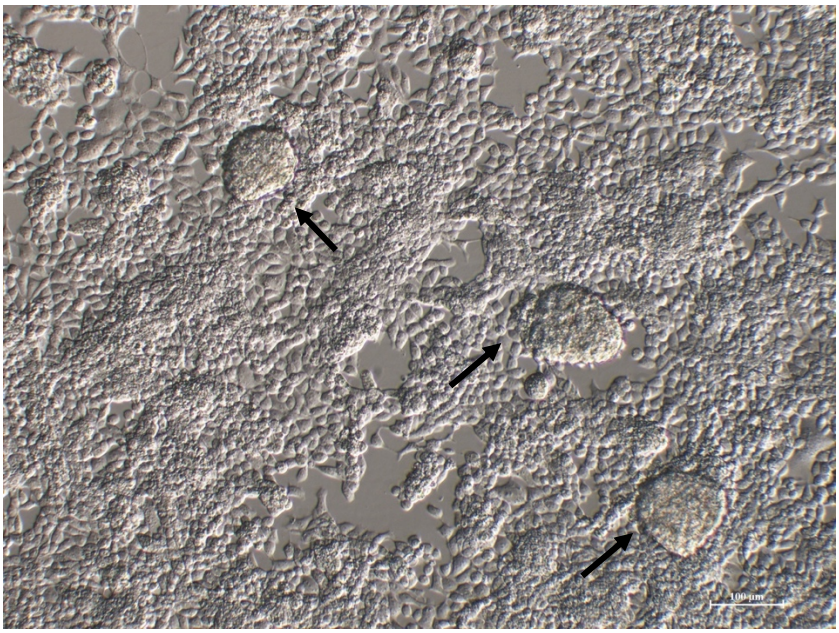
Supplementary Figure 3.1. Concentration and size distribution of EVs released from RL95-2 hormone-treated cells. (**A**) The bars represent the mean concentration (particles/mL) ±SEM of EV sized particles from the SEC fractions 5–8. The treatment groups include estrogen (E2), progesterone (P4), estrogen plus progesterone (E2P4), and the control. Data were from 1 biological replicate and 3 technical replicates from each group. (**B**) The bars represent the mean concentration of the indicated particle size ± SEM from the SEC fractions 5–8. Data are from 1 biological replicate and 3 technical replicates.



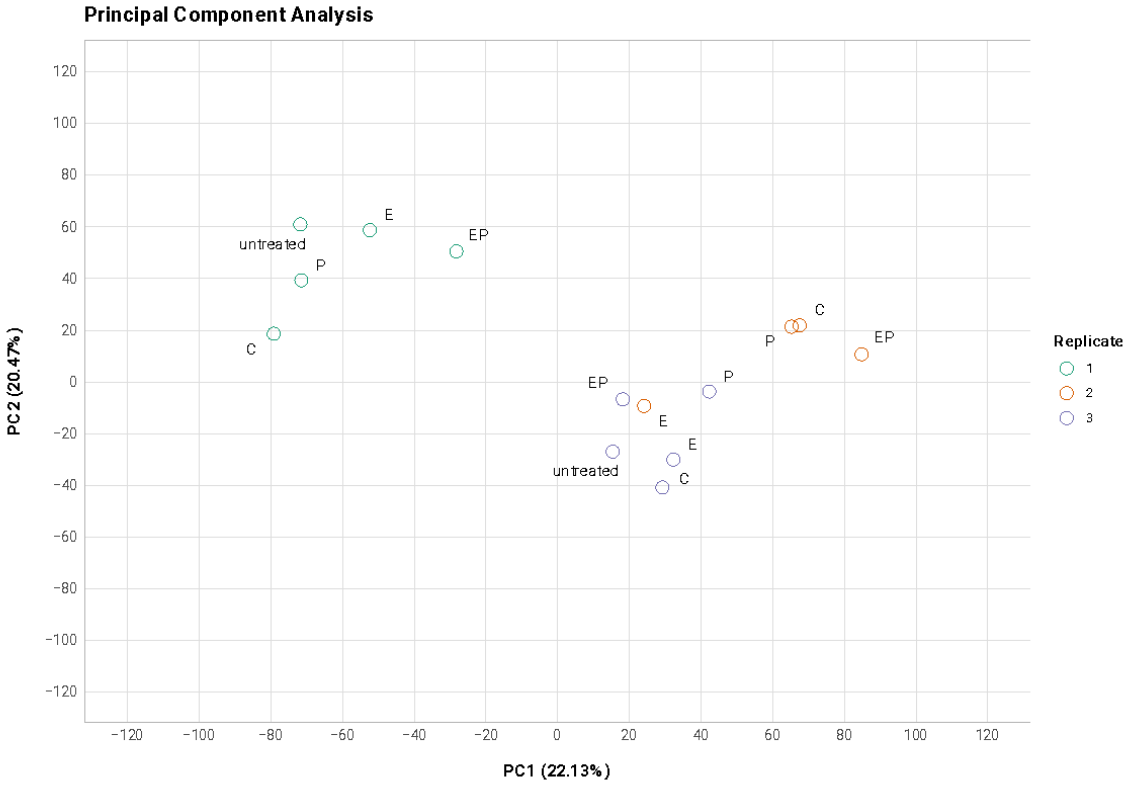
Supplementary Figure 3.2. Example image of JAr Spheroid formation after 24h formation period captured by an inverted microscope.



Supplementary Figure 3.3. Optimisation of binding assay incubation time. Binding percentage of JAr spheroids to RL95-2 monolayer at various incubation times. The height of the bars represents the mean binding percentage from 3 biological replicates and 3 technical replicates. Error bars represent the standard error from the mean.



Supplementary Figure 3.4. Example image of JAr spheroids binding to RL95-2 monolayer after 30 incubation period captured by an inverted microscope. JAr spheroids indicated by black arrows.



Supplementary Figure 3.5. Principal component analysis (PCA) of variable genes in the study groups from 3 replicates with batch effect not adjusted. With the "untreated" group representing JAr cells that haven't been treated with any EVs, "E" group representing JAr spheroids treated with EVs derived from RL95-2 cells treated with Estrogen, "EP" group representing JAr spheroids treated with EVs derived from RL95-2 cells treated with estrogen and progesterone, "C" groups representing JAr spheroids treated with Evs derived from RL95-2 cells treated with the control and "P" group representing JAr spheroids treated with EVs derived from RL95-2 cells treated with progesterone. *n* = 3 for each experimental condition.

Supplementary Table 3.1. Differential expression results of JAr E2P4 v JAr E2.

Entrez Gene ID	Gene symbol	Gene name	log_fc	p_value	fdr
375260	WASH2P	WASP family homolog 2, pseudogene	-7.038	0.025	1.000
162632	USP32P1	ubiquitin specific peptidase 32 pseudogene 1	-5.781	0.014	1.000
100133315	XNDC1N	XRCC1 N-terminal domain containing 1, N-terminal like	-3.488	0.002	1.000
162387	MFSD6L	major facilitator superfamily domain containing 6 like	-1.713	0.045	1.000
116843	SLC18B1	solute carrier family 18 member B1	-1.713	0.013	1.000
3352	HTR1D	5-hydroxytryptamine receptor 1D	-1.660	0.040	1.000
100532726	NDUFC2-KCTD14	NDUFC2-KCTD14 readthrough	-1.561	0.003	1.000
101927220	DEPDC1-AS1	DEPDC1 antisense RNA 1	-1.434	0.038	1.000
25890	ABI3BP	ABI family member 3 binding protein	-1.370	0.030	1.000
255374	MBLAC1	metallo-beta-lactamase domain containing 1	-1.222	0.009	1.000
375791	CYSRT1	cysteine rich tail 1	-1.221	0.045	1.000
124901310	LOC124901310	uncharacterized LOC124901310	-1.197	0.049	1.000
10281	DSCR4	Down syndrome critical region 4	-1.182	0.007	1.000
10815	CPLX1	complexin 1	-1.164	0.032	1.000
51252	FAM178B	family with sequence similarity 178 member B	-1.153	0.027	1.000
9938	ARHGAP25	Rho GTPase activating protein 25	-1.145	0.048	1.000
283518	KCNRG	potassium channel regulator	-1.106	0.014	1.000
151393	RMDN2	regulator of microtubule dynamics 2	-1.051	0.014	1.000
341277	OVCH2	ovochymase 2	1.012	0.036	1.000
9692	PRORP	protein only RNase P catalytic subunit	1.012	0.033	1.000
10965	ACOT2	acyl-CoA thioesterase 2	1.024	0.025	1.000
143282	FGFBP3	fibroblast growth factor binding protein 3	1.024	0.050	1.000
84647	PLA2G12B	phospholipase A2 group XIIB	1.030	0.019	1.000
107984921	LINC01772	long intergenic non-protein coding RNA 1772	1.042	0.049	1.000
254122	SNX32	sorting nexin 32	1.060	0.048	1.000
285368	PRRT3	proline rich transmembrane protein 3	1.095	0.001	1.000

25786	DGCR11	DiGeorge syndrome critical region gene 11	1.128	0.030	1.000
58499	ZNF462	zinc finger protein 462	1.177	0.046	1.000
100271374	RPS27AP5	ribosomal protein S27a pseudogene 5	1.180	0.044	1.000
56107	PCDHGA9	protocadherin gamma subfamily A, 9	1.238	0.044	1.000
51265	CDKL3	cyclin dependent kinase like 3	1.239	0.026	1.000
388553	MEIOSIN	meiosis initiator	1.323	0.014	1.000
64799	IQCH	IQ motif containing H	1.427	0.049	1.000
171391	GATD1-DT	GATD1 divergent transcript	1.464	0.020	1.000
352909	DNAAF3	dynein axonemal assembly factor 3	1.504	0.050	1.000
148523	CIART	circadian associated repressor of transcription	1.542	0.038	1.000
90665	TBL1Y	transducin beta like 1 Y-linked	1.570	0.024	1.000
64852	TUT1	terminal uridylyl transferase 1, U6 snRNA-specific	1.572	0.038	1.000
105377466	LINC02266	long intergenic non-protein coding RNA 2266	1.574	0.022	1.000
113540	CMTM1	CKLF like MARVEL transmembrane domain containing 1	1.813	0.026	1.000
100131094	DPP9-AS1	DPP9 antisense RNA 1	1.832	0.023	1.000
140921	PPP2R5CP	protein phosphatase 2 regulatory subunit B'gamma pseudogene	2.057	0.034	1.000
202658	TRIM39-RPP21	TRIM39-RPP21 readthrough	2.137	0.012	1.000
170591	S100Z	S100 calcium binding protein Z	2.251	0.015	1.000
554225	STRCP1	stereocilin pseudogene 1	2.806	0.025	1.000
341568	OR8S1	olfactory receptor family 8 subfamily S member 1	2.835	0.007	1.000
152302	CIDECP1	cell death inducing DFFA like effector c pseudogene 1	3.217	0.027	1.000
100775107	RBM5-AS1	RBM5 antisense RNA 1	3.789	0.020	1.000
100996928	FMC1-LUC7L2	FMC1-LUC7L2 readthrough	6.702	0.033	1.000
100532735	INO80B-WBP1	INO80B-WBP1 readthrough (NMD candidate)	6.881	0.034	1.000
100128385	FAM225B	family with sequence similarity 225 member B	7.272	0.005	1.000

Supplementary Table 3.2. Differential expression results of JAr E2P4 v JAr P4.

Entrez Gene ID	Gene symbol	Gene name	log_fc	p_value	fdr
54441	STAG3L1	stromal antigen 3-like 1 (pseudogene)	-8.318	0.000	1.000
162632	USP32P1	ubiquitin specific peptidase 32 pseudogene 1	-5.825	0.013	1.000
152831	KLB	klotho beta	-3.475	0.001	1.000
101927124	HEATR5A-DT	HEATR5A divergent transcript	-2.931	0.020	1.000
100287482	SMKR1	small lysine rich protein 1	-2.688	0.001	1.000
2302	FOXJ1	forkhead box J1	-2.273	0.014	1.000
101927220	DEPDC1-AS1	DEPDC1 antisense RNA 1	-1.673	0.017	1.000
93550	ZFAND4	zinc finger AN1-type containing 4	-1.617	0.037	1.000
6571	SLC18A2	solute carrier family 18 member A2	-1.596	0.035	1.000
6517	SLC2A4	solute carrier family 2 member 4	-1.538	0.020	1.000
118812	MORN4	MORN repeat containing 4	-1.537	0.017	1.000
728485	LOC728485	uncharacterized LOC728485	-1.524	0.026	1.000
29767	TMOD2	tropomodulin 2	-1.484	0.044	1.000
283518	KCNRG	potassium channel regulator	-1.474	0.002	1.000
116843	SLC18B1	solute carrier family 18 member B1	-1.395	0.040	1.000
414245	DNAJC9-AS1	DNAJC9 and MRPS16 antisense RNA 1	-1.272	0.044	1.000
56138	PCDHA11	protocadherin alpha 11	-1.232	0.025	1.000
105374085	LOC105374085	uncharacterized LOC105374085	-1.220	0.032	1.000
80206	FHOD3	formin homology 2 domain containing 3	-1.173	0.042	1.000
50515	CHST11	carbohydrate sulfotransferase 11	-1.154	0.009	1.000
151393	RMDN2	regulator of microtubule dynamics 2	-1.114	0.010	1.000
653659	TMEM183BP	transmembrane protein 183B, pseudogene	-1.081	0.005	1.000
8399	PLA2G10	phospholipase A2 group X	-1.072	0.041	1.000
100532726	NDUFC2-KCTD14	NDUFC2-KCTD14 readthrough	-1.065	0.031	1.000
128229	TSACC	TSSK6 activating cochaperone	1.003	0.048	1.000
80115	BAIAP2L2	BAR/IMD domain containing adaptor protein 2 like 2	1.008	0.006	1.000

5296	PIK3R2	phosphoinositide-3-kinase regulatory subunit 2	1.018	0.000	1.000
113457	TUBA3D	tubulin alpha 3d	1.019	0.012	1.000
147798	TMC4	transmembrane channel like 4	1.022	0.004	1.000
105372419	GEMIN7-AS1	GEMIN7 antisense RNA 1	1.071	0.031	1.000
388553	MEIOSIN	meiosis initiator	1.080	0.037	1.000
9901	SRGAP3	SLIT-ROBO Rho GTPase activating protein 3	1.081	0.042	1.000
55753	OGDHL	oxoglutarate dehydrogenase L	1.093	0.035	1.000
254122	SNX32	sorting nexin 32	1.098	0.043	1.000
83473	KATNAL2	katanin catalytic subunit A1 like 2	1.121	0.014	1.000
55096	EBLN2	endogenous Bornavirus like nucleoprotein 2	1.129	0.021	1.000
4485	MST1	macrophage stimulating 1	1.152	0.001	1.000
25960	ADGRA2	adhesion G protein-coupled receptor A2	1.157	0.024	1.000
100130348	TMEM262	transmembrane protein 262	1.158	0.036	1.000
3679	ITGA7	integrin subunit alpha 7	1.169	0.038	1.000
10219	KLRG1	killer cell lectin like receptor G1	1.249	0.049	1.000
1308	COL17A1	collagen type XVII alpha 1 chain	1.260	0.043	1.000
50853	VILL	villin like	1.268	0.017	1.000
151556	GPR155	G protein-coupled receptor 155	1.281	0.023	1.000
25806	VAX2	ventral anterior homeobox 2	1.311	0.001	1.000
100128788	SRRM2-AS1	SRRM2 antisense RNA 1	1.345	0.038	1.000
107984773	LINC01852	long intergenic non-protein coding RNA 1852	1.354	0.050	1.000
102724826	ZNF337-AS1	ZNF337 antisense RNA 1	1.397	0.013	1.000
152877	FAM53A	family with sequence similarity 53 member A	1.414	0.024	1.000
124905202	LOC124905202	uncharacterized LOC124905202	1.415	0.043	1.000
8642	DCHS1	dachsous cadherin-related 1	1.419	0.043	1.000
440952	EIF1B-AS1	EIF1B antisense RNA 1	1.427	0.027	1.000
55507	GPRC5D	G protein-coupled receptor class C group 5 member D	1.446	0.008	1.000
138162	PIERCE1	piercer of microtubule wall 1	1.448	0.016	1.000
101669766	ZNF350-AS1	ZNF350 antisense RNA 1	1.522	0.026	1.000

7352	UCP3	uncoupling protein 3	1.567	0.024	1.000
157739	TDH	L-threonine dehydrogenase (pseudogene)	1.619	0.015	1.000
340351	AGBL3	AGBL carboxypeptidase 3	1.642	0.019	1.000
445329	SULT1A4	sulfotransferase family 1A member 4	1.875	0.010	1.000
100129540	LOC100129540	uncharacterized LOC100129540	1.969	0.015	1.000
30815	ST6GALNAC6	ST6 N-acetylgalactosaminide alpha-2,6-sialyltransferase 6	2.166	0.022	1.000
100129722	STPG3-AS1	STPG3 antisense RNA 1	2.181	0.044	1.000
8676	STX11	syntaxin 11	2.236	0.001	1.000
100130476	WAKMAR2	wound and keratinocyte migration associated lncRNA 2	2.511	0.003	1.000
100507607	NPIPB9	nuclear pore complex interacting protein family member B9	2.916	0.016	1.000
100775107	RBM5-AS1	RBM5 antisense RNA 1	3.289	0.027	1.000
57412	AS3MT	arsenite methyltransferase	5.801	0.023	1.000

Supplementary Table 3.3. Differential expression results of JAr E2 v JAr P4.

Entrez Gene ID	Gene symbol	Gene name	log_fc	p_value	fdr
54441	STAG3L1	stromal antigen 3-like 1 (pseudogene)	-8.432	0.000	1.000
100532735	INO80B-WBP1	INO80B-WBP1 readthrough (NMD candidate)	-7.878	0.016	1.000
100996928	FMC1-LUC7L2	FMC1-LUC7L2 readthrough	-7.377	0.018	1.000
100128385	FAM225B	family with sequence similarity 225 member B	-5.772	0.029	1.000
152302	CIDECP1	cell death inducing DFFA like effector c pseudogene 1	-4.534	0.002	1.000
554225	STRCP1	stereocilin pseudogene 1	-3.140	0.010	1.000
152831	KLB	klotho beta	-2.307	0.006	1.000
6339	SCNN1D	sodium channel epithelial 1 subunit delta	-2.193	0.002	1.000
143903	LAYN	layilin	-1.987	0.019	1.000
2321	FLT1	fms related receptor tyrosine kinase 1	-1.810	0.033	1.000
729873	TBC1D3	TBC1 domain family member 3	-1.788	0.031	1.000
84911	ZNF382	zinc finger protein 382	-1.639	0.022	1.000
91319	DERL3	derlin 3	-1.612	0.050	1.000
644809	PAK6-AS1	PAK6 antisense RNA 1	-1.559	0.021	1.000

7710	ZNF154	zinc finger protein 154	-1.504	0.039	1.000
101928371	LOC101928371	uncharacterized LOC101928371	-1.485	0.037	1.000
6517	SLC2A4	solute carrier family 2 member 4	-1.430	0.026	1.000
883	KYAT1	kynurenine aminotransferase 1	-1.351	0.013	1.000
341277	OVCH2	ovochymase 2	-1.284	0.010	1.000
115948	ODAD3	outer dynein arm docking complex subunit 3	-1.263	0.046	1.000
11182	SLC2A6	solute carrier family 2 member 6	-1.257	0.024	1.000
100533111	ZNF670-ZNF695	ZNF670-ZNF695 readthrough (NMD candidate)	-1.217	0.047	1.000
256006	ANKRD31	ankyrin repeat domain 31	-1.109	0.042	1.000
101927352	PLS3-AS1	PLS3 antisense RNA 1	-1.101	0.039	1.000
100129583	FAM47E	family with sequence similarity 47 member E	-1.013	0.049	1.000
4881	NPR1	natriuretic peptide receptor 1	1.009	0.034	1.000
9901	SRGAP3	SLIT-ROBO Rho GTPase activating protein 3	1.095	0.040	1.000
102724826	ZNF337-AS1	ZNF337 antisense RNA 1	1.162	0.035	1.000
100506083	DDX19A-DT	DDX19A divergent transcript	1.206	0.016	1.000
153478	PLEKHG4B	pleckstrin homology and RhoGEF domain containing G4B	1.244	0.043	1.000
2330	FMO5	flavin containing dimethylaniline monoxygenase 5	1.262	0.039	1.000
105370888	TMEM202-AS1	TMEM202 antisense RNA 1	1.335	0.007	1.000
128229	TSACC	TSSK6 activating cochaperone	1.358	0.010	1.000
339799	EIF3FP3	eukaryotic translation initiation factor 3 subunit F pseudogene 3	1.382	0.031	1.000
101669766	ZNF350-AS1	ZNF350 antisense RNA 1	1.388	0.042	1.000
54843	SYTL2	synaptotagmin like 2	1.392	0.023	1.000
101927559	CEBPB-AS1	CEBPB antisense RNA 1	1.473	0.037	1.000
56102	PCDHGB3	protocadherin gamma subfamily B, 3	1.498	0.041	1.000
340351	AGBL3	AGBL carboxypeptidase 3	1.501	0.032	1.000
107984773	LINC01852	long intergenic non-protein coding RNA 1852	1.729	0.013	1.000
55507	GPRC5D	G protein-coupled receptor class C group 5 member D	1.775	0.002	1.000
728798	FRMPD2B	FERM and PDZ domain containing 2B, pseudogene	1.907	0.009	1.000

3352	HTR1D	5-hydroxytryptamine receptor 1D	1.916	0.023	1.000
124905202	LOC124905202	uncharacterized LOC124905202	1.948	0.007	1.000
968	CD68	CD68 molecule	2.068	0.014	1.000
6939	TCF15	transcription factor 15	2.175	0.022	1.000
8676	STX11	syntaxin 11	2.353	0.001	1.000
9472	AKAP6	A-kinase anchoring protein 6	3.148	0.002	1.000
503569	RGMB-AS1	RGMB antisense RNA 1	3.332	0.008	1.000
57412	AS3MT	arsenite methyltransferase	6.700	0.007	1.000
375260	WASH2P	WASP family homolog 2, pseudogene	7.068	0.024	1.000
723790	H2AC19	H2A clustered histone 19	9.826	0.039	1.000

Supplementary Table 3.4. Differential expression results of Jar C v JAr E2.

Entrez Gene ID	Gene symbol	Gene name	log_fc	p_value	fdr
723790	H2AC19	H2A clustered histone 19	-9.767	0.040	1
10819	OR7E14P	olfactory receptor family 7 subfamily E member 14 pseudogene	-5.047	0.005	1
101060351	TBC1D3K	TBC1 domain family member 3K	-4.502	0.030	1
57156	TMEM63C	transmembrane protein 63C	-2.896	0.004	1
2852	GPER1	G protein-coupled estrogen receptor 1	-2.753	0.007	1
102724105	ZNF528-AS1	ZNF528 antisense RNA 1	-2.680	0.006	1
8557	TCAP	titin-cap	-2.162	0.027	1
643008	SMIM5	small integral membrane protein 5	-2.059	0.020	1
107984773	LINC01852	long intergenic non-protein coding RNA 1852	-2.053	0.005	1
441381	LRRC24	leucine rich repeat containing 24	-2.024	0.009	1
6540	SLC6A13	solute carrier family 6 member 13	-1.938	0.046	1
10581	IFITM2	interferon induced transmembrane protein 2	-1.919	0.049	1
148808	MFSD4A	major facilitator superfamily domain containing 4A	-1.770	0.029	1
100419515	LOC100419515	zinc finger protein 41 pseudogene	-1.768	0.018	1
4922	NTS	neurotensin	-1.489	0.043	1
376497	SLC27A1	solute carrier family 27 member 1	-1.471	0.030	1

54567	DLL4	delta like canonical Notch ligand 4	-1.407	0.010	1
7078	TIMP3	TIMP metallopeptidase inhibitor 3	-1.368	0.014	1
101927401	LOC101927401	uncharacterized LOC101927401	-1.345	0.021	1
4117	MAK	male germ cell associated kinase	-1.322	0.012	1
8858	PROZ	protein Z, vitamin K dependent plasma glycoprotein	-1.302	0.019	1
2122	MECOM	MDS1 and EVI1 complex locus	-1.289	0.001	1
728501	RPL21P75	ribosomal protein L21 pseudogene 75	-1.208	0.031	1
60495	HPSE2	heparanase 2 (inactive)	-1.182	0.048	1
105374085	LOC105374085	uncharacterized LOC105374085	-1.136	0.050	1
155382	VPS37D	VPS37D subunit of ESCRT-I	-1.112	0.044	1
64581	CLEC7A	C-type lectin domain containing 7A	-1.080	0.044	1
283663	LINC00926	long intergenic non-protein coding RNA 926	-1.014	0.028	1
374462	PTPRQ	protein tyrosine phosphatase receptor type Q	1.097	0.038	1
254122	SNX32	sorting nexin 32	1.114	0.038	1
109729127	KRT7-AS	KRT7 antisense RNA 1	1.160	0.026	1
11182	SLC2A6	solute carrier family 2 member 6	1.186	0.032	1
388553	MEIOSIN	meiosis initiator	1.193	0.025	1
883	KYAT1	kynurenine aminotransferase 1	1.215	0.025	1
50487	PLA2G3	phospholipase A2 group III	1.246	0.049	1
246778	IL27	interleukin 27	1.296	0.029	1
10673	TNFSF13B	TNF superfamily member 13b	1.304	0.045	1
107984875	ZNF747-DT	ZNF747 divergent transcript	1.307	0.010	1
102724532	SP2-DT	SP2 divergent transcript	1.321	0.024	1
79630	C1orf54	chromosome 1 open reading frame 54	1.338	0.024	1
256006	ANKRD31	ankyrin repeat domain 31	1.345	0.015	1
26576	SRPK3	SRSF protein kinase 3	1.354	0.048	1
100271374	RPS27AP5	ribosomal protein S27a pseudogene 5	1.380	0.019	1
171391	GATD1-DT	GATD1 divergent transcript	1.408	0.025	1
113675	SDSL	serine dehydratase like	1.464	0.049	1

6339	SCNN1D	sodium channel epithelial 1 subunit delta	1.516	0.028	1
7710	ZNF154	zinc finger protein 154	1.525	0.036	1
644809	PAK6-AS1	PAK6 antisense RNA 1	1.556	0.021	1
6911	TBX6	T-box transcription factor 6	1.689	0.045	1
100861430	PDCD6IPP1	PDCD6IP pseudogene 1	1.752	0.047	1
729873	TBC1D3	TBC1 domain family member 3	1.837	0.027	1
54760	PCSK4	proprotein convertase subtilisin/kexin type 4	1.890	0.030	1
100528064	NEDD8-MDP1	NEDD8-MDP1 readthrough	2.130	0.008	1
375616	KCP	kielin cysteine rich BMP regulator	2.353	0.030	1
79875	THSD4	thrombospondin type 1 domain containing 4	2.767	0.048	1
100775107	RBM5-AS1	RBM5 antisense RNA 1	3.430	0.036	1
54441	STAG3L1	stromal antigen 3-like 1 (pseudogene)	5.255	0.023	1
7803	PTP4A1	protein tyrosine phosphatase 4A1	5.614	0.016	1
91695	RRP7BP	ribosomal RNA processing 7 homolog B, pseudogene	6.921	0.025	1

Supplementary Table 3.5. Differential expression results of JAr C v JAr P4.

Entrez Gene ID	Gene symbol	Gene name	log_fc	p_value	fdr
100532735	INO80B-WBP1	INO80B-WBP1 readthrough (NMD candidate)	-7.946	0.016	0.995
10819	OR7E14P	olfactory receptor family 7 subfamily E member 14 pseudogene	-6.300	0.000	0.995
100631383	FAM47E-STBD1	FAM47E-STBD1 readthrough	-6.289	0.022	0.995
54441	STAG3L1	stromal antigen 3-like 1 (pseudogene)	-3.177	0.006	0.995
152302	CIDECP1	cell death inducing DFFA like effector c pseudogene 1	-3.089	0.007	0.995
152831	KLB	klotho beta	-2.657	0.003	0.995
57156	TMEM63C	transmembrane protein 63C	-2.290	0.023	0.995
22836	RHOBTB3	Rho related BTB domain containing 3	-2.270	0.014	0.995
102724488	SYT15B	synaptotagmin 15B	-2.120	0.027	0.995
8557	TCAP	titin-cap	-2.110	0.032	0.995
441381	LRRC24	leucine rich repeat containing 24	-2.104	0.006	0.995
149478	BTBD19	BTB domain containing 19	-2.031	0.020	0.995

143903	LAYN	layilin	-1.892	0.022	0.995
148808	MFSD4A	major facilitator superfamily domain containing 4A	-1.825	0.026	0.995
128854	TSPY26P	testis specific protein Y-linked 26, pseudogene	-1.792	0.030	0.995
100419515	LOC100419515	zinc finger protein 41 pseudogene	-1.639	0.029	0.995
100885848	PTGES3L	prostaglandin E synthase 3 like	-1.509	0.028	0.995
2569	GABRR1	gamma-aminobutyric acid type A receptor subunit rho1	-1.505	0.048	0.995
29767	TMOD2	tropomodulin 2	-1.490	0.041	0.995
105374085	LOC105374085	uncharacterized LOC105374085	-1.467	0.014	0.995
1006	CDH8	cadherin 8	-1.464	0.039	0.995
54567	DLL4	delta like canonical Notch ligand 4	-1.425	0.009	0.995
165829	GPR156	G protein-coupled receptor 156	-1.355	0.010	0.995
2122	MECOM	MDS1 and EVI1 complex locus	-1.353	0.001	0.995
358	AQP1	aquaporin 1 (Colton blood group)	-1.349	0.027	0.995
64581	CLEC7A	C-type lectin domain containing 7A	-1.340	0.015	0.995
161497	STRC	stereocilin	-1.297	0.035	0.995
494143	CHAC2	ChaC glutathione specific gamma-glutamylcyclotransferase 2	-1.290	0.026	0.995
83595	SOX7	SRY-box transcription factor 7	-1.274	0.042	0.995
60495	HPSE2	heparanase 2 (inactive)	-1.206	0.044	0.995
90485	ZNF835	zinc finger protein 835	-1.186	0.012	0.995
283298	OLFML1	olfactomedin like 1	-1.181	0.031	0.995
3175	ONECUT1	one cut homeobox 1	-1.149	0.003	0.995
629	CFB	complement factor B	-1.124	0.024	0.995
161394	SAMD15	sterile alpha motif domain containing 15	-1.093	0.044	0.995
90167	FRMD7	FERM domain containing 7	-1.091	0.027	0.995
57188	ADAMTSL3	ADAMTS like 3	-1.024	0.012	0.995
149473	CCDC24	coiled-coil domain containing 24	1.001	0.026	0.995
654841	MFF-DT	MFF divergent transcript	1.006	0.015	0.995
4485	MST1	macrophage stimulating 1	1.017	0.002	0.995
80726	IQCN	IQ motif containing N	1.024	0.043	0.995

283629	TSSK4	testis specific serine kinase 4	1.029	0.021	0.995
55507	GPRC5D	G protein-coupled receptor class C group 5 member D	1.037	0.049	0.995
115123	MARCHF3	membrane associated ring-CH-type finger 3	1.055	0.037	0.995
80115	BAIAP2L2	BAR/IMD domain containing adaptor protein 2 like 2	1.065	0.004	0.995
100289092	ATP2A1-AS1	ATP2A1 antisense RNA 1	1.070	0.040	0.995
83473	KATNAL2	katanin catalytic subunit A1 like 2	1.084	0.018	0.995
254122	SNX32	sorting nexin 32	1.152	0.034	0.995
245711	SPDYA	speedy/RINGO cell cycle regulator family member A	1.161	0.012	0.995
81419	OR7E99P	olfactory receptor family 7 subfamily E member 99 pseudogene	1.175	0.011	0.995
387496	RASL11A	RAS like family 11 member A	1.180	0.004	0.995
100506083	DDX19A-DT	DDX19A divergent transcript	1.248	0.013	0.995
2330	FMO5	flavin containing dimethylaniline monoxygenase 5	1.248	0.040	0.995
203100	HTRA4	HtrA serine peptidase 4	1.276	0.014	0.995
152877	FAM53A	family with sequence similarity 53 member A	1.306	0.035	0.995
121268	RHEBL1	RHEB like 1	1.324	0.015	0.995
1308	COL17A1	collagen type XVII alpha 1 chain	1.356	0.030	0.995
157739	TDH	L-threonine dehydrogenase (pseudogene)	1.381	0.036	0.995
153478	PLEKHG4B	pleckstrin homology and RhoGEF domain containing G4B	1.447	0.020	0.995
8676	STX11	syntaxin 11	1.517	0.020	0.995
200728	TMEM17	transmembrane protein 17	1.529	0.041	0.995
26576	SRPK3	SRSF protein kinase 3	1.545	0.030	0.995
114804	RNF157	ring finger protein 157	1.555	0.018	0.995
246778	IL27	interleukin 27	1.657	0.009	0.995
56102	PCDHGB3	protocadherin gamma subfamily B, 3	1.668	0.025	0.995
131096	KCNH8	potassium voltage-gated channel subfamily H member 8	1.693	0.019	0.995
388323	GLTPD2	glycolipid transfer protein domain containing 2	1.813	0.047	0.995
100113407	TMEM170B	transmembrane protein 170B	1.927	0.019	0.995
100130476	WAKMAR2	wound and keratinocyte migration associated lncRNA 2	1.939	0.017	0.995
642658	SCX	scleraxis bHLH transcription factor	1.963	0.028	0.995

102724826	ZNF337-AS1	ZNF337 antisense RNA 1	2.043	0.001	0.995
100861430	PDCD6IPP1	PDCD6IP pseudogene 1	2.051	0.026	0.995
968	CD68	CD68 molecule	2.198	0.010	0.995
6939	TCF15	transcription factor 15	2.292	0.017	0.995
100129722	STPG3-AS1	STPG3 antisense RNA 1	2.569	0.017	0.995
9472	AKAP6	A-kinase anchoring protein 6	2.692	0.006	0.995
100507607	NPIPB9	nuclear pore complex interacting protein family member B9	2.890	0.018	0.995
57412	AS3MT	arsenite methyltransferase	6.402	0.010	0.995

Supplementary Table 3.6. Differential expression results of JAr C v JAr E2P4.

Entrez Gene ID	Gene symbol	Gene name	log_fc	p_value	fdr
100532735	INO80B-WBP1	INO80B-WBP1 readthrough (NMD candidate)	-6.949	0.033	0.999
10819	OR7E14P	olfactory receptor family 7 subfamily E member 14 pseudogene	-6.041	0.001	0.999
2852	GPER1	G protein-coupled estrogen receptor 1	-2.998	0.003	0.999
102724105	ZNF528-AS1	ZNF528 antisense RNA 1	-2.992	0.003	0.999
100128385	FAM225B	family with sequence similarity 225 member B	-2.892	0.048	0.999
6518	SLC2A5	solute carrier family 2 member 5	-2.614	0.038	0.999
102724488	SYT15B	synaptotagmin 15B	-2.578	0.008	0.999
643008	SMIM5	small integral membrane protein 5	-2.097	0.019	0.999
8557	TCAP	titin-cap	-2.085	0.033	0.999
64852	TUT1	terminal uridylyl transferase 1, U6 snRNA-specific	-1.878	0.019	0.999
107984773	LINC01852	long intergenic non-protein coding RNA 1852	-1.678	0.021	0.999
100885848	PTGES3L	prostaglandin E synthase 3 like	-1.678	0.015	0.999
161497	STRC	stereocilin	-1.591	0.012	0.999
3899	AFF3	ALF transcription elongation factor 3	-1.582	0.031	0.999
101927288	MANEA-DT	MANEA divergent transcript	-1.576	0.011	0.999
54567	DLL4	delta like canonical Notch ligand 4	-1.561	0.005	0.999
629	CFB	complement factor B	-1.533	0.003	0.999
7078	TIMP3	TIMP metallopeptidase inhibitor 3	-1.504	0.007	0.999

64581	CLEC7A	C-type lectin domain containing 7A	-1.443	0.009	0.999
445329	SULT1A4	sulfotransferase family 1A member 4	-1.432	0.030	0.999
90485	ZNF835	zinc finger protein 835	-1.410	0.004	0.999
376497	SLC27A1	solute carrier family 27 member 1	-1.408	0.036	0.999
122945	NOXRED1	NADP dependent oxidoreductase domain containing 1	-1.380	0.027	0.999
390215	OR7E145P	olfactory receptor family 7 subfamily E member 145 pseudogene	-1.366	0.032	0.999
23424	TDRD7	tudor domain containing 7	-1.335	0.044	0.999
3745	KCNB1	potassium voltage-gated channel subfamily B member 1	-1.324	0.040	0.999
51088	KLHL5	kelch like family member 5	-1.250	0.016	0.999
494143	CHAC2	ChaC glutathione specific gamma-glutamylcyclotransferase 2	-1.220	0.034	0.999
728501	RPL21P75	ribosomal protein L21 pseudogene 75	-1.166	0.036	0.999
118461	C10orf71	chromosome 10 open reading frame 71	-1.148	0.001	0.999
7006	TEC	tec protein tyrosine kinase	-1.109	0.044	0.999
4117	MAK	male germ cell associated kinase	-1.038	0.044	0.999
55096	EBLN2	endogenous Bornavirus like nucleoprotein 2	-1.035	0.032	0.999
283663	LINC00926	long intergenic non-protein coding RNA 926	-1.032	0.025	0.999
654841	MFF-DT	MFF divergent transcript	1.007	0.015	0.999
135152	B3GAT2	beta-1,3-glucuronyltransferase 2	1.051	0.007	0.999
284393	RPL10P16	ribosomal protein L10 pseudogene 16	1.101	0.035	0.999
203100	HTRA4	HtrA serine peptidase 4	1.103	0.028	0.999
151393	RMDN2	regulator of microtubule dynamics 2	1.130	0.009	0.999
11117	EMILIN1	elastin microfibril interfacer 1	1.139	0.039	0.999
109729127	KRT7-AS	KRT7 antisense RNA 1	1.187	0.022	0.999
283518	KCNRG	potassium channel regulator	1.241	0.007	0.999
101059938	NPIPA7	nuclear pore complex interacting protein family member A7	1.258	0.025	0.999
116443	GRIN3A	glutamate ionotropic receptor NMDA type subunit 3A	1.291	0.048	0.999
8552	INE1	inactivation escape 1	1.327	0.022	0.999
101928108	LY6L	lymphocyte antigen 6 family member L	1.386	0.021	0.999
55815	TSNAXIP1	translin associated factor X interacting protein 1	1.469	0.030	0.999

10815	CPLX1	complexin 1	1.480	0.008	0.999
256227	STEAP1B	STEAP family member 1B	1.512	0.026	0.999
414245	DNAJC9-AS1	DNAJC9 and MRPS16 antisense RNA 1	1.549	0.015	0.999
100532726	NDUFC2-KCTD14	NDUFC2-KCTD14 readthrough	1.598	0.002	0.999
100528064	NEDD8-MDP1	NEDD8-MDP1 readthrough	1.624	0.029	0.999
4825	NKX6-1	NK6 homeobox 1	1.709	0.026	0.999
388588	SMIM1	small integral membrane protein 1 (Vel blood group)	1.835	0.027	0.999
6847	SYCP1	synaptonemal complex protein 1	1.896	0.041	0.999
101927220	DEPDC1-AS1	DEPDC1 antisense RNA 1	1.898	0.007	0.999
101929174	LOC101929174	uncharacterized LOC101929174	1.959	0.008	0.999
2302	FOXJ1	forkhead box J1	2.016	0.026	0.999
100287482	SMKR1	small lysine rich protein 1	2.296	0.005	0.999
100133315	XNDC1N	XRCC1 N-terminal domain containing 1, N-terminal like	2.407	0.033	0.999
101927124	HEATR5A-DT	HEATR5A divergent transcript	2.858	0.022	0.999
54441	STAG3L1	stromal antigen 3-like 1 (pseudogene)	5.140	0.026	0.999
7803	PTP4A1	protein tyrosine phosphatase 4A1	5.167	0.022	0.999
162632	USP32P1	ubiquitin specific peptidase 32 pseudogene 1	6.301	0.007	0.999

Supplementary Table 3.7. Differential expression results of JAr P4 v JAr UN.

Entrez Gene ID	Gene symbol	Gene name	log_fc	p_value	fdr
57412	AS3MT	arsenite methyltransferase	-6.706	0.007	0.528
375260	WASH2P	WASP family homolog 2, pseudogene	-6.645	0.034	0.528
445329	SULT1A4	sulfotransferase family 1A member 4	-3.745	0.000	0.469
100507607	NPIPB9	nuclear pore complex interacting protein family member B9	-3.189	0.009	0.528
100129722	STPG3-AS1	STPG3 antisense RNA 1	-2.933	0.006	0.528
9472	AKAP6	A-kinase anchoring protein 6	-2.708	0.006	0.528
100418961	LOC100418961	aurora kinase A pseudogene	-2.380	0.043	0.534
283971	CLEC18C	C-type lectin domain family 18 member C	-2.215	0.047	0.534

100996425	ARLNC1	androgen receptor regulated long noncoding RNA 1	-2.206	0.033	0.528
107984773	LINC01852	long intergenic non-protein coding RNA 1852	-2.109	0.003	0.528
100527978	TLCD4-RWDD3	TLCD4-RWDD3 readthrough	-1.995	0.018	0.528
389537	OR7E38P	olfactory receptor family 7 subfamily E member 38 pseudogene	-1.877	0.047	0.534
100113407	TMEM170B	transmembrane protein 170B	-1.866	0.022	0.528
441073	RPL26P19	ribosomal protein L26 pseudogene 19	-1.834	0.007	0.528
28968	SLC6A16	solute carrier family 6 member 16	-1.762	0.042	0.531
9047	SH2D2A	SH2 domain containing 2A	-1.760	0.047	0.534
246778	IL27	interleukin 27	-1.725	0.007	0.528
124905202	LOC124905202	uncharacterized LOC124905202	-1.719	0.015	0.528
728798	FRMPD2B	FERM and PDZ domain containing 2B, pseudogene	-1.707	0.019	0.528
101927559	CEBPB-AS1	CEBPB antisense RNA 1	-1.695	0.018	0.528
645158	CBX3P2	chromobox 3 pseudogene 2	-1.665	0.035	0.528
202658	TRIM39-RPP21	TRIM39-RPP21 readthrough	-1.597	0.025	0.528
8676	STX11	syntaxin 11	-1.576	0.016	0.528
55507	GPRC5D	G protein-coupled receptor class C group 5 member D	-1.566	0.004	0.528
340351	AGBL3	AGBL carboxypeptidase 3	-1.558	0.024	0.528
105371730	LOC105371730	uncharacterized LOC105371730	-1.521	0.020	0.528
157739	TDH	L-threonine dehydrogenase (pseudogene)	-1.516	0.021	0.528
440952	EIF1B-AS1	EIF1B antisense RNA 1	-1.455	0.024	0.528
100506083	DDX19A-DT	DDX19A divergent transcript	-1.404	0.006	0.528
7134	TNNC1	troponin C1, slow skeletal and cardiac type	-1.396	0.041	0.528
100289373	UBAC2-AS1	UBAC2 antisense RNA 1	-1.390	0.047	0.534
161145	TMEM229B	transmembrane protein 229B	-1.377	0.021	0.528
100130348	TMEM262	transmembrane protein 262	-1.371	0.014	0.528
153478	PLEKHG4B	pleckstrin homology and RhoGEF domain containing G4B	-1.360	0.027	0.528
1576	CYP3A4	cytochrome P450 family 3 subfamily A member 4	-1.347	0.048	0.534

83657	DYNLRB2	dynein light chain roadblock-type 2	-1.290	0.042	0.531
128229	TSACC	TSSK6 activating cochaperone	-1.241	0.017	0.528
9506	PAGE4	PAGE family member 4	-1.229	0.048	0.534
441161	OOEP	oocyte expressed protein	-1.203	0.044	0.534
197257	LDHD	lactate dehydrogenase D	-1.196	0.002	0.528
57535	ELAPOR1	endosome-lysosome associated apoptosis and autophagy regulator 1	-1.191	0.047	0.534
9120	SLC16A6	solute carrier family 16 member 6	-1.152	0.048	0.534
101927021	ZFAND2A-DT	ZFAND2A divergent transcript	-1.142	0.015	0.528
151556	GPR155	G protein-coupled receptor 155	-1.140	0.040	0.528
25806	VAX2	ventral anterior homeobox 2	-1.007	0.010	0.528
1733	DIO1	iodothyronine deiodinase 1	-1.000	0.037	0.528
83887	TTLL2	tubulin tyrosine ligase like 2	1.005	0.046	0.534
165829	GPR156	G protein-coupled receptor 156	1.020	0.039	0.528
869	CBLN1	cerebellin 1 precursor	1.046	0.021	0.528
57512	GPR158	G protein-coupled receptor 158	1.067	0.041	0.531
320	APBA1	amyloid beta precursor protein binding family A member 1	1.071	0.012	0.528
105370941	LOC105370941	uncharacterized LOC105370941	1.074	0.022	0.528
341277	OVCH2	ovochymase 2	1.084	0.022	0.528
130132	RFTN2	raftlin family member 2	1.161	0.005	0.528
57732	ZFYVE28	zinc finger FYVE-type containing 28	1.169	0.026	0.528
163255	ZNF540	zinc finger protein 540	1.180	0.031	0.528
252969	NEIL2	nei like DNA glycosylase 2	1.184	0.031	0.528
285755	PPIL6	peptidylprolyl isomerase like 6	1.204	0.030	0.528
154091	SLC2A12	solute carrier family 2 member 12	1.253	0.024	0.528
653082	ZDHHC11B	zinc finger DHHC-type containing 11B	1.289	0.015	0.528
57188	ADAMTSL3	ADAMTS like 3	1.298	0.003	0.528
105375304	SNX10-AS1	SNX10 antisense RNA 1	1.386	0.047	0.534
100507633	TNKS2-DT	TNKS2 divergent transcript	1.388	0.039	0.528
101928415	LOC101928415	uncharacterized LOC101928415	1.428	0.025	0.528

84647	PLA2G12B	phospholipase A2 group XIIB	1.432	0.003	0.528
775	CACNA1C	calcium voltage-gated channel subunit alpha1 C	1.444	0.024	0.528
6339	SCNN1D	sodium channel epithelial 1 subunit delta	1.472	0.020	0.528
91683	SYT12	synaptotagmin 12	1.533	0.009	0.528
259217	HSPA12A	heat shock protein family A (Hsp70) member 12A	1.550	0.008	0.528
6517	SLC2A4	solute carrier family 2 member 4	1.615	0.015	0.528
131616	TMEM42	transmembrane protein 42	1.684	0.017	0.528
5172	SLC26A4	solute carrier family 26 member 4	1.731	0.006	0.528
2635	GBP3	guanylate binding protein 3	1.950	0.009	0.528
57161	PELI2	pellino E3 ubiquitin protein ligase family member 2	2.011	0.016	0.528
22836	RHOBTB3	Rho related BTB domain containing 3	2.217	0.016	0.528
105371795	LOC105371795	uncharacterized LOC105371795	2.776	0.002	0.528
1593	CYP27A1	cytochrome P450 family 27 subfamily A member 1	2.892	0.023	0.528
162632	USP32P1	ubiquitin specific peptidase 32 pseudogene 1	5.840	0.011	0.528
54441	STAG3L1	stromal antigen 3-like 1 (pseudogene)	8.290	0.000	0.528

Supplementary Table 3.8. Differential expression results of JAr E2P4 v JAr UN.

Entrez Gene ID	Gene symbol	Gene name	log_fc	p_value	fdr
375260	WASH2P	WASP family homolog 2, pseudogene	-6.615	0.034	0.474
152831	KLB	klotho beta	-3.074	0.002	0.471
124902388	LOC124902388	uncharacterized LOC124902388	-2.226	0.011	0.471
101410533	YTHDF3-DT	YTHDF3 divergent transcript	-2.122	0.028	0.471
100287482	SMKR1	small lysine rich protein 1	-2.080	0.010	0.471
441073	RPL26P19	ribosomal protein L26 pseudogene 19	-2.077	0.003	0.471
445329	SULT1A4	sulfotransferase family 1A member 4	-1.871	0.002	0.471
100532726	NDUFC2-KCTD14	NDUFC2-KCTD14 readthrough	-1.849	0.001	0.471
414245	DNAJC9-AS1	DNAJC9 and MRPS16 antisense RNA 1	-1.778	0.006	0.471
107984539	LINC02371	long intergenic non-protein coding RNA 2371	-1.732	0.040	0.474

256227	STEAP1B	STEAP family member 1B	-1.718	0.012	0.471
388588	SMIM1	small integral membrane protein 1 (Vel blood group)	-1.712	0.038	0.474
101929174	LOC101929174	uncharacterized LOC101929174	-1.579	0.031	0.471
116443	GRIN3A	glutamate ionotropic receptor NMDA type subunit 3A	-1.567	0.017	0.471
284393	RPL10P16	ribosomal protein L10 pseudogene 16	-1.540	0.005	0.471
83657	DYNLRB2	dynein light chain roadblock-type 2	-1.497	0.024	0.471
105373958	RAB17-DT	RAB17 divergent transcript	-1.449	0.026	0.471
643072	BAZ2B-AS1	BAZ2B antisense RNA 1	-1.434	0.045	0.474
4922	NTS	neurotensin	-1.433	0.049	0.475
100506804	TMEM30A-DT	TMEM30A divergent transcript	-1.431	0.036	0.474
161145	TMEM229B	transmembrane protein 229B	-1.396	0.019	0.471
101927220	DEPDC1-AS1	DEPDC1 antisense RNA 1	-1.346	0.049	0.475
284648	LINC01686	long intergenic non-protein coding RNA 1686	-1.344	0.013	0.471
283518	KCNRG	potassium channel regulator	-1.342	0.003	0.471
643246	MAP1LC3B2	microtubule associated protein 1 light chain 3 beta 2	-1.316	0.049	0.475
8552	INE1	inactivation escape 1	-1.287	0.025	0.471
140894	CNBD2	cyclic nucleotide binding domain containing 2	-1.204	0.002	0.471
256380	SCML4	Scm polycomb group protein like 4	-1.203	0.033	0.473
8399	PLA2G10	phospholipase A2 group X	-1.149	0.028	0.471
5971	RELB	RELB proto-oncogene, NF-kB subunit	-1.143	0.012	0.471
100131434	EOLA1-DT	EOLA1 divergent transcript	-1.134	0.042	0.474
255374	MBLAC1	metallo-beta-lactamase domain containing 1	-1.125	0.015	0.471
56138	PCDHA11	protocadherin alpha 11	-1.123	0.040	0.474
151393	RMDN2	regulator of microtubule dynamics 2	-1.089	0.011	0.471
222950	NYAP1	neuronal tyrosine phosphorylated phosphoinositide-3-kinase adaptor 1	-1.082	0.037	0.474
6375	XCL1	X-C motif chemokine ligand 1	-1.034	0.043	0.474
653659	TMEM183BP	transmembrane protein 183B, pseudogene	-1.012	0.008	0.471
388228	SBK1	SH3 domain binding kinase 1	1.006	0.043	0.474
653199	TCAF1P1	TRPM8 channel associated factor 1 pseudogene 1	1.006	0.013	0.471

118126072	GUSBP9	GUSB pseudogene 9	1.009	0.048	0.475
55753	OGDHL	oxoglutarate dehydrogenase L	1.013	0.046	0.474
85446	ZFHX2	zinc finger homeobox 2	1.109	0.024	0.471
84698	CAPS2	calcyphosine 2	1.177	0.032	0.471
130132	RFTN2	raftlin family member 2	1.194	0.004	0.471
56107	PCDHGA9	protocadherin gamma subfamily A, 9	1.244	0.042	0.474
100505576	LINC00672	long intergenic non-protein coding RNA 672	1.302	0.047	0.475
23424	TDRD7	tudor domain containing 7	1.312	0.046	0.474
100131369	DUX4L27	double homeobox 4 like 27 (pseudogene)	1.313	0.026	0.471
147138	TMC8	transmembrane channel like 8	1.318	0.049	0.475
155185	AMZ1	archaelysin family metallopeptidase 1	1.358	0.006	0.471
56128	PCDHB8	protocadherin beta 8	1.371	0.002	0.471
775	CACNA1C	calcium voltage-gated channel subunit alpha1 C	1.469	0.022	0.471
58494	JAM2	junctional adhesion molecule 2	1.478	0.012	0.471
285755	PPIL6	peptidylprolyl isomerase like 6	1.531	0.007	0.471
131616	TMEM42	transmembrane protein 42	1.531	0.028	0.471
101927631	ADNP-AS1	ADNP antisense RNA 1	1.593	0.024	0.471
259217	HSPA12A	heat shock protein family A (Hsp70) member 12A	1.617	0.006	0.471
84647	PLA2G12B	phospholipase A2 group XIIB	1.668	0.001	0.471
9421	HAND1	heart and neural crest derivatives expressed 1	1.679	0.032	0.471
162333	MARCHF10	membrane associated ring-CH-type finger 10	1.704	0.028	0.471
7352	UCP3	uncoupling protein 3	1.790	0.013	0.471
653489	RGPD3	RANBP2 like and GRIP domain containing 3	1.846	0.011	0.471
113540	CMTM1	CKLF like MARVEL transmembrane domain containing 1	1.866	0.022	0.471
128864	C20orf144	chromosome 20 open reading frame 144	1.960	0.007	0.471
217	ALDH2	aldehyde dehydrogenase 2 family member	2.060	0.035	0.474
57161	PELI2	pellino E3 ubiquitin protein ligase family member 2	2.140	0.011	0.471
341568	OR8S1	olfactory receptor family 8 subfamily S member 1	2.169	0.018	0.471
105371795	LOC105371795	uncharacterized LOC105371795	2.289	0.010	0.471

Supplementary Table 3.9. Differential expression results of JAr E2 v JAr UN.

Entrez Gene ID	Gene symbol	Gene name	log_fc	p_value	fdr
91695	RRP7BP	ribosomal RNA processing 7 homolog B, pseudogene	-7.354	0.017	0.860
100532735	INO80B-WBP1	INO80B-WBP1 readthrough (NMD candidate)	-6.829	0.035	0.860
100128385	FAM225B	family with sequence similarity 225 member B	-6.236	0.018	0.860
390790	ARL5C	ADP ribosylation factor like GTPase 5C	-4.602	0.041	0.860
152302	CIDECP1	cell death inducing DFFA like effector c pseudogene 1	-4.298	0.003	0.860
100775107	RBM5-AS1	RBM5 antisense RNA 1	-3.247	0.049	0.860
202658	TRIM39-RPP21	TRIM39-RPP21 readthrough	-2.885	0.001	0.860
445329	SULT1A4	sulfotransferase family 1A member 4	-2.534	0.000	0.860
101928238	ZNF426-DT	ZNF426 divergent transcript	-2.515	0.005	0.860
645158	CBX3P2	chromobox 3 pseudogene 2	-2.384	0.007	0.860
729873	TBC1D3	TBC1 domain family member 3	-2.318	0.008	0.860
441073	RPL26P19	ribosomal protein L26 pseudogene 19	-2.274	0.002	0.860
2321	FLT1	fms related receptor tyrosine kinase 1	-2.177	0.011	0.860
375616	KCP	kielin cysteine rich BMP regulator	-2.131	0.046	0.860
10819	OR7E14P	olfactory receptor family 7 subfamily E member 14 pseudogene	-1.992	0.014	0.860
105377466	LINC02266	long intergenic non-protein coding RNA 2266	-1.959	0.005	0.860
152831	KLB	klotho beta	-1.905	0.018	0.860
26548	ITGB1BP2	integrin subunit beta 1 binding protein 2	-1.873	0.014	0.860
57535	ELAPOR1	endosome-lysosome associated apoptosis and autophagy regulator 1	-1.708	0.010	0.860
107984539	LINC02371	long intergenic non-protein coding RNA 2371	-1.629	0.049	0.860
644809	PAK6-AS1	PAK6 antisense RNA 1	-1.540	0.022	0.860
115948	ODAD3	outer dynein arm docking complex subunit 3	-1.531	0.015	0.860
285148	IAH1	isoamyl acetate hydrolyzing esterase 1 (putative)	-1.457	0.049	0.860
171391	GATD1-DT	GATD1 divergent transcript	-1.445	0.021	0.860
246778	IL27	interleukin 27	-1.364	0.021	0.860
105371730	LOC105371730	uncharacterized LOC105371730	-1.351	0.031	0.860

116842	LEAP2	liver enriched antimicrobial peptide 2	-1.346	0.046	0.860
102723854	LINC01819	long intergenic non-protein coding RNA 1819	-1.333	0.036	0.860
643246	MAP1LC3B2	microtubule associated protein 1 light chain 3 beta 2	-1.331	0.044	0.860
140894	CNBD2	cyclic nucleotide binding domain containing 2	-1.294	0.001	0.860
101929693	RARA-AS1	RARA antisense RNA 1	-1.287	0.023	0.860
59339	PLEKHA2	pleckstrin homology domain containing A2	-1.279	0.039	0.860
342918	C19orf81	chromosome 19 open reading frame 81	-1.249	0.031	0.860
8811	GALR2	galanin receptor 2	-1.200	0.020	0.860
199745	THAP8	THAP domain containing 8	-1.164	0.001	0.860
2745	GLRX	glutaredoxin	-1.141	0.031	0.860
124904009	LOC124904009	uncharacterized LOC124904009	-1.018	0.040	0.860
1506	CTRL	chymotrypsin like	-1.008	0.007	0.860
388228	SBK1	SH3 domain binding kinase 1	1.008	0.043	0.860
221833	SP8	Sp8 transcription factor	1.022	0.001	0.860
656	BMP8B	bone morphogenetic protein 8b	1.030	0.032	0.860
57732	ZFYVE28	zinc finger FYVE-type containing 28	1.077	0.039	0.860
155185	AMZ1	archaelysin family metallopeptidase 1	1.081	0.025	0.860
100130705	ATP6V1FNB	ATP6V1F neighbor	1.087	0.040	0.860
4921	DDR2	discoidin domain receptor tyrosine kinase 2	1.132	0.026	0.860
259217	HSPA12A	heat shock protein family A (Hsp70) member 12A	1.133	0.047	0.860
3213	HOXB3	homeobox B3	1.173	0.040	0.860
84698	CAPS2	calcyphosine 2	1.205	0.028	0.860
4487	MSX1	msh homeobox 1	1.323	0.032	0.860
105370888	TMEM202-AS1	TMEM202 antisense RNA 1	1.404	0.005	0.860
100131369	DUX4L27	double homeobox 4 like 27 (pseudogene)	1.436	0.016	0.860
149465	CFAP57	cilia and flagella associated protein 57	1.476	0.040	0.860
91683	SYT12	synaptotagmin 12	1.481	0.011	0.860
131616	TMEM42	transmembrane protein 42	1.492	0.032	0.860
2635	GBP3	guanylate binding protein 3	1.511	0.040	0.860

285755	PPIL6	peptidylprolyl isomerase like 6	1.519	0.008	0.860
653489	RGPD3	RANBP2 like and GRIP domain containing 3	1.520	0.032	0.860
58494	JAM2	junctional adhesion molecule 2	1.521	0.010	0.860
7352	UCP3	uncoupling protein 3	1.529	0.032	0.860
2824	GPM6B	glycoprotein M6B	1.541	0.034	0.860
162333	MARCHF10	membrane associated ring-CH-type finger 10	1.622	0.037	0.860
50511	SYCP3	synaptonemal complex protein 3	1.668	0.038	0.860
100133315	XNDC1N	XRCC1 N-terminal domain containing 1, N-terminal like	1.705	0.048	0.860
57161	PELI2	pellino E3 ubiquitin protein ligase family member 2	1.729	0.039	0.860
968	CD68	CD68 molecule	1.806	0.025	0.860
105371795	LOC105371795	uncharacterized LOC105371795	2.156	0.015	0.860
101060351	TBC1D3K	TBC1 domain family member 3K	3.884	0.043	0.860
162632	USP32P1	ubiquitin specific peptidase 32 pseudogene 1	5.796	0.012	0.860

Supplementary Table 3.10. Differential expression results of JAr C v JAr UN.

Entrez Gene ID	Gene Symbol	Gene name	log_fc	p_value	fdr
10819	OR7E14P	olfactory receptor family 7 subfamily E member 14 pseudogene	-7.039	0.000	0.523
100532735	INO80B-WBP1	INO80B-WBP1 readthrough (NMD candidate)	-6.896	0.034	0.860
445329	SULT1A4	sulfotransferase family 1A member 4	-3.302	0.000	0.523
57156	TMEM63C	transmembrane protein 63C	-3.189	0.002	0.860
152302	CIDECP1	cell death inducing DFFA like effector c pseudogene 1	-2.853	0.014	0.860
102724105	ZNF528-AS1	ZNF528 antisense RNA 1	-2.704	0.006	0.860
107984773	LINC01852	long intergenic non-protein coding RNA 1852	-2.433	0.001	0.860
2852	GPER1	G protein-coupled estrogen receptor 1	-2.320	0.022	0.860
6540	SLC6A13	solute carrier family 6 member 13	-2.272	0.019	0.860
152831	KLB	klotho beta	-2.255	0.009	0.860
441381	LRRC24	leucine rich repeat containing 24	-2.132	0.006	0.860
148808	MFSD4A	major facilitator superfamily domain containing 4A	-2.050	0.012	0.860
8557	TCAP	titin-cap	-2.025	0.038	0.860

9047	SH2D2A	SH2 domain containing 2A	-1.956	0.031	0.860
441094	NR2F1-AS1	NR2F1 antisense RNA 1	-1.824	0.013	0.860
645158	CBX3P2	chromobox 3 pseudogene 2	-1.792	0.027	0.860
58473	PLEKHB1	pleckstrin homology domain containing B1	-1.769	0.045	0.860
54567	DLL4	delta like canonical Notch ligand 4	-1.762	0.002	0.860
100885848	PTGES3L	prostaglandin E synthase 3 like	-1.608	0.020	0.860
401242	LINC01623	long intergenic non-protein coding RNA 1623	-1.602	0.034	0.860
4922	NTS	neurotensin	-1.520	0.039	0.860
100419515	LOC100419515	zinc finger protein 41 pseudogene	-1.480	0.045	0.860
629	CFB	complement factor B	-1.409	0.006	0.860
103352539	LINC01410	long intergenic non-protein coding RNA 1410	-1.401	0.012	0.860
64581	CLEC7A	C-type lectin domain containing 7A	-1.356	0.014	0.860
155382	VPS37D	VPS37D subunit of ESCRT-I	-1.324	0.018	0.860
8811	GALR2	galanin receptor 2	-1.312	0.013	0.860
728501	RPL21P75	ribosomal protein L21 pseudogene 75	-1.310	0.022	0.860
90485	ZNF835	zinc finger protein 835	-1.309	0.006	0.860
101927288	MANEA-DT	MANEA divergent transcript	-1.239	0.041	0.860
145781	GCOM1	GCOM1, MYZAP-POLR2M combined locus	-1.179	0.049	0.860
149483	CCDC17	coiled-coil domain containing 17	-1.018	0.030	0.860
9235	IL32	interleukin 32	-1.017	0.024	0.860
253152	EPHX4	epoxide hydrolase 4	1.004	0.016	0.860
85366	MYLK2	myosin light chain kinase 2	1.015	0.029	0.860
100289092	ATP2A1-AS1	ATP2A1 antisense RNA 1	1.043	0.042	0.860
57732	ZFYVE28	zinc finger FYVE-type containing 28	1.045	0.046	0.860
84698	CAPS2	calcyphosine 2	1.071	0.049	0.860
130132	RFTN2	raftlin family member 2	1.074	0.008	0.860
4921	DDR2	discoidin domain receptor tyrosine kinase 2	1.089	0.032	0.860
320	APBA1	amyloid beta precursor protein binding family A member 1	1.106	0.010	0.860
59269	HIVEP3	HIVEP zinc finger 3	1.110	0.034	0.860

124900513	LOC124900513	uncharacterized LOC124900513	1.123	0.008	0.860
3213	HOXB3	homeobox B3	1.129	0.047	0.860
55901	THSD1	thrombospondin type 1 domain containing 1	1.133	0.018	0.860
10815	CPLX1	complexin 1	1.137	0.027	0.860
9902	MRC2	mannose receptor C type 2	1.164	0.040	0.860
84647	PLA2G12B	phospholipase A2 group XIIB	1.185	0.012	0.860
56128	PCDHB8	protocadherin beta 8	1.191	0.007	0.860
80726	IQCN	IQ motif containing N	1.289	0.014	0.860
64943	NT5DC2	5'-nucleotidase domain containing 2	1.290	0.048	0.860
656	BMP8B	bone morphogenetic protein 8b	1.297	0.008	0.860
285755	PPIL6	peptidylprolyl isomerase like 6	1.345	0.017	0.860
110806272	BTG3-AS1	BTG3 antisense RNA 1	1.394	0.049	0.860
8174	MADCAM1	mucosal vascular addressin cell adhesion molecule 1	1.414	0.039	0.860
2635	GBP3	guanylate binding protein 3	1.450	0.049	0.860
131616	TMEM42	transmembrane protein 42	1.465	0.035	0.860
102724826	ZNF337-AS1	ZNF337 antisense RNA 1	1.484	0.007	0.860
259217	HSPA12A	heat shock protein family A (Hsp70) member 12A	1.563	0.007	0.860
56131	PCDHB4	protocadherin beta 4	1.574	0.027	0.860
100507582	BHLHE40-AS1	BHLHE40 antisense RNA 1	1.576	0.043	0.860
113540	CMTM1	CKLF like MARVEL transmembrane domain containing 1	1.594	0.047	0.860
101927117	PLCG1-AS1	PLCG1 antisense RNA 1	1.664	0.027	0.860
968	CD68	CD68 molecule	1.936	0.017	0.860
57161	PELI2	pellino E3 ubiquitin protein ligase family member 2	1.987	0.017	0.860
100528064	NEDD8-MDP1	NEDD8-MDP1 readthrough	2.038	0.010	0.860
79875	THSD4	thrombospondin type 1 domain containing 4	2.582	0.049	0.860
1593	CYP27A1	cytochrome P450 family 27 subfamily A member 1	2.783	0.028	0.860
7803	PTP4A1	protein tyrosine phosphatase 4A1	4.826	0.024	0.860
54441	STAG3L1	stromal antigen 3-like 1 (pseudogene)	5.113	0.025	0.860
162632	USP32P1	ubiquitin specific peptidase 32 pseudogene 1	6.316	0.006	0.860

Supplementary Table 3.11. KEGG terms of all pathways identified to be upregulated in the E2P4 treated groups in all comparison groups with the normalised enrichment scores displayed.

KEGG term	EP v E NES	EP v P NES	EP v C NES	EP v UN NES
KEGG_GLYCOSPHINGOLIPID_BIOSYNTHESIS_GLOBO_SERIES	1.632	1.226	1.462	0.450
KEGG_THYROID_CANCER	0.490	0.891	0.687	0.640
KEGG_FC_GAMMA_R_MEDIATED_PHAGOCYTOSIS	0.777	0.797	0.898	0.653
KEGG_PRIMARY_IMMUNODEFICIENCY	0.895	1.058	1.090	0.732
KEGG_NON_HOMOLOGOUS_END_JOINING	0.621	0.831	0.713	0.761
KEGG_GLYCOSPHINGOLIPID_BIOSYNTHESIS_LACTO_AND_NEOLACTO_SERIES	1.085	1.041	1.222	0.764
KEGG_OTHER_GLYCAN_DEGRADATION	1.264	0.918	0.861	0.781
KEGG_B_CELL_RECEPTOR_SIGNALING_PATHWAY	0.628	0.787	1.107	0.839
KEGG_INSULIN_SIGNALING_PATHWAY	0.476	0.661	0.955	0.847
KEGG_PANCREATIC_CANCER	0.492	0.527	0.900	0.857
KEGG_VEGF_SIGNALING_PATHWAY	1.144	1.011	0.754	0.884
KEGG_TOLL_LIKE_RECEPTOR_SIGNALING_PATHWAY	0.960	1.122	1.483	0.905
KEGG_NEUROTROPHIN_SIGNALING_PATHWAY	0.409	0.409	0.846	0.933
KEGG_NITROGEN_METABOLISM	0.961	1.402	0.815	0.961
KEGG_GLIOMA	0.419	0.518	1.104	0.993
KEGG_T_CELL_RECEPTOR_SIGNALING_PATHWAY	0.851	0.575	0.964	1.007
KEGG_NON_SMALL_CELL_LUNG_CANCER	0.667	0.606	0.684	1.028
KEGG_ALDOSTERONE_REGULATED_SODIUM_REABSORPTION	0.546	1.031	0.683	1.062
KEGG_FC_EPSILON_RI_SIGNALING_PATHWAY	1.399	0.771	0.987	1.066
KEGG_INOSITOL_PHOSPHATE_METABOLISM	1.033	0.803	1.327	1.073

KEGG_ERBB_SIGNALING_PATHWAY	0.522	0.927	0.601	1.076
KEGG_COMPLEMENT_AND_COAGULATION_CASCADES	0.792	0.859	1.023	1.076
KEGG_COLORECTAL_CANCER	0.615	0.949	0.903	1.100
KEGG_ENDOMETRIAL_CANCER	0.774	0.999	0.990	1.111
KEGG_ACUTE_MYELOID_LEUKEMIA	0.858	1.095	0.842	1.114
KEGG_AXON_GUIDANCE	0.900	0.661	1.047	1.115
KEGG_PATHWAYS_IN_CANCER	0.590	0.633	0.805	1.134
KEGG_HISTIDINE_METABOLISM	1.067	0.744	1.148	1.152
KEGG_MTOR_SIGNALING_PATHWAY	0.937	0.884	1.062	1.161
KEGG_TASTE_TRANSDUCTION	1.390	1.469	1.332	1.163
KEGG_CHRONIC_MYELOID_LEUKEMIA	0.388	0.695	1.066	1.167
KEGG_CALCIUM_SIGNALING_PATHWAY	0.598	0.760	1.014	1.186
KEGG_RENAL_CELL_CARCINOMA	0.856	0.774	0.677	1.195
KEGG_ABC_TRANSPORTERS	1.025	0.757	1.021	1.222
KEGG_NATURAL_KILLER_CELL_MEDIATED_CYTOTOXICITY	0.842	0.739	0.848	1.225
KEGG_ECM_RECEPTOR_INTERACTION	0.898	1.200	0.712	1.243
KEGG_PROSTATE_CANCER	0.422	0.778	1.021	1.248
KEGG_FOCAL_ADHESION	0.860	0.848	0.858	1.270
KEGG_JAK_STAT_SIGNALING_PATHWAY	1.002	1.122	1.012	1.296
KEGG_MELANOGENESIS	0.861	0.971	0.466	1.304
KEGG_FATTY_ACID_METABOLISM	1.377	0.934	1.477	1.315
KEGG_BETA_ALANINE_METABOLISM	1.474	0.836	1.386	1.373
KEGG_PYRUVATE_METABOLISM	1.056	0.944	1.433	1.389
KEGG_GAP_JUNCTION	0.645	0.885	1.346	1.508

KEGG_LYSINE_DEGRADATION	1.285	1.121	1.382	1.517
KEGG_PHOSPHATIDYLINOSITOL_SIGNALING_SYSTEM	1.326	1.111	1.555	1.538
KEGG_OLFACTORY_TRANSDUCTION	1.375	1.063	1.567	1.544
KEGG_LIMONENE_AND_PINENE_DEGRADATION	1.426	0.709	1.690	1.564
KEGG_BASAL_CELL_CARCINOMA	1.143	1.096	0.738	1.586
KEGG_WNT_SIGNALING_PATHWAY	0.948	1.174	1.074	1.609
KEGG_ASCORBATE_AND_ALDARATE_METABOLISM	1.546	0.957	1.667	1.662
KEGG_TRYPTOPHAN_METABOLISM	1.140	0.994	1.261	1.667

CHAPTER 4

COMPARISON OF URINE EV ISOLATION AND STORAGE METHODS FOR SUBSEQUENT BIOMARKER RESEARCH.

Chapter 4. Comparison of urine EV isolation and storage methods for subsequent biomarker research.

4.1 Authors contribution.

This chapter is presented in a publication format that is currently not intended to be submitted.

4.2 Interconnecting chapters.

After investigating the role of endometrial extracellular vehicles (EVs) in implantation through *in vitro* models in chapter 2 and 3, the current chapter explores the non-invasive biofluid of urine. The earlier *in vitro* model in the previous chapters revealed that the endometrial EV proteome differs under differing hormonal stimulation regimes, suggesting the potential utility of these EVs as biomarkers for identifying the distinct phases of the menstrual cycle. With the aim of establishing proof of concept of a non-invasive EV-based method for identifying the implantation period, the proceeding chapter focuses on optimising the isolation of EVs from urine.

4.3 Chapter aim.

Optimising the isolation of EVs from urine to ensure the repeatability, purity, and storage condition is sufficient for the subsequent investigation into urine EVs as non-invasive biomarker.

4.4 Abstract.

Human urine is a readily available rich source of extracellular vesicles (EVs), and because of their specific, biological relevant cargos, they are a potentially useful source of non-invasive biomarkers that could aid clinical decision-making in a variety of diseases and conditions, including those of reproductive health. However, the isolation of urine EVs (uEVs) is made difficult by various factors, including the abundance of Tamm-Horsfall protein (THP) found within urine, which can polymerize and entraps uEVs. Additionally, non-standardised methodology in uEV handling, isolation, and storage contributes to the challenge. This study aimed to compare two different isolation methods: one incorporating a THP removal step (using NaCl precipitation, differential centrifugation, and size exclusion chromatography- SEC), and another without, which combined differential centrifugation and SEC. Samples were assessed using nanoparticle tracking analysis (NTA) and bicinchoninic acid assay (BCA) to evaluate the protocols' efficacy in separating EV-sized particles from total protein, as well as determining the concentration and size distribution of the resulting isolated uEVs. Additionally, the impact of storage duration at -80°C on both neat urine and pre isolated uEVs in terms of concentration and size distribution was explored. Overall results from this study indicate that the additional salt precipitation step had no effect on uEV concentration yield and size distribution. Furthermore, the findings suggest that long-term storage of neat urine appears to increase the amount of EV-sized contaminants. These results provide valuable insights for uEV biomarker discovery protocols and subsequent translation of uEV in diagnostic applications.

4.5 Introduction.

Urine is a highly advantageous biofluid, serving as an abundant source of biomarkers (1). Its clinical utility is underscored by many advantages, including non-invasive collection, the potential to collect substantial volumes that can be gathered over several time points throughout the day, and even the possibility of home collection (2). Due to these qualities, urinalysis has been an integral part of standard clinical practice (2). Urine itself contains many different components, with Tamm–Horsfall protein being the most abundant protein (50%), followed by albumin (20%) and immunoglobulin (5%) (3). Additionally, other constituents include traces of epithelial and blood cells, bacteria, organic and inorganic molecules, viruses, and importantly, extracellular vesicles (EVs) (4).

Relatively large quantities of these urine EVs (uEVs) originate from urinary tract cells (5), but research has also indicated their origin extends beyond the urinary tract to other non-urinary tract locations (6–8). These uEVs offer an alternate and beneficial source for protein and genomic biomarkers due to their protective encapsulated cargo environment resulting from the bi-layer glycoprotein membrane (9). As a result, the uEVs' proteome and genome are predicted to remain relatively stable post-collection and isolation. Consequently, due to their potential use in clinical situations, it has recently become fundamentally essential to advance and standardise isolation procedures to ensure reproducibility, purity, and yield, thus enabling accurate biomarker discoveries (10).

Currently, various methods exist for the isolation of uEVs, including, ultracentrifugation, filtration, size exclusion chromatography (SEC), precipitation, commercial kits,

hydrostatic filtration dialysis, as well as various combinations of these methods (11). All of these methods have various reported disadvantages and advantages in their use for EV isolation (12). In addition to these isolation methods, numerous handling and collection variations exist (13), which also in turn affect the enrichment of uEVs, leading to the isolation of various subpopulations that could influence downstream analysis and interpretation in both proteomics and transcriptomics (14,15). Presently, there are limited standardised guidelines of isolation, handling, and storage protocols for EVs. Regarding uEVs, the Urine Task Force of the Rigor and Standardization Subcommittee of the International Society for Extracellular Vesicles (ISEV*)* published a position paper in 2021 summarising the current *state of the art* and listing suggestions for improved rigor, reproducibility, and inter-operability in uEV research (15). However, these are merely suggestions based on expert consensus rather than reproducible large-scale studies, making the interpretation, comparison, and repeatability of published results difficult.

Furthermore, the numerous origins and complex composition of urine and uEVs presents additional challenges. For example, uEV isolation is confronted by the potential contamination with non-uEV associated proteins, most predominantly Tamm Horsfall protein (THP), which creates large mesh-like glycoprotein filaments that entrap uEVs (16). This contaminant issue, coupled with substantial intra- and inter-individual variations in urine composition, means that it is doubtful a defined protocol for urine and uEV handling, isolation, and storage will be applicable in all disease conditions and investigations. Nevertheless, reaching an agreed method is particularly important in biomarker discovery studies concerning clinical and preclinical uEV, as new discoveries hold implications for clinical decision-making.

Hence, in this study, the aim was to assess the efficacy of a combined approach involving differential centrifugation and SEC-based methods for the isolation of EVs from urine in the context of our subsequent biomarker discovery investigations. We hereby describe, in the context of optimising methodologies for biomarker discoveries on uEVs, the effects of isolation, storage, and individual variability. Our findings indicate that the combination of differential centrifugation and SEC facilitates effective uEV enrichment and enables the efficient separation of total protein from EV-contained proteins, eliminating the need for an additional clearance step for THP. Furthermore, our results reveal no long-term detrimental effect of storage on urine or uEV at -80°C. This isolation method and resulting uEVs can be utilized for further downstream proteomic and transcriptomic analysis, thereby advancing research towards the identification of uEV biomarkers and their potential application as a soluble non-invasive biopsy.

4.6 Materials and methods.

4.6.1 Urine samples.

Urine samples from healthy women of reproductive age were obtained from Swiss precision diagnostic (SPD) Development Company (Bedford, UK) according to SPD Protocol- 0054, which has SPD Research Ethics approval. Available clinical information of volunteers can be seen in Supplementary Table 4.1. First void urine was donated and cleared of all cells and debris via centrifugation at 400g for 5mins then 1000g for 10 mins with the supernatant transferred into a clean fresh tube after each spin all at 4°C. These cleared sample then were transported at 4°C from Bedford to Sheffield on the same day as donation. Once received at Sheffield the previously mentioned centrifugation steps

were repeated before freezing and storage at -80°C. Participants use in each experiment are indicated in the result figure description.

4.6.2 Differential centrifugation.

Urine was defrosted at room temperature prior to differential centrifugation. Urine was centrifuged for 10min at 1000× g and 4°C in a sigma 11180 swinging rotor centrifuge. The pellet was discarded, and the supernatant was centrifuged again for 10 min at 4,000× g and 4°C, again the pellet was discarded, and finally the supernatant was centrifuged for 10mins at 10,000× g and 4°C. Following centrifugation, the final resulting supernatant was concentrated using a 10kDa ultrafiltration tube (Sartorius, Hampshire, UK) to 500µl. Retentates were then subjected to size exclusion chromatography.

4.6.3 Size exclusion chromatography.

For the preparation of one SEC column, 14-mL of Sepharose CL-2B (GE Healthcare, Uppsala, Sweden) was packed into an empty gravity chromatography column (Bio-rad, Watford, UK). After separation, a nylon net filter was inserted at the ethanol/Sepharose bead interface line at about 10ml. The ethanol was eluted followed by washing the column three times (5ml x3) with molecular grade water then three times (5ml x 3) with Ca^{2+} and Mg^{2+} free Dulbecco's phosphate-buffered saline (Sigma-Aldrich, Dorset, UK). On top of the filter, 0.5 mL of the concentrated urine was loaded and elution fractions of 0.5mL were collected in 20 fractions with a Ca^{2+} and Mg^{2+} free Dulbecco's phosphate-buffered saline eluent. The resulting fractions were stored at −80°C for further EV characterisation.

4.6.4 Salt precipitation.

Salt precipitation was performed on urine samples after the 4000g differential centrifugation step. Sodium chloride (NaCl) (Sigma-Aldrich, Dorset, UK) was added to the 10ml of urine at a concentration of 0.58M (0.338 g in 10ml urine). Samples where then incubated either at room temperature or 4°C for 2 hours. Following this incubation, samples were then centrifuged at 3000g for 25mins at room temperature to pellet sodium chloride and any precipitated particles (as previously described (17)). Supernatant was then transferred to a fresh tube for a final 10,000g centrifugation at 4 °C for 10 min.

4.6.5 Nanoparticle tracking analysis.

For nanoparticle tracking analysis (NTA) (ZetaView PMX 110, Particle Metrix, Meerbusch, Germany) all samples were diluted in milliQ water. Ideal measurement concentrations were found by pre-testing the ideal particle per frame value (140–200 particles/frame). For each measurement, three cycles were performed by scanning 11 cell positions each and capturing 30 frames per position under following settings: Focus: autofocus; Camera sensitivity for all samples: 50; Shutter: 70; Scattering Intensity: detected automatically; Cell temperature: 25°C. After capture, the videos were analysed by the in-built ZetaView Software 8.04.02 SP2 with specific analysis parameters: Maximum size 500, Minimum size 5, Minimum brightness: 25. Hardware: embedded laser: 40 mW at 488 nm; camera: CMOS.

4.6.6 Bicinchoninic acid assay.

Protein concentrations were determined using the bicinchoninic acid assay kit (Pierce™ BCA Protein Assay Kit) and was performed according to the manufacturer's protocol. The standard curve was constructed from a working range of 20–2000 µg/mL bovine serum albumin (BSA). 25 µl of each standard or protein sample were loaded on a 96-well plate followed by addition of 200 µl/well working reagent. The absorbance at 595nm was measured on a EnSight plate reader (Perkin Elmer, OH, United States).

4.6.7 Transmission electron microscopy (TEM).

After SEC, 100µL of the concentrated EVs were mixed with 100µL of 4% paraformaldehyde (Polyscience, Warrington, USA) to fix the EVs. Samples were transported to the Institute of Animal Reproduction and Food Research, Olsztyn, Poland for further analysis. On the day of analysis, 20µL of EVs droplet was covered by a 200-mesh formvar and carbon coated grid (Electron Microscopy Sciences). The EVs droplet was incubated for 20 minutes in room temperature. After 20 minutes, the grid was tapped on filter paper to remove excess PBS. Later the grid was rinsed once by gently touching the surface of the grid on 50µL of ddH_2O droplet and tapping on a filter paper to remove the excess water. For negative staining, the grid was transferred onto a droplet of 4% uranyl acetate (Polysciences, Warrington, USA) for 5 min incubation at room temperature. Samples were observed with a JEM 1400 transmission electron microscope (JEOL Ltd. Tokyo, Japan) at 80 kV, and digital images were acquired with a numeric camera (Morada TEM CCD camera, Olympus, Germany).

4.6.8 Experimental design: Urine EV isolation method comparison.

The experiment aimed to optimise the isolation of uEVs from samples collected from female volunteers. The aim was to determine the SEC fractions containing the highest concentration of EV-sized particles by comparing two distinct methods as well as determining an optimum starting volume to yield enough EVs for further analysis. Method 1, combining differential centrifugation and size exclusion, and method 2, involving a combination of differential centrifugation, salt precipitation and size exclusion chromatography, were assessed. In both methods, urine was thawed at room temperature. In the case of method 1 (Figure 4.1), the urine was divided into 10ml, 5ml and 2.5ml starting sample sizes. These samples underwent a series of differential centrifugation steps, comprising of a centrifugation at 4°C for 10min each at 1000g, followed by 4000g and then 10000g, with the pellet discarded after each spin. The final supernatant was then concentrated to 500µl, as per the methods above. The concentrated samples were subsequently passed through a prepared SEC column, and 20 x 500µl fractions collected. Following this, the samples were frozen at -80°C for subsequent analysis and characterisation.

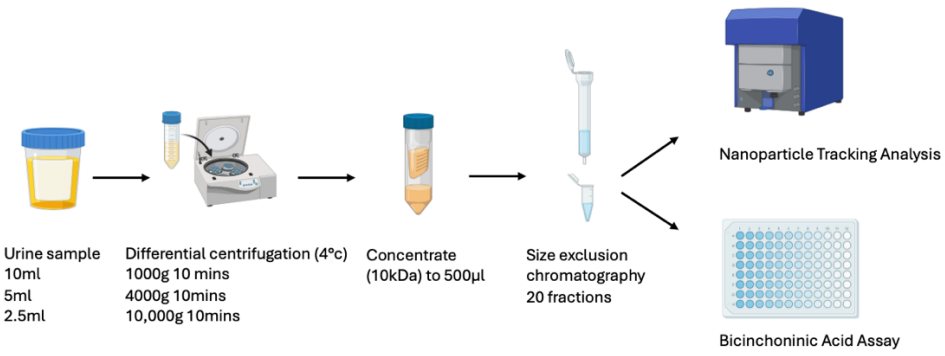


Figure 4.1. Experimental Design for optimisation of EV Particle Isolation from Urine Using a Combination of Isolation Methods of Differential Centrifugation and Size Exclusion Chromatography and Analysis via Nanoparticle Tracking and Bicinchoninic Acid Assay. (Created with BioRender.com).

In method 2 (Figure 4.2), urine was divided into 10ml, 5ml and 2.5ml starting sample sizes. First, differential centrifugation was performed, the same as previously mentioned, but after the 4000g spin and before the 10000g spin, a salt precipitation step was added. For salt precipitation, a final concentration of 0.58M NaCl (Sigma-Aldrich, Dorset, UK) was added to the samples, and they were incubated at either 4°C or at room temperature for 2 hours. Subsequently, the samples underwent centrifugation again at 4°C for 25 minutes at 3000g, followed by a spin at 10,000g for 10 minutes, with the pellet discarded after each spin. The samples were then concentrated to 500µl and passed through a prepared SEC column, collecting 20 x 500µl fractions. Finally, the samples were then frozen at -80°C for further analysis and characterisation.

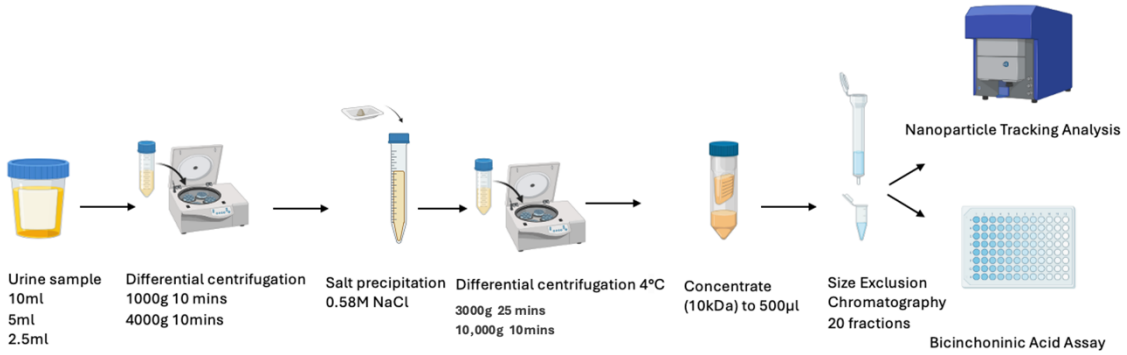


Figure 4.2. Experimental design for benchmarking EV particle isolation from urine Using a Combination of Isolation Methods of Differential Centrifugation, Salt Precipitation and Size Exclusion Chromatography and Analysis via Nanoparticle Tracking and Bicinchoninic Acid Assay. (Created with BioRender.com).

4.6.9 Experimental design: storage comparison.

A storage comparison of uEVs was performed by analysing the NTA results from the urine from the same four volunteers after 1 year of storage in -80°C. The comparison involved both the isolated uEV fraction stored at -80°C for 1 year and the same neat urine stored under the same conditions for 1 year. These results were also compared to those previously obtained, where the uEVs were isolated soon after -80°C storage (Figure 4.3). In all instances, the same isolation method, involving differential centrifugation and SEC, was performed on the same urine volume (10ml). TEM was also performed on samples to confirm morphological presence of EVs in the samples.

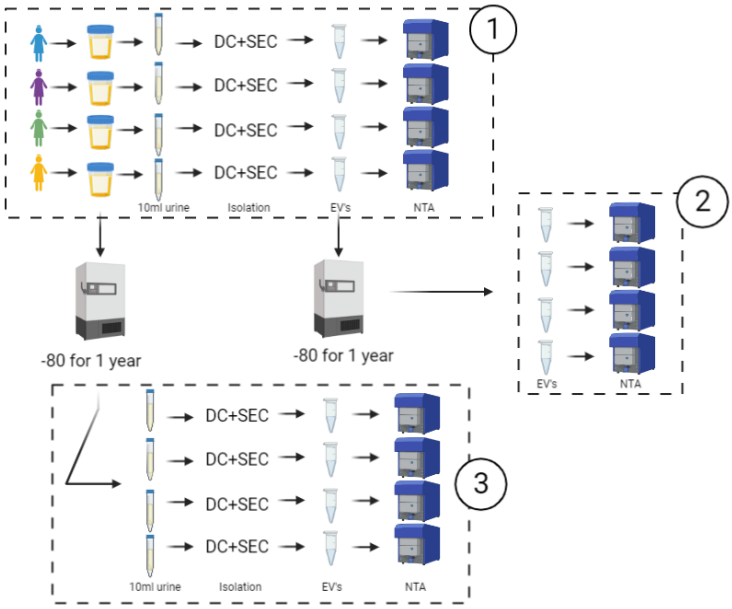


Figure 4.3. Experimental design for storage comparison of urine EVs. 1, represents the urine EVs isolated soon after collection and storage. 2, represents the same EV samples that were stored for 1 year at -80°C. 3, represents the neat urine that was stored for 1 year at -80°C. Isolation method used was differential centrifugation and size exclusion chromatography (DC+SEC). Samples were analysed by nanoparticle tracing analysis (NTA). (Created with BioRender.com).

4.6.10 Statistical analysis.

GraphPad Prism version 9.2.0 was used for all statistical analysis. Statistical test performed on each data set is stated in each figure legend when appropriate. A P value of $P < 0.05$ was considered as significant in all the analysis.

4.7 Results.

4.7.1 Urine EV isolation optimisation method comparison.

To compare particle and protein yield between the two EV isolation methods within each SEC fraction derived from three different starting volumes of urine (10ml, 5ml and 2.5ml), protein quantification using the BCA assay, in addition to the determination of particle concentration by NTA, was performed. Both methods show clear separation between the SEC fractions containing the highest concentration of EV-sized particles and the later fractions exhibiting peak protein concentration (Figure 4.4 and 4.5). While both methods exhibit clear separation between particle-rich and protein-rich fractions, there is a disparity in the specific fractions containing the highest concentrations. In method one, the majority of particles are found in fractions 5-7 (Figure 4.4), whereas method two shows the highest particle concentration in fractions 5-9 (Figure 4.5).

When combining the total concentration of EV-sized particles, no significant difference is observed when comparing the two methods across different starting volumes of urine (Figure 4.6). Further comparison with salt precipitation conducted at both room temperature and 4°c was carried out. However, once again, no significant difference was observed when compared to method 1, whether the salt precipitation was performed at room temperature (Figure 4.7 a) or at 4°C (Figure 4.7 b).

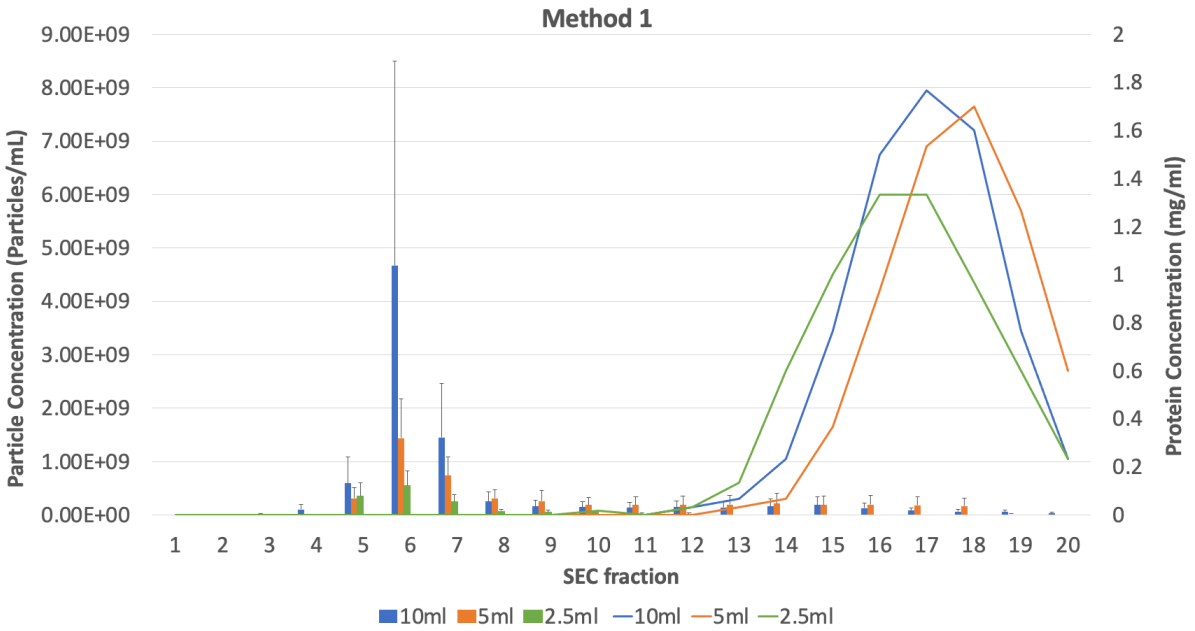


Figure 4.4 Comparison of particle concentration and protein concentration in SEC fractions from different urine starting volumes using isolation method 1. The bars represent the mean concentration (particles/mL) ±SEM of EV-sized particles from the SEC fractions, while the line graph depicts the mean protein concentration in each SEC fraction form the same samples. Data were obtained from 3 biological replicates (volunteers 2, 7, and 3) with 3 technical replicates.

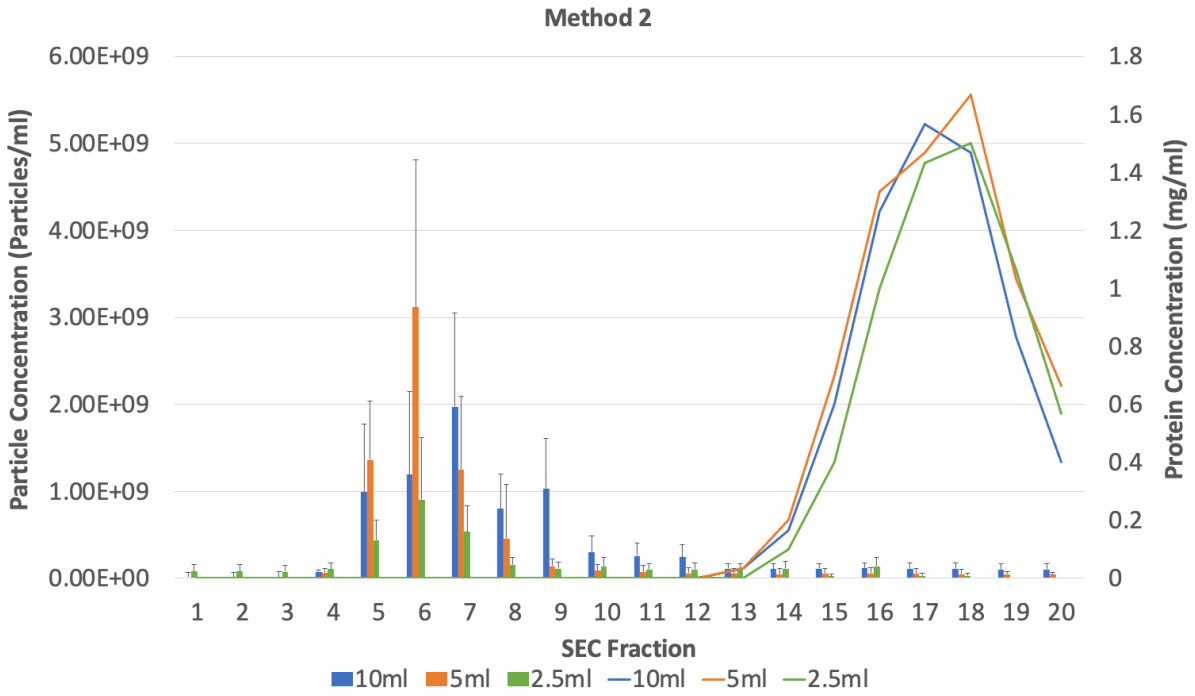


Figure 4.5 Comparison of particle concentration and protein concentration in SEC fractions from different urine starting volumes using isolation method 2. The bars represent the mean concentration (particles/mL) ±SEM of EV-sized particles from the SEC fractions, while the line graph represent the mean concentration of protein in each SEC fraction from the same samples. Data were obtained from 3 biological replicates (volunteers 2,7, and 3) with 3 technical replicates.

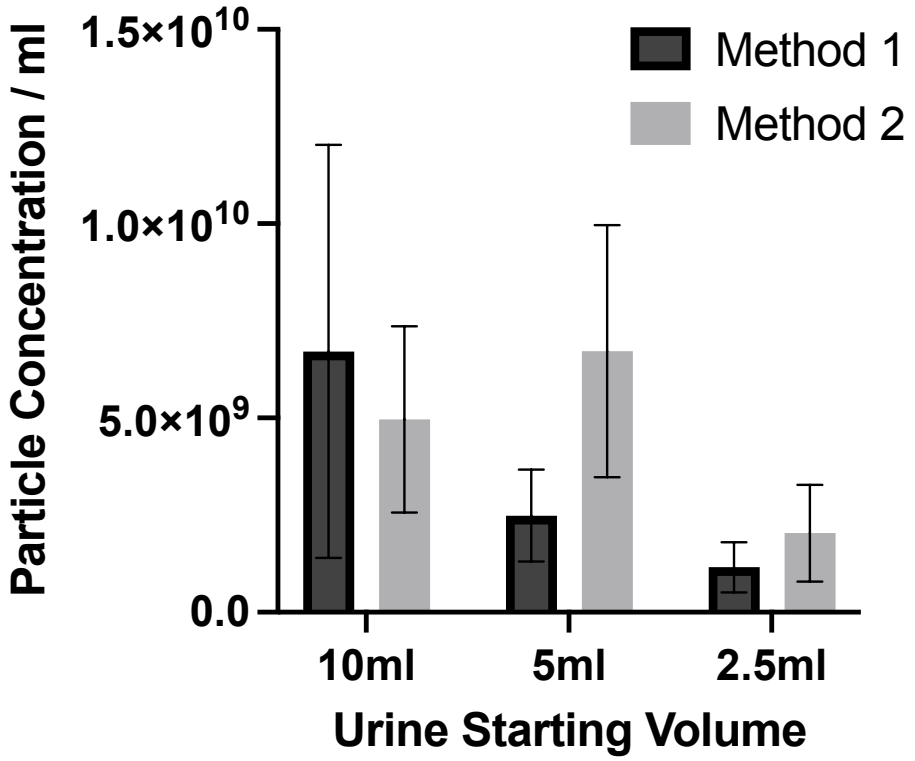


Figure 4.6. Comparison of Particle concentration among the different isolation methods and starting volumes. The bars represent the mean concentration (particles/mL) ±SEM of EV-sized particles from SEC fractions 5–7 for method 1 and 5-9 for method 2. Data were obtained from 3 biological replicates (volunteers 2,7, and 3) and 3 technical replicates for each group. RM two-way ANOVA with Šídák's Multiple Comparisons statistical test was performed, but no significant difference was seen ($P \leq 0.05$).

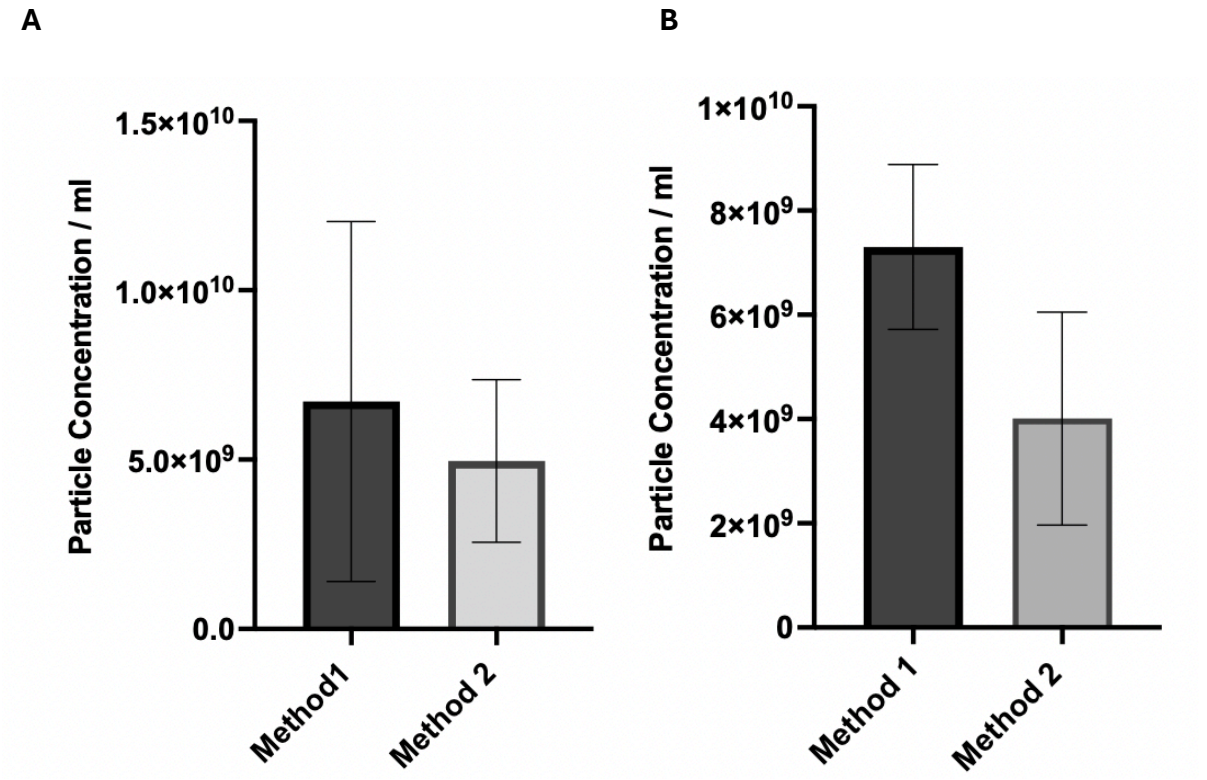


Figure 4.7. Particle concentration comparison of the different isolation methods with a change in the salt precipitation incubation temperature. (A) salt precipitation performed at room temperature and (B) performed at 4°C. The bars represent the mean concentration (particles/mL) ±SEM of EV-sized particles from SEC fractions 5–7 for method 1 and 5-9 for method 2. Both conditions had a urine starting volume of 10ml. Data were obtained from 3 biological replicates (volunteers 2,3 and 7 for A, and volunteers 1, 6 and 4 for B) with 3 technical replicates for each group. Pared T test was performed on each data set, but no statistical significance was seen ($P \leq 0.05$).

4.7.2 Storage comparison.

To assess the stability of uEV-sized particles, the particle number and concentration was measured via NTA analysis in pre-cleared urine. Neat urine was stored at -80°C for 1 year, and uEVs were pre-isolated after a month of storage, then stored at -80°C for 1 year. All samples are derived from the same participants and underwent the same isolation method. A mean uEV particle concentration of $3.25x10^{10} \pm 1.86 x10^{10}$ (SEM) particles per ml was observed in neat urine samples stored for a 1 year at -80°C. In pre-isolated uEVs that had been stored for a year at -80°C, a mean concentration of $1.40x10^{10} \pm 4.51x10^{9}$ (SEM) particles per ml was observed. For samples isolated just a month before storage for a year at-80 °C, the mean concentration was $5.60x10^{9} \pm 2.03 x10^{9}$ (SEM) particles per ml (Figure 4.8). Despite a visual increasing trend in the quantity of uEV-sized particles when stored for a year, especially in neat urine compared to pre-isolate samples, no significant difference was observed. This trend extended to the size distribution, where no significant difference was seen (Figure 4.9).

To visually compare uEV storage conditions and validate previous data obtained by NTA, TEM analysis was performed. In both cases, typical morphological structures were detected (Figure 4.10), but some background debris was also noted in both samples.

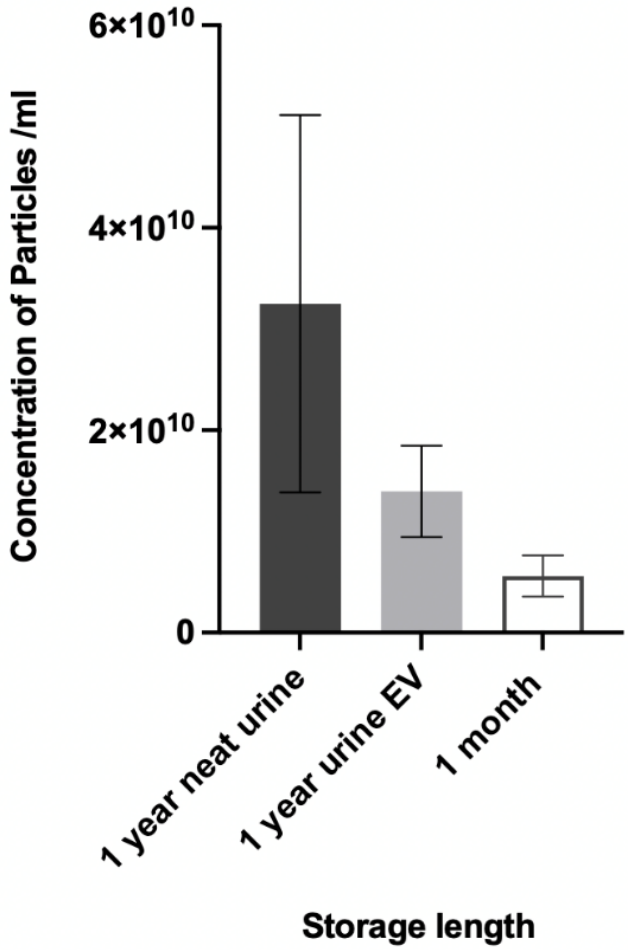


Figure 4.8. Comparison of particle concentration yield under different storage conditions. The bars represent the mean concentration (particles/mL) ±SEM of EV-sized particles from SEC fractions 5–7. Data were obtained from the same four biological replicates (volunteers 1, 2, 4 and 6) with three technical replicates from each group. RM one-way ANOVA with post hoc Tukey statistical test was performed, but no significance was seen ($P \leq 0.05$).

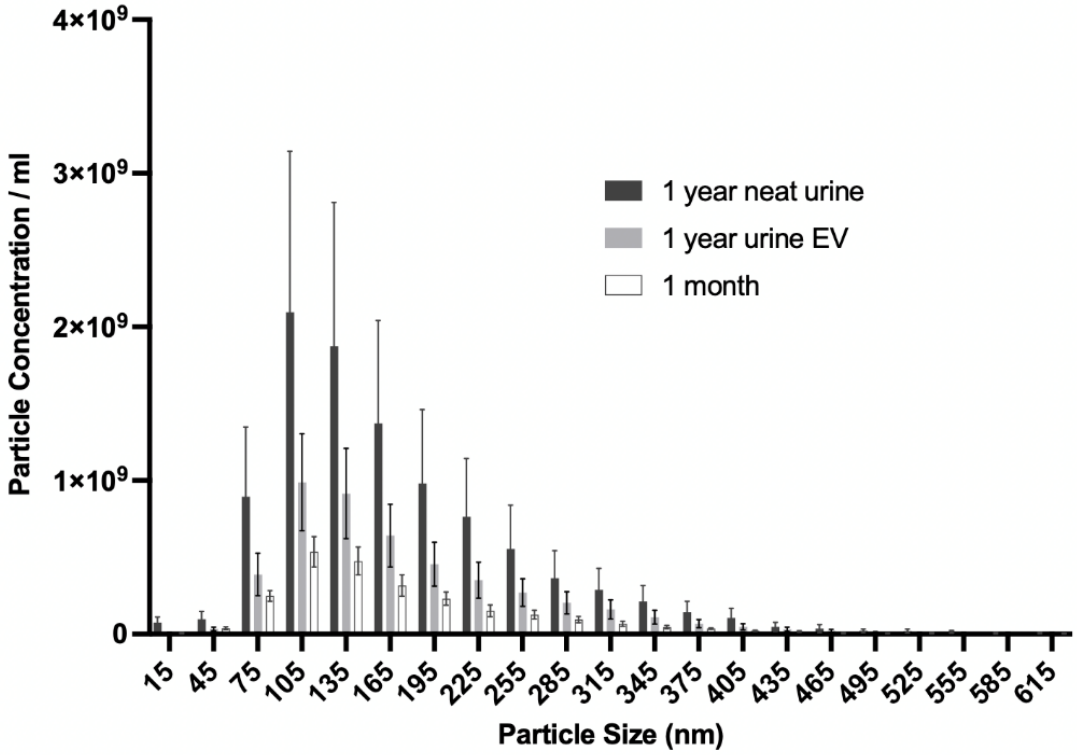


Figure 4.9. Comparison of size distribution under different storage conditions. The bars represent the mean concentration (particles/mL) ±SEM of EV-sized particles from SEC fractions 5–7. Data were obtained from four biological replicates (volunteers 1, 2, 4 and 6) and three technical replicates for each group. RM two-way ANOVA with post hoc Tukey statistical test was performed, but no significance was seen ($P \leq 0.05$).

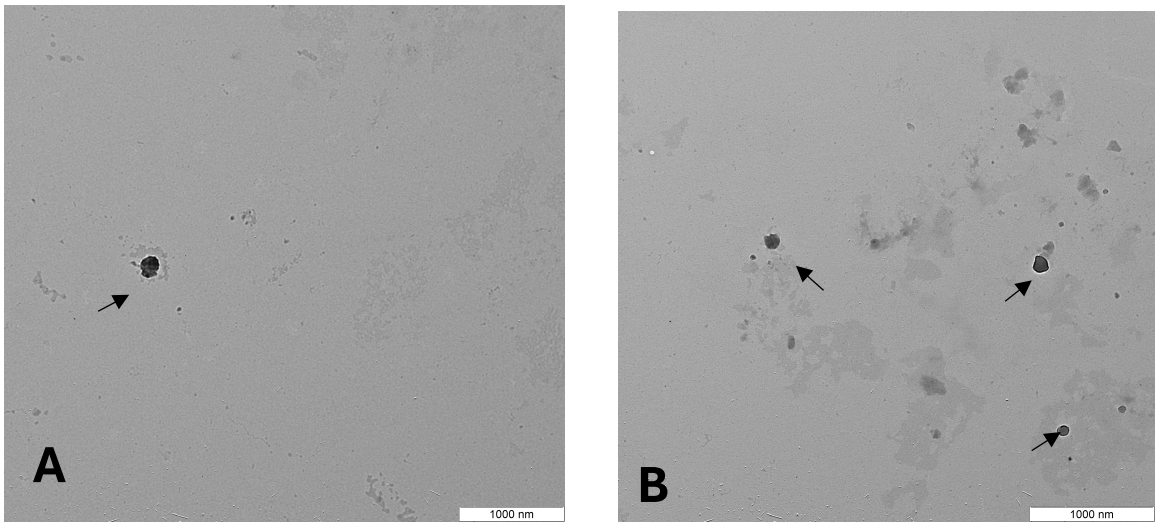


Figure 4.10. TEM Image-based characterisation of uEVs under different storage conditions. Representative TEM images of urine EVs from (A) 1-year neat urine (B) 1-year uEV. Scale bars represent 1000 nm (A, B).

4.8 Discussion.

uEVs have been hypothesised as a valuable biofluid source of potential biomarkers in various conditions, most prominently those affecting the urinary tract (18–20), but also non-urological pathologies (21–24). They hold the potential to complement or replace more invasive diagnostic procedures. However, the translation of potential biomarkers into clinical practice is hindered by the irreproducibility of results due to the lack of standardisation in the field (15). Hence, EV isolation, processing, and handling of biofluids is still a much-needed research area. To contribute to the understanding of uEV isolation, handling, and storage, we compared two different methods of uEV isolation. Both methods involved a combination of differential centrifugation and SEC, with an addition salt precipitation step in one of the groups. We also explored the effect of storage at -80°C, comparing uEVs pre-isolated or stored in neat urine against uEVs isolated after short-term storage. For these experiments, urine was donated from women

of reproductive age, with the intention of using these methods for further research on uEV biomarkers for reproductive health. It is important to note that intrinsic and extrinsic biological differences between samples (such as age, medication, hydration levels, diet, and current sickness) should be considered when interpretating these results, although within this current study it is not statistically possible to account for these differences due to the small sample size. However, we have controlled for technical variations introduced during the collection and processing.

When evaluating and comparing isolation methods in terms of their ability to separate the uEVs from any free proteins, both methods appear successful. This is evident in the combination characterisation graphs (Figure 4.4 and 4.5), illustrating a clear separation between fractions containing increased levels of EV-sized particles and the increase in free proteins levels. In addition to assessing this separation ability, we explored the optimisation of uEV isolation, including the evaluation of different starting volumes. However, when comparing the total concentration of EV-sized particles across varying starting volumes and methods, no significant differences was observed (Figure 4.6). This result contradicts previously published studies demonstrating that total particle count or EV markers increased proportionally to the starting urine volume used (25,26). However, it is important to note that the volumes used in these studies that show a difference between starting volumes utilised considerably higher volumes (800ml Vs 50ml). It is possible that the lack of difference observed in this study could be attributed to the limited variance between volumes, as the assessment of larger volumes was restricted by the limited volume of urine donations received.

Within the literature, the removal of THP appears to be an important step to consider in uEV isolation to maximise yield and purity (16,27,28). Of the reported THP removal methods, Dithiothreitol (DTT) is commonly used (16). However, reports suggest that DTT is a strong reducing agent and can cause remodelling of extracellular protein domains, interfering with the protein's function and downstream analysis (29). An alternative method to DTT is the addition of NaCl, which was used in this study due to it being a simple and less harsh alternative (30). However, surprisingly when comparing the concentration of uEVs in the EV fractions from our method with and without a NaCl THP precipitation step, no significant difference was observed. These results contradict the reported knowledge of THP entrapment on uEV, as it was expected that method one, without a THP removal step, would result in fewer isolated uEVs (31). This opposes results from a study that observed, with the same salt precipitation method, a 10% loss in uEVs when comparing the signal intensity of CD63-immunoreactive band via western blot (17). To investigate if the lack of difference was due the precipitation step being carried out at room temperature rather than at 4°C, as reported by other papers (32), the experiment was repeated. However, this lack of difference between the methods was also observed at this incubation temperature.

This lack of an observable difference could indicate that the importance of a THP removal step is not as vital as once thought. If a study's goal is not to maximise uEV yield but instead to analyse and compares uEVs via omics studies, as in our projected future studies, omitting an additional THP removal step may be advisable to avoid potential contamination or interference from additional chemicals or processing that could affect the resulting uEVs. However, it is worth considering that this lack of difference might be

explained by THP and the entrapped EVs being removed at an earlier stage, before the salt precipitation. Given reports indicating that THP precipitation at low temperatures (27), this could have occurred during the initial centrifugation step after sample thawing. To address this, it has been suggested that warming urine for 5 minutes at 37°C could help avoid such precipitation, with a report showing increased EV recovery with this step (33). Nevertheless, the impact of the warming step on uEV content, structure, and function has not been investigated and hence requires further studies before implementation into a protocol.

Another major consideration when comparing isolation methods with human urine is the vast person-to-person variation in urine composition. Reports indicate that the urine proteome could be influenced by numerous factors stimulated by variances in individuals' regime, such as hydration, diet, exercise, age, gender, and environmental factors, among many others (34). Such variation is evident in our data, as indicated by the large error bars representing the standard error of the mean observed in the replicated data from three different biological repeats, involving three different women. These factors have the potential to influence the amount of uEVs being produced. For instance, within this study, some of the participants were on antibiotics, while others were not, and there was also a variability in hormonal contraception used at the time of collection. Nonetheless, when considering uEVs as a suitable biomarker biofluid, the uEV proteome may be considered highly stable to such variations. This claim is supported by two previous small-scale investigations that report low levels of EV proteome variation (21,35), possibly owing to the protection against degradation provided by the EV lipid bilayer.

The choice of isolation method is not the sole factor to consider when devising a protocol for uEV biomarker discovery; other storage and handling methods can also profoundly affect the resulting uEVs (36,37). When examining the effect of storage, our results show that storage at -80°C, either in neat urine format or after EV enrichment, after 1 year of storage, shows no statistical difference in the concentration of uEVs isolated compared to the same sample isolated a month after storage. Additionally, there were no gross changes in uEVs morphology, as observed by TEM, indicating that the uEVs remain intact in these low-temperature storage conditions for long durations. The data trend suggests an increase in the number of particles after 1 year, particularly in the neat urine format, suggesting that more debris and particles may have broken down and been released during this storage period. However, no statistical difference was observed. It is important to note that NTA was the sole method used to assess the EV concentration in this study, and this method is limited by its lack of specificity to EVs (38). It's also worth considering that the results depicting particle concentration after 1 month of storage are difficult to compare to the others due to possible day- to-day and machine variability, as the samples are being analysed (in the case of the neat urine-stored sample) or reanalysis (in the case of uEV stored sample) a year later.

Nevertheless, another study that assessed uEV concentration after storage via its EV-associated proteins, displayed similar results, with -80°C storage having no effect on EV concentration (39). However, it is important to note that in this study, protease inhibitors were used in the stored sample - a step that wasn't implemented in our study. The use of protease inhibitors in urine to avoid uEV protein degradation has been previously

investigated in studies, but no universal conclusion has been reached. Some studies state that protease inhibitors are essential for preservation (39), while others suggest that EVs can largely resist the endogenous proteolytic activity of urine (40).

In addition to the use of protease inhibitors, other storage variables exist, including an additional vortexing step after thawing. A study has suggested that vortexing significantly increase uEV recovery, with 100% recovery seen at -80°C storage after 7 months (39). This additional step was not implemented in our study due to the unknown of whether vortexing would damage the uEVs or lead to loss of surface or cargo content. Additional studies are needed to determine the effect of this additional step. In summary, in this study, while no significant effect of uEV storage was observed regarding particle concentration and intactness, our data does not provide insight into the storage effect on the stability of uEV function, and surface, or cargo. A comprehensive study investigating the extent the concentration, size, and composition of uEVs are affected by storage time and condition is required to answer these questions.

4.9 Conclusion.

In conclusion, although our study sample is limited, and only a small selection of methods was compared, we demonstrated that uEVs can be efficiently enriched through a two-step combination process of differential centrifugation and SEC. Consistent with other publications, we also demonstrate that ideally, uEVs should be isolated from urine as soon as possible and stored at -80°C to ensure their stability. Overall, this two-step combination method allows for successful isolation of uEVs, which can then be feasibly

analysed further without fear of additional method contaminant, allowing for further biomarker discoveries on an easily assessable non-invasive sample type.

4.10 References.

1. Sequeira-Antunes B, Ferreira HA. Urinary Biomarkers and Point-of-Care Urinalysis Devices for Early Diagnosis and Management of Disease: A Review. Biomedicines. 2023 Mar 29;11(4):1051.

2. Miller IJ, Peters SR, Overmyer KA, Paulson BR, Westphall MS, Coon JJ. Real-time health monitoring through urine metabolomics. Npj Digit Med. 2019 Nov 11;2(1):109.

3. Machii R, Kubota R, Hiratsuka N, Sugimoto K, Masudo R, Kurihara Y, et al. Urinary protein fraction in healthy subjects using cellulose acetate membrane electrophoresis followed by colloidal silver staining. J Clin Lab Anal. 2004;18(4).

4. Aitekenov S, Gaipov A, Bukasov R. Review: Detection and quantification of proteins in human urine. Vol. 223, Talanta. 2021.

5. Svenningsen P, Sabaratnam R, Jensen BL. Urinary extracellular vesicles: Origin, role as intercellular messengers and biomarkers; efficient sorting and potential treatment options. Acta Physiologica. 2020.

6. Cheng Y, Wang X, Yang J, Duan X, Yao Y, Shi X, et al. A translational study of urine miRNAs in acute myocardial infarction. J Mol Cell Cardiol. 2012;53(5).

7. Fraser KB, Rawlins AB, Clark RG, Alcalay RN, Standaert DG, Liu N, et al. Ser(P)-1292 LRRK2 in urinary exosomes is elevated in idiopathic Parkinson's disease. Mov Disord. 2016;31(10).

8. Chattrairat K, Yasui T, Suzuki S, Natsume A, Nagashima K, Iida M, et al. All-in-One Nanowire Assay System for Capture and Analysis of Extracellular Vesicles from an ex Vivo Brain Tumor Model. ACS Nano. 2023;17(3):2235–44.

9. Skotland T, Sagini K, Sandvig K, Llorente A. An emerging focus on lipids in extracellular vesicles. Vol. 159, Advanced Drug Delivery Reviews. 2020.

10. Witwer KW, Buzás EI, Bemis LT, Bora A, Lässer C, Lötvall J, et al. Standardization of sample collection, isolation and analysis methods in extracellular vesicle research. J Extracell Vesicles. 2013 Jan;2(1):20360.

11. Liangsupree T, Multia E, Riekkola ML. Modern isolation and separation techniques for extracellular vesicles. J Chromatogr A. 2021;1636.

12. Wang N, Yuan S, Fang C, Hu X, Zhang Y Sen, Zhang LL, et al. Nanomaterials-Based Urinary Extracellular Vesicles Isolation and Detection for Non-invasive Auxiliary Diagnosis of Prostate Cancer. Vol. 8, Frontiers in Medicine. 2022.

13. Lee, Kim E, Park J, Choi S, Lee MS, Park J. Pre-analytical handling conditions and protein marker recovery from urine extracellular vesicles for bladder cancer diagnosis. PLoS ONE. 2023;18(9 September).

14. Barreiro K, Dwivedi OP, Valkonen S, Groop P, Tuomi T, Holthofer H, et al. Urinary extracellular vesicles: Assessment of pre-analytical variables and development of a quality control with focus on transcriptomic biomarker research. J Extracell Vesicles. 2021 Oct;10(12):e12158.

15. Erdbrügger U, Blijdorp CJ, Bijnsdorp I V., Borràs FE, Burger D, Bussolati B, et al. Urinary extracellular vesicles: A position paper by the Urine Task Force of the International Society for Extracellular Vesicles. J Extracell Vesicles. 2021;10(7).

16. Fernández-Llama P, Khositseth S, Gonzales PA, Star RA, Pisitkun T, Knepper MA. Tamm-Horsfall protein and urinary exosome isolation. Kidney Int. 2010;77:736–42.

17. Kosanović M, Janković M. Isolation of urinary extracellular vesicles from Tamm-Horsfall protein–depleted urine and their application in the development of a lectin-exosome-binding assay. BioTechniques. 2014;57(3).

18. Braun F, Müller RU. Urinary extracellular vesicles as a source of biomarkers reflecting renal cellular biology in human disease. In: Methods in Cell Biology. 2019.

19. Awdishu L, Le A, Amato J, Jani V, Bal S, Mills RH, et al. Urinary exosomes identify inflammatory pathways in vancomycin associated acute kidney injury. Int J Mol Sci. 2021;22(6).

20. Sole C, Cortes-Hernandez J, Felip ML, Vidal M, Ordi-Ros J. MIR-29c in urinary exosomes as predictor of early renal fibrosis in lupus nephritis. Nephrol Dial Transplant. 2015;30(9).

21. Wang S, Kojima K, Mobley JA, West AB. Proteomic analysis of urinary extracellular vesicles reveal biomarkers for neurologic disease. EBioMedicine. 2019;45.

22. Ho DH, Yi S, Seo H, Son I, Seol W. Increased DJ-1 in urine exosome of Korean males with Parkinson's disease. BioMed Res Int. 2014;2014.

23. Sun R, Wang H, Shi Y, Gao D, Sun Z, Chen Z, et al. A Pilot Study of Urinary Exosomes in Alzheimer's Disease. Neurodegener Dis. 2020;19(5–6).

24. Agudiez M, Martinez PJ, Martin-Lorenzo M, Heredero A, Santiago-Hernandez A, Molero D, et al. Analysis of urinary exosomal metabolites identifies cardiovascular risk signatures with added value to urine analysis. BMC Biol. 2020;18(1).

25. Gheinani AH, Vögeli M, Baumgartner U, Vassella E, Draeger A, Burkhard FC, et al. Improved isolation strategies to increase the yield and purity of human urinary exosomes for biomarker discovery. Sci Rep. 2018;8(1).

26. Musante L, Bontha SV, La Salvia S, Fernandez-Piñeros A, Lannigan J, Le TH, et al. Rigorous characterization of urinary extracellular vesicles (uEVs) in the low centrifugation pellet - a neglected source for uEVs. Sci Rep. 2020;10(1).

27. Wachalska M, Koppers-Lalic D, van Eijndhoven M, Pegtel M, Geldof AA, Lipinska AD, et al. Protein Complexes in Urine Interfere with Extracellular Vesicle Biomarker Studies. J Circ Biomark. 2016;5(4).

28. Bjugn R, Flood PR. Scanning electron microscopy of human urine and purified tamm-horsfall's glycoprotein. Scand J Urol Nephrol. 1988;22(4).

29. Musante L, Saraswat M, Duriez E, Byrne B, Ravidà A, Domon B, et al. Biochemical and physical characterisation of urinary nanovesicles following CHAPS treatment. PLoS ONE. 2012;7(7).

30. Yao C, Chen X, Xu Y, Wang F, Ji J, Xu H, et al. Comparing pretreatment strategies to increase the yield and purity of human urinary extracellular vesicles. J Chromatogr B Analyt Technol Biomed Life Sci. 2022;1206.

31. Xu X, Barreiro K, Musante L, Kretz O, Lin H, Zou H, et al. Management of Tamm–Horsfall Protein for Reliable Urinary Analytics. Proteomics - Clin Appl. 2019;13(6).

32. Noonin C, Kapincharanon C, Sueksakit K, Kanlaya R, Thongboonkerd V. Application of tandem fast protein liquid chromatography to purify intact native monomeric/aggregated Tamm–Horsfall protein from human urine and systematic comparisons with diatomaceous earth adsorption and salt precipitation: yield, purity and time-consumption. Anal Methods. 2021;13(30).

33. Armstrong DA, Dessaint JA, Ringelberg CS, Hazlett HF, Howard L, Abdalla MAK, et al. Pre-Analytical Handling Conditions and Small RNA Recovery from Urine for miRNA Profiling. J Mol Diagn. 2018;20(5).

34. Leyla A E, Sander R P, Thang V P, Irene V B, Connie R J. Longitudinal stability of urinary extracellular vesicle protein patterns within and between individuals. Sci Rep. 2021;11(15629).

35. Oeyen E, Willems H, 'T Kindt R, Sandra K, Boonen K, Hoekx L, et al. Determination of variability due to biological and technical variation in urinary extracellular vesicles as a crucial step in biomarker discovery studies. J Extracell Vesicles. 2019;8(1).

36. Maroto R, Zhao Y, Jamaluddin M, Popov VL, Wang H, Kalubowilage M, et al. Effects of storage temperature on airway exosome integrity for diagnostic and functional analyses. J Extracell Vesicles. 2017;6(1).

37. Gelibter S, Marostica G, Mandelli A, Siciliani S, Podini P, Finardi A, et al. The impact of storage on extracellular vesicles: A systematic study. J Extracell Vesicles. 2022;11(2).

38. Bachurski D, Schuldner M, Nguyen PH, Malz A, Reiners KS, Grenzi PC, et al. Extracellular vesicle measurements with nanoparticle tracking analysis–An accuracy and repeatability comparison between NanoSight NS300 and ZetaView. J Extracell Vesicles. 2019;8(1).

39. Zhou H, Yuen PST, Pisitkun T, Gonzales PA, Yasuda H, Dear JW, et al. Collection, storage, preservation, and normalization of human urinary exosomes for biomarker discovery. Kidney Int. 2006.

40. Mitchell PJ, Welton J, Staffurth J, Court J, Mason MD, Tabi Z, et al. Can urinary exosomes act as treatment response markers in prostate cancer? J Transl Med. 2009;7.

4.11 Supplementary material.

Supplementary Table 4.1. Clinical profile of female urine donors. All available data is recorded. Highlighted sample where samples not received or not used in the above experiments.

Volunteer number	Age	Last menstrual period	Cycle day	Hormonal contraceptive	On antibiotics	Menstruating	Peri menopausal	Post-menopausal
1	33	07/02/21	32	YES	NO	NO	NO	NO
2	23	22/02/21	16	NO	NO	NO	NO	NO
3	23	NA*	NA	YES	YES	NO	NO	NO
4	22	NA*	NA	Yes	NO	NO	NO	NO
5	45	07/03/21	4	NO	NO	YES	NO	NO
6	27	11/02/21	28	YES	NO	NO	NO	NO
7	28	06/03/21	5	NO	NO	NO	NO	NO
8	49	16/02/21	23	NO	NO	NO	NO	YES
9	59	NA**	NA	NO	YES	NO	NO	YES
10	47	NA**	NA	NO	YES	NO	NO	YES

*No periods due to contraception

** No periods due to post-menopausal

CHAPTER 5

COMPARISON OF THE MENSTRUAL CYCLE PHASE ON URINE AND URINE EVs.

Chapter 5. Comparison of the menstrual cycle phase on urine and urine EVs.

5.1 Authors contribution.

This work forms part of the article publication **"Exploring Urine Extracellular Vesicles as a Non-Invasive Implantation Window Monitoring Method"** that is currently under review for publication.

5.2 Interconnecting chapters.

After establishing a methodology for isolating EVs that minimally affects uEV structure and content for downstream analysis, as discussed in the in the preceding chapter 4, the focus in this chapter now shifts to comprehensively exploring the proteomic profile of uEVs across the different phases of the menstrual cycle. This chapter parallels the approach taken in Chapter 2, where we explored the endometrial EV proteomic profile during simulated menstrual phases *in vitro*. However, in this chapter, our investigation extends to the non-invasive biofluid of urine. The objective is to unveil potential biomarkers within this biofluid to better identify when the endometrium is most receptive to implantation.

5.3 Chapter aim.

Explore the effects of the menstrual cycle on neat urine and urine EVs using a proteomic approach aiming to characterise and identify potential biomarkers associated with receptivity.

5.4 Abstract.

Progress and advancement in assisted reproductive technologies (ART) and their outcomes are limited by the importance of research of endometrial receptivity being overlooked. Due to endometrial biopsy being invasive and *in vitro* studies lacking reproducibility *in vivo,* urine is an appealing alternative biofluid source for biomarker research as it can be collected in large quantities non-invasively. The discovery of extracellular vesicles (EVs) in urine (uEVs) has also opened a new avenue in biomarker research, with these EVs harbouring thousands of proteins that hold promise for biomarker development. In this study, urine was collected from human female volunteers, and samples representing the different phases of the menstrual cycle were subjected to EV isolation via differential centrifugation and size exclusion chromatography. The resulting uEVs were analysed via Nanoparticle tracking analysis (NTA) to examine the different concentration and size of particles, and proteomic analysis performed using shotgun label-free mass spectrometry on the uEV samples and neat urine samples. Our results showed that uEVs were found in numbers depending on the menstrual cycle phase, but uEV size was not statistically altered during different stages of the menstrual cycle. Proteomics showed 50% of proteins detected in the neat urine were also present in the uEV samples, with 813 proteins being unique in the uEV samples. Proteomics analysis also showed that the menstrual cycle phase affects the uEVs' proteomic profile, with some proteins shown to be significantly upregulated and downregulated during the window of implantation phase of the cycle compared to the other non-receptive periods. This data highlights that uEVs' characteristics are altered depending on the menstrual cycle phase, suggesting the potential of uEVs being used as biomarkers for improving fertility.

5.5 Introduction.

During the history of assisted reproductive technologies (ART), endeavours to improve the outcome rate have mostly been centred on the transfer of high-quality embryos, while the important player of endometrial receptivity has been mostly overlooked (1). In the case of IVF, embryo transfer (ET) must precisely take place when the embryo development and receptive endometrium are in synchrony and compatible (2). Generally, embryo transfer is conducted following the assessment of the endometrial thickness via a transvaginal ultrasound. However, the capability of clinical conventional practices to ascertain the endometrium receptivity to implantation has been questioned (3,4). To combat these shortcomings, the endometrial receptivity array (ERA) was announced in 2011 as a means to establish when the endometrium is receptive to an embryo by utilising molecular genomic arrays to measure the endometrium's proliferation and differentiation and screens for markers of inflammation (5). However, recent retrospective studies and randomised controlled trials have demonstrated no improvement in outcome with the use of ERA, and currently, there is no scientific evidence of it improving IVF outcome (6,7). This lack of a sensitive and reliable assay for determining a receptive endometrium for ET, coupled with the implantation rate in IVF only being around 30% (8), highlights that a clear bottleneck in improving conception outcomes with ART is the ability to tailor embryo transfer timing. An ideal clinical assay would be rapid, objective, accurate, and non-invasive while not reducing the likelihood of implantation.

Examination of human urine is an age-old practice for non-invasive assessment of diseases and diagnosis (9). More recently, proteomic-based methods have increased in

popularity in characterising both the normal urine proteomic profile and in prognosis and therapy responses (10). While proteomic analysis has successfully characterised the normal urine proteomic profile (11,12), female urine profile alterations due to menstrual-cycle related changes have had limited investigations (13,14). Due to the complexity of bio-fluid proteomic profile, along with interfering compounds and individual variations, standardised protocols for sample collecting and handling are essential for translation of proteomic data into clinical practice (15,16). A possible approach is the analysis of biochemical markers, with extracellular vesicles (EVs) being a promising contender. EVs are nano-sized bilayer lipid-membrane particles derived from all cells, containing and constructed of a range of cellular-derived molecules, including lipids, proteins, DNA, messenger RNAs (mRNAs), microRNAs (miRNA), small non-coding RNAs (sncRNAs), and long non-coding RNAs (lncRNAs) (17). Recently, these particles have been explored for exploitation in biomarker discovery for a range of diseases and conditions (18–21).

In reproduction, EVs have been examined in various studies for biomarker discoveries for endometrial receptivity and related conditions in a number of models and sources (22–26). Urine-derived EVs (uEVs) show promise as a useful biofluid for discovering endometrial receptivity biomarkers in clinical settings. Urine can be easily collected in large amounts and at various timepoints without the need for invasive procedures, making it an advantageous option for research (9). Crucially , while the majority of uEVs derive from the kidney and urinary tract, a proportion also stem from distal organs, potentially providing insights into non-urological conditions (27–30). Moreover, uEVs likely to mirror the comprehensive physiological alterations that happen in the body (31),

including the cycling changes of sex hormones. Therefore, uEVs, may provide diagnostic and therapeutic opportunities for endometrial receptivity detection, such as aiding in determining when IVF implantation should occur.

While we have previously demonstrated *in vitro* that the human endometrial cell EV proteomic profile is dependent on the hormones estrogen and progesterone (26), whether the uEV proteomic profile across the human menstrual cycle differs has not been explored to date. Therefore, in this study, we aimed to compare the proteomic profiles across the menstrual cycle both in uEV and neat urine. Through the comparison of neat urine and uEV proteomic profiles, we also hope to demonstrate the advantages of uEV assessment over neat urine assessment. This study has revealed new characteristics and dynamics of uEVs at different phases of the menstrual cycle and thus identified physiological and pathological changes associated with the menstrual cycle as well as indicating a new potential source of receptivity biomarkers.

5.6 Material and methods.

5.6.1 Urine sample collection.

Urine samples were collected according to Swiss Precision Diagnostic (SPD) Protocol-0054, which has SPD Research Ethics approval, and were processed at SPD development company limited in Bedford, UK. Female volunteers were selected according to pre-defined selection criteria. Inclusion criteria were: age 18-45, regular menstrual cycles. Exclusion criteria were: using hormonal systemic birth control in the past 6 months, pregnant or breastfeeding, or using any medication known to alter endocrine system, urinary tract infection in the past 3 months, abnormal urinalysis, and

known reproductive disorders (e.g., endometriosis). First void urine samples were donated every day for 30 days. Samples were not collected when women were menstruating. Urine samples were processed within 3 hours of collection. The volume of the urine samples was measured, and initial centrifugation (Thermo Scientific Sorvall ST 8R centrifuge) in a fixed-angle rotor (Thermo Scientific HIGHConic III Fixed Angle Rotor) at 400g for 5 mins at 4°C was performed, the resulting pellet was discarded, and the supernatant centrifuged at a further 1000g for 5 mins at 4°C. The samples were then aliquoted (15ml aliquots) and stored at -80°C. Samples were then transported to The University of Sheffield in dry ice for further processing and analysis.

5.6.2 Preliminary urinalysis.

All urine samples prior to centrifugation were tested for pH and specific gravity. Specific gravity was measured via the pocket urine specific gravity refractometer (ATAGO Pal-10s cat 4410). The refractometer was set to zero at the beginning of each day before use by wiping the prism clean and applying about 0.3ml of water. The water was left to equilibrate to the temperature of the instrument before zero setting. After zero setting was completed, the prism was cleaned with tissue paper and approximately 0.3ml of urine applied, and the measurement taken (Supplementary Figure 5.1,5.2,5,3). pH measurements were made on a Mettler Toledo InLab expert pro Seven compact pH meter using an Inlab Expert Pro pH probe, which was calibrated at the beginning of each day. After calibration, the pH probe was rinsed and placed into each sample, and the pH value recorded (Supplementary Figure 5.1,5.2,5.3). A quantitative determination of the concentrations of estrone-3-glucuronide (E3G), follicle-stimulating hormone (FSH), and pregnanediol-3- glucuronide (P3G) in the urine samples was carried out retrospectively

using an immunoassay, SPD DELFIA (dissociation-enhanced lanthanide fluorescence immunoassay) assay, for the respective analytes. The profile of urinary luteinizing hormone (LH) in the daily urine samples was obtained using Clearblue digital Ovulation Test (DOT). Ovulation test sticks were inserted into the test holder and 110µl of urine applied and the output from the reader (measured as %A) was recorded. The %a output was directly proportional to LH concentration (Supplementary Figure 5.1, 5.2 and 5.3).

5.6.3 Urine sample cycle day selection.

Urine samples were selected to represent the different phases of the menstrual cycle based on the urinalysis results (Supplementary Figure 5.1, 5.2 and 5.3). Samples represented the proliferative phase were selected to be at least 3 days post menstruation when the progesterone is at the baseline and LH has not peaked. Samples represented ovulation were selected based on LH results, with peak LH urine samples selected as well as 24h and 48h post peak for each of the participants. For the window of implantation, samples were selected to be at least 5 days post-peak LH and while the progesterone is peaking above the levels of estrogen.

5.6.4 Urine EV isolation.

All urine EV's were isolated from a 10ml starting volume of urine. Urine samples received from SPD were defrosted at room temperature followed by differential centrifugation in a Sigma swinging-out rotor centrifuge (catalogue number 11180). First, urine was centrifuged at 1000g for 10 mins at 4°C, the resulting pellet was discarded, and the supernatant was then centrifuged at 4000g for 10mins at 4°C. Again, the resulting pellet was discarded, and the supernatant was then centrifuged at 10,000g for 10 mins at 4°C.

An aliquot of this centrifuged sample was used as the pre-isolation control. The final resulting supernatant was concentrated using a 10kDa ultrafiltration tube (Sartorius, Hampshire, UK) to 500µl. Retentates were subjected to size exclusion chromatography. For the preparation of one size exclusion chromatography (SEC) column, 14-mL of Sepharose CL-2B slurry (GE Healthcare, Uppsala, Sweden) was poured into an empty gravity chromatography column (Bio-Rad, Watford, UK). After settling of the Sepharose beads, a nylon net filter was inserted at the ethanol/Sepharose separation interface at about 10ml. The ethanol preservative was removed from the bead matrix by washing the column with molecular grade water (3 x 5ml) and then with Ca^{2+} and Mg^{2+} free Dulbecco's phosphate-buffered saline (3 x 5ml) (Sigma-Aldrich, Dorset, UK). On top of the filter, 500µl of the concentrated urine was loaded, and fractions of 0.5mL were collected in 20 fractions with 10ml of Ca^{2+} and Mg^{2+} free Dulbecco's phosphate-buffered saline as the eluent. The resulting fractions were stored at −80°C for further EV characterisation. Optimisation determined fractions 6-8 contain the highest concentration of EV sized particles free from protein contaminants, and this strategy was used for all future experiments (Supplementary Figure 5.4). These fractions were then concentrated using a 10kDa ultrafiltration tube (Sartorius, Hampshire, UK) to 300µl and stored at −80°C for further analysis. For the repeatability assessment, a different aliquot from the same urine sample from the same woman was subjected to the same isolation technique on separate days (Supplementary Figure 5.5).

5.6.5 Nanoparticle tracking analysis.

For nanoparticle tracking analysis (NTA) (ZetaView, PMX 110, Particle Metrix, Meerbusch, Germany), all samples were diluted in milliQ water. Ideal measurement concentrations

were found by pre-testing the ideal particles per frame value (140–200 particles/frame). For each measurement, three cycles were performed by scanning 11 cell positions each and capturing 30 frames per position under the following settings: Focus: autofocus; Camera sensitivity for all samples: 50; Shutter: 70; Scattering intensity: detected automatically; Cell temperature: 25 °C. After capture, the videos were analysed by the in-built ZetaView Software 8.04.02 SP2 with specific analysis parameters: maximum size: 500; minimum size: 5; minimum brightness: 25; hardware: embedded laser: 40 mW at 488 nm; and camera: CMOS.

5.6.6 Transmission Electron microscopy (TEM).

After SEC, 100µL of the concentrated EVs was mixed with 100µL of 4% paraformaldehyde (Polyscience, Warrington, USA) to fix the EVs. Samples were transported to the Institute of Animal Reproduction and Food Research, Olsztyn, Poland for TEM analysis. On the day of analysis, 20µL droplet of EVs was covered by a 200-mesh formvar and carbon coated grid (Electron Microscopy Sciences, Pennsylvania, USA). The EV droplet was incubated for 20 min at room temperature. After 20 minutes, the grid was tapped on filter paper to remove excess PBS. Later, the grid was rinsed once by gently touching the surface of the grid onto a 50µL droplet of MilliQ water and then tapped on filter paper to remove the excess water. For negative staining, the grid was transferred onto a droplet of 4% uranyl acetate (Polysciences, Warrington, USA) for 5 min incubation at room temperature. Samples were observed with a JEM 1400 transmission electron microscope (JEOL Ltd. Tokyo, Japan) at 80 kV, and digital images were acquired with a numeric camera (Morada TEM CCD camera, Olympus, Germany).

5.6.7 Proteomic analysis - Label-free liquid chromatography tandem mass spectrometry (LC-MS/MS).

100µL EV samples and 100µl neat urine samples were transported to the Proteomic Core Facility, University of Tartu, Tartu, Estonia on dry ice for proteomic analysis. 1 µg of protein was injected to an Easy-nLC 1000 system (Thermo Scientific). The sample was eluted at 250 nl/min from the trap to a 75 µm ID x 50 cm emitter-column (New Objective) packed with C18 material (3 µm, 300 Å particles, Dr Maisch). The separating gradient was 2-35% B 60 min and 40-100% B 5 min (A: 0.1% formic acid (FA), B: 80% ACN + 0.1% FA). Eluted peptides were sprayed to a Q Exactive Plus (Thermo Fisher Scientific) quadrupole-orbitrap mass spectrometer (MS) using nano-electrospray ionisation at 2.4 kV (applied through liquid-junction). The MS was operated with a top-5 data-dependent acquisition strategy. Briefly, one 350-1400 m/z MS scan at a resolution setting of R=70 000 at 200 m/z was followed by five higher-energy collisional dissociation fragmentation (normalised collision energy of 26) of 5 most intense ions (z: +2 to +6) at R=17 500. MS and MS/MS ion target values were 3e6 and 5e4 with 50 ms injection time. Dynamic exclusion was limited to 40 s.

5.6.8 Proteomic data analysis.

Mass spectrometric raw files were processed with the MaxQuant software package (versions 1.6.15.0 and 2.0.3.0). Methionine oxidation, asparagine and glutamine deamidation and protein N-terminal acetylation were set as variable modifications, while cysteine carbamidomethylation was defined as a fixed modification. Label-free protein quantification (LFQ) was enabled with LFQ and protein minimum ratio count set to 1. Search was performed against *Homo sapiens* reference proteomes, using the

tryptic digestion rule. Peptide-spectrum match and protein false discovery rate (FDR) were kept below 1% using a target-decoy approach. All other parameters were set to default. Protein-coding of significantly altered proteins (SAPs) in Ev's were identified based on a fold change cut-off of 1 and a p-value cut-off of 0.05. An analysis of SAPs was performed in R studio (version 4.2.1) using the Bioconductor "DEP" package (version 3.1.5). Identified duplicates and contaminants were excluded from the list of each sample, and only proteins detected in at least two of the replicates were considered. Gene Ontology (GO) and Kyoto Encyclopedia of Genes and Genomes (KEGG) pathway enrichment analyses were performed by the "clusterProfiler" R package (version 4.4.4). Volcano plots, GO terms, and KEGG pathways were visualised by the "ggplot2" R packages (version 3.3.6).

5.6.9 Data availability.

The mass spectrometry proteomics data was deposited to the ProteomeXchange Consortium via the PRIDE (32) partner repository with the dataset identifier PXD047127 for the urine EV data and PXD047128 for the neat urine data.

5.6.10 Statistical analysis.

GraphPad Prism version 9.2.0 was used for all statistical analysis. Comparison of particle concentration between the hormonal conditions and the control was analysed with repeated measure one-way ANOVA (analysis of variance). When comparing the different sizes and the different treatment groups, a two-way ANOVA with multiple comparisons was performed. All data presented as mean plus/minus standard error (mean ± SE). In all analyses, $p < 0.05$ was considered to be statistically significant.

5.6.11 Experimental design.

Investigating urine EV proteomic profile during the menstrual cycle.

First void urine was collected from 3 female volunteers every day for 30 days. Urine was centrifuged to pellet cells and debris before freezing and stored at -80°C prior to analysis. Aliquots of the urine were analysed retrospectively for hormone markers to determine the individual's hormone profile across the cycle. After determining and selecting the samples that represented the different phases of the menstrual cycle (proliferative, ovulation and window of implantation), EVs were isolated from 10ml of urine via a combination of differential centrifugation and size exclusion chromatography. Samples were analysed via NTA to determine the concentration and size of particles. For characterisation, samples were also analysed via TEM to visually confirm the presence of EVs in the samples. Finally, the EVs were analysed via Label-free liquid chromatography tandem mass spectrometry to compare the EV proteomic profile of the different phases. A graphical representation of this experiment is shown in Figure 5.1 (A).

Investigating neat urine proteomic profile during the menstrual cycle.

From the same urine selected to represent the different phases in the urine EV experiment, the neat urine proteomic profile was also analysed via Label-free liquid chromatography tandem mass spectrometry. The proteomic profiles of the different phases were then compared. A graphical representation of this experiment is shown in Figure 5.1.(B).

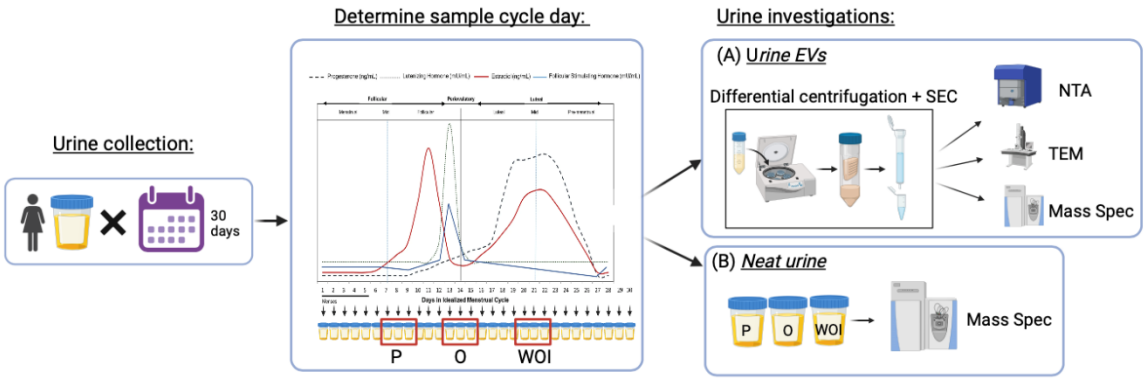


Figure 5.1. Study Experimental Design. Graphical representation of experimental design for investigating the urine EV proteomic profile (A) during the menstrual cycle and the neat urine proteomic profile (B). (Created with BioRender.com).

5.7 Results.

5.7.1 Characterisation of urine EVs.

Purified urine EVs from the proliferative phase were shown to be positive for markers of transmembrane proteins associated with the uEV plasma membrane, CD63 and CD9, which were not seen in the same neat unpurified (UP) proliferative phase urine (Figure 5.2.A). uEVs isolated from the proliferative phase urine were also positive for TSG101, a marker of cytosolic protein recovered in uEVs (Figure 5.2.B), and negative for the negative marker Uromodulin (UMOD), a major urine protein aggregate (Figure 5.2.C). PCA analysis also showed clear separation between the proliferative urine uEV group and the neat unpurified (UP) proliferative phase urine (Figure 5.3). TEM confirmed that urine uEVs were intact, spherical in morphology, and with the expected EV size range within all 3 conditions (Figure 5.4). Combined, these results fulfil the Minimal Information for Studies of Extracellular Vesicles (MISEV) criteria and demonstrate that EVs have been successfully enriched from neat urine samples.

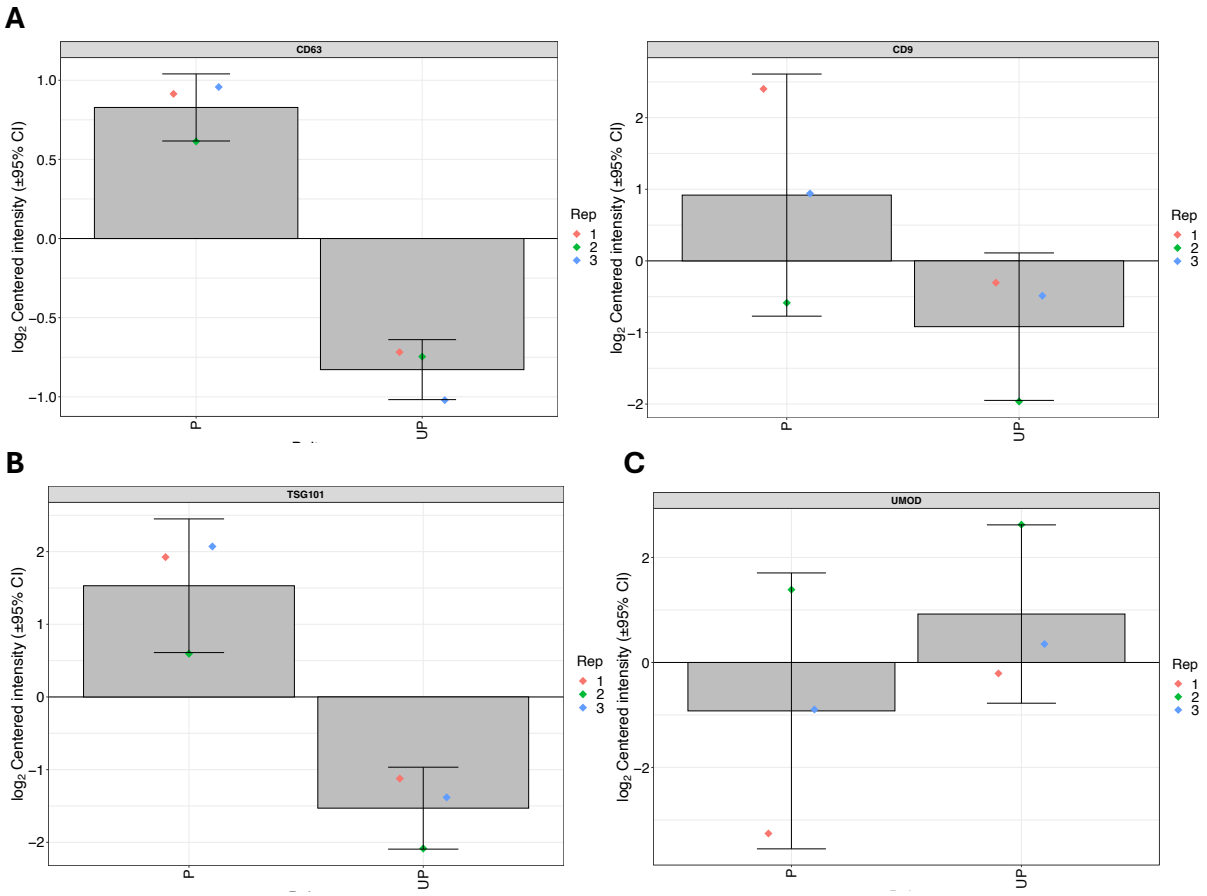


Figure 5.2. Protein content-based uEV characterisation from the Label-free liquid chromatography tandem mass spectrometry data. Bar chart representing the log2 centred intensity of various protein markers in the control as well as the condition media control to validate the presence of EVs according to the MISEV guidelines. A) represents is the intensity of the marker CD63 and CD9 to fulfil the MISEV criteria for markers of transmembrane or GPI-anchored proteins associated to plasma membrane and/or endosomes. B) represents is the intensity of TSG101 to fulfil the MISEV criteria for a marker of cytosolic protein recovered in EVs. C) represents is the intensity of the marker UMOD to fulfil the MISEV criteria for a marker of protein aggregate.

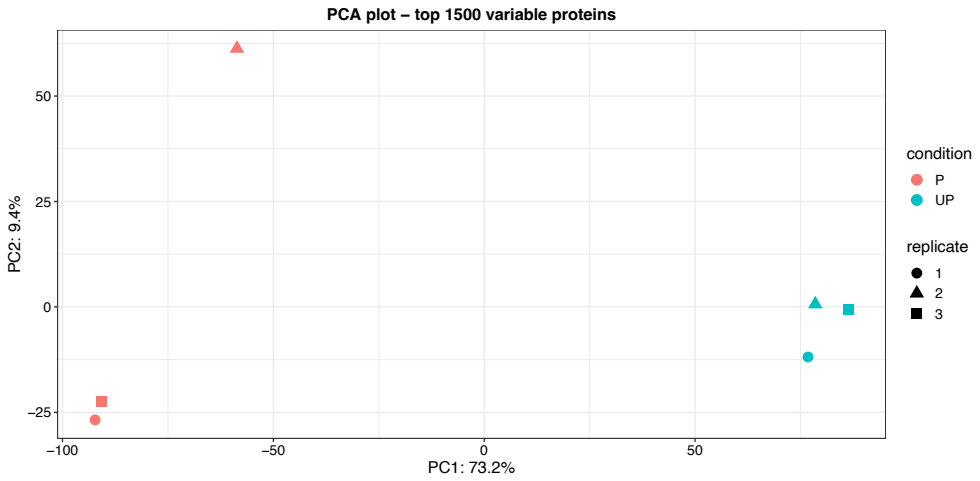


Figure 5.3. Principal component analysis (PCA) of top 1500 variable proteins in the study groups. With P representing the uEVs from the proliferative phase and UP representing the neat impurified (UP) proliferative phase urine.

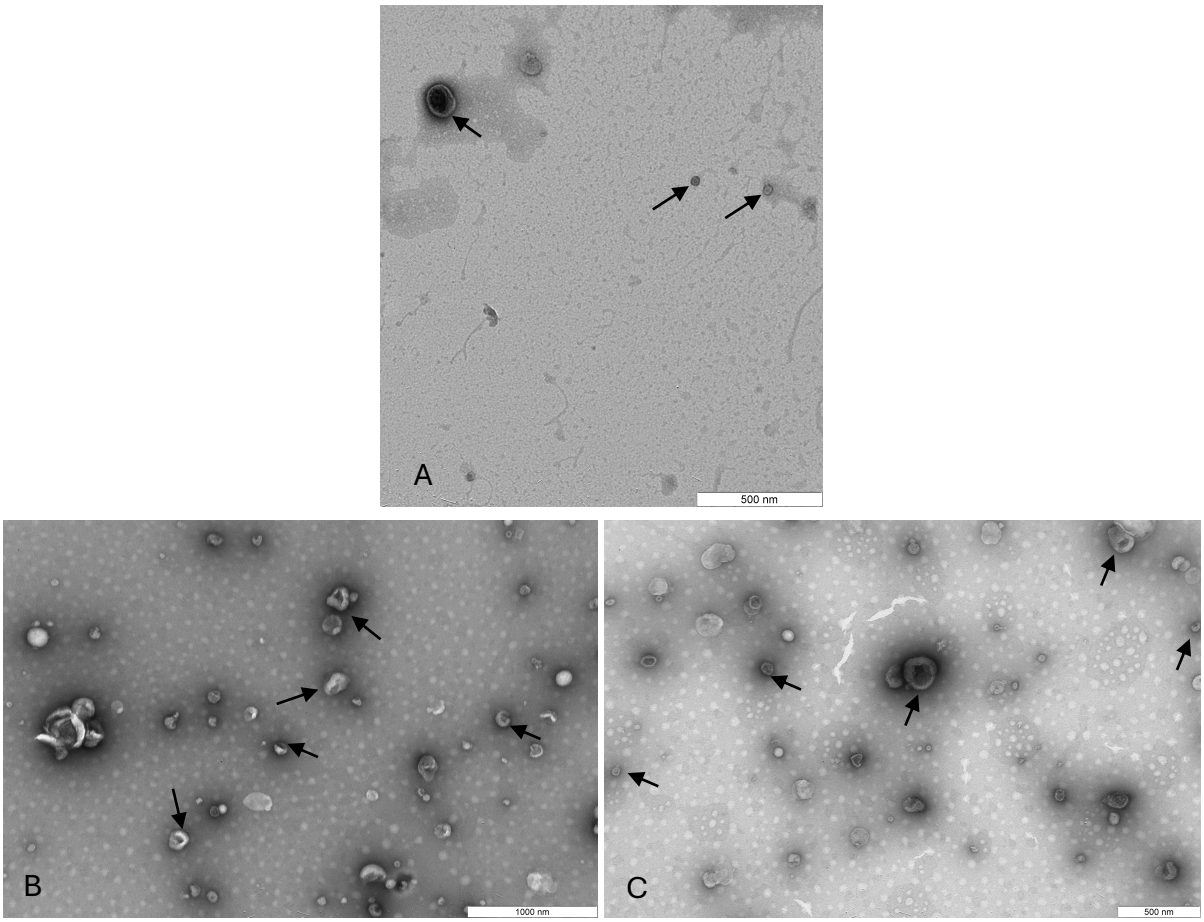
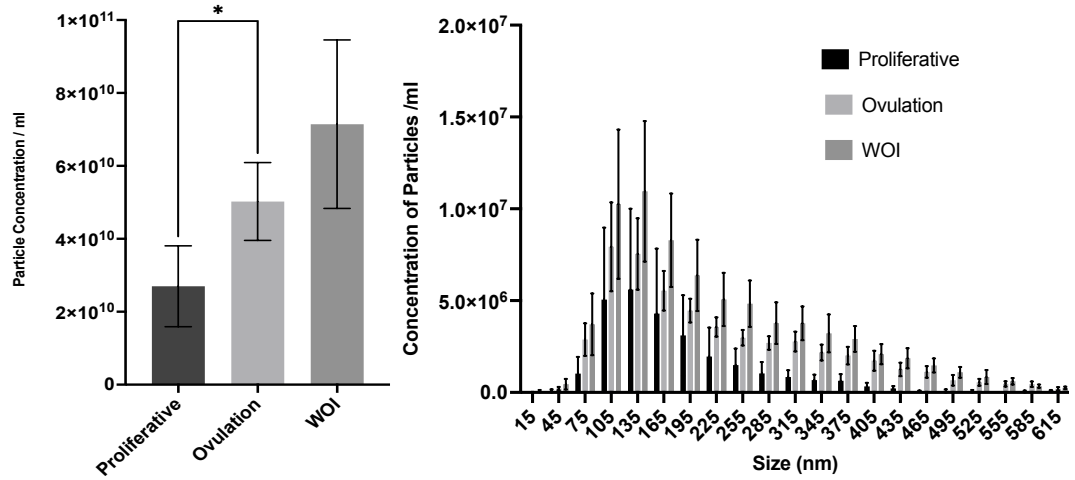


Figure 5.4. Transmission electron microscopy (TEM) Image based characterisation of urine EVs from the different menstrual cycle phases. Representative TEM images of urine EVs from proliferative (A) ovulation (B) and Window of implantation (C) Scale bars: 500 nm (A and C); 1000 nm (B).

5.7.2 Concentration and size distribution of urine EV from the menstrual phases.

To assess the effect of the menstrual cycle on urine EV production, a comparison of the concentration of urine EVs produced from the proliferative phase, ovulation, and window of implantation (WOI) samples was made. The menstrual cycle phases showed a significant difference between the amount of urine EV-sized particles produced from the proliferative and ovulation phases. (Figure 5.5.A). A size comparison analysis of the concentration of particles in the different size classes was also conducted, and the different menstrual phases compared (Figure 5.5.B), but no significant difference was observed.



A B

Figure 5.5. Concentration and size distribution of EVs released from urine EVs from different menstrual cycle phases, obtained from the nanoparticle tracking analysis. (A) The height of the bars represents the mean concentration (particles/ml) of EV sized particles from the pooled urine EV fraction from the different menstrual cycle phases. One-way ANOVA was performed with Tukey post hoc test with significant results marked with 1 asterisk symbol (*) to denote $P \leq 0.05$. (B) The height of the bars represents the mean concentration of the indicated particle size from pooled EV fractions. A two-way ANOVA was performed with Tukey post hoc test, but no results were considered significant ($P \leq 0.05$). Data is from 3 biological replicates and 3 technical replicates, with the error bars represent the standard error from the mean.

5.7.3 Comparative proteomic analysis of urine EVs from the menstrual phases.

A total of 2,262 proteins were identified in all of the uEV samples, with 1,722 of these identified in at least two of the replicates in each condition. Among these proteins, 785 of were common in all three of the phases, with 10 being unique to the proliferative phase group, 71 being unique to the ovulatory phase group, and 221 being unique to the WOI phase group (Supplementary Figure 5.6). A heatmap of the log2 centered intensity of all significant proteins, with the data centered per protein from the 4 experimental conditions, showed a clear grouping of the 3 menstrual phases, with 6 cluster groups showing clear varied intensities between the EV isolated groups (Figure 5.6). There were 9 significantly altered proteins (SAP) identified from the differential enrichment of EV proteins from WOI group compared to O group (supplementary Table 5.3), 3 SAP were identified from differential enrichment of EV proteins from WOI group compared to the P group (Supplementary Table 5.4), and no SAP identified from differential enrichment of EV proteins from P group compared to the O group. In the WOI group compared to the O group, 5 SAP were upregulated and 4 downregulated. In the WOI group compared to the P group, 0 SAP were upregulated and 3 downregulated. Volcano plots of these result show a direct indication of SAPs (Figure 5.7). Proteins identified in the uEVs samples have been associated with the endometrium and implantation, including angiopoietin Like 2 (ANGPTL2) upregulated during the WOI phase compared to the O phase and Keratin 6B (KRT6B) shown to be down regulated during the WOI phase compared to the P phase. To further analyse the biological function of SAPs, GO terms and KEGG pathway enrichment analyses were performed on the two comparison groups (WOIvO and WOIvP) (Figure 5.8 and 5.9). Biological process identified correlated with the known biological function of

uEVs being transport, with the key pathways “ion transport” and “transmembrane transport” identified. KEGG analysis revealed upregulation of “phageosome pathway” in the WOI uEV samples suggesting an innate immunity role of uEVs.

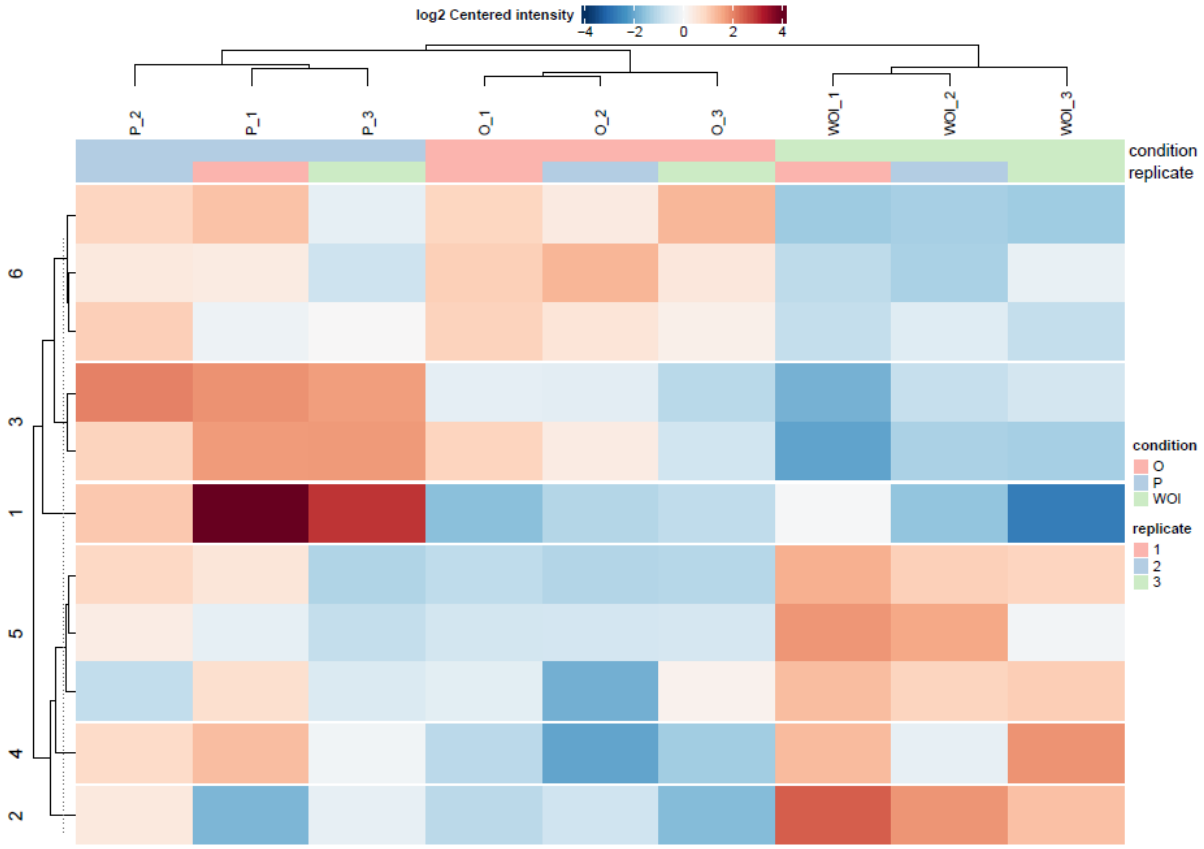
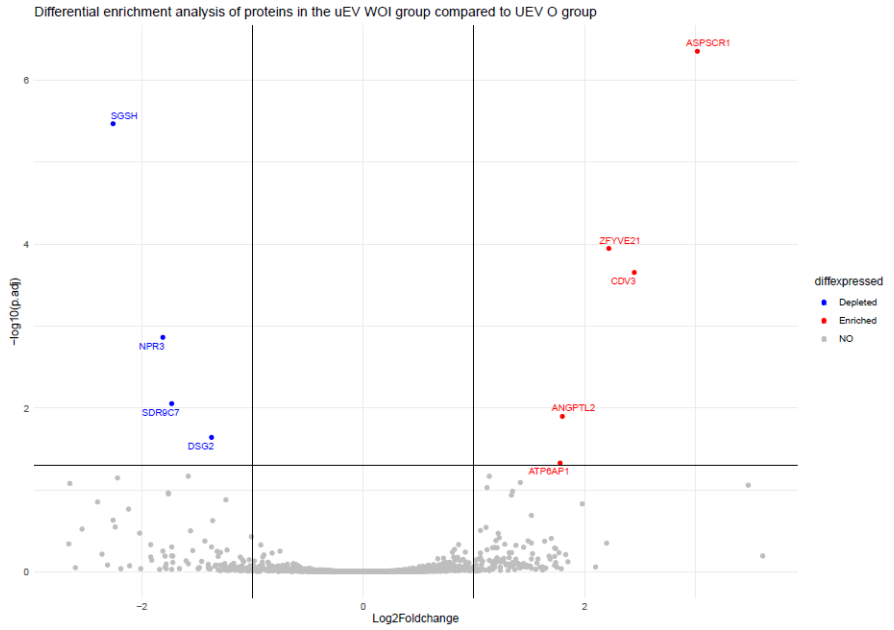
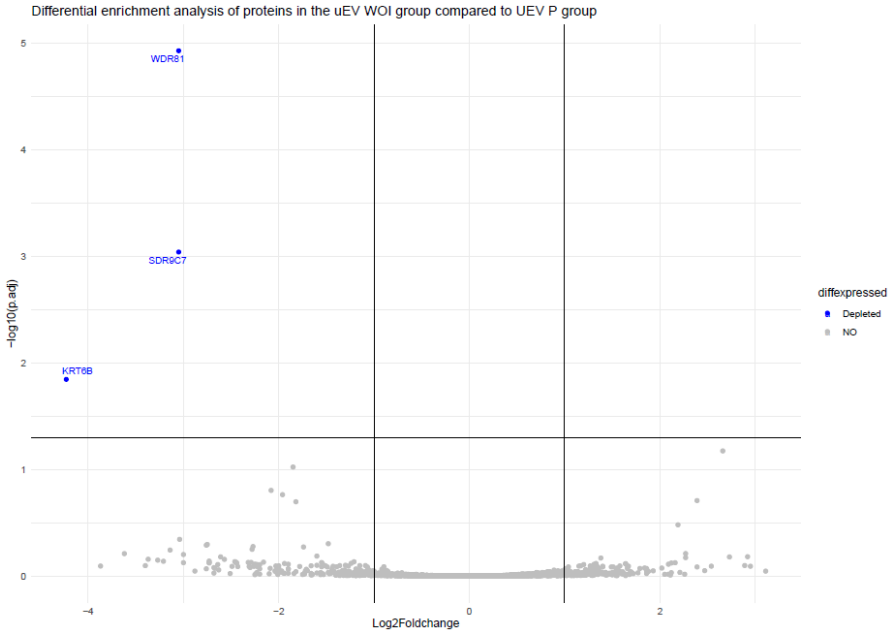


Figure 5.6. Heatmap shows the log2 centered intensity of all significant proteins with the data centred per protein. The rows represent all significant proteins and are clustered in 6 groups by k-means clustering (numbers on the left). O (ovulation group), P (proliferative group) and WOI (window of implantation group). Colours represent the abundance of significantly altered proteins (red: higher; blue: lower) Replicate 1 is from subject 1, replicate 2 is from subject 2, and replicate 3 is from subject 3.

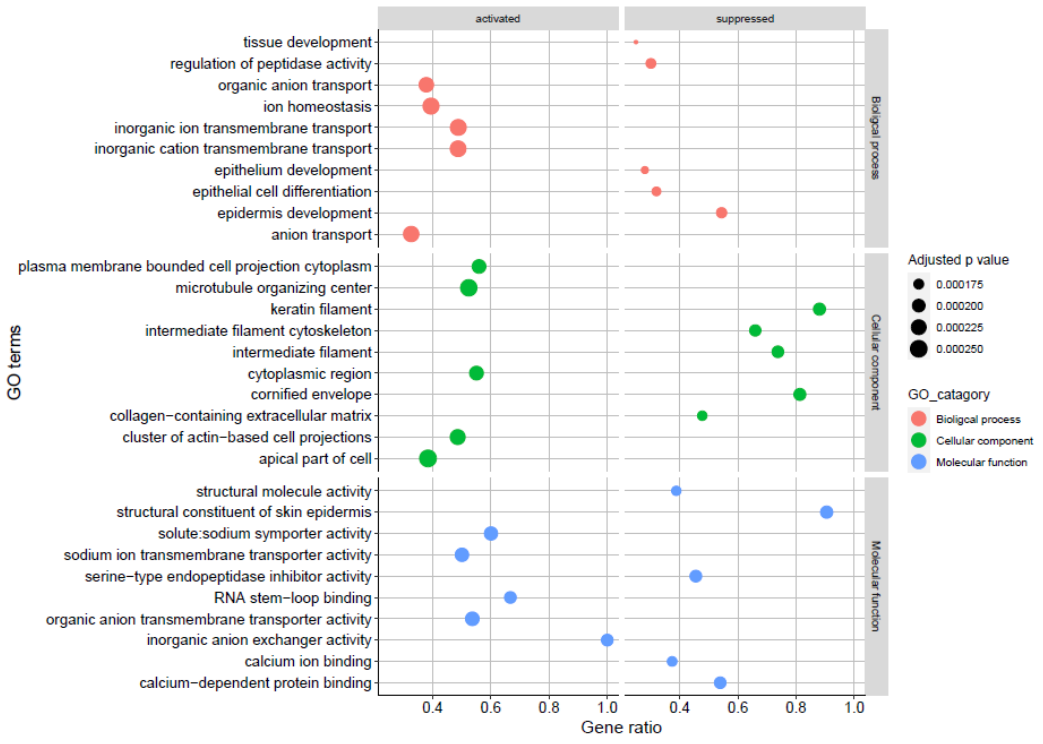


A

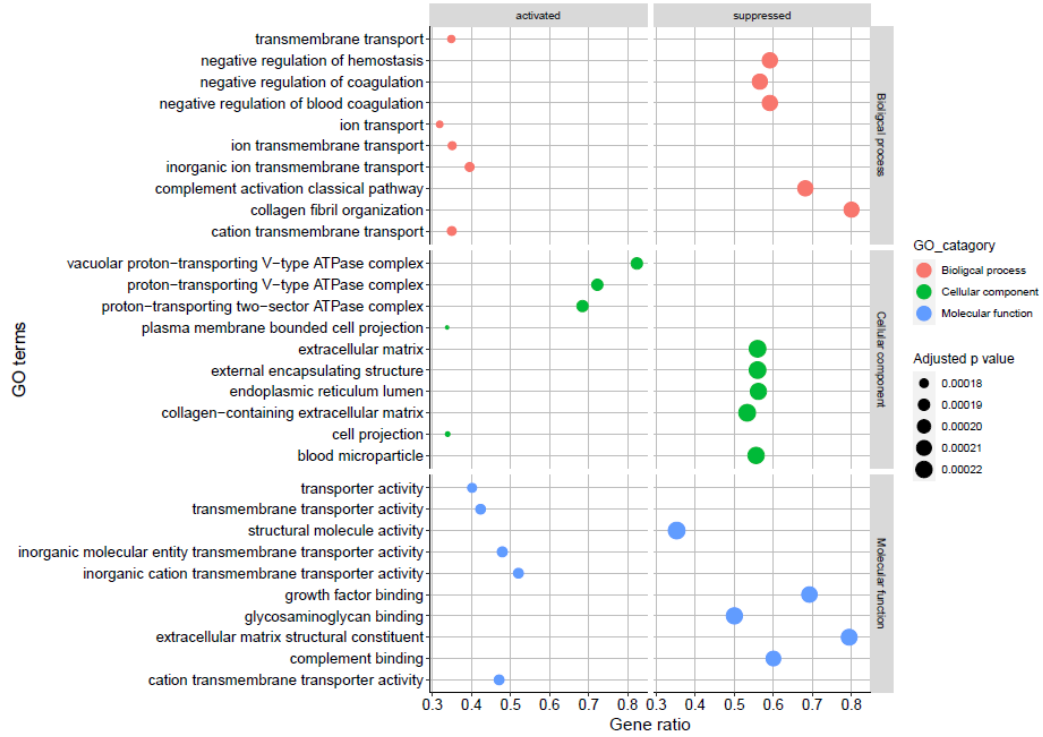


B

Figure 5.7. Differential enrichment of uEV proteins in different comparison groups. (A) Volcano plot of the differentially expressed proteins in the uEV window of implantation group (WOI) compared to the Ovulation group (O), (B) WOI group compared to the progesterone group (P). Adjusted P values (−log10) are plotted against the fold changes (log2). Red dots represent enriched proteins whereas blue dots represent depleted proteins in the respective comparisons.



A



B

Figure 5.8. GO enrichment of SAP in the different comparison groups. (A) WOIvO and (B) WOIvP. Top 5 up and down regulated pathways are represented. The size and colour of points represents the GO category and the q-values respectively.

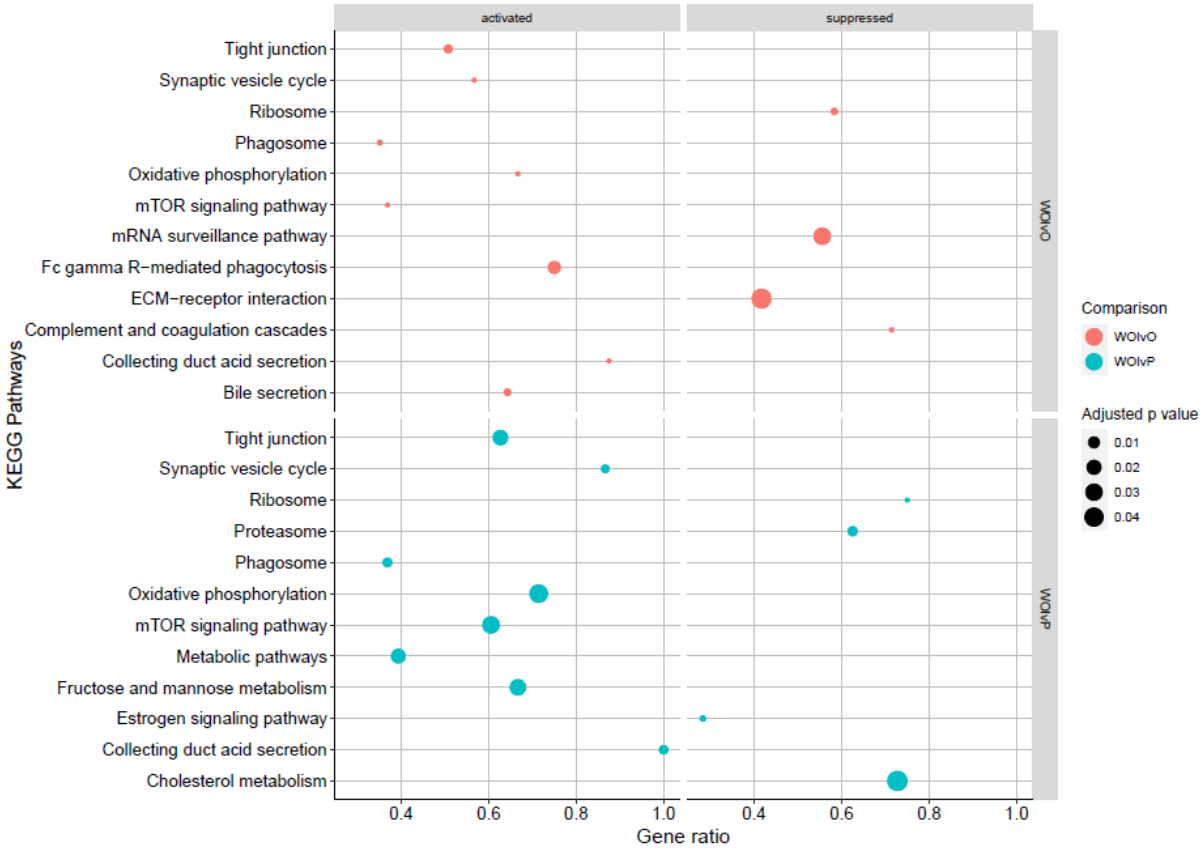


Figure 5.9. KEGG Pathway analysis of SAP in the comparison groups. Pathway analysis of SAP in the comparison groups, the size and colour of points represents the p-values and the comparison groups respectively.

5.7.4 Comparative proteomic analysis of neat urine from the menstrual phases.

To compare the proteomic profile of the neat urine from the different phases of the menstrual cycle, label-free liquid chromatography tandem mass spectrometry analysis was performed on the samples identified to reflect the menstrual cycle phases. A heatmap of the log2-centered intensity of all significant proteins, with the data centered per protein from the 3 neat urine menstrual cycle phases, showed partial grouping of the 3 menstrual phases with 6 cluster groups showing a varied intensities between the urine groups (Figure 5.10). There were 19 significant altered proteins (SAP) identified from the differential enrichment proteins from WOI group compared to O group (Supplementary Table 5.1), 21 SAP identified from differential enrichment of proteins from WOI group compared to the P group (Supplementary Table 5.2), and 35 SAP identified from differential enrichment of proteins from P group compared to the O group. In the WOI group compared to the O group, 9 SAP were downregulation and 10 upregulated (Figure 5.11.a). In the WOI group compared to P group, 5 SAP were downregulated and 16 upregulated (Figure 5.13.b). In the P group compared to the O groups, 11 SAP were downregulated and 5 upregulated (Figure 5.11.c). Key proteins shown to be downregulated associated with the endometrium and implantation include Mucin-16 (MUC16) and integrin Subunit Beta 6 (ITGB6) in the WOI group compared to the O phase. To further analyse the biological function of DEGs, GO terms and KEGG pathway enrichment analyses were performed on the three comparison groups (WOIvO and WOIvP and PvO) (Figure 5.12 and 5.13). GO analysis revealed cellular components including "intracellular non-membrane-bounded organelles," "immunoglobulin complexes," and "collagen-containing extracellular matrix," indicating significant

cellular turnover, immune activation, and tissue remodelling. KEGG pathway analysis of urine proteins during the WOI revealed upregulation in immune processes (e.g., “Phagosome”, “NET Formation”), metabolic activity (e.g., “Oxidative Phosphorylation”), and cellular processes (e.g., “Ribosome”, “mTOR signaling”). GO analysis of the urine proteome during the WOI showed upregulation of the cellular component terms “immunoglobulin complexes” and “collagen-containing extracellular matrix” with downregulation observed in components such as “intracellular vesicles”, “nucleus” and “nucleoplasm”, indicating a complex interplay of immune activation and reduced cellular turnover."

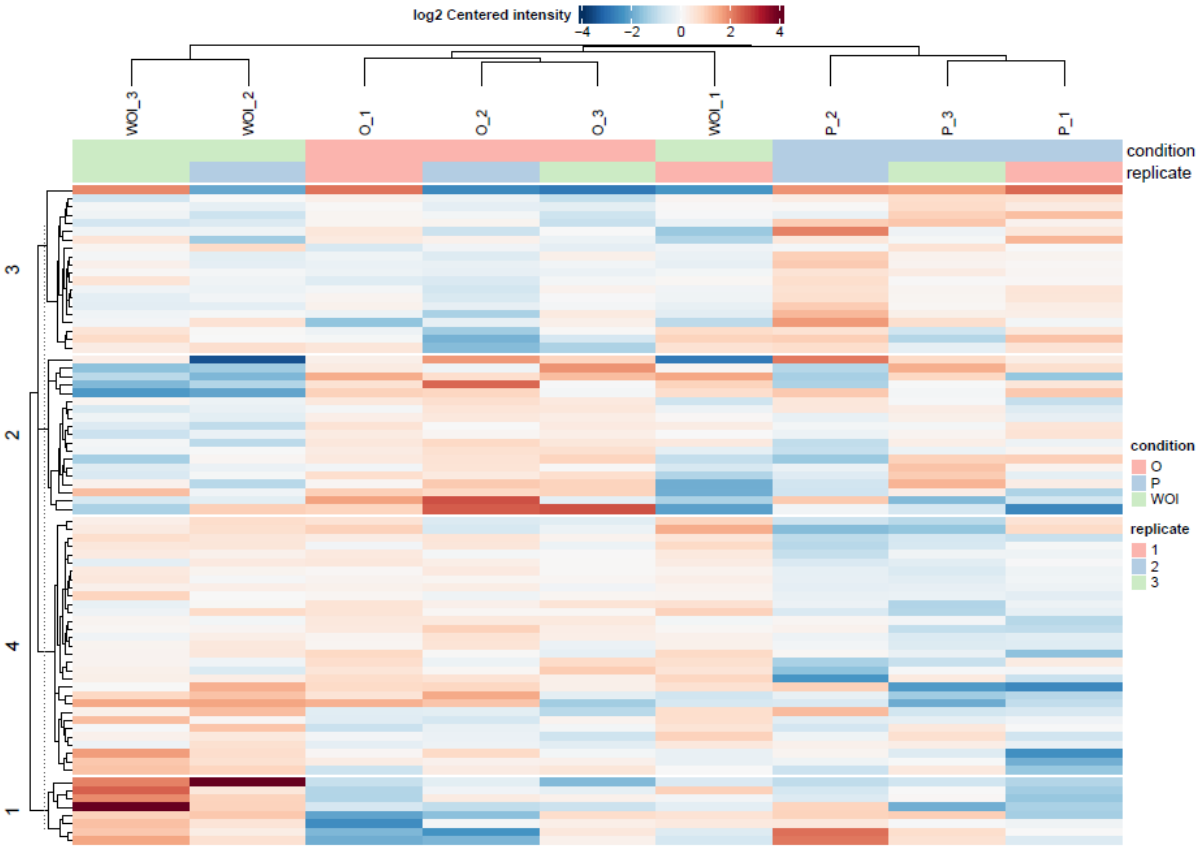
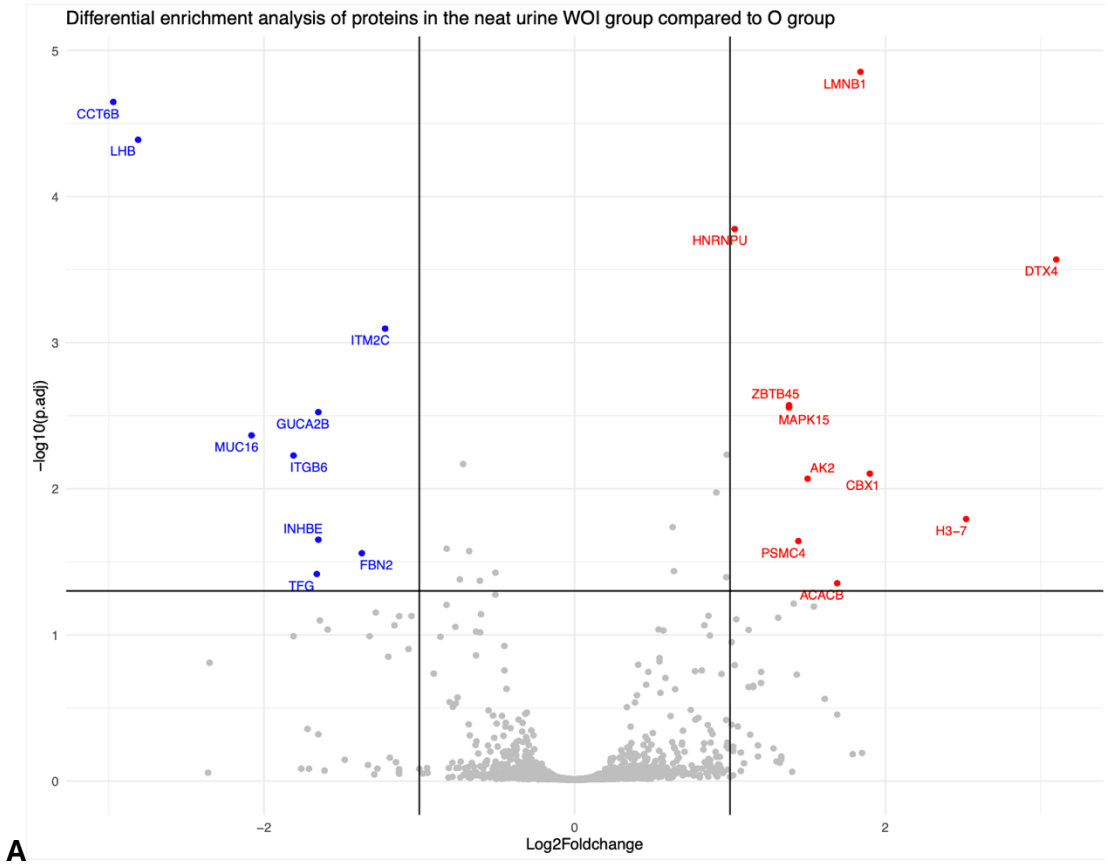
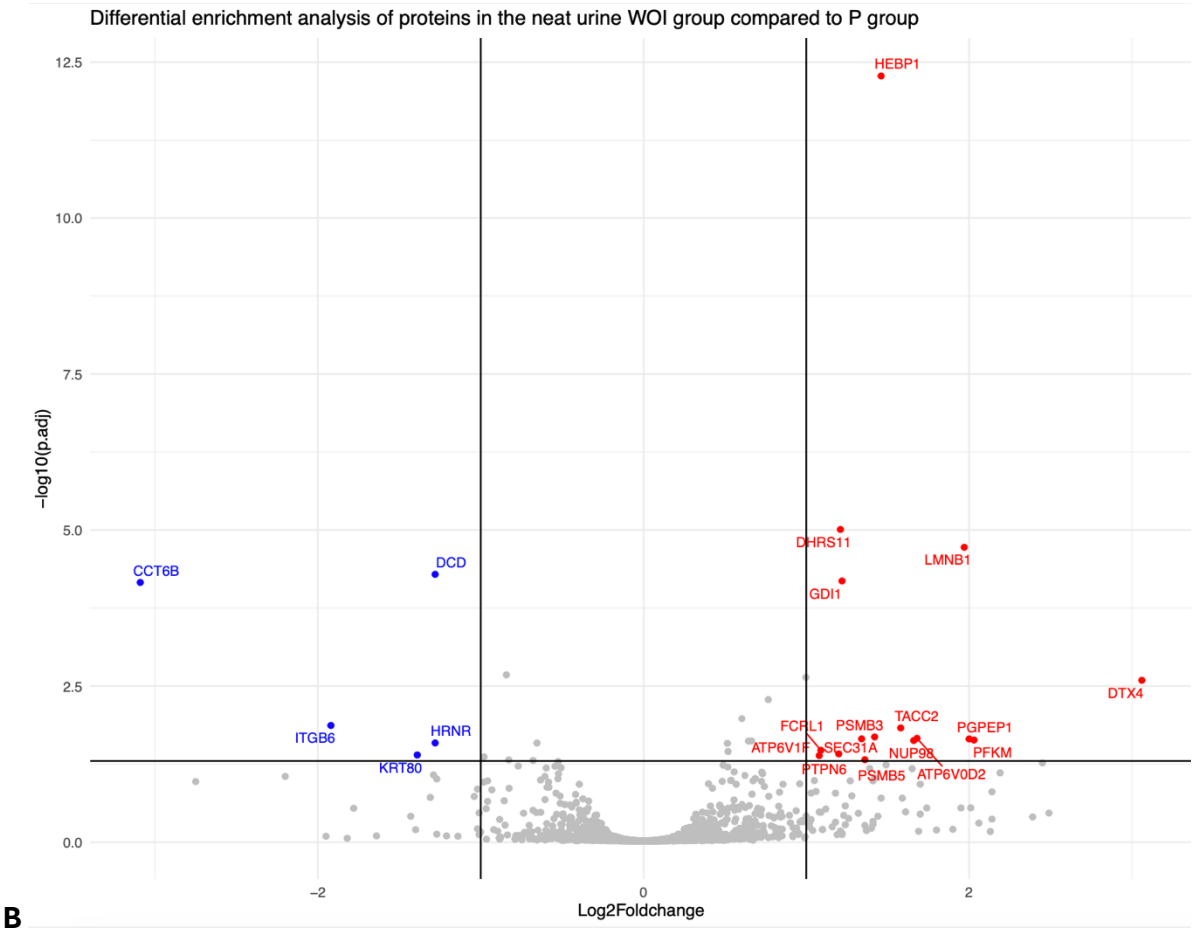
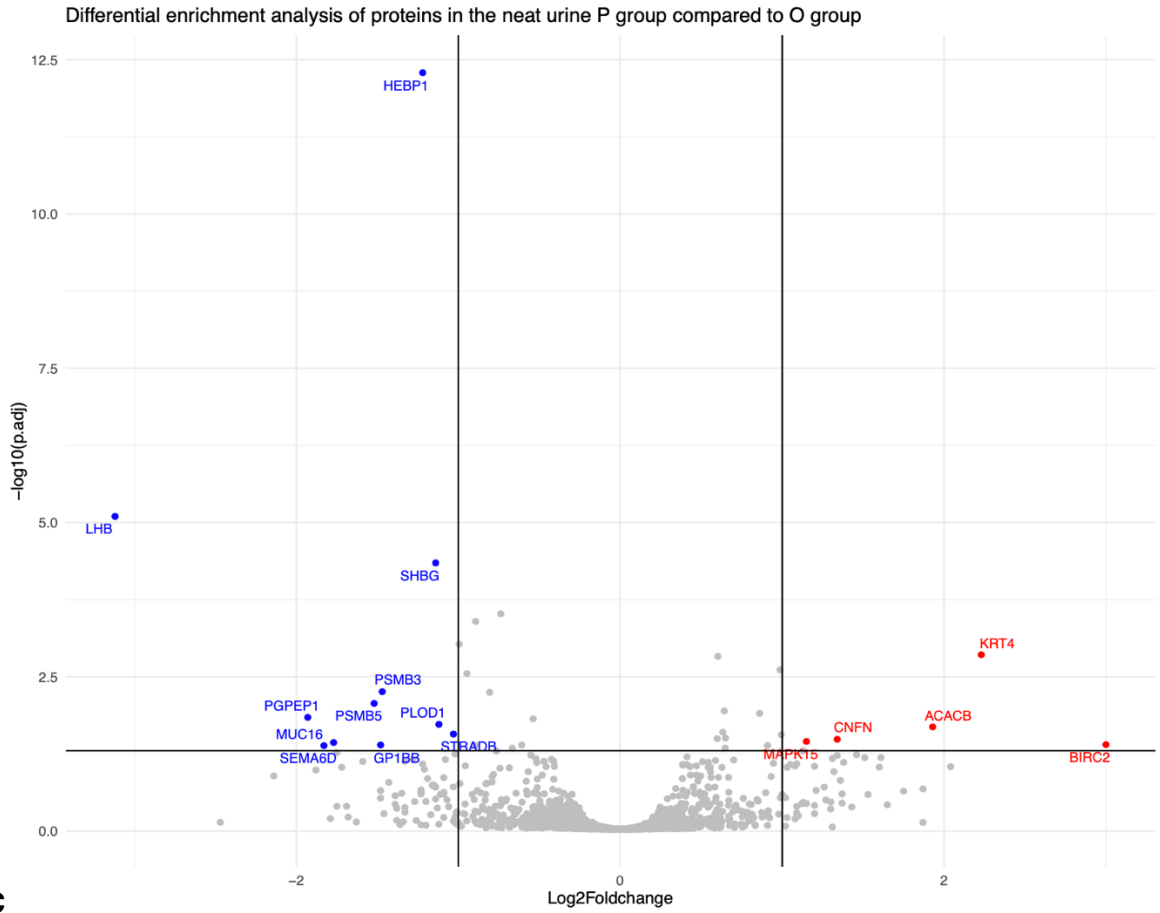


Figure 5.10. Heatmap shows the log2 centred intensity of all significant proteins with the data centered per protein. The rows represent all significant proteins and are clustered in 6 groups by k-means clustering (numbers on the left). O (ovulation group), P (proliferative group) and WOI (window of implantation group). Colours represent the abundance of significantly altered proteins (red: higher; blue: lower). Replicate 1 is from subject 1, replicate 2 is from subject 2, and replicate 3 is from subject 3.

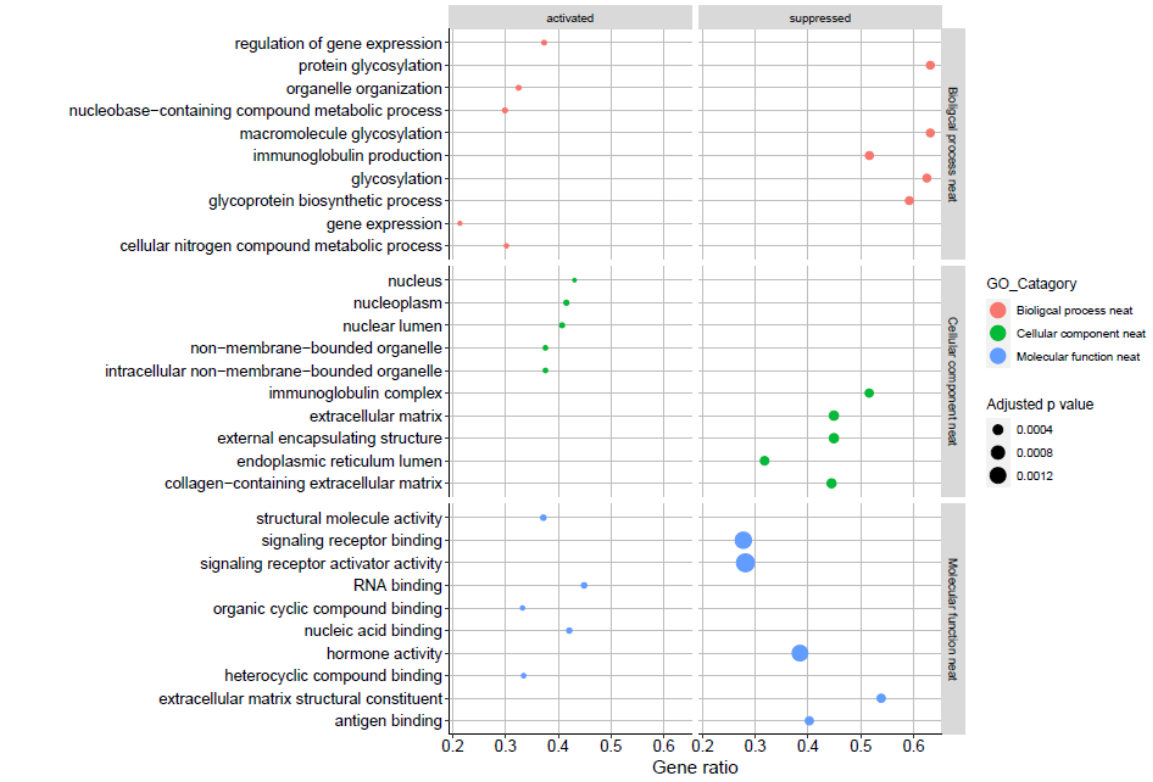

Differential enrichment analysis of proteins in the neat urine WOI group compared to O group
LMNB1
CCT6B
LHB
HNRNPU
DTX4
ITM2C
ZBTB45
MAPK15
GUCA2B
MUC16
ITGB6
AK2
CBX1
INHBE
H3−7
PSMC4
FBN2
TFG
ACACB
−log10(p.adj)
Log2Foldchange
A


Differential enrichment analysis of proteins in the neat urine WOI group compared to P group
HEBP1
DHRS11
LMNB1
CCT6B
DCD
GDI1
DTX4
TACC2
FCRL1
PSMB3
PGPEP1
ITGB6
HRNR
ATP6V1F
SEC31A
PFKM
NUP98
KRT80
PTPN6
PSMB5
ATP6V0D2
−log10(p.adj)
Log2Foldchange
B

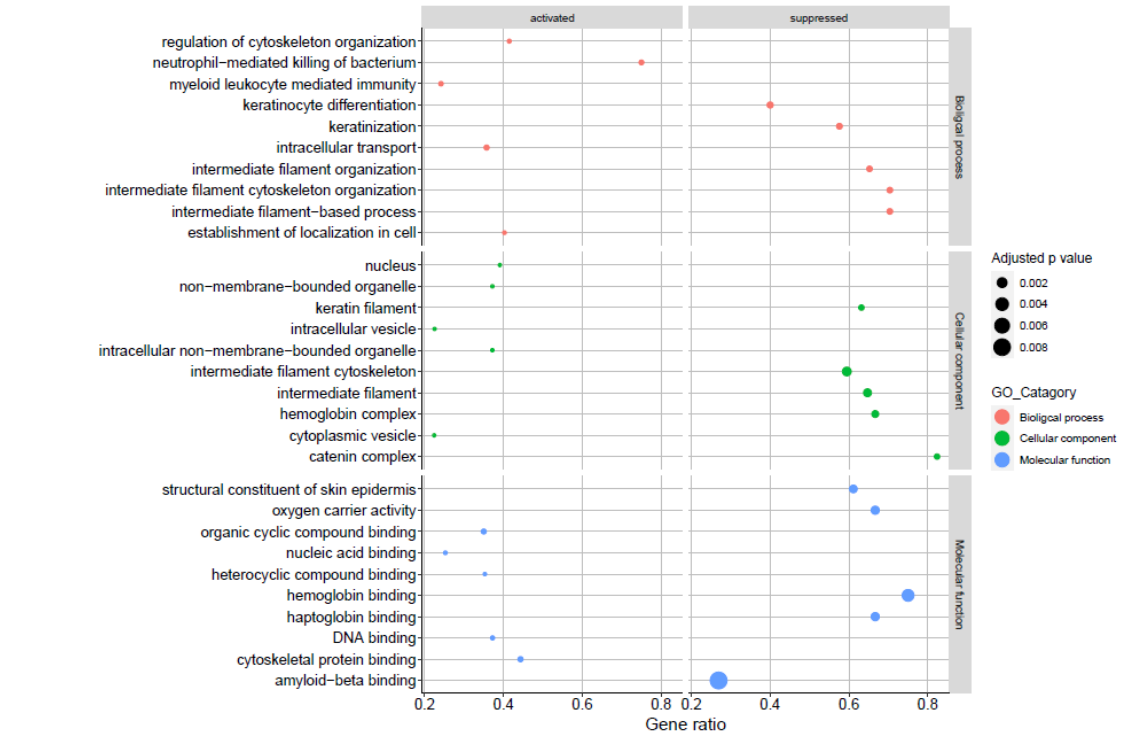


C

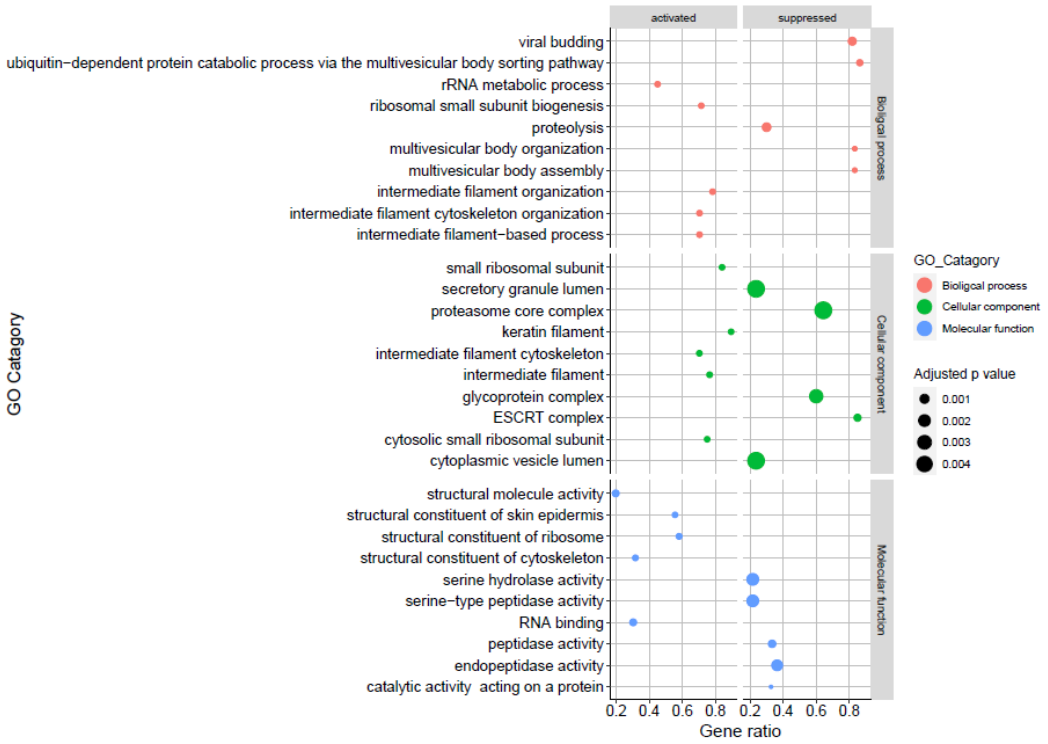
Figure 5.11. Differential enrichment of neat urine proteins in different comparison groups. (A) Volcano plot of the differentially expressed proteins in the window of implantation group (WOI) compared to the Ovulation group (O), (B) WOI group compared to the progesterone group (P) and (C) P group compared to O. Adjusted P values (−log10) are plotted against the fold changes (log2). Red dots represent enriched proteins whereas blue dots represent depleted proteins in the respective comparisons.


activated
suppressed
regulation of gene expression
protein glycosylation
organelle organization
nucleobase−containing compound metabolic process
macromolecule glycosylation
immunoglobulin production
glycosylation
glycoprotein biosynthetic process
gene expression
cellular nitrogen compound metabolic process
Biolgcal process neat
nucleus
nucleoplasm
nuclear lumen
non−membrane−bounded organelle
intracellular non−membrane−bounded organelle
immunoglobulin complex
extracellular matrix
external encapsulating structure
endoplasmic reticulum lumen
collagen−containing extracellular matrix
Cellular component neat
structural molecule activity
signaling receptor binding
signaling receptor activator activity
RNA binding
organic cyclic compound binding
nucleic acid binding
hormone activity
heterocyclic compound binding
extracellular matrix structural constituent
antigen binding
Molecular function neat
0.2
0.3
0.4
0.5
0.6
Gene ratio
GO_Catagory
Biolgcal process neat
Cellular component neat
Molecular function neat
Adjusted p value
0.0004
0.0008
0.0012

A


activated
suppressed
regulation of cytoskeleton organization
neutrophil−mediated killing of bacterium
myeloid leukocyte mediated immunity
keratinocyte differentiation
keratinization
intracellular transport
intermediate filament organization
intermediate filament cytoskeleton organization
intermediate filament−based process
establishment of localization in cell
Biolgcal process
nucleus
non−membrane−bounded organelle
keratin filament
intracellular vesicle
intracellular non−membrane−bounded organelle
intermediate filament cytoskeleton
intermediate filament
hemoglobin complex
cytoplasmic vesicle
catenin complex
Cellular component
structural constituent of skin epidermis
oxygen carrier activity
organic cyclic compound binding
nucleic acid binding
heterocyclic compound binding
hemoglobin binding
haptoglobin binding
DNA binding
cytoskeletal protein binding
amyloid−beta binding
Molecular function
0.2
0.4
0.6
0.8
Gene ratio
Adjusted p value
0.002
0.004
0.006
0.008
GO_Catagory
Biolgcal process
Cellular component
Molecular function

B



C

Figure 5.12. GO enrichment of SAP in the different neat urine comparison groups. (A) WOIvO and (B) WOIvP (C) PvO Top 5 up and down regulated pathways are represented. The size and colour of points represents the GO category and the q-values respectively.

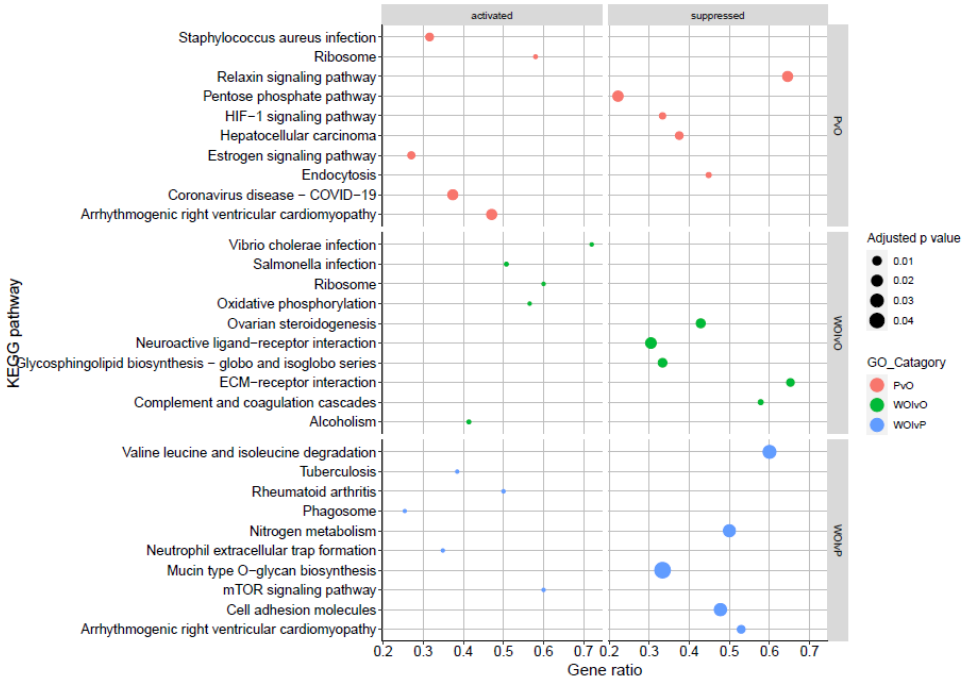


Figure 5.13. KEGG Pathway analysis of SAP in the neat urine comparison groups. Pathway analysis of SAP in the comparison groups, the size and colour of points represents the p-values and the comparison groups respectively.

5.8 Discussion.

This study comprehensively evaluates the proteomic profile of uEVs and neat urine at the different phases of the menstrual cycle to characterise uEVs and to help define novel non-invasive biomarkers of the endometrial receptive period. These biomarkers could aid in implantation success and, consequently, improve pregnancy outcome. The EV isolation method involved a combination of differential centrifugation and SEC, based on previous studies (33) and repeatability assessments (supplementary Figure 5.4 and 5.5). Interestingly, of the 2044 proteins identified in the uEVs, only 90 have also been identified in the top 100 proteins found in EVs (Supplementary Figure 5.7). The presence of these markers further supports their use as indicators of the enrichment of EVs. The additional proteins in EVs could potentially serve as new markers for EVs or more specifically uEVs.

Our study revealed statistically significant variations in uEV concentration when comparing the proliferative phase to the ovulatory phase, highlighting the influence of the menstrual cycle phases. So far, no other studies have compared uEVs concentration across the menstrual cycle or estrous cycle in mammals. However, other studies have instead assessed different biofluids during the menstrual cycle, with varying conclusions on the effect of the menstrual cycle on the EV concentration. For example, in a study looking at human uterine fluid EVs (UF-EVs), no difference was observed between the proliferative and secretory phases (34). In contract, a study on bovine UF-EVs found a significant difference in concentrations when comparing the luteal and follicular phases (25). However, it is important to note that various factors could attribute to these differences between studies, such as the sample biofluid, organism, individual variability between samples, and the EV isolation and quantification method used.

In terms of size distribution, it was observed that all the samples from the different phases were in the expected EV size range, but there was no statistical difference in sizes between the different phases. These results differ from our similar study *in vitro* looking at EVs from RL95-2 endometrial cells conditioned media under hormonal simulation, which showed a significant difference seen between the 135 nm and 165 nm size groups, with more EV being released by the progesterone-treated group compared to the estrogen group or the estrogen plus progesterone group (26). However, it is important to note the major variations in these studies, including the difference in biofluid assessed and the limitations of the method of acquiring this data (NTA). Furthermore, the lack of specificity of NTA means differentiation between non-EV-structures, such as lipoproteins or residual reagent residues, could influence these results. Thus, only limited conclusions can be drawn from this method alone.

Nevertheless, proteomic assessment by mass spectrometry of uEVs allows a broader analysis to be performed. To the best of our knowledge, this is the only human urine EV proteomic profile analysis across the menstrual cycle to date. Proteomics and other 'omics technologies have attracted researchers in biomarker discovery due to their high sensitivity and high throughput capabilities (35). Within the omics field, urine has been commonly examined (36,37), despite, in the case of proteomics, it has previously been believed that the protein concentration in urine is very low in healthy humans. However, recent studies (38,39), including this one, have shown that urine protein is a viable biomarker, with over 2000 proteins detected. The analysis of uEVs allows for better investigation of proteomic changes that could otherwise be masked by high abundance

protein or the heterogeneity of whole neat urine. This is evident in this study, where it was found that just over 50% of proteins detected in the neat urine were also present in the uEV samples. However, 813 proteins were unique in the uEV samples, a finding consistent with other studies comparing neat urine to uEVs (40,41) (Supplementary Figure 5.8). Additionally, 354 proteins discovered in the uEV samples are not found listed in the 3880 proteins currently in the PeptideAtlas database of human urine (42) (Supplementary Figure 5.9). Moreover, there is also a lack of crossover in proteins found to be upregulated or downregulated in the neat urine samples from the different menstrual phases compared to the uEV proteins. Together, these findings highlighting the benefits of uEV in biomarker studies rather than neat urine in revealing proteins that would otherwise be masked. The advantages of uEV over neat urine also extend to limiting the variables in urine affecting the reproducibility of a potential marker. This is due to neat urine harbouring free and active proteases, whereas EVs provide protection against these ubiquitous degraders (43,44). Hence, results from neat urine samples are only comparable to each other, whereas uEVs have advantages due to their unmodified states.

Looking more closely at the individual proteins identified to be altered when comparing the different phases of the menstrual cycle both in the neat urine and the uEVs some interesting proteins associated with the endometrium and/or implantation processes can be seen. This includes the observed downregulation of MUC16 and ITGB6 in urine during the WOI compared to the O phase, which suggests significant changes in endometrial function as it prepares for embryo attachment. MUC16, which typically acts as a protective barrier and facilitates initial embryo contact, may be reduced to transition

the endometrium from a protective state to one more receptive to implantation (45). Similarly, the downregulation of ITGB6, involved in cell adhesion, could reflect integrins' reported role in the necessary modifications in the endometrial decidua matrix to support embryo invasion (46,47). It's assumed these proteins are present in urine as a result of their secretion into the uterine environment, from where they enter systemic circulation and are filtered by the kidneys (48). Unlike some proteins that may be encapsulated in EVs, MUC16 and ITGB6 might be found in the urine in their free form or as part of larger aggregates. This distinction highlights that their presence in urine reflects endometrial changes occurring during the WOI and suggests that neat urine could provide a non-invasive means to monitor endometrial receptivity and adaptation processes associated with implantation.

There were, however, other proteins identified in the uEVs associated with the endometrium and implantation. This includes the detection of ANGPTL2 and KRT6B in uEVs during different phases of the menstrual cycle. ANGPTL2, which is upregulated during the WOI phase compared to the O phase, plays a crucial role in angiogenesis and extracellular matrix remodelling, processes essential for creating a receptive endometrial environment for embryo implantation (49,50). Conversely, KRT6B, a keratin involved in epithelial cell structure (51,52), is downregulated during the WOI phase compared to the P phase, reflecting the transition from endometrial proliferation to a more receptive state for implantation. It's possible these proteins are shed from the endometrium into the systemic circulation and subsequently detected in uEVs. This again highlights the potential of using uEVs as non-invasive biomarkers for monitoring endometrial changes and assessing reproductive health.

While the study identifies several key proteins in uEVs and neat urine, an essential debate persists regarding the origin of these EVs, particularly the limitations imposed by the kidney's filtration process (53,54). The Bowman's capsule, a key component of the nephron, filters blood to form urine, selectively allowing molecules smaller than 8 nm to pass through the glomerular basement membrane and ~32 nm podocyte filtration slits, while retaining larger molecules and particles (55,56). Most EVs range from 30 nm to several hundred nanometers in size, which means they cannot pass through the glomerular filtration barrier intact (57). Therefore, the presence of endometrial associated proteins within uEVs suggests that these EVs might either be smaller subpopulations capable of passing through the filtration barrier or an alternative pathway for their presence in urine. For example, studies suggest that possibly the EVs and larger protein complexes are taken up via active transport by the proximal convoluted renal tubules, bypassing the glomerular filtration barrier, and then secreted into the urine (58,59). Alternatively, possibly larger EVs might be fragmented into smaller vesicles or protein complexes that can pass through the filtration barrier (60,61). Once in the urine, these fragments could reassemble or remain as smaller detectable units (60,61).

Another aspect worth exploring is the presence of receptors for ovarian steroid hormones, such as estrogen and progesterone, in the kidneys and other parts of the urinary system (62). Research indicates that estrogen receptors and progesterone receptors are indeed expressed in various kidney cells, including those in the renal cortex and medulla (63,64). This hormonal influence could impact renal function and the

excretion of reproductive proteins. The bladder and urethra also exhibit the presence of these receptors, which might influence the composition of urine during different phases of the menstrual cycle (65,66). These hormonal interactions can provide additional layers of regulation that affect how endometrial proteins and EVs are processed and detected in the urinary system.

Given the ongoing debate about the origin of EVs and the filtration challenges they face, it is noteworthy that, although no uEV proteins were identified that were also found in our previous endometrial cell EV hormonal experiment (26), rationally, a valuable biomarker for the implantation window may still exist in uEVs based on the clear variation in the proteomic profile when comparing the different phases in the bioinformatic analysis. The origin of the uEVs in this study is not fully understood and requires further investigation. Despite this, the more distinct grouping in the PCA analysis and heatmap cluster analysis of the uEV proteomic profile of the different phases, when compared to the neat urine, suggests that uEVs maybe be more specific in identifying the menstrual phases and, hence, an ideal candidate for further biomarker discovery work.

Finally, to investigate the function of uEVs, GO and KEGG pathway analysis was performed. The majority of the uEV samples from all of the phases were shown to be involved in biological processes related to transport, such as ion transport and transmembrane transport, as expected due to the typical physiological function of EVs (67). Also seen in the KEGG analysis was an activation of the phageosome pathway in the WOI uEV samples. This is an interesting observation as previous studies have identified a role for uEVs in innate immunity. The increase in activation during the WOI also

correlates with EVs from other sources having a suggested functional role in immunity (26), and the well-known role of immunity in implantation (68,69).

In addition to uEVs, our GO analysis of urine proteins during the WOI revealed significant changes in cellular components. Upregulation of components such as "immunoglobulin complexes" and "collagen-containing extracellular matrix" highlights enhanced immune activity and tissue remodelling, which are crucial for implantation (70,71). Conversely, downregulation of components like "intracellular vesicles", "nucleus" and "nucleoplasm" suggests a reduction in cellular turnover or stress responses (71,72). These findings reflect a broader physiological adaptation occurring during the WOI, providing further insight into the role of urine-derived biomarkers in reproductive processes. Nevertheless, it is unclear from this study if the uEVs proteins and free urine proteins are found in the eliminated urine are originating from the urinary system or from circulating EVs, a critical debate within the field as discussed above. The understanding and study of the physiological functions of uEVs are still emerging, and more investigation is required.

However, this study is not without limitations. This includes the limited sample size used in combination with the low detection limit of the mass spec approach employed. The general consensus on label-free quantitative methods is that 10-50 percent of proteins will not be detected due to the MS detection limit (73). Therefore, the upregulated proteins detected in the uEV during the WOI could be speculated to have been identified due to their high abundance. In reality, many other proteins could be altered. Other imitations to considered when interpreting these results are the possible contaminants

during sample collection and processing. The complex nature of the contaminants, including cell debris, proteins, bacteria, and other particles, could affect the uEVs' analysis. This also includes proteins attaching and co-isolating with the EVs, but attaining an uncontaminated pure uEV sample is difficult and demands a vigorous protocol. The suggestion of implementing alkaline washes to minimise protein contaminants should be considered in further uEV isolation workflows for biomarker discovery studies (74).

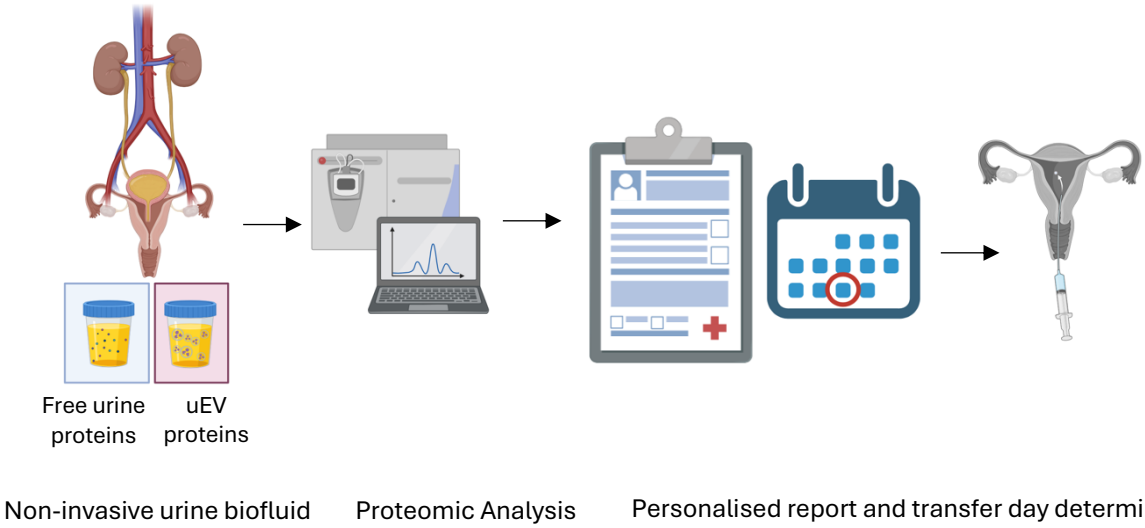


Figure 5.14. Non-invasive urine biofluid proteomic analysis could identify the personalised optimum embryo transfer day, promoting improved implantation outcomes for assisted reproductive technology patients.

In conclusion, this study we examined the potential use of uEVs as a source for optimising urine samples for proteomic profiling and identification of biomarkers for the window of implantation and phases of the menstrual cycle. We demonstrate improved specificity in identifying the different phases of the menstrual cycle in uEVs versus whole neat urine. However, we observed a dramatic decrease in the amount of significantly altered proteins in the uEVs compared to the whole neat urine. Nevertheless, we have demonstrated that uEVs have the capacity to provide a non-invasive source of crucial information regarding identifying the phases of the menstrual cycle, with Figure 5.14 depicting proposed application of non-invasive biofluid of urine analysis in clinical application. However, for clinical application, further studies are required on a larger scale of participants to further characterise potential biomarkers and reduce any inter- and intra-individual variations. These challenges, once answered, will aid in creating a uEV biomarker panel for menstrual phase identification and improving precision medicine approaches.

5.9 References.

1. Galliano D, Bellver J, Díaz-García C, Simón C, Pellicer A. ART and uterine pathology: how relevant is the maternal side for implantation? Hum Reprod Update. 2015 Jan 1;21(1):13–38.

2. Reshef EA, Robles A, Hynes JS, Turocy JM, Forman EJ. A review of factors influencing the implantation of euploid blastocysts after in vitro fertilization. FS Rev. 2022 May;3(2):105–20.

3. Murray MJ, Meyer WR, Zaino RJ, Lessey BA, Novotny DB, Ireland K, et al. A critical analysis of the accuracy, reproducibility, and clinical utility of histologic endometrial dating in fertile women. Fertil Steril. 2004;81(5).

4. Momeni M, Rahbar MH, Kovanci E. A meta-analysis of the relationship between endometrial thickness and outcome of in vitro fertilization cycles. J Hum Reprod Sci. 2011;4(3).

5. Díaz-Gimeno P, Horcajadas JA, Martínez-Conejero JA, Esteban FJ, Alamá P, Pellicer A, et al. A genomic diagnostic tool for human endometrial receptivity based on the transcriptomic signature. Fertil Steril. 2011;95(1).

6. Doyle N, Jahandideh S, Hill MJ, Widra EA, Levy M, Devine K. A Randomized Controlled Trial Comparing Live Birth From SingleI Euploid Frozen Blastocyst Transfer Using Standardized Timing Versus Timing By Endometrial Receptivity Analysis. Fertil Steril. 2021;116(3).

7. Cozzolino M, Diaz-Gimeno P, Pellicer A, Garrido N. Evaluation of the endometrial receptivity assay and the preimplantation genetic test for aneuploidy in overcoming recurrent implantation failure. J Assist Reprod Genet. 2020;37(12).

8. Sun Y, Zhang Y, Ma X, Jia W, Su Y. Determining Diagnostic Criteria of Unexplained Recurrent Implantation Failure: A Retrospective Study of Two vs Three or More Implantation Failure. Front Endocrinol. 2021 Jul 22;12.

9. Miller IJ, Peters SR, Overmyer KA, Paulson BR, Westphall MS, Coon JJ. Real-time health monitoring through urine metabolomics. Npj Digit Med. 2019 Nov 11;2(1):109.

10. Barratt J, Topham P. Urine proteomics: The present and future of measuring urinary protein components in disease. Vol. 177, CMAJ. Canadian Medical Association Journal. 2007.

11. Thongboonkerd V, Mcleish KR, Arthur JM, Klein JB. Proteomic analysis of normal human urinary proteins isolated by acetone precipitation or ultracentrifugation. Kidney Int. 2002;62(4).

12. Castagna A, Cecconi D, Sennels L, Rappsilber J, Guerrier L, Fortis F, et al. Exploring the hidden human urinary proteome via ligand library beads. J Proteome Res. 2005;4(6).

13. Castagna A, Olivieri O, Milli A, Dal Bosco M, Timperio AM, Zolla L, et al. Female urinary proteomics: New insight into exogenous and physiological hormone-dependent changes. Proteomics - Clin Appl. 2011;5(5–6).

14. Shao C, Zhao M, Chen X, Sun H, Yang Y, Xiao X, et al. Comprehensive analysis of individual variation in the urinary proteome revealed significant gender differences. Mol Cell Proteomics. 2019;18(6).

15. Thongboonkerd V. Practical points in urinary proteomics. J Proteome Res. 2007;6(10).

16. Apweiler R, Aslanidis C, Deufel T, Gerstner A, Hansen J, Hochstrasser D, et al. Approaching clinical proteomics: Current state and future fields of application in fluid proteomics. Vol. 47, Clinical Chemistry and Laboratory Medicine. 2009.

17. Yáñez-Mó M, Siljander PRM, Andreu Z, Zavec AB, Borràs FE, Buzas EI, et al. Biological properties of extracellular vesicles and their physiological functions. Journal of Extracellular Vesicles. 2015.

18. Alvarez S, Suazo C, Boltansky A, Ursu M, Carvajal D, Innocenti G, et al. Urinary exosomes as a source of kidney dysfunction biomarker in renal transplantation. Transplant Proc. 2013.

19. Guan M, Chen X, Ma Y, Tang L, Guan L, Ren X, et al. MDA-9 and GRP78 as potential diagnostic biomarkers for early detection of melanoma metastasis. Tumor Biol. 2015;36(4).

20. Jin X, Chen Y, Chen H, Fei S, Chen D, Cai X, et al. Evaluation of tumor-derived exosomal miRNA as potential diagnostic biomarkers for early-stage non-small cell lung cancer using next-generation sequencing. Clin Cancer Res. 2017;23(17).

21. Zhou B, Xu K, Zheng X, Chen T, Wang J, Song Y, et al. Application of exosomes as liquid biopsy in clinical diagnosis. Signal Transduction and Targeted Therapy. 2020.

22. Dissanayake K, Nõmm M, Lättekivi F, Ressaissi Y, Godakumara K, Lavrits A, et al. Individually cultured bovine embryos produce extracellular vesicles that have the potential to be used as non-invasive embryo quality markers. Theriogenology. 2020;149.

23. Pallinger E, Bognar Z, Bodis J, Csabai T, Farkas N, Godony K, et al. A simple and rapid flow cytometry-based assay to identify a competent embryo prior to embryo transfer. Sci Rep. 2017;7:39927.

24. Vilella F, Moreno-Moya JM, Balaguer N, Grasso A, Herrero M, Martínez S, et al. Hsa-miR-30d, secreted by the human endometrium, is taken up by the pre-implantation embryo and might modify its transcriptome. Dev Camb. 2015;142(18).

25. Piibor J, Dissanayake K, Midekessa G, Andronowska A, Kavak A, Waldmann A, et al. Characterization of bovine uterine fluid extracellular vesicles proteomic profiles at follicular and luteal phases of the oestrous cycle. Vet Res Commun. 2023;47(2).

26. Hart AR, Khan NLA, Dissanayake K, Godakumara K, Andronowska A, Eapen S, et al. The Extracellular Vesicles Proteome of Endometrial Cells Simulating the Receptive Menstrual Phase Differs from That of Endometrial Cells Simulating the Non-Receptive Menstrual Phase. Biomolecules. 2023;13(2).

27. Fraser KB, Rawlins AB, Clark RG, Alcalay RN, Standaert DG, Liu N, et al. Ser(P)-1292 LRRK2 in urinary exosomes is elevated in idiopathic Parkinson's disease. Mov Disord. 2016;31(10).

28. Chattrairat K, Yasui T, Suzuki S, Natsume A, Nagashima K, Iida M, et al. All-in-One Nanowire Assay System for Capture and Analysis of Extracellular Vesicles from an ex Vivo Brain Tumor Model. ACS Nano. 2023;17(3):2235–44.

29. Zhang C, Leng W, Sun C, Lu T, Chen Z, Men X, et al. Urine Proteome Profiling Predicts Lung Cancer from Control Cases and Other Tumors. EBioMedicine. 2018;30.

30. Rose JA, Wanner N, Cheong HI, Queisser K, Barrett P, Park M, et al. Flow cytometric quantification of peripheral blood cell β-adrenergic receptor density and urinary endothelial cell-derived microparticles in pulmonary arterial hypertension. PLoS ONE. 2016;11(6).

31. Svenningsen P, Sabaratnam R, Jensen BL. Urinary extracellular vesicles: Origin, role as intercellular messengers and biomarkers; efficient sorting and potential treatment options. Acta Physiologica. 2020.

32. Perez-Riverol Y, Bai J, Bandla C, García-Seisdedos D, Hewapathirana S, Kamatchinathan S, et al. The PRIDE database resources in 2022: A hub for mass spectrometry-based proteomics evidences. Nucleic Acids Res. 2022;50(D1).

33. Yao C, Chen X, Xu Y, Wang F, Ji J, Xu H, et al. Comparing pretreatment strategies to increase the yield and purity of human urinary extracellular vesicles. J Chromatogr B Analyt Technol Biomed Life Sci. 2022;1206.

34. Giacomini E, Scotti GM, Vanni VS, Lazarevic D, Makieva S, Privitera L, et al. Global transcriptomic changes occur in uterine fluid-derived extracellular vesicles during the endometrial window for embryo implantation. Hum Reprod Oxf Engl. 2021;36(8).

35. Hu ZZ, Huang H, Wu CH, Jung M, Dritschilo A, Riegel AT, et al. Omics-Based Molecular Target and Biomarker Identification. In: Methods in Molecular Biology. 2011.

36. Good DM, Zürbig P, Argilés À, Bauer HW, Behrens G, Coon JJ, et al. Naturally occurring human urinary peptides for use in diagnosis of chronic kidney disease. Mol Cell Proteomics. 2010;9(11).

37. Han Y, Quan X, Chuang Y, Liang Q, Li Y, Yuan Z, et al. A multi-omics analysis for the prediction of neurocognitive disorders risk among the elderly in Macao. Clin Transl Med. 2022;12(6).

38. Tomiyama E, Matsuzaki K, Fujita K, Shiromizu T, Narumi R, Jingushi K, et al. Proteomic analysis of urinary and tissue-exudative extracellular vesicles to discover novel bladder cancer biomarkers. Cancer Sci. 2021;112(5).

39. Braun F, Rinschen M, Buchner D, Bohl K, Plagmann I, Bachurski D, et al. The proteomic landscape of small urinary extracellular vesicles during kidney transplantation. J Extracell Vesicles. 2020;10(1).

40. Santucci L, Candiano G, Petretto A, Bruschi M, Lavarello C, Inglese E, et al. From hundreds to thousands: Widening the normal human Urinome. Data Brief. 2014;1.

41. Bruschi M, Ravera S, Santucci L, Candiano G, Bartolucci M, Calzia D, et al. The human urinary exosome as a potential metabolic effector cargo. Vol. 12, Expert Review of Proteomics. 2015.

42. Desiere F, Deutsch EW, King NL, Nesvizhskii AI, Mallick P, Eng J, et al. The PeptideAtlas project. Nucleic Acids Res. 2006;34(Database issue).

43. O'Brien K, Ughetto S, Mahjoum S, Nair AV, Breakefield XO. Uptake, functionality, and re-release of extracellular vesicle-encapsulated cargo. Cell Rep. 2022 Apr;39(2):110651.

44. Hill AF, Pegtel DM, Lambertz U, Leonardi T, O'Driscoll L, Pluchino S, et al. ISEV position paper: extracellular vesicle RNA analysis and bioinformatics. J Extracell Vesicles. 2013 Jan;2(1):22859.

45. Gipson IK, Blalock T, Tisdale A, Spurr-Michaud S, Allcorn S, Stavreus-Evers A, et al. MUC16 Is Lost from the Uterodome (Pinopode) Surface of the Receptive Human Endometrium: In Vitro Evidence That MUC16 Is a Barrier to Trophoblast Adherence1. Biol Reprod. 2008 Jan 1;78(1):134–42.

46. Kumar V, Soni UK, Maurya VK, Singh K, Jha RK. Integrin beta8 (ITGB8) activates VAV-RAC1 signaling via FAK in the acquisition of endometrial epithelial cell receptivity for blastocyst implantation. Sci Rep. 2017 May 15;7(1):1885.

47. Hwang JH, Park MI, Hwang YY, Yoo HJ, Mardon HJ. The characteristics of integrins expression in decidualized human endometrial stromal cell induced by 8-Br-cAMP in in vitro. Exp Mol Med. 2002 Jul 1;34(3):194–200.

48. Julian BA, Suzuki H, Suzuki Y, Tomino Y, Spasovski G, Novak J. Sources of urinary proteins and their analysis by urinary proteomics for the detection of biomarkers of disease. PROTEOMICS – Clin Appl. 2009 Sep;3(9):1029–43.

49. Park YG, Choi J, Seol JW. Angiopoietin-2 regulated by progesterone induces uterine vascular remodeling during pregnancy. Mol Med Rep. 2020 May 27;22(2):1235–42.

50. Thurston G. Role of Angiopoietins and Tie receptor tyrosine kinases in angiogenesis and lymphangiogenesis. Cell Tissue Res. 2003 Oct 1;314(1):61–8.

51. Wang F, Chen S, Liu HB, Parent CA, Coulombe PA. Keratin 6 regulates collective keratinocyte migration by altering cell–cell and cell–matrix adhesion. J Cell Biol. 2018 Dec 3;217(12):4314–30.

52. Ho M, Thompson B, Fisk JN, Nebert DW, Bruford EA, Vasiliou V, et al. Update of the keratin gene family: evolution, tissue-specific expression patterns, and relevance to clinical disorders. Hum Genomics. 2022 Jan 6;16(1):1.

53. Wang J, Liu G. Imaging Nano–Bio Interactions in the Kidney: Toward a Better Understanding of Nanoparticle Clearance. Angew Chem Int Ed. 2018 Mar 12;57(12):3008–10.

54. Adhipandito CF, Cheung SH, Lin YH, Wu SH. Atypical Renal Clearance of Nanoparticles Larger Than the Kidney Filtration Threshold. Int J Mol Sci. 2021 Oct 17;22(20):11182.

55. Du B, Jiang X, Das A, Zhou Q, Yu M, Jin R, et al. Glomerular barrier behaves as an atomically precise bandpass filter in a sub-nanometre regime. Nat Nanotechnol. 2017 Nov;12(11):1096–102.

56. Lahdenkari AT, Lounatmaa K, Patrakka J, Holmberg C, Wartiovaara J, Kestila[Combining Diaeresis] M, et al. Podocytes Are Firmly Attached to Glomerular Basement Membrane in Kidneys with Heavy Proteinuria. J Am Soc Nephrol. 2004 Oct;15(10):2611–8.

57. Zaborowski MP, Balaj L, Breakefield XO, Lai CP. Extracellular Vesicles: Composition, Biological Relevance, and Methods of Study. BioScience. 2015.

58. Naumenko V, Nikitin A, Kapitanova K, Melnikov P, Vodopyanov S, Garanina A, et al. Intravital microscopy reveals a novel mechanism of nanoparticles excretion in kidney. J Controlled Release. 2019 Aug;307:368–78.

59. Williams RM, Shah J, Tian HS, Chen X, Geissmann F, Jaimes EA, et al. Selective Nanoparticle Targeting of the Renal Tubules. Hypertension. 2018 Jan;71(1):87–94.

60. Zuckerman JE, Choi CHJ, Han H, Davis ME. Polycation-siRNA nanoparticles can disassemble at the kidney glomerular basement membrane. Proc Natl Acad Sci. 2012 Feb 21;109(8):3137–42.

61. Huang Y, Wang J, Jiang K, Chung EJ. Improving kidney targeting: The influence of nanoparticle physicochemical properties on kidney interactions. J Controlled Release. 2021 Jun;334:127–37.

62. Thomas W, Harvey BJ. Estrogen-induced signalling and the renal contribution to salt and water homeostasis. Steroids. 2023 Nov;199:109299.

63. Lemale J, Bloch-Faure M, Grimont A, El Abida B, Imbert-Teboul M, Crambert G. Membrane progestin receptors α and γ in renal epithelium. Biochim Biophys Acta BBA - Mol Cell Res. 2008 Dec;1783(12):2234–40.

64. Grimont A, Bloch-Faure M, Abida BE, Crambert G. Mapping of sex hormone receptors and their modulators along the nephron of male and female mice. FEBS Lett. 2009 May 19;583(10):1644–8.

65. Batra SC, Iosif CS. Progesterone Receptors in the Female Lower Urinary Tract. J Urol. 1987 Nov;138(5):1301–4.

66. Diaa E. E. Rizk, Tove Raaschou, Neil Mason, Bertel Berg. Evidence of Progesterone Receptors in the Mucosa of the Urinary Bladder. Scand J Urol Nephrol. 2001 Jan 1;35(4):305–9.

67. Kwok ZH, Wang C, Jin Y. Extracellular vesicle transportation and uptake by recipient cells: A critical process to regulate human diseases. Vol. 9, Processes. 2021.

68. Robertson SA, Care AS, Moldenhauer LM. Regulatory T cells in embryo implantation and the immune response to pregnancy. Vol. 128, Journal of Clinical Investigation. 2018.

69. Mor G, Cardenas I, Abrahams V, Guller S. Inflammation and pregnancy: The role of the immune system at the implantation site. Ann N Y Acad Sci. 2011;1221(1).

70. Mor G, Cardenas I. The Immune System in Pregnancy: A Unique Complexity. Am J Reprod Immunol. 2010 Jun;63(6):425–33.

71. Okada H, Tsuzuki T, Murata H. Decidualization of the human endometrium. Reprod Med Biol. 2018 Jul;17(3):220–7.

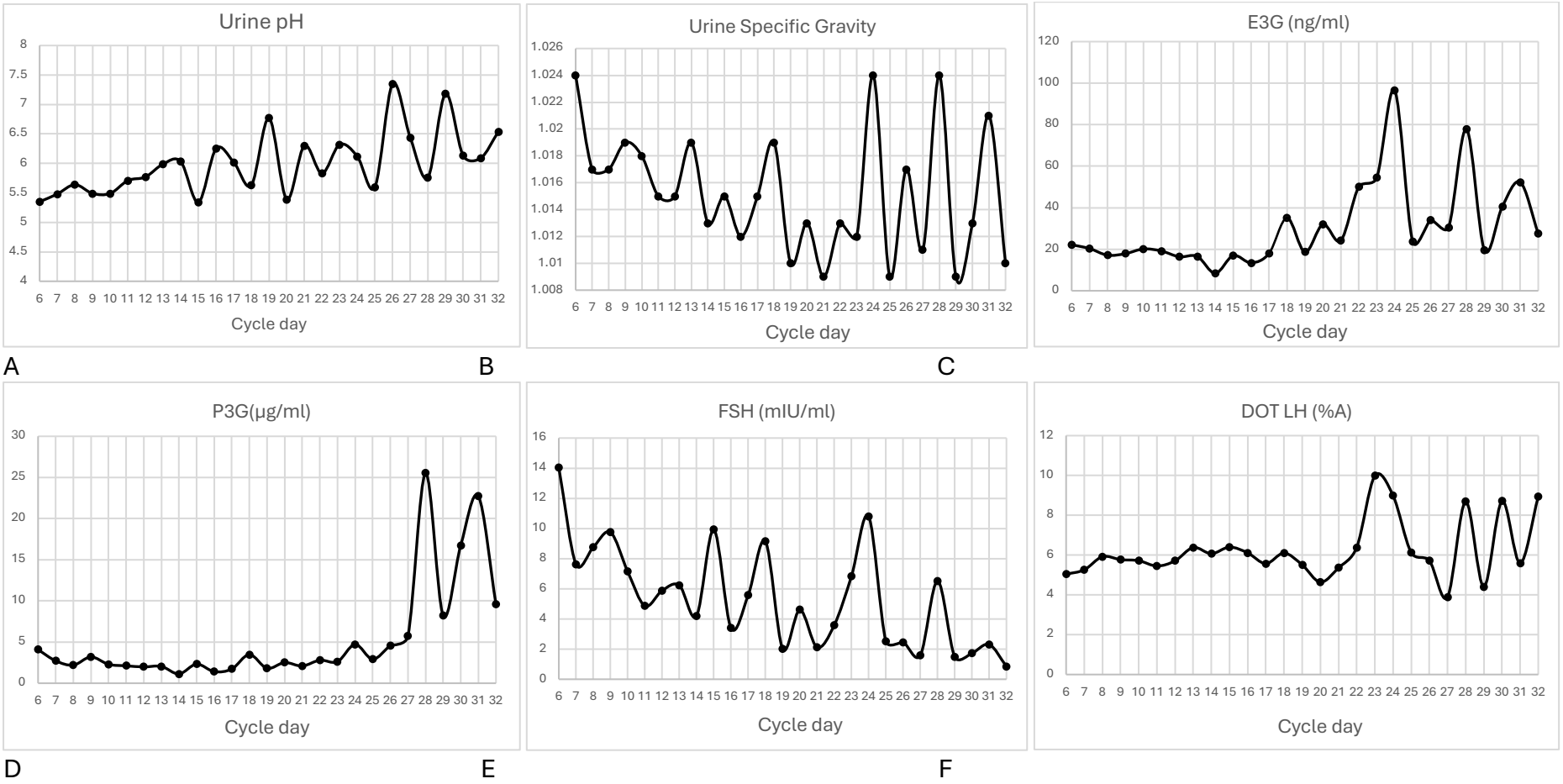
72. Puscheck EE, Awonuga AO, Yang Y, Jiang Z, Rappolee DA. Molecular Biology of the Stress Response in the Early Embryo and its Stem Cells. In: Leese HJ, Brison DR, editors. Cell Signaling During Mammalian Early Embryo Development [Internet]. New York, NY: Springer New York; 2015 [cited 2024 Aug 1]. p. 77–128. (Advances in Experimental Medicine and Biology; vol. 843). Available from: https://link.springer.com/10.1007/978-1-4939-2480-6_4.

73. Lazar C, Gatto L, Ferro M, Bruley C, Burger T. Accounting for the Multiple Natures of Missing Values in Label-Free Quantitative Proteomics Data Sets to Compare Imputation Strategies. J Proteome Res. 2016;15(4).

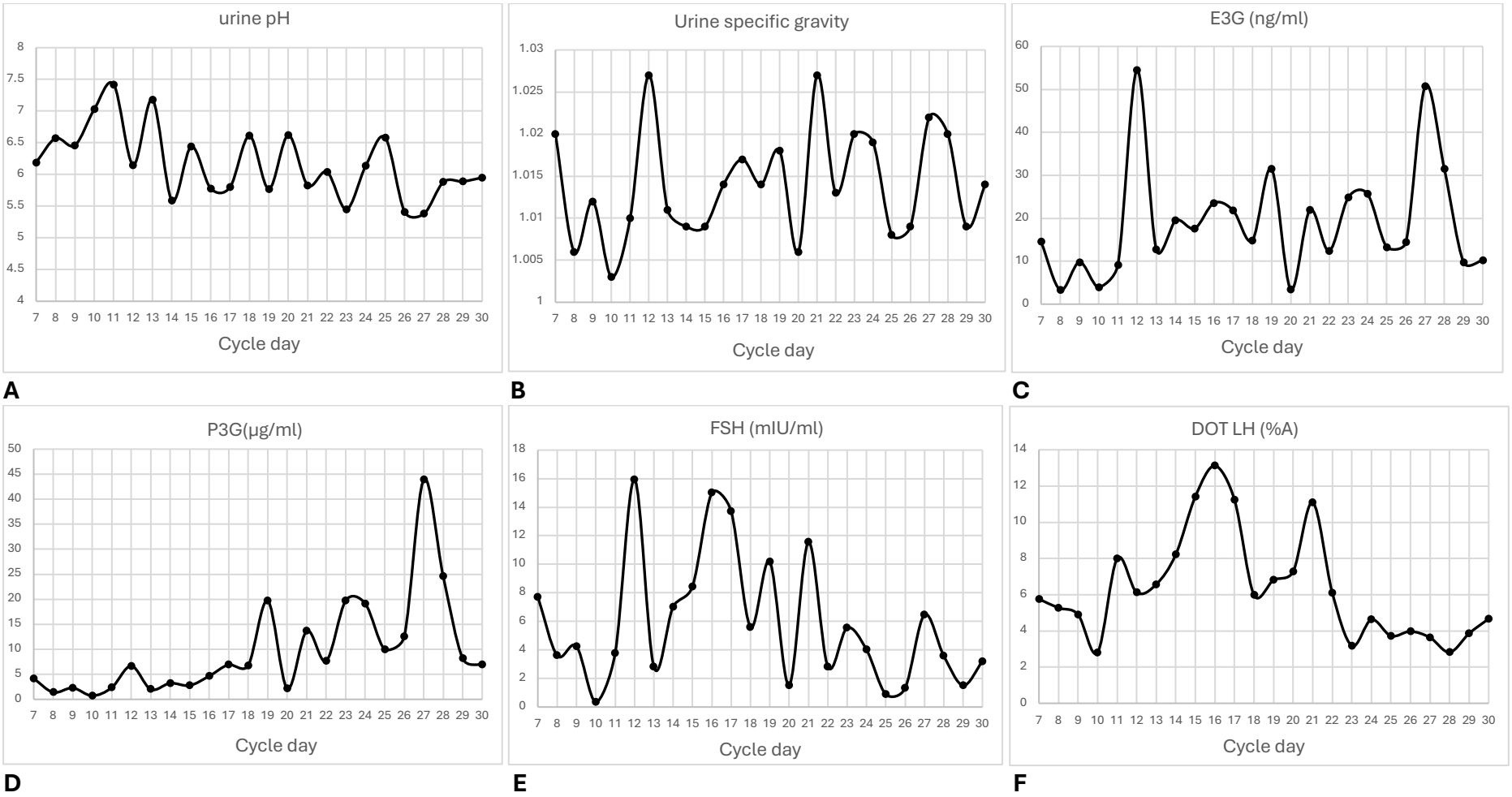
74. Correll VL, Otto JJ, Risi CM, Main BP, Boutros PC, Kislinger T, et al. Optimization of small extracellular vesicle isolation from expressed prostatic secretions in urine for in-depth proteomic analysis. J Extracell Vesicles. 2022;11(2).

75. Heberle H, Meirelles VG, da Silva FR, Telles GP, Minghim R. InteractiVenn: A web-based tool for the analysis of sets through Venn diagrams. BMC Bioinformatics. 2015;16(1).

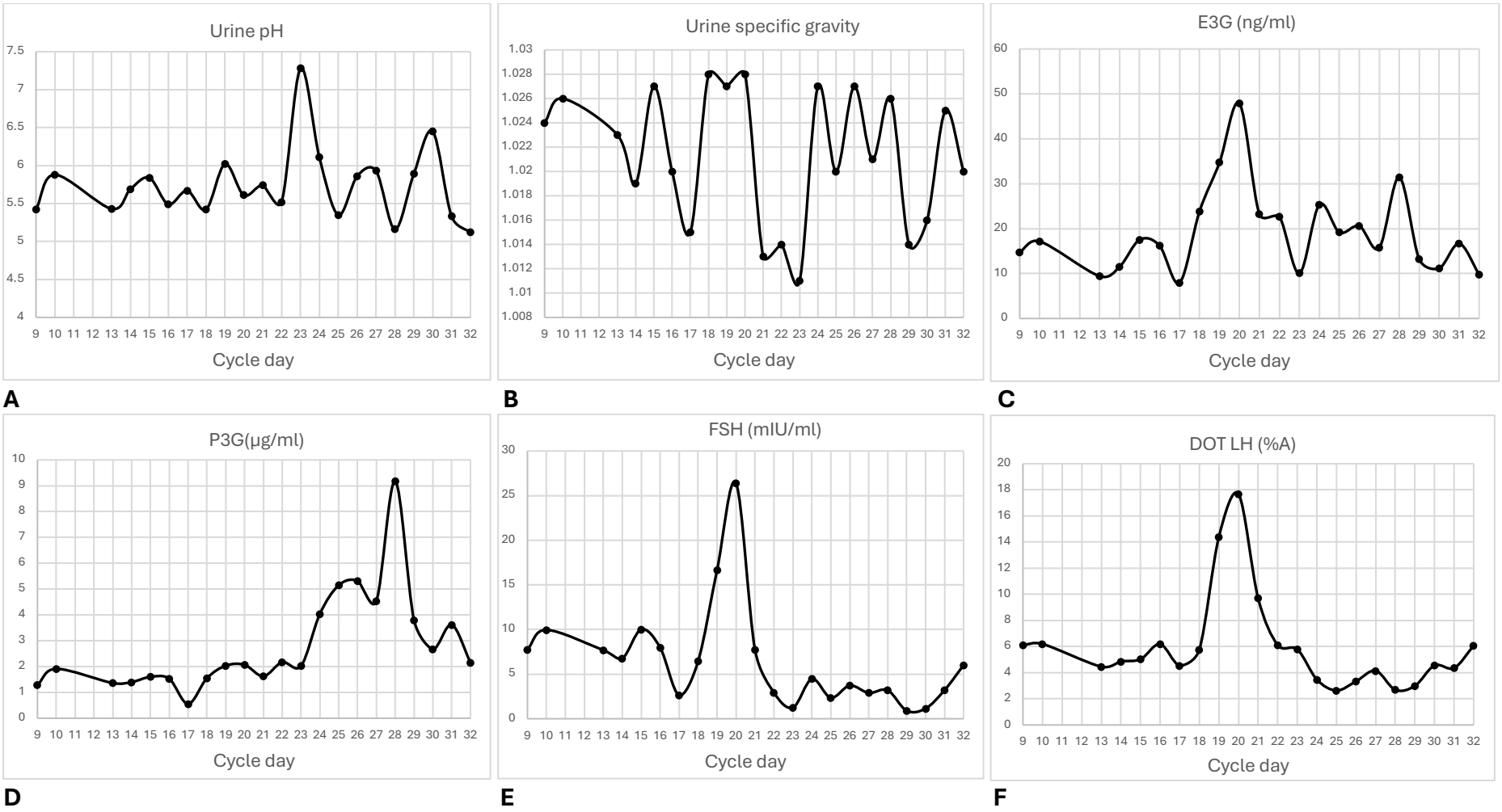
5.10 Supplementary materials.



Supplementary Figure 5.1. Urinalysis of subject 1 urine across the collection period. (A) Depicts the urine pH across the cycle days. (B) Depicts the urine specific gravity across the cycle days. (C) Depicts the concentration of E3G (ng/ml) across the cycle days. (D) Depicts the concentration of P3G (µg/ml) across the cycle days. (E) Depicts the concentration of FSH (mIU/ml) across the cycle days. (F) concentration of LH (%A) across the cycle days.



Supplementary Figure 5.2. Urinalysis of subject 2 urine across the collection period. (A) Depicts the urine pH across the cycle days. (B) Depicts the urine specific gravity across the cycle days. (C) Depicts the concentration of E3G (ng/ml) across the cycle days. (D) Depicts the concentration of P3G (µg/ml) across the cycle days. (E) Depicts the concentration of FSH (mIU/ml) across the cycle days. (F) concentration of LH (%A) across the cycle days.



Supplementary Figure 5.3. Urinalysis of subject 3 urine across the collection period. (A) Depicts the urine pH across the cycle days. (B) Depicts the urine specific gravity across the cycle days. (C) Depicts the concentration of E3G (ng/ml) across the cycle days. (D) Depicts the concentration of P3G (µg/ml) across the cycle days. (E) Depicts the concentration of FSH (mIU/ml) across the cycle days. (F) concentration of LH (%A) across the cycle days.

Supplementary Table 5.1. Differential enrichment of urine proteins of WOI Group compared to O.

Uniport accession	Gene Name	Adjusted p value	Fold change
Q92526	CCT6B	0.013949396	-2.97
P01229	LHB	0.016206562	-2.81
Q8WXI7	MUC16	0.044539522	-2.08
P18564	ITGB6	0.048995664	-1.81
Q92734	TFG	0.086756209	-1.66
Q16661	GUCA2B	0.040552054	-1.65
P58166	INHBE	0.072091892	-1.65
P35556	FBN2	0.077712518	-1.37
Q9NQX7	ITM2C	0.029595502	-1.22
Q00839	HNRNPU	0.0211809	1.03
Q96K62	ZBTB45	0.039216165	1.38
Q8TD08	MAPK15	0.039672616	1.38
P43686	PSMC4	0.072575178	1.44
P54819	AK2	0.055179272	1.5
O00763	ACACB	0.091888019	1.69
P20700	LMNB1	0.011783817	1.84
P83916	CBX1	0.053691036	1.9
Q5TEC6	H3-7	0.065260901	2.52
Q9Y2E6	DTX4	0.023780311	3.1

Supplementary Table 5.2. Differential enrichment of urine proteins of WOI Group compared to P.

Uniport accession	Gene Name	Adjusted p value	Fold change
Q92526	CCT6B	0.011597485	-3.09
P18564	ITGB6	0.039347283	-1.92
Q6KB66	KRT80	0.062559488	-1.39
P81605	DCD	0.010453862	-1.28
Q86YZ3	HRNR	0.052894951	-1.28
Q16864	ATP6V1F	0.063115427	1.08
Q96LA6	FCRL1	0.058424207	1.09
P29350	PTPN6	0.06151384	1.2
Q6UWP2	DHRS11	0.007007253	1.21
P31150	GDI1	0.011350696	1.22
O94979	SEC31A	0.048347916	1.34
P28074	PSMB5	0.067486373	1.36

P49720	PSMB3	0.046731207	1.42
Q9NRV9	HEBP1	0.000208561	1.46
O95359	TACC2	0.040661084	1.58
P52948	NUP98	0.05009687	1.66
Q8N8Y2	ATP6V0D2	0.047904394	1.68
P20700	LMNB1	0.008298118	1.97
Q9NXJ5	PGPEP1	0.048499284	2
P08237	PFKM	0.049539409	2.03
Q9Y2E6	DTX4	0.025039902	3.06

Supplementary Table 5.3. Differential enrichment of urine proteins of P Group compared to WOI.

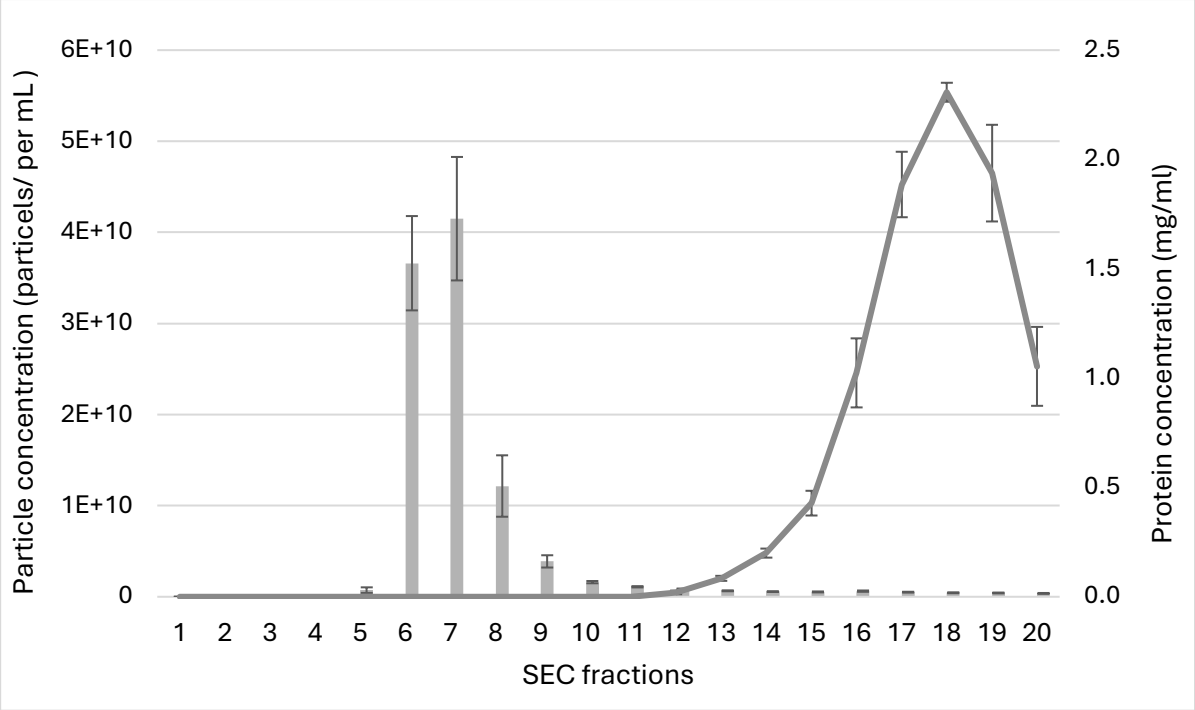
Uniport accession	Gene Name	Adjusted p value	Fold change
P01229	LHB	0.00000797	-3.12
Q9NXJ5	PGPEP1	0.0144	-1.93
Q8NFY4	SEMA6D	0.0413	-1.83
Q8WXI7	MUC16	0.0369	-1.77
P28074	PSMB5	0.00856	-1.52
P13224	GP1BB	0.0403	-1.48
P49720	PSMB3	0.00551	-1.47
Q9NRV9	HEBP1	5.15E-13	-1.22
P04278	SHBG	0.0000452	-1.14
Q02809	PLOD1	0.0187	-1.12
Q9C0K7	STRADB	0.0268	-1.03
Q8TD08	MAPK15	0.0354	1.15
Q9BYD5	CNFN	0.0326	1.34
O00763	ACACB	0.0205	1.93
P19013	KRT4	0.00139	2.23
Q13490	BIRC2	0.0398	3

Supplementary Table 5.4. Differential enrichment of EV proteins of WOI Group compared to O.

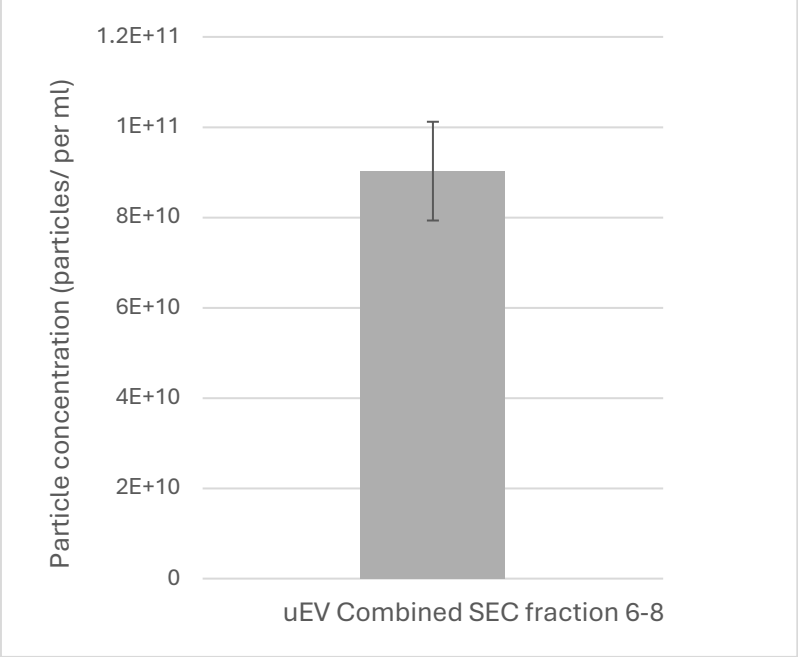
Uniport accession	Gene Name	Adjusted p value	Fold change
P51688	SGSH	0.00000341	-2.26
P17342	NPR3	0.00137	-1.81
Q8NEX9	SDR9C7	0.0088	-1.73
Q14126	DSG2	0.0227	-1.37
Q15904	ATP6AP1	0.0466	1.78
Q8NI99	ANGPTL2	0.0126	1.8
Q9BQ24	ZFYVE21	0.000113	2.22
Q9UKY7	CDV3	0.000222	2.45
Q9BZE9	ASPSCR1	0.000000446	3.02

Supplementary Table 5.5. Differential enrichment of EV proteins of WOI Group compared to P.

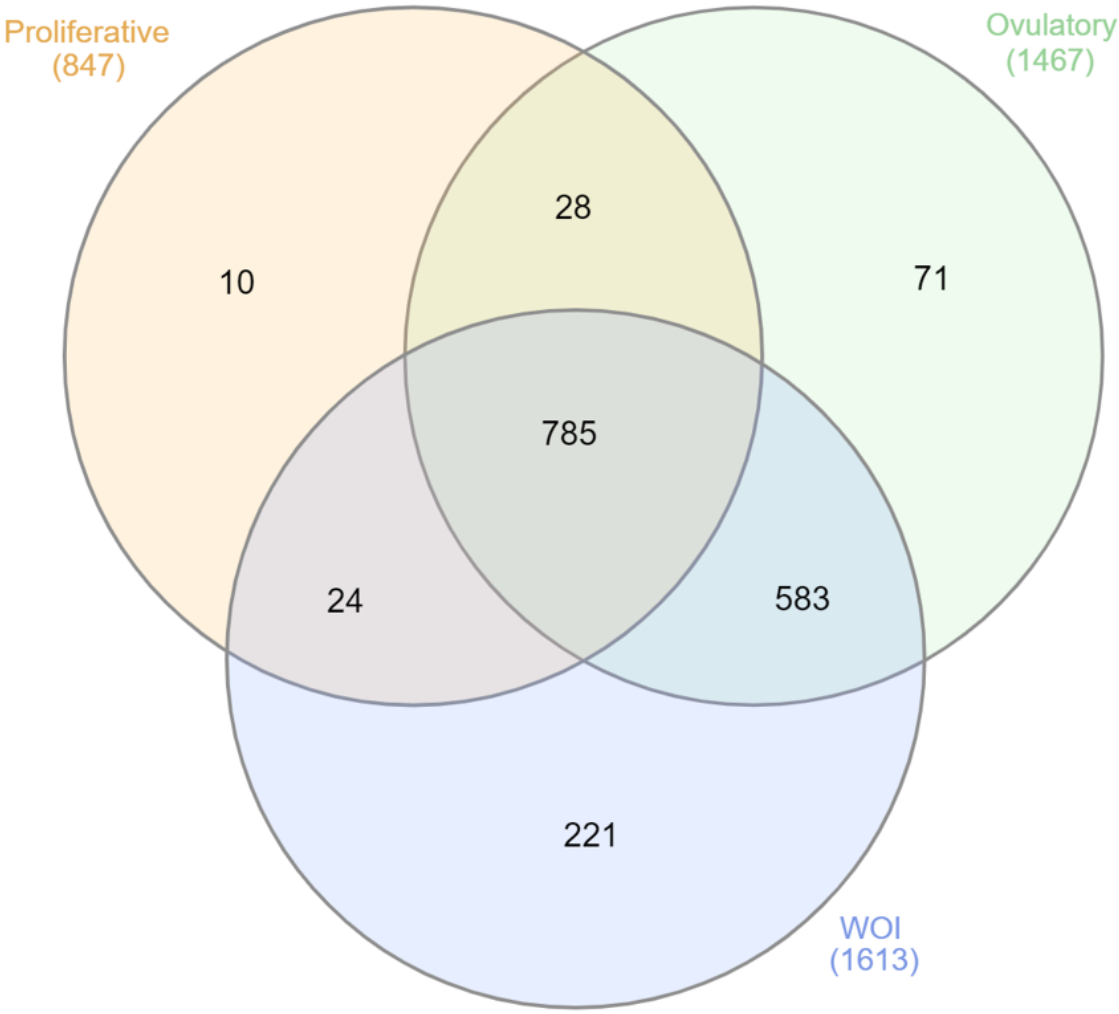
Uniport accession	Gene Name	Adjusted p value	Fold change
P04259	KRT6B	0.0141	-4.23
Q8NEX9	SDR9C7	0.000902	-3.05
Q562E7	WDR81	0.0000117	-3.05



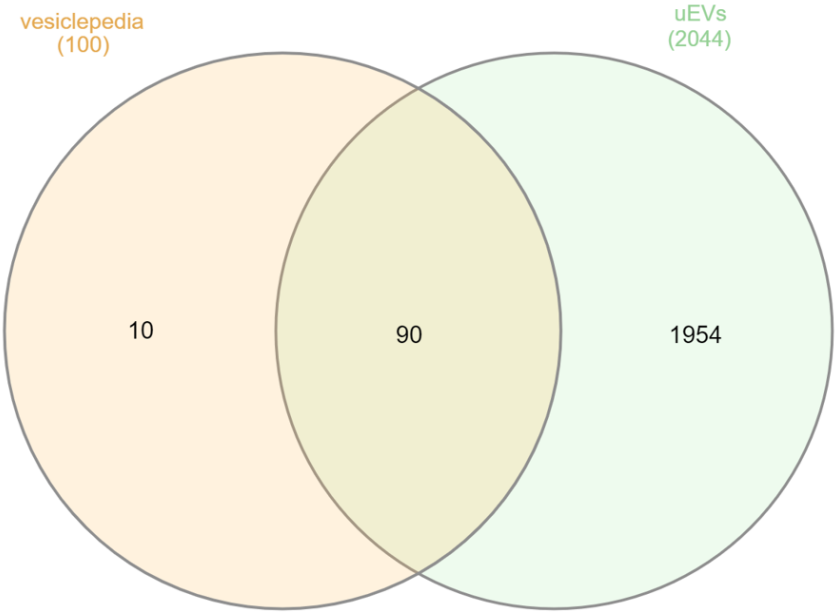
Supplementary Figure 5.4. Isolation of urine extracellular vesicles sized particles using differential centrifugation and size exclusion chromatography. The height of the bars represents the mean concentration (particles/ml) of EVs from 1 biological replicate and 6 technical replicates. The majority of EVs sized particles were eluted in fractions 6-8. The line graph represents the mean concentration of protein (mg/ml) in each SEC fraction from 1 biological replicate and 6 technical replicates. Error bars represent the standard error from the mean.



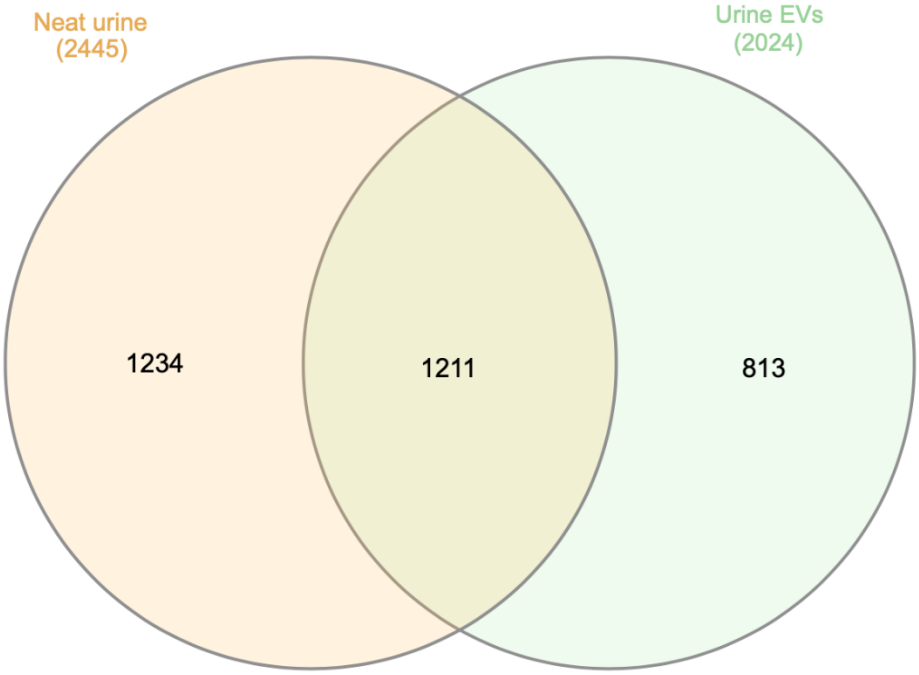
Supplementary Figure 5.5. Combined concentration of EVs for urine from SEC fractions 6-8. The bar represents the mean concentration (particles/mL) ±SEM of EV sized particles from the combined SEC fractions 6–8. Data are from 1 biological replicate and 6 technical replicates.



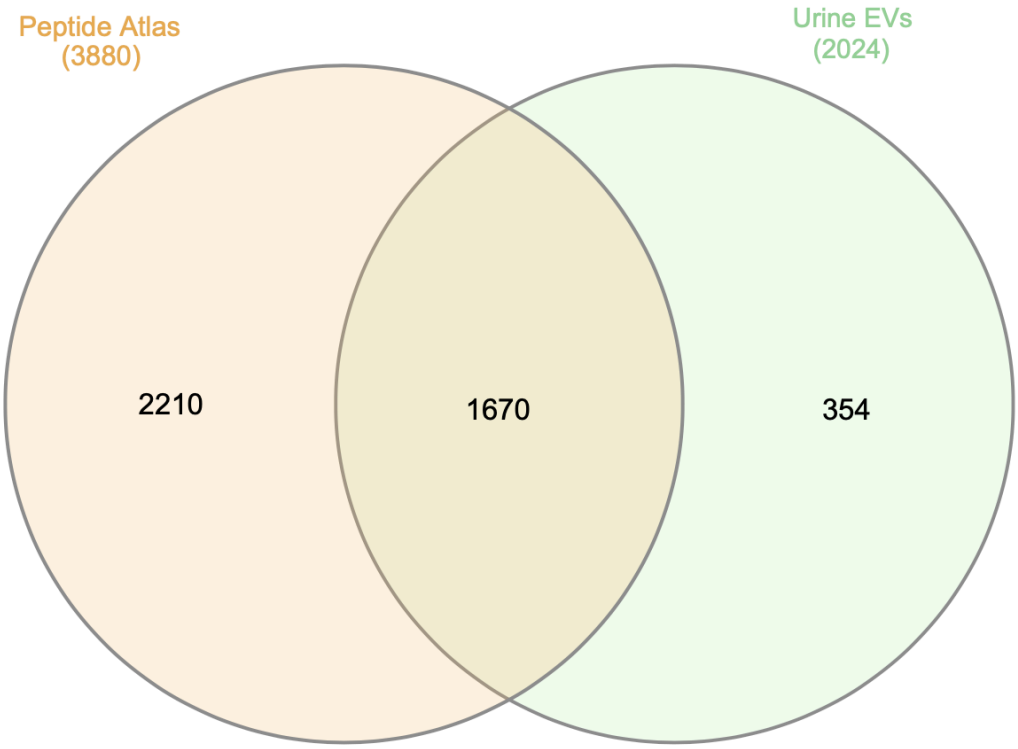
Supplementary Figure 5.6. Venn diagram of uEV proteins in all the comparison groups. Only proteins detected in at least two of the replicates were included. (Made in Heberle, H.; Meirelles, G. V.; da Silva, F. R.; Telles, G. P.; Minghim, R. *InteractiVenn: a web-based tool for the analysis of sets through Venn diagrams*. BMC Bioinformatics 16:169 (2015) (75)).



Supplementary Figure 5.7. Venn diagram of proteins in the uEV groups versus the compared to the top 100 Vesiclepedia EV markers. (Made in Heberle, H.; Meirelles, G. V.; da Silva, F. R.; Telles, G. P.; Minghim, R. *InteractiVenn: a web-based tool for the analysis of sets through Venn diagrams*. BMC Bioinformatics 16:169 (2015) (75)).



Supplementary Figure 5.8. Venn diagram of proteins found in the neat urine versus the number of proteins found in uEVs. (Made in Heberle, H.; Meirelles, G. V.; da Silva, F. R.; Telles, G. P.; Minghim, R. *InteractiVenn: a web-based tool for the analysis of sets through Venn diagrams*. BMC Bioinformatics 16:169 (2015) (75)).



Supplementary Figure 5.9. Venn diagram of proteins reported in peptide atlas human urine 2022-02 database versus the proteins found in uEVs. (Made in Heberle, H.; Meirelles, G. V.; da Silva, F. R.; Telles, G. P.; Minghim, R. *InteractiVenn: a web-based tool for the analysis of sets through Venn diagrams*. BMC Bioinformatics 16:169 (2015) (75)).

CHAPTER 6

RETHINKING ENDOMETRIAL RECEPTIVITY TESTS: A CALL FOR INNOVATION.

Chapter 6. Rethinking endometrial receptivity tests: a call for innovation.

6.1 Authors contribution.

This work forms part of the review article publication "**Rethinking Endometrial Receptivity Tests: A Call for Innovation"** that is currently under review for publication.

6.2 Interconnecting chapters.

Building on the insights gained from preceding chapters, which have revealed that both endometrial and urine EV proteome differs under menstrual cycle hormonal control, and a suggested a functional role, the potential for utilising EVs as receptivity biomarkers has emerged. Thus, the aim of this chapter is to review existing endometrial receptivity assays while also proposing how the future direction of receptivity biomarker research should proceed.

6.3 Abstract.

Despite advances in the fields of reproductive medicine, embryo implantation represents a major bottleneck for infertile patients undergoing assisted reproductive technologies (ART). Currently available endometrial receptivity tests, aim, in the most part, to analyse various panels of genes to determine the implantation window for every patient, and therefore facilitate an optimised and personalised timing for embryo transfer. This seems like a promising solution to implantation failure rates. However, the value of this approach in clinical practice is still unproven. The aim of this review is to analyse the existing assays and their current evidence as well as provide an informed commentary on what an ideal assay should consist of and how the future direction of research should proceed to attain this. As our understanding of the receptive endometrium increases, we envision and advocate for a non-invasive omics-based assay approach for better determining receptivity and the window of implantation, resulting in an increase in positive pregnancy outcomes across populations struggling with fertility.

6.4 Introduction.

The processes leading to successful implantation and subsequent pregnancy are complex and multidimensional, depending on the interplay and communication between the embryo and the receptive endometrium (1). Major advances in preimplantation genetic testing failed to improve the implantation rate of euploid embryos beyond 60% (2), highlighting the importance of the endometrial factor as a major culprit for unsuccessful embryo transfers, rendering the assessment of endometrial receptivity a pivotal determinant of success IVF (3). However, despite

significant advancements in reproductive medicine, endometrial receptivity assessment remains a challenge, often reliant on conventional methods with poor diagnostic accuracy and low predictive powers (4). The current practices and tools available for endometrial receptivity testing, include histological, hormonal, biochemical, imaging modalities, and more recently genomic and proteomic biomarkers; while valuable, present limitations in terms of accuracy, reproducibility, and clinical utility (5). Newer "omics"-based methods have not shown great benefits in terms of improved live birth-rates, highlighting the critical need to re-evaluate and innovate the tools and techniques currently used to assess endometrial receptivity (6).

This opinion paper offers a critical examination of current endometrial receptivity tests and advocates a shift towards more innovative result-driven approaches. We propose that by combining newer, emerging "omics" technologies with artificial intelligence (AI) we can gain a more comprehensive, dynamic, and predictive understanding of endometrial receptivity. We also highlight the need for such a test to be non-invasive in nature to enhance patient experience and facilitate wider adoption in clinical practice.

In this paper, we will highlight the inherent limitations of conventional methods, the opportunities presented by emerging technologies, and the imperative for collaboration among clinicians, researchers, and technology developers to propel the reproductive field towards novel and clinically useful solutions. This call for innovation and a change of approach on endometrial receptivity testing seeks to enhance the efficacy of ART through personalised and optimised testing and treatment strategies. Endometrial receptivity tests are also of significant commercial value. In a landmark deal that was a

massive topic of interest in the reproductive health industry, Igenomix was acquired by Vitrolife in 2019 for a reported $1.48 billion (7). Central to Igenomix's offering, was probably its novel endometrial receptivity array (ERA) test. Hence, improvements and new innovations to pinpoint endometrial receptivity testing seems of significant interest in the reproductive health commercial sector as well. Here, we will outline a roadmap for future research and describe an ideal test and ideas aimed at realising the promise of precise endometrial receptivity tests and personalised embryo transfers.

6.5 Traditional endometrial receptivity timing.

It is well known that implantation success is dependent on a receptive uterus, competent blastocyst, and communication and interaction between the two (8,9). The human endometrium is usually described as refractory except during the mid-luteal phase, a limited time interval in which the endometrium is receptive to implantation, (approximately cycle day 19-24 of a 28 day cycle), called the "window of implantation" (WOI) (10). In hormonal replacement artificial cycles, commonly employed in IVF, the WOI is usually expected to arise 4 -7 days after progesterone administration, with blastocyst transfer typically conducted 5 days after progesterone administration or ovulation (11). During this time, the synchronised competency of an embryo with the receptive endometrium coordinates many molecular pathways in order for a successful pregnancy to occur, along with immunomodulatory regulation of immune factors and the immune microenvironment (8,12,13). Conditions such as recurrent implantation failure (RIF), endometriosis, and unexplained infertility, with probable disruption of the WOI, have prompted efforts to improve the determination of the optimal timing for embryo transfer (14). Currently, as discussed below, determination of endometrium receptivity

for implantation uses mostly histological appearance and imaging. However, over the years, the understanding of endometrial transcriptomics and proteomics for the identification of the implantation window has led to the development of commercial tools to improve implantation rates in assisted reproduction (6). Nevertheless, current evidence of their success is sparse, and herein, the reported effectiveness of such tools will be evaluated, as well as the overall need for more appropriate reliable clinical tools.

6.6 Current practices.

The embryo transfer procedure is a vital step in IVF, conducted to optimise the chances of successful implantation. Correct timing of embryo transfer is critical for success of IVF. One way in which clinicians currently control timing of the transfer often begins with hormonal supplementation (15). Estrogen is commonly used to stimulate endometrial thickening and hence receptivity to the transferred embryo (15). Concurrently, progesterone is also exiguously given for luteal phase support (15). Through this process, the response to hormone therapy is monitored through ultrasound scans and hormone level tests to optimise receptivity (16). Through this monitoring, the day for embryo transfer is meticulously chosen to ensure the endometrium and the developing embryo are in temporal synchrony i.e. a day 5 embryo will be transferred on the fifth day after the first progesterone exposure (15).

However, the dose and timing of hormone treatment has been subject of debate (17). For example, administration of only 2, 4 or 6 mg of estradiol to progesterone for luteal support had no significant effect on pregnancy or implantation rates, however, the lowest dose was been associated with increased miscarriage risk compared with 6 mg

(18).Studies have also suggested that high blood levels of progesterone or premature surge prior to human chorionic gonadotrophin in stimulated and hyper stimulated cycles reduces pregnancy rate (19,20). However other research have stated that there is no correlation between progesterone level and the outcomes of pregnancy (21,22).

Another commonly used method is ultrasound assessments of endometrial thickness, appearance and blood flow (23). There is currently no consensus on the positive or negative predictive values; and diagnostic usefulness of ultrasound endometrial assessments (5,24–26). These conflicting reports have led to suggestion that the future lies in artificial intelligence (AI)-guided ultrasound imaging to improve diagnostics usefulness (27). Clearly, current practices of cycle cancellation based on ultrasound assessment alone are not always justifiable; therefore, better tests that will greatly improve post-test likelihood of ongoing pregnancy are needed.

6.7 Available endometrial receptivity tests.

In recent years, advancements in understanding endometrial transcriptomics and its role in determining the optimal implantation window have fuelled the development of commercial tools aimed at enhancing implantation success and assisted reproduction outcomes (28). This progress has been accelerated by innovation in omics technologies and its resulting data that suggest the timing and duration of the implantation window may vary among women. Researchers have, as a result, pioneered commercially available endometrial receptivity tests, such as the endometrial receptivity array (ERA), Win-Test, RNA-Seq-based endometrial receptivity test (rsERT), ERMap, ERPeak, and beREADY (28). Initially, it was thought that these tests held promise for personalised

approaches for identifying the exact window of implantation, potentially revolutionising assisted reproduction strategies. However, many studies have evaluated the diagnostic usefulness of these tests; and others have looked at whether currently data are robust enough to advocate for routine application in infertile women undergoing assisted conception and those suffering reproductive failure. In this paper we will provide a summary of research that have evaluated the usefulness of available endometrial receptivity tests.

The most published and evaluated of available test is ERA, the only test for which randomised controlled trials (RCTs) exist (see Table 6.1 for a summary of studies on ERA). The ERA, developed by Igenomix (Valencia, Spain), was the first transcriptomic test developed to diagnose the endometrial receptivity status (29). This assay uses next-generation sequencing (NGS) to assess the differential expression of 238 genes with a computational predictor to assess the endometrium status during sampling (29).

The first RCT to evaluate ERA involved 458 women to compare the success of embryo transfer(ET), guided by ERA to that of frozen ET (FET) or fresh embryo transfer (ET) (30). The study showed no significant difference between the methods in terms of pregnancy rate, live birth rate, and implantation rate when an intention-to-treat analyse was performed (30). However, is was shown that the cumulative live birth rate in 12-month period in the ERA group (71.2%) was higher than in FET group (55.4%) and ET group (48.9%) (30). But the usefulness of this study, as well as the study design, is debatable and has been previously critiqued (31,32). This critique summarises that the Standards for Reporting Diagnostic accuracy studies (STARD) standards were not rigidly adhered

to. For example, an inappropriate spectrum of patients whereby only healthy young participants (under the age of 37) were recruited, not, for example, women suffering from recurrent implantation failure, hence not the intended target of add-on procedures and therefore not representative of how such a technology would be utilised in a clinical setting. Another limitation is that apart from interventions compared, the groups were treated differently according to centre protocols. So, although the trial was multicentric, across 16 clinics in Asia, Europe and America, there was deviation from protocol larger than anticipated, along with the lack of control in variation such as progesterone dose, stimulation protocol, and vitrification method, all of which varied subject to the discretion of the centre, creating a heterogeneity in the data. Thirdly, there were more embryo transfers in the ERA group than in the controls, which makes it difficult to interpret the cumulative analysis and thus may be misleading. Further RCT, data pooling, or meta-analysis may reveal different results in terms of ERA clinical advantage.

The diagnostic usefulness of ERA were similar in a more recent RCT (33). Live birth rate was compared from frozen embryo transfer and those undergoing ERA (randomised treatment) in women who had no evidence of recurrent implantation failure (n=767). The live birth rate was not significantly different between those who underwent standard timing (61.9%) and those who had ERA-adjusted timing (58.3%). Confirming the pervious study, that the evidence does not support the use of ERA in a clinical setting.

Table 6.1. Summary of study's assessment of Endometrial Receptivity Array

Study design	Reference	Total Patient population (N number)		Control population not receiving ERA (N number)		Study Recorded Outcome
		RIF	No known conditions	RIF	No known conditions	
Randomised Controlled Trial	Simón et al., 2021 (30)	NA	458	NA	310	PR, LBR, IR
	Doyle et al., 2022 (33)	NA	767	NA	386	LBR,BP_2, CPR
Retrospective	Doyle et al., 2022 (34)	NA	3591	NA	2,284	LBR
	Jia 2022 (35)	172	NA	79	NA	PR
	Eisman et al., 2021 (36)	NA	222	NA	NA	C, PR, LBR
	Bergin et al., 2021 (37)	NA	486	NA	353	LBR
	Fodina, 2021 (38)	253	NA	NA	NA	BP_2, CPR, PL
	Barrenetxa, 2021 (39)	NA	104	NA	NA	LBR
	Cozzolino et al., 2020 (40)	2598	NA	2445	NA	IR PR
	Cohen et al., 2020 (41)	97	NA	NA	NA	CPR, BP_2, IR, LBR, MR
	Neves et al., 2019 (42)	333	NA	227	NA	IR, PR
	Patel et al., 2019 (43)	248	NA	NA	NA	PR, IR, CPR, AR OPR
	Bassil et al., 2018 (44)	NA	556	NA	503	PR
	Tan et al., 2018 (45)	62	26	NA	NA	IR, OPR
	Mahajan, 2015 (46)	186	NA	NA	NA	IR, OPR, PR, MR
	Ruiz-Alonso, 2014 (47)	NA	2445	NA	NA	IR, PR, OPR
Prospective multicentre	Hashimoto et al., 2017 (48)	50	NA	NA	NA	PR
	Ruiz-Alonso et al., 2013 (49)	85	25	NA	NA	PR, IR
Prospective single centre	Saxtorph et al., 2020 (50)	123	NA	NA	37	IR
	Riestenberg et al., 2021 (51)	NA	228	NA	81	LBR

Note: (PR) pregnancy rate, implantation rate (IR) clinical pregnancy rate (CPR) abortion rate (AR) ongoing pregnancy rate (OPR) live birth rate (LBR) biochemical pregnancy (BP_2) pregnancy loss (PL) conception (C) miscarriage rate (MR)

Other available tests include; ERPeak, developed by CooperSurgical, which uses reverse transcription quantitative real-time PCR to analyse 48 genes (52). To assess the effectiveness of this assay on pregnancy outcome, a retrospective cohort study on 1,000 patients with recurrent implantation failure has been reported (53). Here, they showed a significantly elevated live birth rate using ERPeak compared to without it (29.9 % vs 9.7%). A similar test that also uses reverse transcription quantitative real-time PCR is ER Map, produced by iGLS, which instead looks at 184 genes (52). In terms of this test's clinical outcomes, only one retrospective study exists (3). This study also appeared to have promising results, with clinical pregnancy rates being 44.4% in women who had embryo transfer at the time recommended by ER Map, compared to 23.1% when the embryo transfer timing was performed outside the ER Map recommendation, with a reported increase in miscarriage in this group also (20.9% compared to 44.4%) (3). However, it is also important to note that no comparison was made to standard embryo transfer protocol, and, despite positive results from these retrospective studies for both assays, both assays lack randomised controlled trial and prospective studies, so lack robustness and their effectiveness is hard to validate.

Another available test is the Win-Test, with two retrospective studies and one perspective study reported (54). This assay, like the above, uses quantitative real-time PCR for 11 validated genes (54). The prospective study included 217 women with RIF showed that implantation (22.7% vs. 7.2%) and live birth rates (31.8% vs. 8.3%) were significantly higher when the embryo transfer time was adjusted using the Win-Test group compared to the control group using standard embryo transfer protocol (55). In a

further retrospective study that used the Win-test to identify three groups (non-receptive, receptive, and partially receptive) by analysing the genes of endometrial biopsies over a 48h-hour period and the optimum embryo transfer time recommended, the study reported a 21.6% clinical pregnancy per transfer in the non-receptive group and 80% in the receptive group, with the rate differing significantly between the groups (56). However, such a small sample size in the experiment prevented statistical analysis. An additional retrospective study also utilised the Win-Test in its analysis of small non-coding RNAs in endometrial biopsies, comparing results from women with resulting live birth to women with negative hCG, recording 261 sncRNAs that were differentially expressed (57). Though, it should be pointed out, that the above validation studies were all conducted by the same research group, and to improve validation of the Win-Test, future studies from multiple independent centres should be conducted with an increased sample size.

Finally, three other commercially available tests exist, beREADY (Competence Centre on Health Technologies), K-ERT (Yikon), and BioER (Bioarray), all use RNA analysis to evaluate gene expression related to endometrial receptivity. beREADY analyses 67 genes based on an earlier meta-analysis of likely endometrial receptivity biomarkers (58), with the company reporting a 56.7% pregnancy rate among patients with recurrent implantation failure with use of the test, although no clinical data has been published (59). Similarly, K-ERT utilizes RNA sequencing, claiming clinical pregnancy rates exceeding 60% in the recurrent implantation failure population, yet also lacks published peer-reviewed studies (60). Lastly, BioER, employs high-throughput sequencing for over 400 genes, and reports a pregnancy rate ranging from 51% to 63% in recurrent

implantation failure patients, but similar to the others above, lacks published peer-reviewed studies (61).

6.8 What an ideal test needs.

Research within the field of endometrial receptivity biomarker discoveries have all aimed to transfer embryos, the best selection of which is outside the scope of this paper, into an optimal receptive endometrium for implantation success. An ideal endometrial receptivity assay should exhibit very high accuracy and reliability in predicting endometrial receptivity. This requires minimising false positives and negatives to ensure a dependable clinical decision-making tool.

Such a reliable and effective test should have two distinct key clinical applications, including women who have a history of repeated IVF failure and a broad assay for all women undergoing IVF as a standardised screening test. By assisting women with a history of repeated IVF failures, identifying factors contributing to implantation failure is paramount to devise a personalised treatment strategy. In this instance, by accurately assessing endometrial receptivity, clinicians can address underlying issues and optimise the chances of successful embryo implantation in subsequent IVF cycles. Secondly, a broad endometrial receptivity test for all women undergoing IVF as a standardised screening tool could enhance the overall success rate of ART procedures. This approach would facilitate personalised embryo transfer timing, thereby mitigating the risk of implantation failure across the whole diverse patient population. By aiding in the early detection of potential implantation issues, enables early intervention and the generation of personalised plans to optimise reproductive health and fertility outcomes.

An important consideration in an ideal receptivity test assay is the choice of sample type to test. Preferably, a non-invasive material that can be routinely tested in all women undergoing ART, such as saliva, urine and blood plasma or serum, should be used. In addition to selecting a non-invasive material, the test should ideally be seamlessly integrated into the ART protocol, allowing for embryo transfer to occur in the same cycle of testing. While the current available tests performed via endometrial biopsies offer direct sampling, they are invasive, impractical for routine use, and delay optimal transfer until the following cycle. Further metabolic analysis and research on these non-invasive biofluids will provide avenues for further marker discoveries as well as easy integration of such a test into clinical practice for optimal WOI determination. A non-invasive test will not only enhance patient compliance but also facilitate repeated evaluations across different phases of the menstrual cycle. Research has previously underscored the significance of non-invasive approaches, as having significantly higher compliance and uptake rates. For example, computed tomography colonography, had a much higher participation rate than colonoscopy (62). Hence, given the choice, patients would prefer a non-invasive test, a consideration that should be implemented in future endometrial assay development.

Furthermore, in the context of widespread clinical adoption and patient uptake, cost-effectiveness is a crucial consideration for an ideal endometrial receptivity test. A concern is the economic burden of an expensive add-on diagnostic test, even when such will improve pregnancy outcome over the current cost of IVF or repeated rounds of IVF. Ideally, an add-on test should not be employed without sound scientific evidence of high

diagnostic usefulness, measured as ability to generate very much higher post-test, from pre-test probability of pregnancy. An ideal test should offer a favourable balance between diagnostic accuracy and affordability to justify its routine use in clinical practice. A test should enable the first IVF attempt to be the best possible attempt, as for some, depending on the country and financial situation, it may be their only opportunity. Cost-effectiveness analysis should be performed to inform healthcare decision-makers.

6.9 Future direction.

For the development an ideal test with the above characteristic for endometrial receptivity, the future direction of research studies should be carefully considered and criticised. A step-by-step series of investigations should take place, from comprehensive omics investigations, through to the development of a non-invasive test using validated markers, as depicted in Figure 6.1 and hereby outlined.

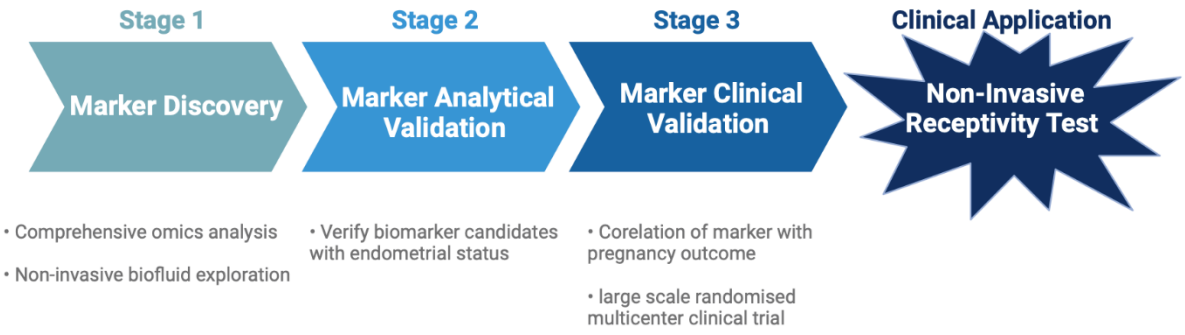


Figure 6.1. Workflow of future direction for the development of an endometrial receptivity test.

Evidence suggests that it is unlikely that a single biomarker will be applicable to be used in identifying the WOI in a clinical setting. The most probable successful assay will be one which consist of a panel of markers for a specific population. The current molecular and non-molecular markers discussed above to determine endometrial receptivity and the WOI have not been built on the knowledge of the mechanism of implantation. Instead, current assays are a result of limited studies and participants that have displayed varying clinical outcomes with their use. A future thorough approach to developing and validating an assay necessitated the discovery of new biomarkers, followed by the association of these biomarkers to endometrial status, and then retrospective and prospective clinical outcomes analysis. Future understanding of endometrial receptivity and discovery of biomarkers likely holds most promise through the integration of omics technologies. Comprehensive omics analyses can uncover novel biomarkers and pathways associated with receptivity, paving the way for more accurate and personalised testing approaches. While estimates suggest that the human genome contains around 23,000 genes, this figure appears insignificant when compared to the variety of the proteome, which is estimated to contain over a million distinct proteins (63). Given this complexity, it is imperative that all omics avenues be thoroughly explored in receptivity biomarker research endeavours. This also includes the analysis of lipids via lipidomics, a method that this far is the least used for endometrial research (64). Additionally, the omics of extracellular vesicles could provide additional advantages in understanding endometrial receptivity, as they serve as crucial mediators of intercellular communication (65,66) and may contain unique molecular signatures reflective of the endometrial microenvironment during the WOI (67–69). Hence, a

broader approach to omics analysis of the endometrium, likely will reveal reliable biomarkers.

One significant limitation regarding existing endometrial receptivity test validation is the difficulty in strict application of the STARD criteria. One example is the difficulty in defining the most appropriate population spectrum. Another is that the ideal spectrum of subjects must be pragmatic, reflecting patients having their first IVF to those who have had repeated IVF failures. Recruitment should be consecutive, and randomisation concealed in each group. Furthermore, apart from the new test and control, all groups should ideally undergo similar IVF protocols across all study clinics and laboratories. Finally cycle cancellation rates and follow-up period should be similar. These trials should be adequately powered to include sufficiently large number of patients. The trial outcomes must be explicit and measurable including sensitivity, specificity, predictive values, likelihood rations, reproducibility, and practical feasibility of these biomarkers in guiding personised fertility treatments. A highly useful test must be able to generate high post-test from pre-test probability of pregnancy and live birth.

However, one of the major challenges obstructing progresses in this field lies in securing funding for the mentioned extensive validation clinical trials required. Without sufficient financial support, researchers may face a catch-22 situation: they need validation studies to prove the efficacy of new biomarkers, yet lack of funding prevents them from conducting these crucial trials. This dilemma risks stagnation in the development of more accurate and reliable tests for endometrial receptivity. Furthermore, the current regulatory landscape, including the Human Fertilisation and Embryology Authority's

(HFEA) traffic light system, poses an additional hurdle (70). While intended to ensure safety and efficacy, this system's strict criteria and slow approval process can supress innovation and impede the introduction of promising new biomarkers into clinical practice (70). Without adequate validation, there remains uncertainty regarding the clinical application of these biomarkers, which is further compounded by regulatory barriers. Thus, it is imperative for stakeholders, including government bodies, private investors, and organisations, to recognise the importance of funding validation studies and collaborate with researchers and fertility specialists to drive advancements in this area of reproductive medicine. Only through financial support, a streamlined regulatory framework, and collaborative partnership can the field overcome these barriers and successfully integrate biomarkers into clinical practice. We encourage this unified approach to ultimately improve outcomes for all individuals seeking fertility treatment.

6.10 Conclusion.

In conclusion, inadequate advancement in the integration of a clinical assay for determining the window of implantation has been made despite advances in the knowledge of the human endometrium physiology and pathophysiology. Whilst there are now available assays and biomarkers for endometrial receptivity, data is insufficient, and recommendation to perform such add-on tests as discussed here in their current state should be avoided. Novel approaches to translate our understanding of the endometrium to clinical testing should be explored. International collaboration and carefully considered randomised clinical trials will be essential to adequately validate a biomarker/biomarker panel in a diverse and well-defined population of participants to bring to fruition a robust test. Given the advancement in omics technologies and our

growing understanding of a receptive endometrium, it is possible to imagine such a non-invasive point-of-care assay with a high-speed result turnaround to enhance embryo transfer occurring in the same cycle of testing. Yet, due to the rising prevalence of couples facing infertility, there is a stronger need than ever to deliver such a tool to clinicians and the public.

6.11 References.

1. Idelevich A, Vilella F. Mother and embryo cross-communication. Vol. 11, Genes. 2020.

2. Cimadomo D, Rienzi L, Conforti A, Forman E, Canosa S, Innocenti F, et al. Opening the black box: why do euploid blastocysts fail to implant? A systematic review and meta-analysis. Hum Reprod Update. 2023 Sep 5;29(5):570–633.

3. Enciso M, Aizpurua J, Rodríguez-Estrada B, Jurado I, Ferrández-Rives M, Rodríguez E, et al. The precise determination of the window of implantation significantly improves ART outcomes. Sci Rep. 2021;11(1).

4. Blesa D, Ruiz-Alonso M, Simón C. Clinical Management of Endometrial Receptivity. Semin Reprod Med. 2014 Jun 24;32(05):410–4.

5. Craciunas L, Gallos I, Chu J, Bourne T, Quenby S, Brosens JJ, et al. Conventional and modern markers of endometrial receptivity: a systematic review and meta-analysis. Hum Reprod Update. 2019 Mar 1;25(2):202–23.

6. Bakkensen JB, Agarwal R, Shapiro M. Recent Advances and Current Perspectives on Endometrial Receptivity. Curr Obstet Gynecol Rep. 2021 Dec;10(4):45–52.

7. Bure. Bures Interim report January-September 2021 [Internet]. Available from: https://storage.mfn.se/3770280e-d639-44f3-a2a3-2fcb0a0a3352/interim-q3-2021.pdf.

8. Teh WT, McBain J, Rogers P. What is the contribution of embryo-endometrial asynchrony to implantation failure? Vol. 33, Journal of Assisted Reproduction and Genetics. 2016.

9. Singh M, Chaudhry P, Asselin E. Bridging endometrial receptivity and implantation: Network of hormones, cytokines, and growth factors. Vol. 210, Journal of Endocrinology. 2011.

10. Harper MJK. 10 The implantation window. Baillieres Clin Obstet Gynaecol. 1992;6(2).

11. Nawroth F, Ludwig M. What is the 'ideal' duration of progesterone supplementation before the transfer of cryopreserved–thawed embryos in estrogen/progesterone replacement protocols? Hum Reprod. 2005 May 1;20(5):1127–34.

12. Wu HM, Chen LH, Hsu LT, Lai CH. Immune Tolerance of Embryo Implantation and Pregnancy: The Role of Human Decidual Stromal Cell- and Embryonic-Derived Extracellular Vesicles. Vol. 23, International Journal of Molecular Sciences. 2022.

13. Dekel N, Gnainsky Y, Granot I, Racicot K, Mor G. The role of inflammation for a successful implantation. Vol. 72, American Journal of Reproductive Immunology. 2014.

14. Franasiak JM, Alecsandru D, Forman EJ, Gemmell LC, Goldberg JM, Llarena N, et al. A review of the pathophysiology of recurrent implantation failure. Fertil Steril. 2021 Dec;116(6):1436–48.

15. Zhang Y, Fu X, Gao S, Gao S, Gao S, Ma J, et al. Preparation of the endometrium for frozen embryo transfer: an update on clinical practices. Reprod Biol Endocrinol. 2023 Jun 8;21(1):52.

16. Sachs-Guedj N, Hart R, Requena A, Vergara V, Polyzos NP. Real-world practices of hormone monitoring during ovarian stimulation in assisted reproductive technology: a global online survey. Front Endocrinol. 2023 Nov 28;14:1260783.

17. Maghraby H, Saleh H, Fourtia IL, Rasheed S, Elmahdy M, Abdelbadie AS, et al. The dilemma of the trigger timing in IVF: a review. Middle East Fertil Soc J. 2024 Jan 20;29(1):8.

18. Tonguc E, Var T, Ozyer S, Citil A, Dogan M. Estradiol supplementation during the luteal phase of in vitro fertilization cycles: A prospective randomised study. Eur J Obstet Gynecol Reprod Biol. 2011;154(2).

19. Bosch E, Labarta E, Crespo J, Simón C, Remohí J, Jenkins J, et al. Circulating progesterone levels and ongoing pregnancy rates in controlled ovarian stimulation cycles for in vitro fertilization: Analysis of over 4000 cycles. Hum Reprod. 2010;25(8).

20. Huang R, Fang C, Xu S, Yi Y, Liang X. Premature progesterone rise negatively correlated with live birth rate in IVF cycles with GnRH agonist: An analysis of 2,566 cycles. Fertil Steril. 2012;98(3).

21. Martínez F, Coroleu B, Clua E, Tur R, Buxaderas R, Parera N, et al. Serum progesterone concentrations on the day of HCG administration cannot predict pregnancy in assisted reproduction cycles. Reprod Biomed Online. 2004;8(2).

22. Venetis CA, Kolibianakis EM, Papanikolaou E, Bontis J, Devroey P, Tarlatzis BC. Is progesterone elevation on the day of human chorionic gonadotrophin administration associated with the probability of pregnancy in in vitro fertilization? A systematic review and meta-analysis. Vol. 13, Human Reproduction Update. 2007.

23. Abdallah Y, Naji O, Saso S, Pexsters A, Stalder C, Sur S, et al. Ultrasound assessment of the peri-implantation uterus: a review. Ultrasound Obstet Gynecol. 2012 Jun;39(6):612–9.

24. Mahutte N, Hartman M, Meng L, Lanes A, Luo ZC, Liu KE. Optimal endometrial thickness in fresh and frozen-thaw in vitro fertilization cycles: an analysis of live birth rates from 96,000 autologous embryo transfers. Fertil Steril. 2022 Apr;117(4):792–800.

25. Chen XT, Sun ZG, Song JY. Does endometrial compaction before embryo transfer affect pregnancy outcomes? a systematic review and meta-analysis. Front Endocrinol. 2023 Nov 14;14:1264608.

26. Xu J, Zhang S, Jin L, Mao Y, Shi J, Huang R, et al. The Effects of Endometrial Thickness on Pregnancy Outcomes of Fresh IVF/ICSI Embryo Transfer Cycles: An Analysis of Over 40,000 Cycles Among Five Reproductive Centers in China. Front Endocrinol. 2022 Jan 24;12:788706.

27. Chen Z, Wang Z, Du M, Liu Z. Artificial Intelligence in the Assessment of Female Reproductive Function Using Ultrasound: A Review. Vol. 41, Journal of Ultrasound in Medicine. 2022.

28. Maziotis E, Kalampokas T, Giannelou P, Grigoriadis S, Rapani A, Anifantakis M, et al. Commercially Available Molecular Approaches to Evaluate Endometrial Receptivity: A Systematic Review and Critical Analysis of the Literature. Diagnostics. 2022 Oct 27;12(11):2611.

29. Díaz-Gimeno P, Horcajadas JA, Martínez-Conejero JA, Esteban FJ, Alamá P, Pellicer A, et al. A genomic diagnostic tool for human endometrial receptivity based on the transcriptomic signature. Fertil Steril. 2011;95(1).

30. Simón C, Gómez C, Cabanillas S, Vladimirov I, Castillón G, Giles J, et al. A 5-year multicentre randomized controlled trial comparing personalized, frozen and fresh blastocyst transfer in IVF. Reprod Biomed Online. 2020.

31. Ben Rafael Z. Endometrial Receptivity Analysis (ERA) test: An unproven technology. Hum Reprod Open. 2021;2021(2).

32. Lensen S, Wilkinson J, van Wely M, Farquhar C. Comments on the methodology of an endometrial receptivity array trial. Vol. 42, Reproductive BioMedicine Online. 2021.

33. Doyle N, Jahandideh S, Hill MJ, Widra EA, Levy M, Devine K. Effect of Timing by Endometrial Receptivity Testing vs Standard Timing of Frozen Embryo Transfer on Live Birth in Patients Undergoing in Vitro Fertilization: A Randomized Clinical Trial. JAMA. 2022;328(21).

34. Doyle N, Combs JC, Jahandideh S, Wilkinson V, Devine K, O'Brien JE. Live birth after transfer of a single euploid vitrified-warmed blastocyst according to standard timing vs. timing as recommended by endometrial receptivity analysis. Fertil Steril. 2022;118(2).

35. Jia Y, Dong YJ, Sha YL, Cai SC, Diao LH, Qiu Z, et al. Effectiveness comparison between endometrial receptivity array, immune profiling and the combination in treating patients with multiple implantation failure. Am J Reprod Immunol. 2022;87(3).

36. Eisman LE, Pisarska MD, Wertheimer S, Chan JL, Akopians AL, Surrey MW, et al. Clinical utility of the endometrial receptivity analysis in women with prior failed transfers. J Assist Reprod Genet. 2021;38(3).

37. Bergin K, Eliner Y, Duvall DW, Roger S, Elguero S, Penzias AS, et al. The use of propensity score matching to assess the benefit of the endometrial receptivity analysis in frozen embryo transfers. Fertil Steril. 2021;116(2).

38. Fodina V, Dudorova A, Erenpreiss J. Evaluation of embryo aneuploidy (PGT-A) and endometrial receptivity (ERA) testing in patients with recurrent implantation failure in ICSI cycles. Gynecol Endocrinol. 2021;37(S1).

39. Barrenetxea G, Romero I, Celis R, Abio A, Bilbao M, Barrenetxea J. Correlation between plasmatic progesterone, endometrial receptivity genetic assay and implantation rates in frozen-thawed transferred euploid embryos. A multivariate analysis. Eur J Obstet Gynecol Reprod Biol. 2021;263.

40. Cozzolino M, Diaz-Gimeno P, Pellicer A, Garrido N. Evaluation of the endometrial receptivity assay and the preimplantation genetic test for aneuploidy in overcoming recurrent implantation failure. J Assist Reprod Genet. 2020;37(12).

41. Cohen AM, Ye XY, Colgan TJ, Greenblatt EM, Chan C. Comparing endometrial receptivity array to histologic dating of the endometrium in women with a history of implantation failure. Syst Biol Reprod Med. 2020;66(6).

42. Neves AR, Devesa M, Martínez F, Garcia-Martinez S, Rodriguez I, Polyzos NP, et al. What is the clinical impact of the endometrial receptivity array in PGT-A and oocyte donation cycles? J Assist Reprod Genet. 2019;36(9).

43. Patel J, Patel A, Banker J, Shah S, Banker M. Personalized embryo transfer helps in improving In vitro fertilization/ICSI outcomes in patients with recurrent implantation failure. J Hum Reprod Sci. 2019;12(1).

44. Bassil R, Casper R, Samara N, Hsieh TB, Barzilay E, Orvieto R, et al. Does the endometrial receptivity array really provide personalized embryo transfer? J Assist Reprod Genet. 2018;35(7).

45. Tan J, Kan A, Hitkari J, Taylor B, Tallon N, Warraich G, et al. The role of the endometrial receptivity array (ERA) in patients who have failed euploid embryo transfers. J Assist Reprod Genet. 2018;35(4).

46. Mahajan N. Endometrial receptivity array: Clinical application. Vol. 8, Journal of Human Reproductive Sciences. 2015.

47. Alonso MR, Díaz-Gimeno P, Gómez E, Rincón-Bertolín A, Vladimirov Y, Garrido N, et al. Clinical efficiency of embryo transfer performed in receptive vs non-receptive endometrium diagnosed by the endometrial receptivity array (era) test. Fertil Steril. 2014;102(3).

48. Hashimoto T, Koizumi M, Doshida M, Toya M, Sagara E, Oka N, et al. Efficacy of the endometrial receptivity array for repeated implantation failure in Japan: A retrospective, two-centers study. Reprod Med Biol. 2017;16(3).

49. Ruiz-Alonso M, Blesa D, Díaz-Gimeno P, Gómez E, Fernández-Sánchez M, Carranza F, et al. The endometrial receptivity array for diagnosis and personalized embryo transfer as a treatment for patients with repeated implantation failure. Fertil Steril. 2013;100(3).

50. Saxtorph MH, Hallager T, Persson G, Petersen KB, Eriksen JO, Larsen LG, et al. Assessing endometrial receptivity after recurrent implantation failure: a prospective controlled cohort study. Reprod Biomed Online. 2020;41(6).

51. Riestenberg C, Kroener L, Quinn M, Ching K, Ambartsumyan G. Routine endometrial receptivity array in first embryo transfer cycles does not improve live birth rate. Fertil Steril. 2021;115(4).

52. Enciso M, Carrascosa JP, Sarasa J, Martínez-Ortiz PA, Munné S, Horcajadas JA, et al. Development of a new comprehensive and reliable endometrial receptivity map (ER Map/ER Grade) based on RT-qPCR gene expression analysis. Hum Reprod. 2018;33(2).

53. Ohara Y, Matsubayashi H, Suzuki Y, Takaya Y, Yamaguchi K, Doshida M, et al. Clinical relevance of a newly developed endometrial receptivity test for patients with recurrent implantation failure in Japan. Reprod Med Biol. 2022;21(1).

54. Haouzi D, Mahmoud K, Fourar M, Bendhaou K, Dechaud H, De Vos J, et al. Identification of new biomarkers of human endometrial receptivity in the natural cycle. Hum Reprod. 2008 Oct 14;24(1):198–205.

55. Haouzi D, Entezami F, Torre A, Innocenti C, Antoine Y, Mauries C, et al. Customized Frozen Embryo Transfer after Identification of the Receptivity Window with a Transcriptomic Approach Improves the Implantation and Live Birth Rates in Patients with Repeated Implantation Failure. Reprod Sci. 2021;28(1).

56. Bissonnette L, Choi J, LeSaint C, Bissonnette F, Kadoch I. Three Different Endometrial Receptivity Profiles Can Be Defined in Patients with Previous Failed Embryo Transfer. Oxf Univ Press. 2019;34:308–209.

57. Drissennek L, Baron C, Brouillet S, Entezami F, Hamamah S, Haouzi D. Endometrial miRNome profile according to the receptivity status and implantation failure. Hum Fertil. 2022;25(2).

58. Altmäe S, Koel M, Võsa U, Adler P, Suhorutšenko M, Laisk-Podar T, et al. Meta-signature of human endometrial receptivity: A meta-analysis and validation study of transcriptomic biomarkers. Sci Rep. 2017;7(1).

59. beREADY - endometrial receptivity test [Internet]. [cited 2024 Feb 14]. Available from: https://www.beready.ee.

60. Endometrial Receptivity Test (YK-ERT) [Internet]. [cited 2024 Feb 14]. Available from: https://en.yikongenomics.com/index.php?m=content&c=index&a=show&catid=9&id=6.

61. Bioarray SL. BioER Endometrial Receptivity Assay. [Internet]. [cited 2024 Feb 14]. Available from: https://bioarray.es/img/cms/BioER (Endometrial Receptivity).pdf.

62. Duarte RB, Bernardo WM, Sakai CM, Silva GLR, Guedes HG, Kuga R, et al. Computed tomography colonography versus colonoscopy for the diagnosis of colorectal cancer: A systematic review and meta-analysis. Vol. 14, Therapeutics and Clinical Risk Management. 2018.

63. Ponomarenko EA, Poverennaya E V., Ilgisonis E V., Pyatnitskiy MA, Kopylov AT, Zgoda VG, et al. The Size of the Human Proteome: The Width and Depth. Vol. 2016, International Journal of Analytical Chemistry. 2016.

64. Demiral İ, Doğan M, Bastu E, Buyru F. Genomic, proteomic and lipidomic evaluation of endometrial receptivity. J Turk Soc Obstet Gynecol. 2015;12(4).

65. Hart AR, Khan NLA, Godakumara K, Dissanayake K, Piibor J, Muhandiram S, et al. The role of extracellular vesicles in endometrial receptivity and their potential in reproductive therapeutics and diagnosis. Reprod Biol. 2022 Jun;22(2):100645.

66. Godakumara K, Dissanayake K, Hasan MM, Kodithuwakku SP, Fazeli A. Role of extracellular vesicles in intercellular communication during reproduction. Vol. 57, Reproduction in Domestic Animals. 2022.

67. Hart AR, Khan NLA, Dissanayake K, Godakumara K, Andronowska A, Eapen S, et al. The Extracellular Vesicles Proteome of Endometrial Cells Simulating the Receptive Menstrual Phase Differs from That of Endometrial Cells Simulating the Non-Receptive Menstrual Phase. Biomolecules. 2023;13(2).

68. Piibor J, Dissanayake K, Midekessa G, Andronowska A, Kavak A, Waldmann A, et al. Characterization of bovine uterine fluid extracellular vesicles proteomic profiles at follicular and luteal phases of the oestrous cycle. Vet Res Commun. 2023;47(2).

69. Muhandiram S, Dissanayake K, Orro T, Godakumara K, Kodithuwakku S, Fazeli A. Secretory Proteomic Responses of Endometrial Epithelial Cells to Trophoblast-Derived Extracellular Vesicles. Int J Mol Sci. 2023;24(15).

70. Macklon NS, Ahuja KK, Fauser BCJM. Building an evidence base for IVF 'add-ons'. Vol. 38, Reproductive BioMedicine Online. 2019.

CHAPTER 7

DISCUSSION AND FUTURE DIRECTION

Chapter 7. Discussion and future direction

7.1 Integrated discussion.

In this thesis, I have consolidated insights gained from the diverse investigations in extracellular vesicles and their implied role in reproductive function. Starting with Chapters 2 and 3 which are centred around the hormonal treatment of RL95-2 cells mimicking the menstrual cycle, the foundations for understanding the complex interplay between endometrial-derived extracellular vesicles (EVs) and trophoblast cells during implantation were explored. Chapters 4 and 5 explored the biofluid of urine and its associated EVs as a potential biomarker for determining a receptive endometrium. Finally, Chapter 6 reviewed current endometrial receptivity tests and explored what the future of endometrial receptivity biomarker research should look like.

7.1.1 Endometrial EVs and trophoblast interaction.

The findings and discussion in Chapter 2 contributed significantly to the understanding of hormonal regulation of endometrial EVs. Our exploration into endometrial EVs under sex hormone influence revealed distinct proteomic changes mirroring the different menstrual cycle phases. Importantly, our research demonstrated that during the receptive phase of the menstrual cycle, endometrial EVs contain proteins related to embryo implantation, endometrial receptivity, and embryo development, as well as crucial pathways involved in immune modulation and implantation processes.

The findings in Chapter 3 corroborated those of Chapter 2 findings. Notably, the study revealed a significant increase in trophoblast binding affinity when co-incubated with

endometrial EVs during the window of implantation (WOI), particularly in the presence of estrogen and progesterone. This finding underscored the potential regulatory roles of hormones in modulating endometrial EVs and influencing trophoblast behaviour during the crucial process of implantation. Despite the absence of significant changes in individual mRNA levels, the increased trophoblast binding affinity suggested the involvement of non-transcriptional or post-transcriptional regulatory mechanisms. GSEA provided an insight into potential pathways involved in trophoblast binding, highlighting pathways associated with cellular adhesion and immune-related pathways.

7.1.2 Urine EV isolation, storage, and optimisation.

Chapter 4 summarised the optimisation of urinary EV (uEV) isolation methods and addressed the critical need for standardised procedures for biomarker discoveries. Interestingly, results revealed an unexpected lack of significant difference in uEV concentration based on whether THP was removed from the urine sample or not. This challenged conventional knowledge and raised questions about the role and need for a THP removal step in uEV isolation. In the exploration of storage conditions, EVs stability was seen when stored at -80°C for 1 year, but a trend was observed suggesting that longer storage of urine introduced more debris and interfering particles. Ultimately, a simple protocol performed on urine as soon as possible after collection would be most suitable for exploring potential biomarkers without introducing contaminants or additional inhibitors.

7.1.3 Urine EV proteomic profiling across menstrual cycle phases.

Chapter 5 explored the novel area of proteomic profiling of uEVs across the female human menstrual cycle, aiming to provide proof of concept evidence for non-invasive biomarkers of endometrial receptivity. The results and analysis highlighted statistically significant variation in uEV concentrations across the menstrual cycle phases, and proteomic analysis uncovered over 2,000 proteins, emphasising uEVs' potential as a source for biomarker discovery. This chapter also discussed the advantage of uEVs over neat urine as the biomarker biofluid source, revealing unique proteins and demonstrating improved specificity in identifying menstrual cycle phases. Further bioinformatic analysis also revealed key pathways known to have roles in transport and immunity, prompting the need for further investigations into their origin and function.

7.1.4 Rethinking endometrial receptivity testing.

Chapter 6 reviewed and examined current endometrial receptivity tests. It was discovered that the currently available tests are not fit for purpose and lack data to support their use in a clinical setting. The chapter discussed how the future of biomarker discovery should be conducted, advocating for clinical validation via large-scale carefully controlled clinical trials. The chapter highted how omics technologies and a growing understanding of the endometrium and implantation will propel research towards an ideal non-invasive reliable assay to determine endometrial receptivity and improve pregnancy outcomes.

7.2 Future direction.

Moving forward, the limitations identified within each chapter underscore the need for addressing these failings and continued research for a profound understanding of EVs in reproductive health and their translation into clinical application. The following future works outline potential avenues for extending the depth and applicability of the present findings.

In terms of subsequent *in vitro* work, it is imperative to expand the scope of the work by increasing the sample size for mRNA sequencing of JAr cells treated with EVs derived from hormone-treated RL95-2 cells. This increase in replicates would be important to increase the robustness of our findings by mitigating potential outliers and revealing potential gene expression patterns and potential transcriptomic response to EVs. Additionally, varying concentrations and treatment duration of EVs could provide an understanding of the mechanism of action of endometrial EVs on trophoblast cells, making them more adhesive to endometrial cells.

While this current work on a single cancerous cell line has provided useful insights, recognising its limitations is essential for advancing our understanding. Future experimentation to understand endometrial EVs should focus on transitioning to incorporating a multicellular model to better simulate the natural endometrium microenvironment. A transition to multicellular models will help bridge the gap between *in vitro* and *in vivo* conditions, offering a more physiological relevant context for investigating EV behaviours and interactions. The suggestion to move forward using a multicellular cell line model over primary cells lines is due to the several advantages they

offer. This includes immortalisation, ensuring indefinite proliferation and consistency, which aids in reproducibility and standardisation of experiments. Additionally, they are cost-effective, easily maintained, and allow for genetic manipulation, facilitating targeted studies of specific genes or pathways. Advantages are also specific to endometrial research, where obtaining samples from women with implantation issues is challenging, in addition to cycle stage variability and individual differences. Additionally, exploring embryonic stem cells (ESCs) could provide even more sophisticated models due to their pluripotency, enabling the creation of cell types that more accurately reflect the endometrial environment, thus enhancing our understanding of EV roles in cellular communication, implantation, and early pregnancy.

In terms of the urine work, while this current study revealed valuable information, a critical limitation is the current sample size. To increase the robustness and wider applicability of our findings, future experiments should be conducted with a larger sample size. This approach will help account for the inherent variability in urine composition among individuals, ensuring that our conclusions and any potential biomarker discoveries are reliable. Additionally, future work should consider exploring other non-invasive biofluids such as saliva and blood, as they offer various advantages over first void urine, such as accessibility and stability of biomarkers. Integrating data from multiple biofluids could enhance the comprehensiveness and clinical relevance of endometrial research.

Finally, a hugely impactful avenue for further research would be collaboration with an IVF clinic to help identify optimum days for embryo transfer to maximise pregnancy

outcome. A useful study would involve participants donating urine on the day of embryo transfer, allowing for the analysis of the urinary extracellular vesicles' proteome. Concurrently, retrospective data on the success of that embryo transfer could be collected, establishing potential correlation between uEV profiles and pregnancy outcomes. Such a collaborative study holds the promise of not only advancing our understanding of uEVs but also providing valuable insights into their potential as biomarkers for endometrial receptivity.

7.3 Conclusion.

In conclusion, these proposed future works aim to build upon the foundation laid out by the current work in this thesis, steering the field towards a more comprehensive understanding of EVs and their clinical relevance in biomarker discoveries within the reproductive field using an abundant and readily available sample such as urine. Such studies would be instrumental in addressing the current lack of reliable and proven receptivity tests in the field to improve embryo transfer and pregnancy outcome for the use of ART techniques to counter the growing global increase in infertility. Building on the works here represents an opportunity to refine methodologies, enhance result validity, and contribute meaningfully to the scientific and clinical community, ultimately advancing our ability to navigate and overcome challenges in reproductive health.

CHAPTER 8

PUBLICATIONS

Chapter 8. Publications.

1) **Hart AR**, Khan NLA, Godakumara K, et al. The role of extracellular vesicles in endometrial receptivity and their potential in reproductive therapeutics and diagnosis. *Reprod Biol*. 2022;22(2):100645. doi:10.1016/j.repbio.2022.100645

2) **Hart AR**, Khan NLA, Dissanayake K, Godakumara K, Andronowska A, Eapen S, Heath PR, Fazeli A. The Extracellular Vesicles Proteome of Endometrial Cells Simulating the Receptive Menstrual Phase Differs from That of Endometrial Cells Simulating the Non-Receptive Menstrual Phase. *Biomolecules*. 2023; 13(2):279. https://doi.org/10.3390/biom13020279

8.1 The role of extracellular vesicles in endometrial receptivity and their potential in reproductive therapeutics and diagnosis.

Reproductive Biology 22 (2022) 100645

Contents lists available at ScienceDirect

Reproductive Biology

journal homepage: www.elsevier.com/locate/repbio

Review

The role of extracellular vesicles in endometrial receptivity and their potential in reproductive therapeutics and diagnosis

Amber Rose Hart[a], Norhayati Liaqat Ali Khan[a,b], Kasun Godakumara[c,d], Keerthie Dissanayake[c,d], Johanna Piibor[d], Subhashini Muhandiram[d], Saji Eapen[e], Paul R. Heath[f], Alireza Fazeli[a,c,d,*]

[a] Academic Unit of Reproductive and Developmental Medicine, Department of Oncology and Metabolism, The Medical School, University of Sheffield, Sheffield, UK
[b] Faculty of Dentistry, Universiti Teknologi MARA (UiTM), Malaysia
[c] Department of Pathophysiology, Institute of Biomedicine and Translational Medicine, Faculty of Medicine, University of Tartu, 14B Ravila, 50411 Tartu, Estonia
[d] Institute of Veterinary Medicine and Animal Sciences, Estonian University of Life Sciences, Tartu, Estonia
[e] SPD Development Company Ltd, Clearblue Innovation Centre, Stannard Way, Priory Business Park, Bedford MK44 3UP, UK
[f] Department of neuroscience, University of Sheffield, Sheffield, UK

ARTICLE INFO

Keywords:
Extracellular vesicles
Embryo
Endometrium
Reproduction
Treatment
Diagnosis

ABSTRACT

Extracellular vesicles (EVs) are small, nanometre sized, membrane-enclosed structures released by cells and are thought to be crucial in cellular communication. The cargo of these vesicles includes lipids, proteins, RNAs and DNA, and control various biological processes in their target tissues depending on the parental and receiver cell's origin and phenotype. Recently data has accumulated in the role of EVs in embryo implantation and pregnancy, with EVs identified in the uterine cavity of women, sheep, cows, horses, and mice, in which they aid blastocyst and endometrial preparation for implantation. Herein is a critical review to decipher the role of extracellular vesicles in endometrial receptivity and their potential in reproductive therapies and diagnosis. The current knowledge of the function of embryo and endometrial derived EVs and their cargoes, with regards to their effect on implantation and receptivity are summarized and evaluated. The findings of the below review highlight that the combined knowledge on EVs deriving from the endometrium and embryo have the potential to be translated to various clinical applications including treatment, a diagnostic biomarker for diseases and a drug delivery tool to ultimately improve pregnancy rates.

1. Introduction

Successful implantation into the uterine wall is critical in the development of the mammalian embryo into a complete organism. However, infertility poses a significant challenge in human reproduction, with epidemiological studies suggesting that merely 30% of all conceptions get clinically recognised [1], with most lost spontaneously. Within couples of reproductive age 55% of those affected by infertility will seek medical services to try and achieve parenthood [2]. Within the UK the use of assisted reproductive technologies (ART) is linked to nearly 3% of births [3]. Despite in the recent decade momentous advances and progression in ART, successful pregnancy rate due to low implantation rate per transferred embryo remains a key setback [4]. This is probably owing to uterine receptivity being suboptimal and inadequate communication between embryo and uterus, despite high-grade morphologically and genetically normal embryos being selected and transferred.

Studies have previously discovered that failure in pregnancy arises mostly during the period of embryo implantation [5]. The complex but vital step of embryo implantation in establishing pregnancy can only occur in a limited window once the unreceptive uterine lining converts to a hospitable environment that is able to receive the embryo [6]. This functional endometrium is established in the secretory phase through the action of progesterone on an estrogen-primed endometrium [7]. During this period, the uterine cavity is prepared to accept a blastocyst and support further implantation through mediation and communication by cytokines (e.g. IL6 [8]), growth factors (e.g. IGF-2 [9]), chemokines (e.g. CX3CL1 [10]) and adhesion molecules (e.g. integrins like αvβ3 [11]). Additionally, as a non-self- entity, due to half of the genetic information coming from the father and unique embryo antigens, the semi-allogenic embryo must also avoid immune system rejection by the mother, demanding complex communication before implantation can occur [12]. Hence, the preparation for receptivity of the endometrium

* Corresponding author at: Academic Unit of Reproductive and Developmental Medicine, Department of Oncology and Metabolism, The Medical School, University of Sheffield, Sheffield, UK.
E-mail address: fazeli@emu.ee (A Fazeli).

https://doi.org/10.1016/j.repbio.2022.100645
Received 16 February 2022; Received in revised form 14 April 2022; Accepted 16 April 2022
Available online 17 May 2022
1642-431X/© 2022 Published by Elsevier B.V. on behalf of Society for Biology of Reproduction the Institute of Animal Reproduction and Food Research of Polish Academy of Sciences in Olsztyn.

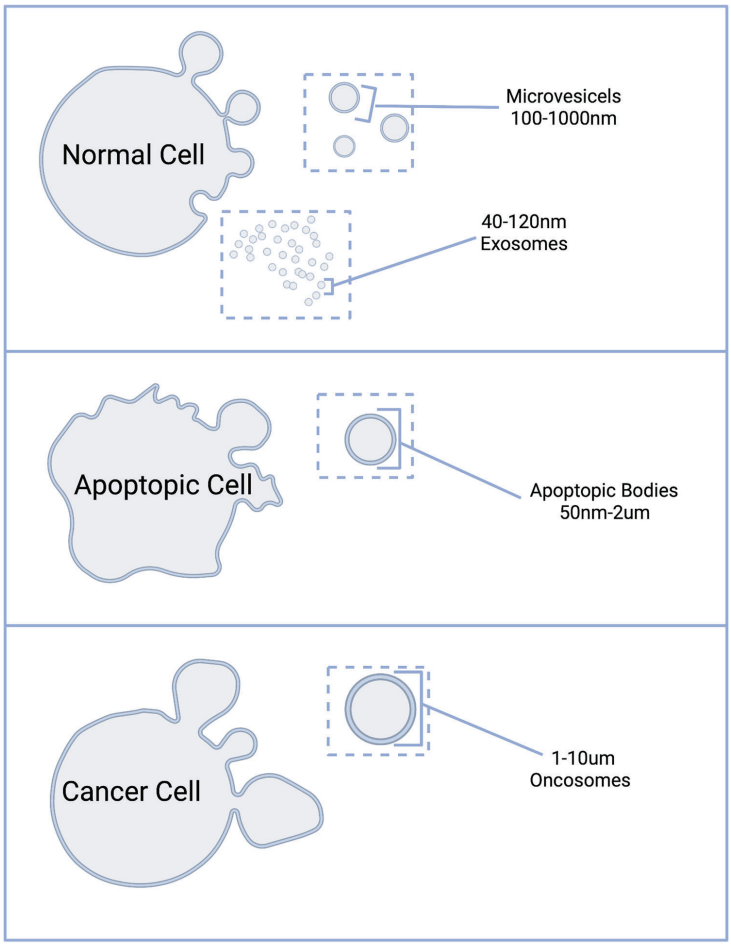


Fig. 1. Extracellular vesicles produced from different cell types vary in size.

is a complex molecular and morphologic course requiring mutual crosstalk between endometrial cells and the embryo [13]. However, little is known about this communication. Previously it has been presumed that the endometrial tissue is passive in its nature and should readily accept an embryo. Outmost the general view was (and probably still is) that the endometrium gets to a receptive stage as a result of the reproductive cycle and the influence of the sex hormones on the endometrial cells. Recent experimental evidence has expanded on this view, confirming a complex mutual communication among the foetal and maternal compartments during implantation in addition to these hormonal effects [14]. A new dogma is emerging that emphasises the role that embryo signals play on preparation of the receptive endometrium for embryo implantation as well as signals produced by the endometrium on initiation of final stages of development of the embryo and its preparation for implantation.

Interaction amongst different cells is understood to rely on different signals, including but not limited to soluble secretory factors like that of cytokines and hormones [15,16]. Several factors, secreted into the uterine environment by the endometrium, regulate implantation by affecting blastocyst development directly and/or by controlling adhesion molecule expression [6]. However, recently the function of extracellular vesicles (EVs) in cell-to-cell interaction in the context of embryo-maternal interactions has been investigated [15,17,18]. From endosomal compartments, factors are thought to be sorted into secretory EVs and transported to targeted tissue in a paracrine way, via the blastocyst, and by the endometrium in an autocrine way [19]. While the cargo of these EVs may be diverse, studies are indicating the mutual crossover of noncoding RNA (ncRNA) from embryo to endometrium as a communication system commanding transcriptomic and epigenomic profile alterations of the maternal system [17,20,21]. Particularly, different kinds of the ncRNA such as microRNA (miRNAs) can be sorted into EVs and transported to the embryo and the endometrium contributing to foetal-maternal interaction [22]. Different miRNA species have been shown to be involved in regulating gene expression associated with embryo implantation, with studies showing their role in blastocyst implantation and uterine receptivity regulation [23].

Recently, within the uterine fluid of women, sheep, cows, horses and mice, EVs have been discovered [24]. Evidence suggests that these

EVs originate from the uterine epithelium with other evidence pointing towards the vesicles being of conceptus origin [25]. Given the hypothetical prominence of EVs in successful pregnancy consequently, isolation and examination of endometrium derived EVs may be a novel substitute for invasive uterine biopsies. This review will carry out a critical analysis of the possible significance of EVs within pregnancy establishment, understanding of EVs heterogeneity and functionality, and their possible impact in the implantation microenvironment. In addition, a discussion on current knowledge of endometrial-derived and embryo-derived EVs role in implantation will be performed. Further examination into the use of these communication factors as potential biomarkers for the evaluation of endometrial physiology and a need for a rapid non-invasive test to assess the receptivity of the endometrium will also be presented.

2. Extracellular vesicles

2.1. Definition and biogenesis of EVs

A general definition of EVs is a membrane-enclosed nano-sized vesicle discharged by a cell that carry DNA, RNA, and proteins between different cells [26]. Most cell types have been shown to discharge EVs, such as haematopoietic cells, B- and T-lymphocytes, endometrial cells, reticulocytes, platelets, mast cells, dendritic cells, neurons, astrocytes, placenta, intestinal epithelial cells, and tumour cells [27]. Membrane-enclosed micro particles isolated first from a variety of biological materials including human seminal plasma [28], animal platelet-free plasma [29], and from various mammalian cell lines, these were presumed to derive from plasma membrane outward budding [30]. Years later Johnstone et al. [31] described in reticulocytes a new theory of active vesicle secretion, here exosomes were described as being discharged via exocytosis [24].

Though EV's have been identified in a range of organisms, they are classified into different categories including microvesicles (MVs), exosomes, and apoptotic bodies, depending on the biogenesis, size and discharge pathway [19]. MVs discharged from budding of plasma membrane facilitated by restructuring of the actin-myosin cytoskeleton, range in size between 100 nm and 1 μm, while the smaller exosomes, originating from the multivesicular endolytic compartment via the merging of the plasma membrane with the multivesicular endosome, range between 40 and 120 nm [19]. Oncosomes, released from cancer cells, range between 1 and 10 μm and apoptotic bodies produced by dying cells range between 50 nm and 2 μm [19] (Fig. 1). The umbrella term, EVs, is often used due to the difficulty in separating the nanoparticles, with all three categories of particles being found in all biological samples.

EVs comprise of cell lineage markers, phosphatidylserine, cell surface receptors, and specialised cell membrane microdomains, hence MVs membrane structure mirrors the parent cell more than those of the exosomes [32]. Regulation of the MV biogenesis is controlled via specific series of molecular occurrences, including acidic sphingomyelinase and AKT activation [33], flux variations in intracellular calcium, and enzymes implicated in upholding the asymmetry of the membrane phospholipid [34]. Unlike the outward budding of MVs, exosomes have a buoyant density and are formed via inward budding of the luminal membrane of endosomal multivesicular bodies [19]. Exosomes are enriched in tetraspanins and their biogenesis is managed by multiple regulatory mechanisms [32]. This includes the endosomal sorting complex required for transport (ESCRT), RabGTPase proteins, syndecan-syntenin-Alix, proteins from the p53/TSAP6 pathway, phospholipase D, ceramide, oligomerization, and neutral sphingomyelinase 2 [32].

2.2. Content and function of EV's

EVs package and transport multiple molecules such as, membrane-bound and soluble proteins, lipids, DNA, and RNA including mRNA and miRNAs [35]. This content varies conditional on the phenotype and origin of the cell, they can then transfer to other cells horizontally, where they become functional [35]. A great diversity of elements has been discovered in EVs from various cells (both prokaryote, non-mammalian and mammalian eukaryotic), this includes around 4400 proteins, 194 lipids, 1639 mRNAs, and 764 miRNAs, illustrating the intricacy of EVs and possible variation in their function [36] (Fig. 2).

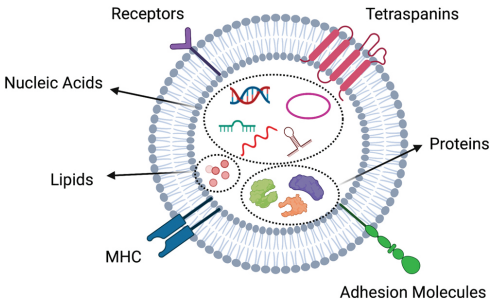


Fig. 2. Schematic representation of Extracellular vesicle structure and content. The phospholipid bilayer is integrated with membrane proteins such as tetraspanins (CD9, CD63, CD81), adhesion molecules (integrins, EpCAM) MHC and receptors. This membrane surrounds the content of nucleic acids (mRNA,miRNA, DNA, LncRNAs, and circRNAs), proteins (HSP70, HSP90, EGFR), and lipids.

Proteomic content of EVs have been extensively investigated owing to their significant role in cell signalling [37]. These studies demonstrated that proteins are transported from one tissue or cell to others by EVs, influencing the bioactivity of the target cells or tissues. EVs have been shown to be enriched in a range of proteins with various functions, for example, heat shock proteins (HSP70 and HSP90) that are involved in the stress response in antigen binding and presentation, and tetraspanins (CD9, CD37, CD53, CD63, CD81, and CD82) which are involved in cell penetration, invasion, and fusion events [38]. Furthermore, endosomal sorting complex proteins needed for exosome release, such as Alix and TSG101, as well as protein markers chaperones are also found [19]. Exosomes have also been shown to contain transmembrane proteins and glycoproteins comparative to the cells they originated from, including integrins, glycoprotein and P-selectin [19]. Furthermore, enriched in EVs are receptors such as membrane trafficking proteins (GTPases, Flotillin and Annexins), epidermal growth factor receptor, cytoskeletal proteins (tubulin and actin), and cytosolic proteins [19].

Besides proteins, EVs also contain a noteworthy component, RNAs, which can integrate into the receiving cells [35]. miRNA are considered to be especially enriched, signifying that EVs could aid in the route of transmission of genetic material between cells [39]. miRNAs can regulate the expression of genes of target cells, with the miRNAs acting intracellularly or discharged in EVs bound or free form [40]. Within pregnancy and implantation, miRNAs have been shown to be isolated from embryo conditioned media and cultured trophoblasts [41]. A variety of RNA and miRNA from embryo and trophoblastic EVs have been identified that have various targets in epithelial and stromal cells [41]. The miRNA targeted genes are thought to control cellular functions like migration and adhesion, implying embryos can alter genomes of the endometrium to improve trophoblast adhesion. Within a study by Cuman et al., it has been shown that secreted miRNA profiles significantly vary among implantation incompetent/competent and developmentally different blastocysts [16]. This included miR-166, that is most highly expressed in non-implanting blastocysts when compared to implanted blastocysts [22]. Further *In vitro* analysis of miR-166 showed that its transfection into human endometrial epithelial cultured cells caused a decrease in trophoblast adhesion to the epithelium [22]. Hence this study indicated embryos only release appropriate signals to aid apposition via modification of the luminal epithelium.

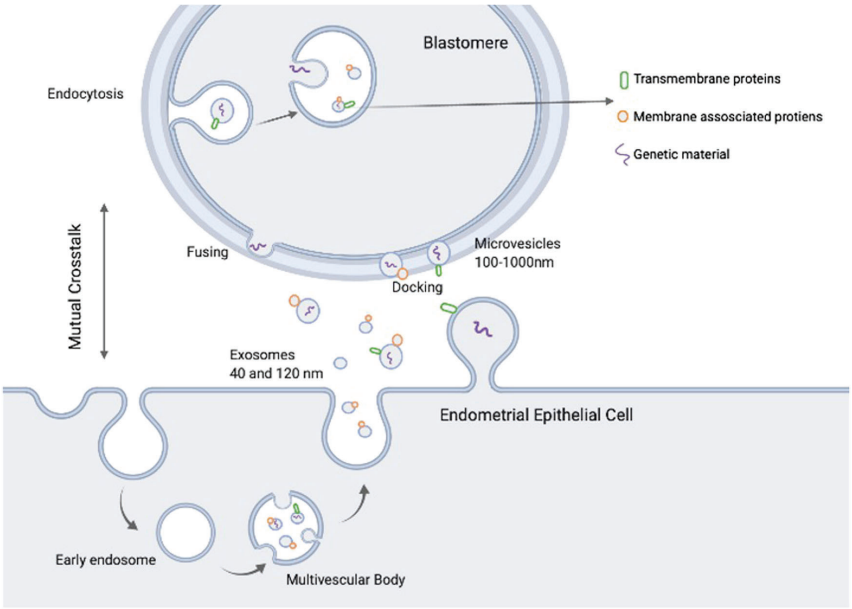


Fig. 3. Embryo-endometrium mutual crosstalk via Exosomes and Microvesicles. Depiction of the production of Exosomes from inward budding of the endosomal membrane and Microvesicles produced from plasma membrane outward budding. Via this mutual communication, EVs can fuse or dock with the membrane or enter via endocytosis with bidirectional movement across the zona pellucida.

EVs are known to have other diverse roles, including angiogenesis stimulation [42], formation of lymphatic vessels [43], and epithelial-mesenchymal transition [44]. In terms of roles within pregnancy and implantation, EVs of placental [45], embryonic and uterine origin [46] are being investigated to improve understanding of their function within uterine receptivity. Within this review the already known roles of EVs within the uterine microenvironment are examined, however it is speculated that these will be the first phases in EVs discovery within the dynamic system of fertility and gestation. We will examine the current literature on potential production of EVs during the window of implantation (WOI) by both embryo and endometrium leading to implantation and establishment of the pregnancy. This information will include, for example, as discussed below, the recently suggested roles of EVs mutual communication between blastocyst and endometrium (Fig. 3).

3. Embryo-derived extracellular vesicles and their potential function

It is apparent that embryos produce EVs and the rate of EVs production as well as type of EVs produced is altered as they undergo development [47–50]. Currently we are not aware what type of EVs are produced or if the cargo of EVs produced changes as embryos develop further. However, embryo derived EVs, seem to have a role as communications vectors within the dialogue of early embryo-maternal communication, as well as embryo-embryo communication and having a regulatory role in the embryo's development (Fig. 3).

First, when thinking about embryo EV uptake or release it's important to consider if EVs can pass through the intact zona pellucida (ZP). The answer to this question lies in the ZP porosity and permeability. It well established that the molecule permeability through the ZP is dependent on the molecule's size and physicochemical factors [51]. For example, hydrophilic–lipophilic properties like that of lipid-containing molecules can penetrate the zona pellucida easily. Therefore, we would expect the same for lipid bilayer membrane EVs. Many studies have supported this theory with EV being shown to pass through the ZP [52,53]. EVs could play a role in the required breakdown of the ZP and hatching for implantation and pregnancy establishment. A recent study has shown that blastocytes are releasing EVs that contain a specific miRNA (miR-378a-3p) and when embryos are supplemented with this miRNA improved hatching is seen and the opposite seen with an inhibitor [54]. These studies highlight that not only EVs are being released from blastocytes and passing through the ZP, but perhaps blastocyte EVs are also acting in an autocrine way and play a crucial role in promoting blastocyst hatching which is an established parameter of embryo quality associated with implantation.

Nevertheless, embryo-derived EVs secretion is dependent on various factors. However, when comparing current published work, there is an agreement that the concentration of embryo derived EVs upsurges in parallel to the embryonic developmental phase. For example, within human embryos it has been shown that day 3 early cleaved embryos compared to the day 5 blastocyst stage, release a lower concentration of EVs [48]. Similarly, it has been shown that conditioned media from embryos that are degenerated after day 8 contained a larger EVs mean concentration opposed to embryos developing into blastocysts on day 8 [47]. Additional factors that affect EVs concentration have also been shown such as the embryo's sex and the in vitro embryo culture conditions. For example, Taqi et al. demonstrated that a higher concentration and larger sized EVs were released by male bovine embryos under 20% O_2 conditions, whereas female bovine embryos released larger and more EVs under 5% O_2 conditions [50]. Similarly, higher concentrations of EVs were shown in bovine embryos at day 7 in comparison to day 3 embryos subjected to 20% oxygen conditions, and the inverse was seen in 5% oxygen conditions [55].

Regarding correlation between embryo competency and embryo derived EVs, studies have also been conducted, with a relationship

Table 1
Current major findings about embryo derived extracellular vesicles.

Subtopic	Key Findings	Reference
EVs derived from in vitro produced embryos	Both IVF and parthenogenetic embryos release EVs but differ in concentration and diameter	[49]
	Bovine somatic cell nuclear transfer embryos secrete EVs, transfer of these EVs to other embryos increased blastocyst formation and quality	[62]
	EVs from parthenogenetic embryos increasing cleavage rate and blastocyst formation in the cloned embryos	[53]
	Labelled embryo derived EVs shown in in vitro cultured human primary endometrial epithelial and stromal cells are uptaken	[48]
	The number and molecular cargo of bovine embryo EVs differed between male and female embryos exposed to environmental stresses.	[50]
	miRNA expression of EVs secreted during blastulation vary depending on embryo quality	[63]
	Bovine embryos under different oxygen tensions changed the EVs concentration and the EVs miRNA contents	[55]
	EVs secreted by pre-implantation bovine embryos can alter the expression of genes of primary oviductal epithelial cells, with the response varying depending on the embryo quality	[58]
	Cultured pre-implantation bovine embryos release EVs with their concentration and size subjective to embryo quality	[47]
EVs derived from in vitro models	Trophectoderm-cells EVs release miRNAs and proteins that stimulate the angiogenesis pathway in maternal endothelial cells	[64]
	Trophoblast spheroids secrete EVs that contain RNA and when incubated with endometrial cells induced down-regulation of transcripts in endometrial cells	[17]
	Multiple signalling pathways may underlie receptor stimulated EVs release besides, or in addition to, calcium.	[65]
	Trophectoderm cells EVs are up taken by endometrial cells and alter transepithelial electrical resistance, and upregulated proteins implicated in embryo attachment, immune regulation and antioxidant activity	[66]
	Trophoblast derived EVs can modify the endometrial gene expression	[20]

between higher concentration of embryo derived EVs and less competent embryos is suggested. For example, using flow cytometry on spent embryo culture medium, there was shown to be a correlation between lower concentration of EVs within embryos ending in pregnancy [56]. However, when considering this study, it should be noted that this study design was based on DNA detection in EVs, with no EVs isolation step, therefore this data could be subjective to a bias selection of EVs subpopulations and that simply incompetent embryos could contain greater apoptotic cells releasing greater volumes of DNA within EVs. Nevertheless, other studies have shown a similar positive correlation between low EVs concentration in media culture leading to pregnancy and higher EVs concentration not leading to pregnancy [57]. Yet a more recent in vitro study utilising bovine embryos the reduction of EVs from the culture media negatively impacted the embryo culture, demonstrated by a reduced blastocyst formation [47].

Embryo-derived EVs have been shown to play a multi-signal messenger part in embryo-maternal communication, with labelled embryo derived EVs shown in in vitro cultured human primary endometrial epithelial and stromal cells [48]. Within this study using non-manipulated human embryos cultured in vitro, it was also shown that Day 3 and day 5 pre-implanted embryos released a heterogeneous population of EVs containing embryonic specific molecules and were shown to be incorporated by an in vitro endometrial epithelial cell line [43]. Crucially, within the protein supplement normally used with embryo culture media, EVs were also found [48]. However, interestingly in the uptake assessment that used EVs isolated from control media containing no embryos but still containing these protein supplements, these EVs were shown to not be up taken by endometrial epithelial cells [48]. More recently it has been shown, in a study examining bovine embryo derived EVs and their effect on oviductal cells, that molecular signatures are displayed by pre-implanted embryos indicating their developmental success, such a signal could be displayed on the surface or within the cargo of EVs [58]. Taken together, this implies the maternal tract is capable of differentiating the EVs origin or molecular content, ultimately regulating embryo EVs uptake by the endometrium. Such results suggest EVs are involved with a maternal-embryo recognition process.

Supporting this in vitro data, a study in sheep demonstrated that EVs harvested on gestation day 14 and derived from elongating conceptuses in vivo are capable of releasing EVs in vitro following 24 h of in vitro embryo culture [59]. Additionally, within this study they showed that in vivo intrauterine instillation of labelled conceptus-derived EVs were up taken by uterine luminal epithelium as well as some glandular epithelial cells but were not detected to be taken up by the uterine stroma or myometrium or any other analysed organ such as the ovaries [59]. These observations demonstrate that EVs uptake is targeted locally to the endometrial epithelium, acting as a new method of cell-to-cell interaction for pregnancy establishment, however, whether these EVs altered the endometrial epithelium gene expression profiles or cell physiology was not investigated.

Embryo derived EVs have also been shown to have a role in embryo-to-embryo communication signalling, with embryo EVs entering embryos via the zona pellucida bringing in new factors for their development. For example, in a study which simulated paracrine communication in a co-culture among different porcine embryos [60] it was demonstrated that the co-culture enhanced significantly the development of in vitro cloned embryos, mirroring previous results by Saadeldin et al. [53]. It was revealed that this communication could be via EVs, with these EVs shown to enclose different pluripotency gene mRNA of which their embryonic expression increased [53]. Similarly, in a different study with bovine embryos, it was shown that labelled PKH67 embryo derived EVs were up taken by zona-intact bovine embryos, and this in addition to embryo derived EVs enriched embryo culture media improved significantly the day 7 and 8 blastocyst rates with a lower apoptotic cell ratio [61].

Generally, the current literature supports the assumption that embryos from the moment of their establishment are producing EVs and releasing it to their environment whether in vivo or in vitro (Table 1). The number, type, and cargo of these EVs are different and is dependent on the embryo developmental stage, embryo gender and embryo's ability for further development. These EVs seems to have a function in communication with other embryos and with the maternal tract.

4. Endometrial derived EVs and their function

Successful pregnancy seems to also necessitate EVs production by the endometrium, with several studies demonstrating endometrial EVs being isolated from bovine [67] human [27] and equine [68] uterine aspirates, mucus, cultured uterine epithelial cells, stromal cells and mesenchymal stromal cells (Table 2).

The initial evidence of existence of endometrial EVs was observed by assessing uterine aspirates. Here EVs positive for tetraspanins, CD9 and CD63 were detected in samples from fertile women within their secretory phase [27]. Via utilisation of cell-surface marker

Table 2
Current major findings about endometrial derived extracellular vesicles.

Subtopic	Key Findings	Reference
EVs obtained from uterine flushing	Uterine flush EVs are up taken by conceptuses trophectoderm cells and the uterine epithelia	[59]
	Progesterone increases the release of EVs from endometrial cells, in addition to increasing the release of miRNAs contained in EVs that target PI3K/AKT and BMP signalling pathways	[74]
	EVs from uterine fluid regulate implantation, with EVs from post-implantation up-regulating the expression of genes related to adhesion molecule and EV's from pre-implantation up-regulating the expression of apoptosis-related genes.	[71]
	Cows' uterine fluid EVs with endometritis impact IVF embryo development with exosomes miRNAs is the main molecule that impeded the quality of IVF embryos	[75]
	EVs isolated from Avian uterine fluid contain proteins that may be essential in the preservation of sperm functions within the female genital tract	[76]
	Endometrial derived EVs transport miRNAs that are internalised by the trophectoderm, influencing the embryo transcriptomic for genes involved in embryonic adhesion	[77]
	Uterine Flush EVs contain various small RNAs that are involved in regulating pathways or processes related to endometrial remodelling and immune processes	[78]
	The transcriptomic cargo of uterine flush EVs reflects the RNA profile of the endometrial tissue as well as changes between the non-receptive and the receptive phase	[79]
	Uterine lavage EVs from fertile versus infertile women contain known predictors of embryo implantation, endometrial receptivity, and implantation success	[46]
Endometrial EVs from in vitro cell models	Endometrial-derived EVs increased adhesion and invasion of human trophectodermal to endometrial epithelium. Transfer of endometrial EV cargo proteins to trophectoderm mediate changes in trophectoderm function was also shown	[80]
	Endometrial derived EVs contain specific miRNA that could be involved in endometrial-embryo cross talk and embryo implantation	[27]
	Endometrial EVs from recurrent implantation failure patients inhibited the functions of trophoblasts by decreasing their proliferation, migration, and invasive capacity.	[81]
	EVs are released by the endometrium, and the miRNA profile of the secreted EVs varies with the physiological states of the uterus	[21]
	Recurrent implantation failure EVs decrease embryo development via inhibition of blastocyst formation, reducing the embryos total cell number and the embryos invasion capability	[82]

immunostaining, EVs were shown to be localised on the luminal epithelial cells apical surface proposing that secreted uterine EVs originated from the endometrial epithelial cells [27]. Also, within this study the miRNA cargo of endometrial derived EVs from the endometrial epithelial cell line, ECC1 was characterised [27]. Of the miRNAs profiled, 214 miRNAs were found in EVs and ECC1 cells, suggesting many host miRNAs are sorted within EVs [27]. However, interestingly the ECC1 derived EV's had 13 unique miRNA transcripts as well as a group of ncRNAs such as small nuclear RNA U6 (involved in the spliceosome), and RNU44 and RNU48 (involved in chemical modifications of other RNAs) [27]. The biological relevance of EVs sorting these ncRNA is unknown but is predicted to target embryo implantation genes. For example, when examining the exosomal miRNAs found most abundantly, (hsa-miR-200c, hsa-miR-17 and hsa-miR-106a), bioinformatic analysis suggests a role for these miRNAs in the implantation biological process [27]. However experimental and mechanistic data on the role of endometrial EVs on the embryo implantation process is still required.

In an in vitro study by Greening et al. it was demonstrated that endometrial derived EVs play an important role in the endometrium-blastocyst interactions within the uterine cavity that is essential for establishing pregnancy, within which these EVs are regulated by hormones and menstrual phases [69]. In this study the proteomic profile of endometrial derived EVs influenced by oestrogen plus progesterone (to mimic the receptive endometrium) and oestrogen (to mimic the proliferative phase) were investigated to study their possible ability to modify trophoblast function [69]. Oestrogen influenced EVs were shown to be enriched with 254 proteins and oestrogen plus progesterone influenced EVs enriched with 126 [69]. Interestingly, oestrogen plus progesterone influenced EVs proteins were related to implantation changes such as adhesion, migration and invasion [69]. These EVs where shown to be up taken by human trophoblast cells and changed their properties, enhancing their adhesion capability at implantation, a response shown to be mediated partly through active focal adhesion kinase (FAK) signalling [69]. Interestingly, FAK is a pathway recently identified in EVs-blastocyst communication and between inner cell mass and the trophectodermal cells [70]. Thus, this study demonstrates endometrial exosomes aid in the endometrial-embryo interactions within a simulated uterine microenvironment.

Similarly, it has been shown in other studies that endometrial EVs play a role in implantation, again with their protein cargo varying during embryo implantation. A study by Kusama et al. , examined effects of bovine intrauterine exosomes on conceptus implantation [71]. This study revealed that numerous proteins are differentially abundantly expressed in the EVs isolated from pre-implantation stage bovine endometrial epithelium in comparison to the post-implantation group [71]. In addition to this, protein analysis was carried out on isolated EVs from bovine uterine flushing fluids during pre- and post-implantation windows [71]. The analysis revealed that the addition of EVs from post-implantation stage to the primary bovine endometrial epithelial cells up regulated the expression of proteins involved in cell adhesion while the pre-implantation endometrial EVs had a greater up regulation of proteins involved in cell apoptosis [71]. These results could suggest a paracrine effect of endometrial EVs in receptivity and implantation regulation, however, these changes might instead just reflect the occurrence of epithelial physiological alterations.

It seems EVs, both from the endometrium and the embryo, have significant functionality in numerous physiological and pathological events within implantation and fertility. Convincing investigations have begun to suggest uses of EVs as possible biomarkers in a clinical setting, such as liquid biopsies in diagnostics [72] and therapeutics [73], suggesting a possible means for helping to defeat infertility.

5. Can endometrial and embryo derived EVs be exploited in diagnostics and treatment?

EV's involvement in a diverse range of pathophysiological processes makes them a promising entity to be utilised in a diagnostic and therapeutic setting. Application of EVs within a clinical setting can be categorised into 4 potential groups of tools. This includes treatment, a diagnostic biomarker for diseases, a drug delivery tool and finally in vaccinations and immune response.

At the onset and during disease, cell physiology, behaviour and metabolism are altered triggering modification in cell's protein content, gene expression and cargo content of cell produced EVs. These alterations therefore make EVs a plausible interesting target as a biomarker in the clinical field. Genomic and proteomic profiling of endometrial EVs in different pathological reproductive conditions has been conducted to help discover these diagnostic biomarkers. This potential of EVs being used as endometrial receptivity biomarkers is further highlighted by a meta-analysis of endometrial tissue implantation-associated genes from nine different studies which showed 28 of 57 receptivity markers transcripts are also found in EVs [83]. Contrary to the investigations of endometrial EVs, very few studies have researched the possibility of embryo derived EVs as a quality biomarker for pre- implanted embryos. It has been reported that EVs composition and secretions are not accidental and can alter depending on internal signalling and external stimulation [84]. Hence embryonic EVs could be used to predict the embryo quality or health. However, it is important to draw attention to the fact that the only method to research mammalian embryo EVs is via in vitro embryo production and culture media analysis. Such methodology results in studies with small sample sizes and contamination with EVs not derived from embryos.

EVs proteomic profiling from uterine fluid has previously helped to identify a protein panel with a 91.7% specificity and sensitivity in differentiating proliferative and receptive phase of samples as well as a 91.7% specificity and 96.6% sensitivity in distinguishing recurrent implantation failure [85]. More recently a study by Rai et al. investigated uterine lavage derived EVs proteome from proven fertile and non-fertile women to provide an insight into endometrial receptivity [86]. Intriguingly, previously known predicted proteins of embryo implantation (PRDX2, IDHC), endometrial receptivity (S100A4, FGB, SERPING1, CLU, ANXA2), and implantation success (CAT, YWHAE, PPIA) were detected in EVs and differed between fertile and non-fertile women [86]. This indicated their potential for diagnostic purposes in endometrial receptivity status and hence pregnancy outcome.

Transcriptomic analysis of endometrial EVs have also been investigated with the goal of classifying new receptivity-associated biomarkers. A study recently profiled small noncoding RNAs (sncRNAs) in endometrial EVs and identified markers of endometrial receptivity and implantation success through analysis of uterine fluid samples from fertile and patients receiving IVF treatment [87]. 12 endometrial EVs-sncRNAs, which are related with biological functions related to immune response, extracellular matrix, and cell junction, were identified as receptivity-associated transcripts in both subject groups. Similarly, in an in vivo mouse study of endometrium EVs MicroRNAs, the upregulation of miR-34c-5p was identified during implantation, suggesting a possible receptivity biomarker for successful embryo implantation [21]. From these studies and others about miRNA, it is reasonable to speculate that in the future, non-invasive EVs-based genomic diagnostics will enable precision health applications.

There are nevertheless endometrial receptivity array (ERA) commercial tests available which, on an endometrial biopsy at the presumed time of WOI, evaluates the gene expression profiles to identify a precise transcriptomic signature to allow a more accurate time of embryo transfer for IVF. However, a recent random control trial based on live birth outcome analysing the use of ERA compared to standardised timing from single euploid frozen blastocyst transfer FBT showed no improvement in live births [88]. Additionally, a recent retrospective study showed that on 488 subjects with recurrent implantation failure (RIF) using an ERA test could not show any improved outcome though use of the test [89]. Collectively these findings suggest that ERA is not yet a reliable tool to improve pregnancy rates, with conditions such as RIF being multi-faceted hence ERA alone does not assist when failure is due to embryo quality or other potential issues with pregnancy establishment. This coupled with the requirement of an invasive endometrial biopsy, EVs could prove as a reliable alternative, by instead assessing the embryos quality through analysis of the EVs being released by the embryo prior to artificial implantation and assessment of endometrial EVs to assess receptivity.

In terms of treatment, EVs have been shown to increase the secretion of proinflammatory cytokines, and therefore this property could be utilised for inflammatory reproductive disease treatment by reducing the absorption or production of EVs. For example, in a study in which endothelial cells were treated with EVs derived from endometrial epithelial cells they displayed an increased release of proinflammatory cytokines such a tumour necrosis factor-alpha as well as a reduction in macrophage-derived chemokines [90]. EVs appear to be emerging frontiers in anti-inflammatory therapy. Within reproduction, the common inflammatory condition, endometritis, could benefit from these emerging therapies, with either anti-inflammatory targeting EVs by surface engineering or cargo loading. Similar to treatment regimens, there is increasing evidence showing that EVs have potential for successful drug delivery mechanism. Since EVs are vesicles for transporting different RNAs and proteins and during pathological conditions as discussed, the speculation of application in drug delivery has gained scientific interest.

Within reproduction, research into the use of EVs as a treatment delivery tool is limited. However, within cancer research this area is progressing owing to EVs numerous advantages over other nanocarriers. For example, the chemotherapy drug doxorubicin (DOX) is used to treat different tumours, however it has multiple side effects including its cardiotoxicity. Encapsulation of DOX within EVs in both in vitro and in vivo experiments have shown to reduce these toxicity effects of the free drug whilst not inhibiting its anticancer effectiveness [91]. Similarly, paclitaxel (PTX), an anti-mitotic chemotherapeutic, loaded into EVs to treat pancreatic cancer cells, showed an improved target cell internalisation via the endocytic pathways and improved its cytotoxicity [92]. Like EVs, liposomes have been used successfully as drug delivery tool, however EVs do have reported advantages over these. For example, in a study which compared the uptake dynamic of exosomes and a liposome nanoparticle via confocal live cell imaging, liposomes were shown to accumulate on the cell surface and only a few being endocytoses after a few hours, whereas the exosomes entered the cells within minutes without accumulation at the cell surface[93]. Such results suggest EVs uptake is more efficient which could then result in an improved cargo delivery and therefore a better delivery system. These advantages of EVs, including their stability, obtainable from multiple sources and having low immunogenicity, shows an opportunity to utilise EVs as a reproductive treatment tool. Perhaps artificial EVs or EVs loaded with a drug could treat and improve the implantation environment, reducing common problems such as recurrent implantation failure and recurrent pregnancy loss.

Overall EVs have the potential to be involved in all aspects of clinical application, but to improve fertility via such applications, it's vital to further increase our knowledge on reproductive tissues EVs biology.

6. Conclusions

For a successful pregnancy, a continuous molecular dialogue is vital, with this communication based on endocrine, paracrine, and autocrine factors. EVs signify a possible direct and dynamic communication method between the embryo and the mother in the development of the blastocyst, embryo modulation of the receptive endometrium, and trophoblast invasion. However, the precise courses of this communication are not fully comprehended, and additional investigations are needed. Improved knowledge of molecular mechanisms facilitating this cross talk could lead to new regulating agent development, with novel diagnostic, biological, and therapeutic possibilities in assisting reproduction and ultimately increasing healthy birth rates. Finally, reliable biomarkers should be confirmed, while various EVs derived molecules have been recognised as possible biomarkers, few are qualified for therapeutic application. However, consensus has established that

EVs are a biological element that could have physiological and diagnostic relevance within pregnancy establishment and so further research into this area is essential.

Funding

This research was funded by the European Union's Horizon 2020 Research and Innovation Programme under COMBIVET ERA Chair grant agreement no. 857418 and a research grant by SPD Development Company Ltd.

CRediT authorship contribution statement

Amber Rose Hart: Conceptualization, Writing – original draft. **Norhayati Liaqat Ali Khan:** Writing – review & editing. **Kasun Godakumara:** Writing – review & editing. **Keerthie Dissanayake:** Writing – review & editing. **Johanna Piibor:** Writing – review & editing. **Subhashini Muhandiram:** Writing – review & editing. **Saji Eapen:** Writing – review & editing, Supervision. **Paul R. Heath:** Writing – review & editing, Supervision. **Alireza Fazeli:** Conceptualization, Writing – review & editing, Supervision, Funding acquisition. All authors have read and agreed to the published version of the manuscript.

Conflicts of Interest

The authors declare no conflict of interest.

Conflict of Interest Statement: All authors have participated in (a) conception and design, or analysis and interpretation of the data; (b) drafting the article or revising it critically for important intellectual content; and (c) approval of the final version. This manuscript has not been submitted to, nor is under review at, another journal or other publishing venue. The authors whose names are listed immediately below have no affiliation with any organization with a direct or indirect financial interest in the subject matter discussed in the manuscript.

References

[1] Jarvis GE. Early embryo mortality in natural human reproduction: What the data say. F1000Research 2016.
[2] Boivin J, Griffiths E, Venetis CA. Emotional distress in infertile women and failure of assisted reproductive technologies: meta-analysis of prospective psychosocial studies. BMJ 2011.
[3] Fertility treatment 2018: trends and figures. Human Fertilisation & Embryology Authority. 2020.
[4] Apter S, Balaban B, Campbell A, Catt J, Coticchio G, Jose de los Santos M, et al. The Vienna consensus: report of an expert meeting on the development of ART laboratory performance indicators. Reprod Biomed Online 2017:494–510.
[5] Wilcox AJ, Baird DD, Weinberg CR. Time of implantation of the conceptus and loss of pregnancy. N Engl J Med 1999.
[6] Ashary N, Tiwari A, Modi D. Embryo implantation: war in times of love. Endocrinology 2018.
[7] Jabbour HN, Kelly RW, Fraser HM, Critchley HOD. Endocrine regulation of menstruation. Endocr Rev 2006;27.
[8] Cork BA, Tuckerman EM, Li TC, Laird SM. Expression of interleukin (IL)-11 receptor by the human endometrium in vivo and effects of IL-11, IL-6 and LIF on the production of MMP and cytokines by human endometrial cells in vitro. Mol Hum Reprod 2002;8(9).
[9] Fowler DJ, Nicolaides KH, Miell JP. Insulin-like growth factor binding protein-1 (IGFBP-1): A multifunctional role in the human female reproductive tract. Hum Reprod Update 2000;Vol. 6.
[10] Hannan NJ, Jones RL, White CA, Salamonsen LA. The chemokines, CX3CL1, CCL14, and CCL4, promote human trophoblast migration at the feto-maternal interface. Biol Reprod 2006;74(5).
[11] He Z, Ma Y, Li L, Liu J, Yang H, Chen C, et al. Osteopontin and integrin αvβ3 expression during the implantation window in IVF patients with elevated serum progesterone and oestradiol level. Geburtshilfe Frauenheilkd 2016;76(6).
[12] Warning JC, McCracken SA, Morris JM. A balancing act: mechanisms by which the fetus avoids rejection by the maternal immune system. Reproduction 2011;141(6):715–24.
[13] Bhagwat SR, Chandrashekar DS, Kakar R, Davuluri S, Bajpai AK, Nayak S, et al. Endometrial receptivity: a revisit to functional genomics studies on human endometrium and creation of HGEx-ERdb. PLoS One 2013.
[14] Modi D, Bhartiya P. Physiology of embryo-endometrial cross talk. Biomed Res J 2015.
[15] Nakamura K, Kusama K, Ideta A, Kimura K, Hori M, Imakawa K. Effects of miR-98 in intrauterine extracellular vesicles on maternal immune regulation during the peri-implantation period in cattle. Sci Rep 2019;9(1).
[16] Massimiani M, Lacconi V, La Civita F, Ticconi C, Rago R, Campagnolo L. Molecular signaling regulating endometrium–blastocyst crosstalk. Int J Mol Sci 2020;21.
[17] Es-Haghi M, Godakumara K, Häling A, Lättekivi F, Lavrits A, Viil J, et al. Specific trophoblast transcripts transferred by extracellular vesicles affect gene expression in endometrial epithelial cells and may have a role in embryo-maternal crosstalk. Cell Commun Signal 2019.
[18] O'Neil EV, Burns GW, Ferreira CR, Spencer TE. Characterization and regulation of extracellular vesicles in the lumen of the ovine uterus. Biol Reprod 2020;102(5).
[19] Zaborowski MP, Balaj L, Breakefield XO, Lai CP. Extracellular vesicles: composition, biological relevance, and methods of study. BioScience 2015.
[20] Godakumara K, Ord J, Lättekivi F, Dissanayake K, Viil J, Boggavarapu NR, et al. Trophoblast derived extracellular vesicles specifically alter the transcriptome of endometrial cells and may constitute a critical component of embryo-maternal communication. Reprod Biol Endocrinol 2021;19(1):115.
[21] Tan Q, Shi S, Liang J, Zhang X, Cao D, Wang Z. MicroRNAs in small extracellular vesicles indicate successful embryo implantation during early pregnancy. Cells 2020.
[22] Cuman C, Van Sinderen M, Gantier MP, Rainczuk K, Sorby K, Rombauts L, et al. Human blastocyst secreted microRNA regulate endometrial epithelial cell adhesion. EBioMedicine 2015.
[23] Zheng Q, Zhang D, Yang YU, Cui X, Sun J, Liang C, et al. MicroRNA-200c impairs uterine receptivity formation by targeting FUT4 and α1,3-fucosylation. Cell Death Differ 2017.
[24] Machtinger R, Baccarelli AA, Wu H. Extracellular vesicles and female reproduction. J Assist Reprod Genet 2021;Vol. 38.
[25] Mishra A, Ashary N, Sharma R, Modi D. Extracellular vesicles in embryo implantation and disorders of the endometrium. Am J Reprod Immunol 2021;85(2).
[26] Xu R, Greening DW, Zhu HJ, Takahashi N, Simpson RJ. Extracellular vesicle isolation and characterization: Toward clinical application. J Clin Investig 2016.
[27] Ng YH, Rome S, Jalabert A, Forterre A, Singh H, Hincks CL, et al. Endometrial exosomes/microvesicles in the uterine microenvironment: a new paradigm for embryo-endometrial cross talk at implantation. PLoS One 2013;8(3):e58502.
[28] Stegmayr B, Ronquist G. Promotive effect on human sperm progressive motility by prostasomes. Urol Res 1982.
[29] Crawford N. The presence of contractile proteins in platelet microparticles isolated from human and animal platelet-free plasma. Br J Haematol 1971.
[30] Trams EG, Lauter CJ, Norman Salem J, Heine U. Exfoliation of membrane ecto-enzymes in the form of micro-vesicles. Biochim et Biophys Acta BBA- Biomembr 1981.
[31] Johnstone RM, Adam M, Hammond JR, Orr L, Turbide C. Vesicle formation during reticulocyte maturation. association of plasma membrane activities with released vesicles (exosomes). J Biol Chem 1987.
[32] Villarroya-Beltri C, Baixauli F, Gutiérrez-Vázquez C, Sánchez-Madrid F, Mittelbrunn M. Sorting it out: regulation of exosome loading. Semin Cancer Biol 2014.
[33] Bianco F, Perrotta C, Novellino L, Francolini M, Riganti L, Menna E, et al. Acid sphingomyelinase activity triggers microparticle release from glial cells. EMBO J 2009;28(8):1043–54.
[34] Piccin A, Murphy WG, Smith OP. Circulating microparticles: pathophysiology and clinical implications. Blood Rev 2007;21(3):157–71.
[35] Yáñez-Mó M, Siljander PRM, Andreu Z, Zavec AB, Borràs FE, Buzas EI, et al. Biological properties of extracellular vesicles and their physiological functions. J Extracell Vesicles 2015.
[36] Kim DK, Kang B, Kim OY, Choi DS, Lee J, Kim SR, et al. EVpedia: an integrated database of high-throughput data for systemic analyses of extracellular vesicles. J Extra Vesicles 2013;2(10).
[37] Yeung CYC, Schoof EM, Tamáš M, Mackey AL, Kjaer M. Proteomics identifies differences in fibrotic potential of extracellular vesicles from human tendon and muscle fibroblasts. Cell Commun Signal 2020;18(1).
[38] Vlassov AV, Magdaleno S, Setterquist R, Conrad R. Exosomes: current knowledge of their composition, biological functions, and diagnostic and therapeutic potentials. Biochim Biophys Acta - Gen Subj 2012;1820(7):940–8.
[39] Huang X, Yuan T, Tschannen M, Sun Z, Jacob H, Du M, et al. Characterization of human plasma-derived exosomal RNAs by deep sequencing. BMC Genom 2013;14(319).
[40] Capalbo A, Ubaldi FM, Cimadomo D, Noli L, Khalaf Y, Farcomeni A, et al. MicroRNAs in spent blastocyst culture medium are derived from trophectoderm cells and can be explored for human embryo reproductive competence assessment. Fertil Steril 2016;105(1):225–35. e3.
[41] Gross N, Kropp J, Khatib H. MicroRNA signaling in embryo development. Biology 2017;6(3):34.
[42] Taraboletti G, D'Ascenzo S, Borsotti P, Giavazzi R, Pavan A, Dolo V. Shedding of the matrix metalloproteinases MMP-2, MMP-9, and MT1-MMP as membrane vesicle-associated components by endothelial cells. Am J Pathol 2002.
[43] Carrasco-Ramírez P, Greening DW, Andrés G, Gopal SK, Martín-Villar E, Renart J, et al. Podoplanin is a component of extracellular vesicles that reprograms cell-derived exosomal proteins and modulates lymphatic vessel formation. Oncotarget 2016.
[44] He S, Chen D, Hu M, Zhang L, Liu C, Traini D, et al. Bronchial epithelial cell extracellular vesicles ameliorate epithelial–mesenchymal transition in COPD pathogenesis by alleviating M2 macrophage polarization. Nanomed Nanotechnol Biol Med 2019.
[45] Han C, Wang C, Chen Y, Wang J, Xu X, Hilton T, et al. Placenta-derived extracellular vesicles induce preeclampsia in mouse models. Haematologica 2020;105(6).

[46] Rai A, Poh QH, Fatmous M, Fang H, Gurung S, Vollenhoven B, et al. Proteomic profiling of human uterine extracellular vesicles reveal dynamic regulation of key players of embryo implantation and fertility during menstrual cycle. Proteomics 2021;21(13–14).

[47] Dissanayake K, Nõmm M, Lättekivi F, Ressaissi Y, Godakumara K, Lavrits A, et al. Individually cultured bovine embryos produce extracellular vesicles that have the potential to be used as non-invasive embryo quality markers. Theriogenology 2020:149.

[48] Giacomini E, Vago R, Sanchez AM, Podini P, Zarovni N, Murdica V, et al. Secretome of in vitro cultured human embryos contains extracellular vesicles that are uptaken by the maternal side. Sci Rep 2017.

[49] Mellisho EA, Velásquez AE, Nuñez MJ, Cabezas JG, Cueto JA, Fader C, et al. Identification and characteristics of extracellular vesicles from bovine blastocysts produced in vitro. PLoS One 2017.

[50] Taqi MO, Saeed-Zidane M, Gebremedhn S, Salilew-Wondim D, Khdrawy O, Rings F, et al. Sexual dimorphic expression and release of transcription factors in bovine embryos exposed to oxidative stress. Mol Reprod Dev 2019.

[51] Turner K, Horobin RW. Permeability of the mouse zona pellucida: a structure-staining-correlation model using coloured probes. J Reprod Fertil 1997;111(2).

[52] Vyas P, Balakier H, Librach CL. Ultrastructural identification of CD9 positive extracellular vesicles released from human embryos and transported through the zona pellucida. Syst Biol Reprod Med 2019;65(4).

[53] Saadeldin IM, Kim SJ, Choi YBin, Lee BC. Improvement of cloned embryos development by co-culturing with parthenotes: A possible role of exosomes/microvesicles for embryos paracrine communication. Cell Reprogram 2014;16(3):223–34.

[54] Pavani KC, Meese T, Pascottini OB, Guan X, Lin X, Peelman L, et al. Hatching is modulated by microRNA-378a-3p derived from extracellular vesicles secreted by blastocysts. Proc Natl Acad Sci 2022(12):119. Available from: 〈https://pnas.org/doi/full/10.1073/pnas.2122708119〉.

[55] Andrade GM, Bomfim MM, del Collado M, Meirelles FV, Perecin F, da Silveira JC. Oxygen tension modulates extracellular vesicles and its miRNA contents in bovine embryo culture medium. Mol Reprod Dev 2019;86:1067–80.

[56] Pallinger E, Bognar Z, Bodis J, Csabai T, Farkas N, Godony K, et al. A simple and rapid flow cytometry-based assay to identify a competent embryo prior to embryo transfer. Sci Rep 2017;7:39927.

[57] Abu-Halima M, Häusler S, Backes C, Fehlmann T, Staib C, Nestel S, et al. Micro-ribonucleic acids and extracellular vesicles repertoire in the spent culture media is altered in women undergoing In Vitro Fertilization. Sci Rep 2017;7:13525.

[58] Dissanayake K, Nõmm M, Lättekivi F, Ord J, Ressaissi Y, Godakumara K, et al. Oviduct as a sensor of embryo quality: deciphering the extracellular vesicle (EV)-mediated embryo-maternal dialogue. J Mol Med 2021;99(5).

[59] Burns GW, Brooks KE, Spencer TE. Extracellular vesicles originate from the conceptus and uterus during early pregnancy in sheep. Biol Reprod 2016;94(56).

[60] Terashita Y, Sugimura S, Kudo Y, Amano R, Hiradate Y, Sato E. Improving the quality of miniature pig somatic cell nuclear transfer blastocysts: aggregation of SCNT embryos at the four-cell stage. Reprod Domest Anim 2011;46(2):189–96.

[61] Pavani KC, Hendrix A, Van Den Broeck W, Couck L, Szymanska K, Lin X, et al. Isolation and characterization of functionally active extracellular vesicles from culture medium conditioned by bovine embryos in vitro. Int J Mol Sci 2019;20(1):38.

[62] Qu P, Qing S, Liu R, Qin H, Wang W, Qiao F, et al. Effects of embryo-derived exosomes on the development of bovine cloned embryos. PLoS One 2017;12(3).

[63] Mellisho EA, Briones MA, Velásquez AE, Cabezas J, Castro FO, Rodríguez-Álvarez L. Extracellular vesicles secreted during blastulation show viability of bovine embryos. Reproduction 2019;158(6).

[64] Bidarimath M, Khalaj K, Kridli RT, Kan FWK, Koti M, Tayade C. Extracellular vesicle mediated intercellular communication at the porcine maternal-fetal interface: a new paradigm for conceptus-endometrial cross-talk. Sci Rep 2017:7.

[65] Conrad KP, Tuna KM, Mestre CT, Banwatt ES, Alli AA. Activation of multiple receptors stimulates extracellular vesicle release from trophoblast cells. Physiol Rep 2020;8(20).

[66] Poh QH, Rai A, Carmichael II, Salamonsen LA, Greening DW. Proteome reprogramming of endometrial epithelial cells by human trophectodermal small extracellular vesicles reveals key insights into embryo implantation. Proteomics 2021;21(13–14).

[67] Nakamura K, Kusama K, Ideta A, Imakawa K, Hori M. IFNT-independent effects of intrauterine extracellular vesicles (EVs) in cattle. Reproduction 2020;159(5).

[68] Almiñana C, Vegas AR, Tekin M, Hassan M, Uzbekov R, Fröhlich T, et al. Isolation and characterization of equine uterine extracellular vesicles: a comparative methodological study. Int J Mol Sci 2021;22(2).

[69] Greening DW, Nguyen HPT, Elgass K, Simpson RJ, Salamonsen LA. Human endometrial exosomes contain hormone-specific cargo modulating trophoblast adhesive capacity: insights into endometrial-embryo interactions. Biol Reprod 2016.

[70] Desrochers LM, Bordeleau F, Reinhart-King CA, Cerione RA, Antonyak MA. Microvesicles provide a mechanism for intercellular communication by embryonic stem cells during embryo implantation. Nat Commun 2016;7:11958.

[71] Kusama K, Nakamura K, Bai R, Nagaoka K, Sakurai T, Imakawa K. Intrauterine exosomes are required for bovine conceptus implantation. Biochem Biophys Res Commun 2018;495(1):1370–5.

[72] Tutrone R, Donovan MJ, Torkler P, Tadigotla V, McLain T, Noerholm M, et al. Clinical utility of the exosome based ExoDx Prostate(IntelliScore) EPI test in men presenting for initial Biopsy with a PSA 2–10 ng/mL. Prostate Cancer Prostatic Dis 2020;23:607–14.

[73] Alvarez-Erviti L, Seow Y, Yin H, Betts C, Lakhal S, Wood MJA. Delivery of siRNA to the mouse brain by systemic injection of targeted exosomes. Nat Biotechnol 2011;29(4).

[74] Burns GW, Brooks KE, O'Neil EV, Hagen DE, Behura SK, Spencer TE. Progesterone effects on extracellular vesicles in the sheep uterus. Biol Reprod 2018;98(5).

[75] Wang X, Tian F, Chen C, Feng Y, Sheng X, Guo Y, et al. Exosome-derived uterine microRNAs isolated from cows with endometritis impede blastocyst development. Reprod Biol 2019;19(2).

[76] Riou C, Brionne A, Cordeiro L, Harichaux G, Gargaros A, Labas V, et al. Avian uterine fluid proteome: Exosomes and biological processes potentially involved in sperm survival. Mol Reprod Dev 2020;87(4).

[77] Vilella F, Moreno-Moya JM, Balaguer N, Grasso A, Herrero M, Martínez S, et al. Hsa-miR-30d, secreted by the human endometrium, is taken up by the pre-implantation embryo and might modify its transcriptome. Dev 2015;142(18).

[78] Xie Y, Liu G, Zang X, Hu Q, Zhou C, Li Y, et al. Differential expression pattern of goat uterine fluids extracellular vesicles miRNAs during peri-implantation. Cells 2021;10(2309).

[79] Giacomini E, Scotti GM, Vanni VS, Lazarevic D, Makieva S, Privitera L, et al. Global transcriptomic changes occur in uterine fluid-derived extracellular vesicles during the endometrial window for embryo implantation. Hum Reprod 2021;36(8).

[80] Evans J, Rai A, Nguyen HPT, Poh QH, Elglass K, Simpson RJ, et al. Human endometrial extracellular vesicles functionally prepare human trophectoderm model for implantation: understanding bidirectional maternal-embryo communication. Proteomics 2019;19(23).

[81] Liu C, Li L, Wang M, Shui S, Yao H, Sui C, et al. Endometrial extracellular vesicles of recurrent implantation failure patients inhibit the proliferation, migration, and invasion of HTR8/SVneo cells. J Assist Reprod Genet 2021;38(4).

[82] Liu C, Yao W, Yao J, Li L, Yang L, Zhang H, et al. Endometrial extracellular vesicles from women with recurrent implantation failure attenuate the growth and invasion of embryos. Fertil Steril 2020;114(2).

[83] Altmäe S, Koel M, Võsa U, Adler P, Suhorutšenko M, Laisk-Podar T, et al. Meta-signature of human endometrial receptivity: a meta-analysis and validation study of transcriptomic biomarkers. Sci Rep 2017;7(1).

[84] Verweij FJ, Bebelman MP, Jimenez CR, Garcia-Vallejo JJ, Janssen H, Neefjes J, et al. Quantifying exosome secretion from single cells reveals a modulatory role for GPCR signaling. J Cell Biol 2018;217(3).

[85] Kasvandik S, Saarma M, Kaart T, Rooda I, Meikas A-V, Ehrenberg A, et al. Uterine fluid proteins for minimally invasive assessment of endometrial receptivity. J Clin Endocrinol Metab 2019.

[86] Rai A, Greening DW, Xu R, Chen M, Suwakulsiri W, Simpson RJ. Secreted midbody remnants are a class of extracellular vesicles molecularly distinct from exosomes and microparticles. Commun Biol 2021;4(1).

[87] Li T, Greenblatt EM, Shin MEJ, Brown TJ, Chan C. Cargo small non-coding RNAs of extracellular vesicles isolated from uterine fluid associate with endometrial receptivity and implantation success. Fertil Steril 2021;115(5):1327–36.

[88] Doyle N, Jahandideh S, Hill MJ, Widra EA, Levy M, Devine K. A randomized controlled trial comparing live birth from singlei euploid frozen blastocyst transfer using standardized timing versus timing by endometrial receptivity analysis. Fertil Steril 2021;116(3).

[89] Cozzolino M, Diaz-Gimeno P, Pellicer A, Garrido N. Evaluation of the endometrial receptivity assay and the preimplantation genetic test for aneuploidy in overcoming recurrent implantation failure. J Assist Reprod Genet 2020;37(12).

[90] Khalaj K, Miller JE, Lingegowda H, Fazleabas AT, Young SL, Lessey BA, et al. Extracellular vesicles from endometriosis patients are characterized by a unique miRNA-lncRNA signature. JCI Insight 2019;4(18).

[91] Toffoli G, Hadla M, Corona G, Caligiuri I, Palazzolo S, Semeraro S, et al. Exosomal doxorubicin reduces the cardiac toxicity of doxorubicin. Nanomedicine 2015;10(19).

[92] Saari H, Lázaro-Ibáñez E, Viitala T, Vuorimaa-Laukkanen E, Siljander P, Yliperttula M. Microvesicle- and exosome-mediated drug delivery enhances the cytotoxicity of Paclitaxel in autologous prostate cancer cells. J Control Release 2015:220.

[93] Heusermann W, Hean J, Trojer D, Steib E, von Bueren S, Graff-Meyer A, et al. Exosomes surf on filopodia to enter cells at endocytic hot spots, traffic within endosomes, and are targeted to the ER. J Cell Biol 2016;213(2).

8.2 The Extracellular Vesicles Proteome of Endometrial Cells Simulating the Receptive Menstrual Phase Differs from That of Endometrial Cells Simulating the Non-Receptive Menstrual Phase.

biomolecules

MDPI

Article

The Extracellular Vesicles Proteome of Endometrial Cells Simulating the Receptive Menstrual Phase Differs from That of Endometrial Cells Simulating the Non-Receptive Menstrual Phase

Amber Rose Hart [1], Norhayati Liaqat Ali Khan [2], Keerthie Dissanayake [3,4,5], Kasun Godakumara [3,4], Aneta Andronowska [6], Saji Eapen [7], Paul R Heath [8] and Alireza Fazeli [1,3,4,*]

[1] Academic Unit of Reproductive and Developmental Medicine, Department of Oncology and Metabolism, The Medical School, University of Sheffield, Jessop Wing, Tree Root Walk, Sheffield S10 2SF, UK
[2] Faculty of Dentistry, University Teknologi MARA (UiTM), Shah Alam 40450, Malaysia
[3] Department of Pathophysiology, Institute of Biomedicine and Translational Medicine, Faculty of Medicine, University of Tartu, Ravila St. 14B, 50411 Tartu, Estonia
[4] Institute of Veterinary Medicine and Animal Sciences, Estonian University of Life Sciences, Kreutzwaldi 62, 51006 Tartu, Estonia
[5] Department of Anatomy, Faculty of Medicine, University of Peradeniya, Peradeniya 20400, Sri Lanka
[6] Institute of Animal Reproduction and Food Research, Polish Academy of Sciences, Juliana Tuwima St. 10, 10-748 Olsztyn, Poland
[7] SPD Development Co., Ltd., Clearblue Innovation Centre, Stannard Way, Priory Business Park, Bedford MK44 3UP, UK
[8] Department of Neuroscience, University of Sheffield, Sheffield S10 2HQ, UK
* Correspondence: alireza.fazeli@emu.ee; Tel.: +372-737-4425

check for updates

Citation: Hart, A.R.; Khan, N.L.A.; Dissanayake, K.; Godakumara, K.; Andronowska, A.; Eapen, S.; Heath, P.R.; Fazeli, A. The Extracellular Vesicles Proteome of Endometrial Cells Simulating the Receptive Menstrual Phase Differs from That of Endometrial Cells Simulating the Non-Receptive Menstrual Phase. *Biomolecules* **2023**, *13*, 279. https://doi.org/10.3390/biom13020279

Academic Editors: Bill Holt and Joaquín Gadea

Received: 9 January 2023
Revised: 23 January 2023
Accepted: 27 January 2023
Published: 2 February 2023

Copyright: © 2023 by the authors. Licensee MDPI, Basel, Switzerland. This article is an open access article distributed under the terms and conditions of the Creative Commons Attribution (CC BY) license (https://creativecommons.org/licenses/by/4.0/).

Abstract: Successful embryo implantation into a receptive endometrium requires mutual endometrial-embryo communication. Recently, the function of extracellular vehicles (EVs) in cell-to-cell interaction in embryo-maternal interactions has been investigated. We explored isolated endometrial-derived EVs, using RL95-2 cells as a model of a receptive endometrium, influenced by the menstrual cycle hormones estrogen (E2; proliferative phase), progesterone (P4; secretory phase), and estrogen plus progesterone (E2P4; the receptive phase). EV sized particles were isolated by differential centrifugation and size exclusion chromatography. Nanoparticle tracking analysis was used to examine the different concentrations and sizes of particles and EV proteomic analysis was performed using shotgun label-free mass spectrometry. Our results showed that although endometrial derived EVs were secreted in numbers independent of hormonal stimulation, EV sizes were statistically modified by it. Proteomics analysis showed that hormone treatment changes affect the endometrial EV's proteome, with proteins enhanced within the EV E2P4 group shown to be involved in different processes, such as embryo implantation, endometrial receptivity, and embryo development, supporting the concept of a communication system between the embryo and the maternal endometrium via EVs.

Keywords: extracellular vesicles; endometrium; receptivity; fertility; proteomics

1. Introduction

The development of the mammalian embryo into a complete organism is dependent on the successful implantation of the embryo into the uterus wall within a limited window of implantation during the menstrual cycle. In humans, the menstrual cycle refers to cyclic changes under the control of several molecules, including the sex hormones, estrogen and progesterone, working in a negative and positive feedback mechanism [1]. These resulting changes in the endometrium lead to a receptive period during the secretory phase for blastocyst arrival and implantation. However, there is only around a 30% chance of conception occurring in one menstrual cycle; such a low percentage is due to many factors including

the short receptive period of 4–5 days [2]. Studies have suggested that by controlling these cyclic changes, the endometrium modulates the uterus environment leading to the secretion of various molecules, factors, and proteins that aid in conception [3]. Accordingly, this complex process of receptive endometrial remodelling and embryo implantation likely requires a sophisticated exchange of signals between embryo and endometrium [4]. However, the mechanisms involved in this process are not yet fully understood.

Recently, extracellular vesicles (EVs), which are lipid bilayer particles secreted into the extracellular space, have been shown to be released from the endometrium and to have a key functional role in cell-to-cell communication, including embryo-maternal interactions [5–8]. The cargos and size distribution of endometrial EVs at different phases of the cycle could affect the functionality of EVs. In terms of the physical properties of vesicles, including size and distribution, these factors previously have been shown to have a determining effect on the recipient cell ability to be internalised [9]. Regarding cargo, endometrial EVs are known to contain various biological molecules, such as proteins, lipids, and nucleic acids, including mRNA, with studies beginning to suggest that they may be up taken by trophoblastic cells, with this content being transferred to the blastocyst to improve or aid in the invasion or adhesion capacity of the embryo during the implantation process [10–12]. The cargos of endometrial EVs, including proteins, DNA, and RNA, have previously been shown in various models [13–15]; however, throughout the menstrual cycle phase of humans, the question remains if the proteomic profile and the size of the endometrial EVs differ or remains constant. This recent experimental data emphasises the role that endometrial signalling may play via EVs on the preparation of the receptive endometrium for embryo implantation. The current investigation builds on this data and aims to identify the characteristics of endometrial EVs at different phases of the menstrual cycle by testing the hypothesis that the characteristics of endometrial EVs change across the different stages of the menstrual cycle. This information has huge potential in clinical applications in therapeutics and biomarker discovery for assisted reproductive treatments.

Many studies have employed in vitro cell culture systems to advance the understanding of the role of EVs in the female reproductive tract and the intercellular communications [8,16,17]. To produce beneficial conclusions from such experiments, it is paramount that cell culture models are optimised for the production and recovery of EVs, whilst mimicking the true in vivo conditions as much as possible. To clarify the mechanisms involved in implantation success and endometrial receptivity, in the present study we isolated EVs secreted by RL95-2 cells under conditions that mimic the menstrual cycle phases and analysed their protein content via proteomic approaches. This study revealed new characteristics and dynamics of endometrial EVs at different phases of the menstrual cycle and thus revealed physiological and pathological changes associated with the menstrual cycle.

2. Materials and Methods

2.1. Cell Culture

Two types of media have been used: (i) Dulbecco's Modified Eagles Medium (DMEM/F12) culture media (Sigma-Aldrich, Dorset, UK), supplemented with 10% fetal bovine serum (FBS) (Sigma-Aldrich, Dorset, UK), 1% L-glutamine (Sigma-Aldrich, Dorset, UK), 1% penicillin (100 IU/mL)/streptomycin (100 µg/mL) (Sigma-Aldrich, Dorset, UK), and 5 µg/mL insulin (human recombinant insulin; Gibco Invitrogen, Roskilde, Denmark); and (ii) Dulbecco's Modified Eagles Medium lacking phenol red (Thermo Fisher, Scotland, UK). The final variation (iii) was phenol red free media (ii) with charcoal stripped FBS (10%) (Sigma-Aldrich, Dorset, UK).

RL95-2 cells obtained from American Type Culture Collection (ATCC, Cat. No. CRL-1671, Teddington, UK) were used to simulate receptive endometrial cells in vitro. RL95-2 cells were cultured in T75 flasks (Greiner, bio-one, Gloucestershire, UK) in culture media (i). Cells were incubated at 37 °C in a 5% CO_2 atmosphere until confluent. At confluence, cells were washed using Ca^{2+} and Mg^{2+} free Dulbecco's phosphate-buffered saline (Sigma-

Aldrich, Dorset, UK). The cells were then harvested using trypsin-EDTA (Sigma-Aldrich, Dorset, UK) and pelleted by centrifugation at 300× *g* for 4 min.

2.2. Differential Centrifugation

Conditioned media was centrifuged for 10 min at 400× *g* at 4 °C in a Sigma swinging-out rotor centrifuge (catalogue number 11,180). The pellet was discarded, and the supernatant was centrifuged for 10 min at 4000× *g* at 4 °C; again the pellet was discarded, and the supernatant was centrifuged for 10 min at 10,000× *g* at 4 °C. The supernatant was then stored at −80 °C for further isolation procedures and experiments. An aliquot was reserved from the control group as a conditioned media control.

2.3. Size Exclusion Chromatography

For the preparation of a size exclusion chromatography (SEC) column, 14-mL of Sepharose CL-2B slurry (GE Healthcare, Uppsala, Sweden) was poured into an empty gravity chromatography column (Bio-Rad, Watford, UK). After settling of the Sepharose beads, a nylon net filter was inserted at the ethanol/Sepharose separation interface at about 10 mL. The ethanol was eluted followed by washing the column with molecular grade water (3 × 5 mL) and then with Ca^{2+} and Mg^{2+} free Dulbecco's phosphate-buffered saline (3 × 5 mL) (Sigma-Aldrich, Dorset, UK). On top of the filter, 0.5 mL of the concentrated conditioned medium was loaded, and fractions of 0.5 mL were collected in 20 fractions with a Ca^{2+} and Mg^{2+} free Dulbecco's phosphate-buffered saline eluent. The resulting fractions were stored at −80 °C for further EV characterisation.

2.4. Nanoparticle Tracking Analysis

All samples were diluted in molecular grade water. Ideal measurement concentrations were found by pre-testing the ideal particles per frame value (140–200 particles/frame). For each measurement, three cycles were performed by scanning 11 cell positions each and capturing 30 frames per position under the following settings: focus: autofocus; camera sensitivity for all samples: 50; shutter: 70; scattering intensity: detected automatically; and cell temperature: 25 °C. After capture, the videos were analysed by the in-built ZetaView Software 8.04.02 SP2 with specific analysis parameters: maximum size: 500; minimum size: 5; minimum brightness: 25; hardware: embedded laser: 40 mW at 488 nm; and camera: CMOS.

2.5. RL95-2 Cell Conditioned Media EV Isolation Optimisation

This experiment was carried out to determine which of the size exclusion fractions contain EV particles. RL95-2 cells were cultured in T75 flasks with complete DMEM culture media until ~70/80% confluent. Cells were washed using DPBS without Ca^{2+} and Mg^{2+} 3 times and FBS free Dulbecco's Modified Eagles Medium (DMEM/F12) culture media added and incubated for 24 h. After 24 h the conditioned media was collected, and differential centrifugation was performed. Conditioned media underwent differential centrifugation followed by concentration using a 10 kDa ultrafiltration tube (Sartorius, Hampshire, UK) to 500 µL. Retentates were subjected to size exclusion chromatography with 20 × 0.5 mL fractions collected. The protein content of the fractions was determined using the bicinchoninic acid assay kit (Pierce™ BCA Protein Assay Kit, Thermo Scientific, Scotland, UK), according to the manufacturer's instructions, and particle concentration was determined by nanoparticle tracking analysis (NTA) (ZetaView, Particle Metrix, Meerbusch, Germany). Experiments were performed in triplicate on 3 different days. From this optimisation, it was determined that fractions 5–8 will be collected as these were shown to contain the highest concentration of EV sized particles free from protein contaminants (Supplementary Figure S1).

2.6. Hormone Treatment of RL95-2 Cells

This experiment was designed to determine the hormonal effect on EVs produced by endometrial cells. RL95-2 cells were cultured in T75 flasks with complete DMEM culture media until ~60/70% confluent. The media was changed after being washed using DPBS without Ca^{2+} and Mg^{2+} 3 times before being incubated with phenol red free DMEM culture media with charcoal stripped FBS (10%) to adapt similar conditions and avoid possible hormone-like (estrogenic) activity of phenol red for 24 h. The appropriate hormone treatment was then added to the cells in phenol red-free DMEM culture media at either a final concentration of 10 nM of progesterone (water soluble, Sigma-Aldrich, Dorset, UK) (P4) or 10 nM of estrogen (water soluble, Sigma-Aldrich, Dorset, UK) (E2) or estrogen (10 nM) plus progesterone (100 nM) (E2P4), as described before [18,19]. A control group containing equal amounts of the solubility complexing agent, cyclodextrin, found within the hormone mixtures was also performed. Following a 24 h incubation period, conditioned media was collected, and differential centrifugation was performed, followed by concentration and size exclusion chromatography, as described above. Samples were then analysed for particle concentration via NTA and protein concentration using the BCA assay. Experiments were performed in triplicates on 3 different days.

2.7. Transmission Electron Microscopy (TEM)

After SEC, 100 µL of the concentrated EVs were mixed with 100 µL of 4% paraformaldehyde (Polyscience, Warrington, PA, USA) to fix the EVs. On the day of analysis, 20 µL of an EVs droplet was covered by a 200-mesh formvar and carbon coated grid (Electron Microscopy Sciences). The EVs droplet was incubated for 20 min at room temperature. After 20 min, the grid was tapped on filter paper to remove excess PBS. Later the grid was rinsed once by gently touching the surface of the grid onto 50 µL of ddH2O droplet and tapped on filter paper to remove the excess water. For negative staining, the grid was transferred onto a droplet of 4% of uranyl acetate (21447 25, Polyscience, Warrington, PA, USA) for 5 min incubation at room temperature. Samples were observed with a JEM 1400 transmission electron microscope (JEOL Ltd., Tokyo, Japan) at 80 kV, and digital images were acquired with a numeric camera (Morada TEM CCD camera, Olympus, Germany).

2.8. Proteomic Analysi—Label-Free Liquid Chromatography Tandem Mass Spectrometry (LC-MS/MS)

EV samples (100 µL each) were transported to the Proteomic Core Facility, University of Tartu, Estonia in dry ice for proteomic analysis. An amount of 1 µg of protein was injected onto an Easy-nLC 1000 system (Thermo Scientific, Scotland, UK). The sample was eluted at 250 nL/min from the trap to a 75 µm ID × 50 cm emitter-column (New Objective, Littleton, CO, USA) packed with C18 material (3 µm, 300 Å particles, Dr Maisch, Ammerbuch, Germany). The separating gradient was 2–35% B for 60 min and 40–100% B for 5 min (A: 0.1% formic acid (FA), B: 80% Acetonitrile (CAN) + 0.1% FA). Eluted peptides were sprayed onto a Q Exactive Plus (Thermo Fisher Scientific, Waltham, MA, USA) quadrupole-orbitrap mass spectrometer (MS) using nano-electrospray ionization at 2.4 kV (applied through liquid-junction). The MS was operated with a top-5 data-dependent acquisition strategy. Briefly, one 350–1400 m/z MS scan at a resolution setting of R = 70,000 at 200 m/z was followed by five higher-energy collisional dissociation fragmentations (normalized collision energy of 26) of the 5 most intense ions (z: +2 to +6) at R = 17,500. MS and MS/MS ion target values were 3×10^6 and 5×10^4, respectively, with a 50 ms injection time. Dynamic exclusion was limited to 40 s.

2.9. Proteomic Data Analysis

Mass spectrometric raw files were processed with the MaxQuant software package (versions 1.6.15.0 and 2.0.3.0). Methionine oxidation, asparagine and glutamine deamidation and protein N-terminal acetylation were set as variable modifications, while cysteine carbamidomethylation was defined as a fixed modification. Label-free protein quantifi-

cation (LFQ) was enabled with LFQ and the protein minimum ratio count set to 1. The search was performed against *Homo sapiens and Bos taurus* reference proteomes, using the tryptic digestion rule. The peptide-spectrum match and protein false discovery rate (FDR) were kept below 1% using a target-decoy approach. All other parameters were default. Protein-coding of significant altered proteins (SAPs) in Evs were identified based on a fold change cut-off of 1 and a *p*-value cut-off of 0.05. An analysis of SAPs was performed in R studio (version 4.2.1) using the Bioconductor "DEP" package (version 3.1.5). Identified duplicates and contaminants were excluded from the list of each sample, and only proteins detected in at least two of the replicates were considered. After a literature review of these proteins enriched in the E2P4 group, 17 were selected for their functional relevance in implantation success and were divided into three groups depending on their involvement in embryo implantation, endometrial receptivity, and embryo development (Table 1). Gene Ontology (GO) and Kyoto Encyclopedia of Genes and Genomes (KEGG) pathway enrichment analyses were performed by the "clusterProfiler" R package (Version 4.4.4). Volcano plots, GO terms, and KEGG pathways were visualized by the "ggplot2" R packages (version 3.3.6). The data sets used and/or analysed during the current study are not currently publicly available, accession numbers have not yet been obtained; at the time of submission, they will be provided during review.

2.10. Statistical Analysis

GraphPad Prism version 9.2.0 was used for all statistical analysis. The comparison of particle concentration between the hormonal conditions and the control was analysed with repeated measure one way ANOVA. When comparing the different sizes and the different treatment groups, a two-way ANOVA with multiple comparisons was performed. All data presented as mean plus/minus standard error (mean ± SE). In all analyses, $p < 0.05$ was considered to be statistically significant.

3. Results

3.1. Characterisation of EVs Released from RL95-2 Cells

Purified EVs were shown to be positive for markers of transmembrane proteins associated with the EV plasma membrane CD9 and CD81 which were not seen in the conditioned media control (Figure 1A). EVs isolated from the control group conditions were also positive for TSG10, a marker of cytosolic protein recovered in EVs (Figure 1B) and negative for the negative marker Calnexin (CANX), a major component of non-EV co-isolated structures (Figure 1C). The PCA analysis also showed clear clustering between the control EV group and the control CM group (Figure 2). Transmission electron microscopy confirmed that EVs were intact, spherical in morphology, and with the expected EV size range within all four experimental conditions (Figure 3). Combined, these results fulfil the minimal information for studies of extracellular vesicles (MISEV) criteria and demonstrate that EVs have been successfully isolated from the endometrial conditioned media.

3.2. Concentration and Size Distribution of EVs Released from Hormone-Treated RL95-2 Cells

To assess the effect of the different menstrual cycle hormones on EV production, a comparison of the concentration of EVs produced from estrogen (E2), progesterone (P4), or estrogen plus progesterone (E2P4)-treated cells were compared to a control group. The addition of the hormones in the three different treatment groups showed no difference between the amount of EV sized particles produced (Figure 4A). A size comparison analysis of the concentration of particles in the different size classes of the particles was also produced and the different treatment groups were compared (Figure 4B). A significant difference can be seen between the 135 nm and 165 nm size groups, with more EV sized particles being released by the P4-treated group compared to the E2 group or the E2P4 group.

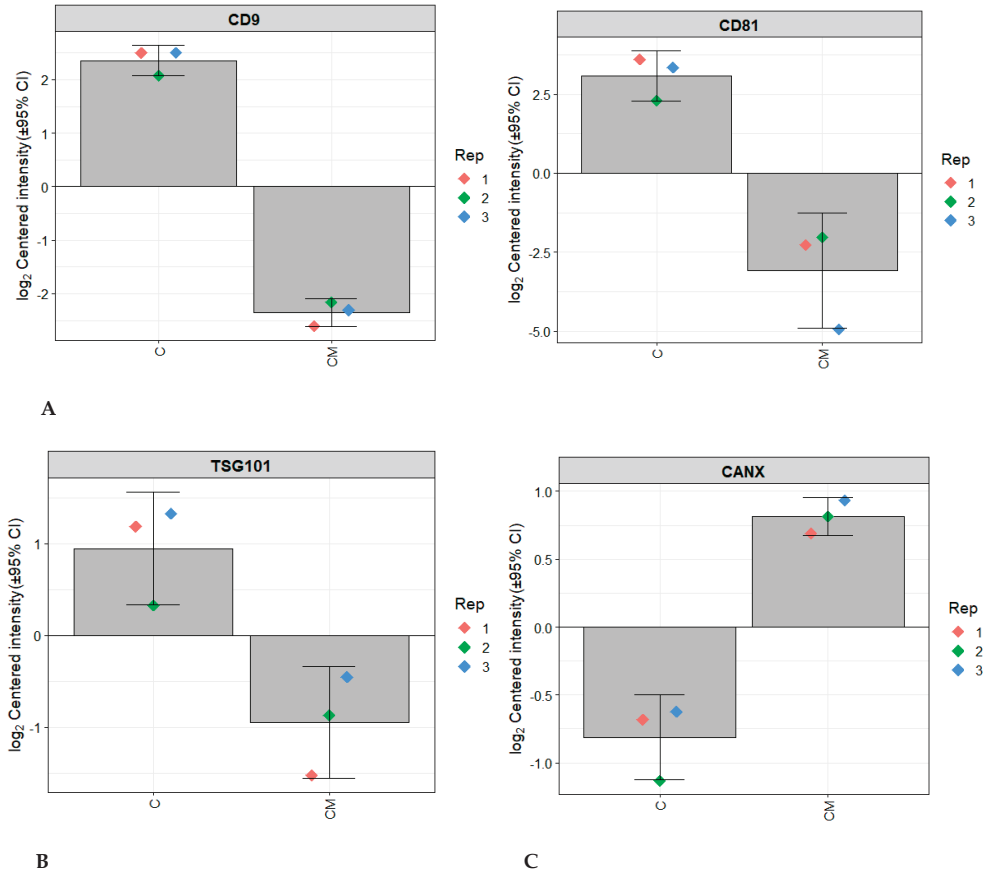


Figure 1. Protein content−based EV characterisation. Graphs representing the log2 centred intensity of various protein markers in the control, as well as the conditioned media control, validating the presence of EVs according to the MISEV guidelines. (**A**) represents is the intensity of the markers CD9 and CD81 to fulfil the MISEV criteria for markers of transmembrane or GPI-anchored proteins associated to plasma membrane and/or endosomes. (**B**) represents is the intensity of TSG101 to fulfil the MISEV criteria for a marker of cytosolic protein recovered in EVs. (**C**) represents is the intensity of the marker CANX to fulfil the MISEV criteria for a marker of a major components of non-EV co-isolated structures.

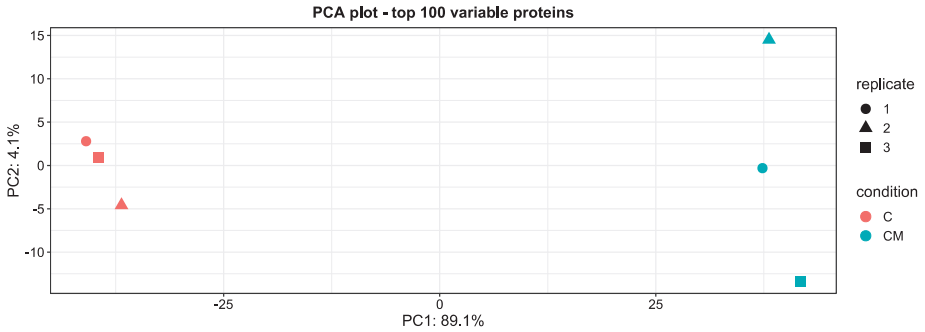


Figure 2. Principal component analysis (PCA) of top 100 variable proteins in the study groups. With C representing the EVs from the control group and CM representing the control conditioned media group. $n = 3$ for each experimental condition.

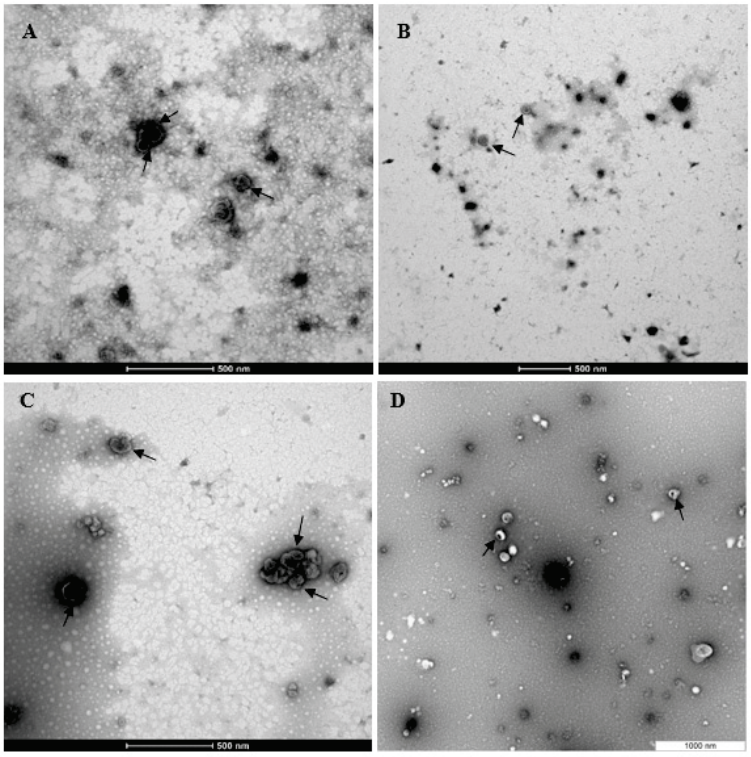


Figure 3. TEM Image based characterization of endometrial EVs from the different hormone treatment groups. Representative TEM images of endometrial EVs from control (**A**), P4 (**B**), E2 (**C**), and E2P4 (**D**). Scale bars: 500 nm (**A**–**C**); 1000 nm (**D**).

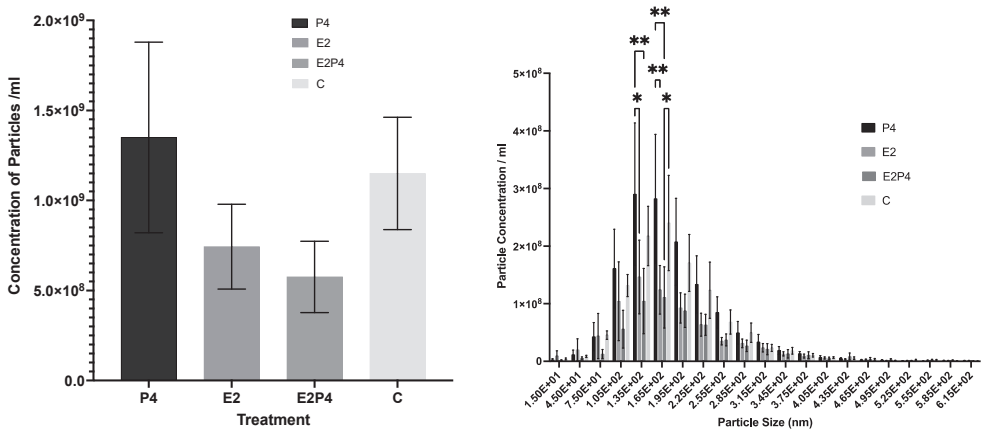


Figure 4. Concentration and size distribution of EVs released from RL95-2 hormone-treated cells. (**A**) The bars represent the mean concentration (particles/mL) ± SEM of EV sized particles from the SEC fractions 5–8. The treatment groups include estrogen (E2), progesterone (P4), estrogen plus progesterone (E2P4), and the control. Data were from 3 biological replicates and 3 technical replicates from each group. (**B**) The bars represent the mean concentration of the indicated particle size ± SEM from the SEC fractions 5–8. The significant difference is marked with 1 asterisk symbol (*) to denote $p \leq 0.05$ and 2 asterisk symbols (**) to denote $p \leq 0.01$. Data are from 3 biological replicates and 3 technical replicates.

3.3. Comparative Proteomic Analysis of Endometrial EVs under Hormonal Treatment

A heatmap of the log2 centred intensity of all significant proteins with the data centred per protein from the four experimental conditions showed a clear grouping of the four experimental conditions with six cluster groups, showing clear varied intensities between the EV isolated groups (Figure 5). There were 60 significant altered proteins (SAP) identified from the differential enrichment of EV proteins from the E2P4 group compared to E2 (Supplementary Table S1), 35 SAP identified from differential enrichment of EV proteins from the E2P4 group compared to the P4 group (Supplementary Table S2), 50 SAP identified from differential enrichment of EV proteins from E2vP4 (Supplementary Table S3), 31 SAP identified from the differential enrichment of EV protein from E2P4vC (Supplementary Table S4), 41 SAP identified from the differential enrichment of EV protein from E2vC (Supplementary Table S5), and five SAP identified from the differential enrichment of EV protein from P4vC (Supplementary Table S6). In the E2P4 group compared to the E2 group, 37 SAP were upregulated and 23 were downregulated. In the E2P4 group compared to the P4 group, 18 SAP were upregulated and 17 were down regulated. Volcano plots of these result show a direct indication of SAP (Figure 6). After a literature review of these proteins enriched in the E2P4 group, 17 were selected for their functional relevance in implantation success and were divided into three groups depending on their involvement in embryo implantation, endometrial receptivity, and embryo development (Table 1).

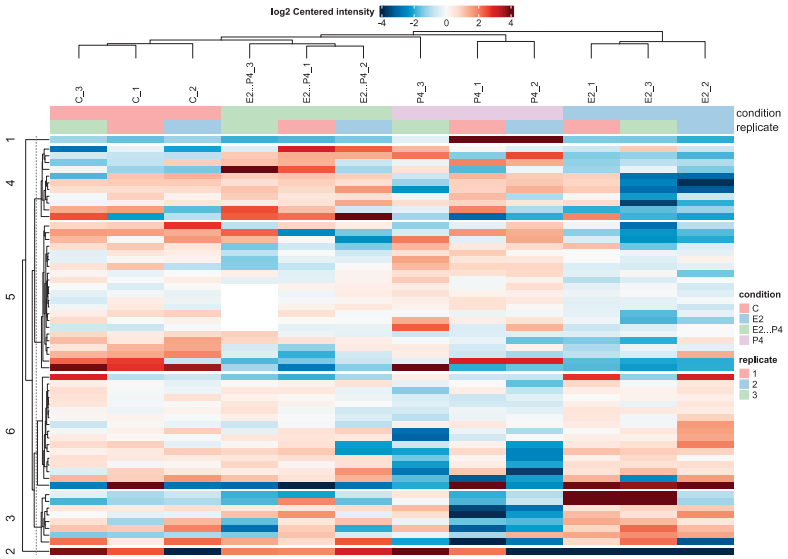
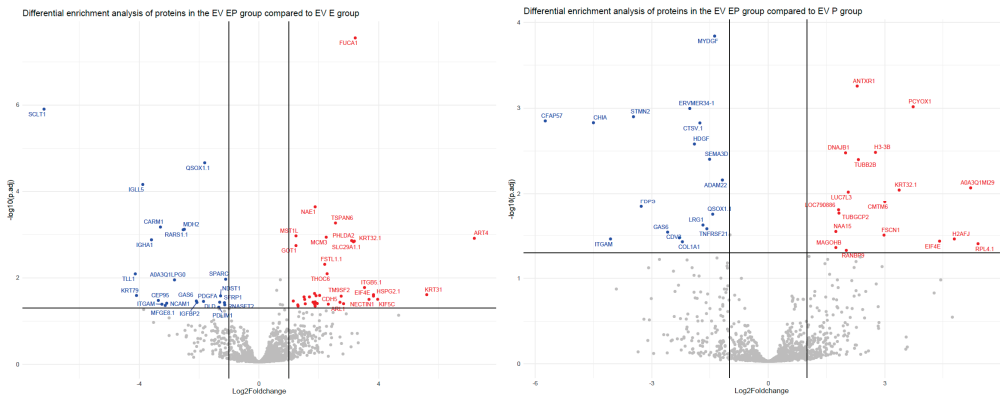


Figure 5. Heatmap shows the log2 centred intensity of all significant proteins with the data centred per protein. The rows represent all significant proteins and are clustered in 6 groups by k-means clustering (numbers on the left). C (control group), E2 (estrogen group), E2 . . . P4 (estrogen and progesterone group), and P4 (progesterone group). Colours represent the abundance of significantly altered proteins (red: higher; blue: lower).



A **B**

Figure 6. *Cont.*

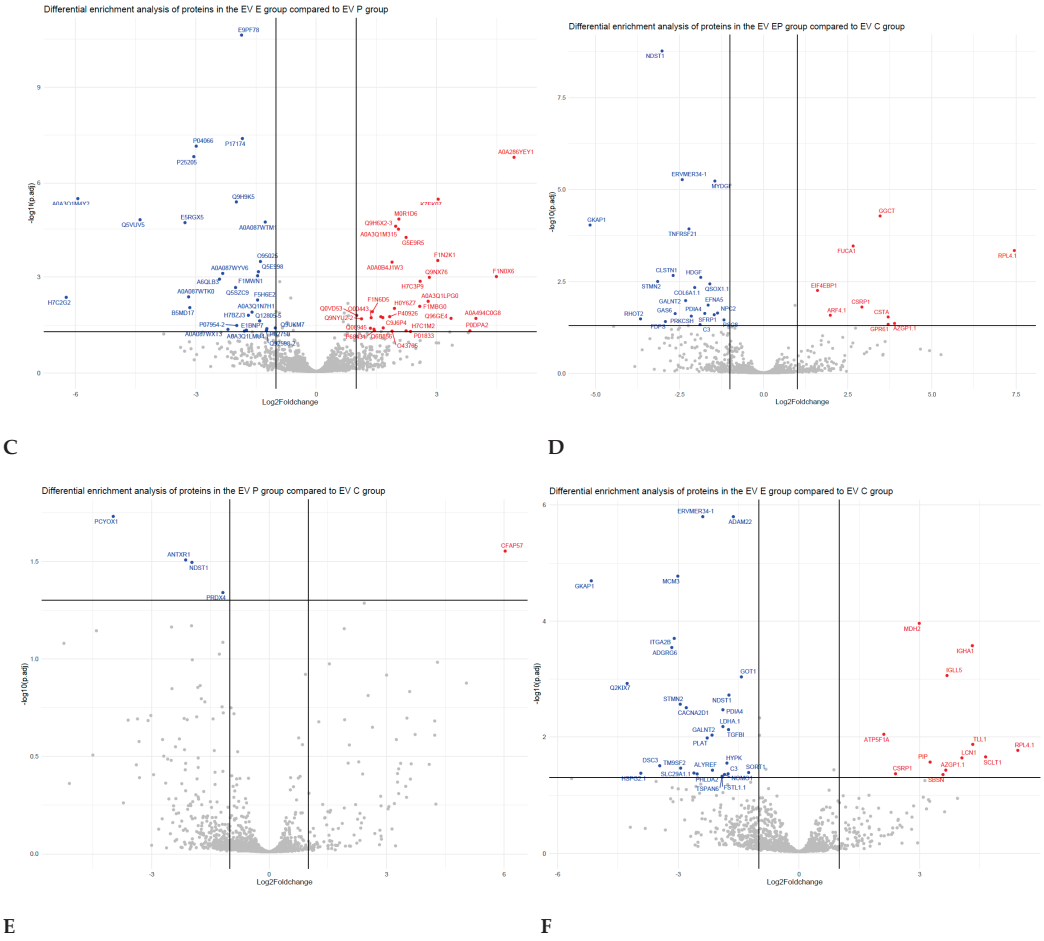


Figure 6. Differential enrichment of EV proteins in different comparison groups. (**A**) Volcano plot of the differentially expressed proteins in the estrogen plus progesterone supplemented groups (E2P4) compared to the estrogen group (E2); (**B**) estrogen plus progesterone supplemented groups (E2P4) compared to the progesterone group (P4); (**C**) estrogen supplemented groups (E2) compared to the progesterone group (P4); (**D**) estrogen plus progesterone group (E2P4) compared to the control (C); (**E**) progesterone (P4) compared to the control (C); and (**F**) estrogen (E2) compared to control. Adjusted *p* values (−log10) are plotted against the fold changes (log2). Red dots represent enriched proteins whereas blue dots represent depleted proteins in the respective comparisons.

Table 1. Proteins differentially enriched in the E2P4 receptive group EVs related to implantation success.

UniProt Accession	Gene Name	Protein Description	Evidence	Reference
	Embryo implantation			
Q6URK6	CDH5	Cadherin-5	CDH5 has been shown to be expressed in the late proliferative phase in the endometrium. A mouse in vitro study has demonstrated that the expression of CDH5 in trophectoderm helps to facilitate embryo implantation.	[20,21]
F1MER7	HSPG2	Basement membrane-specific heparan sulfate proteoglycan core protein	Shown to be an abundant cargo of the luteal phase EVs and have a specific role in embryo implantation. HSPG2 within the uterine epithelium has been shown to facilitate trophoblast attachment and adhesion.	[19,22]
F6RAG5	KIF5C	Kinesin heavy chain isoform 5C	Gene expression increased in embryo-endometrium contact co-cultures, as well as being shown to play a role during different morphogenetic processes in early embryo development.	[23,24]
A0A452DJ21	EIF4E	Eukaryotic translation initiation factor 4E	The expression if EIF4E has been examined in porcine endometrium during implantation, with truncated EIF4E shown to particularly regulate protein synthesis during conceptus attachment at the time of implantation.	[25]
Q58D84	FSTL1	Follistatin-related protein 1	Identified in menstrual fluid samples and is a common inflammatory and repair protein.	[26]
A6QLB3	ITGA2B	Integrin subunit alpha 2b	ITGA2B has been identified during the stages of bovine trophectoderm cell migration and fusion with the uterine epithelial cells.	[27]
Q9NRN7	AASDHPPT	L-aminoadipate-semialdehyde dehydrogenase-phosphopantetheinyl transferase	Found to be upregulated in the endometrium during pregnancy compared to genes during the estrous cycle.	[28]
	Endometrial receptivity			
A0A452DJE0	ACE2	Angiotensin-converting enzyme 2	ACE2 within the female reproductive system is abundantly expressed and is responsible for generating angiotensin, which has been shown to stimulate ovarian follicle growth, ovulation, and oocyte maturation, and is within the human endometrium.	[29]
H7BZJ3	PDIA3	Protein disulfide-isomerase A3	PDIA3 upregulated in fertile endometriums during secretory phase as compared to proliferative phase.	[30]
P00750	PLAT	Tissue-type plasminogen activator	In the reproductive system, PLAT mediates tissue remodelling required for ovulation and endometrial receptivity.	[31]

Table 1. *Cont.*

UniProt Accession	Gene Name	Protein Description	Evidence	Reference
C9JPV1	SLC6A6	Sodium- and chloride-dependent taurine transporter	SLC6A6 gene expression has been shown to be greater in cow endometria in the large preovulatory follicle compared to the small preovulatory follicles. This gene is thought to have a role in amino acid metabolism which is linked to the receptive state of the endometrial tissue.	[32]
A0A087WYV6	TSPAN6	Tetraspanin-6	Found in endometrial exosomes and thought to have functional and regulatory roles.	[33]
M0R1D6	DNAJB1	DnaJ homolog subfamily B member 1	One of many novel genes identified and associated with the biological process of menstrual cycle.	[34]
D6RDI2	LUC7L3	Luc7-like protein 3	Upregulated in human endometrial sample in women who exhibited implantation failure.	[35]
A0A3Q1LMU4	INHBB	Inhibin beta B chain	Known marker gene of decidualization.	[36]
	Embryo development			
P04066	FUCA1	Tissue alpha-L-fucosidase	FUCA1 was seen to be in higher abundance at elongation, as well as upregulated during day 15 of the cycle compared to day 7.	[37,38]
P00338	LDHA	L-lactate dehydrogenase A chain	When LDHA is inhibited, histone lactylation level is reduced and an impaired rate of development of pre-implantation mice embryos is seen.	[39]

To further analyse the biological function of DEGs, GO terms and KEGG pathway enrichment analyses were performed on the three comparison groups (E2P4vE2, E2P4vP4, and E2vP4) and the controls (E2P4vC, E2vC, and P4vC) (Figures 7–9). GO function analysis was conducted first. Regarding the biological process (BP), in E2P4vE2, the enriched SAP were involved in the regulation of cell communication, RNA transport, the movement of the cell or subcellular component, and protein modification (Figure 7A). In E2P4vP4, the SAP were enriched in endosomal transport, dephosphorylation, RNA transport, and mRNA transport (Figure 7B). In E2vP4, the SAP were enriched in protein-containing complex assembly, RNA catabolic process, translation, and mRNA metabolic processes (Figure 7C). In terms of molecular function (MF), in the E2P4vE2 group, enrichment was seen in cytoskeletal protein binding, microtubule binding, and GTPase regulator activity (Figure 7A). In E2P4vP4 the SAP were enriched in phosphatidylinositol phosphate binding, RNA cap binding, and ubiquitin conjugating enzyme activity (Figure 7B). In E2vP4, enrichment was seen in rRNA binding, DNA binding, and translation regulator activity (Figure 7C).

Biomolecules **2023**, *13*, 279

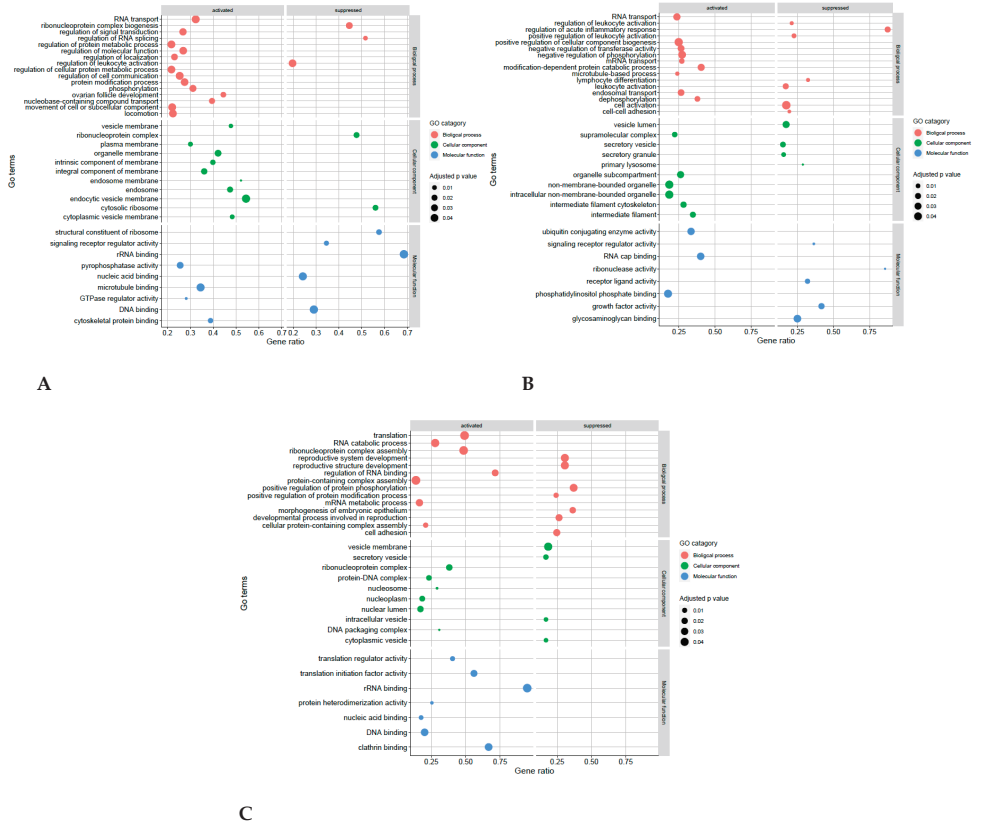


Figure 7. GO enrichment of SAP in the different comparison groups (**A**) E2P4 v E2, (**B**) E2P4 v P4, (**C**) E2vP4. The size and colour of points represents the GO category and the q-values respectively.

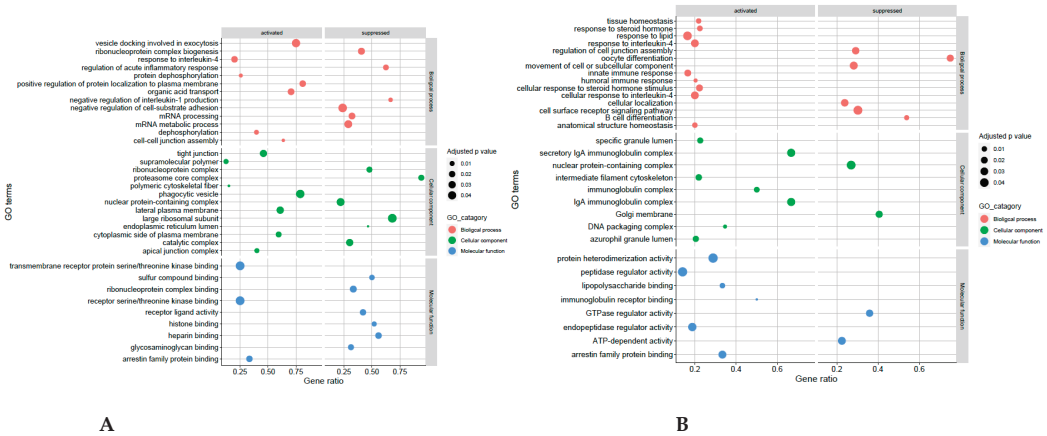
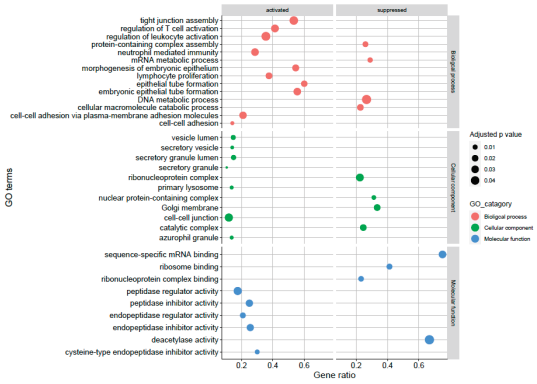


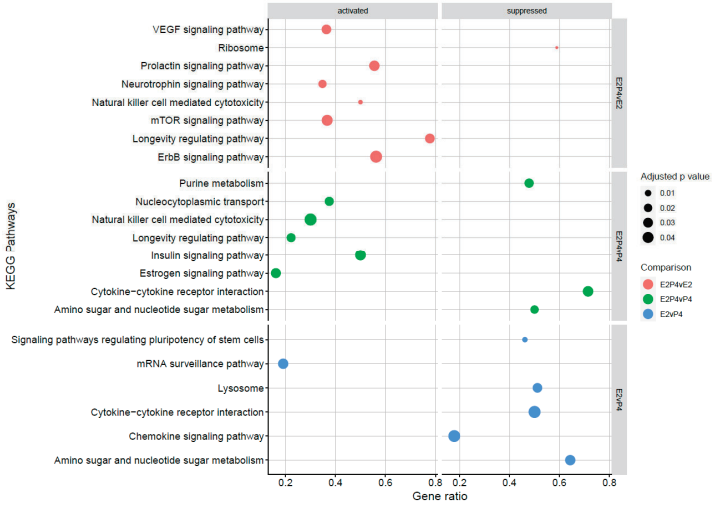
Figure 8. *Cont.*



C

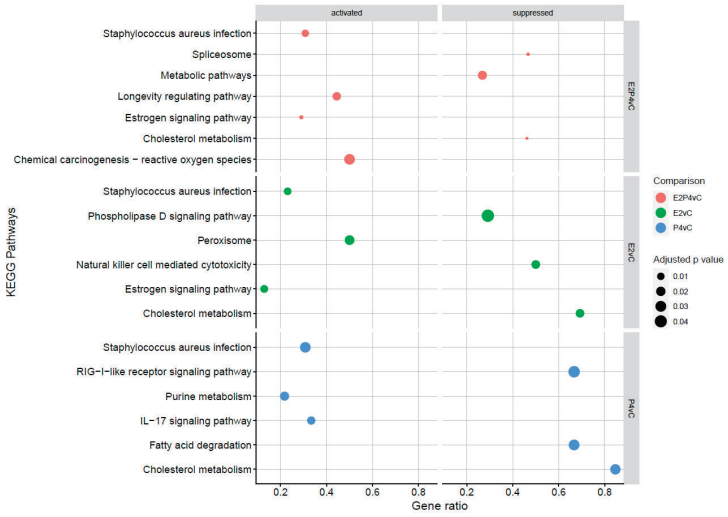
Figure 8. GO enrichment of SAP in the different comparison groups (**A**) E2P4 v C, (**B**) E2 v C, (**C**) P4 v C. The size and colour of points represents the GO category and the q-values respectively.

KEGG pathway analysis showed various pathways enriched in the comparison groups and control (Figure 9A,B). In E2P4vE2, enriched pathways included the mTOR signalling pathway, prolactin signalling pathway, and ErbB signalling pathway. In E2P4vP4, pathways that were intensified included the insulin signalling pathway, natural killer cell mediated cytotoxicity, and estrogen signalling pathway. In E2vP4, supressed pathways included cytokine-cytokine receptor interaction, lysosomes, and chemokine signalling pathways.



A

Figure 9. *Cont.*



B

Figure 9. KEGG Pathway analysis of SAP in the comparison groups and control. (**A**) Pathway analysis of SAP in the comparison groups, the size and colour of points represents the *p*-values and the comparison groups respectively. (**B**) KEGG Pathway analysis of SAP in the treatment groups versus the control, the size and colour of points represents the *p*-values and the comparison groups respectively.

4. Discussion

A successful pregnancy requires a receptive endometrium and a good quality embryo and optimum communication between these two entities. Locally, this complex process involves mutual communication between the incoming embryo and the endometrium in the uterine milieu [40–43]. Recently, it has been suggested that EVs regulate early embryo development as it reaches the uterus, in addition to priming the endometrium for embryo implantation [5,44,45]. The Evs lipid-bilayer protects the cargo, including proteins, from degradation, making them highly stable. However, a complete understanding of EV and their cargo's role in mediating implantation has not been demonstrated. This study comprehensively evaluates the proteome of EVs secreted by RL95-2 cells, an analogue of receptive endometrial epithelial cells, under a hormone stimulation mimicking the menstrual cycle to help begin to define novel biomarkers of endometrial receptivity and implantation success.

RL95 has been used in a number of papers and is a well-established model of a receptive endometrium [46–48]; additionally this cell line has been used in many implantation and adhesion related assays [49–51]. Thus, by using this cell line, we can provide novel insights into the complex process of human embryo implantation regulation. Via this in vitro modulation, discrepancies and variations between endocrinologic milieu Via among the individuals in a population can be avoided. An in vitro endometrial cell culture-based model, despite its simplicity, can offer a simple and a general characterisation and understanding of the EV proteome. Interestingly, 112 proteins were seen to be upregulated in the control EV samples compared to the conditioned medium, and of these proteins only 12 have been previously identified as exosome markers in Vesiclepedia, (ANXA6, ANXA7, ATP1A1, BSG, CD9, FLOT1, GNAS, GNB2, ITGB1, RAB7A, SDCBP, TFRC) (Supplementary Figure S2). The presence of these markers further supports their use as indicators of the enrichment of EVs. The additional 100 proteins enriched in EVs could be additional potential new markers for EVs or endometrial EVs, such as integrin alpha-3, a membrane protein that

regulates multiple biological processes, including cell adhesion, cell differentiation, and cell migration.

Moreover, the results indicate that the effects of all the hormone experimental conditions when compared to the control had no statistically significant differences in terms of EV concentration in vitro. A similar in vitro study showed results comparable to ours in that EVs were secreted in numbers independent of hormonal regulation, with similar concentrations seen between the estrogen and progesterone-treated groups [19]. However, these results and ours contradict those of an in vivo study which demonstrated that P4 increased the concentration of EVs in the uterine lumen [52]. However, it is important to note the different cell lines used when comparing studies, as well as the complex microenvironmental influences from different in vivo models.

In terms of EV size distribution, it was observed that the EV fractions from all four treatment conditions were within the expected EV size range but also, interestingly, there was a significant difference seen between the 135 nm and 165 nm size groups with more EV being released by the P4-treated group compared to the E2 group or the E2P4 group. This could suggest that higher amounts of EVs within this size range in the progesterone group, the hormone most prominent during the secretory phase when the endometrium is fertile, is due to an increase in communication signalling occurring, either sending a signal to the incoming embryo or in an autocrine way for the endometrium to prime itself for the incoming embryo. Alternatively, the larger size could be the presence of more cargo due to induction of secretory activity of the epithelial cells by the progesterone, which indirectly improves communications. However, when interpreting these results, it is Important to remember the limitations of NTA, the lack of specificity means differentiation between non-EV-structures, such as lipoproteins or residual reagent residues, could influence these results. Thus, only limited conclusions can be drawn from this method alone.

4.1. Receptive Phase Endometrial Cell EVs Were Enriched with Proteins Involved in Embryo Implantation

Proteomic assessment by the mass spectrometry of EVs allows a broader analysis to be performed. It has previously been shown that EVs derived from the endometrium can signal to the embryo to promote implantation. However, their composition, function, and influence on the uterine microenvironment and embryo remain unknown. Through proteomic analysis, we identified some key proteins that were significantly increased in E2P4-treated endometrial cell EVs compared to both E2 or P4 endometrial cell derived EVs, and these proteins may have a specific role in embryo implantation. Several of these proteins (including Cadherin-5 "CDH5", heparan sulfate proteoglycan core protein "HSPG2", Kinesin heavy chain isoform 5C "KIF5C" and Eukaryotic translation initiation factor 4E "EIF4E") have previously been identified in various embryo implantation models. Cadherin are cell adhesion molecules of which there are more than eighty members and are key regulators of cell adhesion, sorting and invasion [20]. In the current study, CDH5, was shown to be upregulated in EVs from the E2P4-treated cells, and has similarly been shown to be expressed in the late proliferative phase in endometrial explants [53] as well as endometrial mesenchymal stromal cells [54]. In addition an in vitro mouse study demonstrated that expression of CDH5 in the trophectoderm facilitates embryo implantation [21]. Such studies suggest that the upregulation of CDH5 in EVs specifically in the stimulated receptive period could be contributing to embryo implantation. Of further interest to the developmental progress of pregnancy is our identification of Perlecan (HSPG2) as intrinsic to the EV proteome. This molecule has been shown to be highly regulated at the time of blastocyst apposition and attachment, with previous studies demonstrating this role and its presence in the uterine epithelium [55,56]. All this data point towards the role of the receptive endometrium in contributing to the implantation interface through the release of EVs, potentially by signalling to, and preparing the endometrium to support implantation during this specific period dictated by hormones.

4.2. Receptive Phase Endometrial EVs Were Enriched in Proteins Involved in Embryo Development

The analysis of our dataset from the E2P4 EVs showed further proteins to be increased that are important in embryo development. These include proteins (including, "FUCA1" tissue alpha-L-fucosidase, and "LDHA1" L-lactate dehydrogenase A chain) that have previously been identified in various models assessing embryonic development. For example, the protein FUCA1 was seen in higher amounts in the EV isolated from the receptive phase induced endometrium condition in our study. Interestingly this protein was one of many that have also been seen at a higher level in the uterus of deer while embryos were at elongation rather than during diapause [37]. This suggests that changes occur upon embryo elongation in the uterine environment to support early development and survival, and perhaps our study suggests that endometrial EVs are contributing to transporting these proteins. Additionally, LDHA was seen to be upregulated in the E2P4 group and has also been shown to have a role in embryo development. Within pre-implantation, embryo glycolysis is regulated by LDHA, with LDHA catalysing the conversion of pyruvate to lactate. It has been shown that when LDHA is inhibited, the histone acetylation level is reduced and an impaired rate of development of pre-implantation mice embryos is seen [39]. Taken together this data suggest that endometrial EVs during the receptivity period could contain proteins associated with embryo development and that these are mutually communicated between the embryo and mother.

4.3. Receptive Phase Endometrial EVs Were Enriched in Proteins Involved in Endometrial Receptivity

On further analysis of our dataset, we observed an increase in proteins within E2P4 EVs compared to both E2 or P4 that are important in endometrial receptivity. These include proteins (including and "PLAT" tissue-type plasminogen activator, angiotensin-converting enzyme "ACE2" and inhibin beta B chain "INHBB"), that have previously been identified in various endometrial receptivity models. ACE2 has been found previously to be highly expressed within the reproductive system and is responsible for generating angiotensin using precursor peptides produced locally or taken from the circulation. Angiotensin within various mammalian species is seen to stimulate ovarian follicle growth, ovulation and oocyte maturation, and, within the human endometrium, it is seen at its highest levels during the window of implantation [57]. In addition, it has previously been discovered in airway epithelial cells that estrogen stimulated ACE2 expression, suggesting that the expression seen here also could also be mediated by steroid hormones [58]. However, the precise role of ACEs in the human endometrium is yet to be revealed and more evidence is required. In addition to ACE2, the protein PLAT was also seen to be upregulated in the stimulated receptive phase EVs. Again this protein has also been suggested to have a role in endometrial receptivity with PLAT seen to be involved in the extracellular matrix degradation essential for embryo adhesion and placental angiogenesis [31]. Finally, an increase in INHBB is seen in the receptive phase stimulated EVs. It has been previously reported that INHBB gene expression within the human uterus is related to the onset of decidualization [59], with its expression increasing in human endometrial stromal cells during decidualisation in vitro [60]. In addition to this, a reduced expression and reduced decidualization has been shown in ectopic pregnancies, implying that INHBB expression within human pregnancy is dependent on decidualisation [60]. These studies support the theory that the proteins found within the endometrial EV within the receptive phase have a role in endometrial receptivity too.

4.4. Receptive Phase Endometrial EVs GO Terms and KEGG Pathways Are Associated with Receptivity and Implantation Success

GO and KEGG analyses reinforced the above findings and identified key pathways associated with receptivity and implantation success in the receptive group. In the E2P4 group, in both the E2P4vE2 and E2P4vP4 group, key pathways in immune modulation, specifically natural killer cells, were activated. It has been previously reported that the levels

of NK cells change during the menstrual cycle and pregnancy [61], with increases seen during the secretory phase followed by a peak during the early stages of pregnancy [62]. There are various publications that support the theory that NK cells help in the regulation of pregnancy establishment and maintenance through many mechanisms, such as cytokine production that directly influence trophoblast growth [63], in addition to the vascularization and implantation of the decidua [64], immune modulating protein production that has a role in regulation of the immune response at the maternal-foetal interface [65], as well as the regulation of trophoblast invasion by cell-mediated cytotoxicity [63]. Despite this activation, cytokine-cytokine receptor interaction was shown to be supressed in the E2P4 group. This contradiction has been suggested to derive from the concept that endometrial NK cells are special immature cells that await pregnancy, with the NK cells lacking NK-specific functional phenotype and activity, such as cytokine secretion and cytotoxicity [66]. Hence the activation and suppression of these pathways reflects the phases stimulated in this model, with no influence of pregnancy or embryo stimulus.

In addition to the immune modulation, the KEGG pathway analysis also revealed many pathways known to support implantation in the E2P4 group, including the mTOR signalling pathway and VEGF signalling pathway. The mTOR pathway is known to play a role in cellular functions, such as cell proliferation, differentiation, apoptosis, autophagy, and decidualization [67], all of which are requirements for modulating a receptive endometrium. Similarly to what is seen in our data, it has previously been shown that mTOR increases during the implantation window in mice, with its role in receptivity further highlighted in a study in which an intrauterine injection of an inhibitor of mTOR, rapamycin, compromised the endometrial receptivity in mice [68]. Like mTOR, VEGF is also well reported to have a role in improving endometrial receptivity and facilitating the interactions between the embryo and the endometrium. VEGF, is an endothelial-specific mitogen in vitro, and is a main physiological and pathological angiogenesis regulator in the endometrium [69]. Within rodents, it has been shown that VEGF regulates endometrial vascular permeability and endothelial cell proliferation at the implantation site, indicating a key role of the VEGF pathway in embryonic-endometrial interaction [70,71]. It is well established that expression of VEGF dynamically changes within the oestrus cycle period and has been shown to be highly expressed in the endometrium in the middle stage of secretion, which mimics results seen in this study with the pathways activated in the E2P4 EV group. None of these pathways were seen to be activated in the E2- or P4-only-treated endometrial cell EVs, suggesting that the EV proteome is changing during the menstrual phases but a mechanism of how/if these proteins physiologically affect the endometrium/embryo requires further investigation.

A limitation and implication of interpreting this proteomic data, however, lies in the use of the proteomic method of shotgun label free proteomics. One issue that this approach highlights is that only the most abundant proteins are identified due to limitations in detection methods; hence, further proteins could be identified as being altered in the various groups, had an alternative method been used. This might have identified other pathways or roles that endometrial EVs contribute to during the menstrual cycle. Additionally, the results relate to the sample's total proteome, and it cannot be determined if they are located on the EVs cell surface or exist as cargo. Instead, the results are of a complex total EV proteome and further investigation via other means, such as antibody microarray, would be needed to understand their precise origin (i.e., cargo, surface, or both). Thus, whether these proteins are surface bound or cargos of EVs, and hence how, and if, they are of physiological significance in embryo-maternal signalling, remains an open question.

5. Conclusions

In summary, findings of the present study provide a new insight into the characteristics of EV from endometrial cells under hormonal control. Results from this study have provided new information on the effect menstrual cycles have on EV production, demonstrating a contribution of endometrial-derived EVs to endometrial-embryo cross

talk, showing an effect even without the known contributions of other players, such as spermatozoa, oocyte, and the developing embryo in an environment that is constantly changing and sending and receiving signals. Here the total proteome of endometrial EVs has been shown to be regulated by estrogen and progesterone, as physiologically relevant to the phases of the menstrual cycle. Significantly, our study shows that endometrial EVs within the receptive phase of the menstrual cycle consists of proteins associated with embryo implantation, endometrial receptivity, and embryo development, and key pathways identified in immune modulation and implantation processes. The application of this knowledge may allow EVs to be exploited as an endometrial tissue biopsy alternative and have a range of applications, such as monitoring the window of implantation, identifying the underlying aetiology of recurrent implantation failure, better prediction and increased implantation success in IVF, and enabling the design of non-hormonal-based contraceptives.

Supplementary Materials: The following supporting information can be downloaded at: https://www.mdpi.com/article/10.3390/biom13020279/s1, Figure S1: Isolation of extracellular vesicles sized particles secreted by the endometrial cell line RL95-2 using differential centrifugation and size exclusion chromatography; Figure S2: Ven diagram of proteins enriched in the Control EV group versus the conditioned media control compared to the top 100 Vesiclepedia EV markers; Table S1: Differential enrichment of EV proteins of E2P4 Group compared to E2; Table S2: Differential enrichment of EV proteins of E2P4 Group compared to P4; Table S3: Differential enrichment of EV proteins of E2 Group compared to P4; Table S4: Differential enrichment of EV proteins of E2P4 Group compared to C.; Table S5: Differential enrichment of EV proteins of E2 Group compared to C; Table S6: Differential enrichment of EV proteins of P4 Group compared to C. Reference [72] is cited in the supplementary materials.

Author Contributions: A.R.H.: designed or conceptualized the study; performed experiments, analysis, and interpretation of data; and drafted and revised the manuscript. N.L.A.K.: revised the manuscript. K.D.: assisted in the analysis of data and revised the manuscript. K.G.: assisted in the analysis of data and revised the manuscript. A.A.: assisted in TEM analysis and revised the manuscript. S.E.: revised the manuscript. P.R.H.: designed or conceptualized the study and revised the manuscript. A.F.: designed or conceptualized the study and revised the manuscript. All authors have read and agreed to the published version of the manuscript.

Funding: This research was funded by the European Union's Horizon 2020 research and innovation programme under COMBIVET ERA Chair grant agreement no. 857418 and a research grant by SPD Development Co., Ltd.

Institutional Review Board Statement: Not applicable.

Informed Consent Statement: Not applicable.

Data Availability Statement: The data that support the findings of this study is available from the corresponding author upon reasonable request. The mass spectrometry proteomics data have been deposited to the ProteomeXchange Consortium via the PRIDE [73] partner repository with the dataset identifier PXD039764.

Conflicts of Interest: The authors declare no conflict of interest.

References

1. Reed, B.G.; Carr, B.R. The Normal Menstrual Cycle and the Control of Ovulation. In *Endotext*; MDText.com, Inc.: South Dartmouth, MA, USA, 2021.
2. Taylor, A. ABC of Subfertility: Extent of the Problem. *Br. Med. J.* **2003**, *327*, 434. [CrossRef]
3. Okada, H.; Tsuzuki, T.; Murata, H. Decidualization of the Human Endometrium. *Reprod. Med. Biol.* **2018**, *17*, 220–227. [CrossRef]
4. Bhagwat, S.R.; Chandrashekar, D.S.; Kakar, R.; Davuluri, S.; Bajpai, A.K.; Nayak, S.; Bhutada, S.; Acharya, K.; Sachdeva, G. Endometrial Receptivity: A Revisit to Functional Genomics Studies on Human Endometrium and Creation of HGEx-ERdb. *PLoS ONE* **2013**, *8*, e58419. [CrossRef]
5. Es-Haghi, M.; Godakumara, K.; Häling, A.; Lättekivi, F.; Lavrits, A.; Viil, J.; Andronowska, A.; Nafee, T.; James, V.; Jaakma, Ü.; et al. Specific Trophoblast Transcripts Transferred by Extracellular Vesicles Affect Gene Expression in Endometrial Epithelial Cells and May Have a Role in Embryo-Maternal Crosstalk. *Cell Commun. Signal.* **2019**, *17*, 146. [CrossRef]

6. O'Neil, E.V.; Burns, G.W.; Ferreira, C.R.; Spencer, T.E. Characterization and Regulation of Extracellular Vesicles in the Lumen of the Ovine Uterus. *Biol. Reprod.* **2020**, *102*, 1020–1032. [CrossRef]
7. Nakamura, K.; Kusama, K.; Ideta, A.; Kimura, K.; Hori, M.; Imakawa, K. Effects of MiR-98 in Intrauterine Extracellular Vesicles on Maternal Immune Regulation during the Peri-Implantation Period in Cattle. *Sci. Rep.* **2019**, *9*, 20330. [CrossRef]
8. Dissanayake, K.; Nõmm, M.; Lättekivi, F.; Ord, J.; Ressaissi, Y.; Godakumara, K.; Reshi, Q.U.A.; Viil, J.; Jääger, K.; Velthut-Meikas, A.; et al. Oviduct as a Sensor of Embryo Quality: Deciphering the Extracellular Vesicle (EV)-Mediated Embryo-Maternal Dialogue. *J. Mol. Med.* **2021**, *99*, 685–697. [CrossRef]
9. Caponnetto, F.; Manini, I.; Skrap, M.; Palmai-Pallag, T.; Di Loreto, C.; Beltrami, A.P.; Cesselli, D.; Ferrari, E. Size-Dependent Cellular Uptake of Exosomes. *Nanomed. Nanotechnol. Biol. Med.* **2017**, *13*, 1011–1020. [CrossRef]
10. Li, T.; Greenblatt, E.M.; Shin, M.E.J.; Brown, T.J.; Chan, C. Cargo Small Non-Coding RNAs of Extracellular Vesicles Isolated from Uterine Fluid Associate with Endometrial Receptivity and Implantation Success. *Fertil. Steril.* **2021**, *115*, 1327–1336. [CrossRef]
11. Segura-Benítez, M.; Carbajo-García, M.C.; Corachán, A.; Faus, A.; Pellicer, A.; Ferrero, H. Proteomic Analysis of Extracellular Vesicles Secreted by Primary Human Epithelial Endometrial Cells Reveals Key Proteins Related to Embryo Implantation. *Reprod. Biol. Endocrinol.* **2022**, *20*, 3. [CrossRef]
12. Giacomini, E.; Scotti, G.M.; Vanni, V.S.; Lazarevic, D.; Makieva, S.; Privitera, L.; Signorelli, S.; Cantone, L.; Bollati, V.; Murdica, V.; et al. Global Transcriptomic Changes Occur in Uterine Fluid-Derived Extracellular Vesicles during the Endometrial Window for Embryo Implantation. *Hum. Reprod.* **2021**, *36*, 2249–2274. [CrossRef]
13. Burns, G.W.; Brooks, K.E.; Spencer, T.E. Extracellular Vesicles Originate from the Conceptus and Uterus during Early Pregnancy in Sheep. *Biol. Reprod.* **2016**, *94*, 56. [CrossRef]
14. Almiñana, C.; Vegas, A.R.; Tekin, M.; Hassan, M.; Uzbekov, R.; Fröhlich, T.; Bollwein, H.; Bauersachs, S. Isolation and Characterization of Equine Uterine Extracellular Vesicles: A Comparative Methodological Study. *Int. J. Mol. Sci.* **2021**, *22*, 979. [CrossRef]
15. Nakamura, K.; Kusama, K.; Ideta, A.; Imakawa, K.; Hori, M. IFNT-Independent Effects of Intrauterine Extracellular Vesicles (EVs) in Cattle. *Reproduction* **2020**, *159*, 503–511. [CrossRef]
16. Thippabhotla, S.; Zhong, C.; He, M. 3D Cell Culture Stimulates the Secretion of in Vivo like Extracellular Vesicles. *Sci. Rep.* **2019**, *9*, 13012. [CrossRef]
17. Ng, Y.H.; Rome, S.; Jalabert, A.; Forterre, A.; Singh, H.; Hincks, C.L.; Salamonsen, L.A. Endometrial Exosomes/Microvesicles in the Uterine Microenvironment: A New Paradigm for Embryo-Endometrial Cross Talk at Implantation. *PLoS ONE* **2013**, *8*, e58502. [CrossRef]
18. Yang, H.; Lei, C.; Cheng, C.; Feng, Y.; Zhang, W.; Petracco, R.G.; Sak, S. The Antiapoptotic Effect of Galectin-3 in Human Endometrial Cells under the Regulation of Estrogen and Progesterone. *Biol. Reprod.* **2012**, *87*, 39. [CrossRef]
19. Greening, D.W.; Nguyen, H.P.T.; Elgass, K.; Simpson, R.J.; Salamonsen, L.A. Human Endometrial Exosomes Contain Hormone-Specific Cargo Modulating Trophoblast Adhesive Capacity: Insights into Endometrial-Embryo Interactions. *Biol. Reprod.* **2016**, *94*, 38. [CrossRef]
20. Zhou, W.; Santos, L.; Dimitriadis, E. Characterization of the Role for Cadherin 6 in the Regulation of Human Endometrial Receptivity. *Reprod. Biol. Endocrinol.* **2020**, *18*, 66. [CrossRef]
21. Vilella, F.; Moreno-Moya, J.M.; Balaguer, N.; Grasso, A.; Herrero, M.; Martínez, S.; Marcilla, A.; Simón, C. Hsa-MiR-30d, Secreted by the Human Endometrium, Is Taken up by the Pre-Implantation Embryo and Might Modify Its Transcriptome. *Development* **2015**, *142*, 3210–3221. [CrossRef]
22. Slater, M.; Murphy, C.R. Chondroitin Sulphate and Heparan Sulfate Proteoglycan Are Sequentially Expressed in the Uterine Extracellular Matrix during Early Pregnancy in the Rat. *Matrix Biol.* **1999**, *18*, 125–131. [CrossRef]
23. Sponchiado, M.; Marei, W.F.A.; Beemster, G.T.S.; Bols, P.E.J.; Binelli, M.; Leroy, J.L.M.R. Molecular Interactions at the Bovine Embryo–Endometrial Epithelium Interface. *Reproduction* **2020**, *160*, 887–903. [CrossRef]
24. Dathe, V.; Pröls, F.; Brand-Saberi, B. Expression of Kinesin Kif5c during Chick Development. *Anat. Embryol.* **2004**, *207*, 475–480. [CrossRef]
25. Wollenhaupt, K.; Reinke, K.; Brüssow, K.P.; Albrecht, D.; Tiemann, U.; Seyfert, H.M.; Tomek, W. Natural Occurrence and Physiological Role of a Truncated EIF4E in the Porcine Endometrium during Implantation. *Biochem. J.* **2010**, *432*, 353–363. [CrossRef]
26. Salamonsen, L.A. Menstrual Fluid Factors Mediate Endometrial Repair. *Front. Reprod. Health* **2021**, *3*, 779979. [CrossRef]
27. Imakawa, K.; Bai, R.; Fujiwara, H.; Kusama, K. Conceptus Implantation and Placentation: Molecules Related to Epithelial–Mesenchymal Transition, Lymphocyte Homing, Endogenous Retroviruses, and Exosomes. *Reprod. Med. Biol.* **2016**, *15*, 1–11. [CrossRef]
28. Kim, M.; Seo, H.; Choi, Y.; Shim, J.; Kim, H.; Lee, C.K.; Ka, H. Microarray Analysis of Gene Expression in the Uterine Endometrium during the Implantation Period in Pigs. *Asian-Australas. J. Anim. Sci.* **2012**, *25*, 1102–1116. [CrossRef]
29. Reis, F.M.; Reis, A.M. Angiotensin-Converting Enzyme 2 (ACE2), Angiotensin-(1-7) and Mas Receptor in Gonadal and Reproductive Functions. *Clin. Sci.* **2020**, *134*, 2929–2941. [CrossRef]
30. Rai, P.; Kota, V.; Sundaram, C.S.; Deendayal, M.; Shivaji, S. Proteome of Human Endometrium: Identification of Differentially Expressed Proteins in Proliferative and Secretory Phase Endometrium. *Proteom. Clin. Appl.* **2010**, *4*, 48–59. [CrossRef]

31. Hoirisch-Clapauch, S.; Brenner, B. The Role of the Fibrinolytic System in Female Reproductive Disorders and Depression. *Thromb. Update* **2020**, *1*, 100004. [CrossRef]
32. França, M.R.; da Silva, M.I.S.; Pugliesi, G.; Van Hoeck, V.; Binelli, M. Evidence of Endometrial Amino Acid Metabolism and Transport Modulation by Peri-Ovulatory Endocrine Profiles Driving Uterine Receptivity. *J. Anim. Sci. Biotechnol.* **2017**, *8*, 54. [CrossRef]
33. Koh, Y.Q.; Peiris, H.N.; Vaswani, K.; Reed, S.; Rice, G.E.; Salomon, C.; Mitchell, M.D. Characterization of Exosomal Release in Bovine Endometrial Intercaruncular Stromal Cells. *Reprod. Biol. Endocrinol.* **2016**, *14*, 78. [CrossRef] [PubMed]
34. Groothuis, P.G.; Dassen, H.H.N.M.; Romano, A.; Punyadeera, C. Estrogen and the Endometrium: Lessons Learned from Gene Expression Profiling in Rodents and Human. *Hum. Reprod. Update* **2007**, *13*, 405–417. [CrossRef]
35. Tapia-Pizarro, A.; Figueroa, P.; Brito, J.; Marín, J.C.; Munroe, D.J.; Croxatto, H.B. Endometrial Gene Expression Reveals Compromised Progesterone Signaling in Women Refractory to Embryo Implantation. *Reprod. Biol. Endocrinol.* **2014**, *12*, 92. [CrossRef]
36. Griffiths IV, R.M.; Pru, C.A.; Behura, S.K.; Cronrath, A.R.; McCallum, M.L.; Kelp, N.C.; Winuthayanon, W.; Spencer, T.E.; Pru, J.K. AMPK Is Required for Uterine Receptivity and Normal Responses to Steroid Hormones. *Reproduction* **2020**, *159*, 707–717. [CrossRef]
37. Van der Weijden, V.A.; Bick, J.T.; Bauersachs, S.; Arnold, G.J.; Fröhlich, T.; Drews, B.; Ulbrich, S.E. Uterine Fluid Proteome Changes during Diapause and Resumption of Embryo Development in Roe Deer (*Capreolus capreolus*). *Reproduction* **2019**, *158*, 13–24. [CrossRef]
38. Faulkner, S.; Elia, G.; O'Boyle, P.; Dunn, M.; Morris, D. Composition of the Bovine Uterine Proteome Is Associated with Stage of Cycle and Concentration of Systemic Progesterone. *Proteomics* **2013**, *13*, 3333–3353. [CrossRef]
39. Yang, W.; Wang, P.; Cao, P.; Wang, S.; Yang, Y.; Su, H.; Nashun, B. Hypoxic in Vitro Culture Reduces Histone Lactylation and Impairs Pre-Implantation Embryonic Development in Mice. *Epigenet. Chromatin* **2021**, *14*, 57. [CrossRef]
40. Legato, M.J. *Principles of Gender-Specific Medicine: Gender in the Genomic Era*, 3rd ed.; Academic Press: Cambridge, MA, USA, 2017.
41. Fazeli, A.; Pewsey, E. Maternal Communication with Gametes and Embryos: A Complex Interactome. *Brief. Funct. Genom. Proteom.* **2008**, *7*, 111–118. [CrossRef]
42. Fazeli, A.; Holt, W.V. Cross Talk during the Periconception Period. *Theriogenology* **2016**, *86*, 438–442. [CrossRef]
43. Fazeli, A.; Moein Vaziri, N.; Holt, W.V. Proteomics of the Periconception Milieu. *Proteomics* **2015**, *15*, 649–655. [CrossRef]
44. Hart, A.R.; Khan, N.L.A.; Godakumara, K.; Dissanayake, K.; Piibor, J.; Muhandiram, S.; Eapen, S.; Heath, P.R.; Fazeli, A. The Role of Extracellular Vesicles in Endometrial Receptivity and Their Potential in Reproductive Therapeutics and Diagnosis. *Reprod. Biol.* **2022**, *22*, 100645. [CrossRef]
45. Godakumara, K.; Ord, J.; Lättekivi, F.; Dissanayake, K.; Viil, J.; Boggavarapu, N.R.; Faridani, O.R.; Jääger, K.; Velthut-Meikas, A.; Jaakma, Ü.; et al. Trophoblast Derived Extracellular Vesicles Specifically Alter the Transcriptome of Endometrial Cells and May Constitute a Critical Component of Embryo-Maternal Communication. *Reprod. Biol. Endocrinol.* **2021**, *19*, 115. [CrossRef]
46. Way, D.L.; Grosso, D.S.; Davis, J.R.; Surwit, E.A.; Christian, C.D. Characterization of a New Human Endometrial Carcinoma (RL95-2) Established in Tissue Culture. *In Vitro* **1983**, *19*, 147–158. [CrossRef]
47. Harduf, H.; Goldman, S.; Shalev, E. Human Uterine Epithelial RL95-2 and HEC-1A Cell-Line Adhesiveness: The Role of Plexin B1. *Fertil. Steril.* **2007**, *87*, 1419–1427. [CrossRef]
48. Thie, M.; Denker, H.W. In Vitro Studies on Endometrial Adhesiveness for Trophoblast: Cellular Dynamics in Uterine Epithelial Cells. *Cells Tissues Organs* **2002**, *172*, 237–252. [CrossRef]
49. Harduf, H.; Goldman, S.; Shalev, E. Progesterone Receptor A and C-Met Mediates Spheroids-Endometrium Attachment. *Reprod. Biol. Endocrinol.* **2009**, *7*, 14. [CrossRef]
50. Thie, M.; Herter, P.; Pommerenke, H.; Dürr, F.; Sieckmann, F.; Nebe, B.; Rychly, J.; Denker, H.W. Adhesiveness of the Free Surface of a Human Endometrial Monolayer for Trophoblast as Related to Actin Cytoskeleton. *Mol. Hum. Reprod.* **1997**, *3*, 275–283. [CrossRef]
51. Heneweer, C.; Kruse, L.H.; Kindháuser, F.; Schmidt, M.; Jakobs, K.H.; Denker, H.W.; Thie, M. Adhesiveness of Human Uterine Epithelial RL95-2 Cells to Trophoblast: Rho Protein Regulation. *Mol. Hum. Reprod.* **2002**, *8*, 1014–1022. [CrossRef]
52. Burns, G.W.; Brooks, K.E.; O'Neil, E.V.; Hagen, D.E.; Behura, S.K.; Spencer, T.E. Progesterone Effects on Extracellular Vesicles in the Sheep Uterus. *Biol. Reprod.* **2018**, *98*, 612–622. [CrossRef]
53. Dassen, H.; Punyadeera, C.; Kamps, R.; Klomp, J.; Dunselman, G.; Dijcks, F.; De Goeij, A.; Ederveen, A.; Groothuis, P. Progesterone Regulation of Implantation-Related Genes: New Insights into the Role of Oestrogen. *Cell. Mol. Life Sci.* **2007**, *64*, 1009–1032. [CrossRef]
54. Gargett, C.E.; Schwab, K.E.; Deane, J.A. Endometrial Stem/Progenitor Cells: The First 10 Years. *Hum. Reprod. Update* **2016**, *22*, 137–163. [CrossRef] [PubMed]
55. Yin, Y.; Wang, A.; Feng, L.; Wang, Y.; Zhang, H.; Zhang, I.; Bany, B.M.; Ma, L. Heparan Sulfate Proteoglycan Sulfation Regulates Uterine Differentiation and Signaling during Embryo Implantation. *Endocrinology* **2018**, *159*, 2459–2472. [CrossRef]
56. Carson, D.D.; Tang, J.P.; Julian, J. Heparan Sulfate Proteoglycan (Perlecan) Expression by Mouse Embryos during Acquisition of Attachment Competence. *Dev. Biol.* **1993**, *155*, 97–106. [CrossRef] [PubMed]
57. Henarejos-Castillo, I.; Sebastian-Leon, P.; Devesa-Peiro, A.; Pellicer, A.; Diaz-Gimeno, P. SARS-CoV-2 Infection Risk Assessment in the Endometrium: Viral Infection-Related Gene Expression across the Menstrual Cycle. *Fertil. Steril.* **2020**, *114*, 223–232. [CrossRef]

58. Stelzig, K.E.; Canepa-Escaro, F.; Schiliro, M.; Berdnikovs, S.; Prakash, Y.S.; Chiarella, S.E. Estrogen Regulates the Expression of SARS-CoV-2 Receptor ACE2 in Differentiated Airway Epithelial Cells. *Am. J. Physiol. Lung Cell. Mol. Physiol.* **2020**, *318*, L1280–L1281. [CrossRef]
59. McConaha, M.E.; Eckstrum, K.; An, J.; Steinle, J.J.; Bany, B.M. Microarray Assessment of the Influence of the Conceptus on Gene Expression in the Mouse Uterus during Decidualization. *Reproduction* **2011**, *141*, 511–527. [CrossRef]
60. Horne, A.W.; Van Den Driesche, S.; King, A.E.; Burgess, S.; Myers, M.; Ludlow, H.; Lourenco, P.; Ghazal, P.; Williams, A.R.; Critchley, H.O.D.; et al. Endometrial Inhibin/Activin β-B Subunit Expression Is Related to Decidualization and Is Reduced in Tubal Ectopic Pregnancy. *J. Clin. Endocrinol. Metab.* **2008**, *93*, 2375–2382. [CrossRef]
61. Xu, B.; Wang, J.; Xia, L.; Zhang, D.; Wu, X.; Zhang, A. Increased Uterine NK Cell Numbers and Perforin Expression during the Implantation Phase in IVF Cycles with GnRH Antagonist Protocol. *Sci. Rep.* **2017**, *7*, 39912. [CrossRef]
62. Bulmer, J.N.; Morrison, L.; Longfellow, M.; Ritson, A.; Pace, D. Granulated Lymphocytes in Human Endometrium: Histochemical and Immunohistochemical Studies. *Hum. Reprod.* **1991**, *6*, 791–798. [CrossRef]
63. Lash, G.E.; Otun, H.A.; Innes, B.A.; Percival, K.; Searle, R.F.; Robson, S.C.; Bulmer, J.N. Regulation of Extravillous Trophoblast Invasion by Uterine Natural Killer Cells Is Dependent on Gestational Age. *Hum. Reprod.* **2010**, *25*, 1137–1145. [CrossRef] [PubMed]
64. El-Azzamy, H.; Dambaeva, S.V.; Katukurundage, D.; Garcia, M.D.S.; Skariah, A.; Hussein, Y.; Germain, A.; Fernandez, E.; Gilman-Sachs, A.; Beaman, K.D.; et al. Dysregulated Uterine Natural Killer Cells and Vascular Remodeling in Women with Recurrent Pregnancy Losses. *Am. J. Reprod. Immunol.* **2018**, *80*, e13024. [CrossRef] [PubMed]
65. Fu, B.; Li, X.; Sun, R.; Tong, X.; Ling, B.; Tian, Z.; Wei, H. Natural Killer Cells Promote Immune Tolerance by Regulating Inflammatory TH17 Cells at the Human Maternal-Fetal Interface. *Proc. Natl. Acad. Sci. USA* **2013**, *110*, E231–E240. [CrossRef] [PubMed]
66. Manaster, I.; Mizrahi, S.; Goldman-Wohl, D.; Sela, H.Y.; Stern-Ginossar, N.; Lankry, D.; Gruda, R.; Hurwitz, A.; Bdolah, Y.; Haimov-Kochman, R.; et al. Endometrial NK Cells Are Special Immature Cells That Await Pregnancy. *J. Immunol.* **2008**, *181*, 1869–1876. [CrossRef]
67. Laplante, M.; Sabatini, D.M. Regulation of MTORC1 and Its Impact on Gene Expression at a Glance. *J. Cell Sci.* **2013**, *126*, 1712–1719. [CrossRef]
68. Chen, X.; He, J.; Ding, Y.; Zeng, L.; Gao, R.; Cheng, S.; Liu, X.; Wang, Y. The Role of MTOR in Mouse Uterus during Embryo Implantation. *Reproduction* **2009**, *138*, 351–356. [CrossRef]
69. Salmasi, S.; Sharifi, M.; Rashidi, B. Evaluating the Effect of Ovarian Stimulation and Exogenous Progesterone on CD31-Positive Cell Density, VEGF Protein, and MiR-17-5p Expression of Endometrium Immediately before Implantation. *Biomed. Pharmacother.* **2021**, *133*, 110922. [CrossRef]
70. Rabbani, M.L.; Rogers, P.A.W. Role of Vascular Endothelial Growth Factor in Endometrial Vascular Events before Implantation in Rats. *Reproduction* **2001**, *122*, 85–90. [CrossRef]
71. Shao, L.; Wang, H.; Duan, E.; Zhu, C. Expression of Vascular Endothelial Growth Factor in Rat Uterus during Peri-Implantation. *Chin. Sci. Bull.* **2001**, *46*, 1178–1181. [CrossRef]
72. Heberle, H.; Meirelles, G.V.; da Silva, F.R.; Telles, G.P.; Minghim, R. InteractiVenn: A web-based tool for the analysis of sets through Venn diagrams. *BMC Bioinform.* **2015**, *16*, 169. [CrossRef]
73. Perez-Riverol, Y.; Bai, J.; Bandla, C.; García-Seisdedos, D.; Hewapathirana, S.; Kamatchinathan, S.; Kundu, D.J.; Prakash, A.; Frericks-Zipper, A.; Eisenacher, M.; et al. The PRIDE Database Resources in 2022: A Hub for Mass Spectrometry-Based Proteomics Evidences. *Nucleic Acids Res.* **2022**, *50*, D543–D552. [CrossRef] [PubMed]

Disclaimer/Publisher's Note: The statements, opinions and data contained in all publications are solely those of the individual author(s) and contributor(s) and not of MDPI and/or the editor(s). MDPI and/or the editor(s) disclaim responsibility for any injury to people or property resulting from any ideas, methods, instructions or products referred to in the content.